Characterisation of the T-cell Component of the Lymph Node Microenvironment in Chronic Lymphocytic Leukaemia

Yallop, Deborah

Awarding institution:
King's College London

Characterisation of the T-cell Component of the Lymph Node Microenvironment in Chronic Lymphocytic Leukaemia

Deborah Yallop

A Thesis Presented for the Degree of

Doctor of Philosophy

King's College London

2016

Declaration

I hereby declare that I alone composed this thesis and that the work is my own, except where stated otherwise.

Deborah Yallop

November 2015

Abstract

The aim of this thesis was to characterise the T-cell component of the lymph node (LN) microenvironment in chronic lymphocytic leukaemia (CLL). It is well established that the proliferation of the neoplastic clone in CLL occurs primarily within the secondary lymphoid tissues and that within LNs these cells are in close contact with T-cells and other elements of the microenvironment. First I present a phenotypic study of the T-cells of the CLL LN obtained by fine needle aspiration. I found that, compared to CLL peripheral blood (PB), CLL LNs contain an excess of effector memory CD4+ T-cells and that the LN T-cells express more PD-1 than those from the PB; suggesting ongoing activation. Multiparameter immunofluorescence microscopy on LN biopsy sections showed that proliferating Ki67+ CLL cells are in contact with CD4+ PD-1+ T-cells. Next I sought to characterise the T-cell receptor (TCR) repertoire of flow sorted LN and PB CD4+ T-cells by spectratyping. This revealed oligoclonality in both compartments, with a significant reduction in TCR diversity in the PD-1hi subset. All subsets were skewed compared to healthy age matched PB. The spectratype profiles were distinct between the LN and PB and therefore likely a result of interaction with different antigens. This data was complemented by high throughput sequencing of the TCR, which showed more sequence overlap between 2 LNs taken from the same CLL patient, than between the LN and PB. Finally I present a preliminary *in-vitro* study aimed at recapitulating the events in CLL LNs. This study showed that PD-L1 can be upregulated on PB CLL cells by CD3/CD28 stimulation of accompanying T-cells, and that blocking PD-1 can lead to increased secretion of interferon gamma. Taken together these findings suggest that CLL CD4+ T-cells are subject to chronic activation and have undergone antigen driven oligoclonal expansion within the LN.

Table of Contents

Table of Figures

Table of Tables

Acknowledgments

I am thankful to my supervisors, Professor Stephen Devereux and Dr Andrea Buggins, for giving me the opportunity to work with them in the Rayne Institute, King's College London. I am grateful for their unending support and guidance whilst I undertook this research project and for helping me complete this thesis. Without their vision, hard work and perseverance it would not have been possible.

I acknowledge the British Society of Haematology, who kindly awarded me a start-up grant to undertake this project.

I would like to acknowledge Professor Shaun Thomas who, in the role of postgraduate coordinator, for the duration of my laboratory work, offered me invaluable advice and motivation.

I am thankful for the technical assistance, teaching and camaraderie of my laboratory colleagues; Will Townsend, Marta Pasikowska, Shahram Kordasti, Nicholas Lea, Aytug Kizilors, Jamal Anwar, Costas Chronis, Jane Moorhead, Lok Lam, Winston Vetharoy and especially my friend Emma Hamilton PhD.

I am particularly grateful to Professor Ghulam Mufti, Head of Department, Haematological Medicine, King's College Hospital, for his generosity and support which enabled me to complete this thesis.

I am overwhelmingly thankful to all the patients, who so generously donated samples for research and allowed me to poke needles in their necks, with no benefit to themselves.

I am especially indebted to my friends and clinical colleagues at King's College Hospital; Dr Shireen Kassam, Dr Robin Ireland, Dr Piers Patten and Dr Victoria Potter for helping me achieve this goal and for being nice.

Finally I would like to thank my mum, Paulette, and sister, Becky, for their love regardless of my endeavours, and in loving memory of my Dad, David, who was taken from us too soon.

Abbreviations

Abbreviation	Meaning
7-AAD	7-Amino-Actinomycin D
ABL	Abelson Murine Leukaemia Viral Oncogene Homolog 1
ADP	Adenosine Diphosphate
AID	Activation Induced Deaminase
AIHA	Autoimmune Haemolytic Anaemia
AKT	Protein Kinase B
AMCA	Aminomethylcoumarin Acetate
APC	Allophycocyanin
APC	Antigen Presenting Cell
APRIL	A Proliferation Inducing Ligand
ATM	Ataxia Telangiectasia Mutated
ATP	Adenosine Triphosphate
BAFF	B-Cell Activating Factor
BAFF-R	BAFF Receptor
BAX	Bcl-2 Associated X Protein
BCL	B-Cell Lymphoma
BCL-XL	BCL Extra Large
BCMA	B-Cell Maturation Antigen
BCR	B-Cell Receptor
BCSH	British Committee for Standards in Haematology
BFGF	Basic Fibroblast Growth Factor
BLK	B Lymphocyte Kinase
BM	Bone Marrow
BP	Base Pair
BSA	Bovine Serum Albumin
BTK	Bruton's Tyrosine Kinase
CAR	Chimeric Antigen Receptor

CARD11	Caspase Recruitment Domain Family Member 11
CAV1	Caveolin-1
CCR7	CC Chemokine Receptor 7
CD	Cluster of Differentiation
CDNA	Complementary DNA
CDR	Complementarity Determining Region
CFSE	Carboxyfluorescein Succinimidyl Ester
CLL	Chronic Lymphocytic Leukaemia
CML	Chronic Myeloid Leukaemia
CMV	Cytomegalovirus
CPG	Cytosine-Phosphate-Guanine
CTLA-4	Cytotoxic T-Lymphocyte Antigen 4
CXCR5	CXC Chemokine Receptor 5
CY	Cyanine
DAPI	4',6-Diamidino-2-Phenylindole
DATP	Deoxyadenosine Triphosphate
DCTP	Deoxycytidine Triphosphate
DEPC	Diethylpyrocarbonate
DGTP	Deoxyguanosine Triphosphate
DLBCL	Diffuse Large B-Cell Lymphoma
DMSO	Dimethyl Sulphoxide
DNA	Deoxyribonucleic Acid
DNase	Deoxyribonuclease
DNTP	Deoxyribonucleotide Triphosphate
DTT	Dithiothreitol
DTTP	Deoxythymidine Triphosphate
E2F1	E2F Transcription Factor 1
EDTA	Ethylenediaminetetraacetic Acid
EFS	Event Free Survival
ERK	Extracellular Signal Regulated Kinase

FACS	Fluorescence Activated Cell Sorting
F-Actin	Filamentous Actin
FBC	Full Blood Count
FBS	Foetal Bovine Serum
FC	Fludarabine and Cyclophosphamide
FCR	Fludarabine, Cyclophosphamide and Rituximab
FDC	Follicular Dendritic Cell
FFPE	Formalin Fixed Paraffin Embedded
FISH	Fluorescence In Situ Hybridisation
FITC	Fluorescein Isothiocyanate
FMC7	Flinders Medical Centre 7
FNA	Fine Needle Aspirate
FOXP3	Forkhead Box P3
FSC	Forward Scatter
FYN	Proto Oncogene Tyrosine Protein Kinase Fyn
GC	Germinal Centre
G-CSF	Granulocyte Colony Stimulating Factor
GM-CSF	Granulocyte Macrophage Colony Stimulating Factor
H&E	Haematoxylin and Eosin
HTA	Human Tissue Authority
HUVEC	Human Umbilical Vein Endothelial Cell
ICAM	Intercellular Adhesion Molecule
ICOS	Inducible T-Cell Co-Stimulator
IFN	Interferon
IG	Immunoglobulin
IGH	Immunoglobulin Heavy Chain
IGHV	Immunoglobulin Variable Heavy Chain
IGL	Immunoglobulin Light Chain
IGV	Immunoglobulin Variable Region
IKK	Inhibitor of NF-KB Kinase

IL	Interleukin
ILS-600	Internal Lane Standard 600
IMGT	International ImMunoGeneTics Information System
IRF	Interferon Regulatory Factor
ITAM	Immunoreceptor Tyrosine-Based Activation Motif
IWCLL	International Workshop on Chronic Lymphocytic Leukaemia
KCHFT	King's College Hospital Foundation Trust
KCL	King's College London
KD	Kilodalton
LCK	Lymphocyte Specific Protein Tyrosine Kinase
LDH	Lactate Dehydrogenase
LDT	Lymphocyte Doubling Time
LFA-1	Lymphocyte Function Associated Antigen 1
LN	Lymph Node
LREC	Local Research Ethics Committee
LYN	Tyrosine Protein Kinase Lyn
MAB	Monoclonal Antibody
MALT	Mucosa Associated Lymphoid Tissue
MALT1	MALT Lymphoma Translocation Protein 1
MAP	Mitogen Activated Protein
MAPK	MAP Kinase
MAPKK	MAPK Kinase
MAPKKK	MAPKK Kinase
MBL	Monoclonal B Lymphocytosis
MCL-1	Myeloid Cell Leukaemia 1
MDSC	Myeloid Derived Suppressor Cell
MFI	Mean Fluorescence Intensity
MHC	Major Histocompatibility Complex
MTOR	Mammalian Target Of Rapamycin

MW	Megawatt
NCI	National Cancer Institute
NFAT	Nuclear Factor Of Activated T-Cells
NF-kB	Nuclear Factor Kappa B
NK	Natural Killer Cells
NLC	Nurse Like Cell
NM	Nanometres
NRES	National Research Ethics Service
NT	Nucleotide
OS	Overall Survival
PB	Peripheral Blood
PBMCS	Peripheral Blood Mononuclear Cells
PBS	Phosphate Buffered Saline
PC	Proliferation Centre
PCR	Polymerase Chain Reaction
PD-1	Programmed Death 1
PD-L1	Programmed Death Ligand 1
PD-L2	Programmed Death Ligand 2
PE	Phycoerythrin
PECAM	Platelet Endothelial Cell Adhesion Molecule
PERCP	Peridinin Chlorophyll Protein
PFA	Paraformaldehyde
PFS	Progression Free Survival
PHA	Phytohaemagglutinin
PI	Propidium Iodide
PI3K	Phosphatidylinositol 3-Kinase
PKC	Protein Kinase C
PLC	Phospholipase C
PLL	Prolymphocytic Leukaemia
PMA	Phorbol Myristate Acetate

PMT	Photomultiplier Tube
PV	Polycythaemia Vera
RAG	Recombination Activation Gene
RBC	Red Blood Cell
RhA	Rheumatoid Arthritis
RNA	Ribonucleic Acid
RNASE	Ribonuclease
ROR-1	Receptor Tyrosine Kinase Like Orphan Receptor 1
RPM	Revolutions Per Minute
RPMI	Roswell Park Memorial Institute Medium
RT	Room Temperature
RT	Reverse Transcriptase
SDF	Stromal Derived Factor
SEER	Surveillance, Epidemiology, and End Results Program
SHM	Somatic Hypermutation
SHP	Src Homology Domain Containing Tyrosine Phosphatase
SLE	Systemic Lupus Erythematosus
SLL	Small Lymphocytic Lymphoma
SMIG	Surface Immunoglobulin
SNP	Single Nucleotide Polymorphism
SRC	Proto Oncogene Tyrosine Protein Kinase
SSC	Side Scatter
STAT1	Signal Transducer and Activator of Transcription 1
SYK	Spleen Tyrosine Kinase
TACI	Transmembrane Activator and Calcium Modulator and Cyclophilin Ligand Interactor
TBE	Tris / Borate / EDTA
TBS	Tris Buffered Saline
T_{CM}	Central Memory T-Cell
TCR	T-Cell Receptor

TdT	Terminal Deoxynucleotidyl Transferase
T_{EM}	Effector Memory T-Cell
T_{EMRA}	Terminal Differentiated Effector Memory T-Cell
TFH	Follicular Helper T-Cell
TGF-β	Transforming Growth Factor Beta
TH	Helper T-Cell
TK	Thymidine Kinase
TLR	Toll Like Receptor
T_{NAIVE}	Naïve T-Cell
TNF	Tumour Necrosis Factor
TP53	Tumour Protein 53
TRAF	Tumour Necrosis Factor Receptor Associated Factors
TREG	Regulatory T-Cell
TRITC	Tetramethylrhodamine Isothiocyanate
UK	United Kingdom
US	United States
V/V	Volume / Volume
VCAM	Vascular Cell Adhesion Molecule
VEGF	Vascular Endothelial Growth Factor
VEGFR	Vascular Endothelial Growth Factor Receptor
VOL	Volume
Vβ	Variable Beta
W/V	Weight / Volume
WBC	White Blood Cell
WCC	White Cell Count
WHO	World Health Organisation
WM	Waldenström Macroglobulinaemia
WT	Weight
ZAP-70	Zeta Associated Protein 70
β2-M	Beta-2 Microglobulin

Chapter 1 General Introduction

1.1 Background to Chronic Lymphocytic Leukaemia

1.1.1 Definition

Chronic Lymphocytic Leukaemia (CLL) is a clonal neoplasm of mature B-cells with a characteristic immunophenotype. Malignant B-cells accumulate within the peripheral blood (PB), secondary lymph node tissue (LN), bone marrow (BM) and other organs of affected patients. As the disease progresses this accumulation leads to the clinical features of lymphocytosis, immune dysfunction, lymphadenopathy, splenomegaly, hepatomegaly and ultimately bone marrow failure in advanced disease. In 2008, The International Workshop on Chronic Lymphocytic Leukaemia (iwCLL) updated the National Cancer Institute guidelines to define CLL as a B lymphocytosis with a CLL immunophenotype and an absolute clonal B-cell count of >5000 cells/µl. Previously an absolute lymphocyte count of >5000 cells/µl was used as a diagnostic criteria. This change in classification has resulted in 40% of patients previously labelled as early stage CLL being reclassified as monoclonal B-lymphocytosis of CLL phenotype (MBL) (Shanafelt, Kay et al. 2008).

1.1.2 Epidemiology

CLL is the commonest leukaemia in the western world, accounting for 30% of all cases of leukaemia and 16% of all haematological malignancies. Cancer registration statistics for the United Kingdom (UK) are published by the Office for National Statistics, the Welsh Cancer Intelligence and Surveillance Unit and the Northern Ireland Cancer Registry. The UK incidence of CLL is reported as 3 persons per 100,000 population and there are approximately 3300 new cases diagnosed every year. The United States (US) National Cancer Institute Surveillance, Epidemiology, and End Results Program (SEER) Cancer Statistics Review 1975-2011, reported the age-adjusted incidence rate of CLL at 4.2 per 100,000 per year (Oscier, Dearden et al. 2012). In the UK there is significant geographical variation in CLL incidence, which is reflected by differences in regional demographics. In the most part this is explained by the difference in the mean age of the population in different locations in the UK;

reflecting that the incidence of CLL increases with age. The SEER dataset showed 89% percent of patients are aged over 55 at diagnosis and the median age at presentation is 72. Worldwide epidemiological studies have shown CLL is most common in Caucasians and is 20-30 times less common in India, China and Japan, but no environmental factors have been definitively implicated. CLL is twice as common in males compared to females, which in the most part remains poorly understood. CLL does show a degree of inheritable predisposition with an increased risk of CLL and MBL in first and second degree relatives of patients with CLL (Rawstron, Yuille et al. 2002, Goldin, Landgren et al. 2010). Overall there is a sevenfold increase in the incidence of CLL and more than doubling of the risk of being diagnosed with another lymphoid malignancy, such as lymphoplasmacytoid lymphoma and hairy cell leukaemia, in the relatives of patients with CLL (Goldin, Bjorkholm et al. 2009, Goldin, Landgren et al. 2010). In some families with CLL the phenomenon of genetic anticipation has been documented (Yuille, Houlston et al. 1998, Goldin, Sgambati et al. 1999). To attempt to understand the mechanism behind the familial association several genome wide studies have been undertaken. These have identified a number of single nucleotide polymorphisms (SNP) at multiple susceptibility loci, which seem to correlate with an increased risk of developing CLL (Speedy, Di Bernardo et al. 2014).

1.1.3 Diagnosis

A full blood count (FBC) is one of the most commonly requested blood tests across UK haematology laboratories. Laboratories define the normal range for total lymphocyte counts and participate in national external quality assurance schemes to ensure the validity of the results. Parameters will be set by the laboratory for automated cell counters to trigger a request for a blood film and manual differential count. In CLL the PB lymphocytosis can be just outside the normal range to over a hundred fold above the upper limit. CLL is very commonly detected as an incidental finding from routine blood tests taken for unrelated indications. The PB smear morphology in CLL is characteristic and typically shows a fairly uniform population of small mature lymphocytes with clumped chromatin and a high nuclear to cytoplasmic ratio. Nucleoli are usually small and inconspicuous. So-called "smear cells" are a hallmark feature and relate to the fragility of CLL cells and the content of the cytoskeletal

protein vimentin. (Brown, Hallam et al. 2001). Interestingly the number of smear cells remains constant over time in an individual patient and is an independent prognostic factor (Nowakowski, Hoyer et al. 2007). A typical PB film from a CLL patient is shown in Figure 1-1. There can be a variable number of prolymphocytes present but these must be <10% of total lymphocytes, otherwise a diagnosis of CLL/PLL (prolymphocytic leukaemia) is more appropriate. The blood film can also indicate the degree of anaemia. Anaemia is typically normocytic normochromic when as a consequence of bone marrow involvement, but if the CLL is complicated by autoimmune haemolytic anaemia, spherocytes and polychromasia can be seen. Neutropenia is rare and thrombocytopenia at diagnosis usually indicates advanced disease.
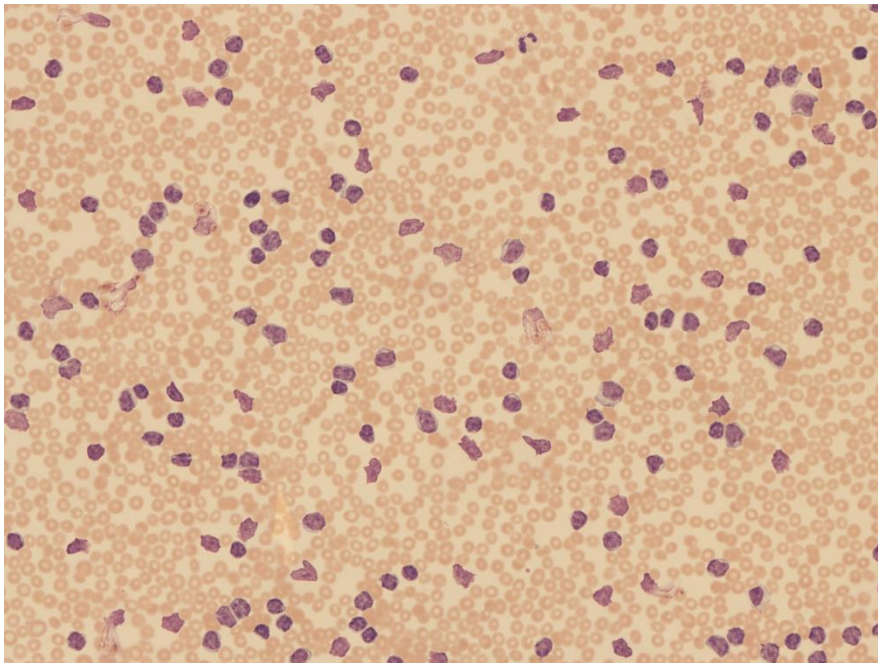
Figure 1-1 PB film in CLL. Magnification x20. Courtesy of King's Haematological Malignancy Diagnostic Centre.

Lymphocytosis and a typical PB film will usually prompt a haematological referral. Many B-cell malignancies can be distinguished by their individual pattern of cell surface markers expression by PB immunophenotyping. The World Health Organisation (WHO) classification of tumours outlines the current diagnostic criteria for the haematological malignancies. The Marsden CLL score has been devised and subsequently revised based on the expression of

the following 5 cell surface markers; weak monotypic surface immunoglobulin, CD5, CD23, weak FMC7 and weak CD22 or CD79b (Matutes, Owusu-Ankomah et al. 1994, Moreau, Matutes et al. 1997). The widely adopted modified scoring system is shown in Table 1-1. A CLL score of 4-5/5 strongly supports the diagnosis of CLL and encompasses 92% of CLL cases.

Table 1-1 Revised CLL scoring system

Surface Marker	Expression Score +1	Expression Score 0
SmIg	Weak	Strong
CD5	Positive	Negative
CD23	Positive	Negative
FMC7	Negative	Positive
CD22 or CD79b	Weak	Strong

In cases where there is diagnostic uncertainty a bone marrow trephine or lymph node biopsy can be performed. The bone marrow is invariably involved in CLL and classically fits two patterns of involvement; either nodular or diffuse infiltration. The presence of pale staining "proliferation centres" (PC) is supportive of the diagnosis. The bone marrow trephine has clinical utility in determining whether PB cytopenias are related to bone marrow failure or autoimmunity. Surgical lymph node biopsy is usually only required for diagnostic purposes in patients where the degree of lymphadenopathy is out of keeping with the PB picture; for example when there is a solitary bulky node, or when a high grade transformation is suspected.

1.1.4 Clinical Features

CLL is characteristically a heterogeneous disease and the way in which the patient presents to the clinician reflects this. 70-80% of new cases are detected incidentally by the presence of isolated lymphocytosis on a FBC performed for an unrelated indication (Oscier, Fegan et al. 2004). Clinical presentations are very variable and reflect the various sequelae of the disease process. Tumour proliferation and bulk can lead to palpable lymphadenopathy, abdominal

discomfort from hepatosplenomegaly or even compressive symptoms, such as dysphagia or cough, from extrinsic pressure from lymph nodes. Bone marrow involvement can lead to symptoms of anaemia with fatigue, shortness of breath or pallor. Non-specific malignancy associated "B-symptoms" frequently reflect disease bulk and include unintentional weight loss and night sweats. Infections are a very common due to the complex immune dysfunction in CLL, and infections are ultimately responsible for up to 50% of CLL deaths (Hamblin 1987). 85% of CLL patients are hypogammaglobulinaemic. Infection risk in CLL correlates with hypogammaglobulinaemia which begins to appear at early stages of the disease (Rozman, Montserrat et al. 1988, Rossi, Sozzi et al. 2009, Morrison 2010). Although depletion of normal B-cells, as a result of expansion of the neoplastic clone, undoubtedly contributes to low immunoglobulin levels, there is also evidence that aberrant expression of CD30 by T-cells supresses immunoglobulin class switching and thus the production of IgG and IgA (Cerutti, Kim et al. 2001). There are numerous defects in cell mediated immunity and T-cell dysfunction which will be discussed later.

1.1.5 Prognosis

Clinical staging systems are extremely useful in dividing the heterogeneous CLL patient population into defined prognostic groups. The two universally accepted CLL staging systems devised by Rai et al (Rai, Sawitsky et al. 1975) and Binet et al (Binet, Auquier et al. 1981) are the best validated tools for predicting prognosis and still play an integral role in clinical decision making. Table 1-2 below shows the staging systems, the percentage of patients that fall into each category and their median survival in the chemotherapy era.

Table 1-2 Rai and Binet CLL clinical staging systems

	Characteristics	% of Patients	Median Survival
Rai Stage			
0	Lymphocytosis	30	12 years
I	Lymphocytosis plus lymphadenopathy	35	9 years
II	Lymphocytosis plus splenomegaly and/or hepatomegaly	25	7 years
III	Lymphocytosis plus Hb <11g/dl	7	5 years
IV	Lymphocytosis plus platelets <100 x10^9/l	3	1 year
Binet Stage			
A	Less than three areas of lymphoid sites involved	65	9 years
B	Three or more areas of lymphoid sites involved	30	5 years
C	Hb <10g/dl or platelets <100 x10^9/l	5	2 years

These clinical staging systems are useful to subgroup individuals with CLL patients but they do not help the clinician predict which individual early stage patient will progress to an advanced clinical stage. The clinical course of CLL generally follows one of four patterns; the first group have stable disease, which changes little over time, these patients do not require chemotherapy and the disease has a little impact on life expectancy. The second group slowly progress over months and years and may eventually require therapy. The third group rapidly progress in weeks resulting in death without treatment. The fourth have a sudden "Richter's" transformation event and rapid deterioration (Zenz, Mertens et al. 2010, Zenz, Gribben et al. 2012). Predicting, at diagnosis which course an individual patient is likely to follow would be invaluable in informing a patient of their prognosis, their likelihood of requiring therapy and their need for monitoring. Age, performance status and sex can add some additional information. Older patients have an overall shorter survival from CLL, but they also have a shorter predicted life expectancy and therefore the biggest impact of shortened survival is apparent in young patients (Jaksic, Vitale et al. 1991). Female patients tend to have a slightly longer survival than males although whether this reflects an intrinsic difference in the biology of the disease remains unclear (Molica 2006). The clinical staging systems do reflect bone

marrow involvement, but morphological features identified prior to bone marrow failure can help predict the aggressiveness of disease. It is evident that patients with a diffuse pattern of bone marrow infiltration have a shorter life expectancy than those with a nodular non diffuse pattern of infiltration (Han, Barcos et al. 1984, Rozman, Montserrat et al. 1984). Markers of the disease kinetics and therefore proliferative index of the disease also correlate with more aggressive disease. Clinically the lymphocyte doubling time (LDT) is a well-established method of identifying patients with aggressive disease, but has the disadvantage of being a retrospective analysis. The LDT is defined as how long it takes for the total lymphocyte count to double in size and a period of time <12 months defines a group of patients with a shorter overall survival and shorter time to treatment than those whose LDT is >12 months. This holds true for all clinical stages of disease (Montserrat, Sanchez-Bisono et al. 1986).

1.1.6 Prognostic Biomarkers

Many biological parameters have been identified which correlate with prognosis in CLL and some can assist in predicting which patients with early stage CLL will progress to advanced disease. These markers may reflect tumour burden, proliferative index or refractoriness to treatment.

1.1.6.1 Serum Markers

A raised lactate dehydrogenase (LDH) is associated with shorter survival in CLL patients (Lee, Dixon et al. 1987) but this is a non-specific marker which is frequently raised in malignancies and in CLL may reflect autoimmune haemolysis. High levels of Beta 2 microglobulin (β2-M) is another non-specific marker of tumour burden which has been independently correlated with a poor outcome in CLL (Hallek, Wanders et al. 1996). The German CLL subgroup and others have also consistently reported that serum thymidine kinase (TK) correlates strongly with outcome, presumably because it reflects overall tumour proliferation (Hallek, Wanders et al. 1996, Konoplev, Fritsche et al. 2010). Recently serum TK was incorporated into a prognostic model based on multivariant analysis of 1948 cases of CLL entered into prospective clinical trials (Pflug, Bahlo et al. 2014). Specific tumour markers are often used in prognostication of malignancies. CLL cells can release membrane proteins into the sera, but validation has proven to be poor between laboratories; due to in part to factors like age of

sample and renal function. Some groups have shown soluble CD23 levels to be predictive of disease progression in stage A CLL and associated with other poor prognosis markers (Sarfati, Chevret et al. 1996, Knauf, Ehlers et al. 1997). Soluble CD44 has also been correlated with advanced disease and shorter progression free survival even within the stage A disease subgroup (Molica, Vitelli et al. 2001).

1.1.6.2 Cell Surface Markers

CD38

High levels of cell surface CD38 expression on CLL cells has been shown to correlate with poor prognosis in numerous studies and is an independent poor prognostic factor (Damle, Wasil et al. 1999, Del Poeta, Maurillo et al. 2001, Ibrahim, Keating et al. 2001, Morabito, Mangiola et al. 2001, Durig, Naschar et al. 2002, Hamblin, Orchard et al. 2002, Krober, Seiler et al. 2002, Morabito, Mangiola et al. 2002). CD38 is a transmembrane protein that is highly conserved in evolution and functions as an enzyme essential in regulating intracellular calcium. As such it has been implicated in many diverse processes from cell activation, proliferation and immune responses to egg fertilisation and muscle contraction (Malavasi, Deaglio et al. 2008). CD38 also has receptor-like properties and with its ligand CD31 is implicated in CLL homing and migration (Deaglio, Aydin et al. 2010). CD38 levels have significant associations with other poor prognosis markers, such as bulky lymphadenopathy, LDT, LDH, β2-M, sCD23, mutation status and cytogenetic abnormalities (Van Bockstaele, Verhasselt et al. 2009). Different groups have chosen different percentage positive cut-off markers to define positivity, which has been a contentious issue. Additionally CD38 has been shown by many groups to be dynamic through the course of the disease (Matrai 2005). Levels of 30%, 20% and 7% have been proposed, as have methods that measure the CD38 mean fluorescence intensity (MFI), but a universal consensus remains unachieved. Some patients have a bimodal CD38 expression, which demonstrates that intraclonal variability can occur within the same patient, it has been suggested the most positive population defines the prognosis (Ghia, Guida et al. 2003, Hayat, O'Brien et al. 2006).

ZAP-70

ZAP-70 (70kd T-cell receptor (TCR) zeta associated protein) is a tyrosine kinase that was originally identified because of its role in T-cell activation. It is normally expressed by T-cells, NK cells, bone marrow pro B-cells and a subset of tonisillar and splenic B-cells (Nolz, Tschumper et al. 2005, Crespo, Villamor et al. 2006, Cutrona, Colombo et al. 2006). Gene expression profiling studies performed on CLL patients initially reported differential expression of ZAP-70 in cases with mutated and unmutated immunoglobulin heavy chain genes (IGHV) (Rosenwald, Alizadeh et al. 2001), however subsequent studies have revealed more discordance (Van Bockstaele, Verhasselt et al. 2009). Its function in CLL appears to be as an adapter protein that enhances B-cell receptor signalling (Chen, Huynh et al. 2008), although it is also believed to play a role in transendothelial migration (Deaglio, Vaisitti et al. 2007). The main limitation of using ZAP-70 as a prognostic marker has been the non-standardisation of its measurement between laboratories.

CD49d

Integrins are surface membrane proteins that are made up of two heterodimers; α and β chains. CD49d is a member of the integrin α chain family and makes up the α4 subunit of the lymphocyte homing receptor α4β1. Expression of CD49d has been shown to correlate with bulky lymphadenopathy, compatible with its function as an adhesion receptor involved in transendothelial migration (Till, Lin et al. 2002). CD49d expression on the CLL B-cell surface has also been shown to promote CLL cell proliferation (Zucchetto, Bomben et al. 2006, Burger 2012). Patients with high levels of CD49d have been shown to have a short survival by several groups (Gattei, Bulian et al. 2008, Rossi, Zucchetto et al. 2008, Shanafelt, Geyer et al. 2008, Nuckel, Switala et al. 2009, Majid, Lin et al. 2011). A recent worldwide collaborative study of over 3000 patients identified a level of CD49d positivity of greater than 30% to be strongest predictor of shorter overall survival and treatment free survival in CLL, independent of CD38 and ZAP-70 (Bulian, Shanafelt et al. 2014). Majid et al reported a correlation between with expression of CD49d and the chemokine receptor CXCR4 suggesting a role in trafficking of CLL cells into lymph nodes (Majid, Lin et al. 2011). CXCR4 expression confers a poor survival

even when associated with good risks factors, such as mutated immunoglobulin (Pepper, Buggins et al. 2015).

1.1.6.3 Cytogenetic Aberrations

Cytogenetic aberrations are very common in CLL, and were first noted in the 1970's. Conventional cytogenetic banding techniques reveals abnormalities in around 40-50% of CLL cases (Juliusson, Oscier et al. 1990). These conventional techniques have a significant lack of sensitivity due to the low mitotic index of the CLL cells *in vitro*. *In vitro* incubation with CpG oligonucleotides and interleukin 2 (IL-2) causes proliferation of CLL cells and has enabled cytogenetic abnormalities to be detected in up to 80% of cases (Dicker, Schnittger et al. 2006).

Fluorescence in situ hybridization (FISH) allow detection of abnormalities of cells in interphase and reveals cytogenetic abnormalities in more than 80% of CLL cases (Dohner, Stilgenbauer et al. 2000). This important study of 325 patients by Dohner et al found several recurring aberrations; 13q deletion in 55%, 11q deletion in 18%, trisomy 12q in 16%, 17p deletion in 7% and deletion 6q in 7%. Interestingly these different abnormalities were correlated with marked differences in the patients survival; 13q deletion (133 months), 11q deletion (79 months), trisomy 12q (114 months), 17p deletion (32 months), normal karyotype (111 months). There have now been many large cohort studies investigating the relative frequency of each abnormality and the consequence of each marker on prognosis (Krober, Seiler et al. 2002, Dewald, Brockman et al. 2003, Glassman and Hayes 2005). This has led to cytogenetic categories being proposed, with 11q- and 17p- poor prognosis and 13q- good prognosis. These abnormalities have provided some new insights into the pathogenesis of CLL. Deletion of 17p deletes the p53 tumour suppressor gene, which plays a role in promoting apoptosis following DNA damage. Of note, purine analogues and alkylating agents require a functioning p53 pathway, which explains the resistance of 17p deleted patients to these chemotherapeutic agents (Dohner, Fischer et al. 1995). Deletion of 11q deletes the ataxia telangiectasia mutated (ATM) gene, which also encodes a protein in the DNA damage response pathway. 11q deleted patients tend to present at a more advanced stage and with bulky lymphadenopathy (Austen, Powell et al. 2005). The role of genes on 13q is less well established but two microRNAs; miR-15a and miR-16-1 are located in this region, which are thought to be involved in regulation of

the bcl-2 (B-cell lymphoma 2) anti-apoptotic pathway (Calin, Dumitru et al. 2002). Deletion of the equivalent region in mice leads to dysregulated B-cell proliferation and the development of a "CLL like" disorder (Klein, Lia et al. 2010).

In addition to the gross structural abnormalities identified by conventional cytogenetics and FISH in CLL, many additional genetic aberrations have now been identified by next generation sequencing. Although point mutations occur commonly in CLL, no single abnormality is present at a high frequency so, unlike disorders such as chronic myeloid leukaemia (CML), polycythaemia vera (PV) and Waldenström macroglobulinaemia (WM), it has not been possible to define a single pathogenic driver. The most frequent and best characterised lesions are those occurring in the NOTCH1, SF3B1 and BIRC3 genes (Fabbri, Rasi et al. 2011, Puente, Pinyol et al. 2011, Wang, Lawrence et al. 2011, Quesada, Conde et al. 2012). NOTCH1 regulates B-cell maturation and NOTCH1 activating mutations have been described in 10% of new CLL cases and up to 20% of relapsed cases; most frequently in unmutated CLL and found in conjunction with trisomy 12. SF3B1 encodes for the subunits of the spliceosome, which controls splicing of genes controlling cell cycle regulation and apoptosis. SF3B1 mutations are found in approximately 10% of new and 17% of progressive cases of CLL (Rossi, Bruscaggin et al. 2011). BIRC3 encodes for an inhibitor of apoptosis protein that binds to tumour necrosis factor receptor-associated factors 1 and 2 (TRAF1 and TRAF2), it also promotes NF-κB (nuclear factor kappa B) signalling and therefore CLL cell survival. BIRC3 mutations therefore constitutively activate the NF-κB pathway and render the cells less chemotherapy sensitive (Rossi, Fangazio et al. 2012). Other mutations such as those of MYD88, which encodes for an adapter of the Toll-like receptor complex, are found at lower frequency (Puente, Pinyol et al. 2011). The presence of point mutations found by whole genome sequencing correlates with clinical parameters such as progression free survival (PFS), overall survival (OS) and the response to therapy, although results to date have been somewhat variable. In a retrospective analysis, NOTCH1 mutated cases were shown to have a poor outcomes equivalent to abnormalities of p53 (Rossi, Rasi et al. 2012).

Another important feature of CLL is the process of clonal evolution where new genetic abnormalities appear during the course of the disease. It is not clear how frequently this occurs

overall, due to the highly selected patient groups analysed in different research studies, but it has been reported in up to 60% of patients. This also has a negative impact on overall prognosis (Oscier, Fitchett et al. 1991, Shanafelt, Witzig et al. 2006, Stilgenbauer, Sander et al. 2007). A better understanding of the heterogeneous clonal evolution is being elucidated by utilising whole genome sequencing (Schuh, Becq et al. 2012, Wu 2012, Kriangkum, Motz et al. 2015, Ojha, Ayres et al. 2015, Vollbrecht, Mairinger et al. 2015).

1.1.6.4 Mutational Status of Immunoglobulin Heavy Chain Genes

Somatic hypermutation is a crucial process in normal B-cell development. In this process antigen is presented to a B-cell within a germinal centre (GC) of the secondary lymphoid tissue, classically by follicular dendritic cells. Affinity maturation is the process by which random somatic mutations occur in the variable region of the B-cells immunoglobulin (IgV) gene to change the antibody's affinity for the antigen. B-cells with a high affinity for an antigen are the population that survive. B-cells which have undergone somatic hypermutation, i.e. have mutated immunoglobulin genes, are therefore generally thought to be post germinal centre antigen experienced B-cells. Initially there was thought to be a lack of somatic hypermutation in CLL and as such it was a disease of pre-follicular B-cells. However important studies revealed there were both somatically mutated and unmutated CLL patients. A cut-off of 98% was subsequently chosen to define two groups of mutated (less than 98% homology to the germline) and unmutated (more than 98% homology to the germline) CLL (Damle, Wasil et al. 1999, Hamblin, Davis et al. 1999). The unmutated group of patients have a significantly shorter survival than the mutated group; median 9 years versus 24 years. This finding has now been consistently shown by many groups (Jelinek, Tschumper et al. 2001, Matrai, Lin et al. 2001, Hamblin, Orchard et al. 2002, Lin, Sherrington et al. 2002, Tobin, Thunberg et al. 2005). There are notable exceptions, there is a subset of mutated CLL cases which express V_H3-21 have a poor survival, comparable to the unmutated group, which may relate to p53 dysfunction (Lin, Manocha et al. 2003, Thorselius, Krober et al. 2006).

1.1.6.5 Telomere Length

Telomeres shorten with each cell cycle division and therefore telomere length is an indicator of a cells proliferative history. In CLL, some groups have demonstrated that patients with high

telomerase activity and therefore shorter telomeres have shorter median survival (Hultdin, Rosenquist et al. 2003, Damle, Batliwalla et al. 2004, Grabowski, Hultdin et al. 2005, Ricca, Rocci et al. 2007, Terrin, Trentin et al. 2007, Roos, Krober et al. 2008, Sellmann, de Beer et al. 2011). Some studies go on to suggest that telomere length can add additional prognostic information to IGHV mutational status (Grabowski, Hultdin et al. 2005, Ricca, Rocci et al. 2007, Britt-Compton, Lin et al. 2012, Lin, Norris et al. 2014, Strefford, Kadalayil et al. 2015).

1.1.6.6 Markers of Angiogenesis

Increased microvascularity of the bone marrow and lymph node in CLL has been reported to correlate with clinical stage and aggressive disease (Kini, Kay et al. 2000). CLL cells are known to produce variable amounts of vascular endothelial growth factor (VEGF) and basic fibroblast growth factor (bFGF), and high levels of these pro-angiogenic molecules correlates with aggressive disease (Molica, Vacca et al. 2002). CLL cells also express VEGF receptors; VEGFR-1 and VEGFR-2; VEGFR-2 levels also correlates with advanced clinical stage and shorter median survival (Ferrajoli, Manshouri et al. 2001).

1.1.7 Treatment of CLL

Treatment of CLL is undergoing a paradigm shift as a result of increased understanding of the pathobiology of the disease. Until very recently CLL has been viewed as an incurable malignancy and treatment solely based on a backbone of conventional cytotoxic chemotherapy. The anti-CD20 monoclonal antibody Rituximab was the first targeted therapeutic agent, which improved survival of CLL patients when used in combination with cytotoxic chemotherapy. The most effective front line chemoimmunotherapy option for fit patients being the fludarabine, cyclophosphamide and rituximab (FCR) combination. Although this regimen can produce deep and durable remissions in a subset of patients, relapses were inexorable. Additionally FCR delivers suboptimal responses in those harbouring TP53 mutations and deletions and is unsuitable for the older patient with comorbidities. Analysis of a subset of cases in the German CLL 8 study, comparing FC and FCR in previously untreated CLL, showed mutations in TP53 predicted for reduced PFS and OS after FCR. There was no role for NOTCH-1 mutation in predicting OS and PFS, whilst those with SF3B1 mutations had a reduced PFS. Given the interactions between mutations and therapy, and the known

confounding effect of underpowered subgroup analyses, it is clear that precisely defining the impact of point mutations on clinical outcome is going to require the analysis of large, complete cohorts of uniformly treated patients.

Now targeted, cellular and immunotherapies in CLL are set to revolutionise the treatment options of the future. This has been driven by the ability to target the B-cell receptor (BCR) signalling pathways in CLL, as well as targeting pro-apoptotic pathways, the cell cycle and disrupting the supportive microenvironment. BCR signalling inhibition has become the fastest growing area for pharmaceutical agents. Two oral agents; Ibrutinib, an inhibitor of Bruton's tyrosine kinase and Idelalisib, an inhibitor of phosphoinositol-3 kinase delta have shown very promising results indeed. These and other molecules directly targeting the BCR signalling pathways are quickly finding their place in the treatment algorithms. The CLL tumour microenvironment is also a very attractive therapeutic target. Lenalidomide has been proven efficacious in CLL. Its mechanism of action of is not entirely clear but its immunomodulatory properties may improve the T-cell defects in CLL. Newer molecules in development include ABT-199 which supress anti-apoptotic proteins such as BCL-2 and so far have given astonishing clinical results. Molecules which inhibit the cell cycle are also being rapidly being developed. Probably one of the most revolutionary developments is that of the chimeric antigen receptor T-cells (CAR T-cells); allogeneic or autologous T-cells are manipulated to express a T-cell receptor (TCR) targeting the CD19 on B-cells leading to removal of CLL cells via their cytotoxic effects.

These new therapeutic strategies are best understood in the context of understanding the pathobiology of CLL and the normal immune system which is discussed below.

1.2 Background to the Normal Immune System

1.2.1 Introduction

In order gain insight into the pathobiology of CLL it needs to be considered in the context of an understanding of the function and maturation of the normal immune system. The human immune system is a highly evolved complex interaction of molecules, cells, tissues and organs together defending the body from pathogenic attack. The system has classically been divided into two; the innate and the adaptive immune system. The innate or non-specific immune system provides the first defence of the body against attack in a non-specific manner. Evolutionarily it precedes the adaptive system and provides no memory. It starts with the most basic physical barriers of skin, mucous membranes, secretions containing soluble anti-bacterial agents and physiological barriers of temperature, pH and oxygen tension, followed by the more advanced processes of phagocytosis by cells such as neutrophils and macrophages. However, it is the adaptive immune system that leads to a specific response against pathogens and "non-self" antigens. Antigen is presented to the immune system, usually within the secondary lymphoid tissues and specific receptors trigger cell priming, activation and differentiation finally leading to a directed effector response to the target site. It is in the understanding this adaptive system and revealing the ways in which it is disrupted that gives a better appreciation of the complex immunopathology displayed in CLL. The aim of this thesis is to specifically focus on the relationship between T and B lymphocytes in CLL.

1.2.2 Normal B-cell Development

In normal adult B-cell development, haematopoietic stem cells differentiate to progenitor B-cells within the bone marrow, where they constitute approximately 2% of the mononuclear cells. The cells mature from progenitor early pro B-cells to late pro B-cells to precursor pre B-cells then to immature B-cells. Immature B-cells are released into the periphery and develop into mature naïve B-cells. These mature B-cells then circulate in the blood and traffic to and within the secondary lymphoid system. The B-cells ultimately differentiate into antibody secreting plasma cells or long-lived memory B-cells, ready to mount an immediate response if the same antigen is reencountered. A summary of stages of B-cell development is shown in Table 1-3.

Table 1-3 Stages of B-cell development. (Adapted from Janet M. Decker, University of Arizona http://www2.nau.edu)

Stages of B-cell Development							
	Stem cell	Early pro B-cell	Late pro B-cell	Large pre B-cell	Small pre B- cell	Immature B-cell	Mature B-cell
Heavy chain genes	Germline	D-J joining	V-DJ joining	VDJ rearranged	VDJ rearranged	VDJ rearranged	VDJ rearranged
Light chain genes	Germline	Germline	Germline	Germline	V-J joining	VJ rearranged	VJ rearranged
Surface Ig	No	No	No	μ chain in pre-B receptor	μ chain in cytoplasm and on surface	Membrane IgM	Membrane IgM and IgD
RAG expression	No	Yes	Yes	No	Yes	Yes	No
Surrogate light chain expression	No	Yes	Yes	Yes	No	No	No
Ig αβ expression	No	Yes	Yes	Yes	Yes	Yes	Yes
BTK	No	Weak	Yes	Yes	Yes	Yes	Yes
Membrane markers	CD34	CD34 CD45 Class II	CD45R Class II CD19 CD40	CD45R Class II CD19 CD40	CD45R Class II CD19 CD40	CD45R Class II IgM CD19 CD40	CD45R Class II IgM IgD CD19 CD21 CD40

1.2.2.1 B-Cell Receptor

In order to trigger a directed immune response, B-cells need to produce an antigen specific receptor and the population of B-cells needs to encompass a vast number of possible pathogens. The BCR determines the cell's antigen specificity. In order to create B-cells with such different specificities, the naïve B-cell rearranges the genes that encode for the BCR. The BCR is composed of a heavy and either a kappa (κ) or lambda (λ) light chain. The immunoglobulin heavy chain gene rearrangement precedes the light chain. There are four segments of genes which encode the BCR. These are the variable (V), diversity (D), joining (J) and constant (C) regions. The V region has 25-100 genes, the D region approximately 25 genes, the J approximately 50 genes. These different genes can be brought together in many different combinations to form vastly different gene sequences to encode the BCR. This process is under strict control by recombination activation genes (RAG-1 and RAG-2). The sequence of events involves a J segment joining to a D segment, looping out the intervening section, then adding the V segment. Additional diversity is caused by the nucleases and ligases which cut and splice the variable sections together, introducing inaccuracies and frameshifts leading to sequences that encode for different amino acids. This process is called junctional diversity. Further alterations in the sequence are caused by deoxyribonucleotidyltransferase inserting random nucleotides, again leading to a shift in the reading frame. If the process is successful the gene encodes for the mu (μ) heavy chain and is expressed with a "surrogate" light chain on the cell surface, this expression triggers the light chain to be rearranged. The resultant B-cell expresses IgM with only one light chain; kappa or lambda. The normal kappa / lambda ratio in adults is 60:40. Therefore at the end of this process each immature B-cell is left with a distinct BCR and the population as a whole covers a huge number of antigen specificities. The stepwise development is shown in Table 1-3.

During B-cell development there is a process of positive and negative selection. Positive selection occurs by antigen independent survival signalling through the BCR. Negative selection occurs when the B-cell BCR binds self-antigen, then the B-cell will then either be deleted, edit its BCR, become anergic or is ignored in a process called central tolerance.

B-cells can come into contact with antigen either directly or via antigen presenting cells (APCs) such as follicular dendritic cells (FDCs) in the B-cell zone of the primary follicle of a lymph node. The diversity of the BCR is broadened further following the B-cell exposure to antigen in the dark zone of the germinal centre. Here the B-cell receives T-cell help, which initiates immunoglobulin class switching of the heavy chain genes and somatic hypermutation of the immunoglobulin variable chain. Both FDCs and T-cells play a role in selecting only the B-cells expressing high affinity BCRs within the light zone. A schema of the germinal centre reaction is shown in Figure 1-2, adapted from Küppers et al (Kuppers 2003).
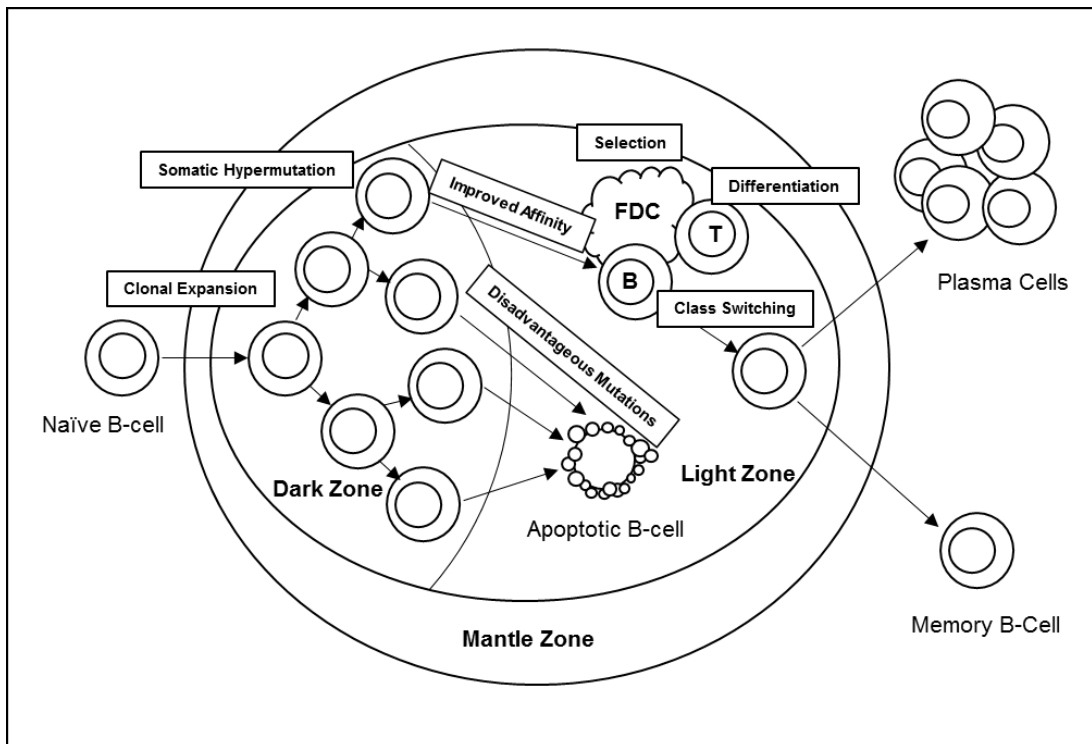
Figure 1-2 The germinal centre reaction of a lymph node. Adapted from Küppers et al.

1.2.2.2 BCR Signalling

On engagement of the BCR by antigen a series of complex downstream signalling events take place. Activation of the BCR leads to recruitment of proto-oncogene tyrosine protein kinase (SRC) family members including tyrosine protein kinase Lyn (LYN), proto-oncogene tyrosine protein kinase Fyn (FYN) and B-lymphocyte kinase (BLK), which phosphorylate CD79a and CD79b via their immunoreceptor tyrosine-based activation motifs (ITAMs). This then leads to recruitment of spleen tyrosine kinase (SYK), Bruton's tyrosine kinase (BTK) and/or phosphatidylinositol 3-kinase (PI3K). Ultimately this leads to calcium mobilisation, downstream activation of mitogen-activated protein (MAP) kinases, RAS, phospholipase C (PLC), protein kinase C (PKC) and caspase recruitment domain containing protein 11 (CARD11). Activation of protein kinase B (AKT), NF-kB or extracellular signal regulated kinase (ERK) pathways lead to cell survival and proliferation (Shaffer, Young et al. 2012).

Figure 1-3 shows a schematic cartoon of chronic active BCR signalling, adapted from Young et al (Young and Staudt 2013). These normal B-cell signalling pathways are becoming increasingly important as targets for therapy in CLL which is revolutionising the treatment paradigm.
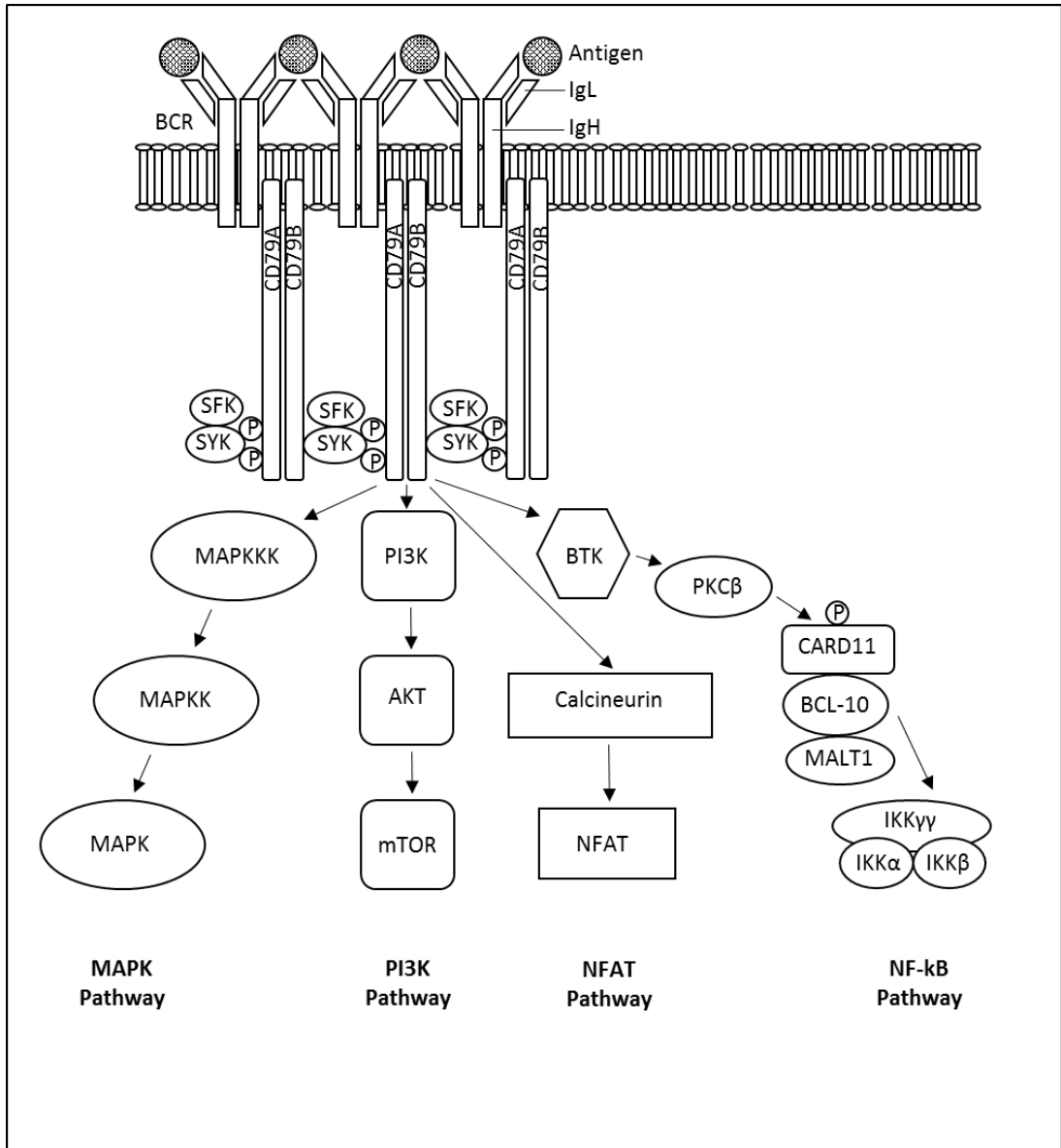
Figure 1-3 Chronic active BCR signalling. Adapted from Young at el.

BTK (Bruton's tyrosine kinase); CARD11 (caspase recruitment domain-containing protein 11); IgH (immunoglobulin heavy chain); IgL (immunoglobulin light chain); IKK (inhibitor of NF-κB kinase); MALT1 (mucosa-associated lymphoid tissue lymphoma translocation protein 1); MAPK (mitogen-activated protein kinase); MAPKK, (MAPK kinase); MAPKKK (MAPK kinase kinase); mTOR (mammalian target of rapamycin); NFAT, (nuclear factor of activated T-cells); PKCβ (protein kinase Cβ).

1.2.2.3 B-cell Activation

T-cell dependant B-cell activation

When B-cells come in contact with antigen via the BCR, the antigen is internalised by endocytosis, processed and the resultant peptides presented to specific T-cells on class II major histocompatibility (MHC) molecules on its surface. This typically occurs in the T-cell zone of the primary lymph node follicle. This results in CD4+ T-helper (Th) and specifically T follicular helper (Tfh) cells, which have specificity for the same antigen, engaging with the peptide on MHC class II via its T-cell receptor (TCR). The engagement of the TCR by the MHC class II in turn leads to cytokine production, including IL-4 and IL-21, which stimulate the B-cell. As part of this process CD40, a member of the tumour necrosis factor (TNF) receptor family expressed on mature B-cells, is engaged by its ligand CD154 (also known as CD40L) on T-cells. CD40L activates the RelA dependant NF-kB canonical and the RelB non-canonical activation pathways. This interaction leads to activation of many signalling pathways which play a crucial role in inducing proliferation, antibody secretion, cytokine production, class switching (of the activated IgM+ B-cells to another isotype), germinal centre formation and ultimately producing long-lived memory B-cells.

T-cell independent B-cell activation

A T-cell independent B-cell response can also occur, but this does not allow efficient class switching or the generation of long-lived memory B-cells. This occurs when antigens, such as foreign polysaccharides, activate the B-cell but the co-stimulatory signals from the T-cell are absent. Therefore activation utilises alternative pathways such as binding of toll-like receptors (TLRS).

1.2.3 Normal T-cell Development

T-cells are a crucial component of the adaptive immune system and cell mediated immunity. T-cell development is complex due to the functional diversity of mature T-cells. All T-cells originate from a lymphoid precursor in the bone marrow but there is subsequent migration to the thymus for further development. T-cell subsets are customarily subdivided according to their function and cytokine production,

1.2.3.1 T-helper Cells

T-helper cells are crucial for the maturation of B-cells into long-lived memory B-cells and plasma cells and are also required for the activation of cytotoxic T-cells. These cells express the glycoprotein CD4 on their surface. They are activated when they engage with peptide presented by MHC Class II molecules on APCs. Once activated, CD4+ Th cells predominantly differentiate into Th1 or Th2. There are also other subtypes including Th17, Th3, Th9 and Tfh cells. The differentiation process is complex and depends upon the cytokine stimulation the T-cell is receiving.

Th1

Th1 cells facilitates the proliferation and expansion of T-cells and plays a critical role in cell mediated immunity; particularly in the clearance of intracellular bacteria and protozoa. They specifically promote macrophages. They are triggered by IL-2 production. Th1 cells produce predominately IL-2, interferon gamma (IFN-γ), tumour necrosis factor beta (TNF-β) and granulocyte macrophage colony-stimulating factor (GM-CSF). Some Th1 cells have cytolytic capacity and can produce perforin, granzyme and express Fas ligand.

Th2

Th2 cells play a role in the host immunity against extracellular pathogens, particularly parasites. They are triggered by IL-4 secretion. They produce IL-4, IL-5, IL-6 and IL-10 and this cell type provides help to activate the B-cell to produce antibody, particularly IgE. They also specifically effect the function of eosinophils, basophils and mast cells.

Th17

Th17 are a relatively recently discovered subset of Th cells which produce IL-17. They mainly produce IL-17, IL-21 and IL-22. They seem to play a critical role in autoimmunity, where Th17 over activity is associated with diseases such as rheumatoid arthritis and psoriasis. Th17 cells expansion is mediated by IL-23 (Zambrano-Zaragoza, Romo-Martinez et al. 2014).

Tfh

Tfh cells are intrinsically involved in the formation of the germinal centre reaction. Defining Tfh cells has been controversial, but they express varying levels of CXC chemokine receptor 5 (CXCR5) and Programmed Death-1 (PD-1) and facilitate the formation of a long-lived B-cell responses and immunoglobulin production (Dorfman, Brown et al. 2006).

1.2.3.2 Regulatory T-cells

Regulatory T-cell (Tregs) account for up to 5% of CD4+ T-cells and express high levels of CD25, forkhead box P3 (Foxp3), CD62 and IL-10. Tregs play an important part of maintaining peripheral T-cell tolerance to self-antigens and protection from autoimmunity. They suppress immune responses and have been correlated with poor prognosis in solid tumours (Wallace, Alcantara et al. 2015).

1.2.3.3 Cytotoxic T-cells

Cytotoxic T-cells express the CD8 glycoprotein on their surface and have a major role in eradicating viruses and tumours. They are activated when they bind antigen presented by MHC Class I molecules, which are present on all nucleated cells. The cytokine profile of CD8+ T-cells subdivides them into Tc1, Tc2 and Tc17 cells. All CD8+ T-cells are cytotoxic, and upon engagement with its target leads to cell death by releasing perforins and granzymes. CD8+ T-cells can also lead to apoptosis via binding of Fas ligand. Cytotoxic T-cells can be subdivided according to their cytokine profile and function. Tc1 cells predominately secrete IFN-γ, Tc2 cells predominately secrete IL-4 and Tc17 cells predominately secrete IL-17.

1.2.3.4 T-cell Receptor

Just like the B-cell, T-cells have a receptor, which defines its specificity for antigen. The T-cell receptor is a heterodimer of either an alpha (α) and beta (β) chain or less commonly a gamma (γ) and delta (δ) chain. The TCR forms a transmembrane signalling complex in conjunction with CD3. The TCR specificity is altered, like the BCR, through random genetic rearrangement of constant and variable domains. The variable domains contain VDJ gene families and the linkage points are called hypervariable regions. The final rearranged segments of DNA, which encode for the antigen binding area is called the complementary-determining region (CDR). It is the third hypervariable region (CDR3), between the V and J region of the β chain, which mostly defines the specificity of the TCR. The differences between the sequence and length of the CDR3 define Vβ families. Some Vβ families are used more frequently than others. This process of TCR rearrangement occurs early in development of the T-cell, before it encounters antigen for the first time. The process was thought to lead to the production of over 10^6 TCRs, but new gene sequencing techniques has suggested this may be much larger (Robins, Campregher et al. 2009). Within the thymus it is estimated that over 95% of T-cells are deleted, some by failure to rearrange their TCR, some by active elimination and some by neglect. T-cells undergo a process of positive and negative selection within the thymus, where T-cells with a high affinity for self-derived peptides die by apoptosis, and low affinity T-cells are released into the periphery.

1.2.3.5 T-cell Activation

Naïve T-cells circulate between the PB and secondary lymphoid tissues under the influence of homing receptors, such as CD62L and CC-chemokine receptor 7 (CCR7) looking for their cognate peptide on the MHC of antigen presenting cells. At this stage these T-cells usually already express either CD4 or CD8 on their surface. CD4+ Th-cells recognise antigenic peptides presented to them by MHC class II molecules found on the surface of APCs such as dendritic cells, B-cells and thymic epithelial cells. Cytotoxic CD8+ T-cells respond to peptides presented to them by Class I MHC molecules and it is by this mechanism that T-cells exert cytotoxicity.

Once the TCR engages its MHC-peptide complex, ligation of other co-stimulatory molecules is required for T-cell activation. The primed T-cell expresses CD28 on its surface which binds to its ligands which are members of the B7 family, including B7-1 (CD80) and B7-2 (CD86) on the surface of the antigen presenting cell. This ligation promotes T-cell IL-2 secretion, activation and survival. Without CD28 ligation the T-cell undergoes apoptosis or is anergic. Activated T-cells also upregulate CD25, which is the alpha chain of the high affinity IL-2 receptor. Once T-cells are activated by antigen they proliferate, producing daughter effector T-cells of the same specificity, which are attracted by chemokines and adhesion molecules to migrate out of the lymph node to the required site of action.

1.2.3.6 Negative regulators of T-cell activation

T-cell activation must also be negatively regulated to attenuate and eventually terminate the T-cell response. Inhibitory T-cell receptors include Cytotoxic T-Lymphocyte Antigen 4 (CTLA-4) and Programmed Death 1 (PD-1).

CTLA-4

CTLA-4 has very high homology with CD28. It is upregulated on activated T-cells and binds to the same B7 family members as CD28, but at a much higher affinity. It negatively regulates the T-cell by decreasing IL-2 production and therefore has a critical role in terminating the immune response (reviewed in (Alegre, Frauwirth et al. 2001, Sharma and Allison 2015). Clearly T-cell activation is in a delicate balance, and most surface CTLA-4 is rapidly endocytosed to prevent early termination of the immune response. Interestingly CTLA-4 deficient mice develop an aggressive lymphoproliferative disorder, due to the lack of a "brake" on the immune system (Waterhouse, Penninger et al. 1995). These findings lead to the hypothesis that CTLA-4 blockade in cancers might allow T-cells to eradicate tumours. A series of murine studies over more than a decade lead to the development of Ipilimumab, a human anti-CTLA-4 antibody (Leach, Krummel et al. 1996, Hurwitz, Yu et al. 1998, van Elsas, Hurwitz et al. 1999, Waitz, Fasso et al. 2012, Zamarin, Holmgaard et al. 2014). This drug was approved by the FDA for treatment of metastatic melanoma in 2011 (Hodi, O'Day et al. 2010, Robert, Thomas et al. 2011).

PD-1

PD-1 has been identified as a critical immune checkpoint regulator and limiter of T-cell responses (Freeman, Long et al. 2000). PD-1 is expressed on activated T-cells, B-cells and macrophages. PD-1 belongs to the immunoglobulin superfamily and has an extracellular IgV domain, a transmembrane region and an intracellular tail with 2 phosphorylation sites; one is an immunoreceptor tyrosine based inhibitory motif and the other an immunoreceptor tyrosine based switch motif (Freeman, Long et al. 2000). Both motifs are phosphorylated on PD-1 ligation, which recruits SHP-2 (Src homology domain-containing tyrosine phosphatase 2) in B-cells and SHP-1 and SHP-2 in T-cells (Okazaki, Maeda et al. 2001, Riley 2009, Yokosuka, Takamatsu et al. 2012). In the B-cell SHP2 activation inhibits downstream BCR signalling by reducing phosphorylation of immunoglobulin β, SYK, PLC, ERK and PI3kinase (Maeda, Scharenberg et al. 1999). TCR signalling is inhibited by reduced phosphorylation of the ZAP-70/CD3zeta signalsome and subsequently reduced downstream signalling to PKCtheta (Sheppard, Fitz et al. 2004).

PD-1 has two known ligands PD-L1 (programmed death ligand 1 also known as B7-H1) and PD-L2. PD-L1 can be upregulated, as a result of IFN-γ secreted by activated T-cells, on tumour cells, epithelial cells B-cells and the T-cells themselves (Dong, Strome et al. 2002).

A simplified schema of the crosstalk between T-cells and the B7-CD28 superfamily is shown in Figure 1-4, adapted from Sharpe et al (Sharpe and Freeman 2002).
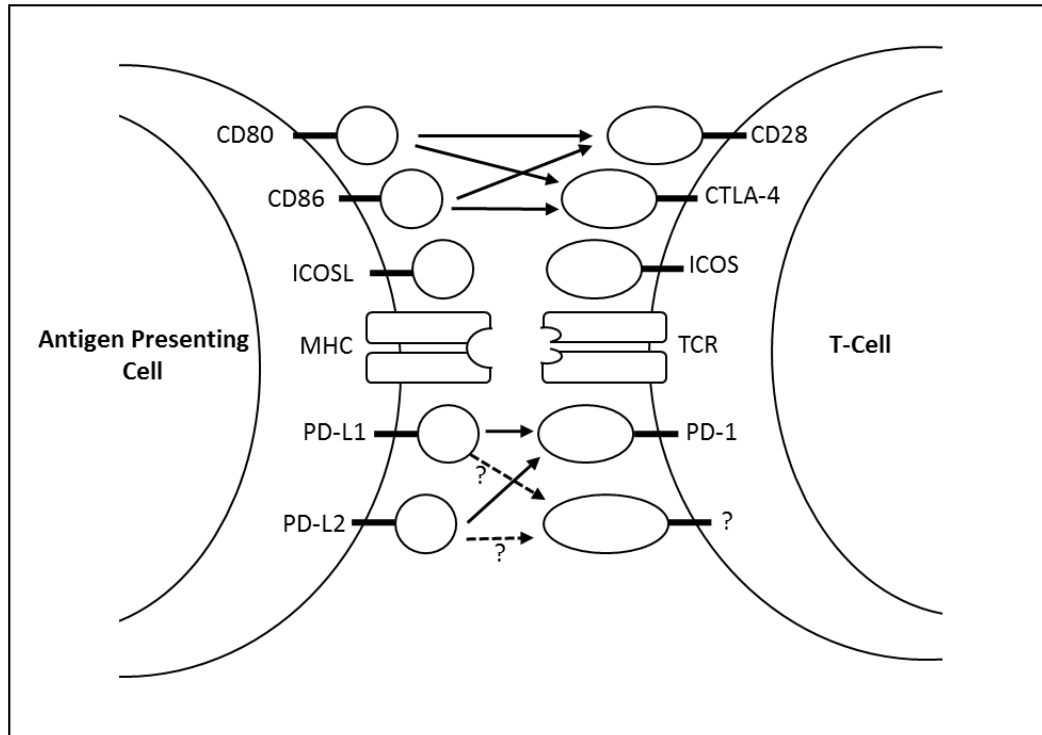
Figure 1-4 B7-CD28 superfamily crosstalk between APC and T-cells. Adapted from Sharpe et al.

1.2.3.7 Memory T-cells

Following most infections, after T-cell activation and proliferation, the pathogen is cleared and the massive T-cell expansion is contracted by apoptosis. Some "memory T-cells" will remain in the lymph node awaiting re-exposure to the same antigen. Both CD4+ and CD8+ T-cells can form memory T-cells, which persist following antigen activation and expand upon re-exposure to their cognate antigen. Memory cells are maintained in part by signalling from FDCs in germinal centres. It is thought memory cell can persist in the absence of the antigen, but it is likely they are periodically re-presented antigen by FDCs. Memory cells can affect a rapid response to re-infection in part through increased expression of accessory molecules such as LFA-1 (lymphocyte function associated antigen 1), LFA-3 and ICAM-1 (intercellular adhesion molecule 1) and by faster triggering into cell division and cytokine secretion. Naïve T-cells have a different phenotype from memory T-cells. In memory T-cells there is a change in isoform of the leukocyte common antigen CD45R, from CD45RA to CD45RO. Naïve T-cells

also express low levels of the adhesion molecule CD44 compared to high levels on memory T-cells. Generally memory T-cells are considered to be either central memory (T_{CM}) or effector memory (T_{EM}) (Sallusto, Lenig et al. 1999). Within these populations the expression levels of the co-stimulatory molecules CD27 and CD28 decrease with differentiation. There has been reported to be significant inter-individual variation in the frequencies of the individual CD4+ and CD8+ subsets, but specifically there are particularly marked differences with advancing age, notably with an overall decrease in the number of naïve cells in the CD8+ pool (Koch, Larbi et al. 2008).

Central Memory T-cells (T_{CM})

The T_{CM} population are antigen primed T-cells, which when they re-encounter their cognate antigen offer B-cell help, stimulate DCs and generate effector T-cells. T_{CM} cells express CCR7, which is the receptor for the chemokines CCL19 and CCL21, they also express CD62L. CD62L, also known as L-selectin, is a cell adhesion molecule whose role, at least in part, is to influence the cells to home to the secondary lymphoid tissue.

Effector memory T-cells (T_{EM})

The T_{EM} population lack both CCR7 and CD62L, but they express CCR1, CCR3, CCR5 receptors which respond to pro-inflammatory chemokines, and therefore mediate inflammatory reactions and cytotoxicity.

The differential expression of CD62L and CCR7 therefore orchestrates the T_{CM} to generally home to the lymph nodes, spleen and blood and T_{EM} to the sites of inflammation and infection in the peripheral tissues.

Terminal Effector memory T-cells (T_{EMRA})

A small population of terminal differentiated effector memory (T_{EMRA}) cells are defined as CD45RA+/CCR7- and expresses CD57. They are cytotoxic and express high levels of perforin and Fas ligand. As such they are highly susceptible to apoptosis.

Exhausted T-cells

In persistent infections there may be eventual "exhaustion" of the effector function and substantial phenotypic and functional abnormalities of the memory T-cells. These memory cells are being continuously stimulated and in contrast to the usual slow turnover of a memory T-cell their proliferation is substantial. As a cell can only undergo a finite number of divisions eventually the telomeres become too short (the so called "Hayflick limit), these cells will eventually be eliminated.

Chronically activated T-cells express PD-1 which has been referred to as a sign of exhaustion. The negative regulatory function of PD-1 suppresses the T-cell function and seems to maintain its dysfunction. If the PD-1 expression is reversed the T-cell function has been shown to be revived. A seminal experiment of mice infected with chronic cytomegalovirus (CMV) infections, showed an improvement in the functionality of memory CD8+ T-cells and clearance of the virus when PD-1 was blocked (Barber, Wherry et al. 2006). PD-1 knockout C57BL/6 mice develop lupus-like autoimmune diseases due to the lack of this crucial negative regulator of the immune system (Nishimura, Nose et al. 1999). Blockade of the PD-1 / PD-L1 axis has generated much interest recently. Anti PD-L1 antibodies have been shown to promote tumour regression in melanoma, bladder cancer, renal carcinoma and non-small cell lung cancer (Brahmer 2012, Powles, Eder et al. 2014). Several anti-PD-1 drugs have reached the clinic since the work in this thesis was undertaken. Pembrolizumab has shown up to a 38% response rate in advanced metastatic melanoma and was FDA approved in September 2014 (Hamid, Robert et al. 2013, Robert, Ribas et al. 2014). Nivolumab showed similar success and was FDA approved in December 2014 for melanoma and March 2015 for lung cancer (Robert, Ribas et al. 2014). (Reviewed by (Sharma and Allison 2015)).

1.3 Pathology of CLL B-cells

1.3.1 Introduction

Malignant CLL B-cells have diverse cytogenetic abnormalities and show immunological heterogeneity. Historically CLL was thought to be a disease of quiescent B-cells and therefore a disease of accumulation, due to a defect in apoptosis, and not a disease of proliferation (Dameshek 1967). This hypothesis was informed by PB studies of circulating CLL cells that found the majority of them to be in the resting, G0 phase, of the cell cycle (Dighiero, Travade et al. 1991). However there is now good evidence that CLL is more dynamic than previously thought. One good piece of evidence that CLL cells have a replicative history comes from the discovery that CLL cells have short telomeres and that cases with the shortest telomeres have the most aggressive disease (Bechter, Eisterer et al. 1998). Single-molecule telomere length and telomere fusion analysis has now been undertaken and the shortest telomere length recorded in human tissue was reported in CLL (Lin, Letsolo et al. 2010).

Additional evidence for proliferation in CLL was provided by the seminal study of Messmer et al, who performed *in vivo* labelling studies, of patients with CLL, using deuterated water ($^2H_20$). Deuterium (^2H) becomes incorporated into the DNA of proliferating CLL cells, so that the degree of ^2H enrichment measured by gas chromatography / mass spectrometry, reflects overall tumour proliferation. The study revealed that the CLL birth rate was up to 1% of the total clone per day (Messmer, Messmer et al. 2005).

1.3.2 Cell of Origin

The malignant transformation of B-cells can occur at any stage in B-cell development. In CLL however, unlike in some other B-cell malignancies, there is not a clear non-malignant B-cell counterpart. Some groups have postulated there may be a distinct CD5+ malignant B lineage cell (Caligaris-Cappio 1996, Dono, Burgio et al. 2007). Others have found there are phenotypic similarities between CLL cells and splenic marginal zone B-cells suggesting an alternative cell of origin (Chiorazzi and Ferrarini 2003). Gene expression profiling of CLL cells has given new insights; malignant CLL B-cells show marked similarities to that of a normal memory B-cells (Klein, Tu et al. 2001, Rosenwald, Alizadeh et al. 2001). In these studies both mutated and

unmutated cases had very similar gene profiles which seemed to dispute the theory that unmutated CLL originated from naïve B-cells as previously hypothesised (Forconi, Potter et al. 2010). Recent studies have found receptor tyrosine kinase-like orphan receptor 1 (ROR-1) on CLL B-cells, which is only usually found on haematogones, opening up an alternative theory of potential cell of origin (Zhang, Chen et al. 2012). More recent detailed flow cytometric studies have revealed that CLL most likely arises from a hitherto unrecognised post germinal centre CD5+ B-cell subset (Seifert, Sellmann et al. 2012). Chiorazzi reviewed the many models of either a single or multiple cell origins of CLL and although this question remains unanswered there is likely to be a multistep process of leukaemogenesis. (Chiorazzi and Ferrarini 2011).

Although CLL cells were originally believed to be quiescent, their phenotype is consistent with ongoing antigenic stimulation as they express a number of markers of antigen exposure / activation, including CD23, CD25, CD69, CD71 and CD27; this is the case for both mutated and unmutated cases (Damle, Ghiotto et al. 2002).

1.3.3 Immunoglobulin Repertoire

Most CLL cells express surface IgM/IgD and this initially was taken as evidence that CLL is a disease of naïve B-cells which had not been exposed to antigen (Coffman and Cohn 1977), but there is now compelling evidence to the contrary. CLL cells show significant skewing in their V_H gene usage and the V_H genes used most frequently are V_H1-69, V_H3-07 and V_H4-34 (Schroeder and Dighiero 1994, Fais, Ghiotto et al. 1998, Hamblin, Davis et al. 1999). This bias would suggest that the B-cell is responding to antigen. Another piece of supportive evidence is that in approximately 50% of CLL cases the immunoglobulin heavy chain shows evidence of somatic hypermutation, as discussed previously this is a process which occurs following antigen exposure (Schroeder and Dighiero 1994, Hashimoto, Dono et al. 1995, Oscier, Thompsett et al. 1997, Fais, Ghiotto et al. 1998). Several studies have also revealed that in subsets of unrelated patients, CLL cells expressed BCRs with a striking homology to each other; so much so as to suggest specificity to the same antigen (Messmer, Albesiano et al. 2004, Tobin, Thunberg et al. 2004, Widhopf, Rassenti et al. 2004, Ghia, Stamatopoulos et al. 2005, Stamatopoulos, Belessi et al. 2007). Stereotyped BCRs occurs in up to a third of CLL

cases (Chiorazzi, Rai et al. 2005, Agathangelidis, Darzentas et al. 2012). This phenomenon could not possibly occur by random chance and the probability independent clones would carry the same BCR would be in the region 1 in 10^{-12}.

1.3.4 BCR Signalling and Antigen Drive

The data discussed above suggests that both mutated and unmutated cases of CLL are both derived from B-cells which have been exposed to antigen and continue to signal through their BCRs by ligand dependant mechanisms and it is becoming increasingly apparent that signalling through the BCR is critical in the pathobiology of CLL (Stevenson, Krysov et al. 2011, Woyach, Johnson et al. 2012). BCR signalling may be additionally enhanced by ZAP-70 expression, which facilitates the recruitment of kinases to the BCR complex (Chen, Huynh et al. 2008).

Unlike in diffuse large B-cell lymphoma (DLBCL), studies to date have not detected a high frequency of activating mutations in the BCR pathway that might lead to independence from antigen (Philippen, Diener et al. 2010). This has led investigators to try and identify putative antigens. Many B-cell malignancies are known to be triggered by chronic stimulation from antigen such as Helicobacter pylori, EBV, hepatitis C. There is also an association with autoimmune disorders such as rheumatoid arthritis (RhA), systemic lupus erythematosus (SLE) and Sjörgren's syndrome (Morse, Kearney et al. 2001, Kuppers 2005). Interestingly BCRs from unmutated CLL cases appear to be polyreactive but some BCRs show affinity for self-antigens (Herve, Xu et al. 2005). These self-antigens include cytoskeletal proteins, such as non-muscle myosin heavy chain IIA, vimentin and cofilin. Additional reactivity has been demonstrated by self-antigens such as the Fc immunoglobulin tail, single stranded DNA, double stranded DNA, lipopolysaccharide, insulin and oxidised low density lipoprotein (Catera, Silverman et al. 2008, Lanemo Myhrinder, Hellqvist et al. 2008, Binder, Lechenne et al. 2010, Chu, Catera et al. 2010).

Other groups have found affinity of BCRs for a variety of non-self-antigens including bacteria, fungal elements and viruses including CMV (Landgren, Rapkin et al. 2007, Kostareli, Hadzidimitriou et al. 2009, Steininger, Rassenti et al. 2009). Hoogeboom et al published a stereotyped mutated BCR IGHV3-7 recognised the antigen beta-(1,6)-glucan (found in yeasts

and filamentous fungi) with high affinity and in fact lead to CLL cell proliferation (Hoogeboom, van Kessel et al. 2013). This gives further weight to the argument that antigen responsiveness in part drives CLL proliferation. Duhren-von Minden et al have fascinatingly published in Nature evidence for BCR activation by antigen independent cell autonomous signalling. They showed that, by binding the CLLs own CDR3 to an epitope in the second framework region, calcium signalling was induced; suggesting an auto-reactive BCR activation. Following on from this study a second group demonstrated CLL BCRs ability to recognise themselves via an epitope of the framework region 3 (Duhren-von Minden, Ubelhart et al. 2012).

1.4 T-cells in CLL

1.4.1 Introduction

It is well established from numerous published studies going back to the 1970's that there are both quantitative and qualitative abnormalities of PB T-cells in CLL. T-cell dysfunction plays a key role in the immunopathology in CLL. In health one role of the T-cells is to identify and eliminate emerging neoplastic clones, but in CLL there is direct evidence that dysregulated T-cells may play a supportive role in sustaining the malignant B-cells. Early studies hypothesised that the expansion of T-cells in CLL was related to a specific anti-leukaemic effect; however the reality is far more complex and the T-cell dysfunction in CLL is manifold. In fact a myriad of T-cell abnormalities have been described in CLL and the precise role they play in the pathogenesis remains to be fully elucidated. Immune suppression is a typical finding in CLL, with an increased risk of infections and a predisposition to second malignancies (Rossi, De Paoli et al. 2008, Morrison 2010, Solomon, Rabe et al. 2013, Riches and Gribben 2014). Haematological autoimmune phenomenon are commonly observed, most frequently autoimmune haemolytic anaemia (Dearden 2008).

T-cells in CLL are part of a complex balancing act. Some appear to be cytotoxic against the tumour and are in part being supressed by the CLL B-cells themselves, some appear to be actively supporting tumour proliferation whilst others are contributing to autoimmune phenomenon. I shall summarise the literature below.

1.4.2 T-cell Accumulation in CLL

In 1973 Wybran et al first published in the Lancet that there was a low proportion of T-cells in CLL patients and that this was a "dilution" effect (Wybran, Chantler et al. 1973). Then in a follow up paper in 1974, Catovsky et al first made the observation that untreated patients with CLL had a markedly expanded T-cell compartment compared to healthy controls (Catovsky, Miliani et al. 1974). In this study, before the advent of flow cytometry, B-cells were identified by indirect immunofluorescence and T-cells by the spontaneous formation of sheep red cell rosettes. By the late 1970's monoclonal antibodies allowed CD4+ and CD8+ T-cell subpopulations to be determined (Kung, Goldstein et al. 1979). One of the first papers utilising this technique to investigate CLL T-cells was Platsoucas et al, they studied 30 untreated CLL cases and found increased T-cell numbers, but a significantly decreased proportion of CD4+ T-cells and a subsequent increased proportion of CD8+ T-cells compared to normal controls. They concluded that the CD4/CD8 ratio was lower in CLL patients than normal controls (Platsoucas, Galinski et al. 1982). Many groups have since investigated the CD4/CD8 ratio in the PB of CLL patients. Kimby et al published a study of 48 untreated patients with CLL, and again found that the total T-cell count was high and the CD4/CD8 ratio was low compared to normal controls; they additionally found the total T-cell numbers were correlated with the size of the CLL clone and that the CD8+ numbers increased and CD4/CD8 ratio decreased with progressive advanced stage disease (Kimby, Mellstedt et al. 1987). Now, an overall increase in CD4 and CD8 numbers with a decreasing ratio with advancing disease has been consistently reported (Herrmann, Lochner et al. 1982, Mills and Cawley 1982, Gonzalez-Rodriguez, Contesti et al. 2010). This mirrors the finding of a reduction in CD4/CD8 ratio found in chronic infections such as CMV. Palmer et al published a study, which showed the relative size of the T-cell component was highest in early stage and good prognosis patients, but nonetheless the total number of T-cells continued to increase with advancing stage (Palmer, Hanson et al. 2008). Nunes et al more recently undertook the largest comprehensive phenotypic analysis of 110 untreated CLL patients. They also demonstrated an expansion of CD4+ and CD8+ T-cells and found that the inversion of the CD4:CD8 ratio was related to the comparatively larger expansion of CD8+ T-cells (Nunes, Wong et al. 2012). In general terms

the total T-cell compartment is reported to be 3 fold larger than in healthy controls, with CD8+ T-cells 4 fold increased and CD4+ T-cells 2.5 fold increased (Mellstedt and Choudhury 2006).

The exact mechanism by which T-cells accumulate in CLL is not well defined. It is not fully known whether the accumulation is a specific TCR dependent response to antigen(s) or superantigen or if the T-cells are non-specifically expanded by chemokines.

Some CLL cells have been shown to aberrantly express BAFF (B-cell activating factor) and *in vitro* studies have shown that BAFF can stimulate T-cells to proliferate (Huard, Schneider et al. 2001, Novak, Bram et al. 2002), by this means T-cells could be chronically stimulated and accumulate in CLL. Borge et al have reported T-cell responses to various chemokines and found that there was migration by CLL T-cells towards CXCL12 (also known as SDF-1; stromal derived growth factor). This migration was impaired in ZAP-70 negative CLL cases, hypothesising that T-cells are encouraged to accumulate in the microenvironment in poor risk ZAP-70 positive cases (Borge, Nannini et al. 2010).

1.4.3 T-helper Perturbations in CLL

Studies analysing CLL T-cell cytokine production have found several deviations from the normal pattern that is observed in healthy controls. Rossmann et al found levels of IL-2, IL-4, TNF-α and GM-CSF to be significantly increased in T-cells from CLL patients (Rossmann, Lewin et al. 2002). The cytokine profiles of T-cells between indolent and advanced disease also shows differences, with the highest levels of IL-2 and IL-4 being present in patients with advanced disease. *In vitro* studies of patients with early stage disease seem to show a bias towards Th1 (IL-2, IFN-γ, TNF-β, GM-CSF) cytokine production over Th2 (IL-4, IL-5, IL-6, IL-10) production and conversely more Th2 in advanced cases (Podhorecka, Dmoszynska et al. 2002). The shift from Th1 to Th2 with advanced disease may play a role in CLL cells escaping immune surveillance (Mellstedt and Choudhury 2006). Interestingly IL-2, IL-4 and TNF-α are thought to support CLL survival *in vitro* (Cordingley, Bianchi et al. 1988, Trentin, Zambello et al. 1994). IL-4 also may assist the transition of CLL cells from resting G0 to G1/S (Luo, Rubio et al. 1991, van Kooten, Rensink et al. 1992) and IFN-γ is reported to rescue CLL cells from apoptosis *in vitro* (Buschle, Campana et al. 1993).

This perturbation in Th polarisation may therefore be, in part, driven by the CLL cells themselves, as their prolife of cytokine expression includes IL-1β, IL-2, IL-4, IL-5, IL-6, IL-8, IL-10, IFN-α, IFN-γ, G-CSF, GM-CSF, TNF-α and TGF-β. Research from our group has previously shown that CLL cells secrete high levels of IL-6, and suggest its role in inhibiting T-cell activation and inducing a Th2 response (Buggins, Patten et al. 2008).

Th17

Il-17 secreting Th17 helper cells have recently been studied by several groups. They have found higher levels of Th17 phenotype T-cells in CLL patients compared to normal controls but that lower numbers correlate with advancing disease (Tang, Niu et al. 2014). Th17 numbers seem to correlate inversely with the proportion of Tregs (Jain, Javdan et al. 2012, Hus, Bojarska-Junak et al. 2013).

Tfh

Little work has focused on the T follicular helper cells in CLL to date. Cha et al defined Tfh as CD4+ CXCR5+ and found these cells to represent 25% of CD4+ T-cells in CLL compared to 8% in normal controls suggesting a role in disease (Cha, Zang et al. 2013). However it must be taken into account that CXCR5 is also expressed on central memory T-cells. Ahearne et al concurred there were increased Tfh cells in CLL PB using a more robust CD4+ CXCR5+ ICOS+ phenotype although they found numbers did not correlate with stage. They went on to investigate their major cytokines produced by Tfh cells, IL-21 and IL-4, and found that these promote leukaemic proliferation (Ahearne, Willimott et al. 2013).

Tregs

Tregs maintain self-tolerance and have a significant role in many cancers. Treg numbers in the PB have been consistently shown to be increased in CLL and correlate with advanced stage disease (Beyer, Kochanek et al. 2005, Giannopoulos, Schmitt et al. 2008, Jak, Mous et al. 2009, Weiss, Melchardt et al. 2011, Biancotto, Dagur et al. 2012, D'Arena, D'Auria et al. 2012, Lad, Varma et al. 2013). Treg numbers seem to predict time to first treatment in low risk patients (D'Arena, D'Auria et al. 2012). The complex T-cell immune deficiency means CLL T-cells do not mount an effective anti-tumour effect may in part be assisted by the increased

Tregs which may exert their effect by downregulating tumour specific effector T-cells (D'Arena, Laurenti et al. 2011). The negative regulator CTLA-4 is expressed at high levels by Tregs and high levels of CTLA-4 was found to be correlated with aggressive disease. Recently an interesting paper by Jitschin et al suggested this may be as a result of an increased number of myeloid derived suppressor cells (MDSCs) which supress T-cell activation and induce Tregs (Jitschin, Braun et al. 2014). Another mechanism by which Tregs may be induced is via CD200. CD200 is an immunomodulatory molecule recently found to be expressed on CLL cells which down regulates Th1 responses and induces Tregs (Kretz-Rommel, Qin et al. 2007, Pallasch, Ulbrich et al. 2009).

1.4.4 Evidence of T-cell Stimulation

Phenotypically the T-cells derived from PB patients with CLL have marked differences from normal controls. These phenotypic changes support the hypothesis that the T-cells are undergoing chronic antigenic stimulation. Several groups have reported an increased T_{EM} phenotype (CD45RA-/CCR7-) in the CD4+ T-cells of CLL patients compared to healthy controls and a relative decrease in naïve T-cells, data confirmed in this thesis (Motta, Chiarini et al. 2010, Walton, Lydyard et al. 2010, Nunes, Wong et al. 2012). By convention these CD4+ T_{EM} cells develop post antigen exposure. Similar findings are reported in the CD8+ T-cells with less naïve subsets in CLL patients than healthy controls (Nunes, Wong et al. 2012).

Many studies have found CD69, HLA-DR and CD95 to be higher on the CD4+ PB cells from CLL patients (Totterman, Carlsson et al. 1989, Scrivener, Kaminski et al. 2001, De Fanis, Dalla Mora et al. 2002). Serrano et al also reported that CD57 was significantly increased in both the CD8+ and CD4+ T-cell populations in CLL patients compared to normal controls (Serrano, Monteiro et al. 1997). CD57, as discussed earlier, is a marker of chronic activation, and is expressed on late effector T-cells, again following antigenic stimulation.

Low expression of the co-stimulatory molecule CD28 in both CD4+ and CD8+ T-cells has been consistently reported and lower levels appear to correspond with more advanced disease (Rossi, Matutes et al. 1996, Rossmann, Jeddi-Tehrani et al. 2003). CTLA-4 is found at higher levels on CLL derived T-cells compared to normal controls and is hypothesised to be a mechanism by which T-cell function is impaired (Frydecka, Kosmaczewska et al. 2004).

Taken together these findings have led to the hypothesis that T-cells in CLL, just like the B-cell have been activated and show features of exposure to antigen.

1.4.5 Functional Abnormalities

The functional T-cell abnormalities in CLL PB have long been appreciated (Chiorazzi, Fu et al. 1979). Much of the observed T-cell dysfunction is thought to be induced by the CLL cells themselves. The dysfunction is at least in part mediated by the cytokine production of the tumour cells such as TNF-β and IL-10 that supress T-cell activation and effector function. I shall outline some of the major abnormalities below.

Exhausted T-cells

More recent evidence, and presented here in this thesis, is that the T-cells appear to have markers of chronic exhaustion such as PD-1, CD244 and CD160 (Xerri, Chetaille et al. 2008, Nunes, Wong et al. 2012, Brusa, Serra et al. 2013, Riches, Davies et al. 2013, Novak, Prochazka et al. 2015, Rusak, Eljaszewicz et al. 2015). Ramsay et al reported PD-1 expression on CD3+ T-cells of CLL patients to be higher than those from normal controls and correlated with poor prognosis (Ramsay, Clear et al. 2012). Brusa et al reported that the PD-1 levels were higher on both the CD4+ and CD8+ PB T-cells than normal controls and that surprisingly all subsets could express PD-1 including naïve T-cells (Brusa, Serra et al. 2013). Nunes et al reported that the emergence of CD8+ PD-1+ T-cells at an early stage were associated with a more aggressive clinical disease (Nunes, Wong et al. 2012). Novak et al added that relapsed refractory patients had the highest number of CD4+ and CD8+ T-cells co-expressing PD-1 (Novak, Prochazka et al. 2015). Rusak et al found a higher frequency of CD4+ PD-1+ T-cells in more aggressive disease and suggested that the higher the numbers at diagnosis the shorter the time to first treatment (Rusak, Eljaszewicz et al. 2015). An apparently contradictory report from Tonino et al found decreased expression of PD-1 on effector CD8+ T-cells in CLL compared to normal controls, which was negatively correlated with absolute T-cell numbers, (Tonino, van de Berg et al. 2012). This result is in contrast to other reports and one explanation for this could be the population under study in this paper was the CMV specific CD8+ population, where they showed the largest T-cell effector expansion.

Riches et al found the "exhausted" CD8+ T-cells to have defective cytotoxicity *in vitro* related to impaired vesicle formation but found these T-cells retained the ability to produce cytokines. Unlike T-cells exhausted from viral infections, CLL derived CD8+ "exhausted" T-cells express high levels of IFN-γ, TNF-α and T-BET which may help protect the cells from apoptosis (Riches, Davies et al. 2013).

Much work has now been focusing on the effects of rescuing PD-1+ T-cells from exhaustion. Gassner et al showed in the TCL-1 mouse model that PD-1 / PD-L1 blockade did aid tumour clearance *in vivo*. (Gassner, Zaborsky et al. 2015). Although this murine model may not reflect the situation in human CLL. Brusa et al reported, in primary CLL cells, that blocking the PD-1 / PD-L1 axis *in vitro*, with an anti-PD-L1 antibody, lead to increased CD8+ IFN-γ expression, and conversely co-culture with recombinant soluble PD-L1 decreased IFN-γ levels, a concept I shall discuss further in this thesis (Brusa, Serra et al. 2013).

CD40:CD40L

It is unknown what role CD40:CD40L interactions between CLL and T-cells occur *in vivo* and several groups have reported a defect in CD40L signalling when PB T-cells are cultured with CLL *in vitro* (Cantwell, Hua et al. 1997, Tretter, Schuler et al. 1998, Kneitz, Goller et al. 1999, Buggins, Patten et al. 2008). The overall T-cell immune deficiency in CLL has in fact been likened to those found in patients that genetically lack CD40L (CD154). Patients with genetic defects of CD40L have the phenotype of reduced secondary immunoglobulins and increased susceptibility to bacterial infection. They also fascinatingly, just like CLL patients, produce auto-antibodies against autoantigens for example those found on red cells and platelets (Hamblin, Oscier et al. 1986, Cantwell, Hua et al. 1997). In CLL there is not a lack of CD154 mRNA; the deficiency has been shown to be secondary to receptor mediated down modulation by CD40 expressing CLL cells. This effect can be overcome by adding a CD40 blocker. Ghia et al suggested a role for the CD40/CD40L interaction by cross linking CD40 on CLL cells *in vitro* and observing an increase in CCL22 expression, which in turn was a chemoattractant to CD4+ CD40L+ CCR4+ T-cells (Ghia, Strola et al. 2002), but in this experiment the CD40 crosslinking would have preventing the downregulation of T-cells. CD40 crosslinking has also

been demonstrated to upregulate anti-apoptotic genes such as survivin (Granziero, Ghia et al. 2001).

Interestingly, when normal T-cells are co-cultured with CLL cells at a ratio of <1:33 (more than 33 CLL cells per T-cell) then they too cannot upregulate CD40L. (Cantwell, Hua et al. 1997) Therefore CLL seems to be a model of acquired CD40L deficiency caused by the CLL cells themselves; reducing the ability of the T-cells to effectively activate and therefore helping the tumour itself to evade attack. In fact many solid tumours express CD40 and this is a postulated mechanism by which tumours regulate their microenvironment by reducing the upregulation of the tumour infiltrating lymphocytes. Examples include breast cancer (Hutchins and Steel 1994), bladder cancer (Ben-Aissa, Paulie et al. 1988) and Kaposi's sarcoma (Pammer, Plettenberg et al. 1996).

Gene Expression

Gene expression profiling studies have revealed additional major differences between T-cells derived from CLL patients and healthy aged matched controls. Gorgun et al found the majority of the differentially expressed genes in the CD4+ compartment to be involved in cell differentiation, and in the CD8+ population to be defects in cytoskeleton formation, vesicle trafficking and cytotoxicity. Interestingly they additionally noted that similar abnormalities could be induced in allogeneic T-cells when co-cultured with CLL cells *in vitro*. This again implicates the CLL cells themselves in dysregulating T-cells; leading to gene expression changes in otherwise healthy T-cells and rendering them functionally deficient (Gorgun, Holderried et al. 2005). Rissiek et al came to the same conclusions; suggesting the CLL cells themselves are inducing T-cell dysfunction over time, by studying T-cell phenotypic changes in patients with all stages of disease from MBL to advanced CLL (Rissiek, Schulze et al. 2014).

Defective Immunological Synapse

Ramsay et al have examined the abnormalities in the physical associations between the T and B-cells in CLL. They have shown the formation of a defective "immunological synapse", when CLL cells are incubated with allogeneic or CLL derived T-cells. There is suppressed actin polymerisation, and decreased recruitment of LFA-1 (Lymphocyte function associated

antigen 1), LCK (lymphocyte specific protein tyrosine kinase) and the TCR to the T-cell synapse. They suggest it is this cytoskeletal defect, which ultimately leads to a defective TCR signalling and therefore impaired downstream functional T-cell responses. They go on to show this defect can be repaired with the use of the immunomodulatory drug, lenalidomide (Ramsay, Johnson et al. 2008). The same group undertook functional assays and found that PD-L1, CD200, CD270 (Herpes virus entry mediator) and CD276 (B7-H3) could induce a similarly impaired immunological synapse formation in allogeneic T-cells (Ramsay, Clear et al. 2012) again suggesting the CLL cells themselves play a role in evading immune surveillance.

1.4.6 CLL TCR Repertoire

The T-cell accumulation in CLL may in part be dependent on TCR engagement but this in itself does not give definitive evidence of a specific response to antigen. Analysis of the TCR repertoire has provided direct evidence of oligoclonality in CLL. The overall TCR repertoire in CLL has marked skewing from normal controls (Forconi and Moss 2015). Wen et al were the first to identify the presence of T-cell clones in the PB of 3 out of 5 stage A CLL patients (Wen, Mellstedt et al. 1990). The presence of T-cells clones in CLL has since been replicated by many groups (Farace, Orlanducci et al. 1994, Serrano, Monteiro et al. 1997, Rezvany, Jeddi-Tehrani et al. 1999, Goolsby, Kuchnio et al. 2000). Several groups have demonstrated a small, but definable population of postulated anti-leukaemic T-cells, these have been the subject of interest especially in the possibility of expanding them by vaccination (Rezvany, Jeddi-Tehrani et al. 2000, Goddard, Prentice et al. 2001, Gitelson, Hammond et al. 2003). Cytotoxic CD8+ T-cells have been reported at low frequency that respond to CLL idiotypic peptide (Trojan, Schultze et al. 2000). However CLL derived T-cells dysfunction seems to render them unable to mount an effective anti-leukaemic effect and they do not explain the marked repertoire skewing in CLL (Christopoulos, Pfeifer et al. 2011).

Nunes et al have shown that in CLL, and other human cancers, there is abnormal degradation of BAX (Bcl-2 associated X protein) protein, and that the derived peptides can be presented to CD8+ T-cells on MHC Class I (Nunes, Miners et al. 2011). *In vitro* studies revealed that these antigen specific T-cells are capable of killing primary CLL cells.

These are several alternative potential mechanisms for driving a skewed T-cell repertoire in CLL. When investigating the overall T-cell repertoire of an elderly CLL patient population it must be remembered that there is known to be marked skewing of the TCR repertoire with normal ageing and as a response to chronic viral infections (Giannopoulos, Schmitt et al. 2008). A full understanding of the aberrations in the TCR repertoire in CLL remains to be defined, but there is mounting evidence that CLL T-cells, just like the B-cells are antigen experienced and subject to chronic stimulation. I shall address this in detail in this thesis.

1.4.7 Pro-tumour Role of T-cells in CLL

Taken together, the above studies show that there is a major T-cell dysfunction in CLL which permits the tumour to evade the immune system and that the CLL cells themselves are in part orchestrating this dysfunction. There is evidence of marked skewing of the TCR repertoire and a small but definable number of CD8+ anti-CLL T-cells. However there is also substantial evidence that CD4+ T-cells are supportive of CLL *in vitro*. It is well established that co-culture of CLL cells with CD4+ T-cells promotes CLL cell survival (Tretter, Schuler et al. 1998, Patten, Devereux et al. 2005). More compelling evidence that T-cell help is key in the development of CLL comes from the murine studies from the Chiorazzi group in New York. They found that CLL engraftment in an immunodeficient mouse was entirely dependent on the addition of activated autologous CD4+ T-cells; again inferring that T-cells are essential for *in vivo* proliferation of CLL cell (Bagnara, Kaufman et al. 2011).

Zangani et al also reported a mouse model where B-cell lymphomas developed and were maintained by CD4+ T-cells with specificity for B-cell self-antigens. This is a very interesting concept. It has been previously shown that idiotypic peptides can be eluted from Class II MHC in B-cell lymphomas. The hypothesis is that B-cells constantly present their own immunoglobulin as unique variable region idiotypic peptides on class II MHC to idiotype specific T-cells to drive lymphomas (Bogen, Malissen et al. 1986). Bogen et al showed that the B-cells are chronically helped by these idiotype specific T-cells to develop into lymphomas. Therefore these idiotypic peptides from the immunoglobulin itself may represent a chronic antigen stimulus to Th cells which, in turn, promotes lymphogenesis (Zangani, Froyland et al. 2007). This of course should not occur if the T-cells are universally tolerant to self-antigens;

but it is known that self T-cells can respond to rarer idiotype peptides from unique N regions or somatic mutations (Bogen, Dembic et al. 1993, Eyerman, Zhang et al. 1996). These self-reactive T-cells are found at low frequency (Snodgrass, Fisher et al. 1992).

Os et al looked further at the role of self-reactive T-cells in CLL. Firstly they showed that resting CLL cells could endocytose, process and present self-antigens on Class II MHC and could receive help from specific CD4+ T-cells. Next they generated T-cell lines by stimulating T-cells with autologous CLL cells. They found these T-cell lines to have specificity for endogenous CLL derived antigens and could support CLL proliferation *in vitro* and in a mouse model. The T-cells had a Th1 phenotype and secreted IFN-γ (Os, Burgler et al. 2013).

Therefore the CD4+ T-cells in CLL are activated and can respond to antigen presented to them by the CLL cells. The actual antigenic stimulus remains unknown and, just like the BCR, several candidates have been put forward. Hall et al suggested, like Os et al, that the CD4+ T-cells were autoreactive, as shown in autoimmune haemolytic anaemia (Hall, Vickers et al. 2005). Alternative theories are that the T-cells are responding to exogenous antigen such as fungal elements, like has been described in the BCR (Hoogeboom, van Kessel et al. 2013).

1.4.8 CMV and CLL

Several groups have investigated the complexity that arises in patients with CLL and co-existing cytomegalovirus (CMV) seropositivity and hypothesised a role for CMV for the CLL T-cell aberrations. CMV is a very common virus, which is known to cause marked perturbation of the normal T-cell pool of otherwise healthy individuals. In a healthy elderly population CMV specific CD8+ T-cells can account for up to half the T-cell repertoire (Khan, Shariff et al. 2002). Mackus et al identified the presence of CD8+ T-cell clones reactive against CMV with a CD45RA+ CD27- cytotoxic phenotype in previously infected CLL patients (Mackus, Frakking et al. 2003). These findings lead to the hypothesis that CMV could be in part responsible for the global T-cell expansion and dysfunction in CLL (Akbar 2010). However it has been acknowledged that the T-cell abnormalities in CLL are not just restricted to CMV seropositive individuals and that there is still a vast T-cell expansion of dysregulated T-cells with abnormal phenotype even in CMV seronegative individuals (Nunes, Wong et al. 2012, Riches, Davies et al. 2013). It is also observed that CMV reactivation is rare in untreated CLL individuals

suggesting an intact T-cell response to the virus. To investigate this in detail, te Raa et al designed a series of experiments to assess the function of T-cells from CMV seropositive CLL patients (te Raa, Pascutti et al. 2014). Firstly, they confirmed the global T- cell dysfunction of the total T-cell pool, as evidenced by finding increased levels of expression of inhibitory markers such as PD-1, CD244 and CD160 on CLL CD8+ T-cells. This was associated with increased levels of IFN-γ and TNF-α, in concordance with previous studies. They then selected CLL CMV specific T-cells using CMV tetramers and found no increase in the inhibitory markers and an intact cytokine production. Additionally, in functional assays using CMV peptide loaded target cells, they found CLL derived CD8+ T-cells to be just as effective at killing as those derived from age matched normal controls and they formed an effective immunological synapse. They concluded there was a preserved CD8+ CMV specific T-cell function on a background of global T-cell dysfunction.

The next question is whether there is any perturbation of CD4+ T-cells as a result of CMV seropositivity. 1 et al initially identified a population of CD4+ CD57+ T-cells in CLL patients which were mainly CD45RO+ CD28- and expressed perforin; suggesting a possible cytolytic function. (Porakishvili, Roschupkina et al. 2001). These CD4+ cells lacked CD69 or HLA-DR. They subsequently published evidence that the CD4+ perforin producing T-cells they identified appear to be CMV specific effector / memory T-cells (Walton, Lydyard et al. 2010). Pourgheysari et al further investigated the CD4+ expansion in CLL patients and found the absolute CD4+ T-cell count in CLL was not influenced by CMV serostatus, but found on average 11% of the CD4+ T-cell pool was CMV specific in previously infected individuals (Pourgheysari, Bruton et al. 2010). They reported, like Porakishvili, that there were more CD4+ CD28- T-cells in CMV seropositive compared to seronegative individuals, but these account for a small proportion of the total CD4+ pool.

Taken together, these studies seem to suggest that CMV is not the reason for the global T-cell dysfunction in CLL; in fact CMV responses may be a remaining intact immunological function in the midst of T-cell dysfunction. This could point to the hypothesis that there is a specific suppression of only certain subpopulations of T-cells by CLL. It is not clear whether there could be other subpopulations of T-cells whose function is unaffected by the CLL clone,

as no other viral response is so immuno-dominant and overrepresented in the T-cell repertoire.

1.4.9 Telomeres

Indirect evidence that the T-cells have a specific active role in CLL comes from studies of telomere length. Just like in CLL cells, T-cells from CLL PB have shorter telomeres than healthy matched controls, indicating that these T-cells have a replicative history. This suggests that the T-cells are proliferating, and not merely bystanders (Roth, de Beer et al. 2008). The shortest T-cells telomeres are also correlated with advanced disease.

1.5 NK Cells

Quantitative and qualitative abnormalities in natural killer (NK) cells seem to be relevant in CLL pathology. A higher NK to CLL B-cell ratio is predictive of longer time to treatment as higher numbers were found in early stage disease and mutated cases (Palmer, Hanson et al. 2008). NK cells derived from CLL patients have long been known to have a lower cytolytic capacity than those found in healthy controls (Kay and Zarling 1987), which could be restored by the addition of IL-2 *in vitro* (Kay and Zarling 1987). More recently CLL derived NK cells have been shown to have defective actin polymerisation and impaired immunological synapse formation (Xing, Ramsay et al. 2010).

1.6 Lymph Node Microenvironment in CLL

1.6.1 Introduction

When PB CLL cells are cultured *in vitro* they die rapidly by apoptosis, even when cultured in media which is usually supportive to human B-cell lines (Collins, Verschuer et al. 1989). This is in contrast to the *in vivo* situation where CLL cells are long-lived. From this it can be inferred that the resistance to apoptosis *in vivo* is not intrinsic to CLL cells, but is dependent on external factors (Ghia, Circosta et al. 2005). It has been shown that co-culture of PB CLL cells with CD4+ T-cells and other components of the tumour microenvironment increases CLL cell survival *in vitro* (Ghia and Caligaris-Cappio 2005, Patten, Devereux et al. 2005). It is also now appreciated that the major site of CLL proliferation is not within the PB but within the secondary

lymphoid organs (Ghia and Caligaris-Cappio 2000, Granziero, Ghia et al. 2001). As the proliferating component of CLL is essentially within secondary lymphoid tissue, it is reasonable to propose that the tumour microenvironment niche here provides a supportive environment for the CLL clone where CLL cells are in close communion with other non-malignant cells such as T-cells, stromal cells and vascular endothelium. It is here that the CLL cells can send and receive signals either via cell to cell contact or by soluble factors with T-cells, dendritic cells and stromal cells.

1.6.2 CLL Cells in the Lymph Node Microenvironment

Investigators have long been asking the question whether CLL cells within the LN are intrinsically different from those of the PB. Several studies have identified differences between the CLL cells derived from the PB compared to those from within the microenvironment.

Proliferation and Anti-apoptosis

Histological studies of CLL lymph nodes have identified pale staining "proliferation centres" or "pseudofollicles"; which some have been likened to malignant germinal centres (Stein, Bonk et al. 1980). Proliferation centres contain large prolymphocytes and paraimmunoblasts, surrounded by smaller lymphocytes. The number and size of these proliferation centres may correlate with aggressive disease, but this has not been a reproducible finding (Bonato, Pittaluga et al. 1998, Asplund, McKenna et al. 2002). Within the proliferation centre there is a higher concentration of Ki-67 positive proliferating cells.

CLL cells derived from lymph nodes express higher levels of E2F1 (E2F Transcription Factor 1), which is a transcription factor that drives cell cycle transition from G1/S. There is also an increase expression of c-MYC target genes compared to the peripheral blood, which drive cell proliferation (Herishanu, Perez-Galan et al. 2011). Proliferating CLL cells express higher levels of survivin (Granziero, Ghia et al. 2001); survivin, or BIRC5, is an inhibitor of apoptosis. There is also upregulation of the anti-apoptotic regulators BCL-XL (B-cell lymphoma extra large) and MCL-1 (myeloid cell leukaemia 1) in the LN compared to PB (Smit, Hallaert et al. 2007).

Mittal et al simultaneously studied gene expression profiles of CLL cells from LN, BM and PB and also found signatures that promote pathways of tumour survival and proliferation within the microenvironment (Mittal, Chaturvedi et al. 2014). There were increased levels of BAFF and APRIL (a proliferation inducing ligand) within the LN and evidence of increased NF-kB activation (Mittal, Chaturvedi et al. 2014). Levels of BAFF and APRIL are postulated to support CLL survival through activation of the NF-kB pathway and patients expressing lower levels have a longer survival (Endo, Nishio et al. 2007, Bojarska-Junak, Hus et al. 2009). BAFF has 3 receptors; TACI (transmembrane activator and calcium modulator and cyclophilin ligand interactor), BCMA (B-cell maturation antigen) and BAFF-R (B-cell activating factor receptor) all of which are activated in CLL lymph nodes.

Gilling et al also examined the differing gene signatures in LN and PB compartments and chose a few genes for further examination. These included Caveolin-1 (CAV1) which was found to be expressed seven fold higher in CLL LNs compared to PB. When they knocked down CAV1 in CLL cells, they demonstrated decreased CLL migration and proliferation. In CAV1 cell line knockdowns the immunological synapse was also impaired implying CAV1 can help the CLL cell escape immune-surveillance (Gilling, Mittal et al. 2012).

Adhesion Molecules and Chemokine Receptors

CLL cells from the lymph node also have differential expression of adhesion molecules and chemokine receptors (Burger 2010). This is thought to be a mechanism by which CLL cells are trafficked into, and remain in lymph nodes; leading to lymphadenopathy in more aggressive disease phenotypes.

CD49d, which enhances cell to cell adhesion via VCAM-1 (vascular cell adhesion molecule 1) and fibronectin on stromal cells is expressed at higher levels in lymph nodes (Ghia, Guida et al. 2003, Jaksic, Paro et al. 2004). Levels of CD49d on CLL cells of the PB are known to correlate with poor prognosis. They also found that CD38, another poor prognostic marker, which forms a macromolecular complex with CD49d, is found at higher levels in LN than PB.

There is also an increase in the lymphocyte homing chemokine CXCL13 on the LN CLL cells (Burkle, Niedermeier et al. 2007). CXCR5 is the receptor for CXCL13 (also known as B-

lymphocyte chemoattractant) and this interaction is another postulated mechanism for attracting CLL cells into the LN. CLL cells directly isolated from the LN also appear to express higher levels of CCL3 and CCL4. CCL3 and CCL4 are cytokines involved in inflammation and chemoattractant to immune cells (Herishanu, Perez-Galan et al. 2011). This data implies the CLL cells are creating their own supportive microenvironment.

CXCL12 (SDF-1), is a chemokine that is chemoattractant to lymphocytes via its ligand CXCR4. CXCR4 has been shown to be expressed at relatively lower levels on proliferating LN CLL cells than PB, which is thought to be due to down-modulation as a result of CXCL12 ligation (Bennett, Rawstron et al. 2007). CXCR4 levels are also known to be downregulated as a result of BCR signalling (Quiroga, Balakrishnan et al. 2009, Vlad, Deglesne et al. 2009). *In vivo* deuterium heavy water labelling studies have now shown a higher uptake in the CLL cells with lower levels of CXCR4 and higher CD38 (Calissano, Damle et al. 2009). This model suggests chemokine attraction, followed by BCR ligation by antigen drives proliferation within the PC of the lymph node.

BCR Signalling and Antigen Drive

Herishanu et al performed gene expression studies on CLL cells from 24 untreated patients taken simultaneously from blood, bone marrow and lymph nodes. They found that the CLL cells within the LN have upregulation of genes associated with BCR signalling and increased NF-kB activation. There was also increased SYK phosphorylation, consistent with antigen dependant BCR signalling within the lymph node (Herishanu, Perez-Galan et al. 2011). In a similar study Mittal et al found in the LN CLL cells there were genetic signatures associated with chronic activation of the BCR (Mittal, Chaturvedi et al. 2014). LN CLL cells have also been shown to have increased levels of the interferon regulatory factor 4 (IRF-4 or MUM-1), which is expressed following somatic hypermutation (Ito, Iida et al. 2002, Soma, Craig et al. 2006).

Clonal Diversity

Several groups have tried to address the question of whether phenotypically different LN and circulating B CLL cells were clonally similar. An early study from Bonato et el, showed there was similar light and heavy chain expression between LN sections and PB (Bonato, Pittaluga et al. 1998). Isobe et al went further and dissected proliferation centres from lymph node sections from 4 patients. They extracted the DNA and showed the clonal diversity was very similar in the LN to the PB (Isobe, Tamaru et al. 2001). Vandewoestyne et al raised the question that not all CLL cells within the PC are in fact proliferating and therefore used laser capture to dissect out proliferation centres and then isolated the specific Ki67+ CD79a+ cells to ask the same question. They compared the IGHV of cells from 7 patients' lymph nodes and compared them to matching PB. They found the overrepresented IGHV clones in the LN mirrored the PB providing evidence the proliferating CLL cells in the LN are clonally related to the PB compartment (Vandewoestyne, Pede et al. 2011).

1.6.3 CLL Cells Sustained by the Microenvironment

Much work has focused on which elements within the LN microenvironment are enabling CLL cells to proliferate and offer protection from apoptosis. Studies by our group and others have shown proliferating CLL cells are in close contact with CD4+ T-cells (Ghia, Strola et al. 2002, Patten, Buggins et al. 2008) and stromal cells (Ruan, Hyjek et al. 2006) within the LN microenvironment. The protective advantage given by co-culture of CLL with CD4+ T-cells has already been discussed. In addition *in vitro* culture models have shown that CLL survival can be prolonged by co-culture with several of the elements found within the CLL microenvironment niche.

Stromal Cells

Stromal cells derived from the bone marrow have been consistently shown to support CLL survival *in vitro* (Panayiotidis, Jones et al. 1996, Lagneaux, Delforge et al. 1999, Kay, Shanafelt et al. 2007). Bone marrow stromal cells appear to activate CLL cells and are themselves activated (Ding, Nowakowski et al. 2009, Lutzny, Kocher et al. 2013). Stromal cells interact with CLL cells through receptors for CXCR4 and CXCR5. CLL cells expressing

CXCR4 are attracted to migrate beneath cells that express its ligand CXCL12 (such as stromal cells) by pseudo-emperipolesis (Burger, Burger et al. 1999). CXCL12 ligation in return induces pro-survival signals and downregulates CXCR4 which is associated with the Ki67+ proliferative CLL pool found in the PC (Burger, Hartmann et al. 2005). Vaisitti et al found that CXCL12 induced migration of CLL cells correlated with higher levels of CD38 (Vaisitti, Aydin et al. 2010). These results suggest that CXCL12 secretion within the microenvironment promotes the accumulation of CLL cells.

Bone marrow stromal cells also express Wnt5a which signals though ROR-1. ROR-1 has recently described to be expressed by CLL cells, suggesting another mechanism by which stromal cells may assist CLL cells survival (Fukuda, Chen et al. 2008). Recently abnormalities of the bone marrow derived stromal cells in CLL patients has also been described (Pontikoglou, Kastrinaki et al. 2013)

Vascular Endothelium

The vascular component of lymph nodes has been reported to be increased in CLL compared to normal nodes (Chen, Treweeke et al. 2000). Our group additionally reported that increased expression of CD31 (PECAM-1 (platelet endothelial cell adhesion molecule) expressed on vascular endothelium) in CLL lymph nodes correlated with CD38 levels and therefore poor prognosis (Patten, Buggins et al. 2008). CD31 is the only known ligand of CD38 and it has been shown that ligation of CD38 with CD31 decreases CLL apoptosis *in vitro* (Deaglio, Aydin et al. 2010, Poggi, Prevosto et al. 2010). These results suggest that CLL cases with poor prognosis, as evidenced by high levels of CD38, are more vascular and provide a more supportive environment to CLL cells. Our group has also directly shown that co-culture of CLL cells and endothelial cells promotes CLL cell survival *in vitro* (Buggins, Pepper et al. 2010).

Follicular Dendritic Cells

There has been some controversy regarding the presence of FDCs within involved CLL lymph nodes, with some studies reporting their occasional presence and others concluding they are absent (Stein, Gerdes et al. 1982, Swerdlow, Murray et al. 1984, Chilosi, Pizzolo et al. 1985, Greil, Gattringer et al. 1986, Ratech, Sheibani et al. 1988). However, co-culture of CLL cells

with immortalised FDCs prolongs CLL survival through CD44 ligation and upregulation of the anti-apoptotic protein MCL-1. (Pedersen, Kitada et al. 2002). CD44 is a receptor for hyaluronic acid that interacts with CD38, CD49d, MMP-9 and ZAP-70 (Zhang, Wu et al. 2013) . It is now known that CD44 forms a macromolecular complex with CD38 CD49d and MMP9 which may influence CLL cell migration, invasion and homing (Buggins, Levi et al. 2011).

Nurse-Like Cells

In an *in vitro* system devised by Burger et al, CLL PB cells were co-cultured for 7-14 days with CD14+ monocytes and they observed monocyte differentiation into large so called "Nurse-like cells" (NLCs). These cells are reported to protect CLL cells from apoptosis (Burger, Tsukada et al. 2000). NLCs, similarly to stromal cells derived from the BM, appear to interact with CLL cells through secretion of CXCL12. Co-culture of CLL cells with NLCs increases the CLL expression of CCL3 and CCL4 which consequently attracts supportive cells such as regulatory T-cells (Burger, Quiroga et al. 2009). These NLCs express also high levels of BAFF and APRIL (Nishio, Endo et al. 2005). The presence, or not, of these cells *in vivo* is controversial*.*

Cytokines

Other mechanisms by which CLL cells can be sustained *in vitro* include co-incubation with a vast array of cytokines, some of which may be produced by cells of the microenvironment. These include IL-4 (Panayiotidis, Ganeshaguru et al. 1993), IL-6 (Reittie, Yong et al. 1996), IL-8 (Francia di Celle, Mariani et al. 1996), IL-10 (Jurlander, Lai et al. 1997), IL-13 (Chaouchi, Wallon et al. 1996), IFN-α (Chaouchi, Wallon et al. 1994), IFN-γ (Buschle, Campana et al. 1993), VEGF (Pepper, Ward et al. 2007) and CXCL12 (O'Hayre, Salanga et al. 2010). Interestingly all of these cytokines have also been shown to be intrinsically produced by CLL cells.

1.6.4 T-Cells Derived from the CLL Microenvironment

There has been extensive research into T-cells found in the PB of CLL patients, however very little research has focused on the T-cells from other compartments which may be distinct.

T-cells in CLL Bone Marrow

Immunohistochemistry studies in the 1980's of found the number of T-cells in the CLL bone marrow to be increased compared to normal controls, and that the T-cells were primarily of the Th-cell phenotype (Pizzolo, Chilosi et al. 1983). Bojarska-Junak looked specifically at the levels of TNF in the PB and BM of CLL patients and found higher levels from the BM compartment than the PB, and levels correlated with poor prognostic factors (Bojarska-Junak, Hus et al. 2008).

T-cells in CLL Lymph Nodes

Swerdlow et al published a series of 9 CLL lymph node biopsies and showed the T-cell component to be up to 15% of the total cell numbers with a preponderance of Th T-cells (Swerdlow, Murray et al. 1984). Another small series have reported up to 35% of lymphocytes being T-cells within CLL lymph nodes, with predominately a Th phenotype (Schmid and Isaacson 1994, Bonato, Pittaluga et al. 1998, Granziero, Ghia et al. 2001). Ghia et al suggested between 5-30% of these CD4+ T-cells expressed CD40L, but this has not been consistently reproduced (Ghia, Strola et al. 2002). Our group have previously published, using multiparameter immunofluorescence microscopy, that within the CLL lymph node microenvironment, proliferating CLL cells are in cellular contact with CD4+ Foxp3- T-cells (Patten, Buggins et al. 2008). These T-cells were CD25+ suggesting an activated phenotype. Lad et al have very recently reported that the number of Tregs in the LN microenvironment is higher than in the PB , data confirmed by this thesis (Lad, Varma et al. 2015). Conversely they found fewer Th17 cells. Their hypothesis is that IL-10 excreting Tregs supress the Th17 cells in this compartment allowing CLL to escape immune surveillance. Brusa et al have also recently published a study of CLL lymph nodes and find the presence of CD4+ PD-1+ T-cells in contact with PD-L1+ CLL cells, data I shall discuss further in this thesis (Brusa, Serra et al. 2013).

1.7 Aim of Thesis

The aim of this thesis is to further characterise the T-cell component of the CLL lymph node microenvironment. Although much is known of the PB T-cells in CLL the specific phenotype of the lymph node infiltrating T-cells has not been fully elucidated. Taken together there is strong evidence that T-cells in CLL, just like the B-cell, have been activated and show features of post antigen exposure. The role of T-cells in CLL is clearly complex, with apparently opposing roles; with CD4+ T-cells supporting the tumour whilst CD8+ T-cells are trying to eliminate the tumour but are hampered by their dysfunction. The CLL cells themselves seem to play a critical role in maintaining the T-cell help and dysfunction simultaneously. Our hypothesis is that the critical interaction between T-cells and CLL are taking place within the supportive LN microenvironment. Therefore the investigation of the specific T-cells found within the lymph node microenvironment forms the basis of this research.

Chapter 2 General Materials and Methods

2.1 Ethics

Peripheral blood (PB) was collected from patients under national research ethics NREC: 08/H0906/94 and from healthy controls under LREC: 02-044. Ethical approval was obtained to perform lymph node fine needle aspirations (LN FNA) on CLL patients for research purposes from the research ethics committee REC: 09/H0805/5. Written informed consent was gained according to the Declaration of Helsinki, 2008. Ethical approval for was obtained for use of surplus anonymous lymph node (LN) biopsy samples for research from the national research ethics service (NRES 08/H0906/94) and local research ethics committee (LREC 02-044).

2.2 Primary Patient Material

2.2.1 Peripheral Blood Sample Collection

Patients with a diagnosis of CLL and healthy controls were invited to take part in the study. They were given a patient information sheet and given adequate time to consider their entry into the study. Written consent was obtained and samples pseudo-anonymised. Up to 40mls PB was collected from CLL patients and healthy controls directly into CLL media (See 2.4.5) and EDTA.

2.2.2 Isolating PB Mononuclear Cells (PBMCs)

CLL PBMCs were isolated from PB using Ficoll Histopaque® (Sigma Aldrich) density centrifugation. 10mls anticoagulated whole blood in CLL media was layered onto 10mls of Histopaque in a 50ml Falcon™ tube (Fisher Scientific) and centrifuged at 400g for 25 minutes at room temperature (RT). The opaque layer at the interface was carefully pipetted into a fresh tube. Cells were washed in PBS and centrifuged 250g for 15 minutes. The cell pellet was resuspended in CLL media. Manual cell counting was performed using a counting chamber (Hawksley), with trypan blue solution as a viability stain.

2.2.3 Cryopreservation of Cells

CLL PBMCs were centrifuged at 200g for 5 minutes and resuspended in a 50% solution (v/v) with RPMI-1640, 40% FCS, 10% DMSO. The cells were aliquoted into 1ml cryovials (Nalgene)

at a concentration of CLL cells $1 \times 10^7 - 10^8$/ml and frozen overnight in a Mr. Frosty™ Freezing Container (Nalgene) at -80°C; which optimally cools by -1°C per minute. The cryovials were then transferred to liquid nitrogen storage tanks within the King's College London (KCL) haemato-oncology tissue bank under the license of the Human Tissue Authority (HTA) (licence 12223, awarded 1st September 2006, unconditional status)

2.2.4 Defrosting Cells

Frozen cryovials were thawed in water bath at 37°C. The cells were added to 10mls of pre-warmed CLL media and pelleted by centrifugation at 200g for 5 minutes, before washing and resuspending in CLL media at desired concentration.

2.2.5 Negative B-cell Isolation

The EasySep® negative selection human B-cell enrichment kit without CD43 depletion (StemCell Technologies) was used to isolate CLL B-cells. The magnetic dextran bioparticles form tetrameric antibody complexes with an anti-dextran antibody and antibodies against CD2, CD3, CD14, CD16, CD56 and glycophorin A on the cells to be removed. This leaves behind the B-cells of interest. CLL PBMCs were resuspended in CLL media at a concentration of 5 x 10^7/ml in a 5ml tube. 50µl of EasySep® negative selection human B-cell enrichment cocktail was added per ml. The mix was incubated for 10 minutes at RT. The EasySep® nanoparticles were mixed by pipetting up and down (not vortexed). 50µl of nanoparticles were added per ml of cells and well mixed. The mix was incubated for 10 minutes at RT. The total volume of cells was made up to 2.5mls with PBS and 2% FCS (magnesium and calcium free). The tube was then inserted into the proprietary magnet for 5 minutes. The negatively selected cells that had not bound to the nanoparticles and been removed by the magnet were then harvested from the tube by inversion.

2.2.6 LN FNA Sample Collection

Patients with a diagnosis of CLL and an easily palpable lymph node were invited to take part in the study. They were given a patient information sheet and given adequate time to consider their entry into the study. Written consent was obtained and samples pseudo-anonymised. The LN FNA was performed by a trained clinician using a 23 gauge needle attached to 10ml syringe. Once the sample was aspirated the needle was washed in CLL media. This was

repeated on average 4 times per patient. The LN FNA was sample centrifuged at 200g for 5 minutes and resuspended in CLL media to a final volume depending on the cell count. Manual cell counting was performed using a counting chamber (Hawksley), with trypan blue solution (Fluka Analytical) as a viability stain.

2.2.7 Lymph Node Sections

Lymph node excision biopsies were performed on CLL patients as part of their routine clinical care. These samples were anonymised before release. FFPE blocks were cut into 3 micron sections and mounted onto glass microscope slides by the Department of Histopathology, King's College Hospital NHS Foundation Trust (KCHFT).

2.3 Reagents

2.3.1 General Chemicals, Consumables and Kits

A list of consumables and manufacturers is provided in Table 2-1.

Table 2-1 General chemicals, consumables and kits

Consumable	Manufacturer
0.1M Dithiothreitol (DTT)	Invitrogen
0.5% Triton	Sigma
10nM dNTP Mix	Invitrogen
10X AccuPrime™ PCR Buffer I (600mM Tris-SO4 (pH 8.9), 180mM (NH4)2SO4, 20mM MgSO4, 2mM dGTP, 2mM dATP, 2mM dTTP, 2mm dCCT, thermostable AccuPrime™ protein and 10% glycerol),	Invitrogen
5% Donkey Serum	Stratech
5X DNA Loading Buffer Blue (bromophenol blue)	Bioline
5X VILO™ Reaction Mix (random primers, MgCl2 and dNTPs in a proprietary buffer formulation), 10X SuperScript® enzyme mix	Invitrogen
7-Amino-Actinomycin (7-AAD)	BD Biosciences

AccuPrime™ Taq DNA Polymerase High Fidelity	Invitrogen
AccuPrime™ Taq DNA Polymerase High Fidelity	Invitrogen
Agarose	Bioline
Annexin V – FITC	BD Biosciences
Annexin V Binding Buffer	BD Biosciences
BD Cytofix/Cytoperm™	BD Biosciences
BD GolgiPlug™	BD Biosciences
BD Perm/Wash Buffer™	BD Biosciences
BD™ CompBeads Anti-Mouse Igk	BD Biosciences
BD™ CompBeads Negative Control	BD Biosciences
Boric Acid	Sigma
Buffer PE (10mM TrisCl, pH 8.5)	Qiagen
Buffer QG (5.5 M guanidine thiocyanate; 20 mM Tris HCl pH 6.6.)	Qiagen
cDNA Buffer (250mM Tris acetate (ph 8.4), 375mM potassium acetate, 40mM magnesium acetate and stabilizer),	Invitrogen
cDNA Synthesis mix	Invitrogen
DAPI	Sigma
DEPC Treated Water	Invitrogen
Dimethyl Sulphoxide (DMSO)	Sigma
Dulbecco's Modified Eagle Medium	Sigma
Dynabeads® Human T-Activator CD3/CD28	Thermo Fisher Scientific
EasyLadder I	Bioline
Ethanol	Fisher Scientific
Ethidium Bromide	Invitrogen
Fixable Viability Dye eFluor® 780	eBioscience
Foetal Calf Serum (FCS)	Sigma
Formamide	Promega

Foxp3 Fixation/Permeabilisation Working Solution	eBioscience
Heparin	Leo Laboratories
Histopaque 1077	Sigma Aldrich
HyperLadder I	Bioline
HyperLadder V	Bioline
ILS-600 (Internal Lane Standard 600)	Promega
L-Glutamine	Sigma
MgSO4 (50mM)	Invitrogen
MinElute Gel Extraction Kit	Qiagen
PEG 8000	Sigma
Penicillin	Sigma
Permeabilisation Buffer	eBioscience
Phase Lock Gel Heavy	5 Prime
Phosphate Buffered Saline (PBS)	Sigma
ProLong® Gold Antifade Reagent	Invitrogen
Random Hexamers (50ng/µl)	Invitrogen
Red Cell Lysis Buffer	eBioscience
RNase H	Invitrogen
RNaseOUT™	Invitrogen
RNeasy® Mini Kit	Qiagen
RPE Buffer	Qiagen
RPMI 1640	Gibco
RW1 Buffer (2.5-10% guanidine thiocyanate, 2.5-10% ethanol)	Qiagen
Streptomycin	Sigma
SuperScript® VILO™ cDNA Synthesis Kit	Invitrogen
ThermoScript™	Invitrogen
Tris Base	Sigma

Trisodium Citrate	Sigma
TRIzol	Invitrogen
Trypan Blue	Fluka Analytical
Tween-20	Sigma
Xylene	Fisher Scientific

2.4 Media / Buffers / Solutions

2.4.1 Phosphate Buffered Saline (PBS)

1 PBS tablet (Sigma) (phosphate buffer, 0.02% (w/v) potassium chloride, 0.8% (w/v) sodium chloride) was dissolved per 200ml of deionised H_2O. PBS was autoclaved prior to storage.

2.4.2 TBE

For 1 litre of 5X stock solution. 54g of Tris base (Sigma), 27.5g of boric acid (Sigma) and 20mls of 0.5M EDTA (pH 8.0) was made up to 1 litre with H_2O.

2.4.3 Citrate Buffer

0.001M citrate buffer was made with 2.94g of trisodium citrate (Sigma) dissolved in 150µl HCL (Fisher Scientific), 1 litre of distilled H_2O and 0.5ml Tween 20 (Sigma) to pH 6.1.

2.4.4 Paraformaldehyde Fixation Buffer (4%)

0.375g paraformaldehyde (Sigma) was dissolved in 1ml distilled water with 10µl 10M KOH in a boiling water bath and diluted in 4mls distilled water and 5mls x2 PHEMS buffer.

2.4.5 CLL Media

1 litre RPMI 1640 + L-glutamine (Sigma) + 100 IU heparin (Leo Laboratories) + 5% FCS (Sigma)

2.4.6 Jurkat Culture Media

1 litre RPMI 1640 + 10% FCS + 100µg/ml penicillin + 100µg/ml streptomycin.

2.5 Cell Culture

2.5.1 CLL PBMC Culture

Frozen cryovials were thawed as in 2.2.4. PBMCs were resuspended at a density of $2x10^6$ cells/ml in CLL media. Cells were incubated in a 5% CO_2 37°C humidified incubator.

For T-cell stimulation experiments cells were cultured in 24 well plates at $1x10^6$ cells per well, resuspended in 500µl of CLL media.

2.5.2 Jurkat Cell Culture

Frozen cryovials were thawed as in 2.2.4. Cells were resuspended in Jurkat media at 1×10^5/ml. 5mls was transferred to a 25ml tissue culture flask (Sigma). Cells were cultured at 5% CO_2 at 37°C in a humidified incubator. The cell culture was split in fresh media every 2 days or when cells $>1 \times 10^6$/ml.

2.6 Antibodies

2.6.1 Flow Cytometry Antibodies

The flow cytometry antibodies and their dilutions are detailed in Table 2-2.

Table 2-2 Flow cytometry antibodies

Antigen	Clone	Conjugation	Volume	Company
CD3	SP34-2	APC-Cy7®	2.5µl	BD Biosciences
CD3	UCHT1	APC-Alexa Fluor® 750	10µl	eBioscience
CD3	UCHT1	V500	5µl	BD Biosciences
CD4	RPA-T4	PE	10µl	AbD Serotec
CD4	RPA-T4	PerCp-Cy5.5	2.5µl	eBioscience
CD5	UCHT2	Pe-Cy7	10µl	BioLegend
CD5	MF7-14.5	APC	5µl	AbD Serotec
CD8	SK1	PE	10µl	BD Biosciences
CD8	OKT8	Pacific Blue™	10µl	eBioscience
CD8	OKT8	eFluor® 450	2.5µl	eBioscience
CD19	SJ25-C1	Pacific Blue™	2.5µl	Invitrogen
CD19	HIB19	eFluor® 450	2.5µl	eBioscience
CD25	BC96	PE	2.5µl	eBioscience
CD25	MEM-181	FITC	5µl	AbD Serotec
CD28	CD28.2	APC	10µl	eBioscience
CD38	HB7	PE	2.5µl	eBioscience
CD45RA	H100	Biotin	1µl	eBioscience
CD49d	44H6	FITC	5µl	AbD Serotec
CD49d	44H6	Biotin	5µl	AbD Serotec
CD62L	DREG-56	APC-Alexa Fluor® 750	10µl	eBioscience
CD68	eBioY1/82A	Biotin	1µl	eBioscience
CD69	FN50	PE	10µl	BioLegend
CD80	2D10	FITC	10µl	BioLegend
CD80	2D10	PE	10µl	BioLegend
CD86	IT2.2	APC	10µl	BioLegend
CD86	IT2.2	PE	10µl	BioLegend
CD127 (IL-7Ra)	eBioRDR5	FITC	2.5µl	eBioscience
CD152 (CTLA-4)	14D3	Biotin	1µl	eBioscience
CD154 (CD40L)	24-31	PE	10µl	eBioscience
CD185 (CXCR5)	51505	Biotin	5µl	R&D Systems
CD197 (CCR7)	3D12	PE	10µl	eBioscience
CD273 (PD-L2)	MIH18	PE	10µl	BD Biosciences
CD274 (PD-L1)	MIH1	FITC	10µl	BD Biosciences
CD279 (PD-1)	MIH4	Alexa Fluor® 647	5µl	AbD Serotec
Foxp3	PCH101	APC	2.5µl	eBioscience
Streptavidin	N/A	FITC	2.5µl	eBioscience
Streptavidin	N/A	PE-Cy7	1µl	eBioscience

2.6.2 Indirect Immunofluorescence Antibodies

Primary antibodies for immunofluorescence microscopy are shown in Table 2-3. Secondary fluorescently conjugated antibodies for immunofluorescence microscopy in Table 2-4.

Table 2-3 Primary antibodies for immunofluorescence microscopy

Antigen	Species	Clone	Dilution	Manufacturer
CD3	Rabbit	Polyclonal IgG	1 in 40	Abcam
CD4	Mouse	IgG1: 4B12	1 in 10	Novocastra
CD4	Rabbit	Polyclonal IgG	1 in 40	Abcam
CD5	Mouse	Monoclonal IgG	1 in 40	Abcam
CD8	Mouse	IgG3: FK18	1 in 30	Thermoscientific
CD23	Goat	Polyclonal IgG	1 in 30	R&D Systems
CD38	Mouse	IgG1	1 in 100	AbD Serotec
CD49d	Rabbit	Polyclonal IgG	1 in 40	AbD Serotec
CD79a	Goat	Polyclonal IgG	1 in 40	Santa Cruz
Ki67	Mouse	IgG1: MM1	1 in 100	Novocastra
Ki67	Rabbit	Polyclonal IgG	1 in 100	Abcam
PD-1	Goat	Polyclonal IgG	1 in 30	R&D Systems
CXCR5	Rat	IgG2: RF8B2	1 in 40	BD Biosciences

Table 2-4 Secondary fluorescently conjugated antibodies for immunofluorescence microscopy

Target	Species	Conjugate	Dilution	Manufacturer
Goat IgG (H+L)	Donkey	Cy™5	1 in 100	Jackson ImmunoResearch
Goat IgG (H+L)	Donkey	FITC	1 in 100	Jackson ImmunoResearch
Mouse IgG (H+L)	Donkey	Cy™3	1 in 100	Jackson ImmunoResearch
Mouse IgG (H+L)	Donkey	DyLight™ 488	1 in 100	Jackson ImmunoResearch
Mouse IgG (H+L)	Donkey	Alexa Fluor® 555	1in 100	Invitrogen
Rabbit IgG (H+L)	Donkey	FITC	1 in 50	Jackson ImmunoResearch
Rabbit IgG (H+L)	Donkey	Cy™3	1 in 100	Jackson ImmunoResearch
Rabbit IgG (H+L)	Donkey	Cy™5	1 in 100	Jackson ImmunoResearch
Rat IgG (H+L)	Donkey	FITC	1 in 50	Jackson ImmunoResearch
Rat IgG (H+L)	Donkey	DyLight™ 549	1 in 100	Jackson ImmunoResearch
Rat IgG (H+L)	Donkey	AMCA	1 in 100	Jackson ImmunoResearch

2.7 Flow Cytometry

2.7.1 Staining Cell Surface Antigens for Flow Cytometry

100µl LN FNA, whole PB or PBMCs were aliquoted into the required 12x75mm round bottom test tubes (BD Falcon, BD Biosciences). Directly conjugated +/- biotinylated antibodies were added at appropriate titrated volume as outlined in Table 2-2. Cells were incubated with the required antibodies for 20-30 minutes at 4°C in the dark. Following this 2mls of ammonium chloride 1X red cell lysis buffer (eBioscience) was added to appropriate tubes and the sample incubated at 4°C for 30 minutes in the dark. Cells were then centrifuged at 200g for 5 minutes at 4°C and washed twice in PBS. If all samples used directly conjugated antibodies, the cells were resuspended in PBS for analysis on BD FACSCanto II. For biotinylated antibodies the appropriate streptavidin-conjugate was added and incubated for a further 10-20 minutes at 4°C in the dark. The cells were then pelleted at 200g for 5 minutes at 4°C and then washed twice in PBS prior to resuspension for analysis.

2.7.2 Foxp3 Intracellular Cell Staining Protocol

Cells were stained for surface antigens according to the staining cell surface antigens protocol above. Following the last wash 1ml of 1X Foxp3 Fixation/Permeabilisation working solution (eBioscience) was added to appropriate tubes and the sample incubated at 4°C for 30 minutes in the dark. The 1X permeabilisation buffer (eBioscience) was added to each tube. Tubes were centrifuged at 200g for 5 minutes at room temperature (RT). The cell pellet was resuspended in 100µl 1X permeabilisation buffer and the directly conjugated antibody added at appropriate volume. The tube was again incubated in the dark at RT for 30 minutes. The cells were then washed and pelleted twice in 1X Permeabilisation buffer and centrifuged at 200g for 5 minutes at RT. The final cell pellet was resuspended in PBS for analysis on the BD FACSCanto II.

2.7.3 Intracellular Cytokine Staining Protocol

Cells were washed twice and resuspended in PBS. 1µl fixable viability dye was added and cells were incubated for 10 minutes at RT. Cells were washed twice and then stained for cell surface antigens as described. Following the last wash cells were resuspended in 250µl BD Cytofix/Cytoperm™ fixation buffer (BD Biosciences) for 20 mins at 4°C. 1ml BD Perm/Wash buffer (x10 perm wash diluted in distilled water) was added and left for 15 min in the dark. Cells were then washed and resuspended in 50µl Perm/Wash buffer. Intracellular antibodies were added at the appropriate volume and incubated for 20 minutes at RT in the dark. Then cells were washed twice in 1ml BD Perm/Wash and resuspended for flow cytometry.

2.7.4 Flow Cytometry Viability Assay

Cell viability was assessed by flow cytometry using Annexin V, conjugated to FITC and 7-AAD (BD Biosciences). Annexin V binds to phosphatidyl serine which moves from the intracellular to extracellular leaflet early in apoptosis. 7-AAD is a DNA dye and therefore binds when the cytoplasm is compromised later in apoptosis. 100µl of Annexin V binding buffer was added to the cells of interest with 2.5µl Annexin V +/- 1µl 7-AAD. Samples were incubated for 15 minutes in the dark. 400µl Annexin V binding buffer is then added prior to analysis by flow cytometry.

For the intracellular cytokine staining panels a viability dye was used to ensure the integrity of the cells under investigation. Fixable viability dye eFluor® 780 (eBioscience) is a viability dye that irreversibly labels dead cells. Unlike 7-AAD, cells can then go on to be washed, fixed, permeabilised, and stained for intracellular antigens.

2.7.5 Compensation Matrix

Either cells or compensation beads were used to create the compensation matrix. The staining protocol was as follows. The beads were vortexed and 60μl of positive and 60μl of negative beads added to each tube. The required volume of antibody was added and the tube incubated at RT for 30 minutes in the dark. The beads were washed in PBS and then centrifuged at 200g for 10 minutes twice. The singly stained beads were then resuspended in PBS and analysed on the BD FACSCanto II to create a compensation matrix.

2.7.6 BD FACSCanto II (BD Biosciences)

The BD FACSCanto II configuration 4-2-2 has 3 lasers allowing 8 colour flow cytometry. The cytometer is set up as shown in Table 2-5. BD Cytometer Set up and Tracking beads (BD Biosciences) were used to validate the cytometers performance. The beads contain equal concentrations of dim, mid-range and bright fluorescent intensities and are used to determine baseline PMT gains and allow performance quality control.

Table 2-5 FACSCanto II configuration

Lasers	Violet	405nm solid state diode, 30mW fibre power output	
	Argon (Blue)	488nm solid state, 20mW laser output	
	Red	633-nm HeNe, 17Mw laser output	
Fluorescence Detectors	8 PMTs in 4-2-2 configuration		
Laser Dyes	Violet	Pacific Blue AmCyan	455nm 488nm
	Blue	FITC PE PerCP or PerCp-Cy5.5 Pe-Cy7	525nm 575nm 678nm / 695nm 785nm
	Red	APC APC-Cy7	660nm 785nm
Detector Bands	Violet	450/50; 502-525nm	
	Blue	530/30; 585/42; >670; 780/60nm	
	Red	660/20; 780/60 nm	

2.7.7 Flow Cytometry Data and Statistical Analysis

Samples were collected and analysed using FACSDiva software (BD Biosciences) and FlowJo (TreeStar). Percentage positivity and/or mean fluorescence intensity (MFI) values were obtained as appropriate. Statistical analysis was performed using GraphPad Prism® (Graph Pad Inc.). For comparisons to be made between paired samples, first a D'Agostino and Pearson omnibus normality test was performed on the whole sample group and then paired t-tests for those that passed and a Wilcoxon matched pairs test for those that did not. A p-value of <0.05 was considered statistically significant. For unpaired comparisons an un-paired t-test was used and again a p-value of <0.05 was considered statistically significant. Results are expressed +/- standard error of the mean.

Chapter 3 Characterisation of the T-cell Component of the CLL Tumour Microenvironment by Immunophenotyping

3.1 Introduction

It is well described that in CLL the malignant B-cell proliferation occurs primarily within the secondary lymphoid tissues, and not in the PB (Ghia and Caligaris-Cappio 2000, Granziero, Ghia et al. 2001). It is here where the CLL cells are in close contact with T-cells and other elements of the supportive microenvironment (Ghia and Caligaris-Cappio 2005, Patten, Buggins et al. 2008) . As outlined in the introductory chapter, PB CLL cells die rapidly when cultured alone *in vitro*, but they can be rescued from apoptosis when co-cultured with cells or cytokines found from within the microenvironmental niche (Collins, Verschuer et al. 1989, Ghia, Circosta et al. 2005). Studies of the T-cell component in CLL have been performed almost exclusively on T-cells derived from the PB and not the actual T-cells that are in close contact with the proliferating cells. It is well described that T-cells from CLL PB show numerous quantitative and qualitative abnormalities with many phenotypic and functional perturbations from T-cells form age matched normals. These have been reviewed in detail in the introductory chapter. Such studies have many, potentially major, limitations and one specific question that has never been answered is: are the CLL PB T-cells the same population of T-cells that are found within the lymph node? It could be speculated T-cells within the lymph node are the CLL specific population, and may be quite different from the PB, or that only a proportion of these T-cells are present in the PB. The aim of this chapter is to phenotype the T-cell component of the lymph node microenvironment and to compare them to the PB T-cells of the same patient taken at the same time using multi-parameter flow cytometry. This will ascertain whether the T-cell populations from these two compartments are phenotypically similar or have a different profile.

3.1.1 Experimental Approach

The first hurdle is to obtain T-cells from the lymph node. The limited work that has been performed to date on this compartment is mainly on surgical lymph node biopsy specimens and this has some specific limitations (Swerdlow, Murray et al. 1984, Schmid and Isaacson 1994, Patten, Buggins et al. 2008). The patients who undergo lymph node biopsies in CLL are by definition a select group. CLL can usually be diagnosed from the PB and this obviates the need for removing lymph node tissue to make a diagnosis. Routinely a lymph node biopsy adds little or nothing that would influence the treatment pathway for an individual patient and therefore is rarely performed. When lymph node biopsies are performed for diagnostic purposes there are usually in specific and unusual circumstances; such when there is lymphadenopathy which is "out of proportion" compared to the PB picture or when there is a solitary large node and a high grade transformation needs to be excluded. Almost exclusively these highly selected patients are of an advanced stage disease and usual require immediate therapy, therefore it can be seen that this group do not reflect the heterogeneity of the CLL population as a whole. In order to address this issue a study could be undertaken where lymph nodes are surgically resected, for research purposes, on an unselected group of CLL patients. The LN in this scenario would have to be disaggregated to allow multiparameter flow cytometry; this process in itself may change the phenotype of the cells of interest. Indeed the most significant limitations remain as the potential ethical and financial barriers of a patient undergoing a surgical procedure solely for research purposes. We therefore decided not to pursue this approach. An alternative and much less invasive method of obtaining cells from a lymph node uses the technique of lymph node fine needle aspiration (LN FNA). This overcomes the problem of patient selection as any CLL patient with an enlarged LN could undergo the procedure. The cells would be fresh, unfixed and potentially could be cell sorted by flow cytometry. The advantages and disadvantages of the source material are outlined in Table 3-1.

Table 3-1 Lymph node source material

T-cell source	Advantages	Disadvantages
Fresh Lymph Node (Disaggregated)	Unfixed tissue Large cell numbers Ability to sort T-cells Matched PB	Very low availability Highly selected population No normal controls Sample processing required
FNA Lymph Node	Better Availability Unfixed tissue Unselected population Ability to sort T-cells Matched PB	Small cell numbers Difficult to extract RNA No normal controls

Initially we embarked on a study to assess the feasibility of performing LN FNA to access and investigate the T-cell component of the lymph node microenvironment. This is a novel approach to obtaining cells from the tumour microenvironment in CLL, which to our knowledge has not been previously reported in the literature. We first undertook a pilot study of settling small numbers of cells onto poly-L-lysine coated slides and then analysing cell types by immunofluorescence microscopy and whilst this was feasible, as will be outlined in chapter 4, the method was considered superfluous when it became evident that sufficient cells would be available to use the more powerful technique of flow cytometry. Another method we considered was to perform a LN FNA cytospin and to then embed the sample in paraffin for sectioning and analysis however this had no advantage over flow cytometry and was not pursued.

3.1.2 Principles of Multiparameter Flow Cytometry

Flow cytometry allows the identification of cells according to their light scatter and by the surface labelling of known antigens on the cell surface with specific antibodies conjugated to a known fluorochrome (Hulett, Bonner et al. 1973). The fundamental principles of the process can be broken down into fluidics, optics, detection and signal processing. The fluidics system takes up the sample into a central channel, which is surrounded by an outer sheath containing fluid moving at a much faster velocity. The velocity differentials allow cells to move though the chamber in single file, this is called hydrodynamic focusing. Each cell is then interrogated by a beam of light or a laser. Light that is scattered forward (forward scatter channel; FSC) gives

information about the cells size. Light scattered sideways (side scatter channel; SSC) gives information regarding the cells granularity. When a cell is labelled with a fluorochrome the light properties of that specific fluorochrome can be exploited. The fluorochrome is excited by a known specific wavelength and then emits light predictably at another known longer wavelength; the excitation and emission spectra. A flow cytometer can be installed with one or several lasers that emit at a known wavelength, to excite a wide variety of fluorochromes in a predictable way. The flow cytometer then detects the signals with a photomultiplier tube (PMT). The detection specificity is controlled by optical filters/dichroic mirror; this allows specified wavelengths of light to pass through to the sample and then another back to the detector. When the emitted light hits a photodetector a small current is generated, with a voltage proportional to the number of photons received by the detector. This can then be graphically represented as a histogram. Detailed post acquisition analysis can then be performed using proprietary software, such FACSDiva (BD Biosciences) or FlowJo (TreeStar).

3.1.2.1 Flow Cytometry Compensation

Appropriate selection of fluorochrome combinations is critical in the design of multiparameter flow cytometry panels (Mahnke and Roederer 2007). The most crucial element to take into consideration when performing multi-colour fluorescence immunophenotyping is spectral overlap (Kalina, Flores-Montero et al. 2012). When a fluorochrome is excited the emission spectra may be detected not only in the primary channel but also by the other detectors, or secondary channels (Baumgarth and Roederer 2000). If not taken into account, this "spillover" would lead to a false positive signal. An example of commonly used fluorochromes excitation and emission spectra and spectral overlap is shown in Figure 3-1.
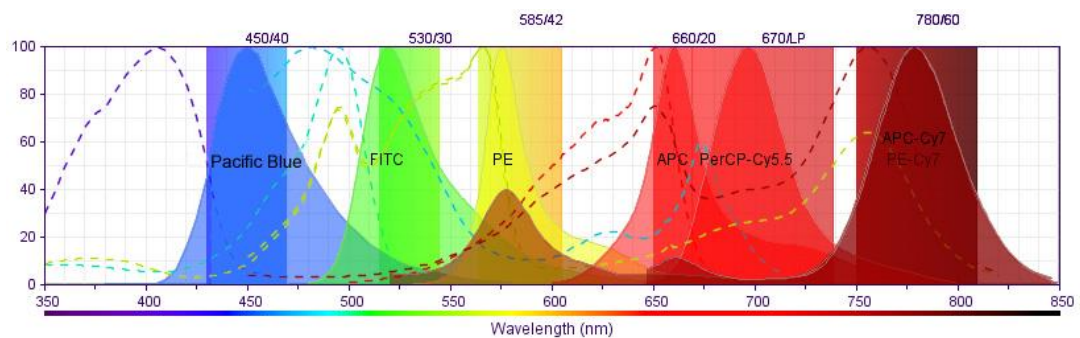
Figure 3-1 Fluorochrome spectral overlaps (Ref: BD Biosciences)

Ideally when choosing fluorochrome combinations for an experiment they would be well apart on the light spectrum and this can be achieved with 2 or 3 colour cytometry. However, in reality, multi-colour experiments give far more powerful data and are thus more commonly undertaken, so overlap is inevitable. Fluorescence compensation applies a mathematical algorithm which calculates how much fluorescence detected in a channel is from the desired fluorochrome and how much is detection is as a result of emission from another unrelated fluorochrome (Tung, Parks et al. 2004). This calculation is possible because the spillover is predictable and therefore can be subtracted after acquisition. The compensation matrix depends on the fluorochrome used, the filters and mirrors of the cytometer, the intensity of the measured signal and the PMT voltages (Kalina, Flores-Montero et al. 2012). Correct compensation is crucial and incorrect compensation, both over- and under- compensation can lead to dramatic errors in results interpretation (Roederer 2001). Compensation is more open to errors when using tandem dyes where one fluorochrome is excited and then transfers the energy across to the coupled dye by fluorescence resonance energy transfer (FRET) as there is more variable spillover (Kalina, Flores-Montero et al. 2012).

3.1.2.2 Designing Multiparameter Flow Cytometry Panels

When designing multi-colour immunophenotyping cytometry panels consideration must be made to the fluorochrome, the cytometer, the antibody and the starting material (Kalina, Flores-Montero et al. 2012). These are summarised in Table 3-2.

Table 3-2 Considerations when designing multiparameter flow cytometry panels

Fluorochrome (Maecker, Frey et al. 2004)	Excitation and emission spectra
	Brightness
	Spillover
	Stability
Cytometer Configuration (Baumgarth and Roederer 2000)	Lasers
	Detectors
	Filters
Antibody (McLaughlin, Baumgarth et al. 2008)	Availability of clones
Starting Material (Wood 2006)	Sample type
	Cell of interest
	Expected antigen expression levels

3.1.3 Multiparameter Flow Cytometry of Lymph Node Fine Needle Aspirates

Immunophenotyping of LN FNA samples has been extensively used by many institutions for the diagnosis of lymphoproliferative disorders and although not universally adopted, it has been validated by many centres, who have found high sensitivity and specificity allowing for identification of the neoplastic clone (Jeffers, Milton et al. 1998, Young, Al-Saleem et al. 1998, Ravinsky, Morales et al. 1999, Meda, Buss et al. 2000, Nicol, Silberman et al. 2000, Sandhaus 2000, Dong, Harris et al. 2001, Kaleem, White et al. 2001, Liu, Stern et al. 2001, Saboorian and Ashfaq 2001, Gong, Williams et al. 2002, Zeppa, Marino et al. 2004, Bangerter, Brudler et al. 2007, Schmid, Tinguely et al. 2010). However, of note, The British Committee for Standards in Haematology (BSCH) guidance entitled the "Best Practice in Lymphoma Diagnosis and Reporting" recommends that "FNA samples should not normally be used as the sole tissue for diagnosis" (Grade B: evidence level III).

3.2 Aim

The aim of this chapter is first to assess the feasibility of performing LN FNAs to obtain T-cells from the CLL tumour microenvironment for analysis. We then plan to undertake multi-parameter flow cytometry on the cells obtained; which allows for a detailed phenotypic analysis on small numbers of cells. We aim to perform a direct comparisons of the phenotype of PB T-cells with the T-cells derived from the LN of the same patient. We additionally aim to compare the phenotype of PB CLL T-cells with those from age matched normal controls.

3.3 Materials and Methods

3.3.1 Ethics

Ethical approval was obtained to perform LN FNAs on CLL patients for research purposes from the research ethics committee REC: 09/H0805/5. PB was collected from patients under national research ethics NREC: 08/H0906/94 and healthy controls under LREC: 02-044. Written informed consent was gained according to the Declaration of Helsinki, 2008.

3.3.2 Primary Patient Material

3.3.2.1 PB Sample Collection

Patients with a diagnosis of CLL and an easily palpable lymph node were invited to take part in the study. Healthy controls were invited to take part in the control arm of the study. They were given a patient information sheet and given adequate time to consider their entry into the study. Written consent was obtained and samples pseudo-anonymised. PB was collected from CLL patients and healthy controls directly into CLL media.

3.3.2.2 LN FNA Sample Collection

CLL patients consenting to the study underwent a LN FNA. The LN FNA was performed by a trained clinician using a 23 gauge needle attached to 10ml syringe. The sample was aspirated and the needle was washed directly into CLL media. This was repeated on average 4 times per patient. The LN FNA was sample centrifuged at 200g for 5 minutes and resuspended in CLL media to a final volume depending on the cell count.

3.3.3 Flow Cytometry Panels

As described the appropriate selection of fluorochrome combinations is critical in the design of multiparameter flow cytometry panels (Mahnke and Roederer 2007). The following panels were developed for the work presented here.

Panel A: T-cell Stimulation and Immune Checkpoint Inhibition.

Fluorochrome	FITC	PE	PerCP-Cy5	Pe-Cy7	APC	APC-Cy7	Pacific Blue
Antigen	CD25	CD40L	CD4	CTLA-4	PD-1	CD3	CD8

Panel B: CLL Prognostic Factors.

Fluorochrome	FITC	PE	Pe-Cy7	APC	Pacific Blue
Antigen	CD25	CD38	CD49d	CD5	CD19

Panel C: Cell Viability.

Fluorochrome	FITC	7-AAD	APC	Pacific Blue
Antigen	Annexin V		CD5	CD19

Panel D: T Follicular Helper Cells 1.

Fluorochrome	PerCP-Cy5	Pe-Cy7	APC-Cy7	Pacific Blue
Antigen	CD4	CXCR5	CD3	CD8

Panel E: T Follicular Helper Cells 2.

Fluorochrome	FITC	PerCP-Cy5	APC	Pacific Blue
Antigen	CXCR5	CD4	PD-1	CD8

Panel F: T Follicular Helper Cells 3.

Fluorochrome	FITC	PerCP-Cy5	APC-Cy7	Pacific Blue
Antigen	CXCR5	CD4	CD3	CD8

Panel G: T-cell Memory Subsets 1.

Fluorochrome	FITC	PE	PerCP-Cy5	Pe-Cy7	APC	APC-Cy7	Pacific Blue
Antigen	CD25	CCR7	CD4	CD45RA	CD28	CD62L	CD8

Panel H: T-cell Memory Subsets 2.

Fluorochrome	FITC	PE	PerCP-Cy5	APC	Pacific Blue
Antigen	CD45RA	CCR7	CD4	CD28	CD8

Panel I: Immune Checkpoint Inhibitors and Ligands 1.

Fluorochrome	FITC	PE	PerCP-Cy5	Pe-Cy7	APC	Pacific Blue
Antigen	PD-L1	CD8	CD4	CD5	PD-1	CD19

Panel J: Immune Checkpoint Inhibitors and Ligands 2.

Fluorochrome	FITC	PE	PerCP-Cy5	Pe-Cy7	APC	Pacific Blue
Antigen	PD-L1	PD-L2	CD4	CD5	PD-1	CD8

Panel K: T Regulatory Cells 1.

Fluorochrome	FITC	PE	PerCP-Cy5	APC	APC-Cy7	Pacific Blue
Antigen	CD127	CD25	CD4	FOXP3	CD3	CD8

Panel L: T Regulatory Cells 2.

Fluorochrome	FITC	PE	PerCP-Cy5	Pacific Blue
Antigen	CD127	CD25	CD4	CD8

3.3.4 Flow Cytometry Antibodies

The flow cytometry antibodies used in this chapter and the volumes per test are detailed in

Table 3-3.

Table 3-3 Flow cytometry antibodies

Antigen	Clone	Conjugation	Volume	Company
CD3	SP34-2	APC-Cy7®	2.5µl	BD Biosciences
CD3	UCHT1	APC-Alexa Fluor® 750	10µl	eBioscience
CD4	RPA-T4	PE	10µl	AbD Serotec
CD4	RPA-T4	PerCp-Cy5.5	2.5µl	eBioscience
CD5	UCHT2	Pe-Cy7	10µl	BioLegend
CD5	MF7-14.5	APC	5µl	AbD Serotec
CD8	SK1	PE	10µl	BD Biosciences
CD8	OKT8	Pacific Blue™	10µl	eBioscience
CD8	OKT8	eFluor® 450	2.5µl	eBioscience
CD19	SJ25-C1	Pacific Blue™	2.5µl	Invitrogen
CD19	HIB19	eFluor® 450	2.5µl	eBioscience
CD25	BC96	PE	2.5µl	eBioscience
CD25	MEM-181	FITC	5µl	AbD Serotec
CD28	CD28.2	APC	10µl	eBioscience
CD38	HB7	PE	2.5µl	eBioscience
CD45	HI30	APC-Alexa Fluor® 750	10µl	eBioscience
CD45RA	H100	Biotin	1µl	eBioscience
CD49d	44H6	FITC	5µl	AbD Serotec
CD49d	44H6	Biotin	5µl	AbD Serotec
CD62L	DREG-56	APC-Alexa Fluor® 750	10µl	eBioscience
CD127 (IL-7Ra)	eBioRDR5	FITC	2.5µl	eBioscience
CD152 (CTLA-4)	14D3	Biotin	1µl	eBioscience
CD154 (CD40L)	24-31	PE	10µl	eBioscience
CD185 (CXCR5)	51505	Biotin	5µl	R&D Systems
CD197 (CCR7)	3D12	PE	10µl	eBioscience
CD273 (PD-L2)	MIH18	PE	10µl	BD Biosciences
CD274 (PD-L1)	MIH1	FITC	10µl	BD Biosciences
CD279 (PD-1)	MIH4	Alexa Fluor® 647	5µl	AbD Serotec
FOXP3	PCH101	APC	2.5µl	eBioscience
Streptavidin	N/A	FITC	2.5µl	eBioscience
Streptavidin	N/A	PE-Cy7	1µl	eBioscience

3.3.5 Staining Cell Surface Antigens for Flow Cytometry

Cells were resuspended in 100µl CLL media and labelled for flow cytometry according to 2.7.1. Directly conjugated +/- biotinylated antibodies were added at appropriate titrated volume as described in Table 3-3 according to the panels outlined in 3.3.3.

3.3.6 Compensation Matrix

Either cells or compensation beads were used to create the compensation matrix. BD™ CompBeads (BD Biosciences) are polystyrene microparticles which are either negative (BD™ CompBeads negative control), and bind nothing, or are anti-mouse Igk (BD™ CompBeads anti-mouse Igk), which will bind any antibody that was raised in a mouse (providing it has an Igk specificity). By this means distinct positive and negative fluorescence can be obtained from the actual fluorochrome used in each experiment to create the compensation matrix. The compensation bead staining protocol is outlined in 2.7.5.

3.3.7 BD FACSCanto II (BD Biosciences)

The BD FACSCanto II configuration 4-2-2 has 3 lasers allowing 8 colour flow cytometry. The cytometer setup is shown in 2.7.6.

3.3.8 Flow Cytometry Data and Statistical Analysis

Samples were collected and analysed using FACSDiva software (BD Biosciences) and FlowJo (TreeStar). Percentage positivity and/or mean fluorescence intensity (MFI) values were obtained as appropriate. Statistical analysis was performed using GraphPad Prism® (Graph Pad Inc.). For comparisons to be made between LN FNA and PB populations, first a D'Agostino and Pearson omnibus normality test was performed on the whole sample group and then paired t-tests for those that passed and a Wilcoxon matched pairs test for those that did not. A p-value of <0.05 was considered statistically significant. For comparison between CLL PB and PB of normal controls an un-paired t-test was used and again a p-value of <0.05 was considered statistically significant. Results are expressed +/- standard error of the mean. Box and whiskers plots show the median and minimum and maximum values.

3.4 Patient Material

3.4.1 Demographics of Patients and Normal Controls

LN FNA and PB sampling was undertaken on 28 patients with a diagnosis of CLL and palpable cervical lymph nodes. The demographics of the patient group are outlined in Table 3-4. An unselected group of serial CLL patients from King's College Hospital Foundation Trust (KCHFT) were invited to take part in the study. Eligibility criteria was a diagnosis of CLL, palpable lymphadenopathy and no treatment within the prior 3 months. Exclusion criteria were anti-coagulated patients, known bleeding disorders and/or evidence of previous or current infection with hepatitis B, C, HIV and/or HTLV-1. Due to the local demographics of CLL patients at KCHFT many patients were excluded due to prior exposure to hepatitis B. This may in part explain the apparent lower incidence of CMV IgG positive individuals as viral infections are often co-existent. PB was additionally sampled from 16 age matched normal controls.

There was no difference in the age of the CLL patients and the normal controls. The median age of patients was 63.5 +/- 11.01 and the median age of controls was 60 +/- 7.90 (p=0.27) see Figure 3-2.
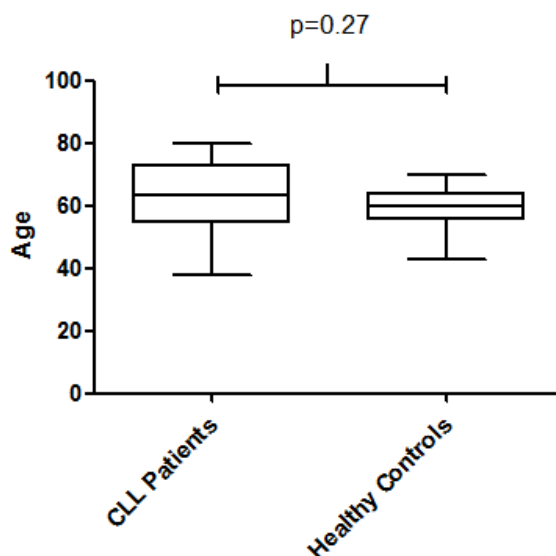
Figure 3-2 CLL patients and healthy control volunteers are age matched
The age of CLL patients (n=28) and healthy controls (n=16) were not statistically different. A D'Agostino and Pearson omnibus normality test was applied prior to un-paired t-test using GraphPad Prism® (Graph Pad Inc.).

Table 3-4 Demographics of CLL patients

Patient Demographics		n = 28	
Age	Years	(38-80)	64
Sex	Male	17	61%
	Female	11	39%
CMV Status	IgG Pos	11	39%
	IgG Neg	15	54%
	Indeterminate	2	7%
Binet Stage	A	10	36%
	B	12	43%
	C	6	21%
Cytogenetics / FISH	Normal	3	11%
	13q-	9	32%
	11q-	3	11%
	17p-	3	11%
	Trisomy 12	4	14%
	Complex	6	21%
CD38 status	<30%	16	57%
	>30%	12	43%
Mutational status	Mutated IGVH <98% homology to germline	5	18%
	Unmutated IGVH >98% homology to germline	20	71%
	Unknown	3	11%

3.5 Results

3.5.1 LN FNA feasibility

A total of 45 LN FNAs were performed on 28 CLL patients. The procedure was well tolerated and was feasible if the palpable lymph node exceeded 1cm. An additional 6 patient samples were unsuitable for processing/analysis; 2 were found to have a high grade transformation, in 2 the total cell count was too low to proceed, in 1 the patient was subsequently found to have co-existing hepatitis infection and in 1 the sample was lost in processing. Cell counting was performed manually using a counting chamber (Hawksley), with trypan blue solution as a viability stain. On average the total cell count was 4.1×10^6 ($1-13 \times 10^6$). Because of the limited number of cells available in a LN FNA, not every panel was performed on every sample.

3.5.2 There is marked T-cell expansion in the PB of CLL patients compared to healthy controls

Initial experiments investigated the T-cell component of CLL PB compared to healthy age matched controls. As a total proportion of PB lymphocytes, the T-cells make up a small percentage in CLL; 3.67% +/- 3.54 (n=15) compared to 75.9% +/- 2.70 in the control population (n=11); p=<0.0001, see Figure 3-3. However the absolute T-cell numbers is statistically much higher in the CLL population compared to normal controls, with the mean total T-lymphocyte count in the CLL group of 4.97×10^9/l +/- 2.16 (n=13) versus 1.47×10^9/l +/-0.57 in the normal controls (n=11), see Figure 3-4. The expansion is in both the CD4 and CD8 compartment. See Figure 3-5 and Figure 3-6. This confirms the findings of many previous studies (Catovsky, Miliani et al. 1974, Herrmann, Lochner et al. 1982, Mills and Cawley 1982, Platsoucas, Galinski et al. 1982, Kimby, Mellstedt et al. 1987, Palmer, Hanson et al. 2008, Gonzalez-Rodriguez, Contesti et al. 2010, Nunes, Wong et al. 2012).

The CD4/CD8 ratio in our CLL patient cohort had a median value of 1.75 +/- 1.982 (n=14), with a wide range (0.59-6.87). The ratio in the normal control group was 2.52 +/- 1.36 (n=11), which was not statistically different from the CLL cohort; p=0.698, see Figure 3-7.

We next investigated whether within the CLL cohort there was a correlation between the CD4/CD8 ratio and the total lymphocyte count, which was not the case; see Figure 3-8.
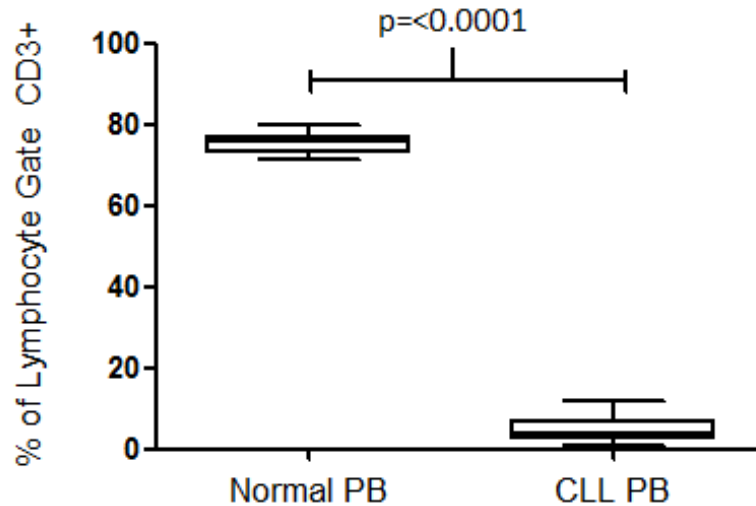
Figure 3-3 Increased percentage of CD3+ T-cells in the lymphocyte gate of normal controls compared to CLL cohort
CD3+ T-cells from the PB of CLL patients (n=15) and normal aged matched controls (n=11) was determined by flow cytometry using the FACSCantoII (BD Biosciences). The lymphocyte gate was based upon the forward and side scatter profile of the sample and then the CD3+ events gated. CD3+ events are presented as a percentage of the lymphocyte gate. Samples were analysed using FACSDiva software (BD Biosciences). A statistical D'Agostino and Pearson omnibus normality test and un-paired t-test was applied using GraphPad Prism® (Graph Pad Inc.). The box and whiskers plots; the box shows the median and 25th to 75th percentile and the whiskers show the minimum to maximum values.
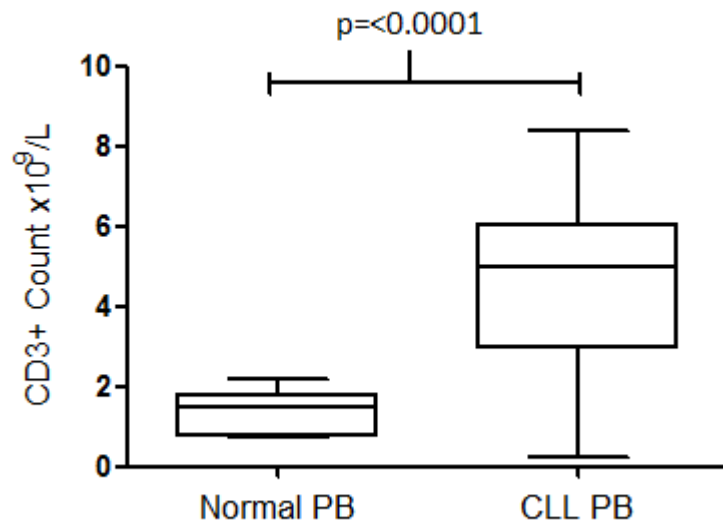
Figure 3-4 Increase in the total CD3+ T-cell count in CLL patients compared to normal controls
The absolute CD3 count was determined from the total lymphocyte count using the ADVIA®
2120i analyzer (Siemens). The total PB CD3+ T-cell count in the CLL cohort (n=13) was
statistically higher than in the normal control cohort (n=11), p=<0.0001.
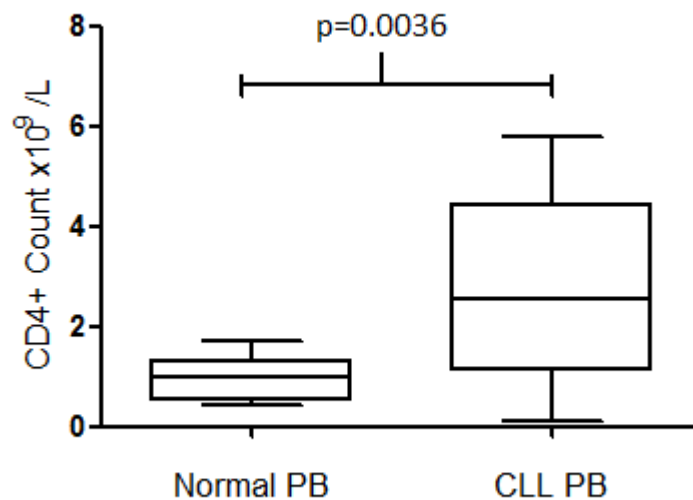
Figure 3-5 The absolute CD4+ count is higher in CLL patients PB than normal controls
The absolute CD4 count was determined from the total lymphocyte count using the ADVIA®
2120i analyzer (Siemens). The total PB CD4+ T-cell count in the CLL cohort (n=13) was
statistically higher than in the normal control cohort (n=11), p=0.0036.
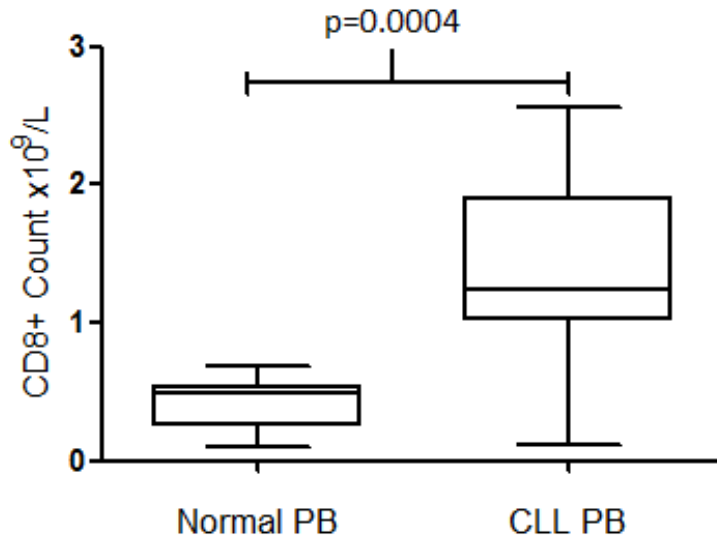
Figure 3-6 There is an expansion in the absolute CD8+ T-cell count in CLL patients compared to normal controls

The absolute CD8 count was determined from the total lymphocyte count using the ADVIA® 2120i analyzer (Siemens). The total PB CD8+ T-cell count in the CLL cohort (n=13) was statistically higher than in the normal control cohort (n=11), p=0.0004.
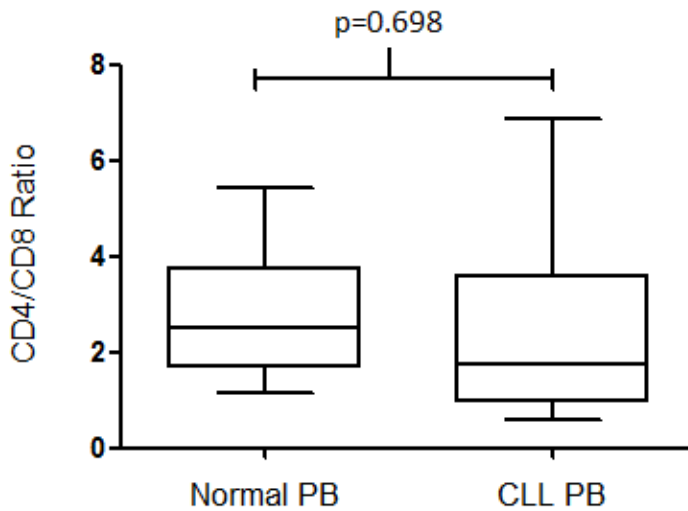
Figure 3-7 There was no difference in PB CD4/CD8 ratio between CLL cohort and healthy controls

PB CD4/CD8 ratios were calculated for normal controls (n=11) and CLL patients (n=14). The median ratio for the cohort of normal controls was 2.52 and for the CLL patients 1.75. There was no difference between the two by an un-paired t-test (p=0.698).
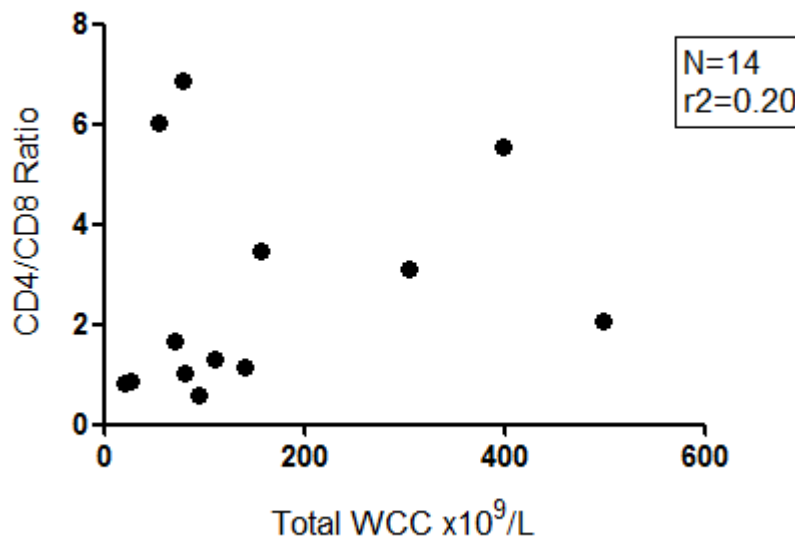
Figure 3-8 There is no correlation between the total WCC and CD4/CD8 ratio in CLL PB
The total WCC was determined using the ADVIA® 2120i analyzer (Siemens). The correlation between the CD4/CD8 ratio and WCC of CLL patients (n=14) was determined by calculating the Pearson correlation coefficient and no correlation was found; Pearson's r=0.2.

3.5.3 CLL LN FNA and PB samples show differences in forward and side scatter reflecting their compartment

Having confirmed the presence of a T-cell expansion in CLL PB, which has been well documented, we next undertook comparative studies of the phenotype of the T-cells taken simultaneously from the PB and LN of CLL patients.

An example forward scatter (FSC) and side scatter (SSC) dot plot from a PB sample is shown in Figure 3-9. There are distinct lymphocyte, monocyte and granulocytic "clouds".
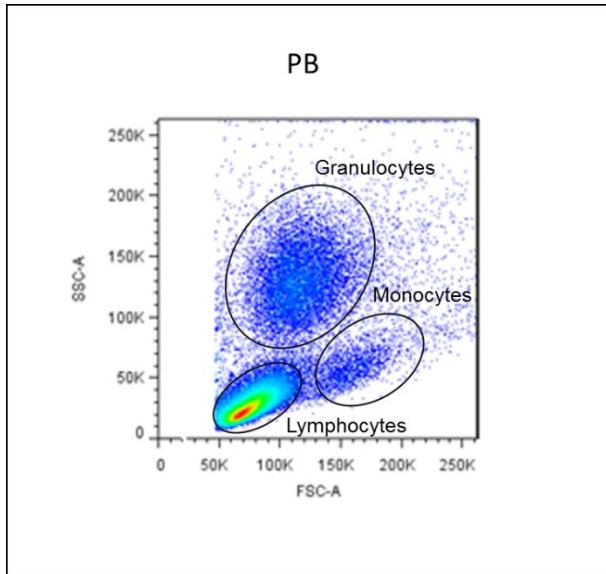
Figure 3-9 Forward and side scatter dot plot of CLL PB
A representative flow cytometry scatter dot plot (FACSDiva) demonstrating the forward (FSC-A) and side scatter (SSC-A) obtained from the PB of a CLL patient. The lymphocyte, monocyte and granulocyte clouds are labelled.

A representative FSC and SSC dot plot of CLL PB and LN FNA sample is shown in Figure 3-10. It can be seen that the scatter plot of the LN FNA lacks the prominent granulocyte and monocyte cloud, giving evidence that the sample is from the LN, which predominately contains lymphocytes.
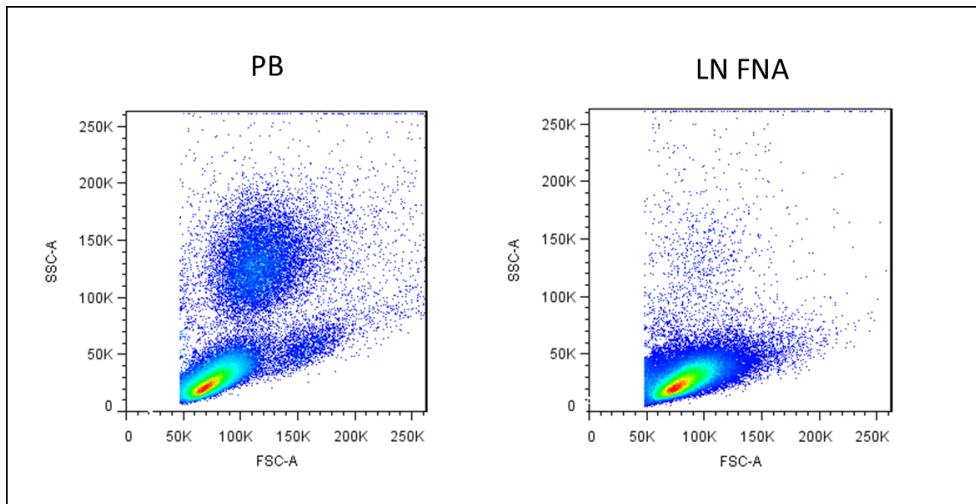
Figure 3-10 Differences in the SSC versus FSC dot plots comparing PB and LN FNA
A representative flow cytometry scatter dot plot demonstrating the forward (FSC-A) and side scatter (SSC-A) obtained from the PB of a CLL patient is shown on the left and on the right the scatter plot obtained from the LN FNA of the same patient. The lack of granulocyte and monocyte cloud can be appreciated in the LN FNA.

3.5.4 There is a higher percentage of CD3+ T-cells in CLL LN FNA samples than the PB

Data from the flow cytometry panels shown in 3.3.3 were used to identify the relative numbers of CD3 (APC-Cy7), CD4 (PerCp-Cy5.5) and CD8 (Pacific Blue) T-cells in the lymphocyte gate of the LN FNA versus PB.

First the CD3+ T-cells were calculated as a percentage of total cells within the lymphocyte gate, see Figure 3-11.
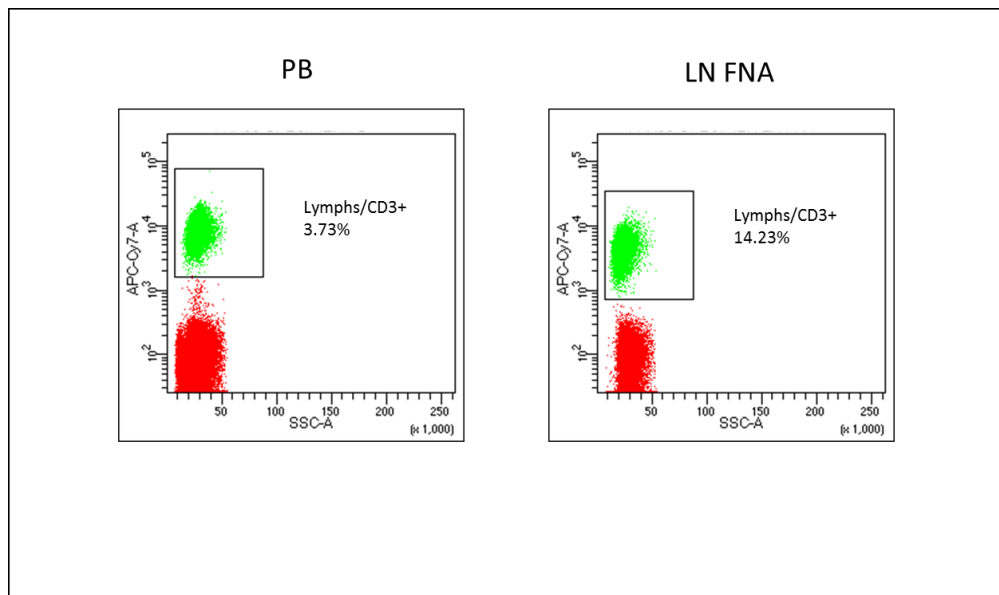
Figure 3-11 Gating of CD3+ T-cells from the lymphocyte gate
Flow cytometry dot plots from PB (left panel) and LN FNA (right panel), from an example CLL patient. The acquisition was gated first on the lymphocyte gate (from the side and forward scatter pattern as described in Figure 3-9) and then on side scatter and CD3+ (APC-CY7). In this example the CD3+ T-cells in the PB account for 3.73% of the lymphocyte gate, and in the LN FNA for 14.23% of the lymphocyte gate.

We found high numbers of CD3+ T-cells within the lymphocyte gate of LN FNAs, which was up to 43% of the total lymphocyte population. This was highly statistically significant compared to the PB, with a mean percentage of CD3+ T-cells in the lymphocyte gate of CLL LN FNAs 17.10% +/- 2.08 compared to 5.51% +/- 1.10 in the PB; p=<0.0001. See Figure 3-12.
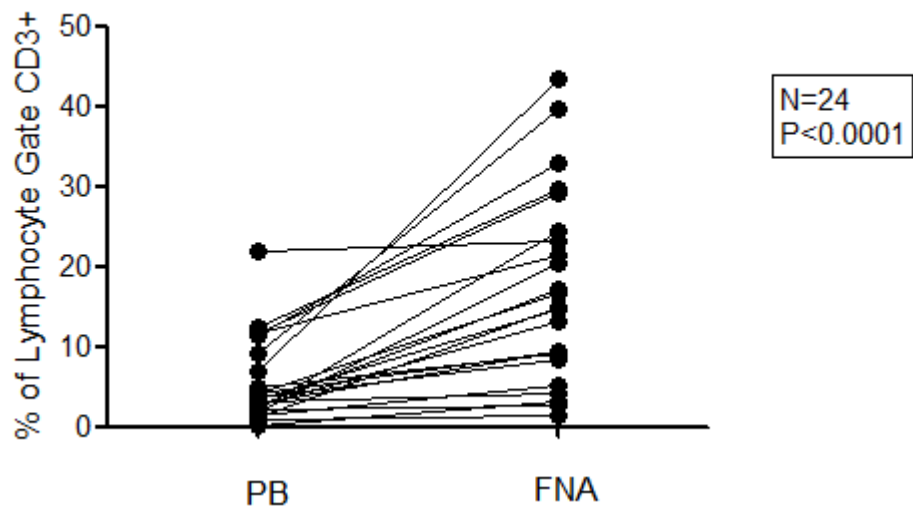
Figure 3-12 The lymphocyte gate contains more CD3+ T-cells in the LN FNA compared to PB
The gating strategy is as described in Figure 3-13. The paired PB and LN FNA data is presented for each CLL patient (n=24). Statistical analysis of all paired PB and LN FNA samples was performed on GraphPad Prism, first with a D'Agostino and Pearson omnibus normality test followed by paired t-test.

3.5.5 The CLL LN FNA has a higher proportion of CD4+ T-cells than the PB

Next we wanted to identify whether these CD3+ T-cells were CD4+ or CD8+. We therefore

gated on the lymphocyte population, CD3+ and then the CD4+ and CD8+ populations. A

typical density flow cytometry dot plot is shown in Figure 3-13.
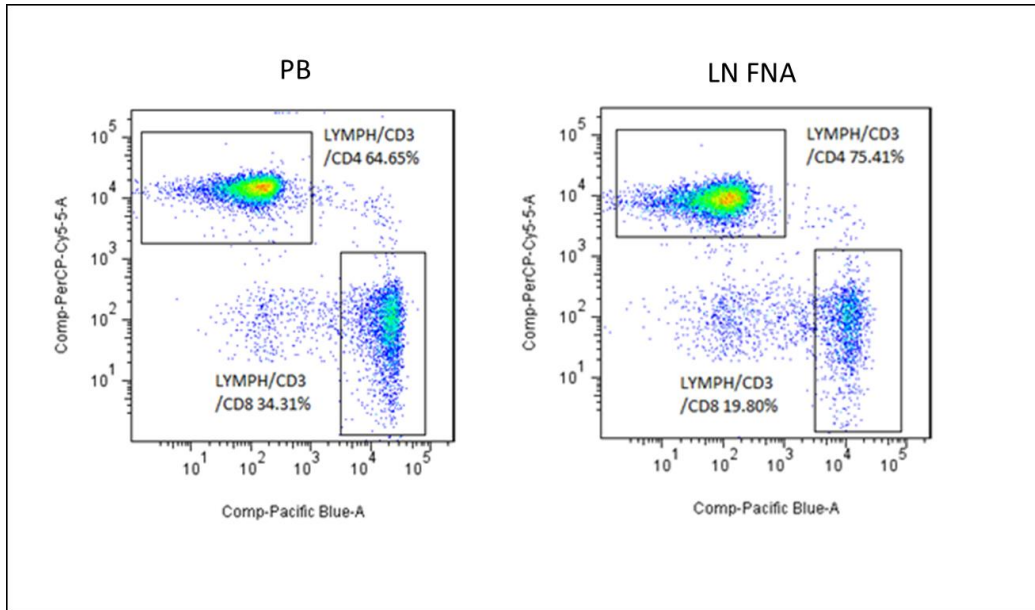
Figure 3-13 Gating strategy for CD4+ and CD8+ T-cells from the CD3+ T-cells in lymphocyte gate

Flow cytometry dot plots from PB (left panel) and LN FNA (right panel), taken from an example CLL patient. The sample was gated first on the lymphocyte gate from the side and forward scatter acquisition plots and then on side scatter and CD3+ (as described in Figure 3-11). This was followed by gating on CD4 (PerCP-Cy5.5) and CD8 (Pacific Blue) subsets. In this example the CD4+ T-cells in the PB account for 64.65% of the CD3+ T-cells, and in the LN FNA for 75.41% of the CD3+ T-cells. Conversely the CD8+ T-cells in the PB account for 34.31% of the CD3+ T-cells and in the LN FNA for 19.80% of the CD3+ T-cells.

We found a much higher percentage of the CD3+ T-cells to be CD4+ in the LN FNA compared to the PB. Within the LN a mean 71.9% +/- 2.08 of the CD3+ cells were CD4+ compared to 60.83% +/- 2.90 in the PB. This was highly statistically significant with a p-value of <0.0001.

See Figure 3-14
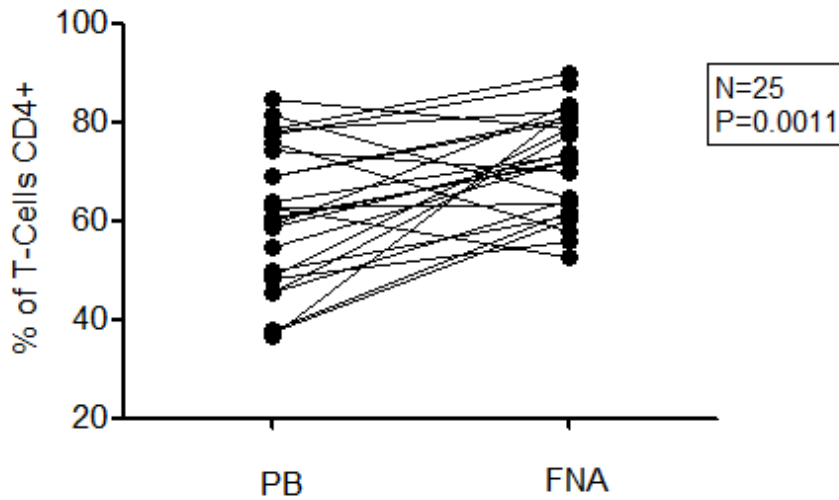
Figure 3-14 CD4+ T-cells were found at relatively higher frequency in the LN FNA compared to PB
The gating strategy is described in Figure 3-13. The paired PB and LN FNA data is presented for each CLL patient (n=25) and statistical analysis as in Figure 3-12.

Conversely, there was a higher proportion of CD8+ cells in the PB compared to the LN; 36.51% +/- 3.07 vs 23.04% +/- 2.08; p=0.0002. See

Figure 3-15.
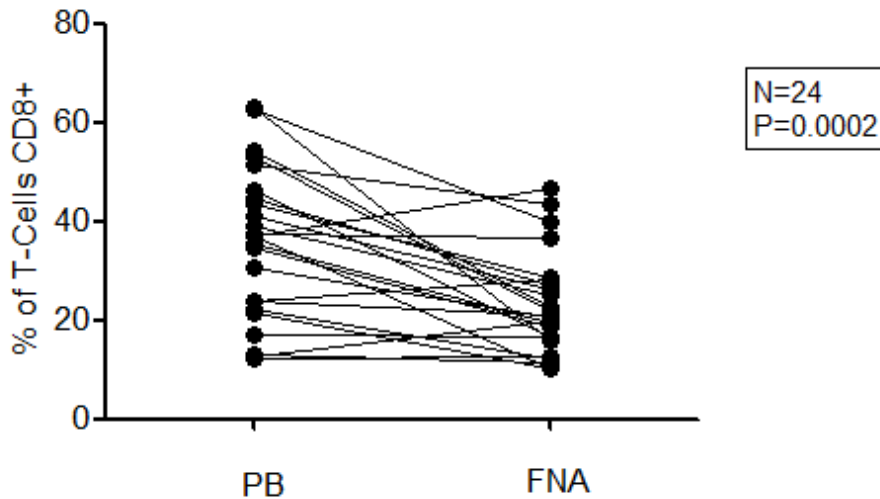
Figure 3-15 CD8+ T-cells were less abundant in lymphocyte gate of the LN FNA compared to PB
The gating strategy is described in Figure 3-13. The paired PB and LN FNA data is presented for each CLL patient (n=24) and statistical analysis as in Figure 3-12.

3.5.6 There is a higher proportion of T-cells in CLL LN FNA compared to PB, biased towards CD4+ effector memory phenotype

Once we established that there is a high proportion of T-cells within the lymphocyte gate of the CLL LN we wanted to investigate their phenotype in more detail. Several groups have reported an increased CD4+ T_{EM} phenotype (CD45RA-/CCR7-) in the PB of CLL patients compared to healthy controls and a relative decrease in naïve T-cells (Motta, Chiarini et al. 2010, Walton, Lydyard et al. 2010, Nunes, Wong et al. 2012). To further delineate the CD4+ phenotype in the CLL LN microenvironment we developed a flow cytometry panel consisting of CD4 (PerCP-Cy5.5), CD8 (Pacific Blue), CD45RA (Pe-Cy7), CD62L (APC-Cy7), CCR7 (PE), CD28 (APC) and CD25 (FITC). This allowed us to differentiate between naïve, T_{EM}, T_{CM}, T_{EMRA} subpopulations. See 3.3.3 Flow Cytometry Panels.

Figure 3-16 shows an example dot plot gating T-cell memory subsets using the following gating strategy: naïve (CD4+/CD45RA+/CCR7+), T_{CM} (CD4+/CD45RA-/CCR7+), T_{EM} (CD4+/CD45RA-/CCR7-), T_{EMRA} (CD4+/CD45RA+/CCR7-).
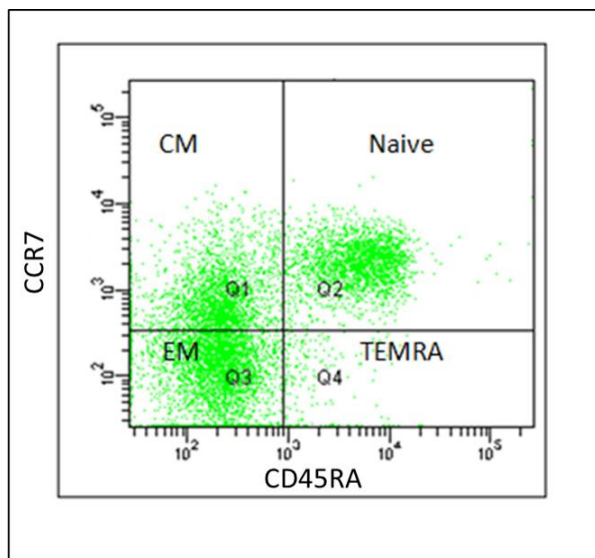
Figure 3-16 Gating strategy for T-cell memory subsets
Flow cytometry dot plots from PB taken from an example CLL patient. The sample was gated first on the lymphocyte gate from the side and forward scatter acquisition plots and then on side scatter, CD3+ followed by CD4 as described in Figure 3-13. CD4+ T-cell memory subsets were then defined according to the expression of CCR7 and CD45RA as follows; naïve (CD4+/CD45RA+/CCR7+), T_{CM} (CD4+/CD45RA-/CCR7+), T_{EM} (CD4+/CD45RA-/CCR7-) and T_{EMRA} (CD4+/CD45RA+/CCR7-).

There was a reduction in the proportion of naïve CD4+ T-cells in the LN compared to PB; LN FNA 9.41% +/- 3.30 vs PB 24.16% +/- 6.10; p=0.002. See Figure 3-17.
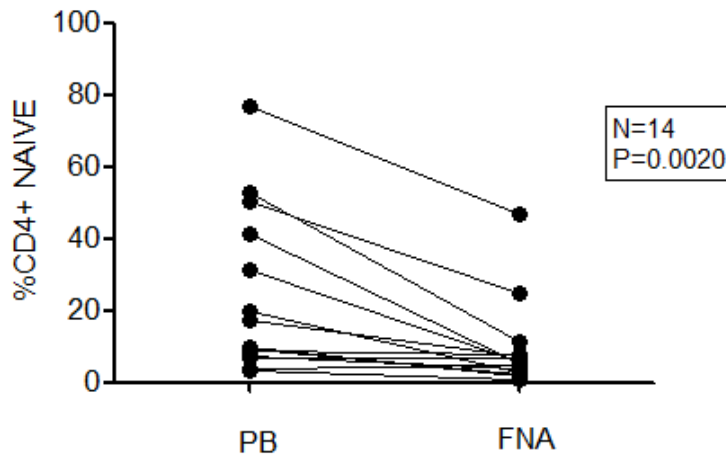
Figure 3-17 There are fewer naïve CD4+ cells in the LN FNA than the PB of the same patient
The gating strategy is as described in Figure 3-16. The paired PB and LN FNA data is presented for each CLL patient (n=14). Statistical analysis as Figure 3-12.

There was also a reduction in the T_{CM} compartment overall in the LN compared to PN; LN FNA 6.79% +/- 3.50 vs PB 11.74% +/- 1.81; p=0.044. See Figure 3-18.
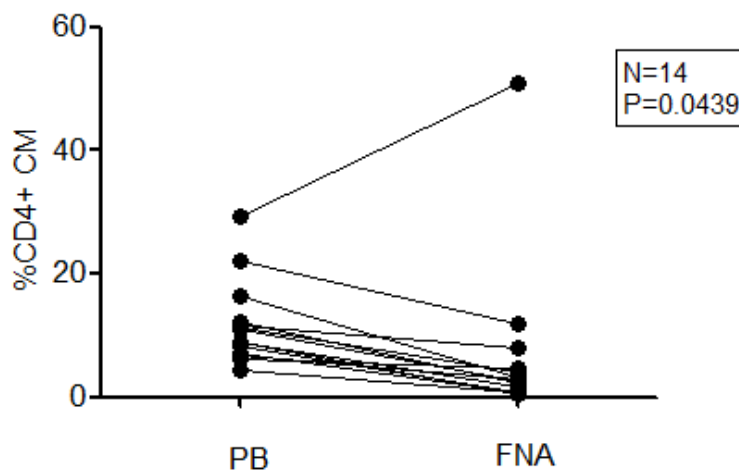
Figure 3-18 There are fewer CD4+ T_{CM} cells in the LN FNA than the PB of the same patient
The gating strategy is as described in Figure 3-16. The paired PB and LN FNA data is presented for each CLL patient (n=14). Statistical analysis as Figure 3-12.

Conversely there was a higher percentage of T$_{EM}$ CD4+ T-cells in the LN compared to PB; LNA FNA 60.35% +/- 4.30 vs PB 48.41 +/- 5.39; p=0.035. See Figure 3-19.
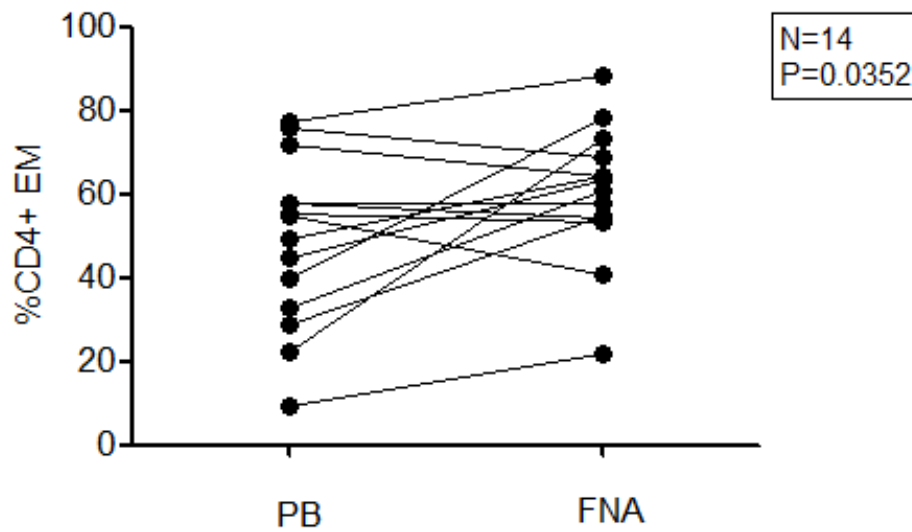
Figure 3-19 There are more CD4+ T$_{EM}$ cells in the LN FNA compared to the PB of the same patient
The gating strategy is as described in Figure 3-16. The paired PB and LN FNA data is presented for each CLL patient (n=14). Statistical analysis as Figure 3-12.

There was also an increased number of T$_{EMRA}$ CD4+ T-cells in the LN compared to PB; LN FNA 23.41% +/- 3.26 vs PB 15.75 +/- 2.77; p=0.022. See Figure 3-20.
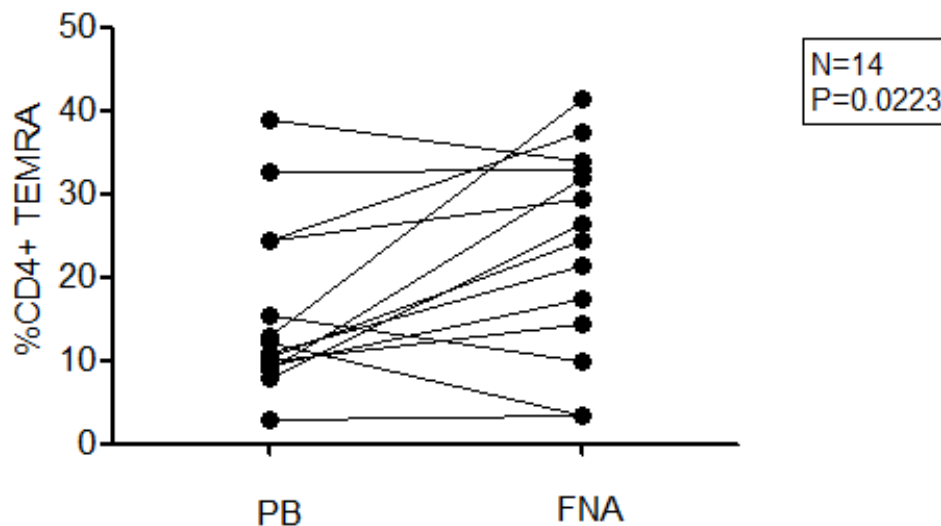
Figure 3-20 There are more CD4+ T$_{EMRA}$ cells in the LN FNA than the PB of the same patients
The gating strategy is as described in Figure 3-16. The paired PB and LN FNA data is presented for each CLL patient (n=14). Statistical analysis as Figure 3-12.

Table 3-5 summarises the results with the mean percentage of CD4+ T-cells that fall into each of these subsets and the differences found between the LN and PB compartments.

Table 3-5 The CD4+ T-cell subsets in CLL PB and LN FNA
Data shows the mean percentage of CD4+ T-cells +/- standard error of the mean that are naïve (CD45RA+/CCR7+), T_{CM} (CD45RA-/CCR7+), T_{EM} (CD45RA-/CCR7-) and T_{EMRA} (CD45RA+/CCR7-). Statistical analysis as in Figure 3-12.

N=14	PB	LN FNA	P Value
Naïve	24.16% +/- 6.10	9.41% +/- 3.30	p=0.002
T_{CM}	11.74% +/- 1.81	6.79% +/- 3.50	p=0.044
T_{EM}	48.41 +/- 5.39	60.35% +/- 4.30	p=0.035
T_{EMRA}	15.75 +/- 2.77	23.41% +/- 3.26	p=0.022

3.5.7 CLL LNs contain relatively higher proportion of Tregs than the PB

After establishing that there were more effector T-cells in the CLL LN FNA than in the PB of the same patient we wanted to look at the Treg subset. Tregs maintain self-tolerance and have a significant role in many cancers. Tregs have been consistently shown to be increased in CLL PB and correlate with advanced stage disease (Beyer, Kochanek et al. 2005, Giannopoulos, Schmitt et al. 2008, Jak, Mous et al. 2009, Weiss, Melchardt et al. 2011, Biancotto, Dagur et al. 2012, D'Arena, D'Auria et al. 2012, Lad, Varma et al. 2013). The initial strategy was to label the cells for Foxp3, which is an intracellular marker. The method is outlined in 2.7.2. This proved to be unfeasible as many more cells were required for the staining controls and as a result this approach substantially limited how many flow cytometric panels could be undertaken on one LN FNA sample. Therefore we switched to a cytoplasmic staining panel where Tregs were defined as CD4+, CD25bright, and CD127dim (Liu, Putnam et al. 2006, Seddiki, Santner-Nanan et al. 2006). This resulted the requirement of many fewer cells and enabled the sample to be effectively split between more panels.

We found that the percentage of the CD4+ T-cells that are Tregs to be significantly increased in the LN compared to the PB; LN FNA 9.51% +/- 1.95 vs PB 5.62% +/- 1.26; p=0.0135. See Figure 3-21
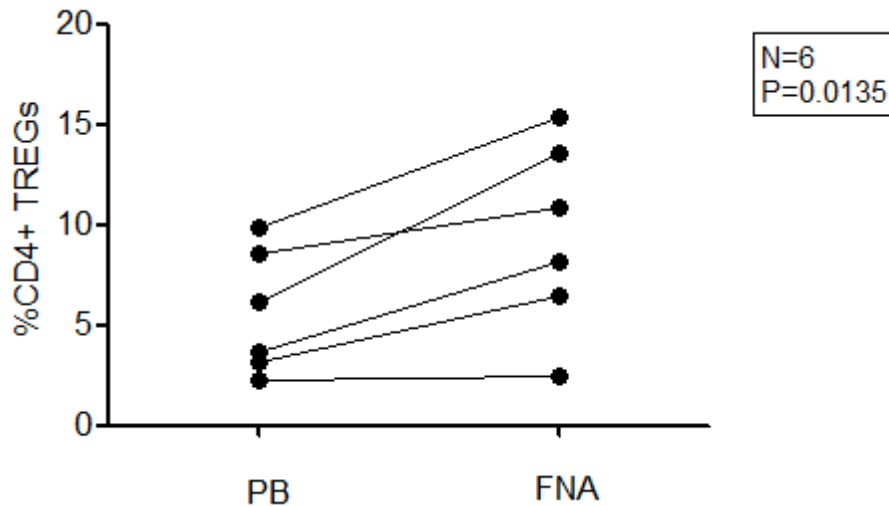
Figure 3-21 There were more Tregs in the CLL LN compared to the PB taken simultaneously The sample was gated on CD4+ T-cells as described in Figure 3-13. Tregs were defined as CD4+/CD25bright/CD127dim. The paired PB and LN FNA data is presented for each CLL patient (n=6). Statistical analysis as Figure 3-12

3.5.8 CLL LN derived T-cells show similar levels of CD25 expression as those from the PB

Our hypothesis was that T-cells from within the tumour microenvironment would be activated, but there is little evidence of this from cells taken directly from the LN. Activated T-cells upregulate CD25, which is the alpha chain of the high affinity IL-2 receptor. Patten et al had described proliferating CLL cells to be in close contact with activated CD4+ CD25+ T-cells in LN biopsy sections (Patten, Buggins et al. 2008), so this marker was preferentially incorporated into the flow panels. We devised a series of panels to investigate activation (CD25, CD40L), co-stimulation (CD28), negative regulation (CTLA-4) and exhaustion (PD-1) on CLL T-cells. The flow cytometry panels used are shown in 3.3.3.

Although there was a surprisingly slight downwards trend, there was no statistically significant difference in the proportion of CD4+ T-cells expressing CD25 in the PB or LN; PB CD4+ T-cells 38.86% +/- 5.65 vs LN 31.17% +/- 3.38; p=0.090. See Figure 3-22.
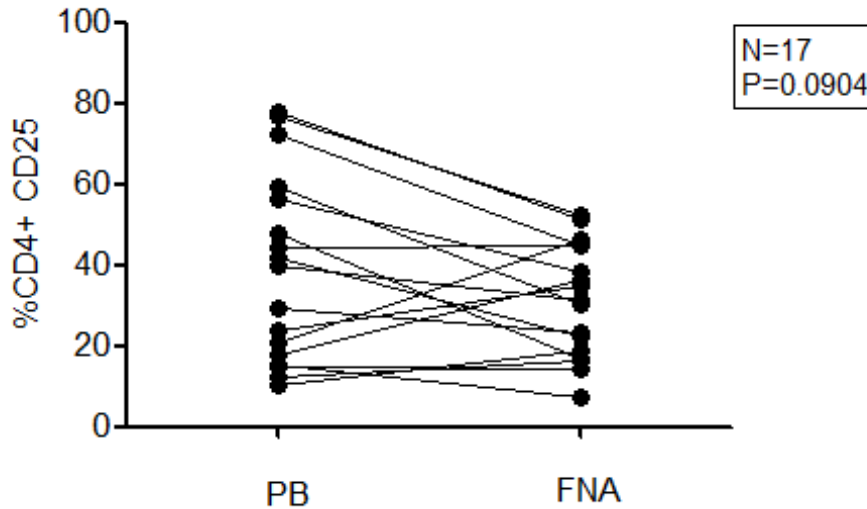
Figure 3-22 There is no difference in the percentage of CD4+ T-cells expressing CD25 in LN FNA or PB
The sample was gated on CD4+ T-cells as described in Figure 3-13 and then sequentially gated on CD4+/CD25+. The paired PB and LN FNA data is presented for each CLL patient (n=17). Statistical analysis as Figure 3-12.

The same held true for the CD8+ T-cells where the CD25 expression level was the same

between compartments: PB CD8+ CD25+ 8.11% +/- 1.83 vs LN CD8+ CD25+ 8.95% +/- 1.39;

p=0.600. Figure 3-23.
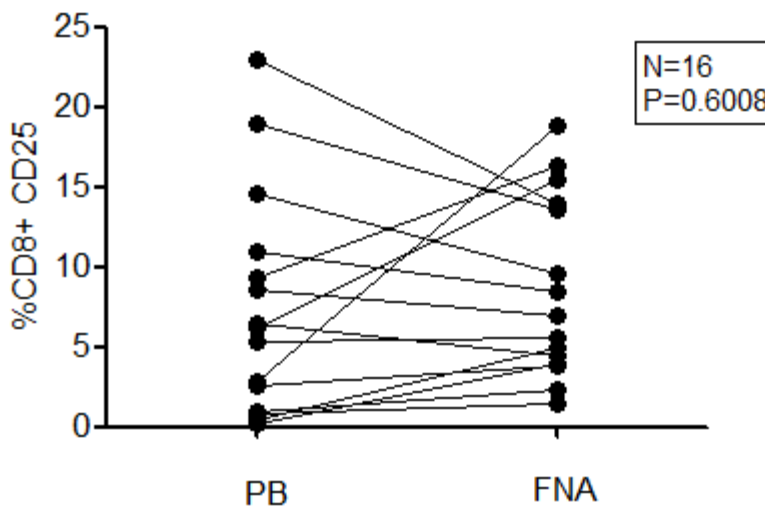
Figure 3-23 There is no difference in the percentage of CD8+ T-cells expressing CD25 between the LN FNA and PB
The sample was gated on CD8+ T-cells as described in Figure 3-13 and then sequentially gated on CD8+/CD25+. The paired PB and LN FNA data is presented for each CLL patient (n=16). Statistical analysis as Figure 3-12.

3.5.9 CD40L expression cannot be detected on resting CLL cells from the PB or LN FNA

Next we looked for evidence of CD40L on the CD4+ T-cells. In the normal human immune response the engagement of the TCR by the MHC class II in turn leads to cytokine production, including IL-4 and IL-21 which stimulate the B-cell. As part of this process CD40 is engaged by its ligand CD40L (CD154) on T-cells. CD40L activates the RelA dependant NF-kB canonical and the RelB non canonical activation pathways. As discussed, in the introductory chapter, there is thought to be an acquired CD40L defect in CLL and the levels of expression in LN derived T-cells is debated. Ghia et al suggested between 5-30% of these CD4+ T-cells expressed CD40L, but this has not been consistently reproduced (Ghia, Strola et al. 2002). We found that levels of CD40L on CLL derived CD4+ T-cells was very low or absent in both the PB and LN FNA. A representative dot plot is shown in Figure 3-24.

To investigate this small shift we analysed the mean fluorescent intensity (MFI) of the CD40L fluorochrome instead of using a more crude percentage value to identify if there was any small difference in expression between compartments.

The MFI CD40L PB CD4+ T-cells was PB CD4+ CD40L 226 +/- 38.32 vs LN CD4+ CD40L 352 +/- 67.1 in the LN; p=0.103. Therefore no difference was demonstrated. See Figure 3-25.
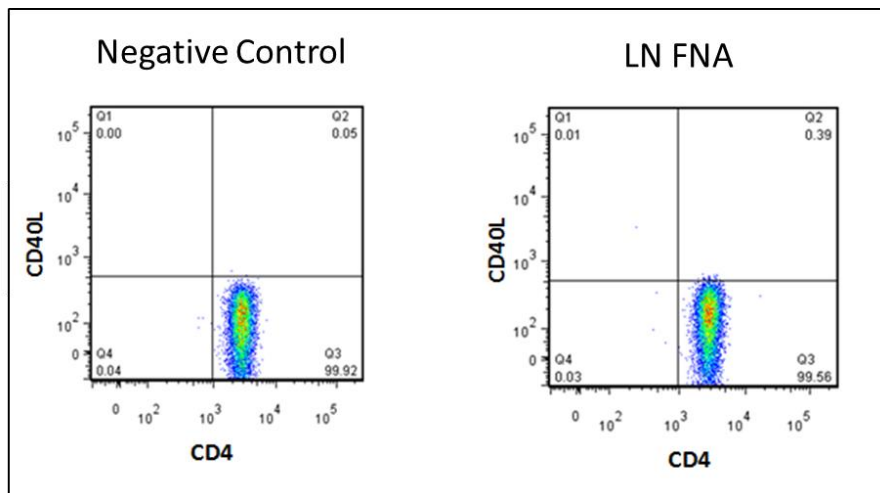
Figure 3-24 CD40L expression in CD4+ T-cells of LN FNA compared to negative control
LN FNA from an example CLL patient. The left panel is a LN FNA labelled with CD3 (APC-Cy7), CD4 (PerCp-Cy5), CD8 (Pacific Blue) excluding the antibody conjugate directed against CD40L (PE). The right panel is labelled in addition with CD40L (PE). The gating strategy for CD4+ T-cells is as in Figure 3-13. The CD4+ CD40L+ gate has very few positive events.
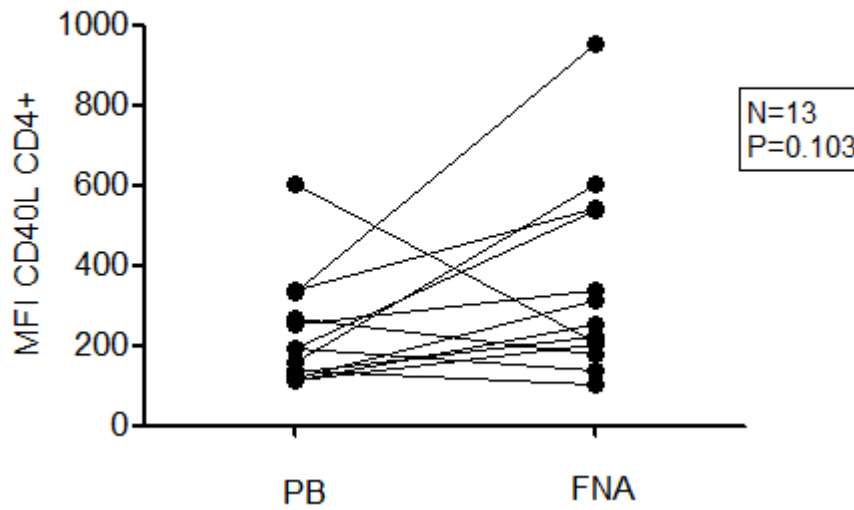
Figure 3-25 There was no upregulation of CD40L in the CLL LN
The sample was gated on CD4+ T-cells as described in Figure 3-13. The MFI of CD40L (PE) was acquired for the total CD4+ T-cell gate. The paired PB and LN FNA data is presented for each CLL patient (n=13). Statistical analysis as Figure 3-12.

3.5.10 Co-stimulatory molecules show differential expression between LN FNA and PB in CLL

Once the TCR engages with the MHC-peptide complex, co-stimulatory molecule ligation is required for T-cell activation. The primed T-cell expresses CD28 on its surface which binds to members of the B7 family, such as CD80 and CD86, on the antigen presenting cell. Lower expression of the co-stimulatory molecule CD28 on both CD4+ and CD8+ PB CLL T-cells has been consistently reported and lower levels appear to correspond with more advanced disease (Rossi, Matutes et al. 1996, Rossmann, Jeddi-Tehrani et al. 2003). Interestingly we found here was higher expression of the co-stimulatory molecule CD28 on both CD4+ and CD8+ T-cells of the LN compared to PB; CD4+ T-cells LN 95.66% +/- 1.47 vs PB 88.97% +/- 3.10; p=0.049. See Figure 3-26. CD8+ T-cells LN 79.81% +/- 3.46 vs 39.64% +/- 6.04; p<0.0001. See Figure 3-27.
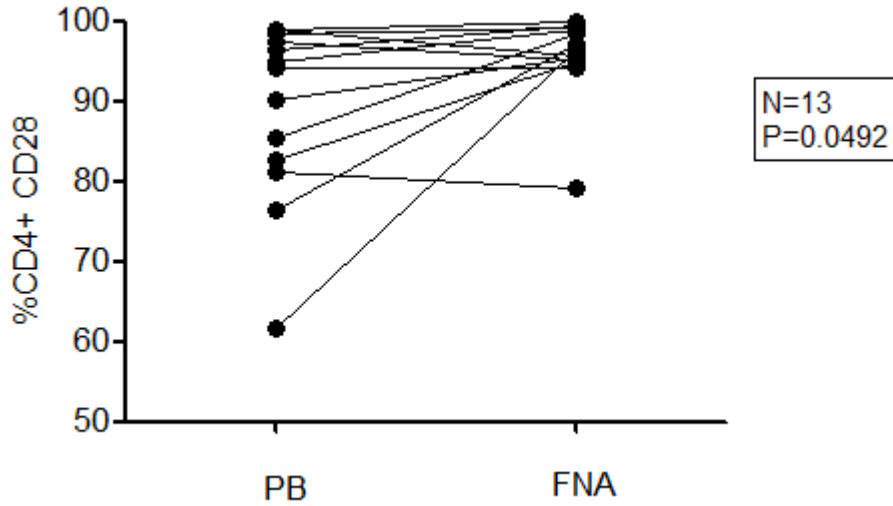
Figure 3-26 There was higher levels of CD28 on CD4+ T-cells in the LN compared to PB
The sample was gated on CD4+ T-cells as described in Figure 3-13 and then sequentially
gated on CD4+/CD28+. The paired PB and LN FNA data is presented for each CLL patient
(n=13). Statistical analysis as Figure 3-12.
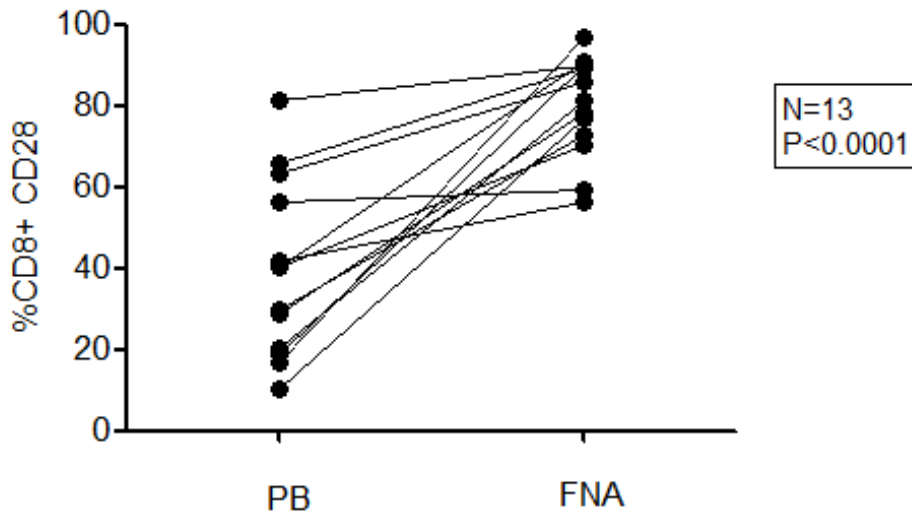
Figure 3-27 There was higher levels of CD28 on CD8+ T-cells in the LN compared to PB
The sample was gated on CD8+ T-cells as described in Figure 3-13 and then sequentially
gated on CD8+/CD25+. The paired PB and LN FNA data is presented for each CLL patient
(n=13). Statistical analysis as Figure 3-12.

3.5.11 Assessment of negative regulators of T-cells

CTLA-4 is a negative T-cell regulator expressed on activated T-cells and binds to the same ligands as CD28. It negatively regulates the T-cell by decreasing IL-2 production and therefore has a critical role in terminating the immune response (Alegre, Frauwirth et al. 2001). We measured CTLA-4 in both CD4+ and CD8+ subpopulations. In the CD4+ population there was a trend toward increased CTLA-4 expression in the LN compartment compared to PB but this was not statistically significant; LN CD4+ CTLA-4 5.40% +/- 2.01 vs PB CD4+ CTLA-4 1.78% +/- 0.46; p=0.076. See Figure 3-28.

There was, however, significantly more expression of CTLA-4 on the CD8+ T-cells in the LN compared to PB; LN CD8+ CTLA-4 21.80% +/- 4.36 vs PB CD8+ CTLA-4 13.05 +/- 3.67; p=0.010. See Figure 3-29.

The increased levels of CTLA-4 in the CLL LN compared to PB are an indication the T-cells are activated in the LN.
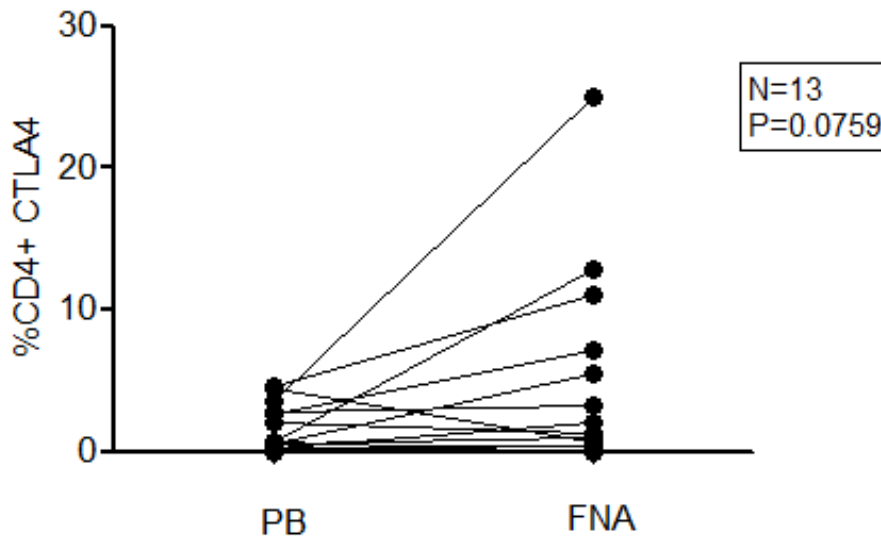
Figure 3-28 There was a trend toward an increase in CTLA-4+ expression on CD4+ T-cells derived from the LN FNA compared to PB
The sample was gated on CD4+ T-cells as described in Figure 3-13 and then sequentially gated on CD4+/CTLA4+. The paired PB and LN FNA data is presented for each CLL patient (n=13). Statistical analysis as Figure 3-12.
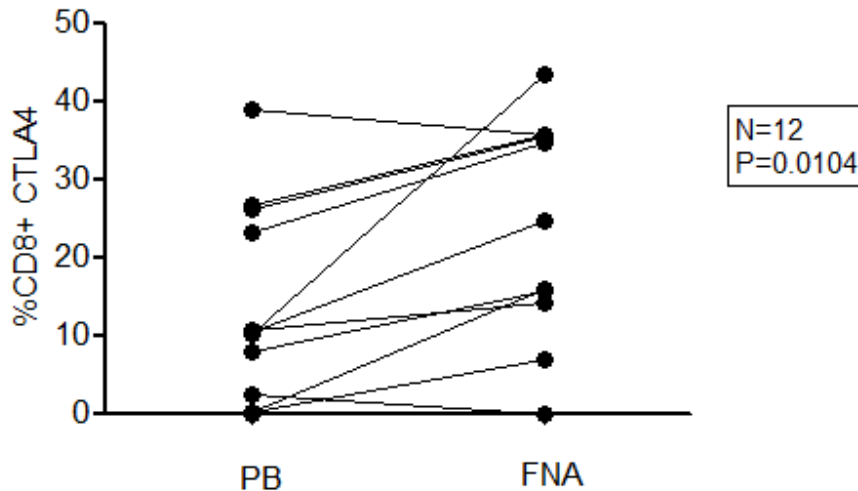
Figure 3-29 There was a statistically higher percentage of CD8+ T-cells that expressed CTLA-4+ in the LN FNA compared to PB
The sample was gated on CD8+ T-cells as described in Figure 3-13 and then sequentially gated on CD8+/CTLA4+. The paired PB and LN FNA data is presented for each CLL patient (n=12). Statistical analysis as Figure 3-12.

3.5.12 PD-1 expression is higher on the PB T-cells of CLL patients than normal controls

Chronically activated T-cells, express the "exhaustion" marker PD-1, whose negative regulatory functions suppresses the T-cell receptor activation. Since the work in this thesis was completed several groups have published that CLL PB T-cells express high levels of PD-1 (Nunes, Wong et al. 2012, Ramsay, Clear et al. 2012, Brusa, Serra et al. 2013, Riches, Davies et al. 2013, Novak, Prochazka et al. 2015, Rusak, Eljaszewicz et al. 2015). We confirm that finding here. There was significantly higher PD-1 expression observed in both CD4+ and CD8+ PB T-cells from CLL PB compared to normals. CLL PB (n=21) CD4+ PD-1+ 31.12% +/- 3.60 vs CD4+ PD-1+ normals (n=11) 17.74% +/- 3.25; p=0.022. See Figure 3-30.
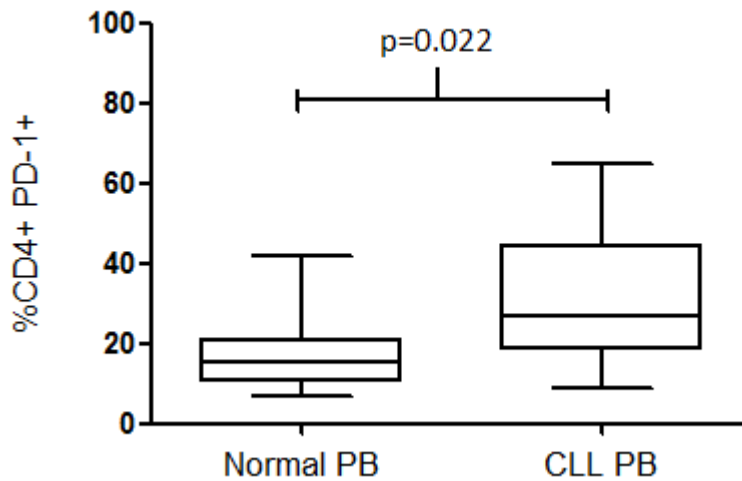
Figure 3-30 There is a higher percentage of PD-1+ CD4+ T-cells in CLL PB compared to healthy controls
The sample was gated on CD4+ T-cells as described in Figure 3-13 and then sequentially gated on CD4+/PD-1+. The unpaired PB data is presented, PB from normal aged matched controls (n=11) and CLL patients (n=21). Statistical analysis as Figure 3-3.

The same was true for the CD8+ component, where higher levels of PD-1 were found on CLL PB derived CD8+ T-cells than normal PB CD8+ T-cells: CLL PB (n=21) CD8+ PD-1+ 41.44% +/- 3.94 vs normal PB (n=11) CD8+ PD-1+ 23.37% +/- 3.81; p=0.006. See Figure 3-31.
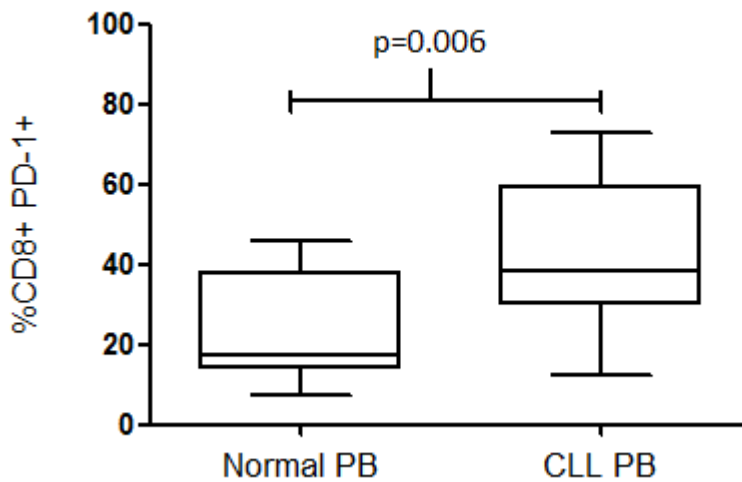
Figure 3-31 There is a higher percentage of PD-1+ CD8+ T-cells in CLL PB compared to healthy controls
The sample was gated on CD8+ T-cells as described in Figure 3-13 and then sequentially gated on CD8+/PD-1+. The unpaired PB data is presented, PB from normal aged matched controls (n=11) and CLL patients (n=21). Statistical analysis as Figure 3-3.

3.5.13 PD-1 expression levels are markedly increased on T-cells derived from the CLL LN compared to PB of the same patient

One of the most striking and previously unreported observations of this study was the significantly increased PD-1 on CLL T-cells of the LN. We found that the level of PD-1 expression on T-cells was much higher in the CLL LN FNA than the corresponding cells of the PB in both the CD4+ and CD8+ T-cells.

Figure 3-32 shows a representative flow cytometry dot plot, showing the shift in MFI of PD-1 on the LN FNA CD4+ T-cells compared to those of the PB.

The MFI of PD-1 in CD4+ T-cells was significantly higher in the CLL LN than the PB; 1272 +/- 180.2 vs 514 +/- 62.2; $p<0.0001$. See Figure 3-33. Also the overall percentage of CD4+ T-cells expressing PD-1 was much higher in the LN than PB; CLL LN CD4+ PD-1+ 56.42% +/- 4.02 vs CLL PB CD4+ PD-1+ 31.12% +/- 3.60; $p<0.0001$. See Figure 3-34.
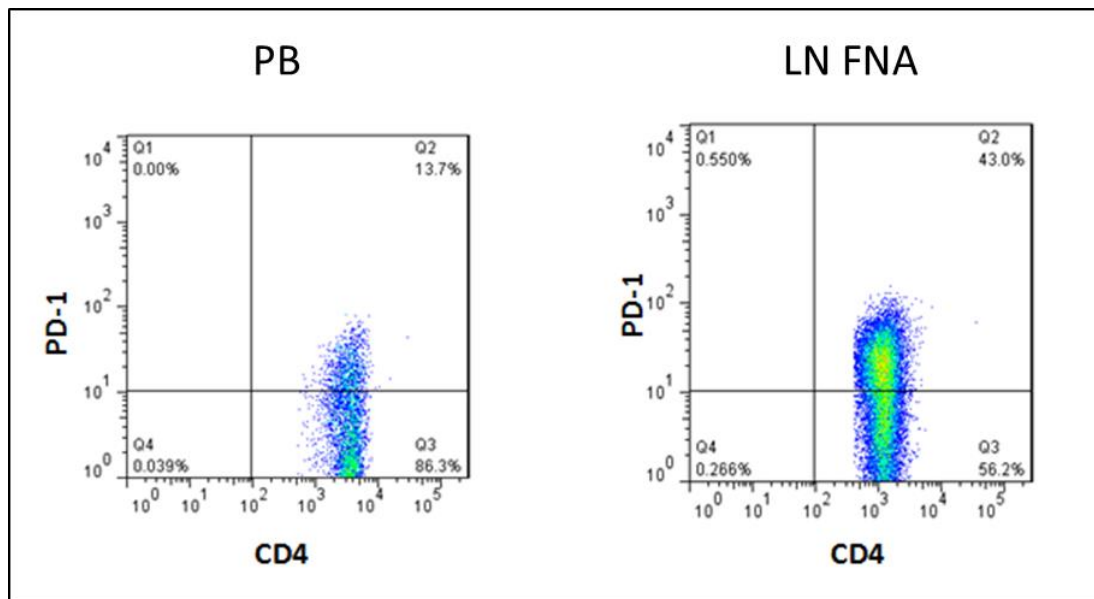
Figure 3-32 Representative dot plot of PD-1+ / CD4+ T-cells of PB compared to LN FNA
Paired PB (left panel) and LN FNA (right panel) from an example CLL patient. The gating strategy for CD4+ T-cells is as in Figure 3-13. The CD4+ PD-1+ gate has more positive events in the LN FNA than the PB and it can be appreciated the PD-1 shifts towards positive in the LN FNA as opposed to a discrete bimodal population of CD4 PD-1+ and PD-1- subpopulations.
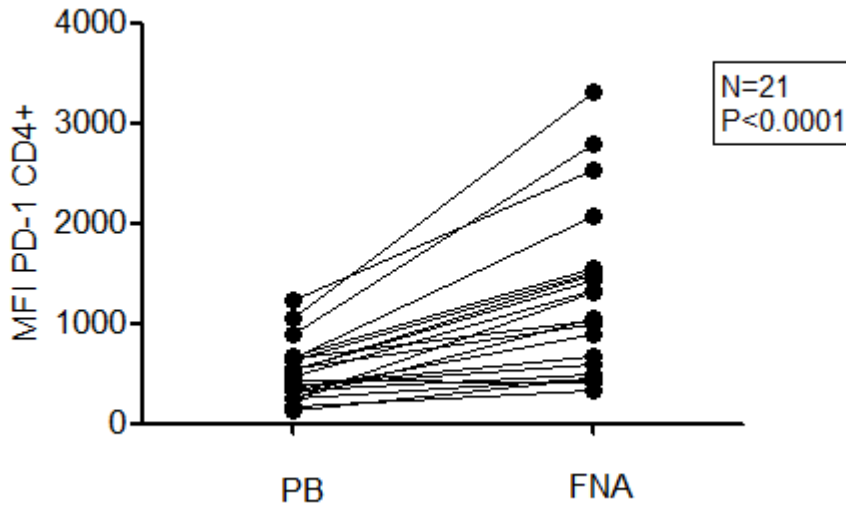
Figure 3-33 The MFI of PD-1 was higher in the LN FNA CD4+ T-cells compared to PB
The sample was gated on CD4+ T-cells as described in Figure 3-13. The MFI of PD-1 was acquired for the total CD4+ T-cell gate. The paired PB and LN FNA data is presented for each CLL patient (n=21). Statistical analysis as Figure 3-12.
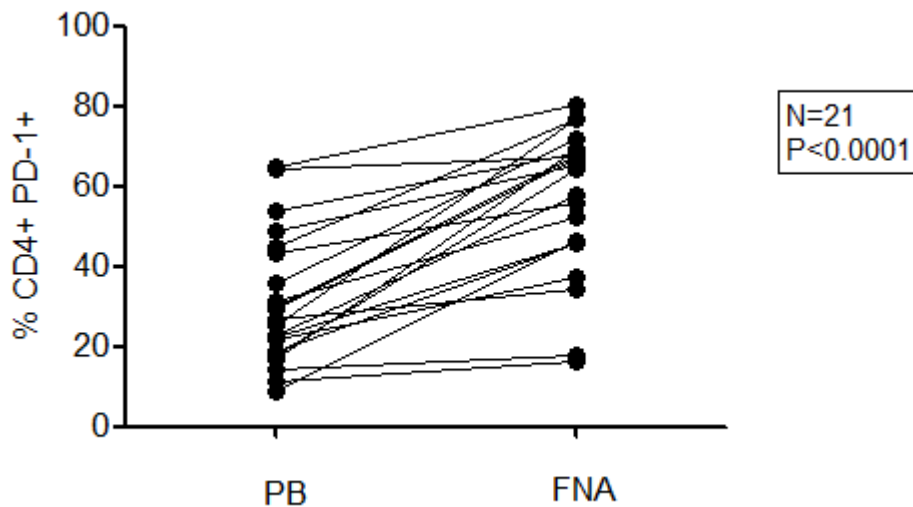
Figure 3-34 There is more PD-1 expressed on the CD4+ T-cells of the LN compared to PB
The sample was gated on CD4+ T-cells as described in Figure 3-13 and then sequentially gated on CD4+/PD-1+. The paired PB and LN FNA data is presented for each CLL patient (n=21). Statistical analysis as Figure 3-12.

This finding was also mirrored in the CD8+ cells where the PD-1 MFI in the LN FNA was much higher than the same cells in the PB; 1615 +/- 218.4 vs 44 +/- 80.9 p<0.0001. See Figure 3-35.
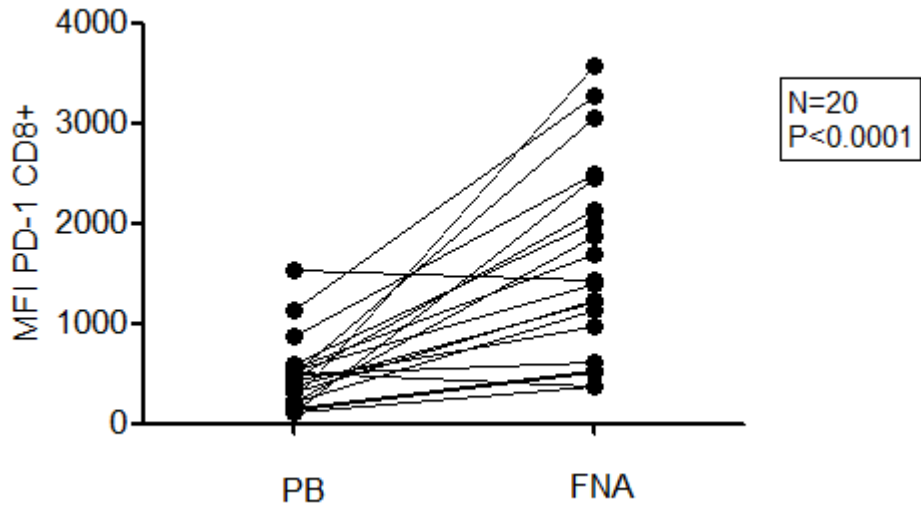
Figure 3-35 The MFI of PD-1 was higher in the LN FNA CD8+ T-cells compared to PB
The sample was gated on CD8+ T-cells as described in Figure 3-13. The MFI of PD-1 was acquired for the total CD8+ T-cell gate. The paired PB and LN FNA data is presented for each CLL patient (n=20). Statistical analysis as Figure 3-12.

There was also an overall increased percentage of PD-1+ CD8 T-cells in the LN vs PB; CLL

LN CD4+ PD-1+ 71.07% +/- 3.54 vs CLL PB CD4+ PD-1+ 41.44% +/- 3.94; p<0.0001. See

Figure 3-36.
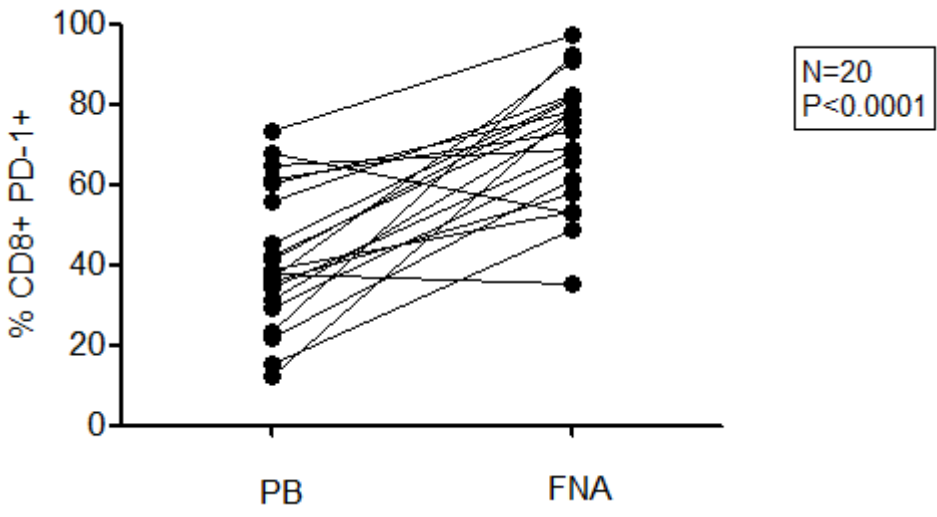
Figure 3-36 There is more PD-1 expressed on the CD8+ T-cells of the LN compared to PB
The sample was gated on CD8+ T-cells as described in Figure 3-13 and then sequentially gated on CD8+/PD-1+. The paired PB and LN FNA data is presented for each CLL patient (n=20). Statistical analysis as Figure 3-12.

3.5.14 The known PD-1 ligands PDL1 and PDL2 are not expressed on resting CLL cells from the PB or LN

PD-L1 and PD-L2 are the known ligands of PD-1, as discussed in the introductory chapter. Therefore we looked for evidence of the PD-L1 and PD-L2 expression on the CLL cells of the PB and LN. The level of expression of PD-L1 was very low in both compartments, with no significant difference between the two. PD-L1 on PB CLL cells vs LN CLL cells: 1.03% +/- 0.59 vs 0.85% +/- 0.69; p=0.78. See Figure 3-37. The positive control experiments for PD-L1 will be discussed in chapter 6 of this thesis.

Figure 3-37 No difference in the level of expression of PD-L1 in the CLL PB or LN FNA
The acquisition was gated first on the lymphocyte gate (from the side and forward scatter pattern as described in Figure 3-9) and then CLL cell population defined as dual CD5+ and CD19+. The CD5+/CD19+/PD-L1+ events were acquired. The PB and LN FNA data is presented for each CLL patient (n=8) and the mean shown. Statistical analysis as Figure 3-12.

PD-L2 expression was not detected at a significant level on CLL cells derived from the PB or the LN. PB CLL cells 0.21% +/- 0.14 compared to LN CLL cells 0.18% +/- 0.10; p=0.74.

3.5.15 PD-1 expression is also identified to be present on CLL cells

Although the primary objective of this work was to study the T-cell compartment in LN and PB, as reported by others, we did detect PD-1 expression by CLL PB B-cells in this study (Xerri, Chetaille et al. 2008, Grzywnowicz, Zaleska et al. 2012, Brusa, Serra et al. 2013). We

therefore went on to study the differential expression of PD-1 on CLL cells of the PB and LN. As was the case for CLL LN derived T-cells, LN CLL B-cells also expressed higher levels of PD-1 compared to the PB; LN CLL PD-1+ 44.68 +/- 4.9 vs PB CLL PD-1+ 32.37 +/- 5.58; p=0.025. See Figure 3-38.

This is of interest because Grzywnowicz et al have previously reported that although there was a higher level of PD-1 transcripts from CLL B-cells compared to normal, they found there was no difference between the CLL PB and BM, confirming again that the LN compartment is a distinct niche (Grzywnowicz, Karabon et al. 2015).
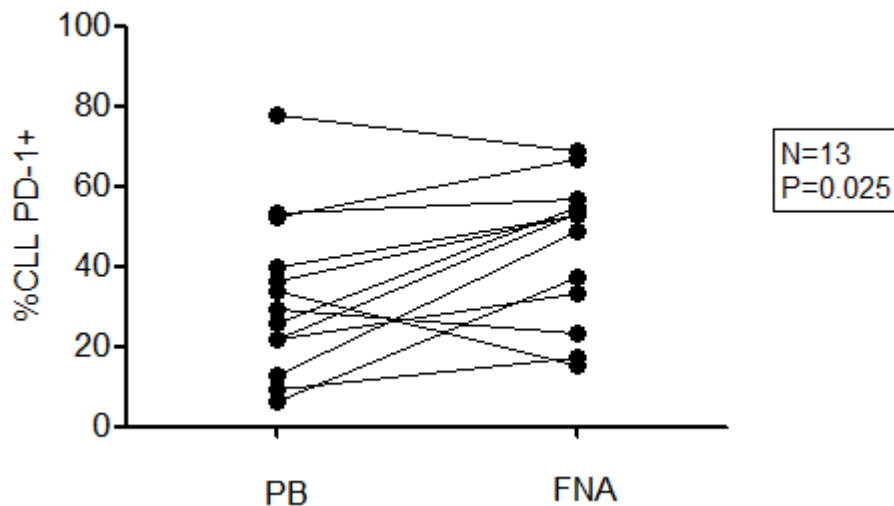
Figure 3-38 Higher frequency of PD-1+ CLL cells in the LN FNA than PB
The sample was gated on CLL cells as described in Figure 3-37 and then sequentially gated on PD-1+. The paired PB and LN FNA data is presented for each CLL patient (n=13). Statistical analysis as Figure 3-12.

3.5.16 There is no difference in T follicular helper cell numbers between CLL PB and LN samples

Little work has focused on the Tfh cells in CLL. Cha et al defined Tfh as CD4+ CXCR5+ and found these cells to represent 25% of CD4+ T-cells in CLL PB compared to 8% in normal controls suggesting a role in disease (Cha, Zang et al. 2013). We also found an increased number of CD4+ CXCR5+ T-cells in the PB of CLL patients (n=12) compared to healthy controls (n=6); 57.9% +/-15.27 vs 8.58% +/-4.20; p=0.0009. See Figure 3-39.
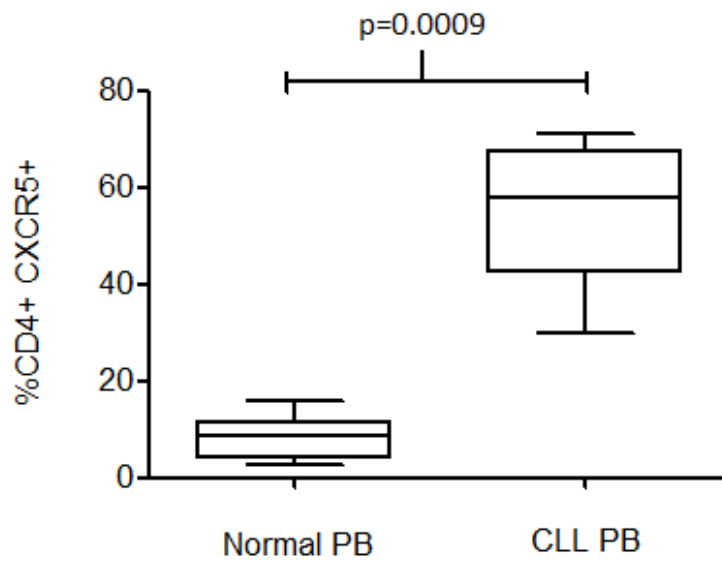
Figure 3-39 Increased CXCR5+ CD4+ cells in CLL PB vs healthy PB
The sample was gated on CD4+ T-cells as described in Figure 3-13 and then sequentially gated on CD4+/CXCR5+. The unpaired PB data is presented, PB from normal aged matched controls (n=6) and CLL patients (n=12). Statistical analysis as Figure 3-3.

When we investigated the same population in the CLL LN FNA we found no difference in the

relative numbers of CXCR5+ CD4+ T-cells whether derived from the PB or LN; 57.90% +/-

15.27 vs 61.30% +/- 25.86; p=1.00. Figure 3-40.
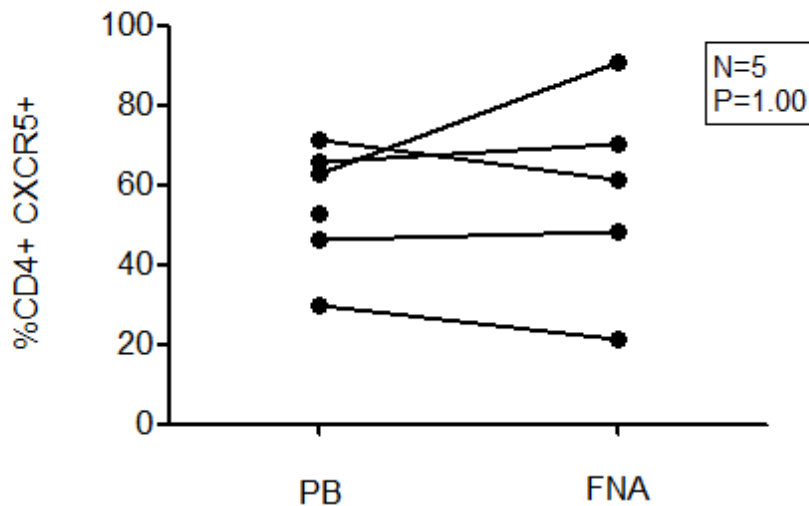
Figure 3-40 There was no difference in the frequency of CD4+ / CXCR5+ T-cells found in the PB or LN FNA in CLL
The sample was gated on CD4+ T-cells as described in Figure 3-13 and then sequentially gated on CD4+/CXCR5+. The paired PB and LN FNA data is presented for each CLL patient (n=5). Statistical analysis as Figure 3-12.

As this was a surprising finding, we questioned whether CD4+ CXCR5+ is a good method of describing Tfh cells. An alternative definition is CD4+ CXCR5+ ICOS+. We did not have access to sufficient LN FNA samples to perform this work by flow cytometry and instead investigated this question using FFPE lymph node biopsy samples, which will be addressed in the next chapter of this thesis. Tfh cells also express PD-1. However if the PD-1 positive cells identified in the study here were all Tfh cells we would be expected to see a differential expression of CXCR5 mirroring the PD-1 results which is not evident.

3.5.17 The impact of CMV seropositivity

Several groups have investigated the PB T-cells of CLL patients with co-existent CMV seropositivity. In a healthy elderly population CMV specific CD8+ T-cells can account for up to half the total T-cell repertoire (Khan, Shariff et al. 2002). As discussed in the introduction of this thesis it has been hypothesised that CMV could be, at least in part, responsible for the global T-cell expansion and dysfunction in CLL (Akbar 2010). However it has been acknowledged that the T-cell abnormalities in CLL are not just restricted to CMV positive individuals and that there is still a vast T-cell expansion of dysregulated T-cells with abnormal phenotype even in CMV seronegative individuals (Riches, Davies et al. 2013). A comparison between the PB and LN T-cell compartments of CLL patients with or without evidence of previous CMV exposure has not been undertaken before.

We wanted to address whether CMV seropositivity influences the T-cell phenotype of the CLL LN microenvironment and whether the "antigen experienced" T-cell phenotype in the LN was restricted to CMV seropositive patients. Firstly we found there was no statistical difference in the size of the T-cell expansion (as a percentage of the total lymphocyte gate) in the CMV seropositive (n=9) or seronegative (n=15) populations: 4.3% +/- 1.2 vs 6.1% +/- 1.8; p=0.696. Figure 3-41.
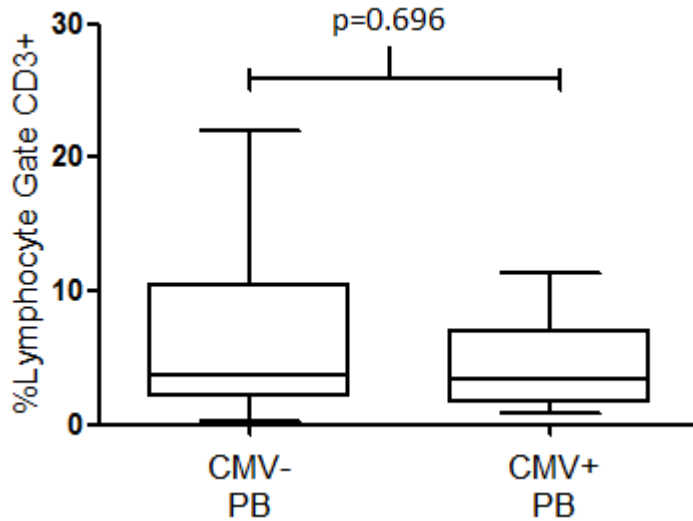
Figure 3-41 The size of the CLL PB CD3+ expansion is not influenced by CMV serostatus
The gating strategy is as in Figure 3-3. The unpaired data of PB CD3+ T-cells are presented as a percentage of the total lymphocyte gate in the CMV seropositive (n=9) and seronegative (n=15) CLL cohorts. Statistical analysis is as Figure 3-3.

The relative size of the CD4 and CD8 expansion in the CLL PB was also the same regardless

of CMV seropositivity: CD4+ CMV seropositive vs CMV seronegative: 58.7% +/- 5.0 vs 64.1%

+/- 4.04; p=0.463. See Figure 3-42. CD8+ CMV seropositive vs seronegative: 36.97% +/- 6.18

vs 34.78% +/- 4.04 p=0.739. See Figure 3-43.
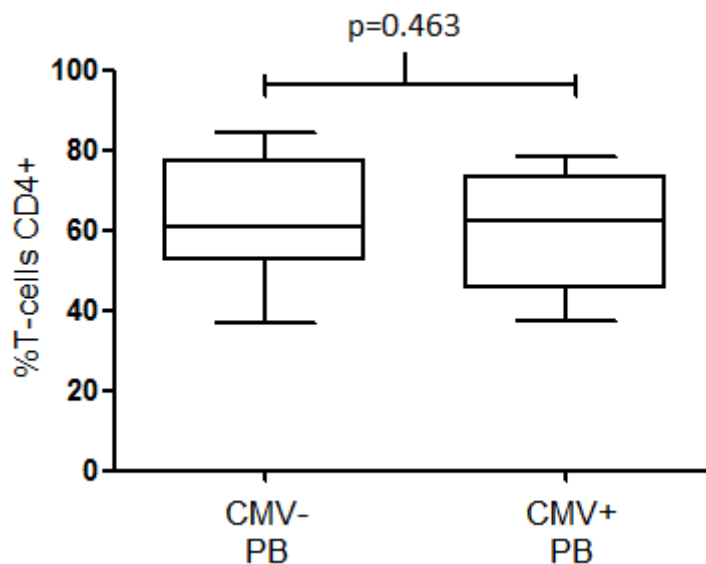
Figure 3-42 The percentage of CD4+ T-cells in CLL PB is not influenced by CMV serostatus
The gating strategy is described in Figure 3-13. The unpaired data of PB CD4+ T-cells are presented as a percentage of the CD3+ T-cells in the lymphocyte gate in CMV seropositive (n=9) and seronegative (n=15) CLL cohorts. Statistical analysis is as Figure 3-3.

CD8+ CMV seropositive vs seronegative: 36.97% +/- 6.18 vs 34.78% +/- 4.04 p=0.739. See
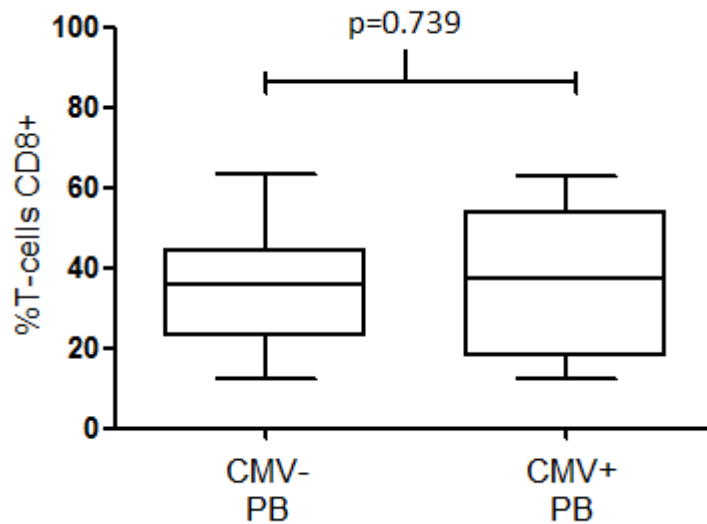
Figure 3-43.

Figure 3-43 The percentage of CD8+ T-cells in CLL PB is not influenced by CMV serostatus
The gating strategy is described in Figure 3-13. The unpaired data of PB CD8+ T-cells are
presented as a percentage of the CD3+ T-cells in the lymphocyte gate in CMV seropositive
(n=9) and seronegative (n=15) CLL cohorts. Statistical analysis is as Figure 3-3.

To determine if there was a relationship between the extended CD4+ T-cell phenotype and

CMV serostatus we compared the number of naïve, T_{CM}, T_{EM} and T_{EMRA} cells between those

subpopulations where the CMV status was known. There was no difference between the

relative percentage of each subpopulation between CMV positive and CMV negative

individuals regardless of whether the T-cells were derived from the PB or LN. See Figure 3-44,

Figure 3-45, Figure 3-46 and Figure 3-47.
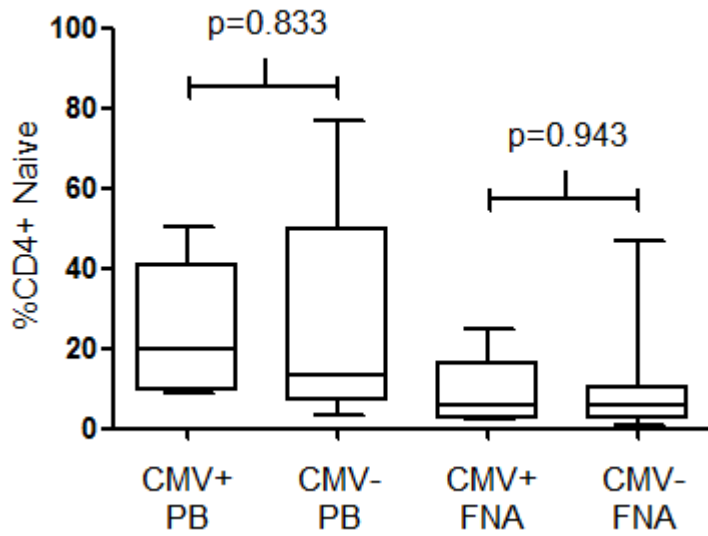
Figure 3-44 CMV serostatus does not influence the percentage of naïve CD4+ T-cells found in the PB or LN of CLL patients

The gating strategy is as described in Figure 3-16. The unpaired data of PB and LN FNA naïve CD4+ T-cells in CMV seropositive (n=5) and seronegative (n=8) CLL cohorts. Statistical analysis is as Figure 3-3.
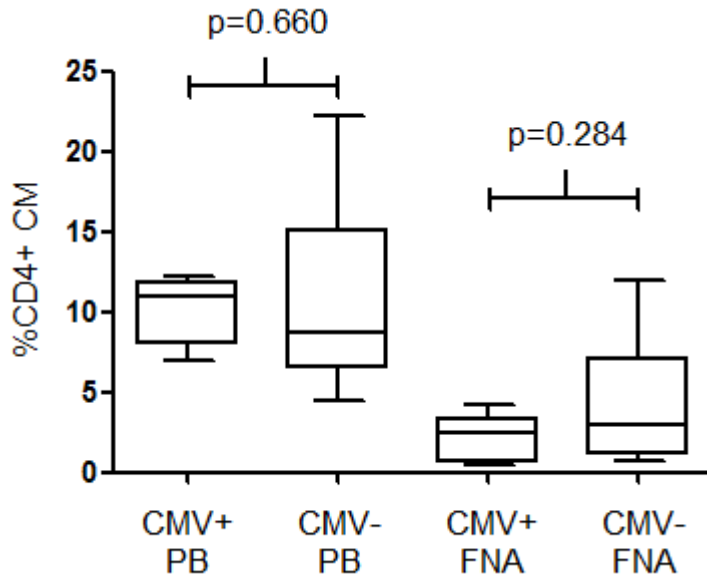
Figure 3-45 CMV serostatus does not influence the percentage of T_{CM} CD4+ T-cells found in the PB or LN of CLL patients

The gating strategy is as described in Figure 3-16. The unpaired data of PB and LN FNA CM CD4+ T-cells in CMV seropositive (n=5) and seronegative (n=8) CLL cohorts. Statistical analysis is as Figure 3-3.
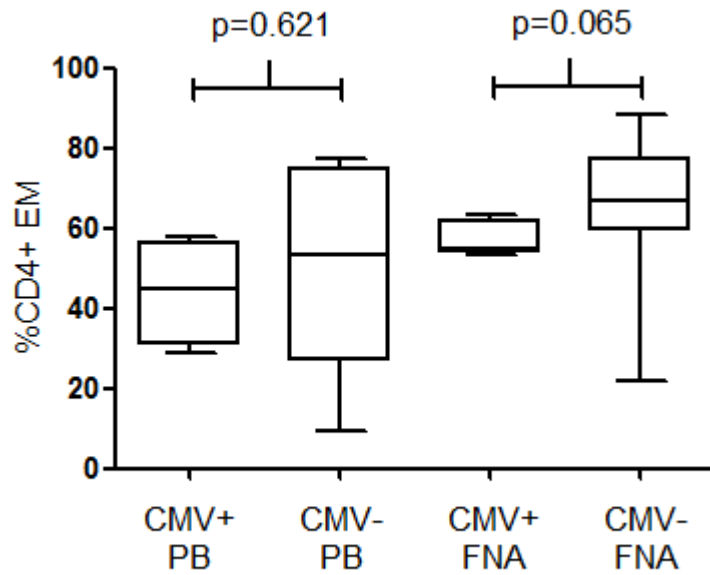
Figure 3-46 CMV serostatus does not influence the percentage of T_{EM} CD4+ T-cells found in the PB or LN of CLL patients
The gating strategy is as described in Figure 3-16. The unpaired data of PB and LN FNA EM CD4+ T-cells in CMV seropositive (n=5) and seronegative (n=8) CLL cohorts. Statistical analysis is as Figure 3-3.
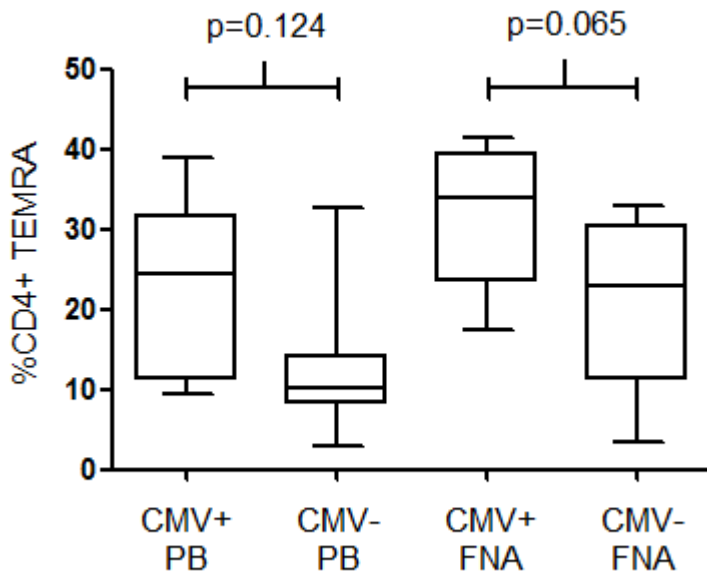
Figure 3-47 CMV serostatus does not influence the percentage of T_{EMRA} CD4+ T-cells found in the PB or LN of CLL patients
The gating strategy is as described in Figure 3-16. The unpaired data of PB and LN FNA TEMRA CD4+ T-cells in CMV seropositive (n=5) and seronegative (n=8) CLL cohorts. Statistical analysis is as Figure 3-3.

There was a possible trend toward more CD4+ T_{EMRA} cells in the PB of previously CMV infected individuals but this did not reach statistical significance; 22.0% +/- 5.15 vs 12.3% +/- 3.16; p=0.124, which may be due small numbers when the subpopulations are divided. Regardless of CMV serostatus there were statistically more effector CD4+ T-cells and fewer naïve in the LN compartment compared to PB across the patients. CMV seronegative patients: Naïve CD4+ T-cells PB vs LN: 26.8% +/- 9.5 vs 10.5% +/- 5.331; p=0.0268. CMV seropositive patients: Naïve CD4+ T-cells PB vs LN: 24.0% +/- 7.8 vs 8.7% +/- 4.2; p=0.0347. Therefore the increased effectors in the LN of CLL patients cannot be explained by previous exposure to CMV.

3.5.18 CMV serostatus did not influence levels of T-cell PD-1 expression

Next we investigated whether the increased number of CD4+ T-cells expressing PD-1 in the LN held true regardless of the CMV serostatus and found that it did. CMV seronegative patients: CD4+ PD-1+ PB vs LN: 26.15% +/- 4.01 vs 55.53% +/- 6.00; p=0.0001. See Figure 3-48. CMV seropositive patients: CD4+ PD-1+ PB vs LN: 36.89% +/- 7.25 vs 55.30% +/- 7.65; p=0.012. See Figure 3-49.
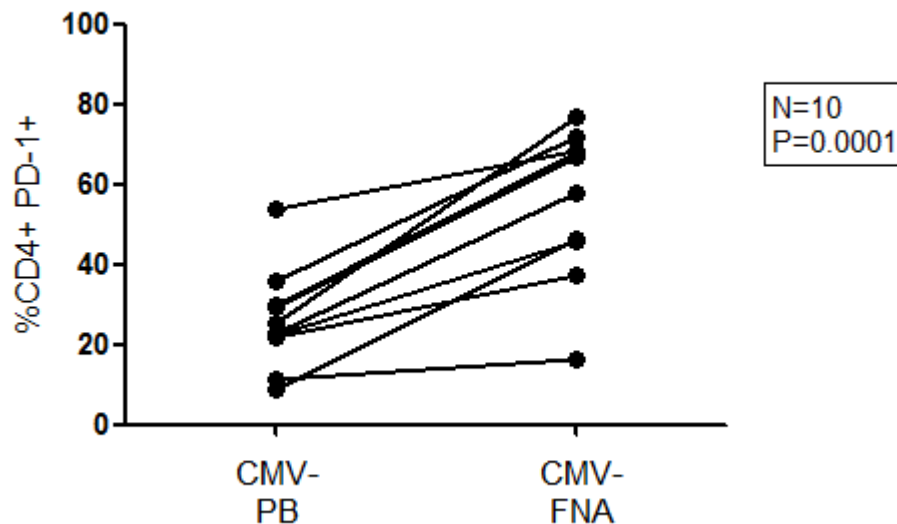
Figure 3-48 PD-1 expression is higher on LN CD4+ T-cells than PB CD4+ T-cells in CMV seronegative CLL patients
The sample was gated as described in Figure 3-30. The paired PB and LN FNA data is presented for each CLL CMV seronegative patient (n=10). Statistical analysis as Figure 3-12.
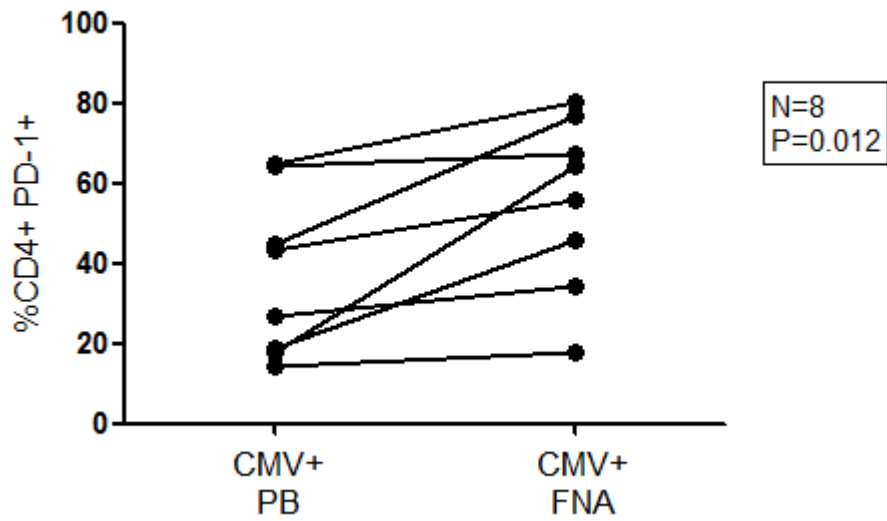
Figure 3-49 PD-1 expression is higher on LN CD4+ T-cells than PB CD4+ T-cells in CMV seropositive CLL patients

The sample was gated as described in Figure 3-30. The paired PB and LN FNA data is presented for each CLL CMV seropositive patient (n=8). Statistical analysis as Figure 3-12.

The same was true for CD8+ T-cells: CMV seronegative patients: CD8+ PD-1+ PB vs LN: 47.65% +/- 4.65 vs 72.32% +/- 5.24; p=0.001. See Figure 3-50. CMV seropositive patients: CD8+ PD-1+ PB vs LN: 39.41% +/- 6.62 vs 73.49% +/- 5.40; p=0.013. See Figure 3-51.
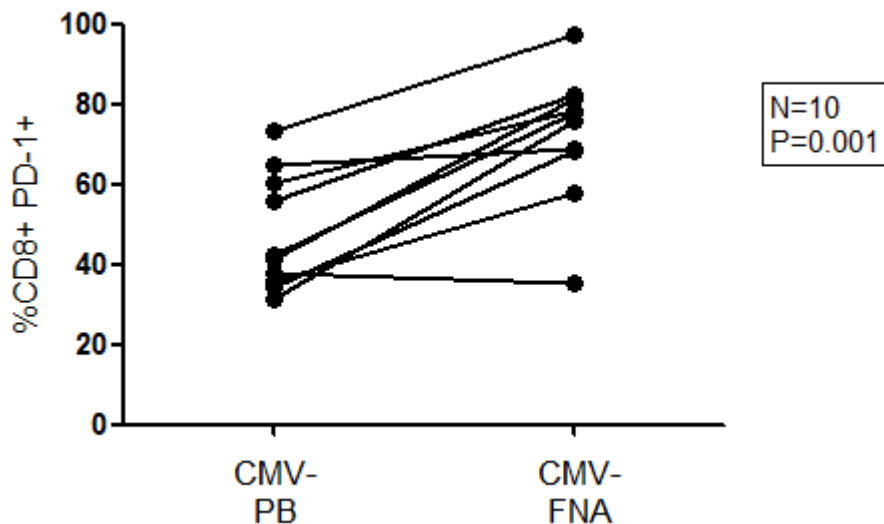
Figure 3-50 PD-1 expression is higher on LN CD8+ T-cells than PB CD8+ T-cells in CMV seronegative CLL patients

The sample was gated as described in Figure 3-31. The paired PB and LN FNA data is presented for each CLL CMV seronegative patient (n=10). Statistical analysis as Figure 3-12.
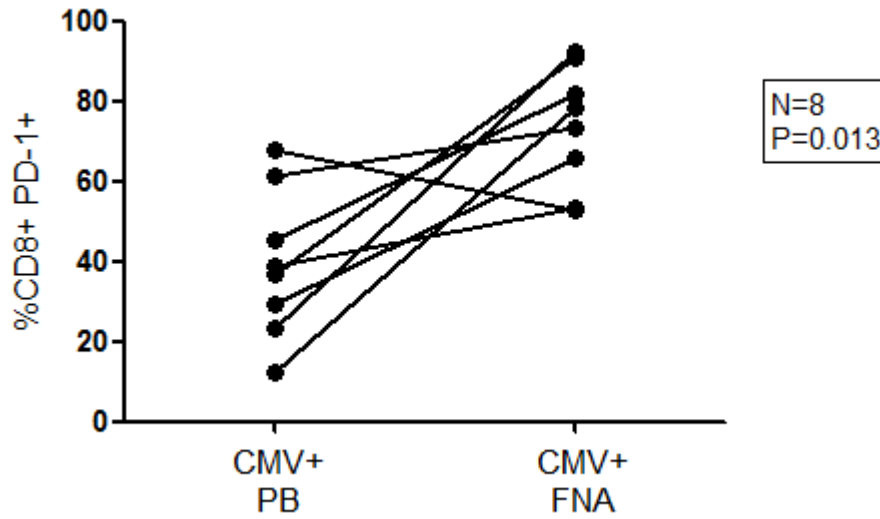
Figure 3-51 PD-1 expression is higher on LN CD8+ T-cells than PB CD8+ T-cells in CMV seropositive CLL patients

The sample was gated as described in Figure 3-31. The paired PB and LN FNA data is presented for each CLL CMV seropositive patient (n=8). Statistical analysis as Figure 3-12.

CMV serostatus made no difference to the percentage of CD4+ PD-1+ cells in the PB of CLL patients: CD4+ PD-1+ CMV seronegative vs seropositive: 26.15% +/- 4.01 vs 36.89% +/- 7.25; p=0.190. The same was true in the LN where there were CMV serostatus made no impact in the size of the CD4+ PD-1+ expansion: CD4+ PD-1+ CMV seronegative vs seropositive: 55.53% +/- 6.00 vs 55.30% +/- 7.65; p=0.981. See Figure 3-52.
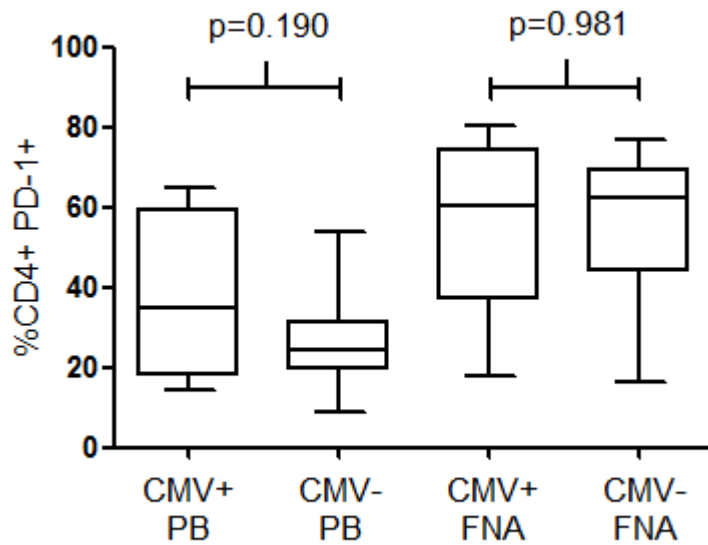
Figure 3-52 CMV serostatus does not impact on levels of PD-1 on CD4+ T-cells in PB or LN
The sample was gated as described in Figure 3-30. The figure shows the unpaired analysis of the data from PB and LN FNA CD4+ PD-1+ T-cells in CMV seropositive (n=8) and seronegative (n=10) CLL cohorts. Statistical analysis is as Figure 3-3.

The same was true for CD8+ T-cells where there was no difference in the percentage of CD8+ PD-1+ cells in the PB of CMV seronegative or seropositive individuals: CD8+ PD-1+ CMV seronegative vs seropositive: 47.65% +/- 4.65 vs 39.41% +/- 6.62; p=0.311.

Again CMV serostatus had no impact on the expansion of CD8+ T-cells expressing PD-1 in the CLL LN: LN CD8+ PD-1+ CMV seronegative vs seropositive: 72.32% +/- 5.24 vs 73.49% +/- 5.40; p=0.880. See Figure 3-53.
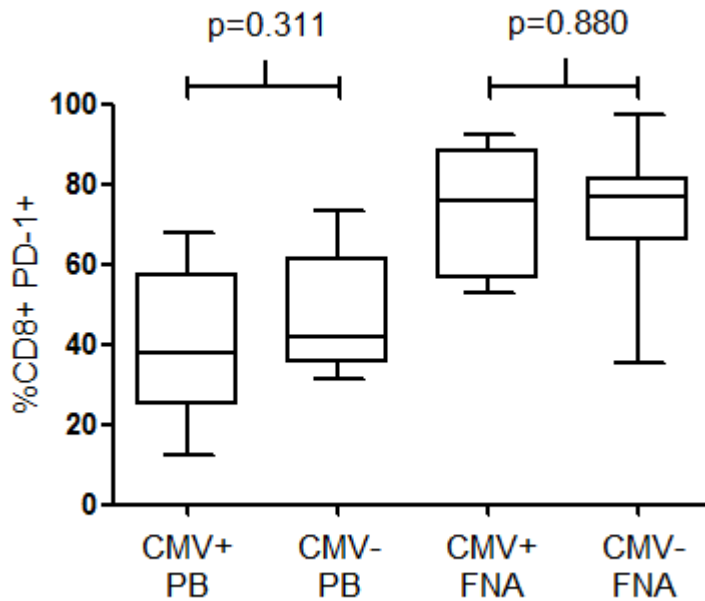
Figure 3-53 CMV serostatus does not impact on levels of PD-1 on CD8+ T-cells in PB or LN compartment
The sample was gated as described in Figure 3-31. The figure shows the unpaired analysis of the data from PB and LN FNA CD8+ PD-1+ T-cells in CMV seropositive (n=8) and seronegative (n=10) CLL cohorts. Statistical analysis is as Figure 3-3.

3.6 Discussion

The work outlined in this chapter has validated the feasibility of the use of LN FNAs to obtain access to the cells of the CLL microenvironment. We were initially anticipating a very low cell yield from this technique and therefore prior to commencing this approach we considered several other methods of analysing small cell numbers. On average the total cell count was 4.1×10^6 which was higher than we anticipated. However, clearly still the majority of these cells were malignant CLL B-cells and there was also some cell loss in processing (cell washing) so not every analysis could be performed on every sample. On reflection some of the initial experiments were too ambitious with the sample being split between too many panels with tubes containing insufficient T-cells for accurate analysis. Therefore this compromised some early analysis, especially when looking to identify infrequent populations, and some of the initial samples were not used optimally.

The aim of this study was to investigate T-cells in an unselected group of CLL patients. As outlined in the introduction, the study of LN biopsy samples generally favours a more advanced and atypical group of CLL patients and we were hoping to avoid this with a LN FNA approach. The demographics of the LN FNA patient group was shown in Table 3-4. The clinical and biological features of our group reflect the heterogeneity of CLL. By definition, there was a slight bias towards patients in the Binet stages B and C groups, as these are the patients with palpable lymphadenopathy. The distribution of cytogenetic abnormalities and mutation status, however, is quite representative of those found in the CLL population as a whole. Of note there is no excess of patients with 11q-, which is most often associated with bulky lymphadenopathy. Therefore we propose a cross section of CLL patients was under evaluation in this study. Of note the CMV IgG positive cohort accounted for only 39% of patients. This might seem low for an elderly unselected CLL population. An explanation for this may be that an exclusion criteria to undergoing a LN FNA included seropositivity for hepatitis B, C or HIV. Due to the local demographics of CLL patients at King's College Hospital many patients were excluded due to prior exposure to hepatitis B, where infection rates amongst our clinical CLL cohort approach 30% (personal correspondence Professor Stephen Devereux) and viral infections are often co-existent. An exclusion criteria to the study was previous treatment for CLL in the past 3 months, unfortunately further details of prior treatment history are unknown and this is a recognised as a limitation.

Firstly we confirmed the findings of many groups that there is an expansion in the T-cell compartment in the CLL PB compared to normal controls (Mellstedt and Choudhury 2006); with a greater than 3 fold expansion in the total lymphocyte count in the CLL group. An overall increase in CD4+ and CD8+ T-cell numbers in CLL PB with a decreasing ratio with advancing disease has been consistently reported (Herrmann, Lochner et al. 1982, Mills and Cawley 1982, Gonzalez-Rodriguez, Contesti et al. 2010, Nunes, Wong et al. 2012). We did not find a difference in the CD4/CD8 ratio between the CLL and the control group; in fact there were some CLL patients with a reversed low ratio and some with a relatively high ratio. Both high and low CD4/CD8 ratios have been previously described in CLL patients. Nunes et al recently reported CD4/CD8 ratios on a cohort of 110 patients and found an inverted ratio in 47%, where a marked CD8+ expansion had a shorter time to first treatment (Nunes, Wong et al. 2012). It

might seem counter intuitive that an increase in CD8+ T-cells associates with a poor prognosis, although it is hypothesised that the decrease in naïve subsets plays a role in rendering the patient immuno-incompetent, unable to mount an effective response to pathogens and new tumour antigens. These T-cells also have markers of "exhaustion", which is discussed below.

Some groups have related the variation in CD4/CD8 ratios to lymphocyte count. We did not find a clear correlation with lymphocyte count. Analysis by stage may only be informative with a larger cohort size. We did not pursue a larger cohort analysis of PB T-cells in CLL as our study was focused on identifying T-cell phenotype changes between the PB and LN compartments in the same patient, it is not a cohort study of the CLL population as a whole, which has been well documented by others.

The first comparative observation between the LN FNA and PB in the CLL cohort was the finding that there was a much higher percentage of CD3+ T-cells found within the lymphocyte gate of the LN FNA compared to PB; on average 18% and up to 43% of the total lymphocyte population were CD3+ T-cells compared to 4% in the PB of the same patients. Of these CD3+ T-cells there was a significant bias towards CD4+ T-cells in the LN FNA compared to PB. These results concurred with the few small histopathology series that have reported the T-cell component of a CLL lymph node to be up to 35% and show bias towards a CD4+ subset (Swerdlow, Murray et al. 1984, Schmid and Isaacson 1994, Bonato, Pittaluga et al. 1998, Granziero, Ghia et al. 2001). Very limited amounts of additional phenotyping has ever been performed on the T-cell compartment of the CLL lymph node and the differences we show here between the PB and LN FNA are being reported for the first time.

We have shown on subset analysis of the CD4+ T-cells that there is a statistically significant increase in number of CD4+ T_{EM} in the LN FNA compared to the PB; 68% versus 44%. The increase in the number of T_{EM} cells is a very significant finding. Other groups have reported that there is an increased number of effector CD4+ and CD8+ T-cells in the PB CLL patients compared to normal controls (Platsoucas, Galinski et al. 1982, Vuillier, Tortevoye et al. 1988, Totterman, Carlsson et al. 1989, Goolsby, Kuchnio et al. 2000, Nunes, Wong et al. 2012), but this has not been reported in the LN. T_{EM} cells lack markers such as CCR7 and CD62L, which

are usually required for efficient trafficking into the lymph node. Therefore CCR7- CD62L- T_{EM} cells, in a normal immune response to an infection, would not gain access and reside in the lymph node, but be directed to the site of infection or inflammation. It could be speculated that these T_{EM} cells are in the lymph node, because it is the lymph node itself that is the site of ongoing antigenic stimulation. There is supportive evidence of this theory from lymph node metastases in solid tumours. In melanoma it has been shown there is an increase in T_{EM} CD8+ T-cells in involved lymph nodes compared to non-involved nodes (Anichini, Scarito et al. 2003) and many groups have shown that in melanoma the T-cell response has specificity for tumour associated antigens (Lee, Yee et al. 1999). So these results support the hypothesis that in CLL the T-cells are responding to antigen within the lymph node. What is not known is the nature of the antigen; whether this is a tumour associated antigen, an autoantigen or an infectious agent remains to be elucidated and is beyond the scope of this study.

Several studies have shown that in otherwise healthy individuals those with CMV seropositivity have a decrease in CD4 and CD8 naïve T-cells and an increase in CD4 and CD8 memory T-cells, and this holds true in both the young and old (Looney, Falsey et al. 1999, Wikby, Johansson et al. 2002, Chidrawar, Khan et al. 2009, Litjens, de Wit et al. 2011). Pourgheysari et al have previously published that the absolute CD4+ T-cell numbers in CLL PB are the same regardless of CMV seropositivity (Pourgheysari, Bruton et al. 2010) and Nunes et al found the CD8+ expansion was not explained by CMV alone (Nunes, Wong et al. 2012). To identify if the skewing of the repertoire towards the T_{EMRA} subset was simply an effect of CMV in our study we compared the relative proportion of these cells in the CMV seropositive and seronegative individuals and found no difference in the relative proportion of CD4+ $T_{naïve}$, T_{CM}, T_{EM} and T_{EMRA} between CMV seropositive or negative patients in any compartment. There may be a trend towards more CD4+ T_{EMRA} in the PB of CMV positive individuals and this would need further investigation in a larger patient cohort. The observation of increased effector cell proportions vs naïve in our study remained between the LN and PB respectively irrespective of CMV serostatus. This gives further evidence that CMV in CLL is not responsible for all the T-cell perturbations.

Next we looked at the Treg subset and found they were significantly over-represented in the LN compared to the PB. Tregs are known to be increased in CLL PB and accumulate as disease progresses although the mechanism is not well understood (Beyer, Kochanek et al. 2005, Giannopoulos, Schmitt et al. 2008, Deutsch, Perry et al. 2009, Jak, Mous et al. 2009, D'Arena, Laurenti et al. 2011, Biancotto, Dagur et al. 2012, Nunes, Wong et al. 2012, D'Arena, Simeon et al. 2013, Lad, Varma et al. 2013). It could be that Treg numbers simply reflect disease burden or that they play a part in its progression. Some groups have suggested they can be used as a prognostic marker; although this doesn't help answer whether they are just innocent bystanders or involved in CLL pathogenesis (D'Arena, Simeon et al. 2013). Our results show they are found a higher frequencies in the LN than the PB. This raises the question what role are they playing in within the LN? Have they merely accumulated as a result of tumour or are they promoting the tumour by dampening down the immune response and allowing tolerance? As they have accumulated within the LN it is suggesting they are playing an active role and are thus a target for future study. A recent publication by Lad et al concurs with the results presented here. They also found a higher proportion of Tregs in the LN of CLL patients compared to the PB (Lad, Varma et al. 2015). They hypothesise that Tregs excrete IL-10 which in turn supress the Th17 cells allowing CLL to escape immune surveillance Some groups have used CD4+ CD25+ alone as a definition of Tregs which is an oversimplification. CD25 is upregulated on activated cells, a report by Jackson et al, has shown that up to 25% of CD4+ T-cells express CD25 in the PB of normal healthy controls (Jackson, Matsumoto et al. 1990). Patten et al previously reported, by immunofluorescence of lymph node sections, that the proliferating CLL cells are in close contact with CD4+ CD25+ but Foxp3-, activated T-cells (Patten, Buggins et al. 2008). Here no difference in the level of CD25+ expression on CD4+ T-cells of the LN FNA compared to PB was identified; 21% versus 18%.

Next we looked for evidence of CD40L on the CD4+ T-cells and almost no expression was seen. As previously discussed, the role of the CD40:CD40L interaction between T and CLL cells *in vivo* is not clear but it is well described that there is a defect in CD40L signalling in CLL. Cantwell et al investigated both PB and splenic CD4+ CLL T-cells and found, following CD3 ligation, no expression of CD40L by flow cytometry. Normal CD4+ T-cells produce CD40L

quickly and transiently upon stimulation. (Castle, Kishimoto et al. 1993, Roy, Waldschmidt et al. 1993). However Cantwell also reported that normal T-cells can acquire a defect in CD40L upregulation in the presence of CLL cells when cultured at ratios of >1:33. This is thought to be due to the expression of CD40 on CLL cells as blocking CD40 reversed the effect. Therefore there is an acquired CD40L defect in CLL (Cantwell, Hua et al. 1997). Our results concur with this finding and call into question the widespread use of CD40L transfected fibroblasts as an *in vitro* "model" of the CLL LN microenvironment.

The next step in this study was to investigate other markers of T-cell activation. Once the TCR engages its MHC-peptide complex, ligation of co-stimulatory molecules is required for T-cell activation. These primed T-cells express CD28 which bind to CD80 and CD86 on the antigen presenting cell which in turn promotes T-cell IL-2 secretion, activation and survival. Without CD28 ligation the T-cell undergoes apoptosis or is anergic. Repeated chronic antigenic stimulation eventually leads to CD28 downregulation and replicative senescence. Many studies have reported that there are increased CD28 negative T-cells in the PB of advanced CLL (Rossi, Matutes et al. 1996, Rossmann, Jeddi-Tehrani et al. 2003). In our study, when the total pool of CLL patients is examined, it appears there are more CD28 negative T-cells in the CLL PB compared to LN, albeit at low frequencies. This was of particular interest because CD28 negative T-cells are known to accumulate in the PB of patients with CMV seropositivity, although not exclusively (Walton, Lydyard et al. 2010, Nunes, Wong et al. 2012).

The next aim of this study was to investigate further the negative T-cell regulators. Following TCR engagement with antigen, T-cells require co-stimulatory signalling through CD28 and CTLA-4 is the negative counter-balance in this system. CTLA-4 also binds to CD80 and CD86 and downregulates the T-cell response. Several groups have reported that CTLA-4 levels were markedly increased on both CD4+, CD8+ T-cells and Tregs in CLL PB compared to healthy controls (Rossmann, Jeddi-Tehrani et al. 2003, Motta, Rassenti et al. 2005). We additionally show here that the cell surface expression of CTLA-4 is found at statistically higher levels in the LN FNA compared to the PB in the CD8+ T-cell subsets. There was also a trend toward increased levels in the CD4+ LN T-cells. The overall level of surface CTLA-4 on the CD4+ population was modest, but this may be a reflection of the fact that the majority of CTLA-

4 is cytoplasmic as it is rapidly endocytosed. Our results suggest that the T-cells are being stimulated in a TCR dependent manner within the LN. Higher levels of CTLA-4 in the LN would suggest that T-cells are being specifically inhibited in this compartment and which would be predicted to lead to T-cell anergy. Of note it has been observed by others that cytoplasmic CTLA-4 is also constitutively activated on Tregs and its expression can be further induced upon T-cell activation (Jonuleit, Schmitt et al. 2001). We did not specifically look at CTLA-4 on Tregs, nonetheless it can be hypothesised that CTLA upregulation on Tregs in the LN may further help CLL evade the immune system. These results would concur with other clinical scenarios where high levels of CTLA-4 have been reported on T-cells, for example in germinal centres, in the skin of patients with graft versus host disease and in the milieu of Hodgkin lymphoma (Vandenborre, Delabie et al. 1998), downregulating T-cell responses. Motta reported, as would be predicted, that blocking CTLA-4 using a monoclonal antibody on CLL derived T-cells resulted in T-cell proliferation (Motta, Rassenti et al. 2005). Therefore this axis has been considered for exploitation for therapeutic purposes. The challenge is manipulating this pathway could lead to unregulated CD4+ and CD8+ T-cell expansions which might be a double edged sword in CLL.

Another important negative T-cell regulator and a marker of T-cell exhaustion is PD-1. PD-1 has been shown to be upregulated in T-cells in response to chronic viral infections including CMV, HIV, adenovirus, hepatitis B and C (Yi, Cox et al. 2010). The theory of T-cell exhaustion, in an intact immune system, is that the T-cell eventually terminates its effective immune response towards the infected cell when it is stimulated over a long period of time and the pathogen is not effectively eradicated. This occurs by PD-1 interaction with its ligands PD-L1 or PD-L2, which leads to reduced signalling through ZAP-70 and PI3k leading to decreased sensitivity to antigenic stimulation (Baitsch, Legat et al. 2012). The PD-1 / PD-L1 axis is thought to be the major T-cell inhibitory pathway (Schietinger and Greenberg 2014). In our study PD-1 expression was significantly increased in both the CD4+ and CD8+ T-cells of LN FNA compared to the PB. This differential expression between the PB and the LN FNA would suggest that the major site where PD-1 is up-regulated is within the lymph node. This result was independent of CMV seropositivity, in keeping with previous reports from the PB (Nunes, Wong et al. 2012). These PD-1+ effector T-cells are then senescent and have low replicative

potential. Very interestingly in viral infections the PD-1 downregulation of the T-cell response can be reversed by blocking PD-1. This has been shown in both CMV and HIV infections where PD-1 blockade effectively leads to reversal of the T-cell exhaustion and allows the T-cell to reinitiate an effective immune response (Trautmann, Janbazian et al. 2006). There is now increasing evidence PD-L1 and PD-L2 is expressed on a variety of solid tumours and this axis can be targeted. PD-L1 / PD-L2 expression correlates with a negative prognosis in several of these malignancies including in ovarian, pancreas and renal cell carcinoma (Okazaki and Honjo 2007). We looked for evidence of PD-L1 or PD-L2 expression on CLL cells but only found very low levels and no difference between compartments. Grzywnowicz et al looked for evidence of PD-L1 on CLL surface and found it to be no different from normal controls although there was a shift in the MFI (Grzywnowicz, Zaleska et al. 2012). Interestingly they found no difference in the quantification of PD-L1 transcripts between CLL and normal B-cells, nor between CLL B-cells from the PB or BM. Our result concurs with the findings published by Xerri at el who found no evidence of PD-L1 on 18 LN sections of CLL/SLL patients (Xerri, Chetaille et al. 2008). A conflicting study has been published by Brusa et al which reported PD-L1 expression on LN CLL sections, where expression was localised in proliferating paraimmunoblasts (Brusa, Serra et al. 2013). Ramsay et al also report expression of PD-L1 by PB CLL cells and that the expression is higher in CLL LNs compared to reactive normal LNs (Ramsay, Clear et al. 2012). The reasons for these conflicting results are unclear but may relate to technical factors, such as cell preparation and antibody specificity.

Since the work on this thesis was completed there has been a huge amount of interest focusing on exploiting the PD-1 / PD-L1 axis in cancers. PD-1 expression has been identified by tumour infiltrating T-cells of many solid tumours. PD-1 blockade was first shown to expand the effector T-cell population and suppress the tumour cells in melanoma and colon cancer cell lines (Iwai, Terawaki et al. 2005, Curran, Montalvo et al. 2010). Since then there have been several clinical trials showing efficacy in, for example, melanoma (Wolchok, Hodi et al. 2013), Hodgkin lymphoma (Ansell, Lesokhin et al. 2015), non-small cell lung cancer and renal cancers (Brahmer 2012). So encouraging have been the results that the PD-1 blocker, Pembrolizumab, has been given advanced FDA approval in melanoma, giving it "breakthrough therapy designation" (Momtaz and Postow 2014). This is a fascinating concept in the context

of CLL, and begs the question what would happens if the CLL PD-1 axis is blocked. Recently a study has reported that the exhausted T-cells can be mimicked in the TCL1 mouse model of CLL and that this phenotype is induced by the tumour cells. They went on to show blockade of the PD-1 / PD-L1 axis can increase the cytotoxic potential of those T-cells (Gassner, Zaborsky et al. 2015). Brusa et al reported, in primary CLL cells, that blocking the PD-1 / PD-L1 axis *in vitro* with an anti-PD-L1 antibody lead to increased CD8+ IFN-γ expression, and conversely co-culture with recombinant soluble PD-L1 decreased IFN-γ levels (Brusa, Serra et al. 2013). This will be addressed further in chapter 6 of this thesis.

One interpretation of the results presented in this chapter is that the PD-1+ T-cells seen are exhausted antigen-stimulated T-cells, it must however also be remembered that PD-1 expression is found at high levels on Tfh cells (Dorfman, Brown et al. 2006). Little work has focused on the Tfh cells in CLL, although Ahearne et al reported increased numbers in CLL PB compared to normal controls (Ahearne, Willimott et al. 2013). The study presented here concurs with this finding where we identify higher levels of CD4+ CXCR5+ T-cells in the PB of CLL patients compared to healthy controls. Ahearne et al went on to investigate their major cytokines produced by Tfh cells, IL21 and IL4, and found that these promote leukaemic proliferation. We further investigated the CD4+ CXCR5+ phenotype by looking in the LN and found no difference between the LN and PB compartment. However we accept that dual positivity of CD4+ and CXCR5+ is an oversimplification of the definition of Tfh cells and that CXCR5 is also expressed on T_{CM} cells. Tfh cells are probably more accurately defined as CD4+ CXCR5+ ICOS+ PD-1hi. We found approximately 60% of CLL PB CD4+ T-cells were CXCR5+ compared to only 30% that were PD-1+. Therefore, by inference, the PD-1+ CD4+ T-cells we have described cannot all be Tfh cells. In the next chapter we study Tfh cells further by analysis on FFPE lymph node sections.

Taken together our results support the hypothesis that in CLL there is a T-cell population that is chronically stimulated by antigen within the lymph node which leads to an accumulation of effector T-cells. Furthermore, the data suggests that in the face of ongoing TCR stimulation there is upregulation of negative T-cell regulators including CTLA-4 and PD-1 which leads to termination of the immune response and renders the T-cell into a state of exhaustion. This

finding was independent of CMV seropositivity. To confirm these findings we sought to validate our results using multi-parameter staining of lymph node sections, which are detailed in the next chapter.

Chapter 4 Investigation of the T-cells in CLL Lymph Nodes by Multi-parameter Immunofluorescence Microscopy

4.1 Introduction

The lymph node fine needle aspirate study outlined in the previous chapter has provided new information on the phenotype of T-cells infiltrating the CLL LN microenvironment. To confirm these findings and to take this work further this chapter investigates a complimentary method of phenotyping the T-cells, and additionally looks for spatial relationships between T-cells and CLL cells within the lymph node microenvironment niche. This work develops the technique of multi-parameter immunofluorescence microscopy on formalin fixed, paraffin embedded (FFPE) lymph node sections. Microscopy on tissue sections has the major advantage that information can be gained regarding the *in vivo* architecture of the lymph node microenvironment and enables the visualisation of and spatial relationships of more than one cell type on a section simultaneously. This can help inform which cell types of interest should be studied further. Additionally it can be possible to locate an antigens cellular localisation. It is well established that cells within the microenvironment promote CLL survival and proliferation including T-cells (Patten, Devereux et al. 2005, Kiaii, Kokhaei et al. 2013). *In vitro* co-culture models attempt to recapitulate the microenvironment but few studies have investigated the *in vivo* architecture of lymph nodes. Previous work from our group provides evidence that proliferating CLL cells are in close contact with CD4+ CD25+ T-cells *in vivo* (Patten, Buggins et al. 2008). The aim of this chapter is to further characterise the LN T-cells and specifically to look for evidence of antigen exposure in these cells and investigate their interaction with proliferating CLL cells.

4.1.1 Experimental Approach

The aim of this chapter is to optimise the technique of multiparameter immunofluorescence microscopy on lymph node sections and then further phenotype the infiltrating T-cells. As the work in chapter 3 identified PD-1 expression to be differentially expressed in CLL PB and LN FNA samples, an overall aim was to confirm the presence of this antigen on the T-cells found within LN biopsy specimens. This would also enable us to identify if there was any spatial

proximity between proliferating Ki67+ CLL cells and PD-1+ T-cells. A supplementary aim was to look for any evidence that these T-cells were infiltrating follicular T-helper (Tfh) cells, which are known to express high levels of PD-1 in normal germinal centres (Dorfman, Brown et al. 2006, Wang, Hillsamer et al. 2011).

The disadvantages of studying FFPE lymph node biopsy sections have been detailed in chapter 3. In summary, access to lymph node excision biopsy specimens is limited as lymph nodes are now rarely removed diagnostically and CLL can usually be diagnosed from the PB obviating the need for removing lymph node tissue. Additionally when lymph nodes are excised it is usually in specific circumstances, such as when a patient presents with out of proportion lymphadenopathy to the WCC or when there is a solitarily large node and a high grade (Richter's) transformation needs to be excluded; which makes this a highly selected population. As a tissue biopsy usually does not alter treatment decisions for an individual patient, it can usually be avoided and therefore access to CLL lymph nodes is limited. In order to overcome this problem we considered the possibility of removing lymph nodes from patients for research purposes only. We did not pursue obtaining ethical approval for such a study as, although there is precedent from other groups, we felt it was inappropriate for patients to undergo such an invasive procedure for the purposes of research alone.

A second option was to prospectively tissue bank fresh frozen lymph nodes removed from patients for diagnostic purposes with matched PB, bearing in mind this only happened in specific circumstances. We have successfully obtained ethical permission for this study although eligible patient numbers are small. Therefore we chose to proceed with utilising the CLL lymph nodes archived by the KCHFT histopathology department, for which we had ethical approval to use surplus material from, in an anonymised fashion. These specimens were all FFPE, which limits the range of investigations that can be performed and we do not have matched PB for comparison, nonetheless the material is still valuable to study.

The archived lymph node tissue sections are a scarce resource and therefore the initial optimisation of cell staining was undertaken using B-cells, selected from previously cryopreserved PBMCs from CLL patients, settled onto slides. This approach enabled the gaining of invaluable experience in the cell staining techniques without wasting primary lymph

node material. This technique, described below, involved settling CLL cells onto poly-lysine slides and indirectly labelling with antibodies conjugated to fluorochromes, allowing for immunofluorescence microscopy.

4.1.2 Immunofluorescence Microscopy

Microscopy has made huge advances from its origins as a simple magnifier to the confocal imaging that can be performed today. Originally it was a single lens system with a fixed tube length; now multiple lenses are configured to provide what is known as "infinity optics". Conventional light microscopy and standard tissue staining techniques allow excellent visualisation of tissues but are limited in that morphology alone is used to distinguish between different cell types. Immunohistochemistry revolutionised light microscopy, allowing specific cell types to be identified by the use of antibodies. However, this still has major limitations in that only one specific marker can be identified at a time on an individual tissue section. Immunofluorescence microscopy allows the visualisation of more than one antigen on the same section by taking advantage of the different light properties of the secondary fluorescent antibodies and the development of filter sets within microscopes. In fluorescence microscopy the target antigen is labelled with a primary antibody which is in turn targeted by a secondary antibody (with specificity to the species of the first), conjugated to a fluorochrome. Specific fluorochromes predictably absorb light and emit light at known wavelengths. Good fluorochromes have a high "quantum yield", meaning that there is a favourable ratio of the emitted light versus absorbed photons, and a barrier filter is used when viewing the specimen so that only the emission spectra is transmitted back to the eyepiece/camera. This allows cells with the attached fluorescent molecules to be visualised against a black background. The principle of immunofluorescence has been discussed in chapter 2.

A graphical schema of the optics of an inverted fluorescence microscope is shown in Figure 4-1.

1. Intermediate image plane phototube
2. Eyepiece
3. Intermediate image plane frontport
4. Intermediate image plane baseport
5. Beam path switch
6. Sideport prisms
7. Tube lens
8. Analyser
9. Reflector module
10. Luminous field diaphragm
11. Aperture diaphragm
12. Filter slider
13. HBO lamp
14. HAL lamp
15. Luminous field diaphragm
16. Polariser
17. Aperture diaphragm
18. Condenser
19. Objective

Figure 4-1 Fluorescence microscope light beam path (Axiovert 200 diagram modified from Carl Zeiss)

4.2 Aim

The ultimate aim of this chapter is to optimise a method of immunofluorescence staining and systematic analysis of FFPE LN sections, in order to assess the phenotype of the infiltrating T-cells and to examine the spatial organisation of these cells in relation to the proliferating tumour cells in CLL.

4.3 Materials and Methods

4.3.1 Ethics

PB was collected from CLL patients with ethical approval NREC: 08/H0906/94 044. Written informed consent was gained according to the Declaration of Helsinki, 2008. Ethical approval was obtained for use of surplus anonymous lymph node biopsy samples for research from the national research ethics service (NRES 08/H0906/94) and local research ethics committee (LREC 02-044).

4.3.2 Patient Material

CLL PBMCs were isolated from PB using Ficoll Histopaque® (Sigma Aldrich) density centrifugation and aliquots were stored frozen in liquid nitrogen as described in 2.2.2. Lymph node excision biopsies were performed on CLL patients as part of their routine clinical care. FFPE blocks were cut into 3 micron sections and mounted onto glass microscope slides by the Department of Histopathology, King's College Hospital NHS Foundation Trust (KCHFT). A total of 15 LN biopsy samples were available in an anonymous fashion.

4.3.3 PBMC Slide Preparation

CLL PBMCs were cultured, after defrosting, in CLL medium at a concentration of 1×10^6/ml as previously described in 2.5.1. B-cells were selected as in 2.2.5. 2×10^6 B-cells were resuspended in 400µl CLL media and dropped onto poly-l-lysine coated slides (Polysine, Menzel-Glaser) within an area bounded by an ImmEdge™ pen (Vector laboratories, Inc.) and allowed to settle for 24 hours at 37°C. Excess media was removed under suction. Cells were fixed with paraformaldehyde for 2 hours. Slides were then washed x3 with PBS. For permeabilisation Triton 0.5% was added for 10 minutes per slide. Slides were then again washed x3 PBS.

4.3.4 FFPE Antigen Retrieval

FFPE sections were dewaxed in xylene (Fisher Scientific) twice for 5 minutes. The slides were then rehydrated in ethanol-water of decreasing grades (100%, 96%, 96%, 70% and 50%) for 10 minutes each. The slides were subsequently washed with water. Antigen retrieval was performed using citrate buffer pH 6.0 in a pressure cooker. Slides were pressure cooked at 15 pounds per square inch for 3 minutes and subsequently cooled in water. This was performed in the KCHFT department of histopathology.

4.3.5 Immunofluorescence Antibodies

The primary antibodies used are listed in Table 4-1. All primary antibodies used on the same section must be raised in a different species to allow detection by species specific secondary conjugates. The secondary fluorescently conjugated antibodies were all raised in donkey and are listed in Table 4-2. The excitation and emission spectra of the secondary antibodies are listed in Figure 3-1. The concentration of antibody that yielded the best signal with the least background fluorescence was determined by serial dilution; these are shown below.

Table 4-1 Primary antibodies for immunofluorescence microscopy

Antigen	Species	Clone	Dilution	Manufacturer
CD3	Rabbit	Polyclonal IgG	1 in 40	Abcam
CD4	Mouse	IgG1: 4B12	1 in 10	Novocastra
CD4	Rabbit	Polyclonal IgG	1 in 40	Abcam
CD23	Goat	Polyclonal IgG	1 in 30	R&D Systems
CD38	Mouse	IgG1	1 in 100	AbD Serotec
CD49d	Rabbit	Polyclonal IgG	1 in 40	AbD Serotec
CD79a	Goat	Polyclonal IgG	1 in 40	Santa Cruz
Ki67	Mouse	IgG1: MM1	1 in 100	Novocastra
Ki67	Rabbit	Polyclonal IgG	1 in 100	Abcam
PD-1	Goat	Polyclonal IgG	1 in 30	R&D Systems
CXCR5	Rat	IgG2: RF8B2	1 in 40	BD Biosciences

Table 4-2 Secondary fluorescently conjugated antibodies for immunofluorescence microscopy

Target	Species	Conjugate	Dilution	Manufacturer
Goat IgG (H+L)	Donkey	Cy™5	1 in 100	Jackson ImmunoResearch
Goat IgG (H+L)	Donkey	FITC	1 in 100	Jackson ImmunoResearch
Mouse IgG (H+L)	Donkey	Cy™3	1 in 100	Jackson ImmunoResearch
Mouse IgG (H+L)	Donkey	DyLight™ 488	1 in 100	Jackson ImmunoResearch
Mouse IgG (H+L)	Donkey	Alexa Fluor® 555	1in 100	Invitrogen
Rabbit IgG (H+L)	Donkey	FITC	1 in 50	Jackson ImmunoResearch
Rabbit IgG (H+L)	Donkey	Cy™3	1 in 100	Jackson ImmunoResearch
Rabbit IgG (H+L)	Donkey	Cy™5	1 in 100	Jackson ImmunoResearch
Rat IgG (H+L)	Donkey	FITC	1 in 50	Jackson ImmunoResearch
Rat IgG (H+L)	Donkey	DyLight™ 549	1 in 100	Jackson ImmunoResearch
Rat IgG (H+L)	Donkey	AMCA	1 in 100	Jackson ImmunoResearch

4.3.6 Immunofluorescence Labelling

Following optimisation the final method for immunofluorescence staining of settled PBMCs and antigen retrieved FFPE lymph node sections is described below.

A circle was drawn onto the slide around the visible specimen with ImmEdge™ pen (Vector laboratories Inc.). The sections were next pre-hydrated in PBS for 30 minutes. The PBS was removed and 5% donkey serum (Jackson ImmunoResearch) added for 1 hour at 4°C to block non-specific antibody binding. Primary antibodies were diluted in PBS as listed in Table 4-1. A final volume of 400µl was added to each slide, which was incubated for 2 hours at RT. Primary antibodies were removed by washing the slide for 10 minutes in PBS 3 times. The secondary antibodies were diluted according to Table 4-2 and 400µl of final solution was added to each slide, which was incubated for 2 hours at RT in the dark. Samples were again washed for 10 minutes in PBS 3 times. Slides were carefully dried and a mounted with a coverslip using ProLong® gold antifade reagent (Invitrogen). Negative, single and multiply stained slides were prepared for each sample. For the multi-parameter staining experiments, all secondary antibodies were added to the negative and single labelled controls to control for non-specific binding.

4.3.7 Microscopy and Image Acquisition

Multi-parameter fluorescence microscopy was performed using the Zeiss Axiovert 200 inverted microscope system (Carl Zeiss MicroImaging). The microscope is fitted with the following objectives; LD Plan-NeoFluor 20x/0.4, Plan-Apochromat 40x/1.0 oil iris, Plan-Apochromat 100x/1.0 oil iris. The microscope is fitted with four filter cube sets allowing a maximum of four colour visualisation, the set up allows for visualisation with DAPI, FITC, Cy3 and Cy5. Therefore a single slide can be labelled with a maximum of four fluorochromes (antigens). The filter cubes must be manually put in place to acquire the image produced by the associated fluorochrome. There will be some spectral overlap as other fluorochromes present on the slide may also be excited / visualised to some extent depending on the wavelength. A single image is captured for each fluorochrome through the appropriate filter and then the final image is constructed by overlaying the images generated from each fluorochrome. The exposure times were optimised for minimal autofluorescence and then

consistently applied across the sections. Random microscope fields for each slide were chosen for image capture, avoiding areas of haemorrhage. Images were captured using AxioCam MRm high resolution microscopy camera (Carl Zeiss MicroImaging) and image analysis was performed on AxioVisonLE software (Carl Zeiss MicroImaging) and NIS Elements AR Microscope Imaging Software (Nikon Corporation, Tokyo, Japan).

4.4 Results 1 – Optimisation Experiments

4.4.1 Immunofluorescence labelling of settled cells

Due the limited availability of the primary lymph node tissue samples we first undertook optimisation experiments by indirect immunofluorescence labelling of CLL cells settled on poly-lysine slides. Initially we opted to use directly conjugated antibodies but this method did not provide an adequate fluorescent signal for detection (data not shown). A combination of CD5, CD79a, CD38, CD49d and Ki67 primary antibodies were used to optimise the technique as these antibodies have been successfully used previously in our laboratory. The major technical challenges of this pilot was ensuring that the immunofluorescence staining was specific, with positive and negative controls showing no non-specific binding. An example matrix of controls is shown in Table 4-3 below. This shows that for dual antigen staining on a single specimen an additional 4 control slides were required.

Table 4-3 Immunofluorescence control slide matrix
Five slides are required for adequate positive and negative controls of two colour immunofluorescence staining on slides. Matrix is as follows: A1 (negative control), A2 (DAPI and both secondary antibodies), A3 (DAPI and primary 1 and both secondary antibodies), A4 (DAPI, primary 2 and both secondary antibodies), A5 (DAPI, primary 1 and 2 and both secondary antibodies).
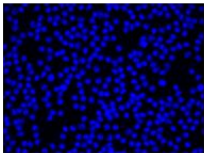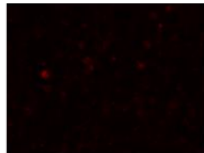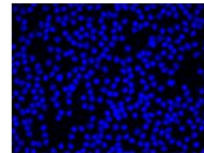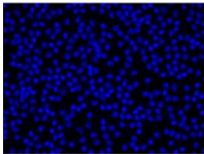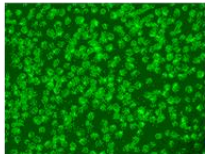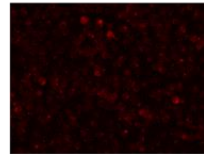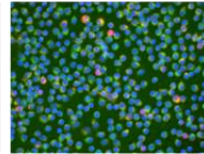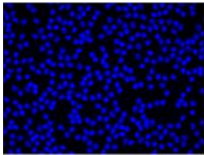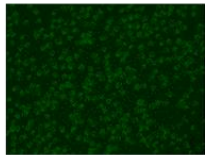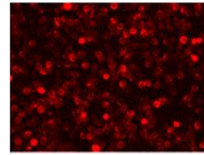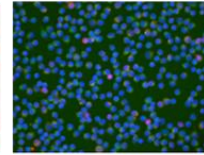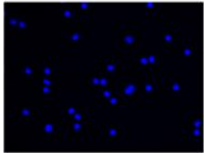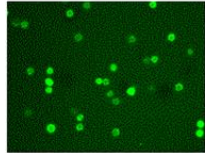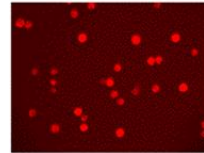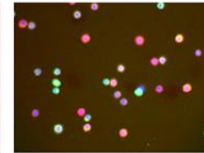
Slide	DAPI	Primary 1	Primary 2	Secondary to Primary 1	Secondary to Primary 2
A1	-	-	-	-	-
A2	✓	-	-	✓	✓
A3	✓	✓	-	✓	✓
A4	✓	-	✓	✓	✓
A5	✓	✓	✓	✓	✓

Images were captured for each of the control slides separately, using all the filters of the microscope with the exposure time optimised and then consistently applied. The manual nature of the specific microscope set-up in our laboratory made controlling the exposure times a critical step in the image acquisition. Initially optimising controls and non-specific binding of secondary antibodies to cells in the absence of a primary antibody was problematic. This was overcome by a series of stepwise experiments changing incubation times, adding an additional blocking step with donkey serum and from gaining technical expertise with the microscope. An example of the acquired images from the matrix in above Table 4-3 is shown in Table 4-4 below, showing successful staining of settled PBMCs.

Table 4-4 Staining matrix of settled CLL B-cells on slides
Selected CLL B-cells were allowed to settle for 24 hours and labelled as described. Positive and negative control slides are stained as per the matrix outlined in Table 4-3. Multi-parameter fluorescence microscopy was performed using the Zeiss Axiovert 200 inverted microscope system (Carl Zeiss MicroImaging). A single image is captured for each fluorochrome through the appropriate filter and then the final overlay image is constructed by overlaying the images generated from each fluorochrome channel. The exposure times were optimised for minimal autofluorescence and then consistently applied across the sections. Images were captured using AxioCam MRm high resolution microscopy camera (Carl Zeiss MicroImaging).

Slide	Channel			
	DAPI	Secondary 1	Secondary 2	Overlay
DAPI No Primaries Secondaries 1&2				
DAPI Primary 1 Secondaries 1&2				
DAPI Primary 2 Secondaries1&2				
DAPI Primaries 1&2 Secondaries 1&2				

4.4.2 Fluorescence labelling of lymph node sections

Once the technical skills of slide labelling were achieved the next step was to successfully singly label FFPE lymph node sections with fluorescence markers. The multiparameter immunofluorescence staining of FFPE lymph node posed many technical challenges that were not experienced to such a degree with settled cells on slides. The first issue encountered was that of autofluorescence. Autofluorescence is well known to create significant issues in fluorescence microscopy and is based on the fact that many biological molecules have inherent fluorescent properties and the emission spectra tends to wide compared to the narrow spectra of fluorescence probes (Van de Lest, Versteeg et al. 1995). Significant molecules in human tissues exhibit this phenomenon including elastin, collagen, fibronectin and lipofuscin; this is natural fluorescence. Formaldehyde has properties of fixative-induced fluorescence, this is caused when aldehydes react with amines and proteins resulting in a fluorescent product which is seen in the green (FITC) channel (Billinton and Knight 2001). The best ways of minimising this issue is by carefully choosing the excitation wavelength, excitation power and microscope aperture, fluorochrome and to perform filtering during image acquisition. If a weak fluorochrome is used or an antigen expressed at low density it can be difficult to visualise on a background of autofluorescence. If these considerations are not taken into account misinterpretation of results can result. FFPE lymph node samples exhibit high levels of autofluorescence, which is most significantly related to formaldehyde and also elastin and collagen in blood vessel walls and which can be visualised readily.

Figure 4-2 is a cautionary example, where a slide section image is captured with no primary or secondary fluorescence antibody present at all. This image is obtainable simply by increasing the cameras exposure time in the FITC channel.
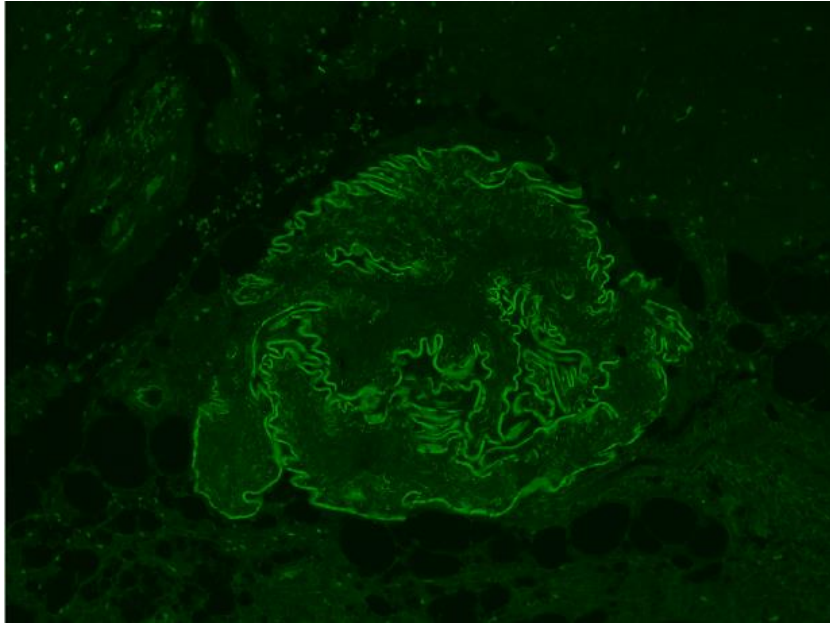
Figure 4-2 Autofluorescence in unstained CLL lymph node in FITC channel, magnification x10
This example FFPE section of a CLL lymph node was dewaxed, rehydrated and antigen retrieved using a citrate buffer as described. Multi-parameter fluorescence microscopy was performed directly using the Zeiss Axiovert 200 inverted microscope system (Carl Zeiss MicroImaging). No primary of secondary antibodies are present. This image was captured in the FITC channel using the AxioCam MRm high resolution microscopy camera (Carl Zeiss MicroImaging) demonstrating autofluorescence.

This highlights the need for strict negative controls in all fluorescence experiments. Several technical protocols are available to try and reduce the fixative induced fluorescence, for example using sodium borohydride or trypan blue. During this period of initial optimisation experiments CLL lymph node sections and normal reactive lymph nodes were labelled with antibody combinations previously used in our laboratory.

Figure 4-3 shows the successful labelling of CLL B-cells with CD23 using a donkey anti-goat Cy5 secondary antibody. The negative controls showed no background fluorescence.

Following considerable optimisation, single immunofluorescence staining of CD4 in a CLL LN is shown in Figure 4-4 using the Cy3 channel.
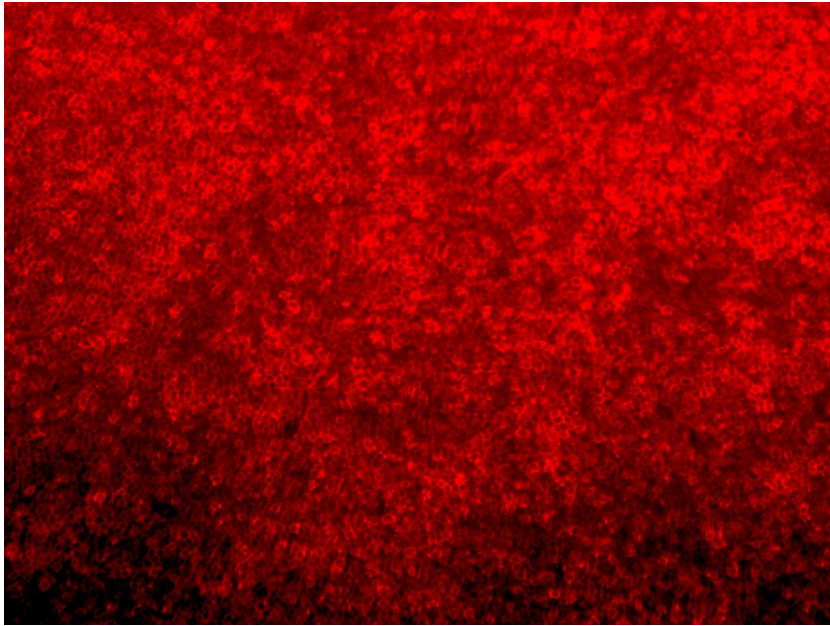
Figure 4-3 CD23+ CLL cells labelled with Cy5 (red), magnification x10
This example CLL LN FFPE section was processed as described in Figure 4-2. The sample was labelled with the primary antibody CD23 (goat) and the secondary antibody conjugated to Cy5 (donkey anti-goat IgG). This image was captured in the Cy5 channel using the AxioCam MRm high resolution microscopy camera. The negative controls showed no background fluorescence.
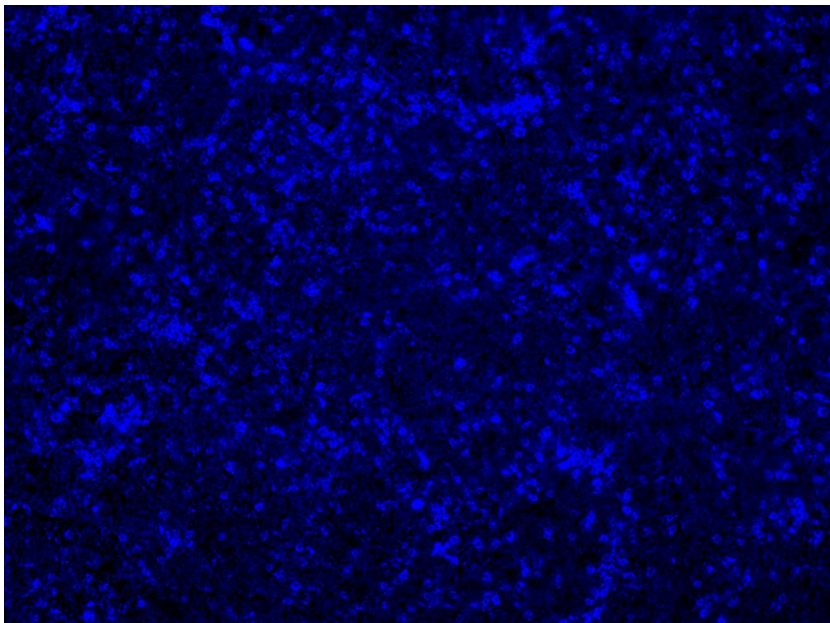
Figure 4-4 CD4 labelled with Cy3 (blue) in a CLL lymph node, magnification x10
This example CLL LN FFPE was labelled with the primary antibody CD4 (mouse) and the secondary antibody conjugated to Cy3 (donkey anti-mouse IgG). This image was captured in the Cy3 channel using the AxioCam MRm high resolution microscopy camera. The negative controls showed no background fluorescence.

In order to validate the findings from the LN FNA analysis in chapter 3, we next sought to

optimise PD-1 labelling. Successful staining with PD-1 in the Cy5 channel is shown in a normal

lymph node in Figure 4-5 and a CLL lymph node section is shown in Figure 4-6.
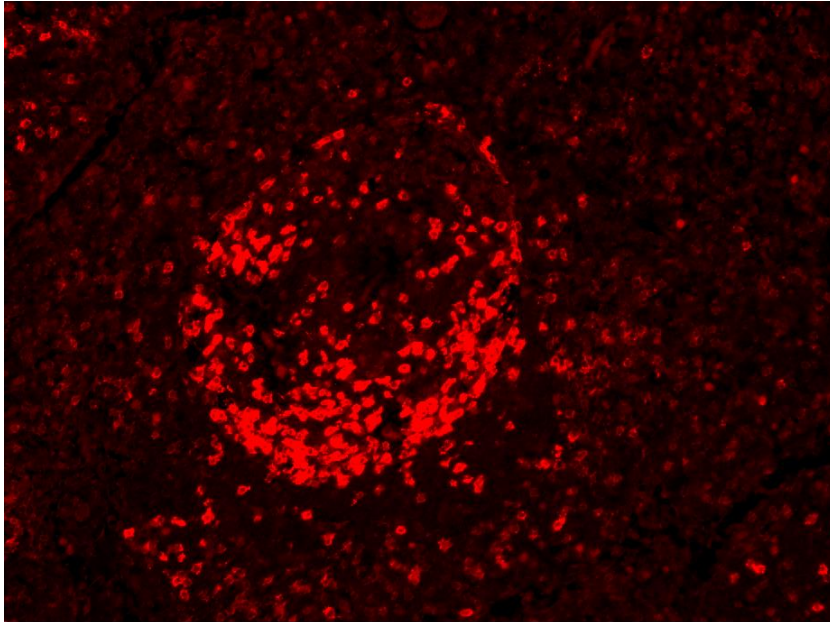
Figure 4-5 PD-1 labelled with Cy5 (red) in a normal reactive lymph node, magnification x10
This example normal reactive LN FFPE was labelled with the primary antibody PD-1 (goat)
and the secondary antibody conjugated to Cy5 (donkey anti-goat IgG). This image was
captured in the Cy5 channel using the AxioCam MRm high resolution microscopy camera.
The negative controls showed no background fluorescence.
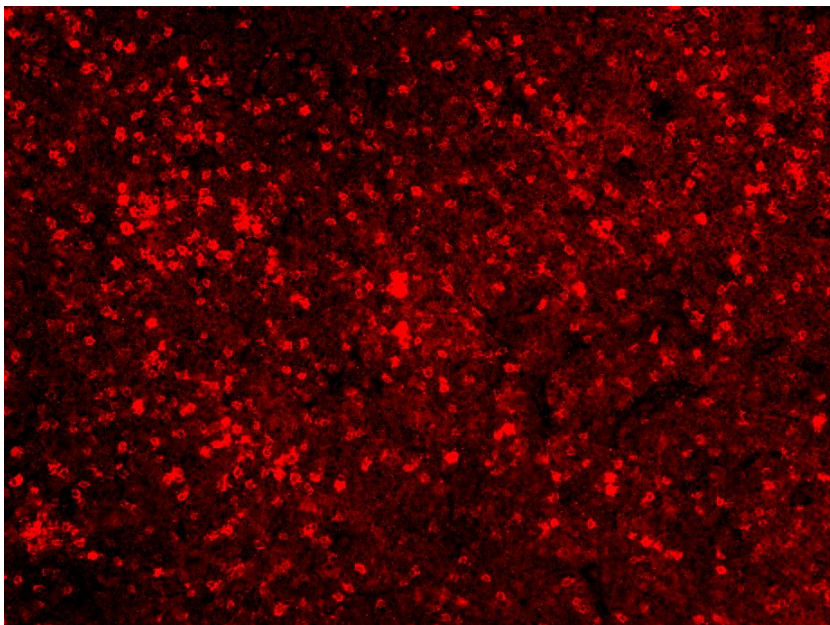
Figure 4-6 PD-1 labelled with Cy5 (red) in a CLL lymph node, magnification x10
This example CLL LN FFPE was labelled with the primary antibody PD-1 (goat) and the
secondary antibody conjugated to Cy5 (donkey anti-goat IgG). This image was captured in
the Cy5 channel using the AxioCam MRm high resolution microscopy camera. The negative
controls showed no background fluorescence.

The most striking visual observation of the PD-1 fluorescence pattern in CLL was the apparently random, less bright and diffuse expression in CLL compared to the bright and organised pattern in the normal reactive node, where the structure of a reactive germinal centre can be observed.

As the ultimate aim of this study was to examine the relationship between proliferating CLL cells and T-cells we decided to utilise Ki67 as a marker of proliferation. Ki67 was first optimised using the secondary donkey anti-rabbit antibody conjugated to Cy3. However this was subsequently substituted by donkey anti-rabbit FITC secondary antibody. As discussed autofluorescence is most marked in the FITC channel, therefore as Ki67 has a very specific nuclear staining pattern it was much easier to identify genuinely positive cells from the background of autofluorescence than when FITC was used for a cytoplasmic antigen. Post-acquisition image analysis was made much less complicated following this change.

A normal reactive lymph node, shown in Figure 4-7, is labelled with Ki67 in (FITC). This image clearly shows the architecture of a normal germinal centre. Figure 4-8 and Figure 4-9 shows the Ki67+ distribution in a representative CLL sample.
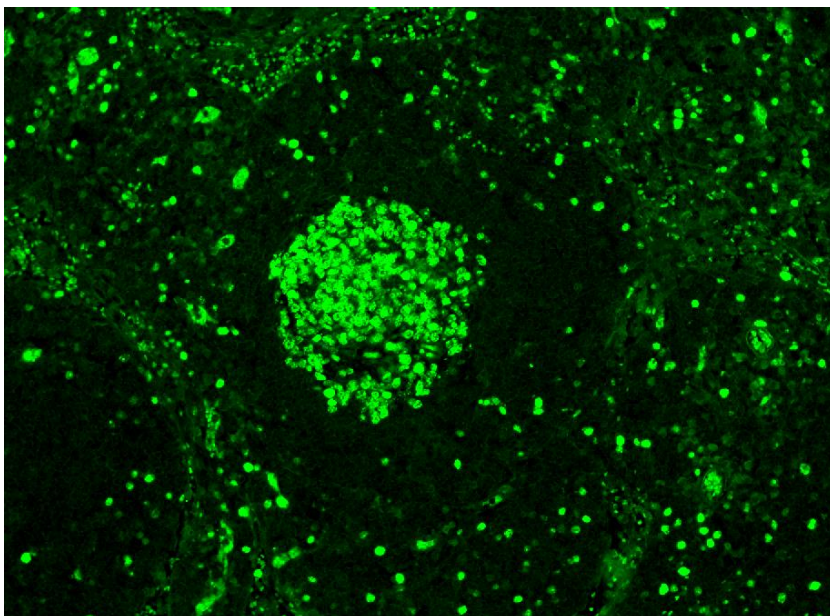
Figure 4-7 Ki67 green labelled with FITC (green) in a normal germinal centre, magnification x10
This example normal reactive LN FFPE was labelled with the primary antibody Ki67 (rabbit) and the secondary antibody conjugated to FITC (donkey anti-rabbit IgG). This image was captured in the FITC channel using the AxioCam MRm high resolution microscopy camera. The negative controls showed minimal background autofluorescence.
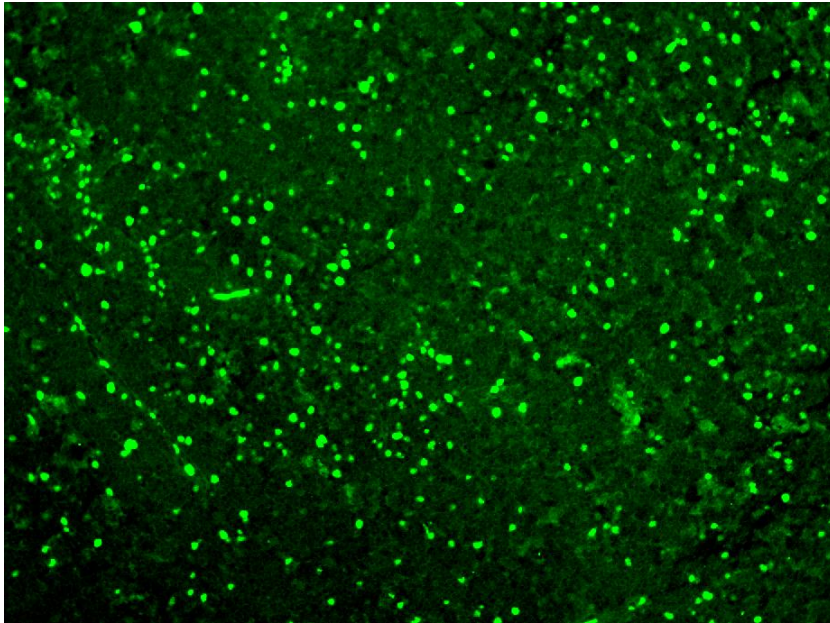
Figure 4-8 Ki67 cells labelled with FITC (green) in a CLL lymph node, magnification x10
This example CLL LN FFPE was labelled with the primary antibody Ki67 (rabbit) and the secondary antibody conjugated to FITC (donkey anti-rabbit IgG). This image was captured in the FITC channel using the AxioCam MRm high resolution microscopy camera. The negative controls showed minimal background autofluorescence.
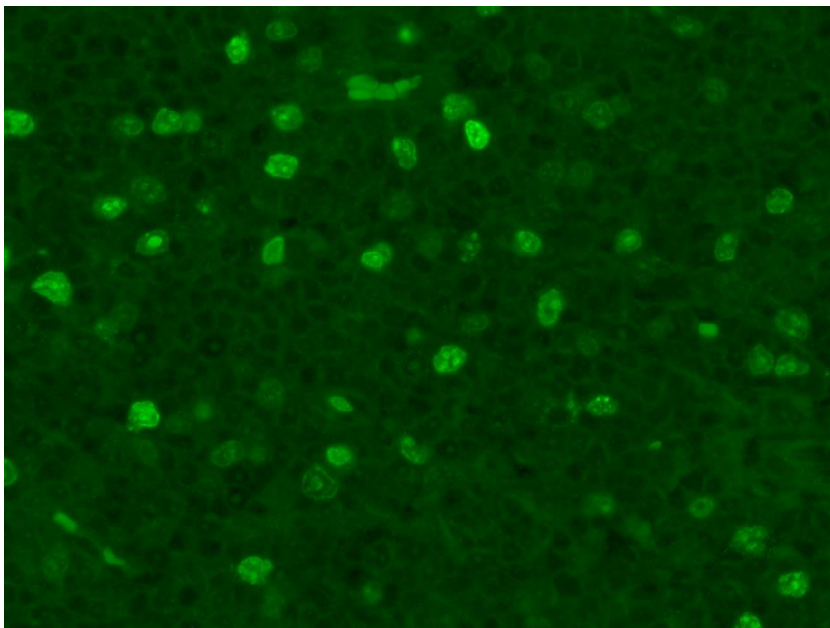
Figure 4-9 The nuclear staining of Ki67 can be appreciated at high power, magnification x 40
High power visualisation of the CLL LN shown in Figure 4-8.

The normal reactive lymph node, shown in Figure 4-7, labelled with Ki67, shows the architecture of a normal reactive germinal centre. This pattern was in stark contrast to the diffuse fluorescence pattern seen in CLL in Figure 4-8 and Figure 4-9. In all the cases examined the pattern was visually comparable between lymph nodes of different patients. No residual normal germinal centres were seen in any of the CLL cases in this study. Additionally there was no clear evidence of areas with a higher concentration of Ki67 cells, which may have been anticipated to correlate with "proliferation centres", which can be identifiable as pale staining areas by conventional immunohistochemistry using Haematoxylin and Eosin (H&E).

4.4.3 Multiparameter immunofluorescence of lymph node sections

Following on from the single labelling studies, we proceeded to dual and triple labelling of the tissue sections. Figure 4-10 and Figure 4-11 shows the successful staining of CLL LNs with CD23+ and proliferating Ki67+ cells in the same section.
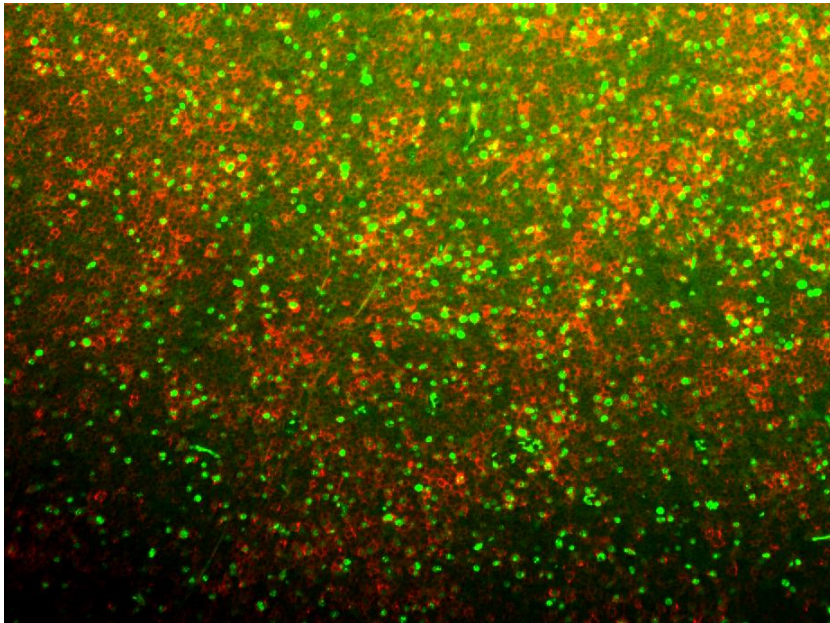
Figure 4-10 CD23 labelled with Cy5 (red) and Ki67 labelled with Cy3 (green) in a CLL lymph node, magnification x10
This example CLL LN FFPE was labelled with two primary antibodies; CD23 (goat) and Ki67 (rabbit) and both secondary antibodies, one conjugated to Cy5 (donkey anti-goat IgG) and the other to FITC (donkey anti-rabbit IgG). Images were captured in the Cy5 and FITC channels using the AxioCam MRm high resolution microscopy camera. The negative controls showed minimal background autofluorescence. The Image shown is the overlay from the two images acquired and visualised using AxioVisonLE software.
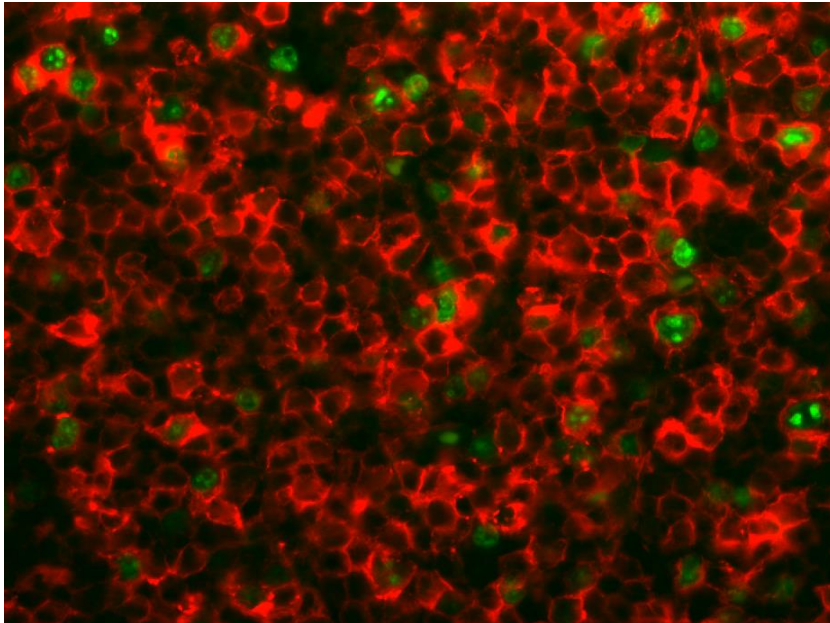
Figure 4-11 CD23 labelled with Cy5 (red) and Ki67 labelled with Cy3 (green) in a CLL lymph node, magnification x40
High power visualisation of the CLL LN shown in Figure 4-10.

Next we performed dual labelling of CD4+ cells and Ki67. A normal reactive lymph node is

shown in Figure 4-12 and a CLL lymph node in Figure 4-13.
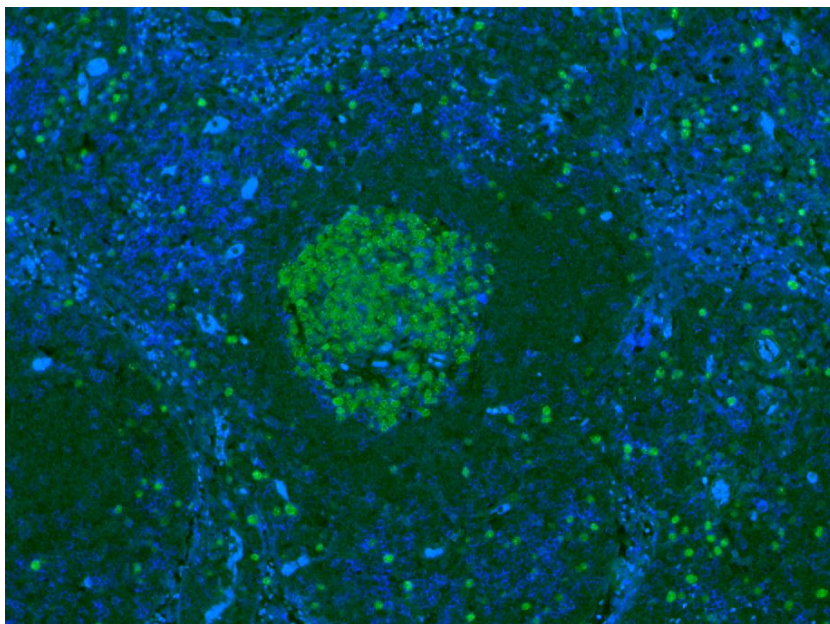
Figure 4-12 Ki67 labelled with FITC (green) and CD4 with Cy3 (blue) in a normal lymph node, magnification x10
This example normal reactive LN FFPE was labelled with two primary antibodies; Ki67 (rabbit) and CD4 (mouse) and both secondary antibodies, one conjugated to FITC (donkey anti-rabbit IgG) and the other to Cy3 (donkey anti-mouse IgG). Images were captured in the FITC and Cy3 channels using the AxioCam MRm high resolution microscopy camera. The negative controls showed minimal background autofluorescence. The Image shown is the overlay from the two images acquired and visualised using AxioVisonLE software.
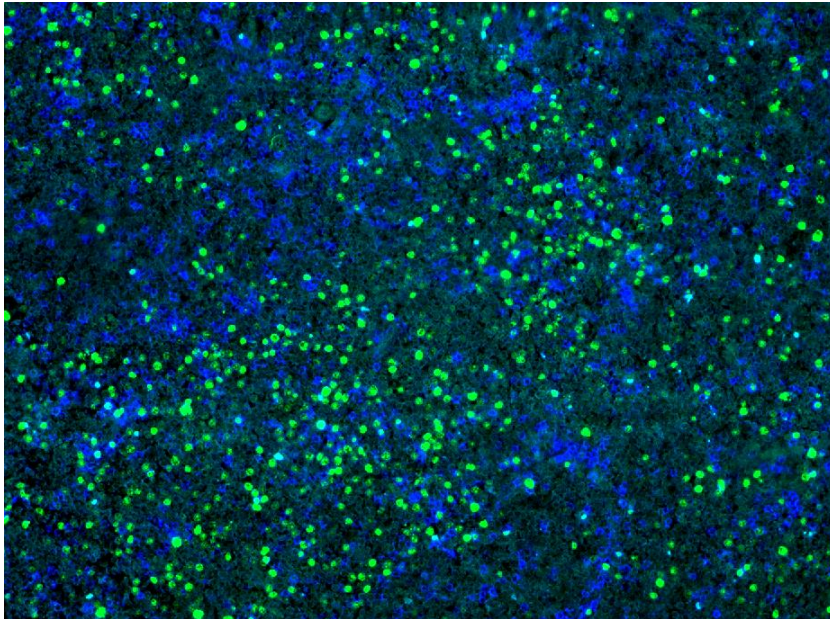
Figure 4-13 Ki67 labelled with FITC (green) and CD4 with Cy3 (blue) in a CLL lymph node, magnification x10
This example CLL LN FFPE was labelled with two primary antibodies; Ki67 (rabbit) and CD4 (mouse) and two secondary antibodies, one conjugated to FITC (donkey anti-rabbit IgG) and the other to Cy3 (donkey anti-mouse IgG). Images were captured in the FITC and Cy3 channels using the AxioCam MRm high resolution microscopy camera. The negative controls showed minimal background autofluorescence. The Image shown is the overlay from the two images acquired and visualised using AxioVisonLE software.

Following this, CLL lymph node sections were successfully labelled with 3 markers. First

CD23, CD4 and Ki67, see Figure 4-14. This shows the close proximity of Ki67+ CLL cells with

CD4+ T-cells, as previously reported by our group (Patten, Buggins et al. 2008).
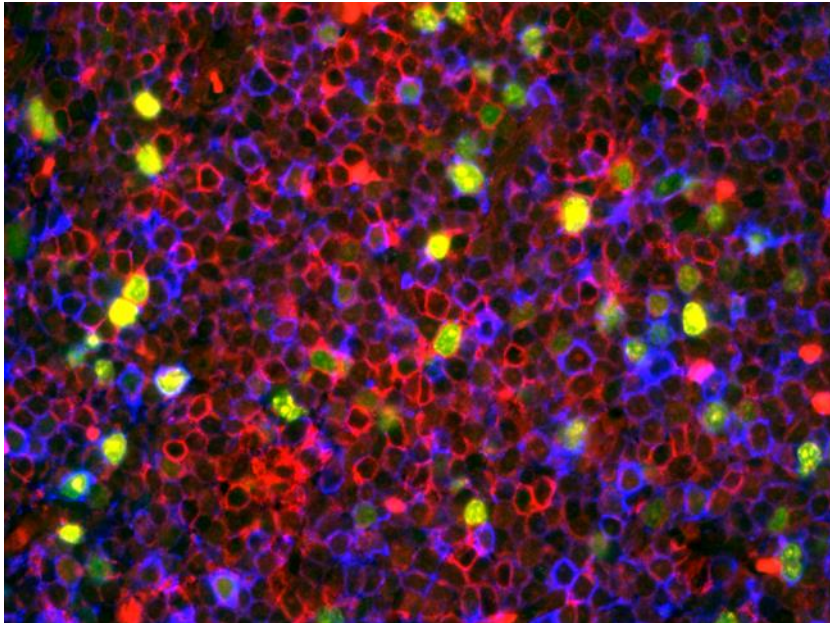
Figure 4-14 CLL lymph node triple labelled with CD23 (red), CD4 (blue) and Ki67 (green), magnification x40

This example CLL LN FFPE was labelled with three primary antibodies; CD23 (goat), Ki67 (rabbit) and CD4 (mouse) and three secondary antibodies, one conjugated to Cy5 (donkey anti-goat IgG), one to FITC (donkey anti-rabbit IgG) and the other to Cy3 (donkey anti-mouse IgG). Images were captured in the Cy5, FITC and Cy3 channels using the AxioCam MRm high resolution microscopy camera. The negative controls showed minimal background autofluorescence. The Image shown is the overlay from the three images acquired and visualised using AxioVisonLE software.

As the main purpose of this work was to investigate PD-1hi T-cells we next optimised the multicolour staining with PD-1. PD-1 and Ki67 dual labelling in a normal germinal centre is shown in Figure 4-15 and a representative CLL lymph node in Figure 4-16.
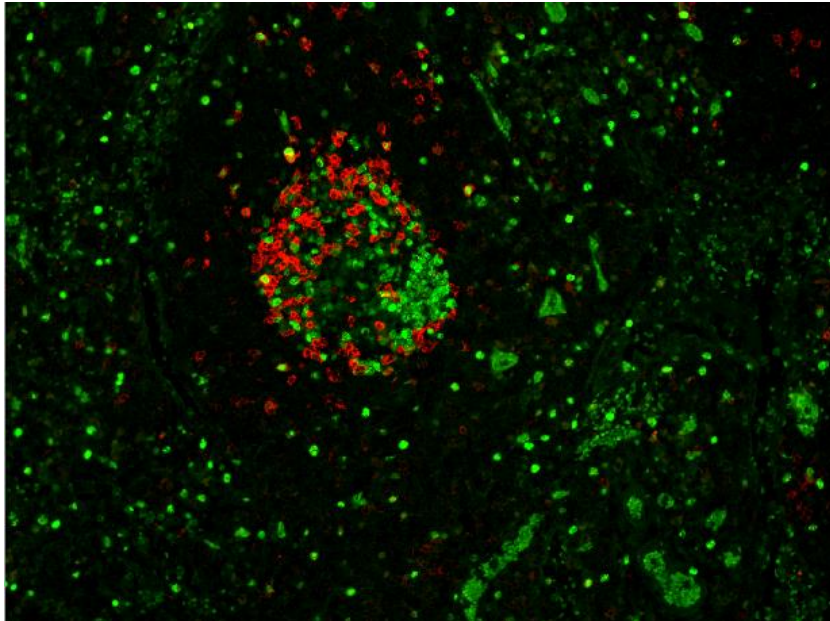
Figure 4-15 Ki67 labelled with FITC (green) and PD-1 labelled with Cy5 (red) in a germinal centre of a normal lymph node, magnification x10

This example normal reactive LN FFPE was labelled with two primary antibodies; Ki67 (rabbit) and PD-1 (goat) and two secondary antibodies, one conjugated to FITC (donkey anti-rabbit IgG) and the other to Cy5 (donkey anti-goat IgG). Images were captured in the FITC and Cy5 channels using the AxioCam MRm high resolution microscopy camera. The negative controls showed minimal background autofluorescence. The Image shown is the overlay from the two images acquired and visualised using AxioVisonLE software.
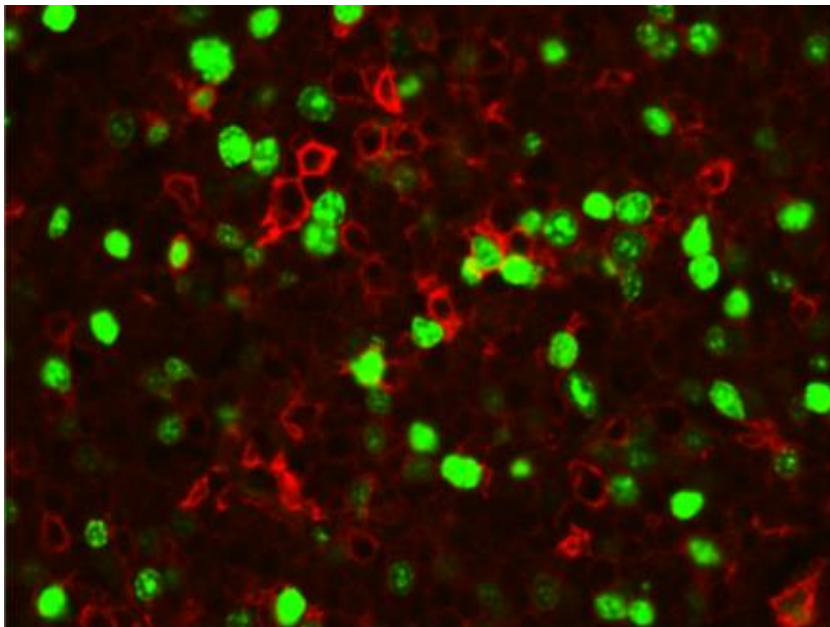
Figure 4-16 Ki67 labelled with FITC (green) and PD-1 labelled with Cy5 (red) in a CLL lymph node, magnification x40

High power visualisation of the CLL LN shown in Figure 4-15.

Finally we successfully simultaneously stained CD4, PD-1 and Ki67 on the same slide. All the appropriate positive and negative controls were performed for each channel (data not shown).

Figure 4-17 and Figure 4-18 shows a normal germinal centre and the relationship between T-cells, PD-1+ cells and Ki67 cells can be readily appreciated. Interestingly a distinct pattern of cellular distribution can be seen in the normal germinal centre. The germinal centre itself shows polarity, with the Ki67 (green) cells localised in the dark zone and the PD-1hi (red) T-cells (blue) are localised in the light zone, consistent with previous publications (De Silva and Klein 2015).
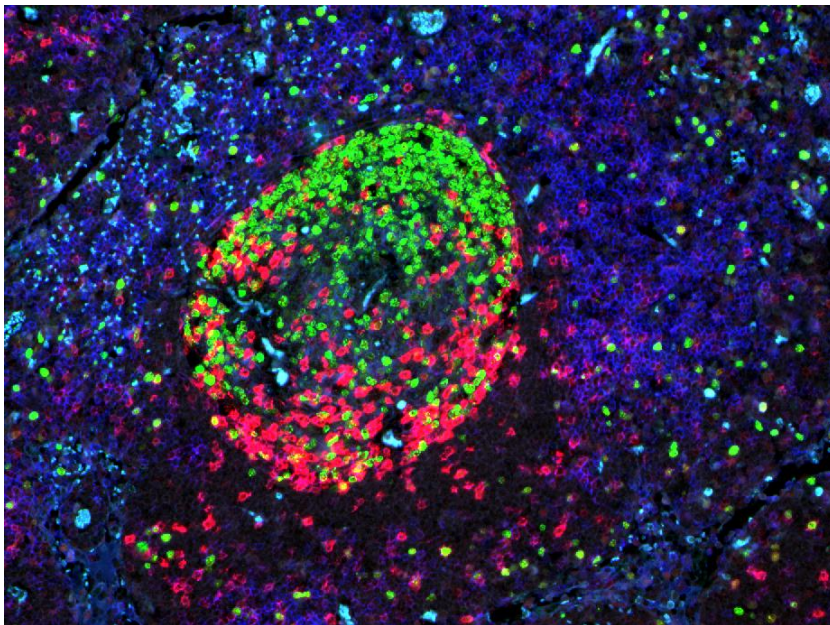
Figure 4-17 Normal germinal centre in a reactive lymph node. Ki67 (green), CD4 (blue) and PD-1 (red), magnification x10
This example reactive normal LN FFPE was labelled with three primary antibodies; Ki67 (rabbit), CD4 (mouse) and PD-1 (goat) and three secondary antibodies, one conjugated to FITC (donkey anti-rabbit IgG), one to Cy3 (donkey anti-rabbit IgG) and the other to Cy5 (donkey anti-goat IgG). Images were captured in the FITC, Cy3 and Cy5 channels using the AxioCam MRm high resolution microscopy camera. The negative controls showed minimal background autofluorescence. The Image shown is the overlay from the three images acquired and visualised using AxioVisonLE software.
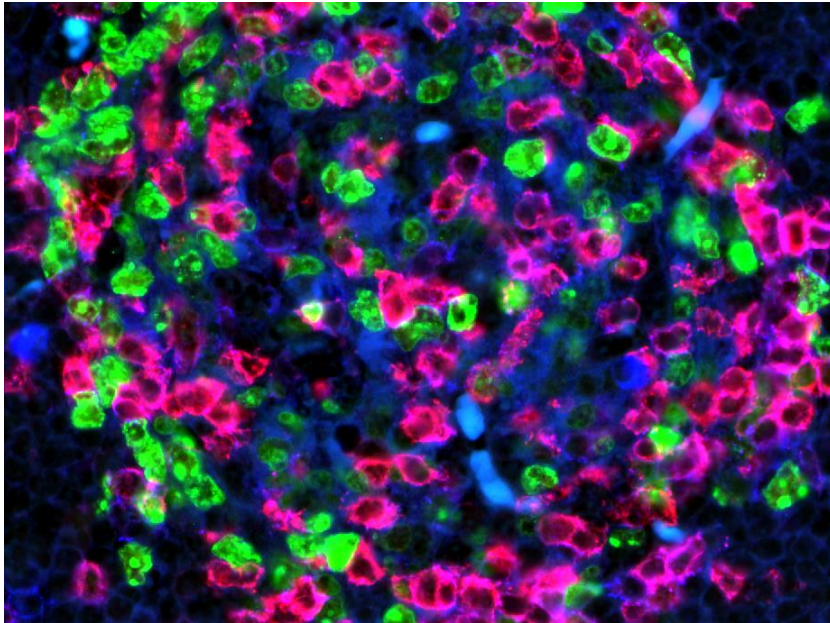
Figure 4-18 Normal germinal centre in a reactive lymph node. Ki67 (green), CD4 (blue) and PD-1 (red), magnification x40. The blue and red positive cells (CD4 and PD-1) are pink/purple. High power visualisation of the germinal centre of the normal reactive LN shown in Figure 4-17. The overlay image in higher magnification shows clearly the cells that are CD4+ and PD-1+ are pink/purple.

The ultimate aim of this work was to stain a CLL lymph node with CD4, PD-1 and Ki67, this would enable analysis of the spatial interactions between these cell types.

Figure 4-19 and Figure 4-20 show a representative example of the staining pattern in a CLL lymph node. Here the distinct normal germinal centre pattern cannot be appreciated. Once this technical method was optimised, it enabled the successful staining of multiple CLL LN samples from different patients to be undertaken.
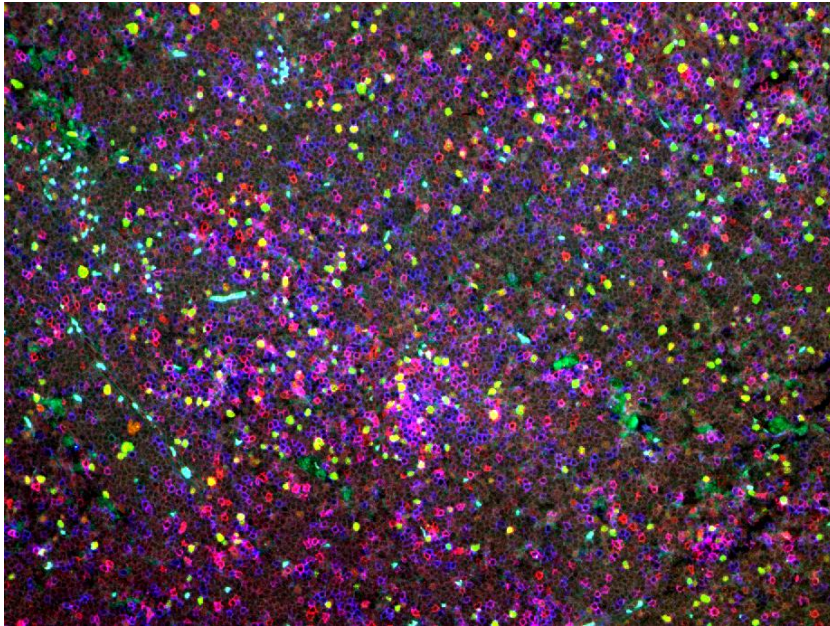
Figure 4-19 CLL lymph node stained for Ki67 labelled with FITC (green), CD4 with Cy3 (blue) and PD-1 with Cy5 (red), magnification x10.

This example CLL LN FFPE was labelled with three primary antibodies; Ki67 (rabbit), CD4 (mouse) and PD-1 (goat) and three secondary antibodies; conjugated to FITC (donkey anti-rabbit IgG), Cy3 (donkey anti-rabbit IgG) and Cy5 (donkey anti-goat IgG). Images were captured in the FITC, Cy3 and Cy5 channels using the AxioCam MRm high resolution microscopy camera. The blue and red positive cells (CD4 and PD-1) are pink/purple. The negative controls showed minimal background autofluorescence. The Image shown is the overlay from the three images acquired and visualised using AxioVisonLE software.
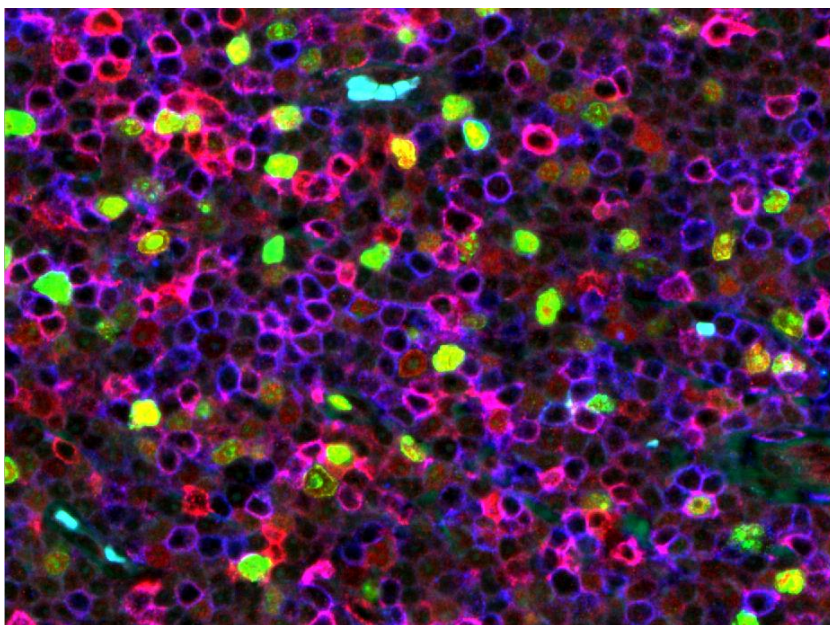
Figure 4-20 CLL lymph node stained for Ki67 labelled with FITC (green), CD4 with Cy3 (blue) and PD-1 with Cy5 (red), magnification x40.

High power visualisation of the CLL LN shown in Figure 4-19. The overlay image in higher magnification shows clearly the cells that are CD4+ and PD-1+ are pink/purple.

4.5 Results 2 - Image Analysis

4.5.1 Analysing co-expression of CD4 and PD-1 on FFPE LN samples

Once the technique of antibody staining method on FFPE lymph node samples was optimised, patient samples were processed in a consistent manner going forward. The first question we wanted to answer was identify whether the CD4+ T-cells in the lymph node biopsy sections also expressed PD-1 as found in the LN FNA samples. To address this we had to adopt a robust method of analysing the immunofluorescence images. The methods for approaching this type of study are not uniform and extreme caution must be adopted when analysing images. Images from unselected fields were captured, excluding areas with extensive haemorrhage and therefore high background autofluorescence. The images were acquired from the microscope camera and stored as proprietary Zeiss "zvi" files, these were then exported as uncompressed lossless Tagged Image File Format (tiff) files. It must be realised that if any compressed format of image is used data from the image is lost and integrity of analysis compromised. "Lossy" compression is a feature of many file formats including "Jpeg" (Joint Photographic Experts Group) and these should not be used (Kabachinski 2007). It is also important to remember that the actual images are black and white and that the red/blue/green channels are entirely artificial overlays on the image for visualisation purposes. Therefore these potential pitfalls must be guarded against when analysis is undertaken. Identifying and mastering a method to analyse the images to answer specific questions was technically challenging. The AxioVisonLE software (Carl Zeiss MicroImaging) did not have adequate functionality to enable this work. Therefore we decided to proceed with initial analysis using visual inspection of the image and manual counting of positive cells as previously published (Patten, Buggins et al. 2008). This proved to be very time consuming and difficult to validate. Subsequently we had access to use the facilities at the Nikon Imaging Centre at King's College London (KCL). The NIS Elements AR Microscope Imaging Suite offered the best software solution for our needs.

Here I shall summarise the image analysis technique we employed. Initially the "threshold" of the image needs setting; put simply this step informs the software which area of the image is "positive" (i.e. antigen present) and which is "negative" (antigen absent). The thresholding can be set to inform the software when the image intensity is too bright or too dim to be considered

- 184 -

positive; thus demarcating the image assigned as "positive" and defining an area of interest. Where there are two fluorochromes on a slide there will be two associated image layers; one for fluorochrome/antigen 1 and one for fluorochrome/antigen 2. Thresholding is performed separately for each layer of an image and in the NIS software these images are called "binary layers". Each thresholded binary layer can be assigned a colour for convenience and for ease of visualisation; these layers can then be saved for later analysis. The binary layers can be converted to "regions of interest" or "objects". The region of interest can be refined mathematically to exclude areas that are judged too big or too small according to the users own defined parameters. Objects can be assigned an individual number to "tag" them, which enables cell counting and for individual cells to be analysed, this can then be manually verified on the image.

Once the user has defined two binary layers (regions of interest or objects) the software can compare the two layers to look for overlap and therefore infers the presence of two antigens on same cell. The software generates the Boolean "AND"; forming a new layer of the intersection from the two layers. It can also generate the Boolean "OR"; and a new layer is formed where either of the two layers are present. If individual cells on a slide have been defined as objects the thresholded region of interest of the second or third layer can be overlaid and the software can then calculate the number of objects (cells) that intersect with defined regions of interest. This quantitates whether two or three fluorochromes do or do not overlap on a cell of interest. Figure 4-21 shows the stepwise approach.
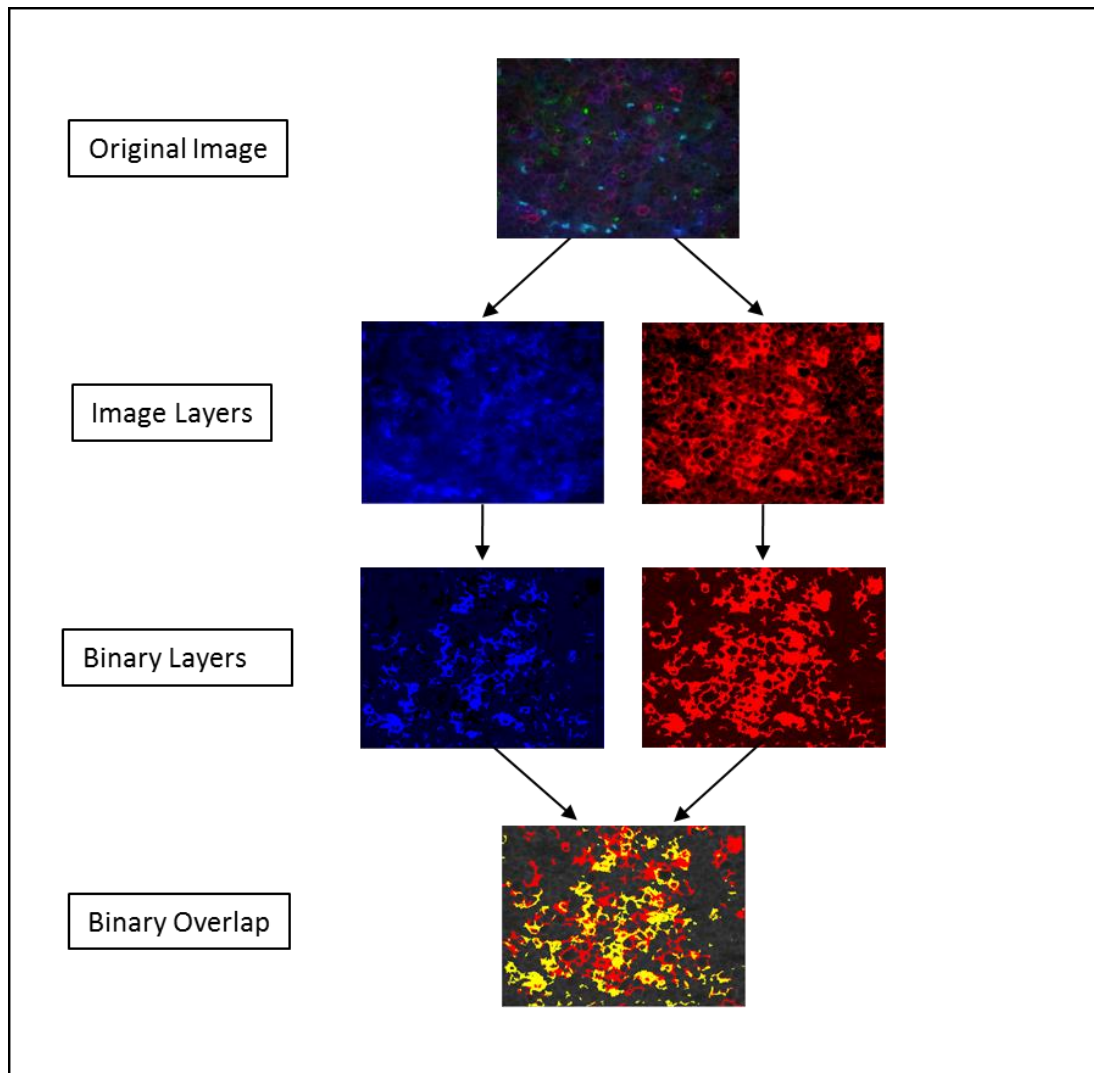
Figure 4-21 Thresholding and Overlap
The original image is first split into its image layers from the time of acquisition. The image layers are converted to binary layers by thresholding the images. The two binary layers are combined and an overlap is produced (visualised in yellow).

4.5.2 CD4+ and PD-1+ co-expression on FFPE LN samples mirrors the findings of the LN FNA

The first analysis we performed was to confirm whether the CD4+ T-cells in the LN biopsy sample co-expressed PD-1. Nine individual CLL lymph nodes from different patients were examined. A median of 7 different fields were analysed per patient (range 4-15). Each experiment was repeated on average twice.

The data for each patient analysed is shown in Figure 4-22. Every dot represents an individual field in that patient.
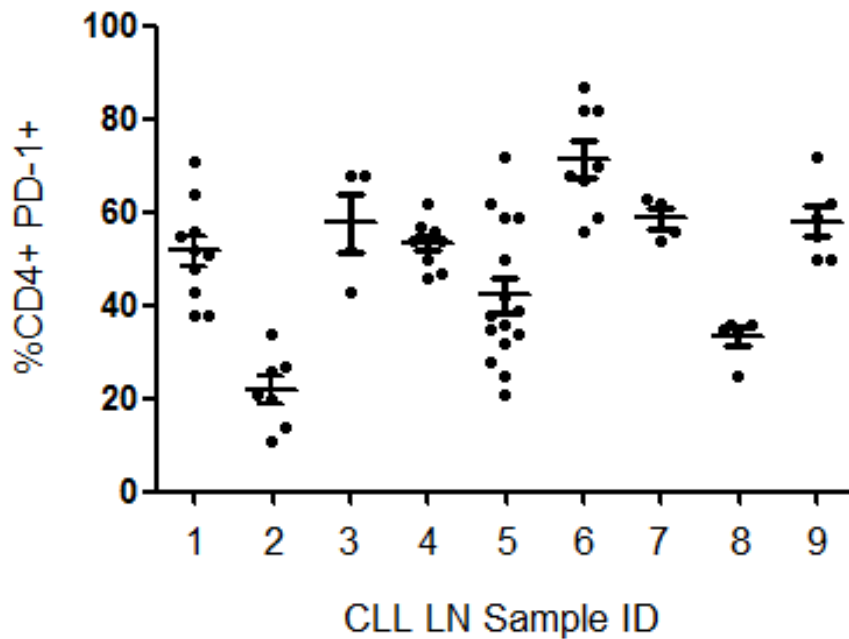
Figure 4-22 Percentage of CD4+ T-cells expressing PD-1 across the 9 CLL samples.
Slides were labelled for CD4 and PD-1 as described in Figure 4-19. Nine individual CLL lymph nodes were examined (CLL LN sample ID 1-9). Binary layers of CD4+ and PD-1+ were constructed as described in Figure 4-21 and analysed using NIS Elements AR Microscope Imaging Suite. A median of 7 random fields were analysed per sample (range 4-15). Each experiment was repeated on average twice. Each data point represents the percentage of CD4+ T-cells that are also PD-1+ in each individual field. The number of CD4+ PD-1+ T-cells per image was normally distributed both within patient samples and between patients by a D'Agostino and Pearson omnibus normality test.

The number of CD4+ PD-1+ T-cells per image was normally distributed both within patient samples and between patients by D'Agostino and Pearson omnibus normality test.

Overall a median of 49.77% +/- 4.99 of the CD4+ T-cells were PD-1 positive. This compared to 56.42% +/- 4.02 in the fresh LN FNA sample data presented in chapter 3. An unpaired t-test was used to compare the number of CD4+ PD-1hi T-cells observed in the LN FNA study from chapter 3 and the LN FFPE samples presented here. There was no statistical difference between the median number of CD4+ PD-1+ T-cells found in the LN FNA study (n=21) compared to the FFPE (n=9); p=0.40), confirming the validity of the FNA results. See Figure 4-23.
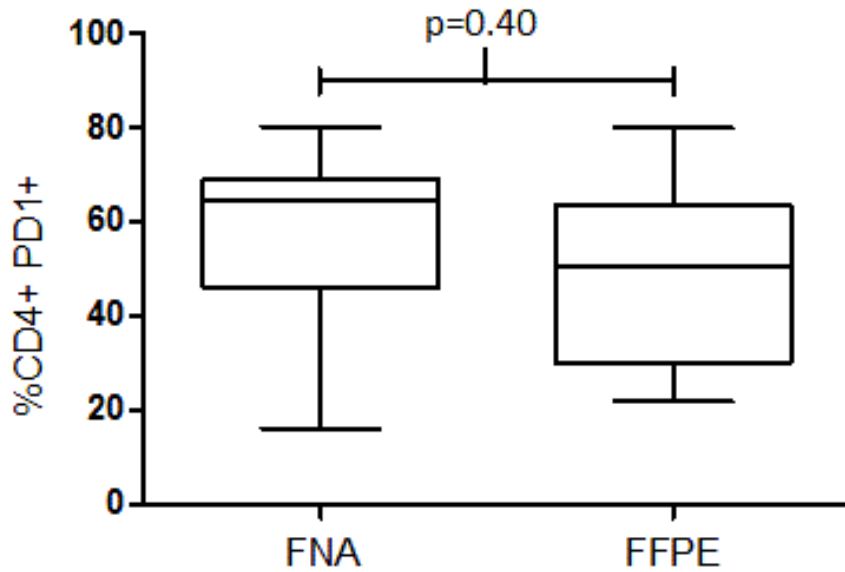
Figure 4-23 Comparison between percentage CD4+ T-cells expressing PD-1 in fresh LN FNA samples and FFPE LN biopsy sections.
By flow cytometry, 56.42% +/- 4.02 of LN FNA CD4+ T-cells were also PD-1+ (n=21) (data set presented in Chapter 3, Figure 3-34). This compares to 49.77% +/- 4.99 in the FFPE LN samples (n=9), data set presented in Figure 4-22. There was no difference between these two methods; p=0.40. Statistical analysis was with a D'Agostino and Pearson omnibus normality test and unpaired t-test.

4.5.3 The majority of Ki67+ cells in CLL lymph node are contacting a CD4+ PD-1+ T-cell

The next question was whether the CD4+ PD-1+ T-cells were in close contact with Ki67+ proliferating CLL cells. To address this a binary layer was made for the intersection of CD4+ AND (Boolean) PD-1+ areas as above. Then a binary layer was made of the Ki67+ cells. Several algorithms were tried to make the Ki67 binary layer, before an optimal method was devised.

As stated previously Ki67 was visualised in the FITC channel, and images in this channel have the disadvantage of unavoidable background autofluorescence. This can be manually visually overcome, as the Ki67 is a very specific staining pattern; but the software cannot easily make this distinction. Therefore when the FITC positivity was assigned by thresholding alone then the background autofluorescence was also included in the binary layer. Therefore, two methods of analysis had to be employed. Firstly the image was thresholded and then the "region of interest" identified manually. There needed to be a stringent deletion of thresholded areas inappropriately assigned as a region of interest. The software can be programmed to

ignore regions of interest below and above a defined size, which are deemed too small or too big to represent a cell, although this did not negate the requirement of a manual sense check. As all the individual Ki67+ cells can be identified as distinct objects by eye, we therefore manually assigned the genuine individual cells onto the thresholded layer. The objects were then dilated to increase the size of the region of interest to that of the whole cell. At the end of this process a layer was formed with multiple cells identified as Ki67+. The software then tagged the cells and assigned each individual Ki67+ cell a cumulative number and a new image layer is formed. The Boolean AND / OR script can then be applied to this layer and another layer with a defined region of interest. We therefore asked whether there was any overlap with the Ki67 layer and the CD4+ PD-1+ binary layers. Figure 4-24 shows the stepwise process in undertaking this analysis.
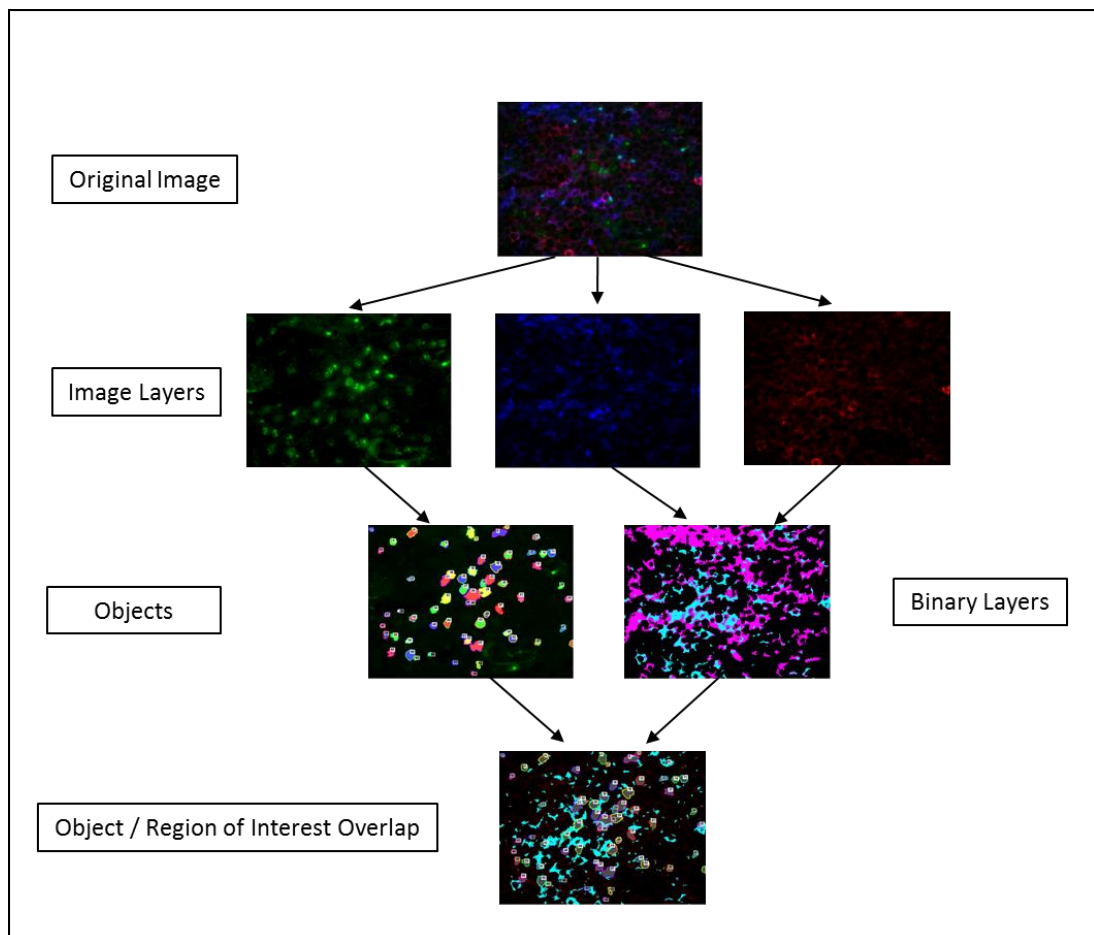
Figure 4-24 Objects and Regions of interest
The original image is split into its original layers and thresholded to produce binary layers as before. The Ki67 layer is converted to numeric objects. The overlapping binary of CD4 AND PD-1 is defined as the region of interest. Then the number of objects (Ki67 cells) that overlap with the region of interest (CD4+/PD-1+ cells) can be calculated.

The software generates a spreadsheet of all Ki67+ cells overlapping with cells that are CD4+ AND PD-1. We can therefore calculate the median percentage of the total number of Ki67+ cells that were touching a CD4+ / PD-1+ T-cells per field.

Six individual patients lymph node samples were examined, once again on average on two separate occasions, with a median of number of fields analysed per sample being 6 (range 4-10). The data derived from the 6 patients is shown in Table 4-5 and Figure 4-25.

Table 4-5 Analysis of Ki67 on CLL FFPE sections
FFPE CLL lymph node sections from 6 individual patients (CLL1-6) were analysed. Slides were labelled as described in Figure 4-19. Binary layers were made and overlapping objects (Ki67+ cells) and regions of interest (CD4+ AND PD-1+ cells) were calculated as described in Figure 4-24 using NIS Elements AR Microscope Imaging Suite. A median of 6 random fields were analysed per sample.

Sample	Mean number of Ki67+ cells per field	Mean number of Ki67+ cells touching CD4+/PD-1+ per field	Mean number of Ki67 cells not touching CD4+/PD-1+ per field	Mean percentage of Ki67 touching CD4+/PD-1+
CLL1	53.6	34.8	18.8	63.4%
CLL2	62.7	36.7	26.0	61.7%
CLL3	19.5	14.5	5	66.7%
CLL4	111.7	101.4	10.3	91.1%
CLL5	47.7	37.7	10	77.2%
CLL6	18.3	15.8	2.5	85.0%

There was a median of 50.65 Ki67+ cells per field (range 18-111). The mean percentage of Ki67+ cells overlapping with a CD4+ / PD-1+ T-cell in the whole population was 74.18% +/- 14.01. See Figure 4-25.
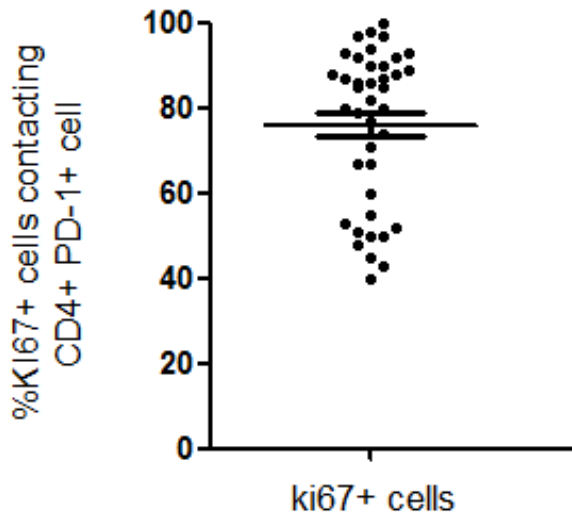
Figure 4-25 Percentage of Ki67+ cells overlapping with a CD4+ PD-1+ T-cell
Experimental details as described in Table 4-5. This data here shows a mean percentage of
74.18% of Ki67+ cells overlap with a CD4+ / PD-1+ T-cell across all fields examined (n= 40)
from the total patient cohort (n=6).

The range of Ki67+ cells per field was large but there was no correlation between number of

Ki67+ cells per field and likelihood of touching a CD4+ PD-1+ T-cell (r=0.259) see Figure 4-26.
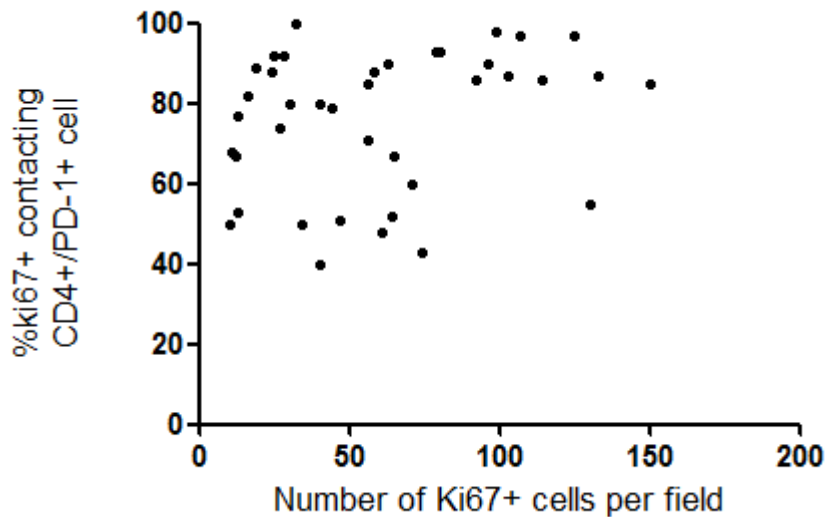
Figure 4-26 No correlation between number of Ki67+ cells per field and the likelihood of
touching a CD4+ PD-1+ T-cell
The correlation between the number of Ki67+ cells per field and the percentage of Ki67+
touching a CD4+ PD-1+ T-cell across all 40 fields was determined by calculating the Pearson
correlation coefficient, no correlation was found; Pearson's r=0.259.

4.5.4 The majority of PD-1+ T-cells in CLL LN samples do not have a Tfh phenotype

The normal germinal centre is shown in Figure 4-17. It can be seen that the distribution of the CD4+ PD-1+ T-cells in the normal reactive lymph node is vastly different to that in the CLL lymph node shown in Figure 4-19. In the reactive lymph nodes germinal centres Ki67+ proliferating cells can be clearly visualised organised into a distinct structure with a surrounding polar halo of CD4+ PD-1+ T-cells; conversely there is no such clear organisational structure to the CLL lymph node. It can also be readily appreciated that the intensity of PD-1 fluorescence in the normal germinal centre appears much higher than that seen in the CLL lymph node. The PD-1 very bright T-cells in the light zone of a normal germinal centre are the Tfh cells. Wang et al designated these cells as PD-1^{+++} memory T-cells; they localise to the rim of the germinal centre and co-express CXCR5 and CXCR4 (Wang, Hillsamer et al. 2011). These Tfh cells produce IL-21 and CXCL13 and offer B-cell help. Tfh cells are critical in the normal B-cells development as discussed in the introductory chapter. They provide differentiation signals to germinal centre B-cells and mediate the selection of high affinity B-cell clones allowing them to become mature plasma cells (Linterman 2014). Tfh cells have recently been reported to be found at in increased numbers in the PB of CLL patients compared to healthy controls (Ahearne, Willimott et al. 2013), data we confirmed in the previous chapter.

To confirm the presence of CD4+ cells with the phenotype of the Tfh in normal lymph nodes, and to look for evidence of Tfh cells in CLL lymph nodes we initially chose to use the marker CXCR5 in combination with PD-1 (Schaerli, Willimann et al. 2000, Haynes, Allen et al. 2007, Wang, Hillsamer et al. 2011). We quickly ran into problems as CLL cells also express CXCR5 making the image analysis technically very difficult, see Figure 4-27.
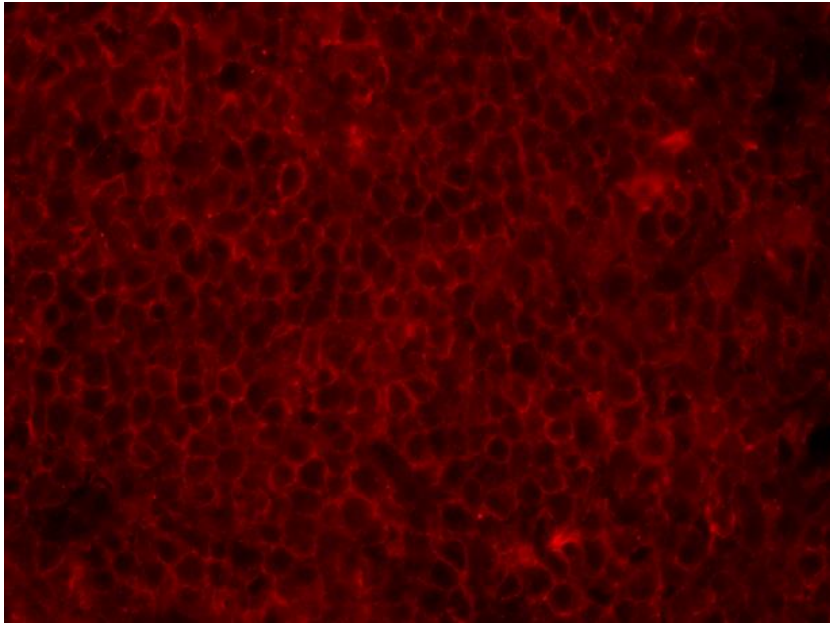
Figure 4-27 CXCR5 staining of a CLL LN with DyLight™ 549 (red) reveals all cells to be positive
This example CLL LN FFPE was labelled with the primary antibody CXCR5 (rat) and the secondary antibody conjugated to DyLight™ 549 (donkey anti-rat IgG). This image was captured in the Cy3 channel using the AxioCam MRm high resolution microscopy camera, magnification x10. All cells appear red. The negative controls showed no background fluorescence.

Therefore to move this work forward we chose to substitute CXCR5 with ICOS which is also a marker of Tfh cells (Schaerli, Willimann et al. 2000, Akiba, Takeda et al. 2005).

This labelling was conducted by Dr William Townsend, a Clinical Research Fellow in our group. A comparison was made between the percentages of CD4+ PD-1hi T-cells which co-express ICOS in normal germinal centres and CLL patients. Lymph nodes from 6 CLL patients were labelled with CD4, PD-1 and ICOS. A median of 5 fields were examined per patient (range 4-5). The analysis was undertaken by creating binary layers of the individual markers and looking for overlap as described. In CLL PD-1 positivity was observed in 54.17% +/- 4.26 of the CD4+ T-cells, confirming the results reported above on separate cohort of CLL LN samples.

This also adds further validation to the results already presented, as these experiments were performed and analysed by a different operator. ICOS+ was present on 9.0% +/-2.33 of the CLL CD4+ PD-1+ cells (range 2-16%). Therefore 91% of the CD4+ PD-1+ T-cells are not ICOS+ and therefore do not represent Tfh cells in the CLL LN.

In the normal reactive lymph nodes microscopy fields from the germinal centre and non-germinal centre were analysed (n=6). PD-1 was expressed on 49% +/- 5.26 of the CD4+ T-cells of the normal germinal centre. Of the CD4+ T-cells 33.0% +/-5.24 were dual PD-1+ and ICOS+ and therefore these are Tfh cells. In the non-germinal centre areas only 0.46% +/- 0.23 CD4+ cells also co-expressed PD-1+ and ICOS+.

These results confirm that in the normal germinal centre there is a high number of Tfh cells which is in contrast to CLL where the PD-1+ CD4+ T-cells more closely resemble the T-cells of the normal inter-follicular areas. See Figure 4-28.
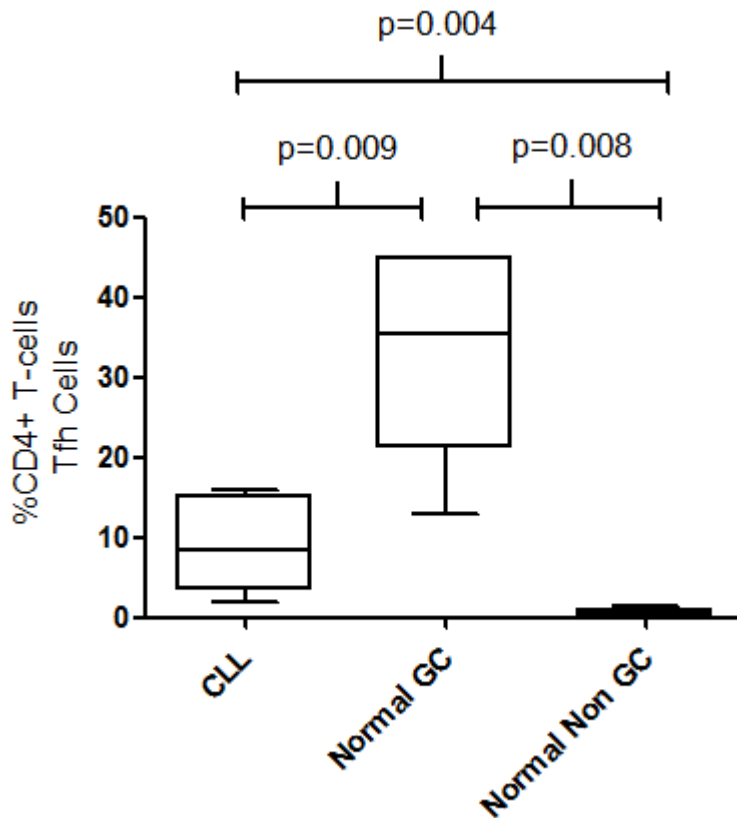
Figure 4-28 The majority of CD4+ T-cells in the CLL LN are not Tfh cells
FFPE CLL LN sections from 6 individual patients and 6 normal reactive LN were analysed. Slides were labelled with CD4, PD-1 and ICOS. Binary layers of CD4+, PD-1+ and ICOS were constructed as described in Figure 4-21 and analysed using NIS Elements AR Microscope Imaging Suite. Tfh cells are defined here as CD4+/PD-1+/ICOS+. A median of 5 fields were examined per slide. In the normal reactive LN, fields were assigned visually to be germinal centres (GC) and non-germinal centres (Non GC). In the normal GC 33.0% +/-5.24 of CD4+ T-cells are Tfh cells whereas in the non-germinal centre areas they account for only 0.46% +/- 0.23 (p=0.08). In the CLL sample Tfh cells accounted for 9.0% +/-2.33 of the CD4+ T-cells.

4.6 Discussion

The aim of the work outlined in this chapter was to complement the findings described in chapter 3. The results from the lymph node FNA phenotyping informed the choice of antigens investigated here. Firstly, the aim was to confirm the presence of CD4+ PD-1+ T-cells in the CLL lymph node and to investigate the spatial relationship between the different cell types. CD4+ T-cells are known to be in close contact with proliferating B-cells but little more is known of the phenotype of these T-cells (Patten, Buggins et al. 2008). Since the flow cytometry studies described in chapter 3 indicated that CLL LNs contain numerous CD4+ PD-1hi T-cells, we investigated whether it was these cells that contact proliferating CLL cells. In a normal germinal centre, antigen responsive helper T-cells supply growth promoting signals to B-cells, so in this study we sought to determine whether the same process might occur in CLL LNs. Multiparameter immunofluorescence microscopy of FFPE lymph nodes sections is technically challenging, however we were able to develop a robust method of immunostaining, image acquisition and systematic analysis of the resulting data.

This work confirmed that there is a high level of PD-1 expression on CD4+ T-cells in CLL lymph nodes. This confirms the results presented in chapter 3 and the study by Xerri et al who previously demonstrated PD-1 to be present on CLL LN sections. It also complements the data presented here and from recent studies which have found PD-1 to be expressed at higher levels on the T-cells of the PB in CLL patients compared to normal controls (Nunes, Wong et al. 2012, Ramsay, Clear et al. 2012, Brusa, Serra et al. 2013, Riches, Davies et al. 2013, Novak, Prochazka et al. 2015, Rusak, Eljaszewicz et al. 2015).

Our group had previously reported that the T-cells within the CLL LN express the activation marker CD25 and these results give further evidence of T-cell activation. Brusa et al recently published that levels of PD-1 increase with T-cell activation with CD3/CD28 beads, data which is confirmed in chapter 6 of this thesis. Our data shows that PD-1 is increased in CLL CD4+ T-cells of the LN and this suggests that there is *in vivo* T-cell activation ongoing in the LN.

Brusa also showed that the PD-1 T-cells within the lymph node are in contact with PD-L1+ CLL cells (Brusa, Serra et al. 2013). We have additionally demonstrated that the CD4+ PD-1+ T-cells are not simply in contact with CLL B-cells but they contact the proliferating

component of the CLL lymph node microenvironment. We have specifically shown that the CD4+ PD-1+ T-cells are in contact with Ki67+ B-cells, suggesting a specific recruitment to the tumour. Two groups have reported that PD-1 positivity in CLL lymph nodes has two patterns diffusely positivity or locally concentrated within proliferation centres in CLL when using standard immunohistochemistry techniques (Ahearne, Willimott et al. 2013, Brusa, Serra et al. 2013). These patterns could not be demonstrated by immunofluorescence in our study or in the Brusa paper. This may be in part because immunofluorescence is technically not feasible at the low power magnifications that are required to visualise proliferation centres. To try and overcome this we hypothesised that fields with a relatively higher number of Ki67 positive events per field may represent a proliferation centre. Therefore we looked to identify whether in fields with a low number of Ki67+ cells they were less likely to be in contact with CD4+ PD-1+ T-cells compared to areas which were presumed to be proliferation centres with a higher number of Ki67+ cells. We found there was no correlation between number of Ki67+ cells per field and the likelihood that the Ki67+ cells were in contact with a CD4+ PD-1+ T-cell.

The next question we asked was whether the CLL CD4+ PD-1+ T-cells were Tfh cells like those of the normal germinal centre reaction. Wang et al reported, in normal lymph nodes that there was heterogeneous expression of PD-1+ T-cells (Wang, Hillsamer et al. 2011). They described the very bright PD-1+ T-cells of the germinal centre as PD-1^{+++}. Wang identified these germinal centres PD-1^{+++} cells to be Tfh cells. In addition they identified PD-1^{dim} T-cells which they designated as PD-1$^{low(+)}$ and PD-1$^{medium(+)}$. Whilst the PD-1^{+++} Tfh cells stimulated the germinal centre B-cells, the PD-1^{dim} population were Th1 and Th17 cells which were located in the mantle zone and appear to restrains the B-cell helper function to prevent an excessive antibody response. In our study we also observed that the PD-1+ T-cells of the CLL lymph node were visually much less bright than the PD-1^{+++} cells of the normal germinal centre. Therefore this suggests that the CLL PD-1+ T-cells are not Tfh but may reflect the PD-1^{dim} population of the normal lymph node. With this knowledge we perhaps could have designed experiments to assess the relative brightness of the PD-1 in normal and CLL lymph nodes for an accurate comparison. This was not feasible retrospectively, at least in our study, as the image acquisition was not set up for inter-sample comparisons. The sections were of slightly variable thickness and the samples acquired at different times so although internal

controls were strict, direct comparison between slides of fluorescence intensity would not be scrupulously robust. A future direction would be to design the experiments to allow a comparison of the relative pixel intensity of the PD-1+ cells. Nevertheless the visually lower intensity of the PD-1+ T-cells in CLL lymph nodes gives a clue that the CLL PD-1+ T-cells are probably not predominately Tfh. We confirmed this assumption with immunofluorescence experiments incorporating co-staining with ICOS. We found that only a small proportion of the PD-1+ CD4+ cells co-expressed ICOS and therefore the majority of these cells were not Tfh cells. A median of 9% of the cells had the phenotype of Tfh cells. The significance of this is not clear and a direct comparison with a normal lymph node is difficult, where the PD-1^{+++} Tfh cells reside in discrete germinal centres. As discussed, Ahearne et al have reported an increased number of circulating CD4+ CXCR5+ ICOS+ Tfh cells in CLL patients compared to normal controls. They also demonstrated that IL-21 and IL-4, which are the major cytokines secreted by Tfh cells, promote CLL proliferation *in vitro* (Ahearne, Willimott et al. 2013). We have also shown in the proceeding chapter evidence of increased CD4+ CXCR5+ T-cells in CLL PB compared to age matched controls. The mechanism for the Tfh accumulation is unknown but may be as a result of the CLL cell secreting favourable cytokines into the tumour microenvironment. We have previously reported that CLL cells secrete high levels of IL-6 which is required for Tfh cell development (Buggins, Patten et al. 2008, Eto, Lao et al. 2011). Clearly the field of research of Tfh cells in CLL requires further study.

This chapter has confirmed the presence of CD4+ / PD-1+ cells residing in the CLL lymph node and in contact with proliferating Ki67+ CLL cells. It has also shown that the majority of these CD4+ T-cells do not have the phenotype of Tfh cells. PD-1 is known to be upregulated on T-cells in response to TCR stimulation and our results therefore suggest this stimulation is ongoing in the LN. In the next chapter we address whether we can provide any direct evidence that the PD-1+ CD4+ T-cells have an antigen specific response by studying their T-cell receptor repertoire.

Chapter 5 Investigating the T-cell Receptor Repertoire in CLL Lymph Nodes

5.1 Introduction

The work outlined in chapters 3 and 4 suggests that CLL lymph node T-cells are phenotypically different from those in normal LNs and the CLL PB compartment. The observation that there is a high proportion of effector memory T-cells that express markers of chronic activation, such as PD-1 further suggests that these cells may have undergone an antigen specific response. As discussed earlier, there is evidence that just like the BCR the TCR in CLL shows evidence of an antigenic response; as CLL PB derived T-cells show a skewed TCR repertoire.

The BCRs in CLL are generally polyreactive and some show affinity for self-antigens; including antigens derived from apoptosis, such as cytoskeletal proteins, non-muscle myosin heavy chain IIA and vimentin (Herve, Xu et al. 2005). BCR reactivity has also been identified to the Fc immunoglobulin tail, single stranded DNA, double stranded DNA, lipopolysaccharide, insulin and oxidised low density lipoprotein (Catera, Silverman et al. 2008, Lanemo Myhrinder, Hellqvist et al. 2008, Binder, Lechenne et al. 2010, Chu, Catera et al. 2010). Other groups have found affinity of BCRs for a variety of non-self-antigens including bacteria, fungal elements and viruses including CMV (Landgren, Rapkin et al. 2007, Kostareli, Hadzidimitriou et al. 2009, Steininger, Rassenti et al. 2009). In regard to the TCR it has been exclusively studied within the PB compartment, where there are major perturbations in the TCR repertoire of CLL patients compared to healthy controls. Oligoclonality has been identified in both the CD4+ and CD8+ compartments. The presence of T-cells clones in CLL has been reported by many groups (Wen, Mellstedt et al. 1990, Farace, Orlanducci et al. 1994, Serrano, Monteiro et al. 1997, Rezvany, Jeddi-Tehrani et al. 1999, Goolsby, Kuchnio et al. 2000). A comprehensive explanation for this remains to be fully elucidated and although several groups have identified putative candidates the issue is still hotly debated and the mechanisms of antigenic drive remains elusive.

Several groups have demonstrated a small, but definable population of postulated anti-leukaemic T-cells with a measurable specific tumour driven antigen response (Rezvany,

Jeddi-Tehrani et al. 2000, Goddard, Prentice et al. 2001, Gitelson, Hammond et al. 2003). These CD8+ cytotoxic T-cells have been the subject of interest especially with regard to the possibility of expanding them by vaccination. The repertoire of the CD4+ T-cells has been the subject of limited study, but is of interest due to the observation that these T-cells are supportive *in vitro* to the CLL clone (Patten, Buggins et al. 2008).

As previously noted, CLL is generally a disease of the elderly and when investigating the T-cell repertoire of an elderly patient population it must be remembered that there is known to be marked skewing of the TCR repertoire as a consequence of normal ageing and previous exposure to common viral infections. CMV is a ubiquitous beta herpes virus that has a prevalence of approximately 70% of 70 year olds and is known be very immuno-dominant on the normal immune system (Savva, Pachnio et al. 2013). In a healthy elderly population CMV specific CD8+ T-cells can account for up to half the T-cell repertoire (Khan, Shariff et al. 2002). As discussed in the introduction chapter several groups have investigated the hypothesis that CMV could be in part responsible for the global T-cell expansion and dysfunction in CLL (Akbar 2010). However, it has been acknowledged that the T-cell abnormalities in CLL are not just restricted to CMV seropositive individuals and that there is still a vast T-cell expansion of dysregulated T-cells with abnormal phenotype even in CMV seronegative individuals (Riches, Davies et al. 2013). te Raa et al recently published a study whereby they selected CMV specific T-cells from CLL patients, using CMV tetramers, and found a preserved CD8+ CMV specific T-cell function on a background of T-cell dysfunction. Therefore they hypothesised that the CLL cell induced T-cell suppression is not global and there may be specific suppression of T-cell subsets by the CLL within the microenvironment (te Raa, Pascutti et al. 2014). We have shown in chapter 3 that the phenotypic changes in CLL T-cells are not restricted to CMV seropositive individuals.

Research has not focused on the TCR repertoire from T-cells from with lymph nodes due to the lack of availability of material; however there is evidence from some solid cancers that T-cells derived from within the tumour microenvironment have a more skewed TCR repertoire compared to the PB. For example, Sfanos et al, have published that CD8+ T-cells obtained from prostate glands infiltrated with prostatic cancer have an oligoclonal repertoire, to an as

yet unknown antigen (Sfanos, Bruno et al. 2009). Moreover the CD8+ T-cells expressed high levels of PD-1, suggesting a chronically antigen stimulated phenotype. Similarly, tumour infiltrating oligoclonal T-cells have been found in ovarian cancer (Pappas, Jung et al. 2005), gastric and colorectal patients (Matsutani, Shiiba et al. 2004, Sherwood, Emerson et al. 2013). A meta-analysis of 126 studies has been published which reviewed the literature of the impact of tumour infiltrating T-cells, B-cells, NK cells and macrophages in a variety of cancers (Fridman, Pages et al. 2012). In the solid tumour setting, high levels of infiltrating cytotoxic T-cells, Th1 and memory T-cells have a positive impact on patient survival. Although the scenario is not directly comparable to CLL where the immune system is itself the tumour, host, defender and supportive microenvironment, nonetheless we can learn from these studies in terms of experimental approach and technical application.

Several studies are now incorporating the utility of high throughput sequencing (HTS) to investigate the TCR repertoire in health and disease; and this emergent technology has given in further insights into the vast TCR diversity, which in the PB of healthy subjects is estimated to be in the order of 20-100 million clonotypes (Arstila, Casrouge et al. 1999, Robins, Campregher et al. 2009). Our collaborators at Adaptive Biotechnologies® have published several recent studies and proposed new methods for the quantification and analysis of the TCR repertoire of tumour immune infiltrates in a variety of cancers (Robins, Ericson et al. 2013).

A full understanding of the aberrations in the TCR repertoire in CLL remains to be defined, but there is mounting evidence that CLL T-cells, just like the B-cells are antigen experienced. In this chapter the aim is to analyse the TCR repertoire of CD4+ T-cells derived from the CLL LN microenvironment and compare it to the repertoire found in the PB. Our hypothesis is that the TCR repertoire of the high frequency PD-1hi LN and PB T-cells will show evidence of greater antigen specificity than the PD-1lo counterparts and that they are therefore antigen driven within the lymph node.

This hypothesis could be addressed by a variety of different experimental approaches.

5.2 Experimental Approach

5.2.1 TCRVβ Repertoire Assessment

Before proceeding with the analysis of the LN TCR repertoire we assessed the various methods. These are reviewed below (Six, Mariotti-Ferrandiz et al. 2013).

1. **Flow Cytometry**

Monoclonal antibodies are available to some of the TCRVβ subgroups and have been used to study the TCR repertoire (Faint, Pilling et al. 1999). The TCR repertoire can then be expressed in terms of family usage. This approach is limited by the availability of antibodies and the inability to detect junctional diversity. One publication has suggested that just 364 T-cell events need to be captured to calculate divergence by this method (Ciupe, Devlin et al. 2013).

2. **Micro-array**

The micro-array method is a direct method of assessing the repertoire without PCR. RNA is isolated and cDNA constructed. The double stranded cDNA is biotinylated and the in vitro transcription product cRNA isolated. The cRNA is then hybridised to a gene chip of random oligonucleotides. The diversity of the TCR can then be inferred from the number of hybridised oligonucleotides (Ogle, Cascalho et al. 2003, Bonarius, Baas et al. 2006)

3. **Quantitative Reverse Transcriptase Polymerase Chain Reaction**

Many PCR methods have been employed to try and assess TCR repertoire. Constant and variable family-specific primers can be used to amplify the CDR3, as it is the CDR3 region of the β chain defines the specificity of the TCR. One of the limitations of this approach is the potential for amplification bias with multiple primer sets.

Ligation anchored PCR is a method of amplifying cDNA with an unknown 5' sequence. An oligonucleotide (the anchor), which has no sequence homology to the gene of interest, is ligated to the first strand cDNA using RNA T4 ligase. The anchor oligonucleotide has a 5' phosphorylation and a 3' ddC, to ensure the ligation can only occur in one direction. Next a PCR can be performed using two primers – one to the anchor and the other to the sequence

of interest (Troutt, McHeyzer-Williams et al. 1992). In this scenario one primer is to the anchor oligonucleotide and the other to the constant region of the TCRVβ.

Matsutami et al described a cDNA restriction digest and an adapter ligated PCR with one set of primers, where one primer is ^{32}P labelled. The PCR products are fractionated by agarose gel electrophoresis and the size of each fragment is compared to known lengths for each TCRVβ family and densiometric quantification of signal intensity used to quantify the product. This is technically difficult and the use of radiolabelled primers reduces the general utility of this method (Matsutani, Oishi et al. 1994).

To try and remove the need for a radiolabelled primer Matsutami et al developed a microplate based assay. First RNA is extracted and transcribed into cDNA. Then a universal adapter is ligated onto the 5' end of the resultant cDNA. The adapter allows for a universal PCR amplification of all the TCRVβs. The PCR products are then biotinylated. Microplate wells are coated with TCRVβ specific oligonucleotide probes in water soluble carbodiimide. The PCR products are allowed to hybridise to the plate and the amount can be measured by a quantitative ELISA and automated colorimetric methods (Matsutani, Yoshioka et al. 1997)

4. Spectratyping

At the time of this study spectratyping (also known as Immunoscope technology), was the most common method of assessing the TCRVβ repertoire (Cochet, Pannetier et al. 1992, Pannetier, Cochet et al. 1993). DNA or cDNA is used as a PCR template where primers cross the V, D, J and C regions of the TCRVβ chain and encompass the CDR3. One primer is to the constant region and the other to one of the Vβ families. As the TCR gene size varies according to its mutated sequences different length PCR products will result. As the genetic rearrangement is random, the PCR product lengths should fall into a Gaussian distribution and should differ from each other by 3 nucleotides. PCR fragment length distribution analysis measures the CDR3 length of each TCR within Vβ families. Fragment length distribution analysis can assess the normal distribution of the repertoire. Any over represented lengths in a population will deviate the eight peak bell-shaped distribution curve which suggests skewing in the repertoire, due to an over represented TCR in the population. Both oligoclonal or clonal expansions of T-cells disrupts the bell shape curve (Cochet, Pannetier et al. 1992). This

method is not quantitative but allows for assessment of diversity. Analysis of spectratype data is typically judged subjectively and although statistical analysis tools have been developed, they have not been widely adopted (Wu, Chillemi et al. 2000, Lu, Basu et al. 2004, He, Tomfohr et al. 2005). Clearly primer design is a key issue in spectratyping studies. Primers need to encompass the VDJ gene segments, the number of primers pairs should be as minimal as possible and the resultant PCR product be of a reasonable size. The European BIOMED-2 collaborative group have published a standardised Vβ primer set which it recommends for assessing T-cell clonality; see Table 5-6. The conventional PCR methodology uses 24 Vβ family forward primers and one common Cβ reverse primer. In order that the resultant fragments can be sized, the Cβ primer is conjugated to a FAM reporter molecule, and an analysing platform, such as Genetic Analyser (Applied Biosystems), is used to size the resultant products by fluorescence-based capillary electrophoresis. In order to size the fragments a fluorescently labelled size standard ladder (such as ILS-600, Promega) is added to the amplified PCR product mix; this enables the software to size the fragments against the known lengths in the ladder. The ILS-600 (Internal Lane Standard 600) is a double stranded DNA ladder consists of 22 fragments between 60bp and 600bp asymmetrically labelled with carboxy-X-rhodamine. Formamide is used as a denaturing agent in the mix. The mix is moved through a polymer filled capillary (multiple capillaries per machine) by electrophoresis. The Genetic Analyser then records the fluorescent intensity as a function of time and wavelength and can size fragments up to 12000bp. Enumeration and sizing of the individual fragments is then analysed on software program such as GeneMapper (Applied Biosystems) allowing graphical and statistical analysis.

5. **Sanger Sequencing**

Capillary based Sanger sequencing individually sequences each TCR present in a sample. The Sanger method first requires a sequence amplification step where the input DNA is fragmented and cloned into bacterial vectors. Then a reverse strand synthesis is undertaken with DNA polymerase using a known priming sequence. The sequence can be elucidated by the combining deoxy-nucleotides (dNTPs) and modified and labelled dideoxy-nucleotides (ddNTPs). Sequencing reactions utilise three of the four dNTPs (combination of dATP, dGTP, dCTP, dTTP) and one of four is a labelled ddNTPs (ddATP, ddGTP, ddCTP or ddTTP). The

addition of the ddNTP to the sequence causes a non–reversible termination of the sequence as it does not have the 3' hydroxyl group which is needed to form a phosphodiester bond. The resulting DNA fragments are heat denatured and separated by electrophoresis (Sanger, Nicklen et al. 1977). This fundamental method has been enhanced and adapted allowing a PCR amplification and a single tube reaction with automated capillary based electrophoresis technology. This method, called dye-terminator sequencing, uses different fluorescent labels for each of the four ddNTPs; which can be detected by the emission of light at different wavelengths (Smith, Sanders et al. 1986). Fully automated methods have subsequently been developed and several methods now do not require prior amplification. The main limitation continues to be the size limit and insufficient power to sequence fragments that alter by just one nucleotide. It is only possible to sequence up to 384 sequences of between 600-1000bp in parallel and the error rate is between 1 in 10^4 and 1 in 10^5 (Kircher and Kelso 2010). Therefore its utility in assessing the whole TCR repertoire is limited and it can only be effectively used to selectively characterise the TCR sequence of clones identified by other techniques such as flow cytometry or spectratyping. Direct sequencing of 10^2-10^3 TCRs has been undertaken by this method but is not routinely a useful approach due to cost and time (Six, Mariotti-Ferrandiz et al. 2013).

6. **High Throughput Sequencing**

High throughput sequencing is an emerging technology to investigate the TCR repertoire. This PCR based technology allows the parallel direct sequencing of the total TCR repertoire, which may be up to 10^6-10^7 clonotypes (Arstila, Casrouge et al. 1999). Unlike Sanger sequencing, HTS can sequences millions of TCRs simultaneously, from which the diversity of the CDR3 can be assessed as well as the relative frequency within a population. Whereas spectratyping looks for overrepresented TCR clones by virtue of the size of the PCR product, HTS can sequence each and every individual receptor. Comparative studies of spectratyping and HTS show very similar CDR3 distributions (Ademokun, Wu et al. 2011, Six, Mariotti-Ferrandiz et al. 2013). This new technology still requires validation and is not universally accepted technology for accurate TCR repertoire assessment due to high rates of sequencing error and complex bioinformatics (Bolotin, Mamedov et al. 2012). Robins et al first published an

assessment of the TCR repertoire in healthy subjects using the Illumina Genome Analyser platform whilst our studies were underway (Robins, Campregher et al. 2009).

There are three main technologies currently leading the field to sequence the TCR repertoire: 454 (Roche), MiSeq/HiSeq (Illumina) and Ion Torrent (Life Technologies). Figure 5-1, adapted from Baum et al and Bolotin et al, is an illustrative schema of the different technologies (Baum, Venturi et al. 2012, Bolotin, Mamedov et al. 2012).

The first step in the process is TCR cDNA amplification (A); the 454 and Illumina use a universal 5' primer (M1) whereas Ion Torrent requires a multiplex V and J primer set because the fragments need to be short (150-200 base pairs (bp)) for the Ion Torrent platforms bead based PCR. Next the resultant fragments are immobilised prior to amplification (B). The 454 and Illumina can immobilise larger fragments than the Ion Torrent. The 454 and Ion Torrent use a bead technology and emulsion PCR, whereas Illumina uses a cluster on a glass slide and bridge PCR. The 454 and Ion Torrent elongates the sequence using one nucleotide (nt) at a time (dATP, dCTP, cTTP or dGTP) and every time a new nucleotide is incorporated a pyrophosphate (PPi) and a proton (H+) is released (C). The 454 detects the pyrophosphate by using sulfurylase and luciferase enzymes which emit light which is then detected on a bead array. The Ion Torrent detects the proton by measuring a resultant change in pH on a transistor chip (D). The Illumina platform adds in all of the nucleotides simultaneously but as they are fluorescently labelled and irreversibly blocked, only one nucleotide can be added per cycle (C), the fluorescence from the specific nucleotide that was incorporated can then be detected on the slide.
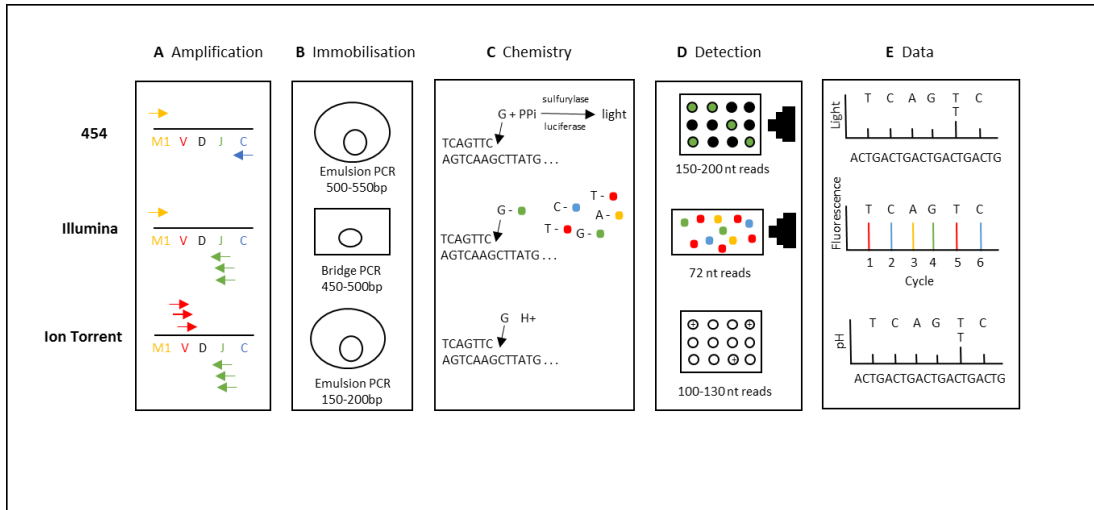
Figure 5-1 Methods of analysing the TCR by HTS. Adapted from Baum et al and Bolotin et al.

Because a direct comparison was needed in our study, the method of assessing the TCR repertoire needed to be able to be comparative but not necessarily quantitative. Our initial approach was that of a cDNA ligation technique with a single primer set PCR to avoid any PCR bias, but this proved to be unreliable (discussed below). Subsequently we decided to undertake conventional TCRVβ spectratyping, as this was the gold standard validated technique for assessing the TCR at the time of study. HTS was subsequently undertaken in a pilot study as the technology became available to us.

5.2.2 Starting Material

Following identification of the most appropriate methodology for assessing the TCR repertoire, the next step was to choose the best primary starting material. The major advantages and disadvantages of each tissue have been previously discussed and are reviewed again in Table 5-1.

Table 5-1 Starting material

T-cell source	Advantages	Disadvantages
FFPE lymph Node	Samples available Normal controls available Ability to laser dissect PCs	Anonymous samples No matched PB Highly selected population Fixed sample Unable to extract RNA Difficulty sorting T-cells
Fresh Lymph Node	Unfixed tissue Large cell numbers Ability to sort T-cells Ease of RNA extraction Matched PB	Low availability Highly selected population No normal controls
FNA Lymph Node	Better availability Unfixed tissue Unselected population Ability to sort T-cells Matched PB	Small cell numbers Difficult to extract RNA No normal controls

The most straightforward approach would have been to have paired fresh lymph node biopsy samples and peripheral blood, but the lack of availability was a major stumbling block and the highly selected population that undergo lymph node biopsy could bias the study. FFPE LN samples were already available, but only available to us in an anonymised fashion without clinical details or paired PB. Additionally sorting cells and extracting quality RNA from FFPE, although not impossible, is technically difficult. Laser dissection microscopy can be employed on FFPE sections although very small numbers of cells are extracted.

Vandewoestyne et al dissected out proliferation centres in CLL by laser pressure catapulting and sorted the Ki67+ subset in order to sequence the IgVH (Vandewoestyne, Pede et al. 2011). This group stated that extracting genomic DNA (gDNA) from 2000 cells gave a

Gaussian distribution of the IGHV, however using gDNA as a template to assess the TCR repertoire has flaws. The rearranged TCR are of course structurally different from the genomic template and even though there is not the added complexity of affinity maturation as seen in the BCR, using DNA as a templates does not exclude the TCRs that are rearranged but not expressed. Nonsense mRNA molecules, on the other hand, are quickly degraded (Wang, Vock et al. 2002, Bhalla, Gudikote et al. 2009). Recent evidence from HTS reveals marked differences in the reported TCR repertoire depending on whether cDNA or gDNA were used as starting material; with under and over representation of transcripts (Desmarais 2012). Hedegaard et al have also recently published their experience of HTS using DNA and RNA extracted from FFPE compared to fresh frozen samples. They compared several methods of DNA and RNA extraction and outline the inaccuracies in sequencing that can arise from the fragmentation and chemical modifications that can occur to nucleic acids post fixation. They found, by pairwise analysis, that whole exome sequencing of extracted DNA showed only a 70-80% concordance between fresh and FFPE samples. The concordance was superior when RNA was used as a template but they recognise RNA extraction from FFPE is more challenging (Hedegaard, Thorsen et al. 2014). Despite the technical challenges, RNA extraction from FFPE for TCR repertoire analysis has been reported as feasible by several groups (O'Shea, Hollowood et al. 1996, Le Gal, Widmer et al. 2007).

Weighing up the advantages and disadvantages we decided to use RNA as a starting material. Despite the potential ability to extract RNA from FFPE we decided that as the studies main aim was to be comparative between compartments, the lack of matched PB and the difficulties in extracting RNA from paraffin made the utility of this approach less attractive. We therefore made the decision to use fresh LN FNA and PB as starting material. This had the major advantage of matched fresh samples allowing for RNA extraction. There was also the ability to control cell numbers, samples could be obtained from an unselected CLL population and this study was ethically approved. The strongest power of this approach was the potential to be able to sort T-cells in a comparable way between sample types; we could also utilise flow sorting to look at subpopulations of T-cells and compare them between compartments. In addition, results could be compared to those from normal PB. The disadvantage of small

amounts of starting material would need to be overcome, especially when sorting cells and extracting RNA.

5.2.3 Flow Cytometric Cell Sorting

Flow cytometric cell sorting allows the isolation and collection of fluorescently labelled cells. The basic principles of flow cytometry principles have been reviewed in chapter 3. Flow cytometric cell sorters differentiate cell populations by exactly the same principle. In addition, this system allows subpopulations of cells to be defined and then collected according to their fluorescent cell surface labelling. The cells are first immunofluorescently labelled by the conventional method. The properties of the cell population of interest are inputted into the software to define which populations are to be collected. The BD FACSAria (BD Biosciences) sorter can simultaneously sort 4 defined populations, assuming there is no conflicting overlap between collection subsets. The sample is loaded onto the FACSAria and the fluidics system moves cells from the sample injection chamber into the cuvette flow cell where the stream is hydrodynamically focused and the cell within it is interrogated and subsequently either collected or sent to waste, depending on the parameters that have been defined for the sort. For the collection or "sort" to take place so called "drop drive" energy is applied to the flow stream to split it into highly uniform droplets containing a cell. When a cell is detected, and it meets the criteria for collection, an electrical charge is applied to the stream at exactly the moment the droplet is about to break off. The resultant droplet, containing only the cell, has then gained a charge. The droplet then passes between two strongly charged deflection plates and depending on the droplets charge polarity it is attracted or repelled left or right by different degrees into a waiting collection tube. The FACSAria allows a differential charge to be applied to each droplet containing the specified cell population to be collected. A non-charged droplet passes into the central waste collector. By this method, four populations of cell can be simultaneously collected and the remaining cells discarded.

5.3 Aim

The major question we wanted to answer in this study was whether the high frequency PD-1+ T-cells found in the lymph node had a skewed TCR repertoire and therefore evidence of a specific antigen driven response. In order to elucidate this we chose to undertake TCRVβ

repertoire analysis on the PD-1hi and PD-1lo CD4+ subsets of the LN and PB and look for skewing of the repertoire in each subset by conventional spectratyping. We were specifically interested in the CD4+ T-cells as these T-cells are supportive of CLL *in vitro*. The CD8+ T-cells were also selected for future work. We also sought to identify whether the PD-1hi T-cells were a different population from the PD-1lo T-cells and whether the T-cells within the PB were the same or a distinct population from the LN. In order to perform TCR analysis on a subset of T-cells the individual populations were first sorted by flow cytometry.

5.4 Materials and Methods

5.4.1 Ethics

Ethical approval was obtained to perform LN FNAs on CLL patients for research purposes from the research ethics committee REC: 09/H0805/5. PB was collected from patients under national research ethics NREC: 08/H0906/94. PB was collected from healthy controls under LREC: 02-044. Written informed consent was gained according to the Declaration of Helsinki, 2008.

5.4.2 Primary Patient Material

5.4.2.1 Peripheral Blood

PB was collected from CLL patients undergoing LN FNA and from healthy controls directly into CLL media or EDTA as described in 2.2.1.

5.4.2.2 LN FNA

Patients with a diagnosis of CLL and an easily palpable lymph node were invited to take part in the study. They were given a patient information sheet and given adequate time to consider their entry into the study. Written consent was obtained and samples pseudo-anonymised. The LN FNA was performed using a 23 gauge needle attached to 10ml syringe. Once the sample was aspirated and the needle washed directly into CLL media. This was repeated on average 4 times per patient.

5.4.3 Jurkat Cells

Jurkat cells were donated by Dr Shahram Kordasti and cultured as in 2.5.2. Cells were resuspended in Jurkat media at 1 x 10^5/ml. 5mls was transferred to a 25ml tissue culture flask (Sigma). Cells were cultured at 5% CO_2 at 37°C in a humidified incubator. The cell culture was split in fresh media every 2 days or when cells >1 x10^6/ml.

5.4.4 Antibodies for FACS Cell Sorting

The antibodies used for cell sorting were are shown in Table 5-2.

Table 5-2 Antibodies for flow cytometric sorting

Antigen	Clone	Conjugation	Volume	Company
CD4	RPA-T4	PE	10µl	AbD Serotec
CD8	OKT8	Pacific Blue™	10µl	eBioscience
CD279 (PD-1)	MIH4	Alexa Fluor® 647	5µl	AbD Serotec

5.4.5 Staining Cell Surface Antigens for Flow Cytometry

Cells were resuspended in 100µl PBS and labelled for flow cytometry according to 2.7.1. Directly conjugated antibodies were added at appropriate titrated volume as described in Table 5-2.

5.4.6 FACS Sorting

Cells were sorted using the BD FACSAria flow cytometer with technical assistance from Winston Vetharoy. Cells were sorted from the lymphocyte gate. Cells were defined as CD4+/PD-1hi, CD4+/PD-1lo. CD8+/PD-1hi, CD8+/PD-1lo. Sorted cells were collected directly into CLL media and their post purity was checked by flow cytometry. The cells were subsequently centrifuged at 200g for 5 minutes and the cell pellet resuspended in 0.5ml TRIzol® for subsequent RNA extraction.

5.4.7 RNA Extraction

Several methods of RNA extraction were optimised. Initially mRNA was extracted using a direct method and subsequently a total RNA extraction; described below.

5.4.7.1 Direct mRNA Isolation Protocol

1. **Preparation of Lysate from Cell Suspension**

Cells were pelleted by microcentrifugation at 200g for 5 minutes. Cells were then washed in PBS and re-pelleted by microcentrifugation 200g 5 minutes. 300µl Invitrogen Dynabeads lysis/binding buffer (Invitrogen) was added to the cell pellet. The solution was repeatedly passed through an RNAse free plugged pipette tip until the solution became viscous which confirmed complete lysis.

2. **Preparation of Dynabeads Oligo(dT)$_{25}$**

Dynabeads Oligo(dT)$_{25}$ (Invitrogen) were prepared before use. First they were vortexed to resuspend them and then 20µl was transferred to a RNase free 1.5 ml microcentrifuge tube. This was placed on the proprietary magnet and when suspension was clear (about 30 seconds), the supernatant was removed. The beads were washed by resuspending in 50µl lysis/binding buffer and then replaced on the magnet ready for use.

3. **Direct mRNA Isolation**

The sample lysate was added to the prepared Dynabeads Oligo(dT)$_{25}$ and resuspended by pipetting. The tube was then continuously mixed on rotating mixer for 5 minutes at RT to allow the polyA tail of the mRNA to hybridize to the oligo(dT)25 on the beads. Beads were magnetically removed and then the bead/mRNA complex were washed twice with 600µl Washing Buffer A and twice with 300µl Washing Buffer B (Invitrogen) at RT. The magnet was used to separate the beads from the solution between each washing step. Finally the beads were washed and resuspended in 50µl cDNA synthesis buffer ready for cDNA first strand synthesis.

5.4.7.2 Total RNA Extraction

A method for total RNA extraction was optimised for the FACS sorted samples stored in TRIzol® (Invitrogen) (Chomczynski and Sacchi 1987). A combined TRIzol®/RNeasy® Extraction Protocol was developed and described here.

Two different hybrid methods utilising the RNeasy® Micro kit (Qiagen) were used. The first method utilised the Phase Lock Gel Heavy (5 Prime) product to ensure no contamination of

the organic phase and the aqueous phase, the second method did not use the gel tubes and prove to be robust.

The following procedure was performed in a fume hood where no post PCR products were handled. Samples in TRIzol® were either used directly or thawed from -80°C. 0.2ml of chloroform was added per 1ml TRIzol® homogenate. The sample in TRIzol® was shaken vigorously for approximately 15 seconds and then left to stand at RT for 3 minutes.

For the samples extracted using the Phase Lock Heavy Gel tube (5-Prime), the gel tube was first prepared by pre-centrifugation at 12000g for 3 minutes at RT. Then the sample was loaded into the Phase Lock tube. Whether the Phase Lock tube was used or not the extraction continued as per the RNeasy® Mini Kit (Qiagen) protocol as follows.

Samples were centrifuged at 12000g for 15 minutes at 4°C. The aqueous phase was then removed carefully by aspiration and transferred to a new RNAse free tube. The sample volume was noted and an equal volume of 70% ethanol was added slowly. The sample, including any precipitation that had occurred, was loaded into an RNeasy® column on a collection tube and centrifuged at 8000g for 30 seconds. The flow-through was discarded and the sample sat on a new collection tube. 700µl RW1 buffer (2.5-10% guanidine thiocyanate, 2.5-10% ethanol) was added to the column and centrifuged again for 30 seconds at 8000g. The flow-though was discarded and the column seated on a new collection tube. Ethanol was added to the RPE buffer and 500µl was added to the column which was again centrifuged for 30 seconds at 8000g. This was repeated but with a 2 minute centrifugation, discarding the flow-through between steps. The tube was then centrifuged empty in a new collection tube for a further 1 minute to remove any remaining buffer in the column. The column was transferred to the final collection tube and 30µl of RNase-free water added to the column membrane. The sample was left for 2 minutes at RT before a final centrifuge of 1 minute at 8000g to elute the RNA. 1µl of RNA was used to quantify the product using a spectrophotometer (NanoDrop, Thermo Scientific) and the remainder was stored at -80°C or used immediately for downstream applications.

5.4.8 RNA Quantification

The NanoDrop spectrophotometer was used to quantify the RNA concentration and measure its purity and integrity. First the upper and lower optical surfaces were cleaned. The NanoDrop was initialised and a blank measurement performed on 1 µl of deionised water pipetted onto the lower optical surface. 1µl of the RNA was then pipetted onto the lower surface and measurement performed using the NanoDrop propriety software in nucleic acid mode. This calculates the nucleic acid concentration (Gallagher and Desjardins 2006).

5.4.9 First Strand cDNA Synthesis

First strand cDNA synthesis was performed originally using ThermoScript™ (Invitrogen) and subsequently by SuperScript® VILO™ cDNA synthesis kit (Invitrogen) due to the improved yields obtained using this protocol.

1. **ThermoScript™ cDNA synthesis**

In an RNase-free 0.2ml thin walled tube (StarLab) the RNA was added to 1µl random hexamers (50ng/µl) and 2µl 10nM dNTP mix and made up to 12µl with DEPC treated water. This was incubated at 65°C for 5 minutes then transferred onto ice. 8µl of cDNA synthesis mix was added which is made up of 4µl 5X cDNA buffer (250mM Tris acetate (ph 8.4), 375mM potassium acetate, 40mM magnesium acetate and stabilizer), 1µl 0.1M DTT, 1µl RNaseOUT™(40U/µl), 1µl DEPC water and 1µl ThermoScript™ RT. The tube was incubated for 25°C for 10 minutes, then 50°C for 45 minutes and finally the reaction was terminated by incubation at 85°C for 5 minutes. 1µl of RNase H was added and incubated for 20 minutes at 37°C. The resultant cDNA was subsequently used immediately for downstream reactions or stored at -20°C.

2. **SuperScript® VILO™ cDNA synthesis**

In an RNase-free 0.2ml thin walled tube (StarLab) the RNA was added to 4µl 5X VILO™ reaction mix (random primers, MgCl$_2$ and dNTPs in a proprietary buffer formulation), 2µl 10X SuperScript® enzyme mix and made up to 20µl with DEPC treated water. The contents were gently mixed and incubated at 25°C for 10 minutes, then at 42°C for 60 minutes. The reaction

was terminated by incubating at 85°C for 5 minutes. The resultant cDNA was subsequently used immediately for downstream reactions or stored at -20°C.

5.4.10 Ligation of Novel Oligonucleotide to Single Stranded cDNA

For the ligation anchored PCR experiments the following optimised method was used. The cDNA was washed and then resuspended in x1 NEB reaction buffer (50 mM Tris-HCl, pH 7.8, 10 mM MgCl2, 10 mM DTT, 1 mM ATP). 10µl of 100pmol oligonucleotide for ligation was added with 25% (w/v) PEG 8000 and 1µl T4 RNA ligase (NEB). The oligo for ligation was phosphorylated at the 5'end and 3'ddC and is shown in Table 5-3.

The ligation mix was incubated at 22°C for 72 hours.

Table 5-3 Ligation PCR oligonucleotide and primer design

	Sequence
Oligonucleotide for ligation	5' (PHO)TAGGATCTGGGACGGATGGC(3'ddC) 3'
TCR Forward Primer	5' CTCAAACACAGCGACCTCGG 3'
Oligo Reverse Primer	5' GCCATCCGTCCCAGATCCTA 3'

5.4.11 Polymerase Chain Reaction Methods

The PCR methodologies were subject to numerous modifications and optimisation steps and the final methods are presented below. The final method used for TCR Vβ TCR repertoire spectratyping is method 4.

1.   Ligation Anchored PCR

cDNA was washed in x1 PCR buffer and was added to 5µl 10x PCR buffer (without Mg), 1.5µl 50Mm MgCl, 1µl 10mM dNTP mix, 0.4µl and Platinum Taq DNA polymerase (5U/µL). Forward and reverse primers were added. Primers used are detailed in Table 5-3. DEPC treated water was added to make up to final volume 50µl.

The PCR was undertaken using a Veriti® 96-well thermal cycler (Applied Biosystems) according to the following program:

1. Hot start: 94°C 2 minutes

2. Denaturation: 94°C 30 seconds ⎫

3. Annealing: 55°C 30 seconds ⎬ X30 cycles

4. Elongation: 72°C 108 seconds ⎭

5. Final elongation 72°C 5 minutes

6. Hold 4°C

2. PCR Housekeeping Gene (Beta Actin)

The beta actin primer set is shown in Table 5-4. The PCR was undertaken in 0.2ml thin walled tubes (StarLab). To each tube 2 µl of cDNA was mixed with 12.5µl TaqMan® Gene Expression Master Mix (AmpliTaq Gold® DNA Polymerase, Uracil-DNA glycosylase, dNTPs (with dUTP), ROX™ Passive Reference, and optimized buffer components), 2.5µl β actin forward primer, 2.5µl β actin reverse primer and the final volume was made up to 25µl with water.

The PCR was undertaken using a Veriti® 96-well thermal cycler (Applied Biosystems) according to the following program:

1. 94°C 30 seconds ⎫

2. 55°C 30 seconds ⎬ X 40 Cycles

3. 72°C 108 seconds ⎭

4. Hold 4°C

Table 5-4 Beta actin primer set

β actin Primers	Sequence
Forward	5' TGGCGCTTTTGACTCAGGAT 3'
Reverse	5' GGGATGTTTGCTCCAACCAA 3'

3. PCR Housekeeping Gene (Abl)

The Abl (Abelson murine leukaemia viral oncogene homolog 1) primer set is shown in Table 5-5. The PCR was undertaken in 0.2ml thin walled tubes (StarLab). To each tube 2µl of cDNA was mixed with 12.5µl TaqMan® Gene Expression Master Mix (AmpliTaq Gold® DNA

Polymerase, Uracil-DNA glycosylase, dNTPs (with dUTP), ROX™ Passive Reference, and optimized buffer components), 2.5μl Abl forward primer, 2.5μl Abl reverse primer and the final volume was made up to 25μl with water.

The PCR was undertaken using a Veriti® 96-well thermal cycler (Applied Biosystems) according to the following program:

1. $50°C$ 2 minutes

2. $95°C$ 10 minutes

3. $95°C$ 15 seconds

4. $60°C$ 1 minute

X 40 Cycles

5. Hold $4°C$

Table 5-5 Abl primer set

Abl Primers	Sequence
Forward	5' GATACGAAGGGAGGGTGTACC A 3'
Reverse	5' CTCGGCCAGGGTGTTGAA 3'

4. PCR TCRVβ Repertoire

The final method for assessing the TCRVβ repertoire by PCR using AccuPrime™ Taq DNA Polymerase High Fidelity (Invitrogen) is outlined below.

The 24 forward Vβ primer and Cβ reverse primer sequences are detailed in Table 5-6. The Cβ primer was FAM labelled for subsequent analysis.

The PCR was undertaken in a 96 well plate (Applied Biosystems). To each well the cDNA was mixed with 2.5μl of 10X AccuPrime™ PCR Buffer I (600mM Tris-SO_4 (pH 8.9), 180mM $(NH_4)_2SO_4$, 20mM $MgSO_4$, 2mM dGTP, 2mM dATP, 2mM dTTP, 2mm dCCT, thermostable AccuPrime™ protein and 10% glycerol), 2μl forward primer, 2μl reverse primer, 0.2μl AccuPrime™ Taq DNA Polymerase High Fidelity (5U/μl), 1μl $MgSO_4$ (50mM) and the final volume was made up to 25μl with water.

The PCR was undertaken using a Veriti® 96-well thermal cycler (Applied Biosystems) according to the following program:

1. Hot start: 95°C 5 minutes

2. Denaturation: 94°C 45 seconds

3. Annealing: 60°C 45 seconds   X40 cycles

4. Elongation: 72°C 90 seconds

5. Final elongation 72°C 5 minutes

6. Hold 4°C

Table 5-6 Vβ primer set for TCR sequencing

Primer	Sequence
Vβ1	5′ GTAGTGCGATGGCCAGTCCGCACAACAGTTCCCTGACTTGC 3′
Vβ2	5′ GTAGTGCGATGGCCAGTGGCCACATACGAGCAAGGCGTCGA 3′
Vβ3	5′ GTAGTGCGATGGCCAGTCGCTTCTCCCGGATTCTGGAGTCC 3′
Vβ4	5′ GTAGTGCGATGGCCAGTTTCCCATCAGCCGCCCAAACCTAA 3′
Vβ5	5′ GTAGTGCGATGGCCAGTAGCTCTGAGCTGAATGTGAACGCC 3′
Vβ6	5′ GTAGTGCGATGGCCAGTTCTCAGGTGTGATCCAAATTCGGG 3′
Vβ7	5′ GTAGTGCGATGGCCAGTCCTGAATGCCCCAACAGCTCTCTC 3′
Vβ8	5′ GTAGTGCGATGGCCAGTCCATGATGCGGGGACTGGAGTTGC 3′
Vβ9	5′ GTAGTGCGATGGCCAGTTTCCCTGGAGCTTGGTGACTCTGC 3′
Vβ10	5′ GTAGTGCGATGGCCAGTCCACGGAGTCAGGGGACACAGCAC 3′
Vβ11	5′ GTAGTGCGATGGCCAGTTGCCAGGCCCTCACATACCTCTCA 3′
Vβ12	5′ GTAGTGCGATGGCCAGTTGTCACCAGACTGGGAACCACCAC 3′
Vβ13	5′ GTAGTGCGATGGCCAGTCACTGCGGTGTACCCAGGATATGA 3′
Vβ14	5′ GTAGTGCGATGGCCAGTGGGCTCGGCTTAAGGCAGACCTAC 3′
Vβ15	5′ GTAGTGCGATGGCCAGTCAGGCACAGGCTAAATTCTCCCTG 3′
Vβ16	5′ GTAGTGCGATGGCCAGTGCCTGCAGAACTGGAGGATTCTGG 3′
Vβ17	5′ GTAGTGCGATGGCCAGTCTGCTGAATTTCCCAAAGAGGGCC 3′
Vβ18	5′ GTAGTGCGATGGCCAGTTGCCCCAGAATCTCTCAGCCTCCA 3′
Vβ19	5′ GTAGTGCGATGGCCAGTTCCTCTCACTGTGACATCGGCCCA 3′
Vβ20	5′ GTAGTGCGATGGCCAGTTCTCAATGCCCCAAGAACGCACCC 3′
Vβ21	5′ GTAGTGCGATGGCCAGTTCCAACCTGCAAGGCTTGACGACT 3′
Vβ22	5′ GTAGTGCGATGGCCAGTAAGTGATCTTGCGCTGTGTCCCCA 3′
Vβ23	5′ GTAGTGCGATGGCCAGTGCAGGGTCCAGGTCAGGACCCCCA 3′
Vβ24	5′ GTAGTGCGATGGCCAGTCCCAGTTTGGAAAGCCAGTGACCC 3′
Cβ	5′ CAGTGTGCAGCGATGACCGGGCTGCTCCTTGAGGGGCTGCG 3′

5.4.12 TBE Agarose Gel

PCR products were run on a 2% TBE (Tris/Borate/EDTA) agarose gel to ensure successful amplification prior to running on the Genetic Analyser (Applied Biosystems). The gel was made up with 150ml 1X TBE (5-Prime) and 3g agarose (Bioline), which was microwaved for 3 minutes, left to cool and then 10µl ethidium bromide (10µl/ml) was added. The gel was run

at 150V for 1-2 hours. 5X DNA loading buffer blue (bromophenol blue) (Bioline) and HyperLadder I or V (Bioline) were used for visualisation and product sizing.

5.4.13 DNA Gel Extraction

MinElute Gel Extraction Kit (Qiagen) was used to extract DNA from the gel. The PCR product of interest on the gel was excised using a scalpel. The gel was weighed and 3 volumes of Buffer QG (Qiagen) was added per 1 volume of 2% gel (100mg gel = 100µl). This was incubated for 10minutes at 50°C to dissolve the gel. pH was corrected with 3M sodium acetate as required. Isopropanol was added at equivalent gel volume. The sample was added to the MinElute spin column, inside a collection tube and centrifuged for 1 minute. The flow through was discarded and 500µl of Buffer QG was added and the tube centrifuged again. Then 750µl of Buffer PE (Qiagen) was added and centrifuged again. To elute the DNA 10µl of Buffer EB (10nM TrisCl, pH 8.5) was added and the tube was left to stand for 1 minute before centrifuging for 1 minute. The eluted DNA was collected for downstream applications.

5.4.14 PCR Product Sequencing

The cleaned PCR products were sent to Geneservice™ (Source Bioscience) for Sanger sequencing. They undertake a plasmid based protocol using the primers we provided.

5.4.15 TCRVβ Spectratyping Fragment Analysis

The Genetic Analyser 3130XL (Applied Biosystems) was used to size PCR products. To each well of a 96 well plate (Applied Biosystems) 1µl of the FAM labelled PCR product was added to 0.8µl ILS-600 (Internal Lane Standard 600, Promega) and 8.8µl formamide. The plate was incubated at 95°C for 3 minutes before being run on the Genetic Analyser; a fluorescence-based capillary electrophoresis system, as described above.

5.4.16 TCRVβ Spectratyping Profile Analysis

Once the CDR3 amplicons were sized using the Genetic Analyser, the data was analysed using the GeneMapper Software (Applied Biosystems). The software generates a graphical spectratyping prolife usually consisting of 8 (5-10) major peaks each representing a CDR3 length differing from the next by 3 nucleotides. The fluorescence intensity is representative of the frequency of the CDR3. A spectratyping profile is produced for each of the 24 TCRVβ

families. An example of a spectratype prolife for one Vβ family from one sample is shown in Figure 5-2 below. The Bell shaped curve represents the normal distribution.
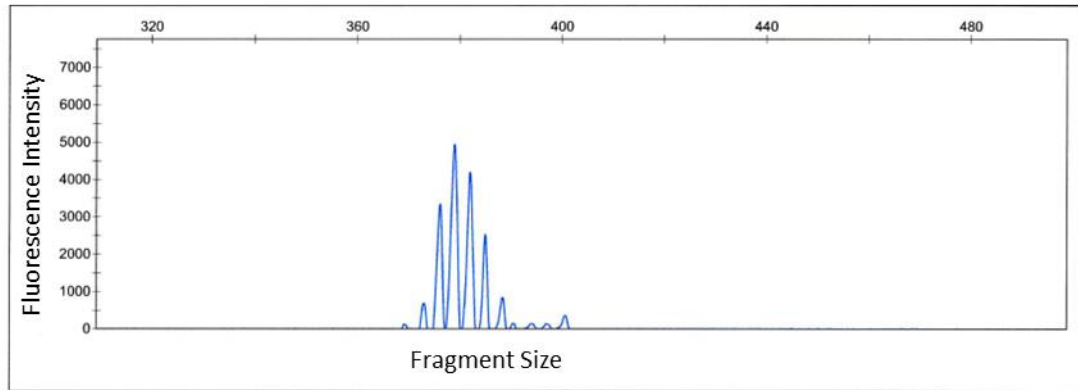
Figure 5-2 Typical TCRVβ spectratype profile
This is an example spectratype profile from one TCRVβ family visually represented using GeneMapper Software (Applied Biosystems). A normal TCRVβ spectratype prolife consists of 8 (5-10) major peaks each representing a CDR3 length (fragment size) differing from the next by 3 nucleotides. The fluorescence intensity is representative of the frequency of the CDR3. The Bell shaped curve confirms the normal distribution.

There is no universally accepted method of spectratyping profile analysis and a range of methods have been employed. Some groups have used visual assessment (Ferrand, Robinet et al. 2000, Kook, Risitano et al. 2002), whilst others have adopted scoring methods (Bomberger, Singh-Jairam et al. 1998, Wu, Chillemi et al. 2000, Peggs, Verfuerth et al. 2003). Ciupe et al in the department of mathematics at Virginia Tech have described a mathematical method of assessing the deviance of spectratypes form the normal repertoire. They used computational mathematics to calculate the Kullback-Leibler divergence to ascertain the difference of the TCRVβ profile from a normal reference (Ciupe, Devlin et al. 2013). We employed two complementary scoring methods adapted from the published literature (Wu, Chillemi et al. 2000, Lu, Basu et al. 2004, Le, Melenhorst et al. 2011). Spectratype profiles were compared for their complexity (number of discrete peaks) and diversity (skewing of the distribution) (Ciupe, Devlin et al. 2013). A complexity score was derived by assigning the spectratype of each subfamily a score of 0-5, dependent on the number of discrete peaks, and then multiplying by the number of TCRVβ families. Spectratypes with >5 peaks were given the maximum score of 5 and no peaks 0. The total complexity score is out of 120 (24x5) (Wu, Chillemi et al. 2000, Lu, Basu et al. 2004). A diversity score was used to ascertain skewed

profiles and a score of 1 given for a single peak being >x2 the height of the next second highest peak. The total diversity score was calculated by summating the scores for all the TCRVβ families, with 24 being the most skewed profile and 0 the least. An example of the scoring is shown in Figure 5-3.
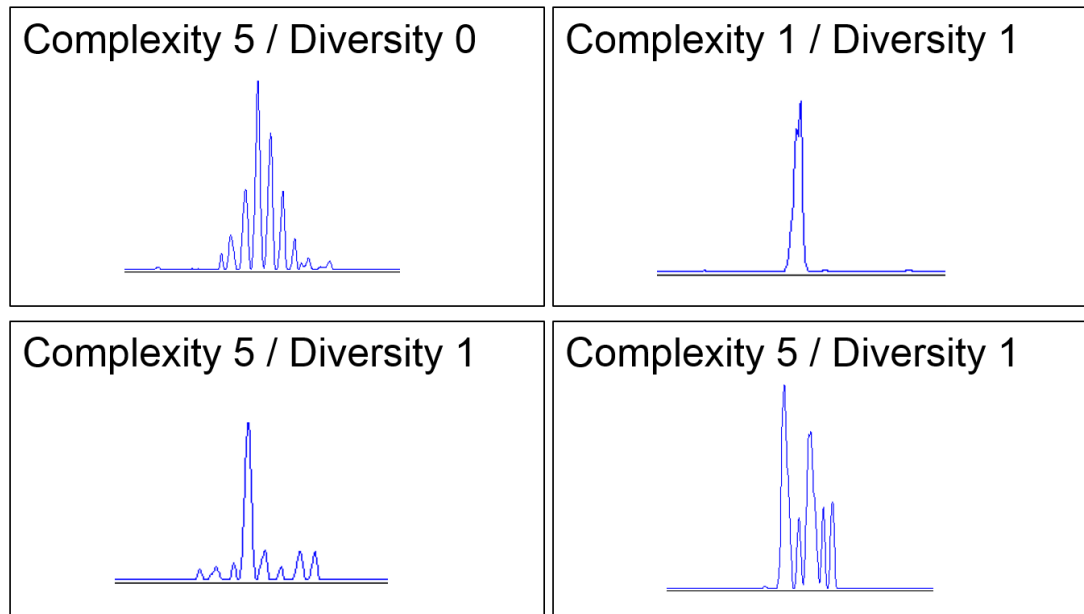
Figure 5-3 Spectratype scoring system
Spectratype profiles are visually assessed for their complexity (number of discrete peaks) and diversity (skewing). The complexity of a TCRVβ spectratype is derived by assigning a score of 0-5, dependent on the number of discrete peaks in the profile. Spectratypes with >5 peaks are given the maximum score of 5 and no peaks 0. The maximum complexity score across the 24 TCRVβ families is 120 (24x5). A diversity score of 1 is assigned to a skewed spectratype profile when a single peak is >x2 the height of the next second highest peak. A total diversity score is calculated by summating the scores for all the TCRVβ families, with 24 being the most skewed profile and 0 the least. The panels above show four examples of differing spectratype profiles and the associated complexity and diversity scoring.

5.4.17 Statistical Analysis

Statistical analysis of the diversity or complexity scores was performed using GraphPad Prism® (Graph Pad Inc.). For paired comparisons to be made between LN FNA and PB populations a paired t-tests was performed and a p-value of <0.05 was considered statistically significant. For comparison between un-paired sample an unpaired t-test was used and again a p-value of <0.05 was considered statistically significant. Results are expressed +/- standard error of the mean. Box and whiskers plots show the median and minimum and maximum values. The statistical analysis used for HTS data is described in the text.

5.4.18 High Throughput Sequencing Analysis

cDNA samples were sent to Adaptive Biotechnologies® using propriety plates. Amplification and sequencing of TCRVβ CDR3 was performed using the immunoSEQ Platform (Adaptive Biotechnologies®, Seattle, WA). TCRVβ CDR3 regions were amplified using a bias controlled high throughput multiplex PCR on the Illumina platform. TCRVβ CDR3 sequences from Adaptive Biotechnologies are defined according to the International ImMunoGeneTics (IMGT) collaboration nomenclature (Yousfi Monod, Giudicelli et al. 2004). Results were made available through the ImmunoSEQ analyser software. The immunoSEQ Platform combines multiplex PCR with high throughput sequencing and a sophisticated bioinformatics pipeline for TCRVβ CDR3 analysis (Robins, Campregher et al. 2009, Carlson, Emerson et al. 2013). The software allows repertoire characterisation, clone tracking and clone identification.

5.5 Results

5.5.1 Demographics of patients and normal controls for spectratyping

The demographics of the CLL patients studied for TCRVβ repertoire by spectratyping is shown in Table 5-7. An additional patient consented to this study and underwent FNA and cell sorting but was subsequently identified to be hepatitis B positive and were therefore excluded. PB from six aged matched normal controls was also taken. The mean age for CLL patients was 61 years +/- 2.07 compared to 58 years +/- 5.05 for healthy controls. There was no statistical difference between the ages p= 1.00, see Figure 5-4.

Table 5-7 Demographics of CLL patients for spectratyping

	Age	Sex	CMV	EBV	Binet	CD38%	Cyto/FISH	Mutational Status
CLL1	38	F	NEG	POS	C	98	17p-	Mutated
CLL2	64	M	POS	POS	C	87	Trisomy 12	Unmutated
CLL3	64	M	NEG	POS	B	57	17p-	Unmutated
CLL5	74	M	POS	POS	C	62	13q-	Unmutated
CLL6	57	M	NEG	POS	A	0	13q-	Mutated
CLL 7	52	M	NEG	POS	A	0	13q-	Mutated
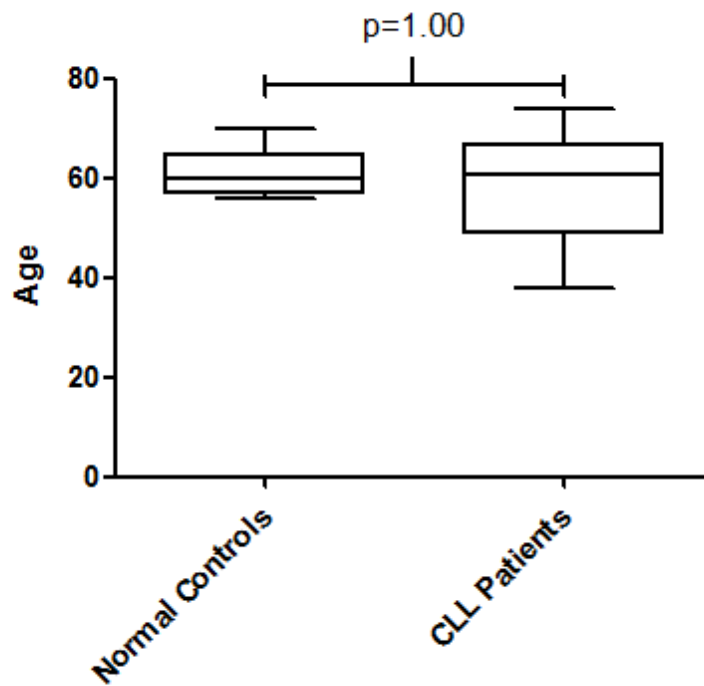
Figure 5-4 Age demographics of patients and normal controls
Age of CLL patients (n=6) and healthy controls (n=6). A D'Agostino and Pearson omnibus normality test was applied prior to un-paired t-test using GraphPad Prism® (Graph Pad Inc.).

5.5.2 Ligation anchored PCR

Our initial experimental approach to sequencing the TCR was to undertake the ligation anchored PCR method. The design was to ligate a unique oligonucleotide sequence to the single stranded cDNA with a 5' phosphorylation and a 3' ddC, to ensure the ligation can only occur in a one direction. We designed a unique oligonucleotide which had no sequence homology to the TCRVβ in the human genome using NCBI BLAST (Basic Local Alignment Search Tool). Next we chose a primer for the constant region of the CDR3 of the TCR and a complimentary primer to the bespoke oligonucleotide. The oligonucleotide and primer design is shown in Table 5-3.

As a proof of principle we used the Jurkat cell line for initial ligation experiments. Jurkat cells are an immortalized human T-cell line from a patient with T lineage acute lymphoblastic leukaemia. Jurkat cells were grown in cell culture as described in 2.5.2. The mRNA was directly isolated according to the Dynabeads® mRNA Direct™ protocol from 1×10^6 cells described in 5.4.7.1. First strand cDNA synthesis was then undertaken according to the ThermoScript™ cDNA synthesis protocol described in 5.4.9. A control PCR of a housekeeping gene was undertaken using beta actin (primers kindly donated by Dr Costas Chronis) as described in 5.4.11. This required several optimisation steps. A successful amplification of actin is shown in Figure 5-5.
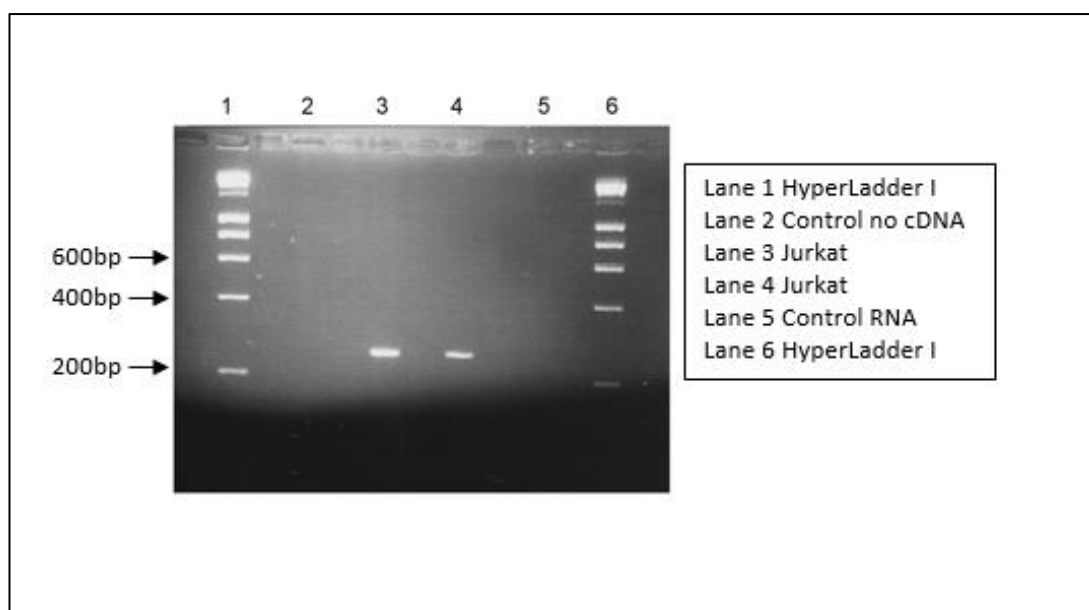
Figure 5-5 Actin in successfully amplified in Jurkat cell line

mRNA was directly isolated from $1x10^6$ cells Jurkat cells, then first strand cDNA was synthesised and a PCR of the actin gene was undertaken as described. The PCR products were run on a TBE gel with ethidium bromide. The gel was run at 150V for 2 hours. Lanes 1&6 show the sizing ladder (HyperLadder I, Bioline), lane 2 is a negative control (no cDNA), lanes 3&4 show the PCR product (actin) in Jurkat cDNA, lane 5 is a negative control (Jurkat RNA).

The Oligonucleotide ligation took many optimisation steps before a PCR product was successfully amplified using the novel TCR primers. A literature review was undertaken to find ways to optimise the ligation. Table 5-8 summarises the published methods. We repeated a series of experiments altering the amount of oligo, total volume, buffer, concentrations of magnesium, PEG, BSA and T4 ligase. We additionally undertook a series of temperature gradient modifications. The successfully optimised ligation method is described in 5.4.10.

Table 5-8 Review of published methods for ligation anchored PCR

Source	Amount Anchor	Volume	Buffer Constituents									
			Tris-HCL	pH	MgCl2	BSA	PEG	Hexamine Colbat Chloride	ATP	DTT	T4 Ligase
Troutt (Troutt, McHeyzer-Williams et al. 1992)	10pM	10µl	50Mm	8.0	10mM	10µg/ml	8000 25% (wt/vol)	1mM	20µM		20U (1 µl)
Ansari-Lari (Ansari-Lari, Jones et al. 1996)	100pM	10µl	50mM	8.0	10mM	10µg/ml	8000 25% (wt/vol)	1mM	20µM		20U (1 µl)
Zhang (Zhang, Kaur et al. 2002)	25nM	20µl	50mM	7.5	10mM	60µg/ml	Suggested	Suggested	1mM	10mM	10U (0.5 µl)
NEB protocol		10µl	50mM	7.8	10mM		8000 25% (wt/vol)	1mM	1mM	10mM	20U (1 µl)

The negative control for the ligation TCR PCR was cDNA made from selected CLL B-cells. B-cell selection method is described in 2.2.5. Clearly B-cells should not amplify a TCR even after a successful anchor ligation. A control PCR using actin was undertaken to prove cDNA was extracted successfully from the B-cells. A successful amplification of the Jurkat TCR and the positive and negative controls are shown in Figure 5-6.
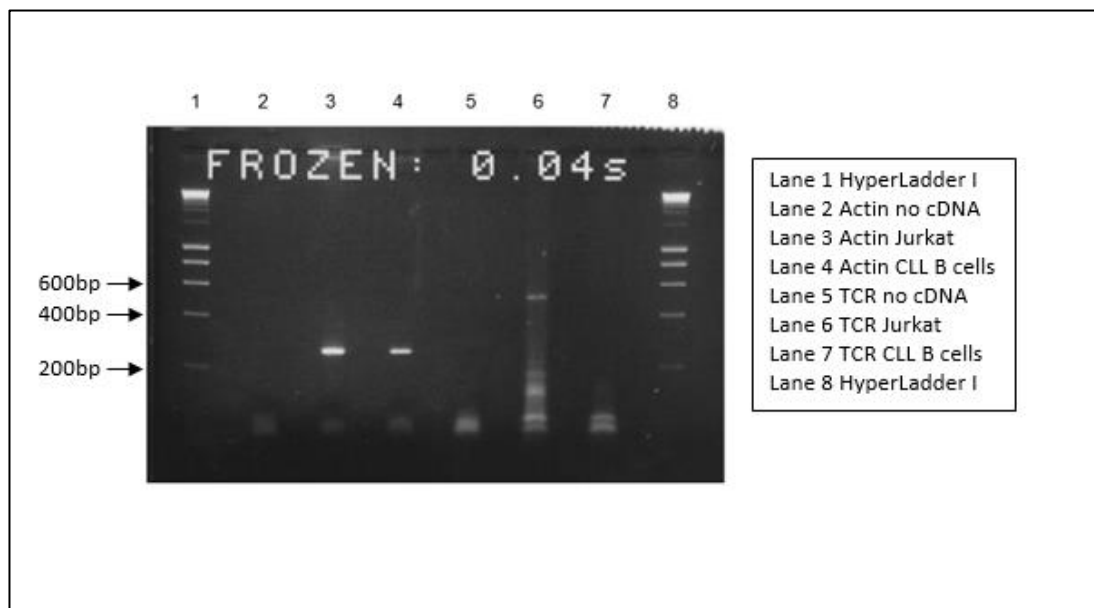
Figure 5-6 Successful TCR amplification in Jurkat cell line (lane 6)
RNA was isolated from 1×10^6 cells Jurkat cells and selected CLL B-cells. First strand cDNA was synthesised and the oligonucleotide ligation undertaken as described. PCR was undertaken to control gene actin and to the TCR (using the TCR forward primer and the ligated oligonucleotide as a reverse primer). The PCR products were run on a TBE gel with ethidium bromide. The gel was run at 150V for 2 hours. Lanes 1&8 are the sizing ladder (HyperLadder I, Bioline), lane 2 is the actin PCR negative control (no cDNA), lane 3 is the actin PCR product in Jurkat cDNA, lane 4 is the actin PCR product in CLL B-cells cDNA, lane 5 is the TCR PCR negative control (no cDNA), lane 6 is the TCR PCR product in Jurkat cDNA, lane 7 is a TCR negative control (CLL B-cells).

The band presumed to be representing the TCR of the Jurkat in lane 6 was cut out of the gel and cleaned up as in 5.4.13. In order to optimise the yield the cleaned up PCR product was amplified with a further 20 PCR cycles. The band was then cut out and cleaned up again. The result PCR product is shown on the gel photo in Figure 5-7.
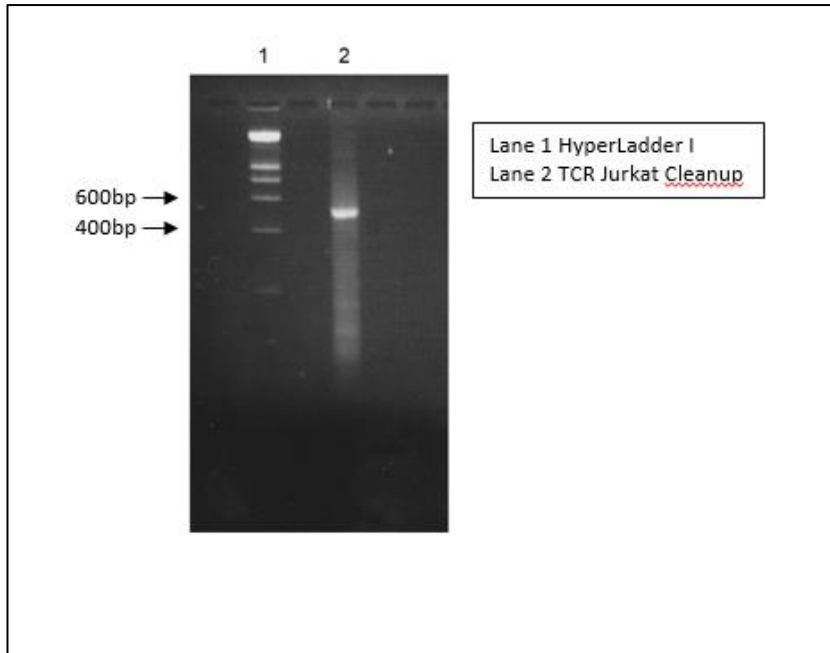
Figure 5-7 Lane 2 shows the cleaned up Jurkat TCR PCR product
The TCR PCR product in Figure 5-6 was excised from the gel and cleaned up using the MinElute Gel Extraction Kit (Qiagen) as described. The cleaned up PCR product was amplified with a further 20 PCR cycles. The resultant PCR products were run on a TBE gel with ethidium bromide. The gel was run at 150V for 2 hours. Lanes 1 is the sizing ladder (HyperLadder I, Bioline), lane 2 is the TCR PCR product.

5.5.3 Gene sequencing of TCRVβ

The cleaned PCR product was sent to Geneservice^{TM} (Source Bioscience) for Sanger sequencing as described in 5.4.14. They undertake a plasmid based protocol using the primers we provided. The sequence was returned as 503bp. A snapshot of the sequence is shown in Figure 5-8.
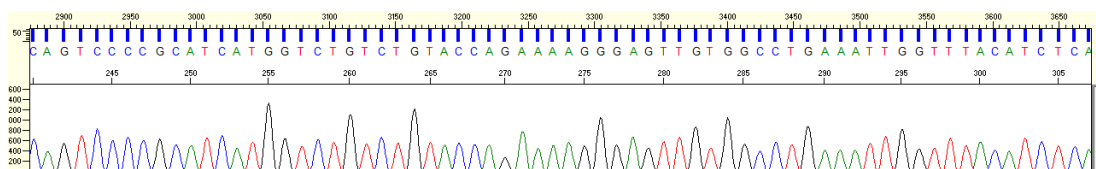
Figure 5-8 Snapshot of sequencing data of PCR product
The TCR PCR product from the Jurkat cell line from Figure 5-7 was sent to Geneservice^{TM} (Source Bioscience) for Sanger sequencing using a plasmid based protocol. The sequence was returned was 503bp.

The full sequence is shown in Figure 5-9. We used the sequence identification tool NCBI BLAST to find matching sequences in the human genome database (RefSeq Genome). The database identified the sequence as Homo sapiens T-cell receptor beta locus (TRB) on chromosome 7 family TCRVβ 12. This confirms that the oligo ligation PCR worked and the TCR could be successfully amplified.

Homo sapiens T cell receptor beta locus (TRB) on chromosome 7
Sequence ID: ref|NG_001333.2| Length: 684973 Number of Matches: 6

Range 1: 395467 to 395761 GenBank Graphics ▼ Next Match ▲ Previous Match

Score	Expect	Identities	Gaps	Strand
538 bits(291)	7e-150	293/295(99%)	0/295(0%)	Plus/Minus

```
Query  82     aaanTGNTGGCACAGAAGTACACAGCTGAGTCCCTGGGTTCTGAGGGCTGGATCTTCAGA  141
              ||| || ||||||||||||||||||||||||||||||||||||||||||||||||||||
Sbjct  395761  AAACTGCTGGCACAGAAGTACACAGCTGAGTCCCTGGGTTCTGAGGGCTGGATCTTCAGA  395702

Query  142    GTGGAGAATGATGCATTAGGCATCTTAGCTGAGAATCGATCCTCGGGCATCCCTGAATCA  201
              ||||||||||||||||||||||||||||||||||||||||||||||||||||||||||||
Sbjct  395701  GTGGAGAATGATGCATTAGGCATCTTAGCTGAGAATCGATCCTCGGGCATCCCTGAATCA  395642

Query  202    TCTATCGGAACGTTGTTGTTAAAGTAAATGAGCAACTCCAGTCCCCGCATCATGGTCTGT  261
              ||||||||||||||||||||||||||||||||||||||||||||||||||||||||||||
Sbjct  395641  TCTATCGGAACGTTGTTGTTAAAGTAAATGAGCAACTCCAGTCCCCGCATCATGGTCTGT  395582

Query  262    CTGTACCAGAAAAGGGAGTTGTGGCCTGAAATTGGTTTACATCTCAGAGTCACTTCTTGT  321
              ||||||||||||||||||||||||||||||||||||||||||||||||||||||||||||
Sbjct  395581  CTGTACCAGAAAAGGGAGTTGTGGCCTGAAATTGGTTTACATCTCAGAGTCACTTCTTGT  395522

Query  322    CCCATCTCTGTCACCTCATGGCGGGGTGACTGGATAACTCCAGCATCTGTATGCT  376
              ||||||||||||||||||||||||||||||||||||||||||||||||||||||||
Sbjct  395521  CCCATCTCTGTCACCTCATGGCGGGGTGACTGGATAACTCCAGCATCTGTATGCT  395467
```

Figure 5-9 BLAST search
The Jurkat TCR PCR product sequence obtained from Geneservice™ was searched for homology to known sequences in the human genome database (RefSeq Genome) using the NCBI BLAST sequence identification tool NCBI BLAST. The database identified the sequence as Homo sapiens T-cell receptor beta locus (TRB) on chromosome 7 family TCRVβ 12.

Despite the ultimately successful ligation of an oligo to the single stranded cDNA for TCR amplification the technique was time consuming, inconsistent and required a large amount of starting cDNA. The ligation was never successfully undertaken in primary patient material from normal controls or CLL patients (data not shown). The fundamental unanswered question remained - how efficiently was the cDNA being ligated? It follows that even if a very small percentage of the total Jurkat cDNA was successfully ligated this could enable amplification of the single clonal TCR. In contrast if only a proportion of the cDNA was ligated in a primary patient sample, with a diverse repertoire, then the whole TCR would not be represented. The question of ligation efficiency could potentially be answered by undertaking Jurkat cDNA spiking experiments. Nevertheless even if we did manage to construct a complete TCRVβ

library, a method for repertoire analysis would still need to be devised. Therefore we did not pursue this experimental approach any further for our study and instead proceeded with standard TCRVβ spectratyping.

5.5.4 TCRVβ spectratyping in primary patient material

TCRVβ spectratyping is the gold standard technique for assessing the TCR repertoire. We chose to assess the TCRVβ repertoire in CD4+ T-cells from the PD-1hi and PD-1lo populations from the PB and LN to look for inter-patient variations. This would be achieved by flow sorting the desired subpopulations, extracting total RNA and undertaking a PCR amplification of the 24 TCRVβ families before assessing the resultant fragment sizes on the Genetic Analyser. Initial experiments were again focused on optimising the method.

5.5.5 Jurkat cell TCRVβ spectratyping

As the ligation experiments and gene sequencing had confirmed the clonal TCR expression in the Jurkat cells we decided to use this cell line for initial TCRVβ spectratyping. This would provide a positive control for the presence of a clonal TCR and a negative control for the remaining Vβ families. We could also identify the cell number of Jurkats required to extract RNA and make cDNA successfully. cDNA was made from 5×10^5, 5×10^4, 1×10^4 and 1×10^3 Jurkat cells as described in 5.4.9. Abl was used as a housekeeping gene and PCR was undertaken as outlined in 5.4.11. Abl was successfully amplified in all 4 dilutions. A caveat is this experiment could not prove that 1000 cells would be adequate for successful amplification in primary patient material as cell lines do not express the same amount of RNA as primary patient T-cells.

Next we undertook the TCRVβ PCR using the 24 family specific primers as described in 5.4.11. As would be predicted, only one lane revealed an amplified product; which confirmed the clonal TCR production of the Jurkat cell line. We ran the samples on the Genetic Analyser and generated a dominant peak in one family confirming the clonal TCR. Figure 5-10 shows the presence of a dominant clonal peak. The two smaller peaks are likely PCR artefacts.
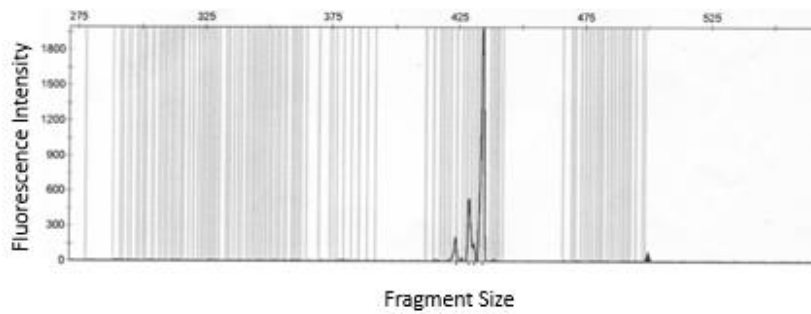
Figure 5-10 Dominant peak in Jurkat Vβ spectratype profile
mRNA was isolated from Jurkat cells and TCRVβ spectratyping was performed as described. The FAM labelled CDR3 PCR products were sized using the Genetic Analyser 3130XL (Applied Biosystems), and the data was visualised using the GeneMapper Software (Applied Biosystems). The PCR product size and fluorescence intensity is displayed, representative of the frequency of the CDR3. The dominant peak here represents the Jurkat TCR.

5.5.6 Cell sorting for TCRVβ spectratyping of primary patient T-cells

Subsets of CD4+ and CD8+ PD-1hi and PD-1lo T-cells were sorted from PB and LN FNA by

FACS as described in 5.4.6. Table 5-9 shows the total numbers of cells of each subpopulation

collected in the sort for each CLL patient.

Table 5-9 Total cell numbers of T-cell sub-populations collected in FACS sort
Subsets of CD4+ and CD8+ PD-1hi and PD-1lo T-cells were sorted from PB and LN as described using the BD FACSAria (BD Biosciences). Cells were sorted from the lymphocyte gate and populations defined as CD4+/PD-1hi, CD4+/PD-1lo, CD8+/PD-1hi, CD8+/PD-1lo.

Sample	CLL 1		CLL 2		CLL 3		CLL 5		CLL 6		CLL 7	
	PB	FNA	PB	FNA	PB	FNA	PB	FNA	PB	FNA	PB	FNA
CD4+ PD-1hi	10000	63427	42082	36276	36900	14612	21959	25409	4130	28299	15860	23595
CD4+ PD-1lo	10000	38179	31072	10535	54400	12797	31037	9425	8999	32595	36600	13446
CD8+ PD-1hi	10000	19810	10011	5643	10060	3348	6158	3559	4215	16364	24611	8221
CD8+ PD-1lo	10000	4787	18083	628	18200	1461	56982	2700	4166	3165	13924	1982

Statistical analysis using GraphPad showed a normal distribution of cells collected of each

CD4+ T-cell subpopulation within and between patients. The mean number of PB CD4+ PD-

1hi cells was 21822 +/- 6127. The mean number of PB CD4+ PD-1lo cells was 28685 +/-

7004. The mean number of LN CD4+ PD-1hi was 31936 +/- 6919. The mean number of LN

CD4+ PD-1lo was 19496 +/- 5112. There was no statistical difference in the number of cells

in each subpopulation. See Figure 5-11 and Figure 5-12
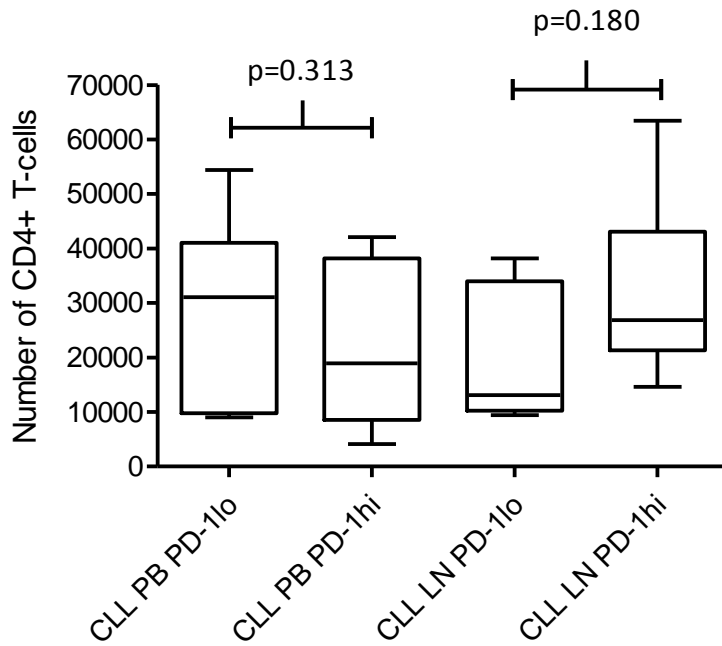
Figure 5-11 Number of each CD4+ T-cell subset in CLL FACS sort
CD4+ T-cells were sorted from PB and LN as described in Table 5-9. A statistical D'Agostino and Pearson omnibus normality test and un-paired t-test was applied using GraphPad Prism®. There was no statistical difference in the number of cells sorted from each subset.
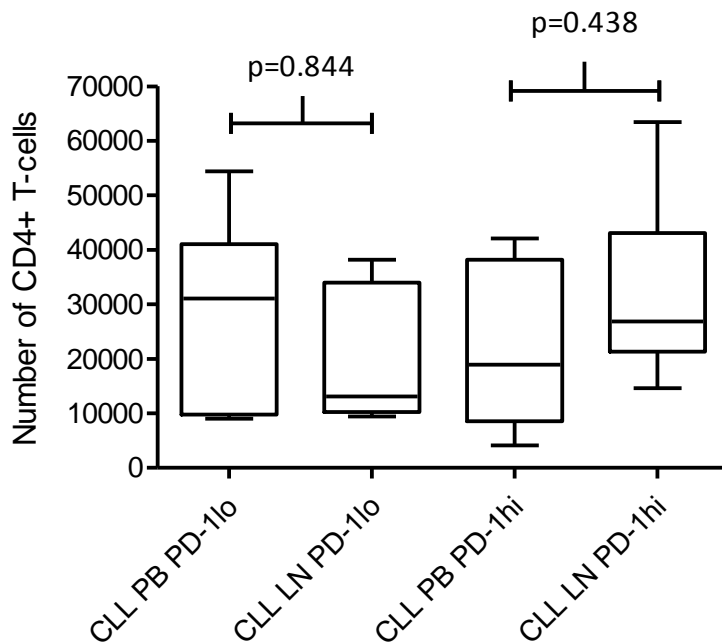
Figure 5-12 No difference in the number of cells sorted of each subpopulation
CD4+ T-cells were sorted from PB and LN as described in Table 5-9. A statistical D'Agostino and Pearson omnibus normality test and un-paired t-test was applied using GraphPad Prism®. There was no statistical difference in the number of cells sorted from each subset.

The total cell numbers collected from the PB of normal controls is shown in Table 5-10.

Table 5-10 Number of sorted cells from healthy control PB
Subsets of CD4+ and CD8+ PD-1hi and PD-1lo T-cells were sorted from PB of normal controls as described using the BD FACSAria (BD Biosciences). Cells were sorted from the lymphocyte gate and populations defined as CD4+/PD-1hi, CD4+/PD-1lo, CD8+/PD-1hi, CD8+/PD-1lo.

	Normal 1	Normal 2	Normal 3	Normal 4	Normal 5	Normal 6
CD4+ PD-1hi	10000	5547	3110	13000	18000	10000
CD4+ PD-1lo	10000	59732	80216	86000	88462	10000
CD8+ PD-1hi	6129	2279	5376	19500	6600	n/a
CD8+ PD-1lo	12572	13388	40702	13700	64000	n/a

There was no statistical difference between the number of cells collected from the PB of CLL patients and normal controls as shown in Figure 5-13.
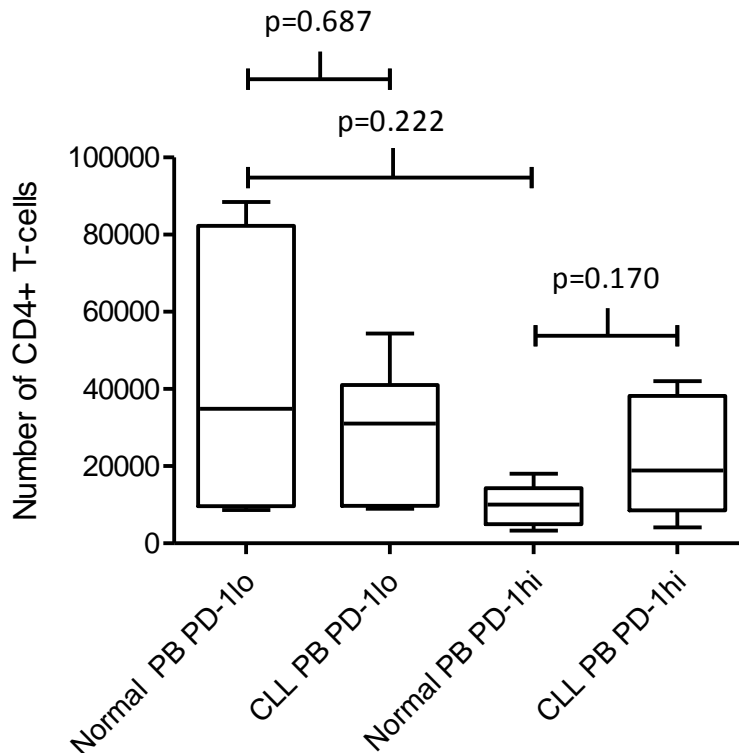
Figure 5-13 Number of sorted CD4+ PB cells normal vs CLL
CD4+ T-cells were sorted from PB from normal controls and CLL patients as described in Table 5-9. A statistical D'Agostino and Pearson omnibus normality test and un-paired t-test was applied using GraphPad Prism®. There was no statistical difference in the number of cells sorted from the PB of normal controls and CLL patients of any CD4+ subset.

5.5.7 RNA quantification

The amount of RNA was quantified using the NanoDrop as described in 5.4.8. The amount of RNA extracted from the flow sorted cells is shown in Table 5-11.

Table 5-11 Quantity of RNA extracted
CD4+ T-cells were sorted from PB and LN as described in Table 5-9. The number of cells sorted from each subset (CD4+/PD-1hi or CD4+/P1-lo) from both PB and LN is shown, with the corresponding quantity of RNA extracted in ng, as recorded using the NanoDrop (Thermo Scientific).

Sample	PB CD4 PD-1hi		PB CD4 PD-1lo		LN CD4 PD-1hi		LN CD4 PD-1lo	
	Cells	RNA ng	Cells	RNA ng	Cells	RNA ng	Cells	RNA ng
CLL1	10000	118	10000	448	63427	121	39179	157
CLL2	42082	78	31072	60	36276	47	10535	42.3
CLL3	36900	57	54400	444	14612	n/a	12797	57
CLL5	21959	199	31037	n/a	25409	504	9425	144
CLL6	4130	406	8999	261	28299	173	32595	280
CLL7	15860	102	36600	87	23595	113	13446	115

The technology relies on the surface tension of the drop forming a liquid column between the upper and lower optical measurement surfaces. The NanoDrop then measures the absorbance between 200nm and 350nm. The concentration of RNA can then be determined by the Beer-Lambert Law of the linear change in absorbance and concentration. The absorbance ratio at 260nm and 280nm is then quantified. RNA has maximal absorbance at 260nm and proteins, particularly aromatic amino acids absorb light at 280nm. Therefore the 260/280 ratio can be used to assess purity; where a ratio of 2 indicate pure RNA (Desjardins and Conklin 2010). There were some quality assurance issues with the NanoDrop machine in our laboratory at the time of measurement. Detergent cleaning which interferes with the liquid column formation, may have been the cause of the problem (Desjardins and Conklin 2010). With this caveat I present the data recorded.

The mean RNA quantity from each subpopulation of CD4+ T-Cells was as follows: PB CD4+ PD-1hi 160ng +/- 53; PB CD4+ PD-1lo 260ng +/- 84; LN CD4+ PD-1hi 191ng +/- 81; LN CD4+

PD-1lo 132.6ng +/- 35. There was no statistical difference between these amounts. See Figure 5-14.

The mean quantity of RNA extracted from normal control PB CD4+ PD-1hi was 356ng +/- 237 and PB CD4+ PD-1lo 192ng +/- 61. There was no statistical difference between these values p=1.00. There was also no statistical difference between the amount of RNA extracted from the PB subpopulations of CLL and normal controls: CD4+ PD-1hi PB CLL 160ng +/- 53 vs controls 356ng +/- 237; p=0.548. CD4+ PD-1lo PB CLL 260ng +/- 84 vs controls 192ng +/-61; p=1.00.
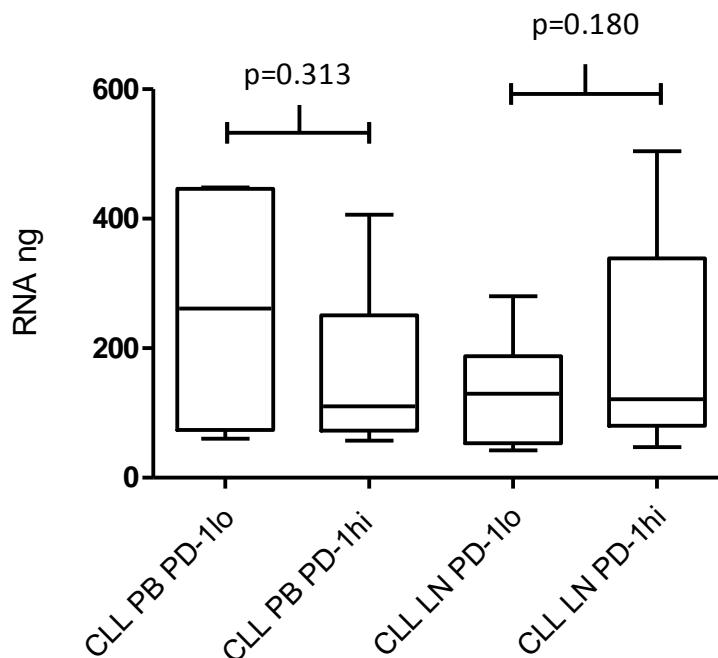
Figure 5-14 Quantity of RNA extracted from each CD4+ T-cell subpopulation in CLL patients CD4+ T-cells were sorted from PB and LN as described in Table 5-9. The quantity of RNA from each subset (CD4+/PD-1hi or CD4+/P1-lo) from both PB and LN is shown, as recorded using the NanoDrop (Thermo Scientific). A statistical D'Agostino and Pearson omnibus normality test and un-paired t-test was applied using GraphPad Prism®. There was no statistical difference in the quantity of RNA from any of the sorted CD4+ populations.

5.5.8 PCR of control housekeeping genes from sorted subpopulations

cDNA was synthesised from the RNA from each CD4+ T-cell subpopulation. Every cDNA sample was checked for integrity with the amplification of a housekeeping gene prior to the TCRVβ PCR as outlined in 5.4.11. The PCR underwent multiple optimisation steps and the

experiments were repeated with stepwise changes in the protocol due to the inability to consistently amplify PCR products. Whilst attempting to ascertain the reasons for the technical failures we used the human immortalized myeloid leukaemia cell line K562 as a positive control (donated by Dr Shahram Kordasti). Several issues were uncovered and it was finally determined the most significant problem was the intermittent use of a specific PCR thermal cycler in our laboratory which was not performing optimally. Figure 5-15 shows a representative example of the gel electrophoresis of successfully amplified Abl in all four CLL PB and LN CD4+ subpopulations from one patient.
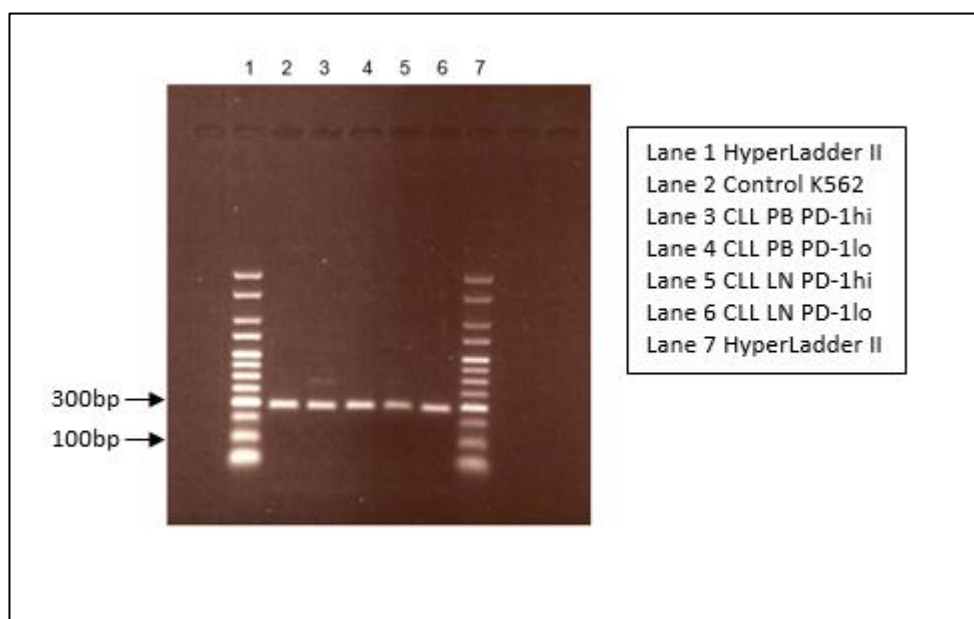
Figure 5-15 Abl amplification in PB and LN sorted CD4+ cell populations
RNA was extracted, first strand cDNA was synthesised and a PCR of the control gene abl was undertaken, as described, from the sorted CD4+ PD-1hi and PD-1lo populations from the PB and LN. The PCR products were run on a TBE gel with ethidium bromide. The gel was run at 150V for 1 hour. Lanes 1&7 show the sizing ladder (HyperLadder II, Bioline), lane 2 is an internal abl control with K562 (a non T-cell cell line), lanes 3-6 show the abl PCR product in all 4 sorted CD4+ populations (CLL PB CD4+/PD-1hi, CLL PBCD4+/PD-1lo, CLL LN CD4+/PD-1hi, CLL LN CD4+/PD-1lo).

5.5.9 TCRVβ PCR products were successfully amplified from the sorted cell populations

Following successful Abl amplification, the cDNA from each subpopulation was used to undertake the 24 individual PCR reactions, one for each TCRVβ family. The products of every individual population (24 families x4 sorted populations x6 patients) were ran on a gel prior to analysis in the Genetic Analyser. A representative gel electrophoresis of the resultant 24

TCRVβ family products from the CD4+ PD-1hi and PD-1lo subpopulations from the PB and LN of one patient is shown in Figure 5-16.
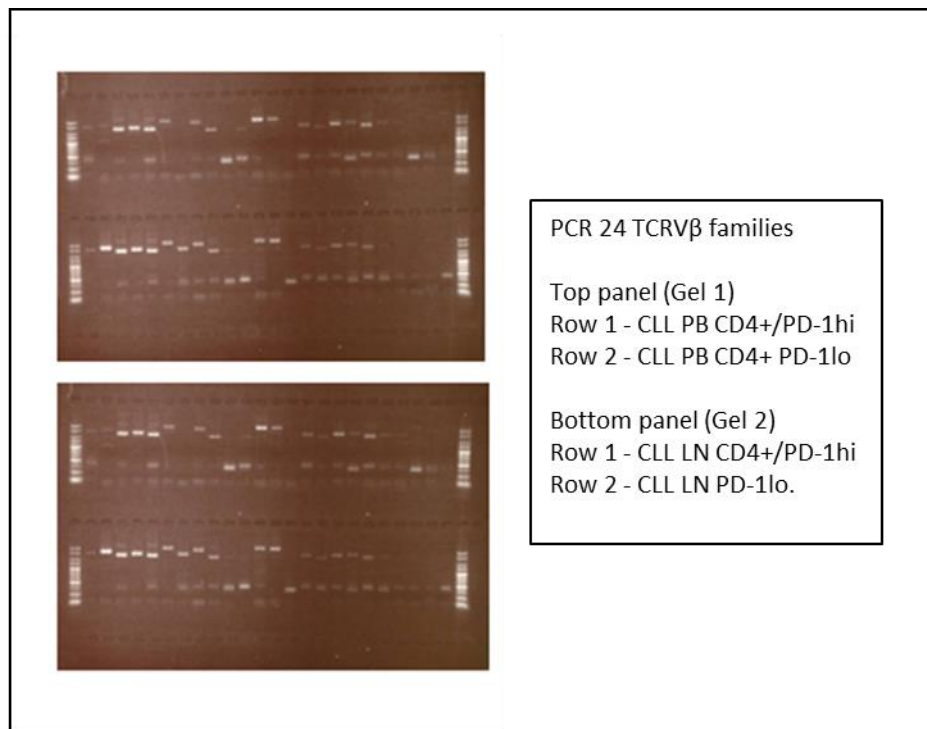
Figure 5-16 Representative figure from one patient showing 24 TCRVβ families amplification in the 4 sorted CD4+ T-cell populations
In this example RNA was extracted from the sorted CD4+ subpopulations from the CLL PB and LN as described. Then first strand cDNA was synthesised and TCRVβ PCR performed using 24 Vβ family specific forward primers and a constant FAM labelled reverse Cβ primer. The PCR products were run on a TBE gel with ethidium bromide. The gel was run at 150V for 1 hour. The photograph of the gels show the PCR products from the 24 Vβ family primers (1-24 left to right). The top panel (Gel 1) shows PCR products from the CLL PB CD4+/PD-1hi samples, the second row shows CLL PB CD4+ PD-1lo. The bottom panel (Gel 2) shows, in the first row, CLL LN CD4+/PD-1hi, and in the second row CLL LN PD-1lo. PCR products can be appreciated in all rows.

5.5.10 TCRVβ spectratyping

The resultant PCR products were subsequently run on the Genetic Analyser as described in 5.4.15. Initially not every Vβ family produced a spectratype profile and the technique required considerable optimisation. In some instances this was secondary to sample overload in the capillary electrophoresis and selected samples were re-run at a lower dilution. For some samples not every Vβ family generated a spectratype profile; this may be due to differences in Vβ usage. An example spectratyping profile from CLL PB is shown in Figure 5-17 and a normal PB in Figure 5-18.
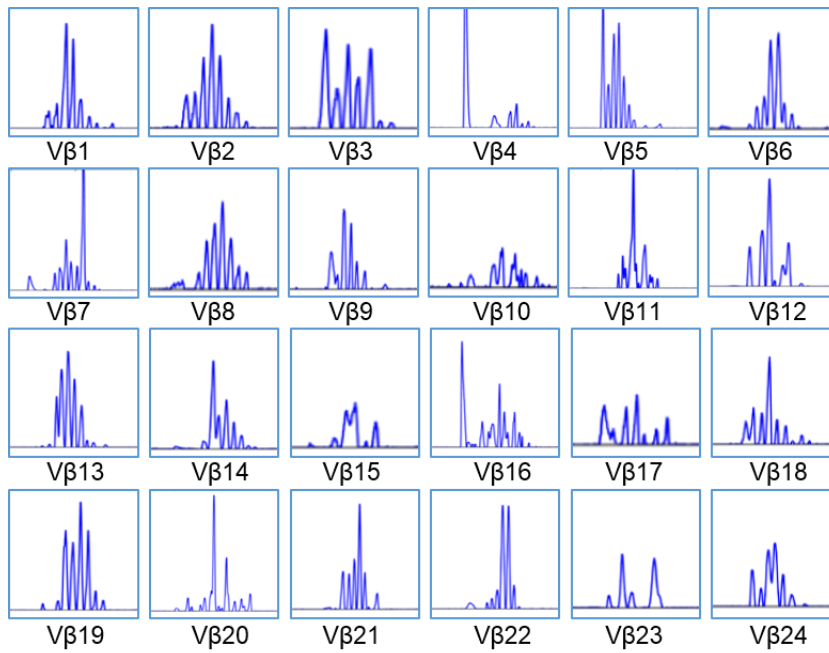
Figure 5-17 Example Vβ spectratype profile from CLL PB.
This is an example Vβ spectratype profile, from each of the 24 Vβ families (labelled Vβ1-24), from a sorted CD4+ population from the PB of a CLL patient. The GeneMapper Software generates a graphical spectratyping prolife usually consisting of 8 (5-10) major peaks each representing a CDR3 length differing from the next by 3 nucleotides. The fluorescence intensity is representative of the frequency of the CDR3. A spectratyping profile is produced for each of the 24 TCRVβ families. As described previously a bell shaped curve represents a normal distribution.
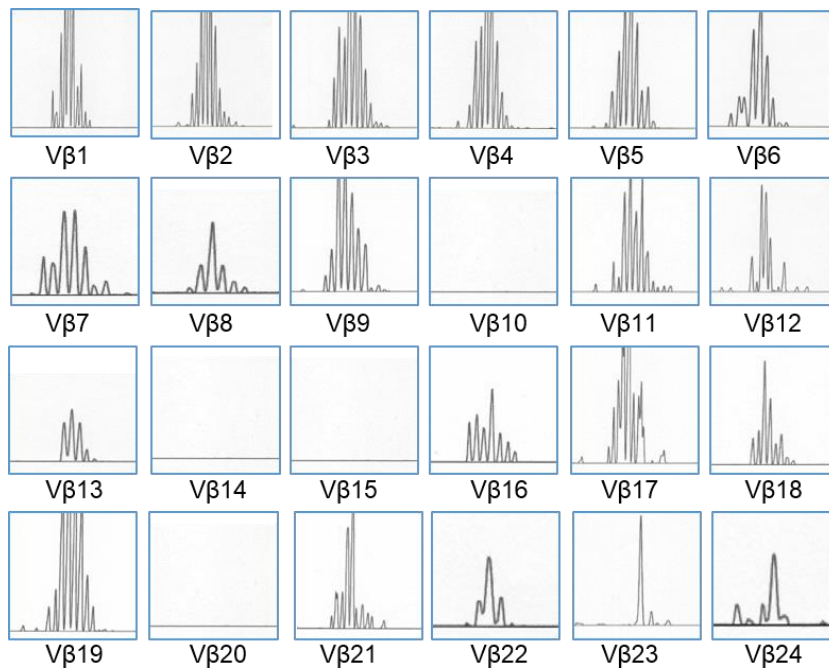
Figure 5-18 Example Vβ spectratype profile from normal PB.
This is an example Vβ spectratype profile, from each of the 24 Vβ families (labelled Vβ1-24), from a sorted CD4+ population from the PB of a normal control generated as described in Figure 5-17.

5.5.11 Diversity and complexity scores

The diversity and complexity scores for each TCRVβ spectratype were calculated for each subpopulation as outlined in 5.4.16. In summary, a complexity score was derived by assigning the spectratype of each Vβ family a score of 0-5, depending on the number of discrete peaks, and then multiplying by the number of Vβ families (n=24). Spectratypes with >5 peaks were given the maximum score of 5 and those with no peaks scored 0, giving a maximum score for the most complex repertoire of 120 (5x24). A diversity score was used to quantify the degree of skewing within the repertoire. A score of 1 was given for a peak that was more than twice the height of the second next highest peak and overall diversity calculated by adding the scores for all the Vβ families, therefore a score of 24 is highly skewed and 0 not skewed. **A higher diversity score thus signifies a less diverse repertoire**. The calculated scores for the 4 CD4+ subpopulations of the 6 CLL patients PB and LN samples is shown in Table 5-12.

Table 5-12 Diversity and complexity scores from CD4+ PD-1hi and PD-1lo populations from CLL PB and LN
CD4+/PD-1hi and CD4+/PD-1lo T-cells were FACS sorted from 6 CLL patients PB and LN as described in Table 5-9. TCRVβ spectratyping was performed as described and spectratype profiles generated as in Figure 5-17. Diversity and complexity scores for each TCRVβ spectratype from all the subpopulations from each patient are shown below. The complexity score was derived by assigning the spectratype of each Vβ family a score of 0-5, depending on the number of discrete peaks, and then multiplying by the number of Vβ families (n=24, maximum score 120). The diversity scoring system assigns a score of 1 for a peak that is more than twice the height of the second next highest peak. The overall diversity score calculated by adding the scores for all the Vβ families (n=24, maximum score 24).

Patient	PB CD4 PD-1hi			PB CD4 PD-1lo			LN CD4 PD-1hi			LN CD4 PD-1lo		
	Number of cells	Complexity Score	Diversity Score	Number of cells	Complexity Score	Diversity Score	Number of cells	Complexity Score	Diversity Score	Number of cells	Complexity Score	Diversity Score
Patient 1	10000	79	23	10000	77	16	10000	76	20	10000	92	12
Patient 2	4130	39	24	8999	68	20	28299	71	21	13446	74	11
Patient 3	21959	39	23	31037	62	22	25409	70	23	9425	62	22
Patient 4	15860	67	16	36600	87	9	23595	49	21	13446	59	15
Patient 5	36900	95	15	54400	93	7	14612	95	20	12797	70	20
Patient 6	42082	91	18	31072	102	14	36276	78	23	10535	89	16

The diversity results for each individual is easier to interpret when displayed graphically. The data can be shown for each individual patient as a "spectratype heat map".

In Figure 5-19 each individual CLL patient is represented by a chart of 24x4 boxes; where the 4 rows represent the 4 sorted CD4+ T-cell populations: PB PD-1hi, PB PD-1lo, LN PD-1hi and LN PD-1lo and the 24 columns are the 24 TCRVβ families. The individual boxes represent the diversity (or skewing) of each TCRVβ family repertoire. A black box represents a skewed repertoire, a grey box a non-skewed repertoire and a white box represents no spectratype profile for that Vβ family. The calculated complexity score (x/120) is displayed in the final column.

Figure 5-20 shows the same data but divided by the sorted CD4+ population of interest. Each chart represents a population of interest; PB PD-1hi, LN PD-1hi, PB PD-1lo and LN PD-1lo from top to bottom. The 6 rows of each chart are the 6 individual patients and the 24 columns are the TCRVβ families.

Figure 5-21 compares the skewing of the repertoire of the CLL PB and normal PB in the CD4+ PD-1hi and CD4+ PD-1lo populations. The populations of interest are CLL PB PD-1hi, Normal PB PD-1hi, CLL PB PD-1lo and Normal PB PD-1lo from top to bottom. The 6 rows of each chart are the 6 individual patients and the 24 columns are the Vβ families.
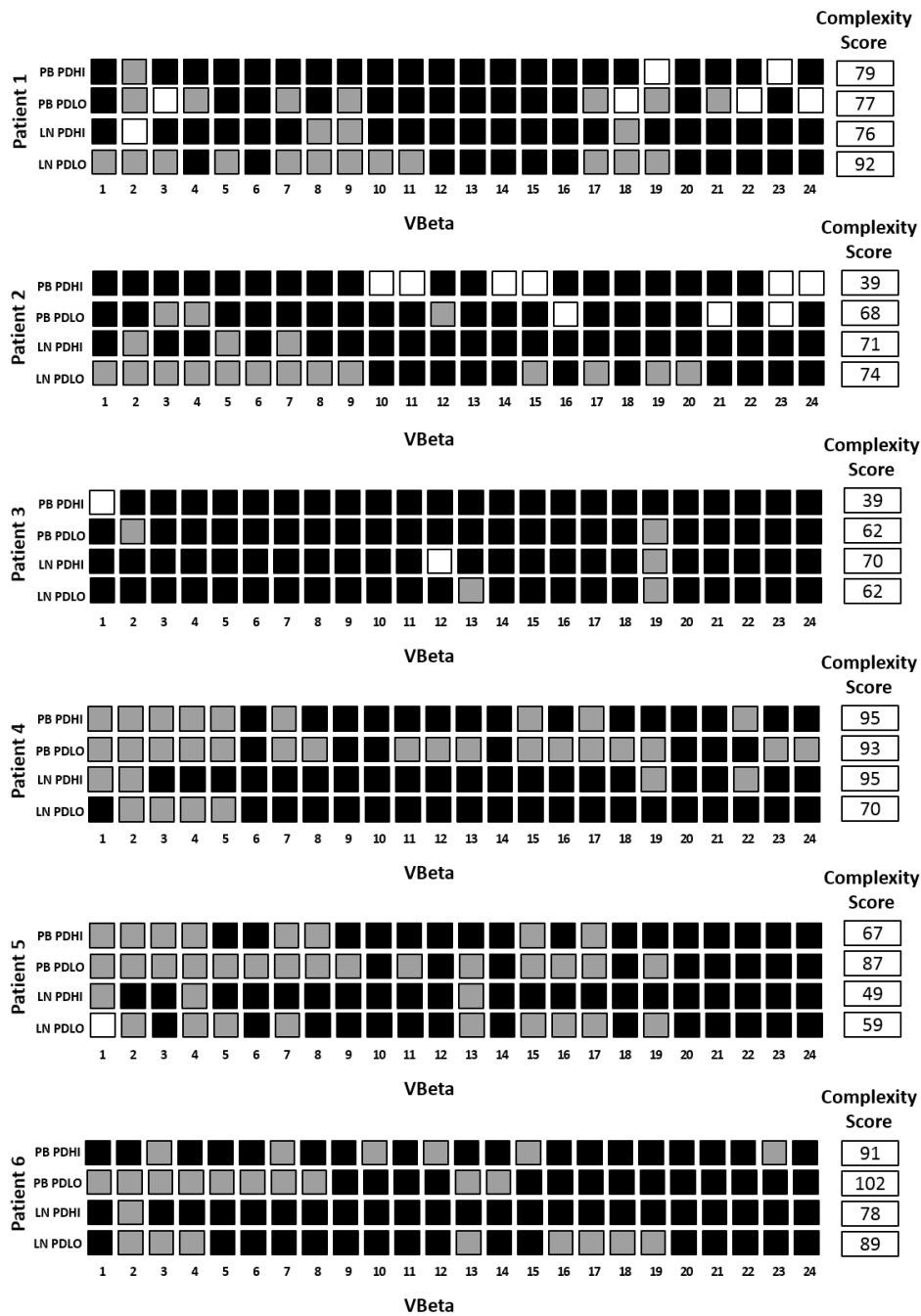
Figure 5-19 The overall diversity of the TCRVβ families from PD-1hi and PD-1lo PB and LN subpopulations in 6 CLL patients

Each individual CLL patient's complete spectratype scoring data (Patient 1-6, top to bottom) is represented by 24x4 boxes; where the 4 rows represent the 4 sorted CD4+ T-cell populations: PB PD-1hi, PB PD-1lo, LN PD-1hi and LN PD-1lo and the 24 columns are the 24 TCRVβ families. The individual boxes represent the diversity (or skewing) of each TCRVβ family repertoire. A black box represents a skewed repertoire, a grey box a non-skewed repertoire and a white box represents no spectratype profile for that Vβ family. The calculated complexity score (x/120) is displayed in the final column.
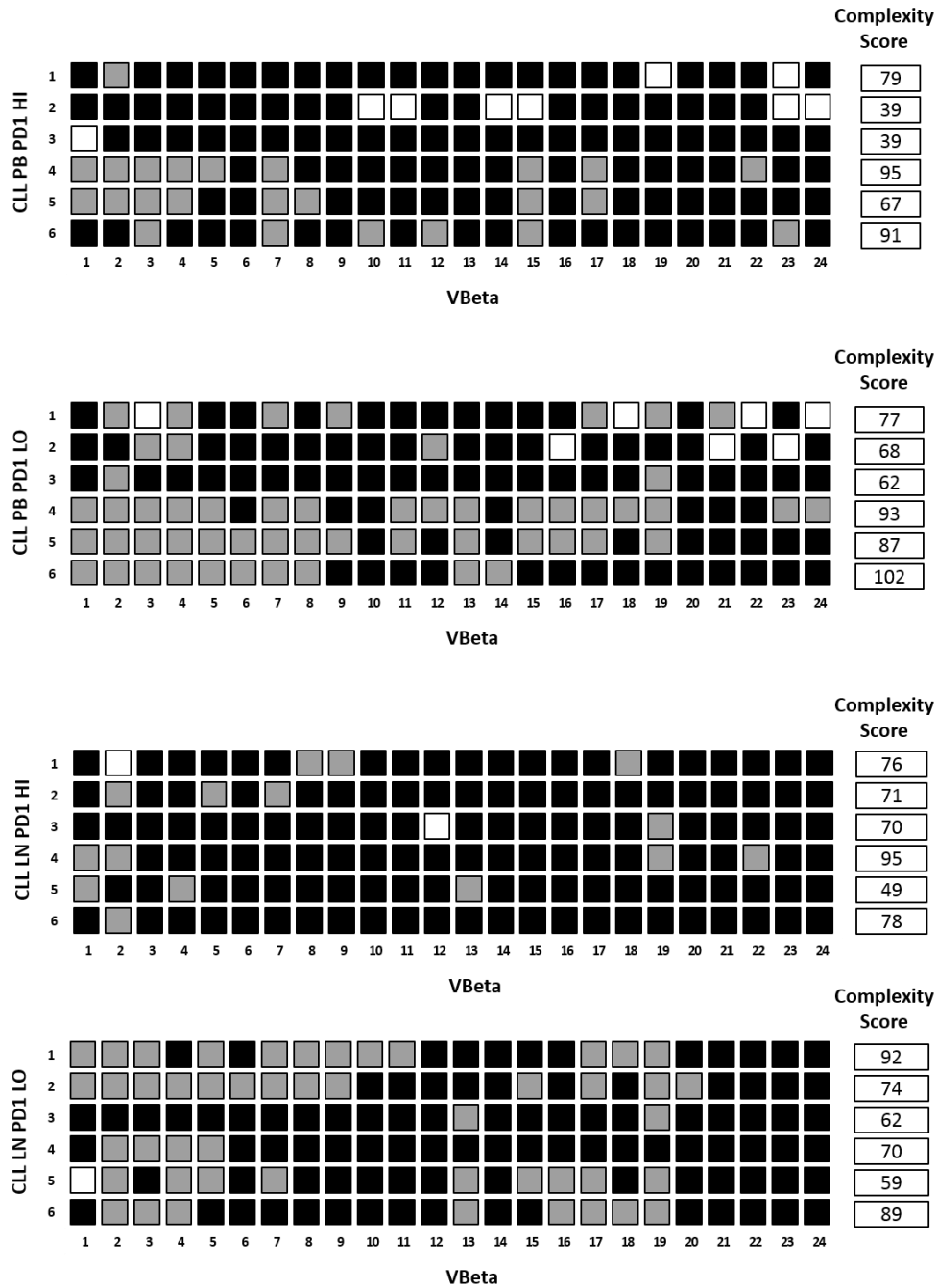
Figure 5-20 The diversity of the TCRVβ from PD-1hi and PD-1lo PB and LN subpopulations in 6 CLL patients

This figure shows the same complete spectratyping data of the cohort as presented in Figure 5-19 but each panel represents the sorted CD4+ population of interest; PB PD-1hi, LN PD-1hi, PB PD-1lo and LN PD-1lo from top to bottom. The 6 rows of each chart are the 6 individual patients and the 24 columns are the TCRVβ families. The individual boxes represent the diversity (or skewing) of each TCRVβ family repertoire. A black box represents a skewed repertoire, a grey box a non-skewed repertoire and a white box represents no spectratype profile for that Vβ family. The calculated complexity score (x/120) is displayed in the final column.
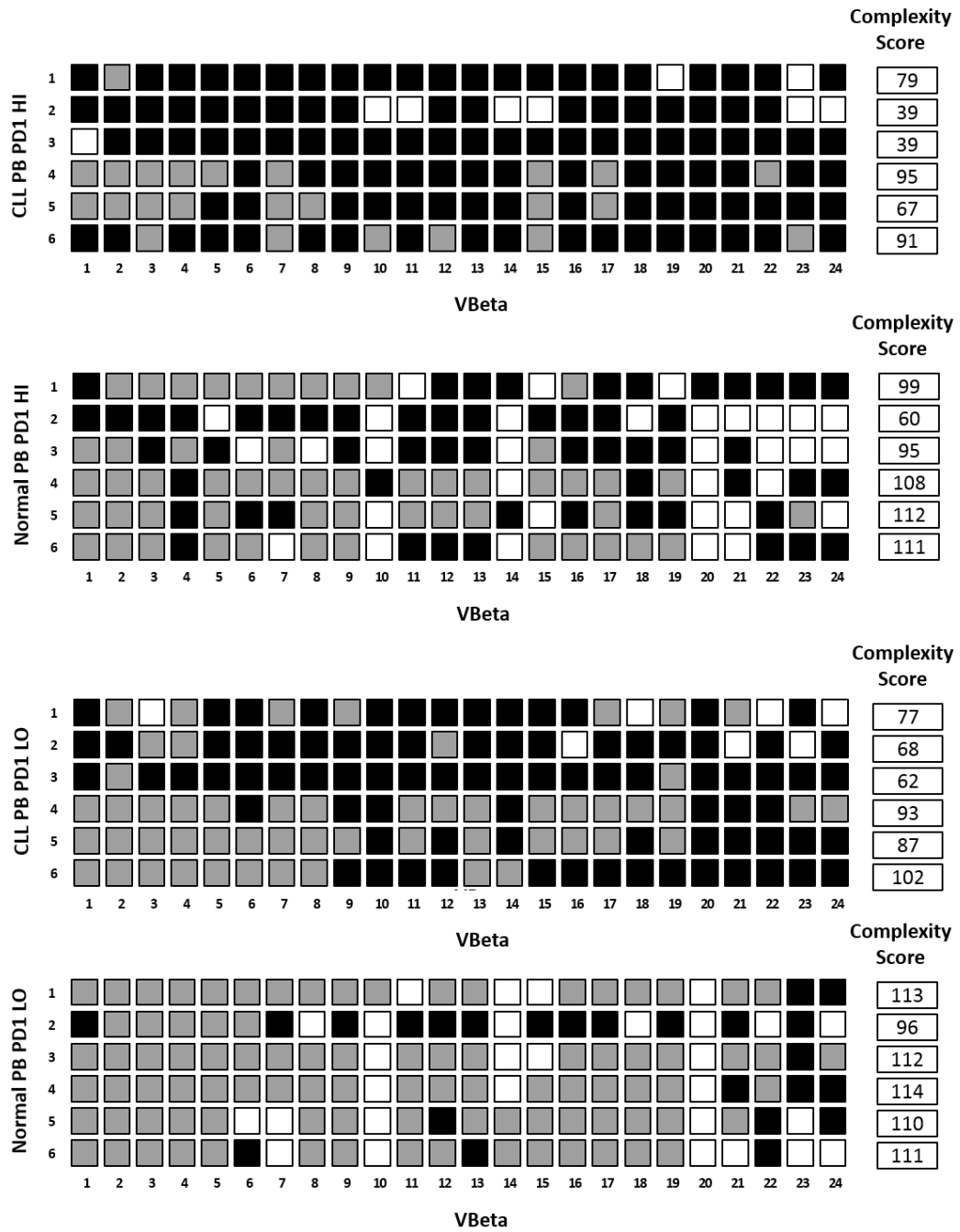
Figure 5-21 A comparison of the overall TCRVβ diversity in the PB PD-1hi and PD-1lo subpopulations of 6 CLL patients and normal controls

This figure shows the complete spectratyping data of the CD4+ sorted subpopulations from the PB of CLL patients and normal controls. Each panel represents the sorted CD4+ population of interest; CLL PB PD-1hi, Normal PB PD-1hi, CLL PB PD-1lo and Normal PB PD-1lo from top to bottom. The 6 rows of each chart are the 6 individual patients and the 24 columns are the Vβ families. The individual boxes represent the diversity (or skewing) of each TCRVβ family repertoire. A black box represents a skewed repertoire, a grey box a non-skewed repertoire and a white box represents no spectratype profile for that Vβ family. The calculated complexity score (x/120) is displayed in the final column.

5.5.12 There is increased skewing of the TCRVβ spectratype in PD-1hi T-cells compared to PD-1lo T-cells in both LN and PB compartments in CLL

Analysis of this data showed there was a significant reduction in overall TCR diversity (i.e. the diversity score is higher and repertoire is more skewed) in the PD-1hi subset in both CLL compartments compared to PD-1lo T-cells; PB PD-1hi vs PD-1lo (19.83+/-1.62 vs 14.67+/-2.42; p=0.005); LN PD-1hi vs PD-1lo (21.33+/-0.56 vs 16.00+/-1.77; p=0.022) See Figure 5-22.
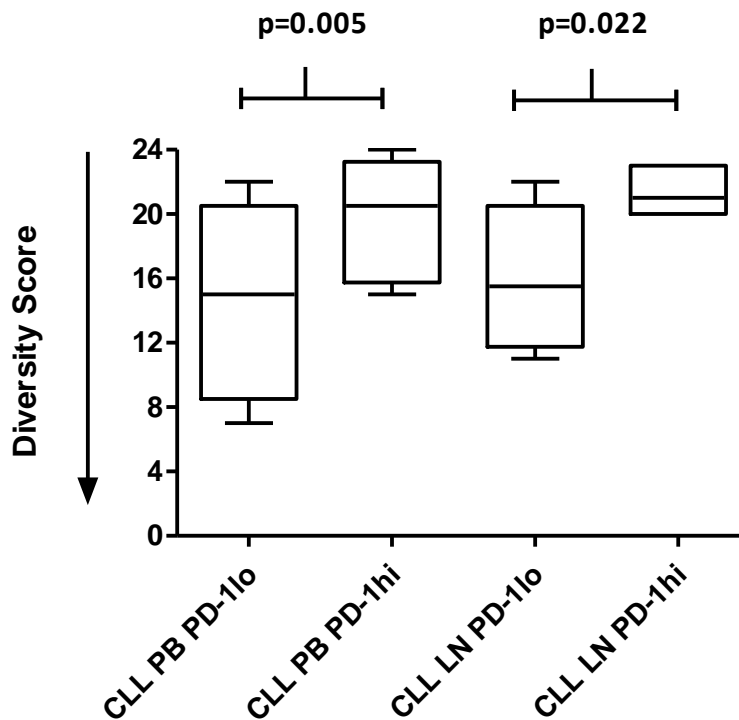
Figure 5-22 There is more skewing in the CD4+ PD-1hi T-cells than CD4+ PD-1lo T-cells of both PB and LN in CLL

A total TCRVβ spectratype diversity score was calculated for each sorted CD4+ subpopulation (CLL PB PD-1lo, CLL PB PD-1hi, CLL LN PD-1lo and CLL LN PD-1hi) from all 6 CLL patients, as in Table 5-12. Statistical analysis was performed with a D'Agostino and Pearson omnibus normality test and a paired t-test using GraphPad Prism®. There was a significant reduction in overall TCR diversity (i.e. the diversity score is higher and repertoire is more skewed) in the PD-1hi subset compared to PD-1lo in both CLL PB (p=0.005) and LN (p0.022).

There was no difference between the diversity in CLL PB PD-1hi T-cells and LN PD-1hi T-cells; PB PD-1hi vs LN PD-1hi (19.83+/-1.62 vs 21.33+/-0.56; p=0.39) or CLL PB PD-1lo T-cells and LN PD-1lo T-cells; PB PD-1lo vs LN PD-1lo (14.67+/-2.42 vs 16.00+/-1.77; p=0.69). See Figure 5-23.
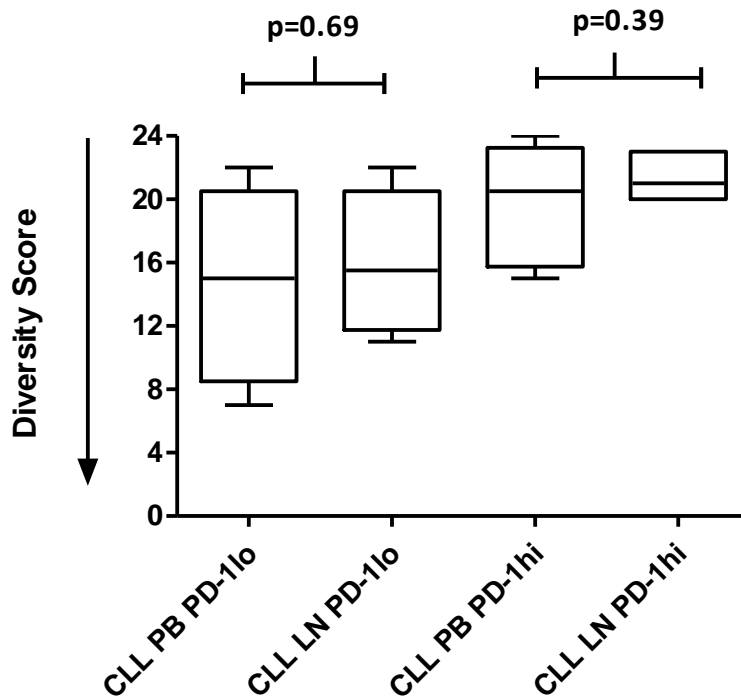
Figure 5-23 The CLL CD4+/PD-1hi population are skewed whether derived from the PB or LN
The total TCRVβ spectratype diversity score for each sorted CD4+ subpopulation (CLL PB PD-1lo, CLL PB PD-1hi, CLL LN PD-1lo and CLL LN PD-1hi) from all 6 CLL patients, was calculated and analysed as in Figure 5-22. There was no difference in the overall TCR diversity score for the CD4+/PD-1hi subset whether the cells were derived from the CLL PB or LN (p0.39).

This demonstrates that the PD-1hi T-cells have a more skewed TCRVβ spectratype than PD-1lo T-cells whether they are in the LN or PB. However we know from our data in chapter 3, there is a significantly larger proportion of PD-1hi T-cells in the LN compared to PB, and therefore the TCR repertoire is more skewed in the LN.

No significant differences in TCR complexity score was observed between the PD-1hi and PD-1lo populations; PB PD-1hi vs PB PD-1-lo (68.33+/-10.10 vs 81.50+/-6.23; p=0.057); LN PD-1hi vs LN PD-1-lo (73.17+/-6.07 vs 74.33+/-5.58; p=0.859). See Figure 5-24.
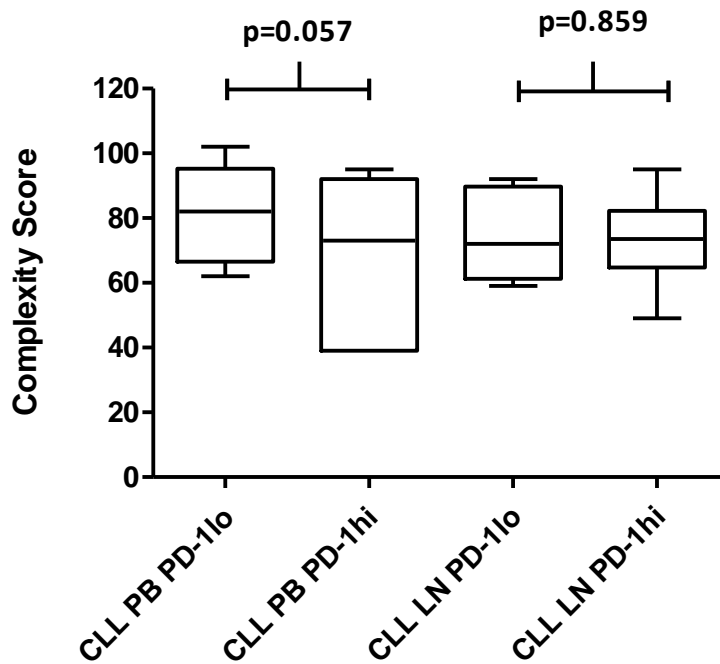
Figure 5-24 The complexity score was the same in all subpopulations of CLL
A total TCRVβ spectratype complexity score was calculated for each sorted CD4+ subpopulation (CLL PB PD-1lo, CLL PB PD-1hi, CLL LN PD-1lo and CLL LN PD-1hi) from all 6 CLL patients, as in Table 5-12. Statistical analysis was performed with a D'Agostino and Pearson omnibus normality test and a paired t-test using GraphPad Prism®. No significant difference in the TCRVβ complexity score was observed between any subpopulation.

5.5.13 There is skewing of the TCRVβ spectratype in PD-1hi CD4+ T-cells compared to PD-1lo CD4+ T-cells in normal PB

In order to see whether it held true that PD-1hi T-cells are skewed in the normal controls we compared the diversity and complexity scores of PB CD4+ PD-1hi and PB CD4+ PD-1lo subsets in the normal controls. There was a higher diversity score, and therefore less diversity, in the PB CD4+ PD-1hi T-cells than the PB CD4+ PD-1lo T-cells. Mean diversity scores PB CD4+ PD-1hi vs PB CD4+ PD-1lo: 12.67 +/- 2.54 vs 5.00 +/- 2.46; p=0.035). See Figure 5-25.
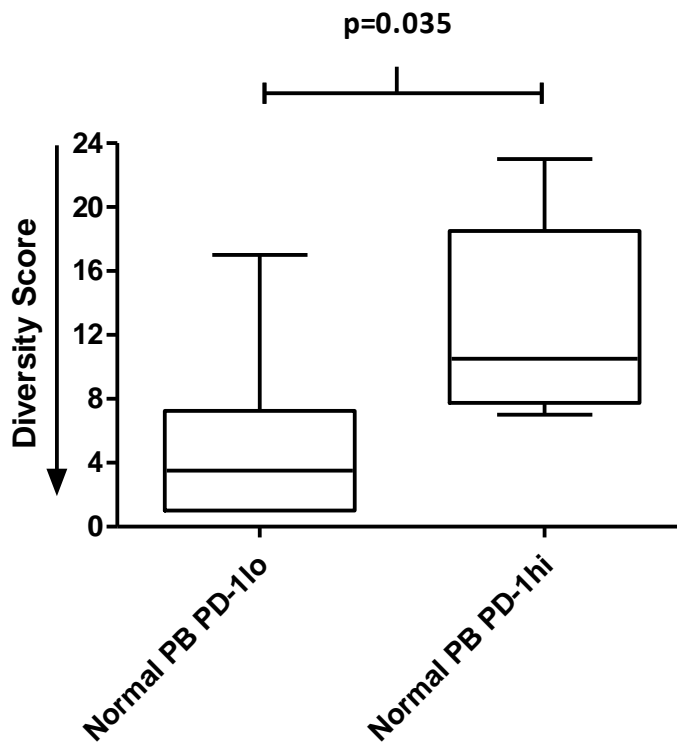
Figure 5-25 Decreased diversity score in the PD-1lo CD4+ T-cells in normal PB
A total TCRVβ spectratype diversity score was calculated for each sorted PB CD4+ subpopulation, (PD-1lo and PB PD-1hi) from the cohort of normal controls (n=6). Statistical analysis was performed with a D'Agostino and Pearson omnibus normality test and a paired t-test using GraphPad Prism®. There was a significant reduction in overall TCR diversity (i.e. the diversity score is higher and repertoire is more skewed) in the PD-1hi subset compared to PD-1lo; p=0.035.

There was also a trend towards, but not statistically significant, less complexity in the PB CD+ PD-1hi T-cells than the PB CD4+ PD-1lo: PB CD4+ PD-1hi vs PB CD4+ PD-1lo: 96.67 +/- 7.75 vs 109.3 +/- 2.73; p=0.063. See Figure 5-26.

This demonstrates that there is evidence of skewing in the PD-1hi, antigen experienced CD4+ T-cells, as would be predicted, but complexity of the repertoire is maintained overall.
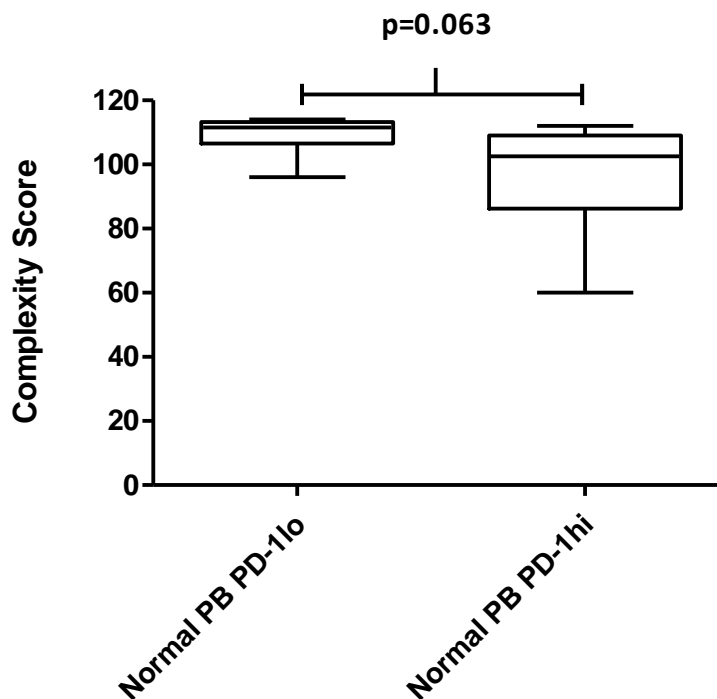
Figure 5-26 Complexity is preserved in the PD-1hi CD4+ T-cells of normal PB
A total TCRVβ spectratype complexity score was calculated for each sorted PB CD4+ subpopulation, (PD-1lo and PB PD-1hi) from the cohort of normal controls (n=6). Statistical analysis was performed with a D'Agostino and Pearson omnibus normality test and a paired t-test using GraphPad Prism®. There was a trend towards less complexity in the PB CD+ PD-1hi T-cells than the PB CD4+ PD-1lo T-cells; p=0.063.

5.5.14 There is increased skewing of the CLL PB TCRVβ spectratype compared to age matched normal controls in both PD-1hi and PD-1lo CD4+ T-cell subsets

From the normal control data presented above we demonstrate that there was a higher diversity score and thus more skewing in the TCRVβ repertoire of PB CD4+ PD-1hi T-cell subsets compared to CD4+ PD-1lo T-cells in normal individuals. Next we wanted to ascertain whether the degree of skewing of the PB TCRVβ repertoire in PD-1hi CD4+ subset of CLL patients and normal controls was the same.

We found the diversity of the TCRVβ to be even more skewed in CLL PB PD-1hi CD4+ T-cells than in the equivalent PD-1hi cells in normal PB. CLL PB CD4+ PD-1hi vs normal PB CD4+ PD-1hi: 19.83 +/- 1.62 vs 12.67 +/- 2.54; p=0.039). Additionally the CLL PB PD-1lo CD4+ T-cell population was more skewed than the normal counterpart. CLL PB CD4+ PD-1lo vs normal PB CD4+ PD-1lo: 14.67 +/- 2.48 vs 5.00 +/- 2.46; p=0.019. See Figure 5-27.
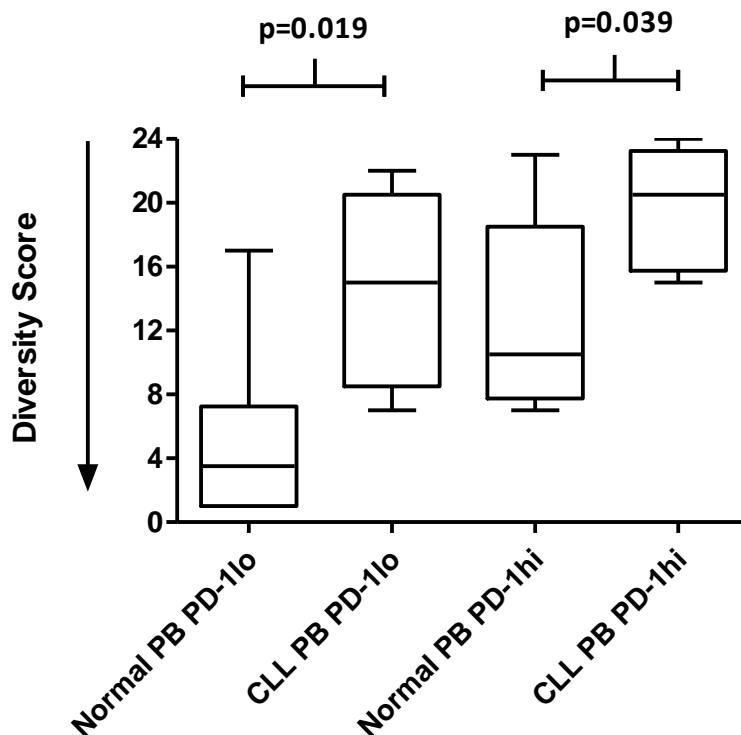
Figure 5-27 CLL CD4+ T-cells have more skewing than normal PB
A total TCRVβ spectratype diversity score was calculated for each sorted PB CD4+ subpopulation, (PD-1lo and PB PD-1hi) from the cohort of CLL patients (n=6) and normal controls (n=6). Statistical analysis was performed with a D'Agostino and Pearson omnibus normality test and an un-paired t-test using GraphPad Prism®. The diversity of the TCRVβ was more skewed in CLL PB PD-1hi CD4+ T-cells than in the equivalent PD-1hi cells in normal PB; p=0.039. Additionally the CLL PB PD-1lo CD4+ T-cell population was more skewed than the normal counterpart; p=0.019.

This confirms more skewing of the CD4+ TCRVβ repertoire overall in CLL compared to age matched normal controls, with evidence in both the CD4+ PD-1hi and PD-1lo T-cells.

There was also less complexity in the TCRVβ repertoire of CLL PD-1hi CD4+ T-cells compared to normal controls. Normal PB CD4+ PD-1hi vs CLL PB CD4+ PD-1hi: 96.67 +/- 7.75 vs 68.33 +/- 10.10; p=0.05. The same was true for the PD-1lo subset; where there was more complexity in the TCRVβ repertoire of normal PD-1lo CD4+ T-cells compared to the same population in CLL. Normal PB CD4+ PD-1lo vs CLL PB CD4+ PD-1lo: 109.30 +/- 2.73 vs 81.50 +/- 6.23; p=0.02. See Figure 5-28.

This is in keeping with the published data that there is oligoclonality of the CLL PB TCR (Forconi and Moss 2015).
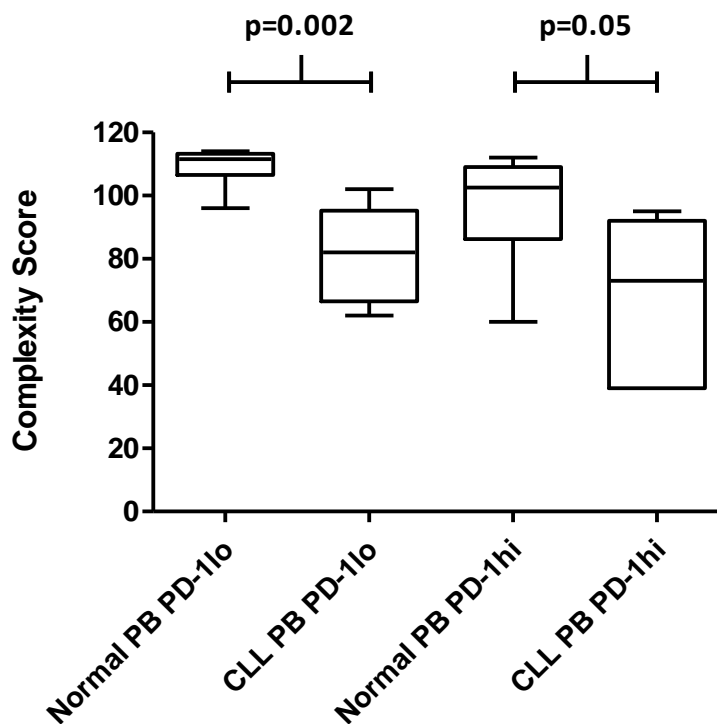
Figure 5-28 TCRVβ repertoire in normal PB is more complex than in CLL
A total TCRVβ spectratype complexity score was calculated for each sorted PB CD4+ subpopulation, (PD-1lo and PB PD-1hi) from the cohort of CLL patients (n=6) and normal controls (n=6). Statistical analysis was performed with a D'Agostino and Pearson omnibus normality test and an un-paired t-test using GraphPad Prism®. The complexity of the TCRVβ was less in CLL PB PD-1lo CD4+ T-cells than in the equivalent PD-1lo cells in normal PB; p=0.002. The same was true between CD4+ PD-1hi T-cells; p=0.05.

5.5.15 TCRVβ family skewing

It has been shown here that the CD4+ TCR Vβ repertoire in the PD-1hi subset of CLL is more skewed than the PD-1lo subset in both PB and LN and that the PD-1hi subset of normal controls is more skewed than the PD-1lo population. In addition, the overall PB CD4+ TCRVβ repertoire of patients with CLL is less complex than normal controls. A graphical representation of the frequency of PB CD4+ TCRVβ family skewing across the CLL and normal control cohorts is shown in Figure 5-29. It can be seen that across the CLL cohort there is an increased frequency of TCRVβ family skewing in both the PD-1hi and PD-1lo subpopulations compared to normal controls with no clear pattern.
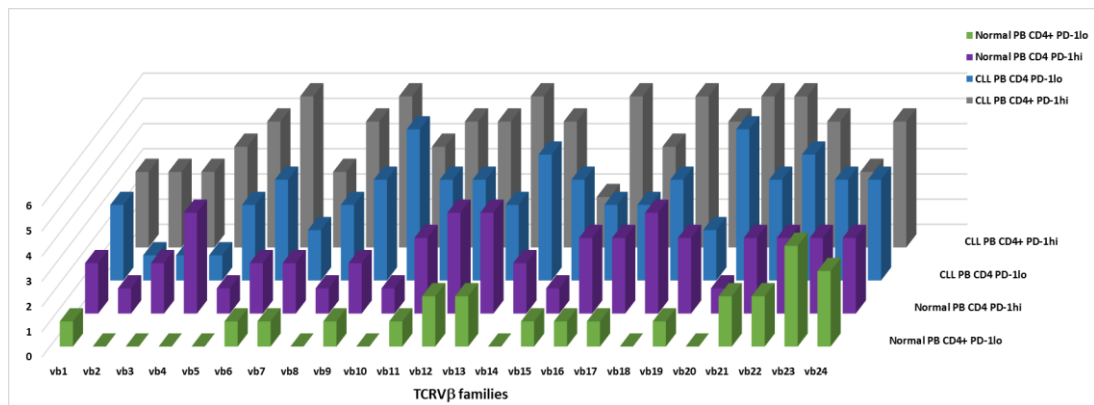
Figure 5-29 The frequency of TCRVβ family skewing of PB CD4+ T-cells across the cohort is greater in CLL patients (n=6) than in normal controls (n=6) in both PD-1hi and PD-1lo subpopulations

In this graphical representation of the total PB cohort of 6 CLL patients and 6 normal controls, each TCRVβ family in a subpopulation (normal PB CD4+ PD-1lo (green), normal PB CD4+ PD-1hi (purple), CLL PB CD4+ PD-1lo (blue) or CLL PB CD4+ PD-1hi (grey)) can be skewed to a maximum score of 6 (representing the cohort of 6 individuals under study). As an example, the green bars above represent the CD4+ PD-1lo samples from the normal PB (n=6). If, as shown here, the TCRVβ family vb1 was skewed in one sample out of the total 6 it scores 1. However if the same family was skewed in 2 out of 6 samples it would have scored 2 (as in vb12) and if every sample skewed that TCRVβ family then it would have scored 6 out of 6. The height of the bar therefore represents the number of individuals in the cohort of 6 that skewed that TCRVβ family. Visually it can be seen that the CLL PB samples have a higher frequency of skewing of TCRVβ families than the same CD4+ T-cells from the normal controls.

In this study we are primarily interested in the CLL cohort. A graphical representation of the frequency of TCRVβ family skewing across the CD4+ PD-1hi and PD-1lo subpopulations from the LN and PB CLL cohort is shown in Figure 5-30. Each column represents the frequency of skewing of the CD4+ TCRVβ family across all 6 CLL patients in the PB and LN PD-1hi and PD-1lo compartments. It can be seen that all families show a degree of skewing across the cohort and no families are unaffected.
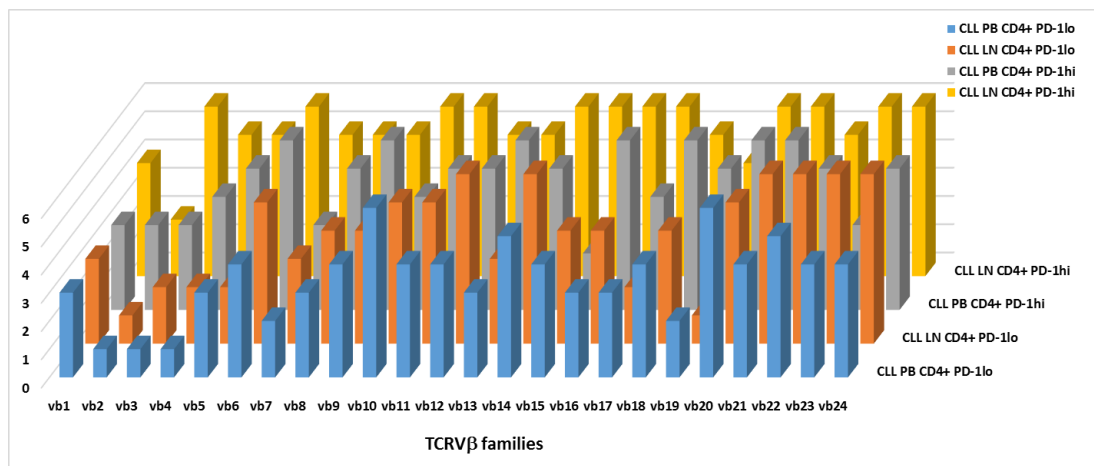
Figure 5-30 Frequency of skewing of the TCRVβ families in CLL CD4+ PB and LN subpopulations; n=6
The frequency of skewing is as described in Figure 5-29. Here it can be seen that there is skewing across all TCRVβ families in all 4 CLL CD4+ subpopulations, PB PD-1lo (blue), LN PD-lo (orange), PB PD-1hi (grey), LN PD-1hi (yellow).

For clarity this data is split into 3 comparisons of interests, looking specifically at comparisons with the CD4+ PD-1hi population. Figure 5-31 shows just the frequency of TCRVβ skewing for the LN PD-1hi and PD-1lo CD4+ T-cells subpopulations. Figure 5-32 shows the CLL PB CD4+ PD-1hi and PB PD-1lo subpopulations. Figure 5-33 shows the CLL LN CD4+ PD-1hi and PB PD-1hi subpopulations.
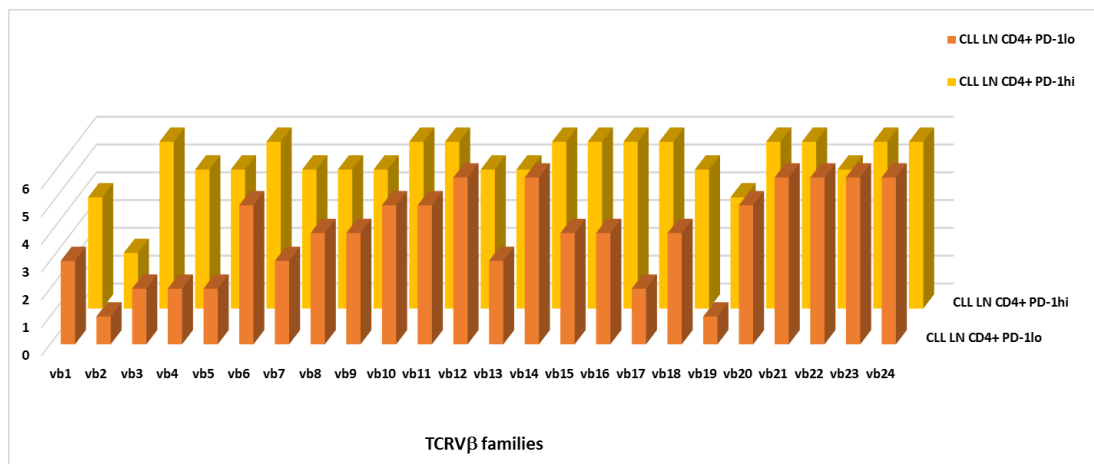
Figure 5-31 Frequency of skewing of the TCRVβ families in LN PD-1hi compared to PD-1lo subpopulations; n=6
The frequency of skewing is as described in Figure 5-29. Here it can be seen that there is skewing across all TCRVβ families in both CLL LN CD4+ subpopulations, LN PD-lo (orange), and LN PD-1hi (yellow).
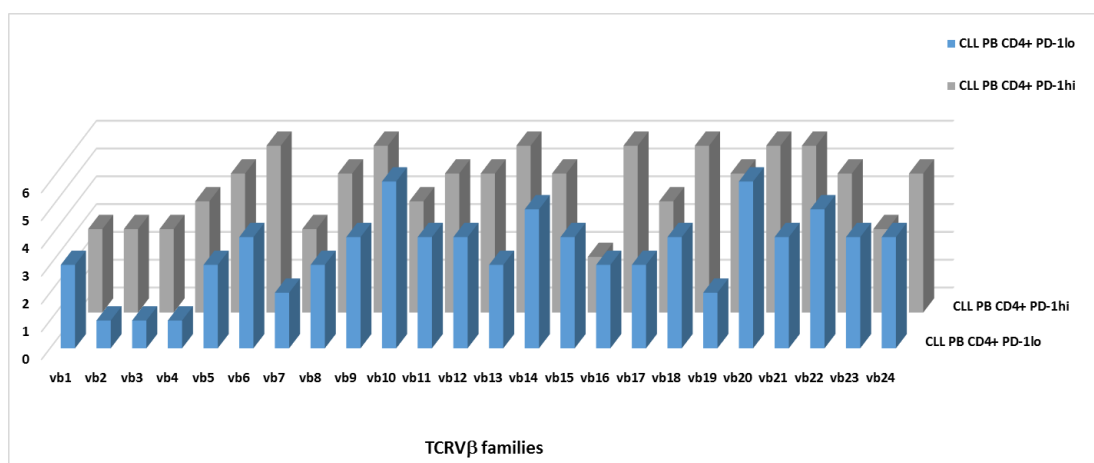
Figure 5-32 Frequency of skewing of the TCRVβ families in CLL PB PD-1hi vs PD-1lo subpopulations; n=6
The frequency of skewing is as described in Figure 5-29. Here it can be seen that there is skewing across all TCRVβ families in both CLL PB CD4+ subpopulations, PB PD-1lo (blue) and PB PD-1hi (grey).
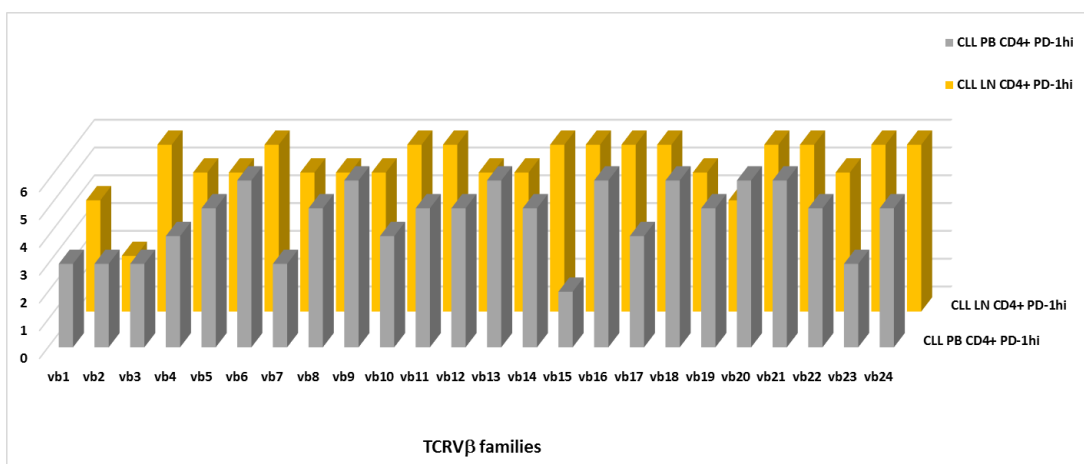
Figure 5-33 Frequency of skewing of the TCRVβ families in CLL LN CD4+ PD-1-hi vs CLL PB CD4+ PD-1hi subpopulations; n=6.
The frequency of skewing is as described in Figure 5-29. Here it can be seen that there is skewing across all TCRVβ families in both CLL CD4+ PD-1hi subpopulations, PB PD-1hi (grey) and LN PD-1hi (yellow).

This data shows that in this cohort of 6 patients, any of the TCRVβ families can be skewed, but gives no further information. We wanted to know whether the TCRVβ family skewing was concordant in the different populations and compartments within an individual patient.

5.5.16 Concordance of skewing

In order to determine whether the events causing skewing of the TCRVβ repertoire were specific to the LN, or part of a more general process in a patient, we estimated the "concordance of skewing" in the PB and LN subpopulations for each individual patient.

To calculate the concordance of skewing we constructed an algorithm that asked if the spectratype profile is skewed in "population 1" of an individual was it also skewed in the same way, (i.e. with the same peaks), in "population 2" of the same individual.

Specifically the first analysis sought to determine if a TCRVβ family was skewed in LN CD4+ PD-1hi population was it also skewed in the same way for LN CD4+ PD-1lo population?

This required visualisation of each spectratype profile and scoring "yes" or "no" if the spectratype profile was skewed in the same way. From this, an overall "concordance of skewing" can be calculated a percentage across the repertoire.

The scoring system is shown in Figure 5-34.
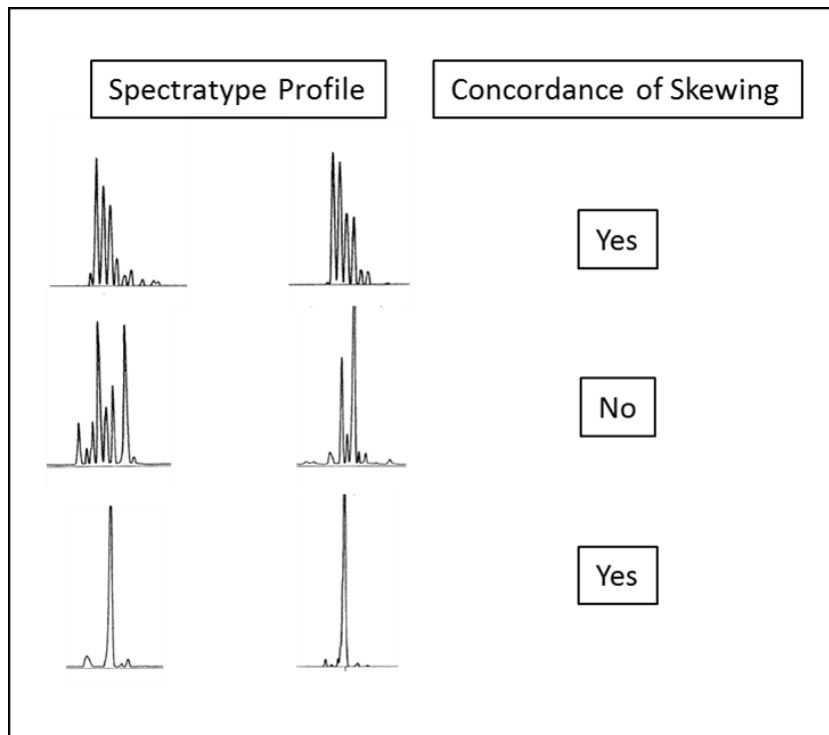
Figure 5-34 Scoring the concordance of skewing
Concordance of skewing is scored by visually assessing if two spectratype profiles are skewed in the same way or not and scoring "yes" or "no". All example pairs shown above are a comparison of the spectratype profiles from the same TCRVβ family from matched samples from the same patient. In the top and bottom panels the concordance of skewing is "yes" as both paired spectratype profiles are skewed in the same way. In the middle panel, the concordance of skewing is "no" as although both spectratypes are skewed, the same peak is not skewed and therefore they are not concordant.

First we compared the CD4+ PD-1hi and PD-1lo populations of the LN, and found the concordance of skewing for the cohort to be 59.8% +/- 4.09. Next we asked if the spectratype profile was skewed in the same way between the PB CD4+ PD-1hi and PB CD4+ PD-1lo T-cell subpopulations. The concordance of skewing was 71.5% +/- 4.96 for the cohort. Finally we wanted to compare the profile skewing of the CD4+ PD-1hi populations of the LN and PB. The concordance of skewing for the cohort was the lowest at 49.5% +/- 10.47.

This would suggest different families are being used in the PB and LN. Additionally there is less concordance of skewing between the PD-1hi and PD-1lo subsets of the LN than the same comparison in the PB; p=0.039.

Figure 5-35 shows the overall concordance of skewing for these 3 comparisons
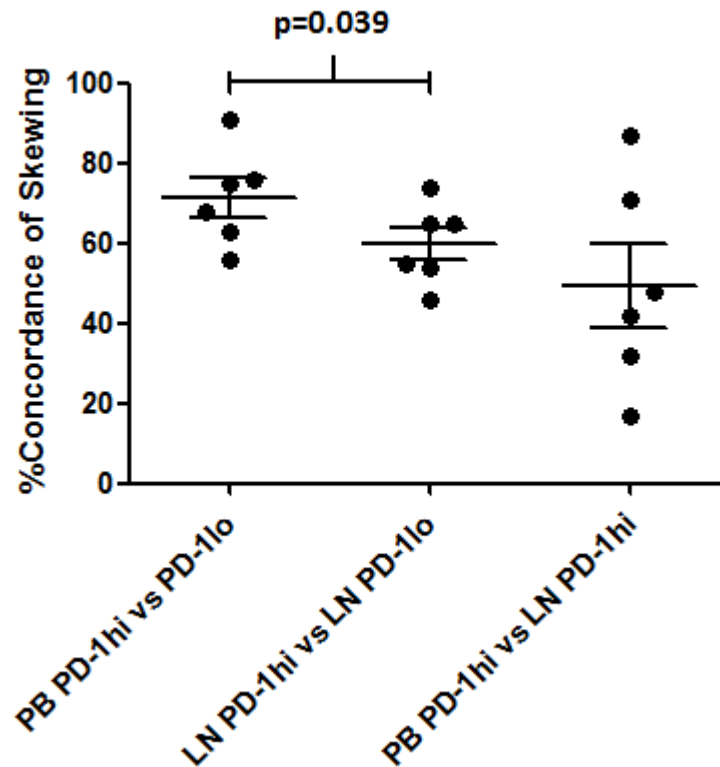
Figure 5-35 Concordance of skewing of TCRVβ spectratyping profiles of CLL CD4+ PD-1+ T-cells from different compartments
Concordance of skewing for each spectratype was calculated according to Figure 5-34. From this a percentage of concordance of skewing was calculated for all TCRVβ families in a sample. The concordance of skewing was highest between the CLL PB CD4+ PD-1hi and PD-1lo populations and lowest between the PB CD4+ PD-1hi and LN CD4+ PD-1hi T-cell subpopulations.

This analysis strongly suggests that the TCR repertoire of the PD-1hi population in the LN and PB are distinct and likely originate through interaction with different antigens.

5.5.17 High throughput TCRVβ sequencing

Our spectratyping results have shown that the CD4+ TCRVβ repertoire is skewed in the PB and LN in CLL, and for the first time we have shown that the diversity was even more skewed within the PD-1hi population. The PD-1hi population of T-cells predominate in the LN and therefore the TCR diversity was most skewed in this compartment. The skewing occurred across all TCRVβ families and although the concordance of skewing strongly suggested differences between the PB and LN, the resolution of spectratype analysis means that we were unable to make a definitive statement about this. In order to further address this point

we employed the emerging technology of high throughput sequencing of the TCR CDR3. Using this technique we could ascertain commonality in the TCRVβ repertoire of the CD4+ T-cells derived from the PB and LN at the level of the individual TCRVβ CDR3. Additionally, we sought to compare the TCRVβ repertoire of a patients PB and 2 separate lymph nodes taken from the same patient at the same time. From this we could identify whether there is any commonality in the TCRVβ repertoire between two different LNs and the LN and PB. Identification of T-cell clonality within the LN would provide evidence that the T-cells are specially proliferating within the LN in response to cognate antigen in a TCR specific manner.

This work was undertaken in partnership with Dr Marta Pasikowska, a post-doctoral scientist in our laboratory and our collaborators at Adaptive Biotechnologies.

Note the TCRVβ nomenclature from Adaptive Biotechnologies is IMGT (Robins, Campregher et al. 2009, Yassai, Naumov et al. 2009).

5.5.18 Demographics of patients and normal controls for HTS

HTS of the TCRVβ was performed on FACS sorted CD4+ T-cells from a separate cohort of 6 patients paired LN and PB. The Demographics of the patients is shown in Table 5-13.

Table 5-13 Demographics of CLL patients for HTS

	Age	Sex	CMV	Binet	CD38%	Cyto/FISH	Mutational Status
CLL8	75	F	POS	B	0	Normal	Unmutated
CLL9	66	M	NEG	C	3	Normal	Unmutated
CLL10	72	M	POS	B	18	11q-	Unmutated
CLL11	53	F	NEG	A	0	Normal	Mutated
CLL12	46	M	UNK	B	5	Normal	Unmutated
CLL 13	74	M	UNK	A	13	13q-	Mutated

5.5.19 Average Vβ gene usage differs between CLL and normal PB

The first analysis used the HTS technology to look at the total CD4+ TCRVβ repertoire in CLL and normal PB, to validate the technology. We wanted to look for evidence of over or underused TCRVβ families in the CD4+ T-cells of CLL PB compared to normal controls. The results are graphically represented in Figure 5-36. The orange bars are selected CD4+ T-cells from normal controls, the blue bars PB from CLL patients. Figure 5-36 shows the frequency of usage of an individual TCRVβ as a percentage of the total TCRVβ usage. It can be seen that the CLL cases appear to have a different pattern of TCRVβ usage than the wild type TCR, with over and under used TCRVβ families.
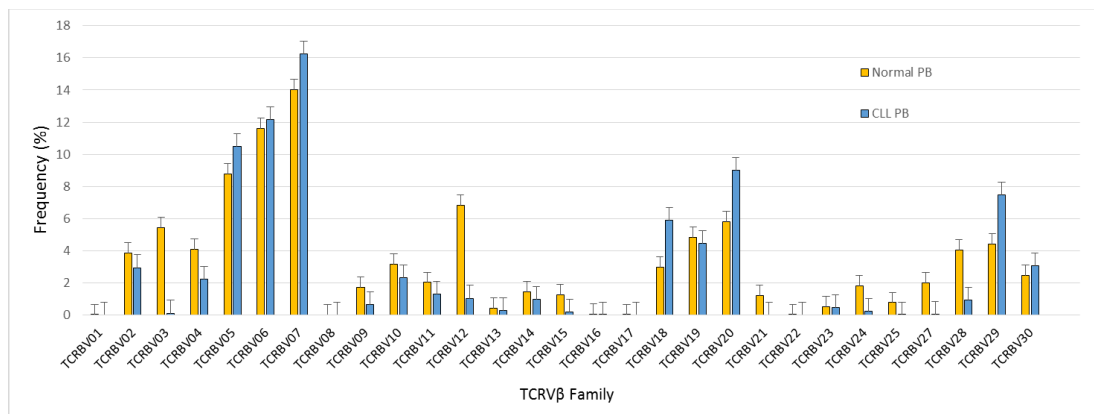
Figure 5-36 Frequency of TCRVβ family usage in normal CD4+ PB T-cells (n=6) and CLL PB T-cells (n=6)
cDNA from flow sorted CD4+ T-cells from 6 PB normal controls (orange bars), and 6 CLL patients (blue bars) were sent to Adaptive Biotechnologies® for amplification and sequencing of TCRVβ CDR3 using the immunoSEQ Platform. TCRVβ CDR3 regions were amplified using a bias controlled high throughput multiplex PCR. TCRVβ CDR3 sequences are defined according to the IMGT collaboration nomenclature. Data was analysed through the ImmunoSEQ analyser software. The bars show the frequency of usage of an individual TCRVβ as a percentage of the total TCRVβ usage. It can be seen that the CLL cases appear to have a different pattern of TCRVβ usage than the wild type TCR, with over and under used TCRVβ families.

This data shows there is divergence of the CD4+ TCRVβ repertoire in the PB CLL compared to normals in this cohort. This is fascinating and potentially a very significant result, however as the cohort size is small, this requires further study in a larger cohort analysis.

This set of experiments has provided evidence that the HTS method worked and allowed us to go on to perform comparative experiments in individual patients to assess differences in the TCRVβ usage between the CD4+ PB and LN.

5.5.20 There is commonality of TCRVβ family usage between CD4+ T-cells from CLL PB and LNs

We next directly compared the overall CD4+ TCRVβ family usage between CLL patients PB and LN, shown graphically in Figure 5-37. The blue bars are the TCRVβ families from the CD4+ T-cells derived from PB and the green bars are the CD4+ TCRVβ families from the LN. This shows a commonality in the frequency of TCRVβ family usage between the PB and LNs across the cohort.
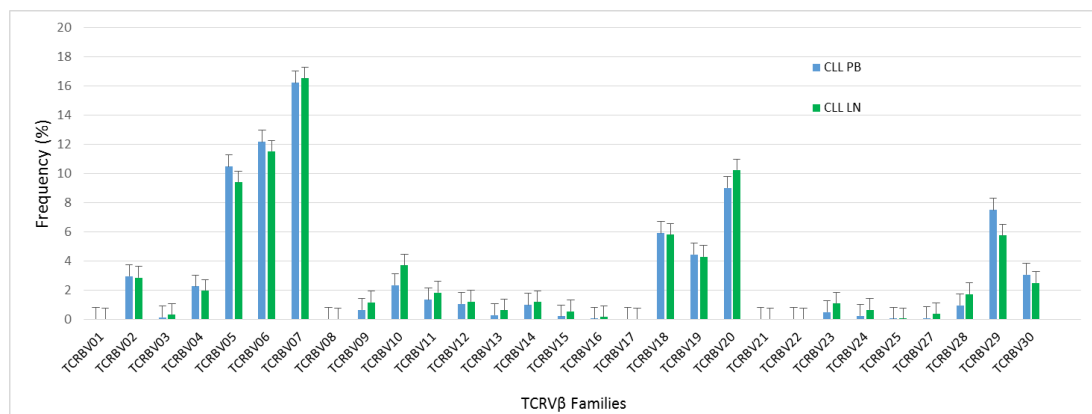
Figure 5-37 Frequency of sorted CD4+ T-cells TCRVβ family usage in matched CLL PB and LN (n=6)
HTS of the TCRVβ was undertaken on matched flow sorted CD4+ T-cells from CLL PB and LN (n=6) and analysed as described in Figure 5-36. The blue bars represent the frequency of TCRVβ family usage from the CD4+ T-cells derived from PB and the green bars from the LN.

These results tell us which families are used and gives quantitative data of the frequency of usage. However, it does not tell us about the complexity i.e. number of unique sequences within the family. In order to assess the complexity of the repertoire we assessed the number of individual productive unique sequences across all TCRVβ families from CLL patients PB and LN.

We found the median number of unique sequences in the CD4+ cells from CLL PB was no different to that in the LN: 5490 +/- 3052 vs 7913 +/- 2466, n=6; p=0.834. See Figure 5-38.
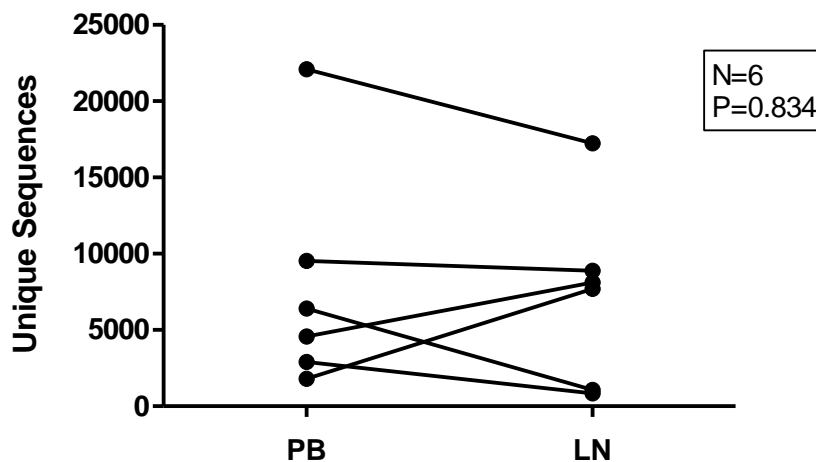
Figure 5-38 No difference in the number of unique sequences (complexity) of the CD4+ TCR repertoire in CLL PB and LN by HTS
HTS of the TCRVβ was undertaken on matched flow sorted CD4+ T-cells from CLL PB and LN (n=6) and analysed as described in Figure 5-36. The number of unique sequences identified in the CD4+ sample from the CLL PB was no different to that in the LN; p=0.834.

Therefore the number of unique sequences was the same whether the CD4+ T-cells were derived from the PB or the LN. This confirms that the CLL repertoire complexity is maintained between the PB and LN, supporting the data from the spectratyping.

5.5.21 The starting number of T-cells is proportionate to the number of unique sequences derived

It would be expected that the number of unique sequences would be less with fewer cell numbers. To confirm this PB CD4+ T-cells were sorted in different quantities prior to HTS TCRVβ sequencing. The starting number of T-cells positively correlated the number of unique sequences identified; shown in Figure 5-39. This analysis was kindly provided by Adaptive Biotechnologies. Therefore to mitigate for this bias in this study we sorted equal number of CD4+ T-cells from PB and LN.
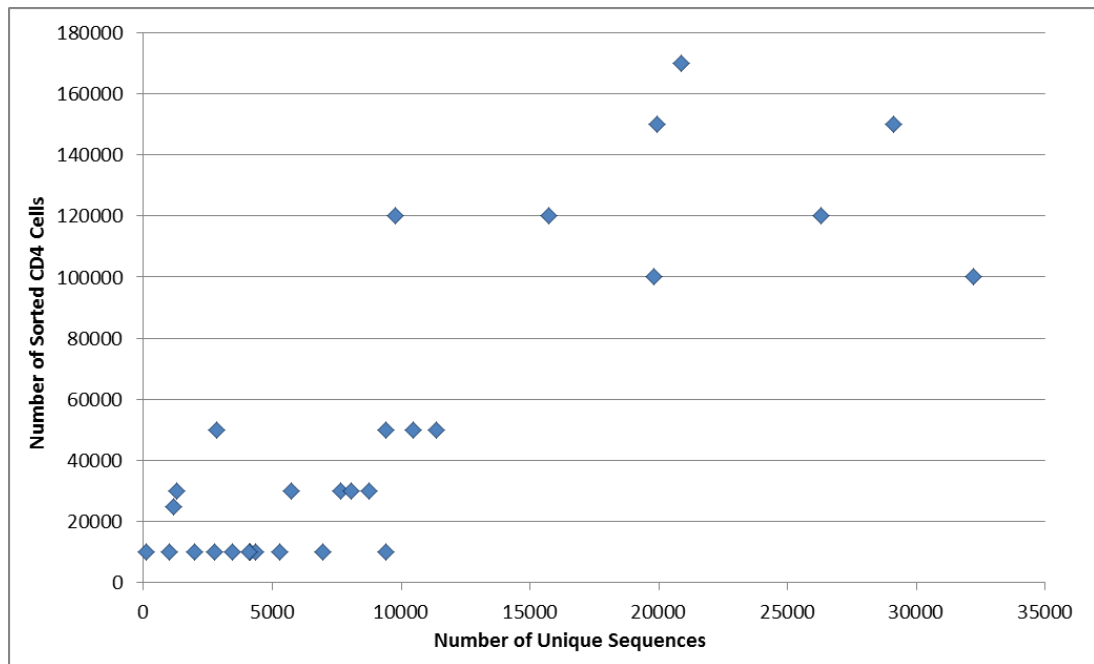
Figure 5-39 Number of unique sequences correlates with starting CD4+ cell number.
HTS of the TCRVβ was undertaken on flow sorted CD4+ T-cells from normal control PB (n=25) and analysed as described in Figure 5-36. The number of unique sequences correlates with the number of sorted CD4+ T-cells. Analysis courtesy of Adaptive Biotechnologies.

5.5.22 There is more clonality of the CD4+ T-cells from the LN FNA than the PB

The advantage of HTS over spectratyping is that the frequency of each of the unique sequences can be determined. This gives direct evidence of clonality. The spectratyping data found more skewing in the LN compared to PB; which is a presumed surrogate for clonality. Therefore, using HTS, we investigated the skewing of the TCRVβ repertoire by quantifying the actual number of over-represented individual sequences, i.e. identifying clonotypes.

The mathematical techniques underlying this analysis are complex and beyond the scope of this thesis. In brief, this involves the assessment of entropy, a technique derived from information theory, which quantifies the predictability of information. When assessing immune repertoires Shannon entropy is a measure of diversity within a complex data set. Samples with high entropy have a greater diversity of sequence, conversely samples with low entropy have sequences that share nucleotide homology. Entropy is calculated by summing the frequency of each clone, multiplied by the log of the same frequency of all productive reads of the sequence. This value is normalised based on the total number of productive sequences and subtracted from 1. Therefore entropy takes into account the variation of clone frequency.

The resultant equation to calculate clonality is 1-(entropy)/log2(number of productive unique reads). This generates a relative "clonality" value (Robins, Campregher et al. 2009). A value of 1 is a clonal repertoire and a value of 0 completely random. Values approaching 1 have a few predominant clones or are more oligoclonal. Adaptive Biotechnologies report a median clonality score of adult TCR repertoire as 0.075. The analysis of clonality in our samples was performed by Dr David Hamm at Adaptive Biotechnologies.

Both the CD4+ T-cells derived from the PB and LN in our study have median clonality values >0.075, confirming they are more oligoclonal than normal PB. Our results additionally reveal a higher clonality score in the LN than the PB, revealing for the first time the CD4+ TCRVβ repertoire is more oligoclonal in the LN than PB in CLL. See Figure 5-40. We repeated the LN and PB sampling on two occasions for the 6 patients. This data further supports the hypothesis that there is antigen driven expansion of T-cells within the LN.
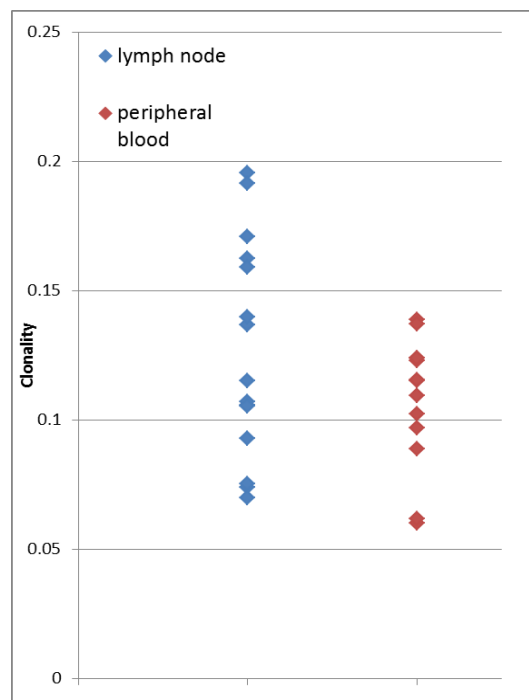
Figure 5-40 The CLL LN CD4+ T-cells are more clonal than those derived from the PB
HTS of the TCRVβ was undertaken on matched flow sorted CD4+ T-cells from CLL PB and LN (n=6) and analysed as described in Figure 5-36. The experiment was repeated on 2 separate occasions. A clonality score was calculated by Adaptive Biotechnologies with the following equation; 1-(entropy)/log2(number of productive unique reads). A value of 1 is a clonal repertoire and a value of 0 completely random. Adaptive Biotechnologies report a median clonality score of an adult TCR repertoire as 0.075. Data shown here shows a higher clonality score in the CLL CD4+ T-cells derived from the LN than the PB. Analysis courtesy of Adaptive Biotechnologies.

5.5.23 CLL CD4+ T-cells derived from LNs have more commonality of TCR usage with each other than with matched PB

To identify whether the CD4+ T-cell clones in the CLL LN showed commonality between LNs of the same patient, we sampled 2 separate LNs from the same patient at the same time. We then looked for overlapping sequences between the 2 LNs. In addition we compared the CD4+ LN derived clones with matched PB, to identify whether the same clones were present in the LN and PB. This enabled the analysis of the frequency of overlapping sequences between the two compartments and to identify whether the same clones are present in the LN and PB.

A representative example is graphically illustrated in Figure 5-41. Each dot represents a TCR clonotype. It can be seen visually that there appears to be more common T-cell clones between the 2 LNs than either LN with the PB.
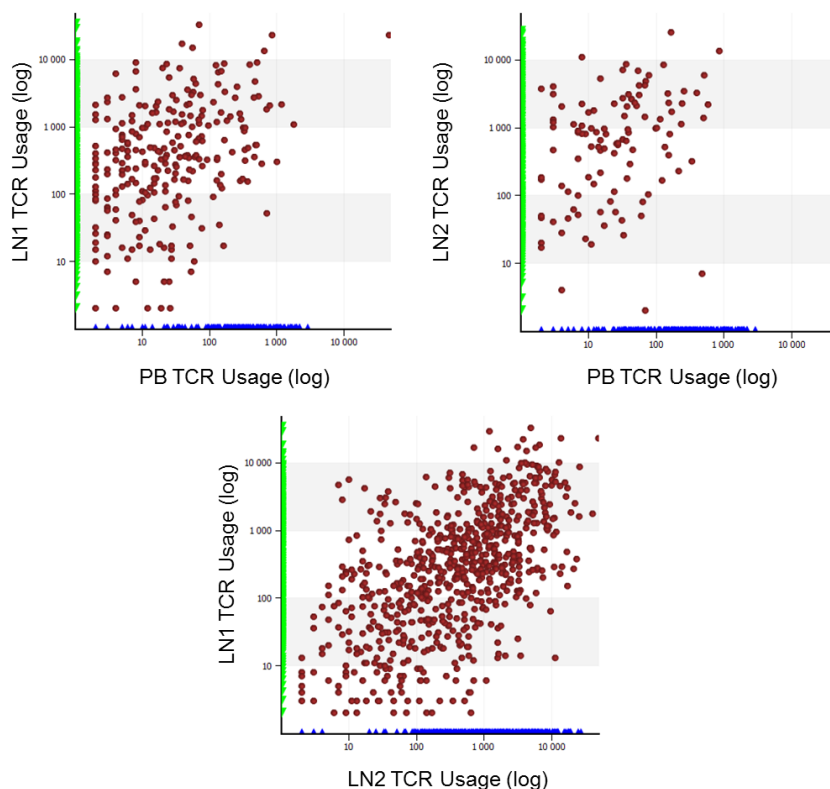
Figure 5-41 More commonality of TCR usage between two separate LNs from same patient than between the LN and matched PB
HTS of the TCRVβ was undertaken on matched flow sorted CD4+ T-cells from CLL PB and 2 separate LNs taken at the same time. Analysis was as described in Figure 5-36. Data shown here is a graphical comparison of TCR usage of the CD4+ T-cells from the PB and 2 LNs (LN1 and LN2) of a single individual. Each dot represents the frequency of a TCR clonotype. It can be seen visually that there appears to be more common T-cell clones between the 2 LNs than between either LN with the PB.

Statistical analysis showed the mean "overlap score" between the sequences in LN1 and LN2 was 0.331 and between LN1 and PB was 0.151; p=0.0064.

The overlap score in immunoSEQ analyser, defines the extent to which clonotypes are observed to be shared between two samples. It is a sum of the counts for all shared sequences observed in sample A and sample B (in our first example LN1 and LN2) divided by the total number of counts of all sequences in both samples.

We went on to repeat this experiment with 4 more patients on up to two occasions. The results confirm there is more commonality of TCRVβ usage between two LNs in the same patient than between LNs and PB, as the overlap score is higher in the LN-LN comparison than LN-PB of the same patient. See Figure 5-42
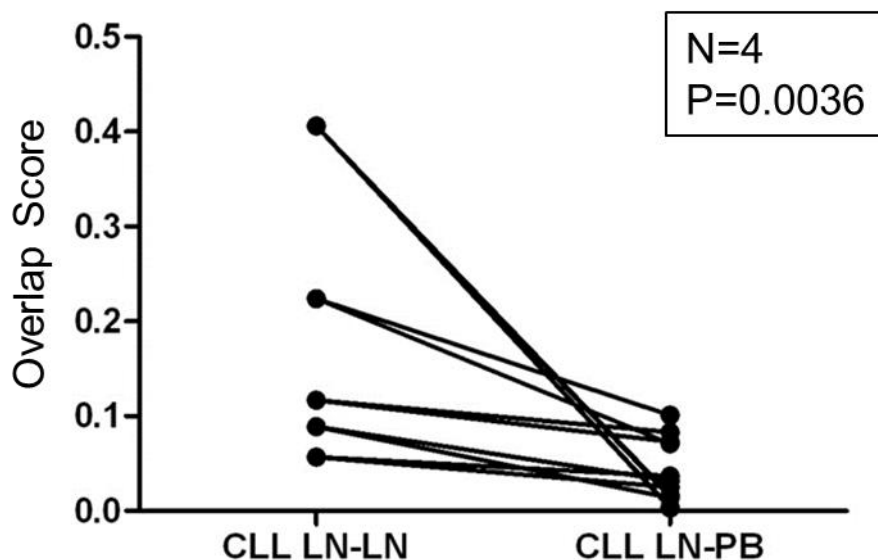
Figure 5-42 More overlapping TCR sequences (a higher overlap score) between two LNs than between LN and PB
Comparison of TCRVβ usage from CD4+ T-cells from CLL PB and 2 separate LNs taken at the same time from 4 individuals. Experimental detail as in Figure 5-41. An overlap score is derived using the immunoSEQ analyser, which defines the extent to which clonotypes are observed to be shared between two samples. This is calculated as a sum of the counts for all shared sequences observed in sample A and sample B divided by the total number of counts of all sequences in both samples. The overlap score is higher in the LN-LN comparison than LN-PB of the same patient. Analysis courtesy of Adaptive Biotechnologies.

5.6 Discussion

There is compelling evidence for an antigenic drive in CLL and the preceding chapters have presented indirect phenotypic evidence for antigenic stimulation of the CD4+ T-cells within the lymph node CLL microenvironment. As discussed in chapter 1, there are postulated mechanisms by which T-cells could accumulate in CLL and we have speculated that T-cells could be attracted into the microenvironment by both TCR dependant and independent means. The observation of high frequency PD-1hi T-cells in the LN supports the theory that there is an antigen drive of T-cells within the lymph node; which operates via a TCR dependant mechanism. The aim of the work in this chapter was to find direct evidence of specific T-cell accumulation in the lymph node by investigating the T-cell receptor repertoire. We approached this problem in several ways. The initial approach was using a ligation oligo PCR method. This method would allow the variable CDR3 to be amplified using a single primer pair. It is well established that different PCR primer pairs have differential amplification efficiency, which can introduce bias and therefore this method would potentially reduce this. The technique however was technically challenging and successful ligation was difficult to replicate consistently. Several methods of optimising the ligation were undertaken as reviewed in Table 5-8 and evidence for successful ligation and amplification of the TCR in the Jurkat cell line is presented here. A potential shortcoming in this method is that the ligation efficiency was unknown and therefore there may be significant bias introduced if only a small percentage of the cDNAs are ligated to the oligo. In the Jurkat experiment this would be unknown as there was only one TCR mRNA as starting material, therefore even if only a relatively small percentage of resultant cDNA molecules were ligated the PCR would still amplify the solitary TCR. In primary patient material, where there are many thousands of potential T-cell receptors, if the efficiency of ligation was not 100% then the whole repertoire could be non-specifically, randomly skewed. This could make comparisons between samples impossible. To assess the ligation efficiency we could have ligated a "wild type" TCRVβ repertoire to look for diversity. Alternatively Jurkat spiking experiments with known amounts of starting RNA could have been tried.

To determine the best method to adopt we clarified exactly the question we were addressing. In this case we wanted to examine the TCR repertoire of CD4+ PD-1hi and PD-1lo cells between different compartments within the same patients. Therefore the fundamental analysis was a paired comparison. By choosing conventional spectratyping we would utilise multiple primers pairs, which may amplify variably, and this is only of concern in a quantitative study. However our primary analyses were comparative and therefore the relative inefficiency of one pair of PCR primers versus another would, in the end, be applied consistently across all groups and therefore the bias would not favour one group. This would lead to a specific and constant bias and not non-specific random bias as may have occurred with the inefficient oligo ligation method. Therefore we felt this potential limitation was acceptable. The potential impact of primer bias in the HTS setting is discussed later.

An unavoidable limitation with any pooled cDNA PCR method is that the starting quantity of mRNA molecules may not be consistent, even with the same number of starting T-cells. Some T-cell subsets have different amounts of mRNA which can be up or down-regulated by microenvironmental factors (Paillard, Sterkers et al. 1988), therefore if one of our sorted subsets of T-cells had a higher level of mRNA TCR expression than another the relative proportion of cDNA entering the PCR reaction from those cells could bias the result. To identify the amount of starting material we measured the total RNA extracted, which may not reflect the TCR mRNA. This limitation could potentially be overcome by single cell PCR or by using gDNA. The disadvantage of using gDNA has already been discussed, but the major disadvantage is that this method takes no account of whether there is a resultant functional rearranged TCR expressed by the T-cell (Desmarais 2012).

As our study was not designed to compare quantitative information about the frequency of a TCRVβ family usage, but was simply looking for diversity of the repertoire, the impact of these potential PCR biases were considered acceptable. Therefore we decided to proceed with TCRVβ spectratyping using RNA as the starting material. This technique was well validated in the literature and the resultant PCR fragments could be analysed in a consistent and comparative way. This study therefore gives information on the presence of CDR3s of different

lengths (complexity of the repertoire) and skewing of a profile (diversity) but does not provide quantitative frequency of a specific TCR family usage.

LN and PB starting material was obtained freshly and FACS cell sorting was utilised to collect CD4+ T-cells, which were PD-1hi or PD-1lo. For the initial FACS sorts we attempted to collect 10000 cells of each population of CD4+ PD-1hi, CD4+ PD-1lo, from both the PB and LN FNA of CLL patients and PB of healthy controls. This would then rule out the potential criticism of using unequal cell numbers for assessing the TCR. However this was technically challenging as the sort had to be interrupted 3 times to remove the tubes. This compromised the ability to collect cells from very small samples such as LN FNA where cells were invariably lost during the processing. Therefore in later experiments the total sort was collected. Regardless, there was no statistical difference in the number of T-cell sorted from CLL patients and normal controls in all subpopulations. There was a trend towards more PD-1hi T-cells isolated from the CLL patients vs normal PB. This was due to the length of time it took to sort PD-1hi T-cells from whole PB, which were found at relatively low frequency and large volumes of whole blood were required. In retrospect we could have performed a T-cell enrichment step prior to the sort but we wanted all samples to be handled in a consistent manner. If the fewer number of PD-1hi T-cells from normal controls led to a bias in the results then the normal control (with less cell numbers) would be anticipated to be more skewed i.e. have a less diverse repertoire than the CLL PD-1hi cells. In fact the opposite is true and the CLL PD-1hi T-cells were more skewed than the normal control PB despite more cells entering the experiment. This adds more power to the result as the expectation would be the bias favours the opposite result to be true. The only place this bias could therefore have had an impact was between diversity of the normal control PD-1hi and PD-1lo populations, which was not the question this study was aiming to answer. The normal control showed that 10,000 input T-cells enabled a normally distributed spectratype prolife. In two of the six normal control cases <10,000 cells were collected in the PB PD-1hi subset. There was skewing of the profile in these cases, as there was in PD-1hi subset where more than 10,000 cells were collected. There is published data which concurs with our findings that PD-1hi cells have skewed repertoires (Lin, Peacock et al. 2007, Gros, Robbins et al. 2014), nonetheless cell numbers cannot be entirely excluded as a confounding variable in these two cases.

Overall our results have provided evidence for skewing of the CD4+ TCRVβ spectratype in the PD-1hi T-cells compared to PD-1lo T-cells in both LN and PB compartments in CLL. There was also increased skewing of the CLL CD4+ PB TCRVβ repertoire compared to age matched normal controls of both the PD-1hi and PD-1lo CD4+ T-cell subsets. Overall complexity of the CD4+ TCRVβ repertoire in CLL was the same between the PD-1hi and PD-1lo populations, but there was lower complexity of the TCRVβ repertoire overall in CLL PB compared to age matched controls.

As we have demonstrated in chapter 3, it is within the lymph node that PD-1+ T-cells accumulate and therefore it is here that the repertoire is most skewed. This data was backed up with evidence from our HTS study that showed that there was skewing of the overall TCRVβ repertoire in CLL CD4+ PB T-cells, with apparent over and under usage of certain TCRVβ families, although this needs further elucidation in a larger cohort study. There were the same number of unique sequences in the CD4+T-cells whether derived from the LN or PB, however there was more clonality (less diversity) within the LN than the PB. Additionally when 2 LNs from the same patient were compared with the PB there was more overlapping sequence homology between the CD4+ T-cells derived from the 2 LNs than with the PB. Taken together this suggests that it is in the LN where the CD4+ T-cells are specifically responding to a common antigen.

In contrast to spectratyping, the HTS technology can be used to quantitate frequencies of TCRVβ usage and of individual clonotypes. HTS is an emerging technology for examining the TCR repertoire and there are many complexities and caveats that must be taken into consideration when attempting to quantify the TCR repertoire. HTS was first designed to sequence large regions of the genome, not very short CDR3 regions of the TCR which are not only different to the germline DNA but also highly variable (Robins 2013). A major problem is to accurately quantify the number and size of each of millions of TCRs. There are both biological and technical reasons for the difficulties encountered. From a technical perspective when sequencing the TCR there is the PCR enrichment step, which has the potential to introduce amplification bias and this is more critical here where quantification analysis is undertaken. If gDNA is used as the template a multiplex PCR amplification is employed in

order to capture all the VDJ rearrangements. One primer set PCR amplification is not possible as the distance between the constant and J region is too large and there is not enough homology between the V and J regions (Robins, Campregher et al. 2009, Sherwood, Desmarais et al. 2011). Therefore errors may be introduced from differences in the amplification efficiency of certain primer pairs. In order to try an overcome this Carlson et al have developed a solution whereby they generated a complete set of synthetic TCRVβ molecules. As the precise quantity of the synthetic TCRVβ that enters the PCR is known it can be ascertained which primer pairs under or over amplify the product relative to the others. Then the amount of primer is titrated up or down in a sequential fashion until nearly all the bias is removed and any remaining differences were removed by a mathematical algorithm (Carlson, Emerson et al. 2013). Quantitative PCR amplification is much easier if the starting target material is mRNA. This is because the introns have been removed and there is a constant region 3' of the J region in the transcript. The PCR amplification can then have a single constant universal primer at the 5' end and a multiplex of Vβ primers although this of course can still add in amplification bias it is much smaller than in a complex multiplex PCR (Robins 2013).

An alternative option would be to use 5' RACE-PCR (Rapid Amplification of cDNA Ends) sequencing, which removes primer bias but is not without limitations as there are potential biases dependant on transcript length and GC content. The PCR itself can introduce random errors and these sequence errors are compounded with each PCR cycle. However it must be remembered that these one off sequence errors effect an exponentially smaller fraction of the total PCR pool with every cycle. Biological factors can also play a key role in introducing errors. Firstly RNA is difficult to work with as it degrades quickly and there is a variable amount of mRNA produced by different T-cell subsets as stated earlier. This may introduce an unwanted amplification bias from one subset of T-cells. Some groups have introduced T-cell line spiking experiments but no robust method has been described to overcome this problem and T-cell lines themselves have high quantities of mRNA compared to primary T-cells (Robins, Desmarais et al. 2012). When HTS is used to assess the TCR repertoire there are further considerations to take into account associated with the technology chosen (Bolotin, Mamedov et al. 2012, Robins 2013). When sequencing gDNA code errors can usually be readily

detected. However when sequencing highly variable low frequency regions, such as the TCR, sequencing errors may be missed and inaccurately assigned as a distinct TCRs which in reality may only vary from each other by one nucleotide (Baum, Venturi et al. 2012). Therefore small errors artificially introduced may lead to the generation of a false interpretation of TCR diversity. The 454 and Ion Torrent platforms lead to a high rate of insertions and deletions (indels) due to their defective ability to sequence homopolymers. This occurs because on these platforms, as discussed earlier, sequencing does not terminate after the addition of a single nucleotide, as occurs on the Illumina platform. Therefore the same nucleotide needs to be sequentially added again and again in adjacent positions to sequence the homopolymeric stretch. When the number of nucleotide additions are measured either by light (454) or redox (Ion Torrent) the total number of nucleotides may be incorrectly calculated. This is because the light or redox signal is not entirely linearly proportionate to the number of nucleotides added and this can result in frameshift errors (Loman, Misra et al. 2012). This leads to a particular problem when sequencing the TCR because the D segment often contain homopolymer stretches of G nucleotides. The Illumina platform causes less indels (as the sequencing is terminated every time a nucleotide is added) but it is still susceptible to position dependent errors which are then consistently layered in the same region (Nakamura, Oshima et al. 2011). In HTS single template molecules are sequenced many times which means that an error is then compounded. Sanger sequencing has the advantage that the large number of template molecules means the occasional sequence error is of lower impact (Baum, Venturi et al. 2012). Bolotin et al recently published a comparative study of these three HTS technologies; they sequenced the same TCR rearranged genes from replicate samples and found profound discrepancies in terms of diversity and abundance (Bolotin, Mamedov et al. 2012). They go on to suggest biological and computational mechanisms to identify true variance from sequence artefacts. It is clear a cross platform collaborative approach is needed to address these issues.

Therefore these issues need to be fully resolved before HTS is universally adopted as the gold standard for TCR analysis. Nonetheless since the work presented here was complete significant developments in bioinformatics have made HTS of the TCRVβ a more attractive. The HTS results in our study complemented the spectratyping data. We have found that the

overall TCRVβ family usage by CD4+ T-cells is similar between the LN and PB but that overall there is more clonality in the LN derived CD4+ T-cells compared to PB. Importantly, there was more similarities between 2 distinct lymph nodes from the same patient, than between the LN and PB suggesting there may be a different antigenic drive between compartments.

Taken together, the work here has confirmed that the PD-1hi subset of CD4+ T-cells in CLL show evidence of TCR oligoclonality and these cells predominate in the LN. This suggests that within the LN there are antigen specific interactions that lead to the expansion of certain T-cell clones within the LN. The nature of the antigen and the role these cells play in disease pathogenesis is, however, uncertain. This is an important question given the increasing interest in harnessing tumour infiltrating lymphocytes in cancer therapeutics, and the availability of antibodies that block the PD-1 / PD-L1 axis. Preliminary experiments that explore this are presented in the next chapter.

Chapter 6 An *in vitro* model of CLL LN T-cells and effects of blocking the PD-1 / PD-L1 axis

6.1 Introduction

In the preceding chapters it has been shown that T-cells derived from CLL LN show a different phenotype to those found in the PB of the same patient. CD4+ T-cells accumulate in the LN of CLL patients and these cells show a phenotype of chronic antigenic stimulation. We have hypothesised that these phenotypic changes provide evidence of T-cell activation and antigen experience that occurs within the LN. As previously outlined, it is accepted that it is within the LN that CD4+ T-cells make contact with CLL cells and the tumour proliferates. We have shown that the Ki67+ proliferating CLL cells are in close contact with PD-1+ CD4+ T-cells. Therefore it may be considered appropriate to suggest that functional studies of T-cells in CLL should only be undertaken utilising these T-cells derived from the tumour microenvironment. An obvious question is whether a co-culture system between autologous CD4+ T-cells derived from the LN could protect CLL cells from apoptosis and promote their proliferation *in vitro* without prior stimulation. Or indeed whether the CD8+ PD-1+ T-cells could be rescued from exhaustion and mount an anti-tumour response. Ideally this could be achieved by setting up a series of co-culture experiments with autologous T-cells derived from both the LN and PB. Unfortunately this was not feasible due to the small numbers of T-cells which could be sorted from the LN FNA sample. Therefore methods were designed to try and recapitulate the tumour microenvironment using T-cells sourced from the PB. Activated CD4+ T-cells co-cultured with CLL cells is an established method of maintaining CLL cells in culture. Our group and others have previously reported the use of CD3/CD28 bead stimulated T-cells to protect CLL cells from apoptosis *in vitro* (Patten, Devereux et al. 2005, Prieto, Sanchez et al. 2005). Os et al also reported that CLL cells proliferative in response to specific T-cell help (Os, Burgler et al. 2013). This approach has therefore been used to *in vitro* model the tumour microenvironment.

In this pilot study we first sought to identify whether pre-stimulating PB T-cells changes their phenotype to one comparable to those found in the LN. We specifically were interested in mimicking the PD-1hi phenotype. In health, PD-1 is known to be inducible upon stimulation

and during chronic infection (Agata, Kawasaki et al. 1996, Barber, Wherry et al. 2006). As part of the normal immune response engagement of PD-1 by its ligands, PD-L1 or PD-L2, leads to negative regulation of the immune system, with decreased cell proliferation and inhibition of cytokine production (Freeman, Long et al. 2000, Latchman, Wood et al. 2001). The changes are hierarchical where first there is loss of proliferation, then inhibition of IL-2 production, TNFα before IFN-γ, accompanied by expression of PD-1, LAG-3, TIM-3 and CTLA-4 (Wherry 2011). These changes have already been shown in CLL derived T-cells where "exhausted" PD-1+ CD4+ and CD8+ T-cells secrete low levels of IFN-γ and TNF (Riches, Davies et al. 2013). Interestingly in our study despite the high levels of PD-1 we did not detect high levels of PD-L1 on resting CLL cells from either the LN or PB in keeping with Xerri et al. (Xerri, Chetaille et al. 2008). This is in contrast to the TCL-1 transgenic mouse model of CLL that has constitutive PD-L1 expression on the tumour cells (Gassner, Zaborsky et al. 2015). Therefore, following establishment of an *in vitro* model, the next aim of this study is to identify whether stimulating T-cells *in vitro* increases the PD-L1 or PD-L2 levels on CLL cells.

Our next aim was to block PD-1 and assess the phenotypic changes induced. Huge interest has been generated in the possibility of harnessing the PD-1 / PD-L1 axis to restore T-cell function to aid the clearance of viruses, and more recently cancers. Barber et al authored the seminal paper in Nature which used an anti PD-L1 blocking antibody to restore function of exhausted CD8 T-cells to clear mice chronically infected LCMV (Barber, Wherry et al. 2006). PD-1 / PD-L1 blockade in lymphoid malignancies is a less straightforward proposition; here the cells are both the immune system and the malignant tumour. Hodgkin disease is the lymphoma where PD-L1 blockade is the most well studied, but here lies a very specific scenario. The Reed-Sternberg cells harbour 9p24.1 amplifications; which encodes for PD-L1 and leads to its constitutive activation; independent of T-cell stimulation and IFN-γ. Several groups have reported that tumour infiltrating lymphocytes in Hodgkin lymphoma express PD-1, and that the number of PD-1+ T-cells is an independent negative prognostic factor for OS (Muenst, Hoeller et al. 2009). Early phase studies of the anti-PD-1 drug Nivolumab in Hodgkin lymphoma have shown an 87% response rate (Ansell, Lesokhin et al. 2015).

In CLL the unanswered question is what happens when T-cells are playing dual roles; where the CD4+ T-cells may be supporting the tumour survival and a proportion of cytotoxic T-cells may be directed against the tumour; PD-1 blockade may be a double edged sword. Therefore in this study we set out to block the PD-1 / PD-L1 axis in primary CLL cells in culture and assess the phenotypic changes this induces on both the CD4 and CD8 T-cells.

6.1.1 Experimental Approach

In this chapter we plan to identify whether the T-cell phenotype of CLL LN is mimicked by stimulating T-cells derived from previously cryopreserved CLL PBMCs. This would support the rationale of using stimulated PB derived CLL T-cells as *in vitro* model for the LN microenvironment, which then gives weight to using this approach for *in vitro* functional studies and investigation of the PD-1 / PD-L1 axis.

T-cell stimulation can be undertaken by several means. We chose to use CD3/CD28 bead stimulation, as this was the method our group previously published to activate T-cells and which supported CLL cells *in vitro* (Patten, Devereux et al. 2005). The proprietary Dynabeads® are superpara-magnetic polymer beads coated with mouse anti-human IgG monoclonal antibodies against CD3 and CD28. The CD3 antibody is specifically directed against the epsilon chain of human CD3. These beads are designed to mimic the *in vivo* physiologic stimulation of T-cells by APCs; although clearly this is still a non-specific method of TCR stimulation. These activated T-cells have been shown to produce IL-2, GM-CSF, IFN-γ and TNF (Bonyhadi, Frohlich et al. 2005) and it is established that IFN-γ induces PD-L1 in the normal immune system (Dong, Strome et al. 2002). We are interested in identifying if PD-L1 can be upregulated on CLL cells by stimulating the T-cells to produce IFN-γ. In order to investigate the effects of T-cell stimulation we planned to undertake time course experiments; harvesting the T-cells at 24 hours, 48 hours and 5 days post stimulation to identify the most appropriate length of time for T-cell stimulation. We went on to look at blocking the PD-1/PD-L1 axis *in vitro* using a monoclonal antibody against PD-1.

6.2 Aim

Therefore the primary aim of this chapter is to assess whether stimulating CLL PB T-cells can lead to phenotypic changes that mimic the CD4+ T-cells found in CLL LN FNAs from our data presented in chapter 3. Following this we plan to investigate the effects of blocking the PD-1 / PD-L1 axis *in vitro*.

6.3 Materials and Methods

6.3.1 Ethics

Patients with a diagnosis of CLL were invited to take part in the study. Ethical approval for this study was granted under NREC: 08/H0906/94 044. Patients were given the patient information sheet and adequate time to consider their entry into the study. Written informed consent was gained according to the Declaration of Helsinki, 2008.

6.3.2 Primary Patient Material

PB was collected from CLL patients and PBMCs isolated by Ficoll Histopaque® (Sigma Aldrich) density centrifugation as described in 2.2.1. PBMCs were previously cryopreserved and thawed on the day of the experiment.

6.3.3 PBMC Culture

PBMCs were cultured in 24 well plates at 1×10^6 cells per well, resuspended in 500µl of CLL media. Cells were cultured for 24 hours, 48 hours and 5 days in a humidified CO_2 incubator at 37°C.

6.3.4 CD3/CD28 Stimulation of T-cells

Dynabeads® Human T-Activator CD3/CD28 magnetic beads (Fisher Scientific) were used to stimulate T-cells. These beads are superparamagnetic polymer beads of a uniform size coated with monoclonal antibodies against CD3 and CD28. Prior to use Dynabeads® were resuspended in the vial by vortexing. The beads were washed by aliquoting the desired amount into an equal volume of buffer and mixing. The tube was then placed on the magnet (DynaMag™) for 1 minute and the supernatant discarded. The washed beads were then resuspended in the same volume of culture medium as they were initially suspended in. 10µl of beads were incubated per 1×10^6 cells. Incubation of the cells was undertaken in the

humidified CO_2 incubator at 37°C with the beads for 24 hours, 48 hours and 5 days. At the required time-point, cells were harvested and beads were removed by vigorously pipetting the sample. Then the sample was placed back in the magnet for 2 minutes. The supernatant containing the washed activated cells was then transferred to a fresh tube for flow cytometry.

6.3.5 Blocking PD-1

Functional grade anti-human PD-1 (eBioscience) was used to block PD-1 in culture. 10µg of anti-PD-1 was used per 1 x10^6 cells. The J116 monoclonal antibody inhibits PD-1 signal transduction but does not block binding of the PD-L1 ligand. The blocking antibody was added immediately prior to the anti-CD3/CD28 beads were added to the PBMCs in culture at time 0. Cells were harvested at 24 hours, 48 hours and 5 days. Effective PD-1 blocking using this method has been published by several groups (Dong, Strome et al. 2002, Saudemont, Jouy et al. 2005, Jurado, Alvarez et al. 2008).

6.3.6 Intracellular Cytokine Measurement

For those experiments were intracellular cytokines were to be measured, Brefeldin A (BD GolgiPlug™) was added to the PBMCs in culture 12 hours prior to harvesting the cells, at a volume of 1µl per well. Brefeldin A is a protein transport inhibitor and blocks the intracellular transport *in vitro*, as a result cytokines can accumulate in the cells enabling their detection by flow cytometry.

6.3.7 Flow Cytometry Antibodies

Flow cytometry antibodies used in this chapter are detailed in Table 6-1.

Table 6-1 Flow cytometry antibodies

Antigen	Clone	Conjugation	Volume	Company
CD3	UCHT1	V500	5µl	BD Biosciences
CD4	RPA-T4	PE	10µl	AbD Serotec
CD4	RPA-T4	PerCp-Cy5.5	2.5µl	eBioscience
CD5	UCHT2	Pe-Cy7	10µl	BioLegend
CD5	MF7-14.5	APC	5µl	AbD Serotec
CD8	OKT8	Pacific Blue™	10µl	eBioscience
CD8	OKT8	eFluor® 450	2.5µl	eBioscience
CD19	SJ25-C1	Pacific Blue™	2.5µl	Invitrogen
CD19	HIB19	eFluor® 450	2.5µl	eBioscience
CD25	MEM-181	FITC	5µl	AbD Serotec
CD28	CD28.2	APC	10µl	eBioscience
CD69	FN50	PE	10µl	BioLegend
CD152 (CTLA-4)	14D3	Biotin	1µl	eBioscience
CD154 (CD40L)	24-31	PE	10µl	eBioscience
CD273 (PD-L2)	MIH18	PE	10µl	BD Biosciences
CD274 (PD-L1)	MIH1	FITC	10µl	BD Biosciences
CD279 (PD-1)	MIH4	Alexa Fluor® 647	5µl	AbD Serotec
IFN-γ	G2-4	FITC	5µl	eBioscience
Streptavidin	N/A	FITC	1 µl	eBioscience

6.3.8 Flow Cytometry Panels

The following flow cytometry panels were developed for the work presented here.

Viability Panel

Fluorochrome	FITC	PE	APC	7-AAD	Pacific Blue
Antigen	Annexin V	CD4	CD5		CD8

Stimulation Panel A

Fluorochrome	FITC	PE	PerCP-Cy5	PE-Cy7	APC	Pacific Blue
Antigen	PD-L1	PD-L2	CD4	CD5	PD-1	CD8

Stimulation Panel B

Fluorochrome	FITC	PE	PerCP-Cy5	APC	Pacific Blue
Antigen	CTLA-4	CD40L	CD4	PD-1	CD8

Stimulation Panel C

Fluorochrome	FITC	PE	PerCP-Cy5	PE-Cy7	APC	Pacific Blue
Antigen	CD25	CD69	CD4	CD5	CD28	CD8

Stimulation Panel D

Fluorochrome	FITC	PE	PerCP-Cy5	APC	APC-Cy7	Pacific Blue
Antigen	IFN-γ	CD69	CD4	CD8	Viability	CD3

Stimulation Panel E

Fluorochrome	FITC	PE	PerCP-Cy5	Pe-Cy7	APC	APC-Cy7	Pacific Blue
Antigen	PD-L1	PD-L2	CD4	CD5	PD-1	Viability	CD19

6.3.9 Staining Cell Surface Antigens for Flow Cytometry

Cells were resuspended in 100µl CLL media and labelled for flow cytometry according to 2.7.1. Directly conjugated +/- biotinylated antibodies were added at appropriate titrated volume as described in Table 6-1 according in the panels outlined in 6.3.8. Viability of cells was checked using Annexin V as per 2.7.4.

6.3.10 Intracellular Cytokine Staining

For the intracellular cytokine staining panels a viability dye was used to ensure the integrity of the cells under investigation. Fixable viability dye eFluor® 780 (eBioscience) is a viability dye that irreversibly labels dead cells. Unlike 7-AAD, cells can then go on to be washed, fixed, permeabilised, and stained for intracellular antigens. The method for intracellular cytokine staining is as follows. Cells were washed twice and resuspended in PBS. 1µl fixable viability dye was added and cells were incubated for 10 minutes at RT. Cells were washed twice and then stained for cell surface antigens as previously described. Following the last wash cells were resuspended in 250µl BD Cytofix/Cytoperm™ fixation buffer (BD Biosciences) for 20 mins at 4°C. 1ml BD Perm/Wash buffer (x10 perm wash diluted in distilled water) was added to cells and incubated for 15 minutes in the dark. Cells were then washed and resuspended in 50µl Perm/Wash buffer. Intracellular antibodies were added at the appropriate volume and incubated for 20 minutes at RT in the dark. Then cells were washed twice in 1ml BD Perm/Wash and resuspended for flow cytometry.

6.3.11 Compensation Matrix

Either cells or compensation beads were used to create the compensation matrix. As outlined in 2.7.5.

6.3.12 BD FACSCanto II (BD Biosciences)

The BD FACSCanto II configuration 4-2-2 has 3 lasers allowing 8 colour flow cytometry. The cytometer setup is shown in 2.7.6.

6.3.13 Flow Cytometry Data and Statistical Analysis

Samples were collected and analysed using FACSDiva software (BD Biosciences). Percentage positivity and/or mean fluorescence intensity (MFI) values were obtained as appropriate. Statistical analysis was performed using GraphPad Prism® (Graph Pad Inc.). For comparisons to be made between samples from the same patient, first a D'Agostino and Pearson omnibus normality test was performed on the whole sample group and then paired t-tests for those that passed and a Wilcoxon matched pairs test for those that did not. A p-value of <0.05 was considered statistically significant. For comparison between un-paired t-test was used and a p-value of <0.05 was considered statistically significant. Results are expressed +/- standard error of the mean.

6.4 Patient Material

6.4.1 Demographics of Patients

PB sampling was undertaken on 13 patients with a diagnosis of CLL. The demographics of the patient group are outlined in Table 6-2.

Table 6-2 Demographics of CLL patients

Patient Demographics		n = 13	
Age	Years	44-79	65
Sex	Male	8	62%
	Female	5	38%
CMV Status	IgG Pos	0	0%
	IgG Neg	10	77%
	Unknown	3	23%
Binet Stage	A	5	38%
	B	5	38%
	C	3	24%
Cytogenetics / FISH	Normal	3	23%
	13q-	3	23%
	11q-	4	31%
	17p-	0	0%
	Trisomy 12	3	23%
CD38 status	<30%	9	69%
	>30%	4	31%
Mutational status	Mutated IGVH <98% homology to germline	3	23%
	Unmutated IGVH >98% homology to germline	9	69%
	Unknown	1	8%

6.5 Results

6.5.1 T-cells are viable after 48 hours of culture following stimulation

CLL autologous T-cells were stimulated in culture with CD3/CD28 beads, as described in 6.3.4, for up to 5 days. CLL and T-cell viability was checked at time points 0 hours, 24 hours, 48 hours and 5 days using Annexin V and 7-AAD by flow cytometric analysis. Cell viability was universally >95% at 48 hours. At the 5 day time point cultured PBMCs were >50% positive for Annexin V and 7-AAD and therefore this time point was not used.

6.5.2 Activation markers can be induced on PB CLL T-cells by CD3/CD28 bead stimulation

We measured the levels of activation in the CLL autologous T-cells at baseline and at 24 and 48 hours of stimulation with CD3/CD28 beads. This was to validate that the stimulation was successful. CD69 levels increased after 24 hours and further still after 48 hours of stimulation in both the CD4+ and CD8+ T-cell populations. See Figure 6-1. CD4+ CD69+ post 24 hours culture without stimulation vs CD3/CD28 stimulation; 2.69% +/- 0.95 vs 58.12% +/- 5.30; n=13, p=<0.0001. CD4+ CD69+ post 48 hours culture without stimulation vs stimulation; 3.46% +/- 1.02 vs 68.82% +/- 5.23; n=9, p=<0.0001.
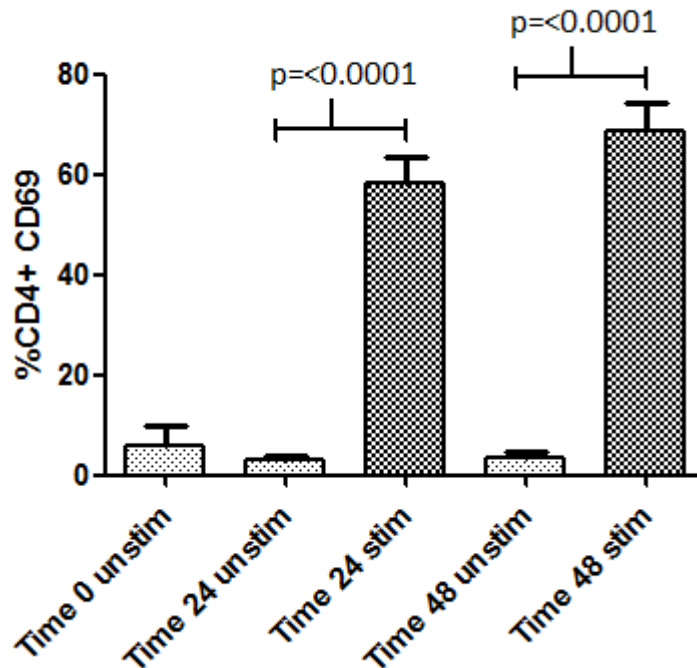
Figure 6-1 CD69 is upregulated on CD4+ T-cells from CLL PB following CD3/CD28 stimulation at 24 hours and further still at 48 hours

CLL autologous PB T-cells were stimulated in culture with Dynabeads® Human T-Activator CD3/CD28 magnetic beads (Fisher Scientific). 10µl of beads were incubated per 1×10^6 cells. At the required time-point, cells were harvested and beads were removed prior to flow cytometry. Levels of CD69 were measured on CD4+ T-cells at time 0 (Time 0), 24 hours (Time 24) and 48 hours (Time 48), with CD3/CD28 beads (stim) and without (unstim). The percentage of CD4+ T-cells that expressed CD69+ increased after 24 hours of stimulation (n=13, p=<0.0001) and further still after 48 hours (n=9, p=<0.0001). Statistical analysis of all paired samples was performed on GraphPad Prism, first with a D'Agostino and Pearson omnibus normality test followed by paired t-test.

The same was true of CD8+ T-cells, which significantly upregulated CD69 after CD3/CD28 stimulation at 24 hours and further still at 48 hours. See Figure 6-2. CD8+ CD69+ 24 hours no stimulation vs CD3/CD28 stimulation; 4.76% +/- 1.96 vs 52.07% +/- 6.09; n=13, p=<0.0001. CD8+ CD69+ 48 hours no stimulation vs stimulation; 10.03% +/- 2.79 vs 81.03% +/- 4.37; n=9, p=<0.0001.
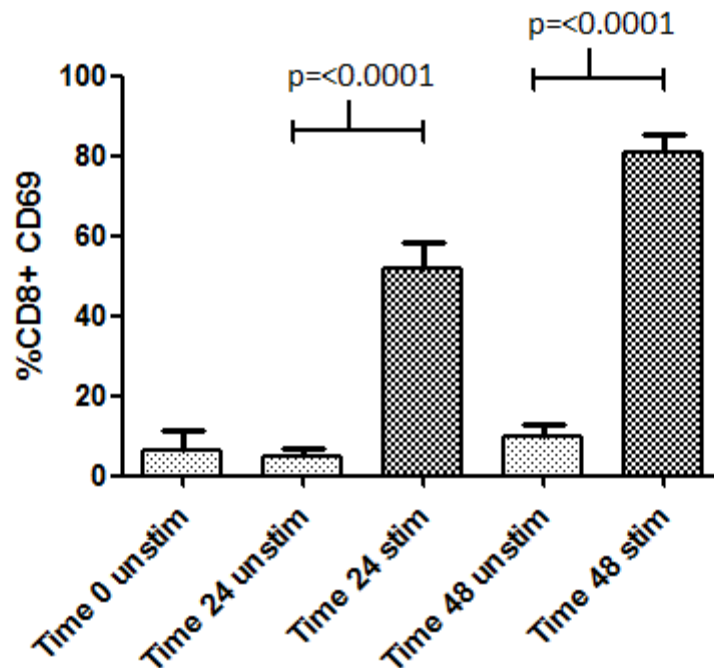
Figure 6-2 CD69 is upregulated on CD8+ T-cells from CLL PB following CD3/CD28 stimulation CLL autologous PB T-cells were stimulated as in Figure 6-1. Levels of CD69 were measured on CD8+ T-cells at time 0 (Time 0), 24 hours (Time 24) and 48 hours (Time 48), with CD3/CD28 beads (stim) and without (unstim) by flow cytometry. The percentage of CD8+ T-cells that expressed CD69+ increased after 24 hours of stimulation (n=13, p=<0.0001) and further still after 48 hours (n=9, p=<0.0001). Statistical analysis as Figure 6-1.

CD25 was also upregulated by CD3/CD28 stimulation on both CD4+ and CD8+ T-cells. See

Figure 6-3 and Figure 6-4. CD4+ CD25+ 24 hours unstimulated vs CD3/CD28 stimulation;

11.41% +/- 1.69 vs 60.09% +/- 6.38; n=12, p=<0.0001. CD4+ CD25+ 48 hours of unstimulated

vs CD3/CD28 stimulation; 7.48% +/- 1.02 vs 85.38% +/- 3.50; n=9, p=<0.0001. CD8+ CD25+

24 hours unstimulated vs CD3/CD28 stimulation; 3.67% +/- 1.15 vs 37.88% +/- 6.31; n=12,

p=<0.0001. CD8+ CD25+ 48 hours unstimulated vs CD3/CD28 stimulation; 9.33% +/- 2.48 vs

78.31% +/- 6.56; n=9, p=<0.0001.
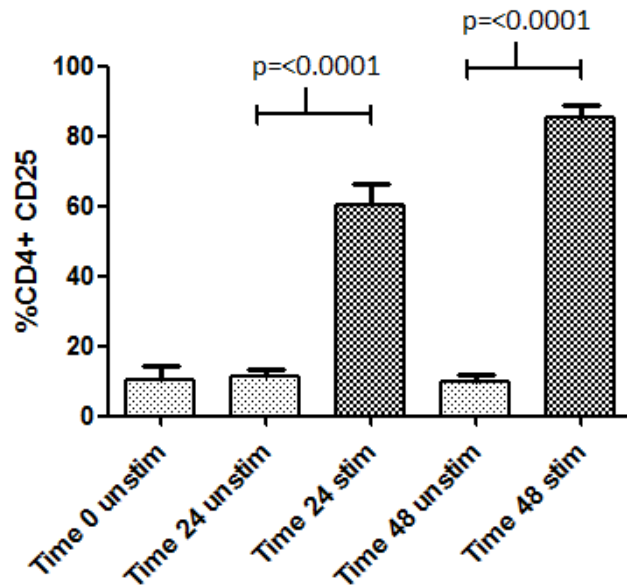
Figure 6-3 CD25 is upregulated on CD4+ T-cells from CLL PB following CD3/CD28 stimulation
CLL autologous PB T-cells were stimulated as in Figure 6-1. Levels of CD25 were measured on CD4+ T-cells at time 0 (Time 0), 24 hours (Time 24) and 48 hours (Time 48), with CD3/CD28 beads (stim) and without (unstim) by flow cytometry. The percentage of CD4+ T-cells that were CD25+ increased after 24 hours of stimulation (n=12, p=<0.0001) and further still after 48 hours (n=9, p=<0.0001). Statistical analysis as Figure 6-1.
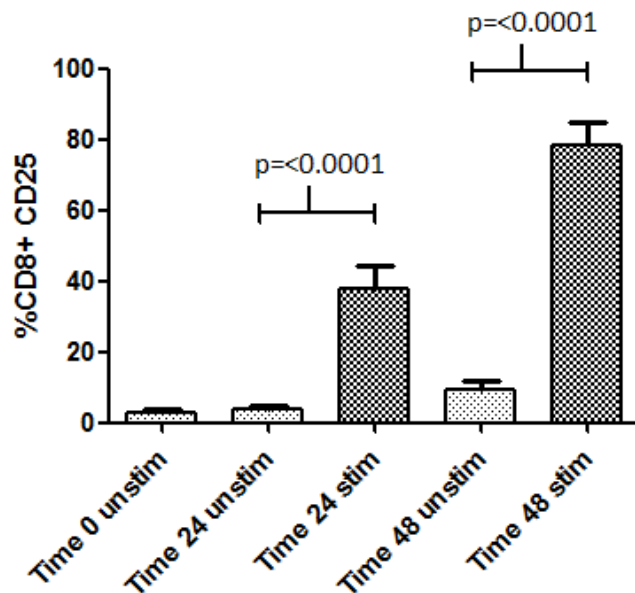
Figure 6-4 CD25 is upregulated on CD8+ T-cells from CLL PB following CD3/CD28 stimulation
CLL autologous PB T-cells were stimulated as in Figure 6-1. Levels of CD25 were measured on CD8+ T-cells at time 0 (Time 0), 24 hours (Time 24) and 48 hours (Time 48), with CD3/CD28 beads (stim) and without (unstim) by flow cytometry. The percentage of CD8+ T-cells that were CD25 increased after 24 hours of stimulation (n=12, p=<0.0001) and further still after 48 hours (n=9, p=<0.0001). Statistical analysis as Figure 6-1.

6.5.3 Negative regulators of the immune system upregulate upon T-cell CD3/CD28 stimulation

CTLA-4 increases on activated CD4+ T-cells and we confirm here that stimulation of CLL T-cells by CD3/CD28 increases levels of CTLA-4. See Figure 6-5. CD4+ CTLA-4+ 24 hours unstimulated vs CD3/CD28 stimulation; 11.25% +/- 3.72 vs 29.41% +/- 5.94; n=13, p=0.0013. CD4+ CTLA-4+ 48 hours unstimulated vs CD3/CD28 stimulation; 24.30% +/- 7.98 vs 58.07% +/- 8.16; n=11, p=0.0005.
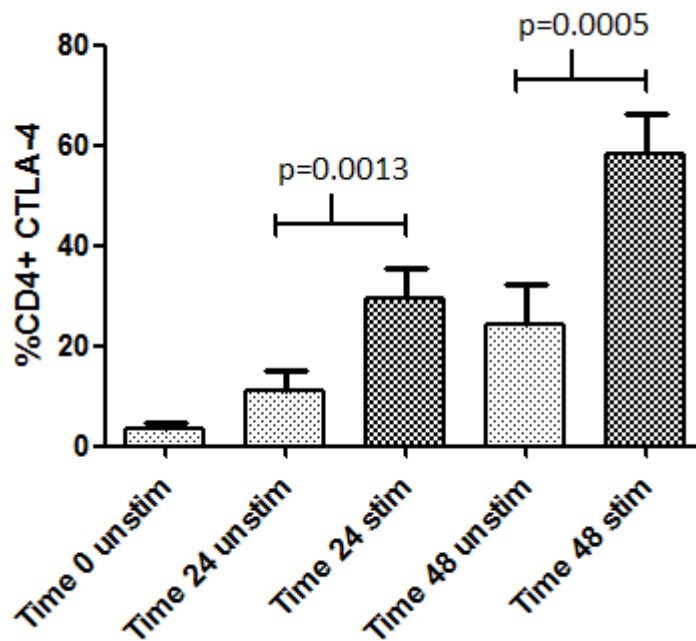
Figure 6-5 CTLA-4 is upregulated on CD4+ T-cells from CLL PB following CD3/CD28 stimulation

CLL autologous PB T-cells were stimulated as in Figure 6-1. Levels of CTLA-4 were measured on CD4+ T-cells at time 0 (Time 0), 24 hours (Time 24) and 48 hours (Time 48), with CD3/CD28 beads (stim) and without (unstim) by flow cytometry. The percentage of CD4+ T-cells that expressed CTLA-4 increased after 24 hours of stimulation (n=12, p=0.0013) and further still after 48 hours (n=9, p=0.0005). Statistical analysis as Figure 6-1.

6.5.4 PD-1 can be induced on CLL T-cells by CD3/CD28 bead stimulation

Importantly we wanted to identify whether PD-1 could be induced by CD3/CD28 bead stimulation and found this to be the case for both the CD4+ and CD8+ populations. See Figure 6-6. CD4+ PD-1+ 24 hours unstimulated vs CD3/CD28 stimulation; 43.43% +/- 7.38 vs 70.28% +/- 7.41; n=9, p=0.0002. CD4+ PD-1+ 48 hours unstimulated vs CD3/CD28 stimulation; 41.85% +/- 9.27 vs 81.92% +/- 5.68; n=9, p=0.0008.
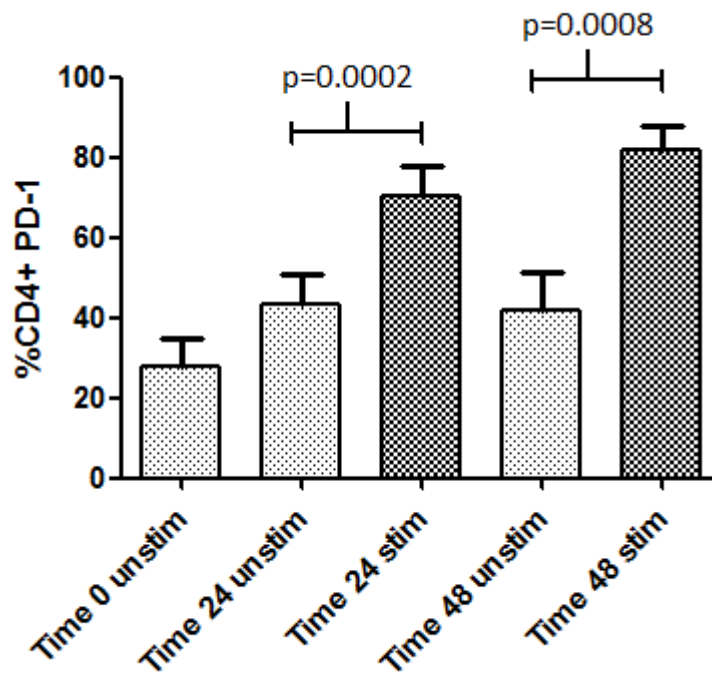
Figure 6-6 PD-1 is upregulated on CD4+ T-cells from CLL PB on CD3/CD28 stimulation
CLL autologous PB T-cells were stimulated as in Figure 6-1. Levels of PD-1 were measured on CD4+ T-cells at time 0 (Time 0), 24 hours (Time 24) and 48 hours (Time 48), with CD3/CD28 beads (stim) and without (unstim) by flow cytometry. The percentage of CD4+ T-cells that expressed PD-1 increased after 24 hours of stimulation (n=9, p=0.0002) and further still after 48 hours (n=9, p=0.0008). Statistical analysis as Figure 6-1.

The same was found in CD8+ T-cells. See Figure 6-7. CD8+ PD-1hi 24 hours unstimulated vs CD3/CD28 stimulation; 55.65% +/- 5.53 vs 71.47% +/- 4.59; n=9, p=0.0195. CD8+ PD-1hi 48 hours unstimulated vs CD3/CD28 stimulation; 56.04% +/- 8.06 vs 88.80% +/- 5.49; n=9, p=0.0011.
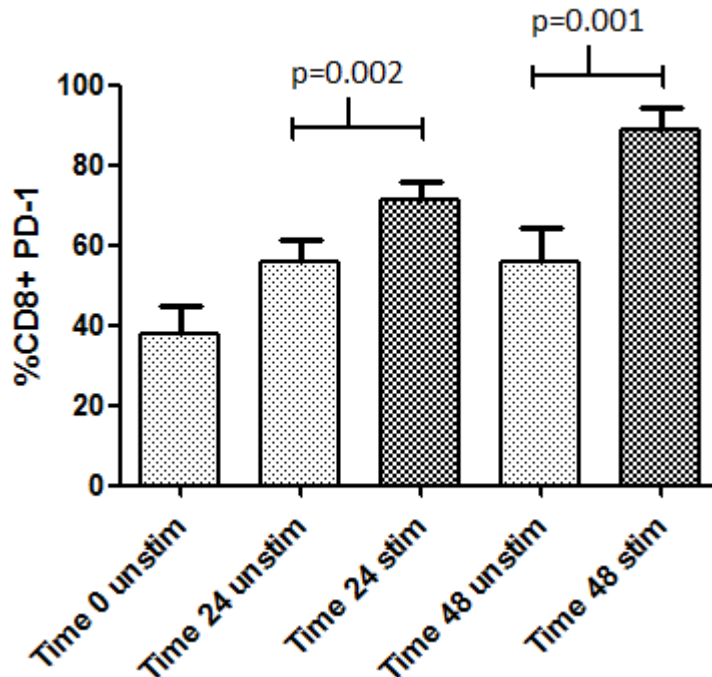
Figure 6-7 PD-1 is upregulated on CD8+ T-cells from CLL PB on CD3/CD28 stimulation
CLL autologous PB T-cells were stimulated as in Figure 6-1. Levels of PD-1 were measured on CD8+ T-cells at time 0 (Time 0), 24 hours (Time 24) and 48 hours (Time 48), with CD3/CD28 beads (stim) and without (unstim) by flow cytometry. The percentage of CD8+ T-cells that expressed PD-1 increased after 24 hours of stimulation (n=9, p=0.002) and further still after 48 hours (n=9, p=0.001). Statistical analysis as Figure 6-1.

6.5.5 Resting levels of CD25 were higher on T-cells from cryopreserved CLL PBMCs compared to fresh whole blood and CD3/CD28 bead stimulation raised the level of CD25 higher still

Next we planned to compare whether the activation state of the stimulated T-cells was comparable to the *in vivo* T-cells derived from the LN FNA presented in chapter3. It was not possible to match the samples as the LN FNA data was historical from chapter 3 where the resting LN FNA cells had been compared with resting PB cells. The same patients with palpable LNs willing to undergo matched FNA and PB sampling were not available at the final stages of the project, therefore it was necessary to utilise the LN FNA data from chapter 3 and

compare it with activated PB from another cohort of patients. As the work presented in this chapter is from a different cohort of patients and also the cells have been handled differently, i.e. in this chapter the PB cells are derived from previously cryopreserved PBMCs, we needed to undertake an analysis to control for the effect of both different unmatched patient cohorts and cryopreservation.

First we compared the activation phenotype of the fresh PB T-cells from chapter 3 the previously cryopreserved PB samples from this chapter. In chapter 3 we found no difference in the expression of CD25 in the fresh PB T-cells compared to the LN FNA T-cells. Interestingly, here we found there was statistically less CD25 expression on the CD4+ T-cells that had been previously cryopreserved compared to our fresh PB control samples. CD4+ CD25 cryopreserved (n=8) vs fresh (n=17) PB; 12.98% +/- 4.70 vs 38.86% +/- 5.65; p=0.0057. See Figure 6-8. Unfortunately as the patients were not matched and the cohort is reasonably small, it cannot clearly be demonstrated that this is not simply a cohort effect. However, this result does concur with other studies where cryopreservation has been shown to lead to a downregulation of CD25 (Golab, Leveson-Gower et al. 2013).
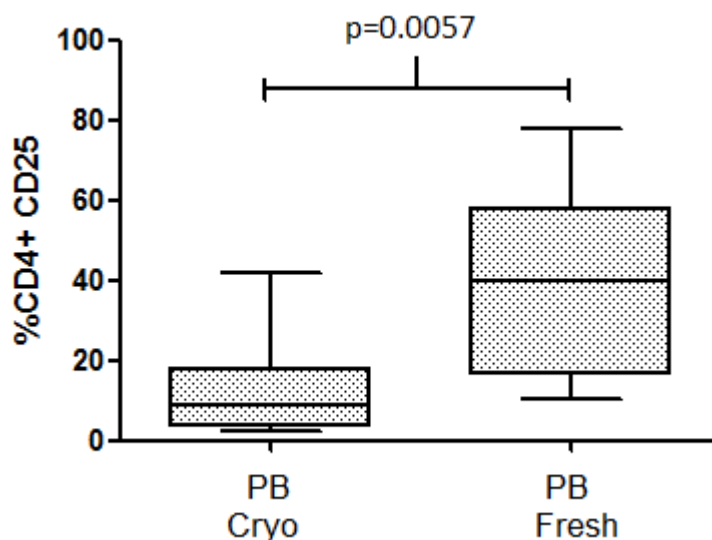
Figure 6-8 CD25 was present on a smaller percentage of CLL PB CD4+ T-cells when cells had been previously cryopreserved compared to fresh PB
In chapter 3 we reported by flow cytometry that 38.86% +/- 5.65 of PB CD4+ T-cells (PB fresh) were also CD25+ (n=17). In the previously cryopreserved CD4+ T-cells presented here (PB Cryo) only 12.98% +/- 4.70 of CD4+ T-cells express CD25 (n=8). This reached statistical significance; p=0.0057. Statistical analysis was with a D'Agostino and Pearson omnibus normality test and unpaired t-test.

We went on to compare whether the amount of CD25 on stimulated T-cells mimicked the LN

T-cells. We found that there was a marked increase in expression of CD25+ on previously

cryopreserved PB CD4+ T-cells following 24 hours of CD3/CD28 bead stimulation compared

to baseline, and that although the baseline levels were lower than that found in the LN, the

activation lead to levels exceeding that in the LN FNA sample. CD4+ CD25+ LN (n=17) vs PB

CD3/CD28 stimulation for 24 hours (n=12); 31.17% +/- 3.38 vs 60.09% +/- 6.39; p=0.0010.

See Figure 6-9.
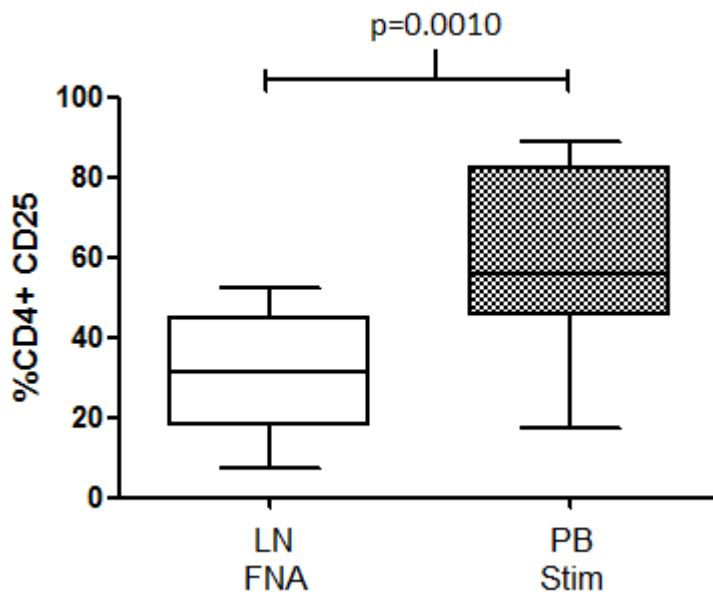
Figure 6-9 CLL CD4+ T-cells that have been stimulated with CD3/CD28 beads have a higher
percentage that are CD25+ compared to fresh LN FNA CD4+ T-cells
CLL autologous PB T-cells were stimulated as in Figure 6-1. Levels of CD25 were measured
on CD4+ T-cells after 24 hours of stimulation (PB stim). The level of CD25 was compared to
that found on the unstimulated fresh CD4+ T-cells from the LN of CLL patients from Chapter
3 (LN FNA). Statistical analysis was with a D'Agostino and Pearson omnibus normality test
and unpaired t-test. There was statistically higher percentage of CD4+/CD25+ T-cells in the
PB stim sample than the LN FNA; p=0.0010.

6.5.6 Levels of CTLA-4 on CD4+ T-cells were the same on fresh and cryopreserved PB but CD3/CD28 bead stimulation does not mimic the levels found in the LN

Unlike for CD25 we found baseline levels of CTLA-4 were the same on PB CD4+ T-cells whether they were previously cryopreserved or fresh and that CTLA-4 on CD4+ T-cells increased upon stimulation to levels higher than that found on the CD4+ T-cells derived from fresh CLL LN FNA. See Figure 6-10. Cryopreserved PB CD4+ CTLA-4 (n=10) vs fresh PB (n=13); 3.38% +/- 1.30 vs 1.77% +/- 0.46; p=0.779. LN CD4+ CTLA-4+ (n=13) vs PB CD4+ CTLA-4+ stimulated for 24 hours (n=13); 5.40% +/- 2.01 vs 29.40% +/- 5.94; p=0.0008.
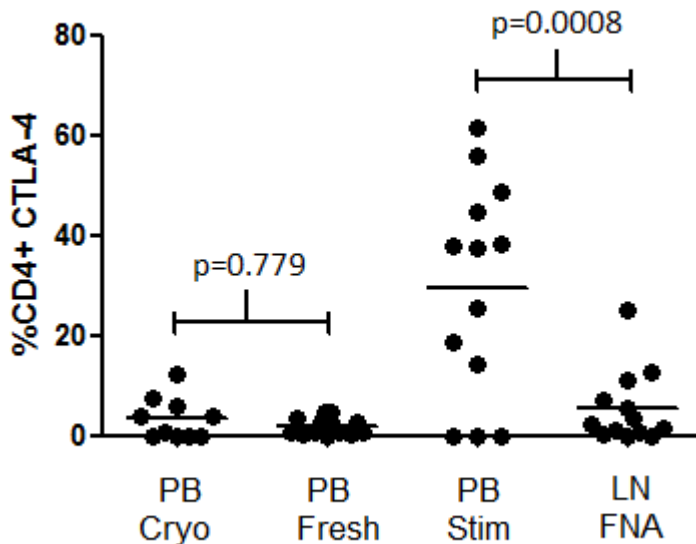
Figure 6-10 CTLA-4 expression is similar between CD4+ PB cells whether or not previously cryopreserved
In chapter 3 we reported by flow cytometry that 1.77% +/- 0.46 of PB CD4+ T-cells (PB fresh) were also CTLA-4+ (n=13). In the previously cryopreserved CD4+ T-cells presented here (PB Cryo) 3.38% +/- 1.30 of CD4+ T-cells express CTLA-4 (n=10). This was not statistically significantly different; p=0.779. CLL autologous PB T-cells were stimulated as in Figure 6-1. Levels of CTLA-4 were measured on CD4+ T-cells after 24 hours of stimulation (PB stim). The level of CTLA-4 was compared to that found on the unstimulated fresh CD4+ T-cells from the LN of CLL patients from Chapter 3 (LN FNA). There was statistically higher percentage of CD4+/CTLA-4+ T-cells in the PB stim sample (n=13) than the LN FNA (n=13); p=0.0008. Statistical analysis was with a D'Agostino and Pearson omnibus normality test and unpaired t-test.

6.5.7 CD3/CD28 bead stimulation upregulates PD-1 on PB T-cells to levels similar to those found in LN FNA

We have shown that PD-1 is upregulated on T-cells following CD3/CD28 bead stimulation on PB derived T-cells. Therefore we next wanted to answer whether this is this similar to that seen on LN derived T-cells. Again we initially wanted to ascertain whether the number of CD4+ PD-1+ cells was the same whether fresh or cryopreserved cells were used and found this was the case. CD4+ PD-1+ fresh PB cells (n=21) vs previously cryopreserved (n=7); 31.12% +/- 3.59 vs 27.83% +/- 7.08; p=0.671. Next we investigated whether the 24 hour CD3/CD28 stimulated PB CLL CD4+ T-cells expressed the same amount of PD-1 as LN FNA derived T-cells and found they did. Stimulated PB CLL CD4+ T-cells (n=9) vs LN FNA (n=21); 70.28% +/- 7.42 vs 56.42% +/- 4.023 vs; p=0.118. See Figure 6-11.
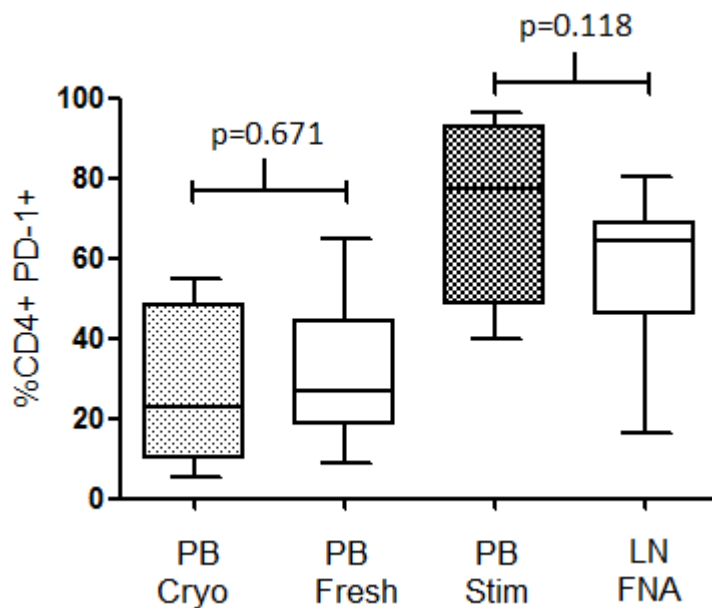
Figure 6-11 The level of PD-1 expression on CD4+ T-cells is unaffected by cryopreservation, and stimulation of T-cells with CD3/CD28 beads for 24 hours increases PD-1 levels on CD4+ T-cells to the same level as found on LN FNA derived CD4+ T-cells.
In chapter 3 we reported by flow cytometry that 31.12% +/- 3.59 of PB CD4+ T-cells (PB fresh) were also PD-1+ (n=21). In the previously cryopreserved CD4+ T-cells presented here (PB Cryo) 27.83% +/- 7.08 of CD4+ T-cells express PD-1 (n=7). This was not statistically significantly different; p=0.671. CLL autologous PB T-cells were stimulated as in Figure 6-1. Levels of PD-1 were measured on CD4+ T-cells after 24 hours of stimulation (PB stim) (n=9). The level of PD-1 was compared to that found on the unstimulated fresh CD4+ T-cells from the LN of CLL patients (n=21) from Chapter 3 (LN FNA) and were found to be similar; p=0.118. Statistical analysis was with a D'Agostino and Pearson omnibus normality test and unpaired t-test.

Next we asked the same question of CD8+ T-cells. Again we wanted to ascertain whether the number of CD8+ PD-1hi cells was the same whether fresh or cryopreserved cells used and we found the baseline levels of PD-1 to be the same. CD8+ PD-1hi fresh PB cells (n=20) vs previously cryopreserved (n=7); 41.44% +/- 3.94 vs 37.87% +/- 7.13; p=0.599.

Next we showed that stimulating the PB T-cells with CD3/CD28 beads for 24 hours increases the PD-1 levels on CD4+ T-cells to those equivalent to the LN FNA. Stimulated PB CLL CD8+ T-cells (n=9) vs LN FNA CD8+ T-cells (n=20); 71.47 +/- 4.59 vs 71.07% +/- 3.54 vs; p=1.00. See Figure 6-12.
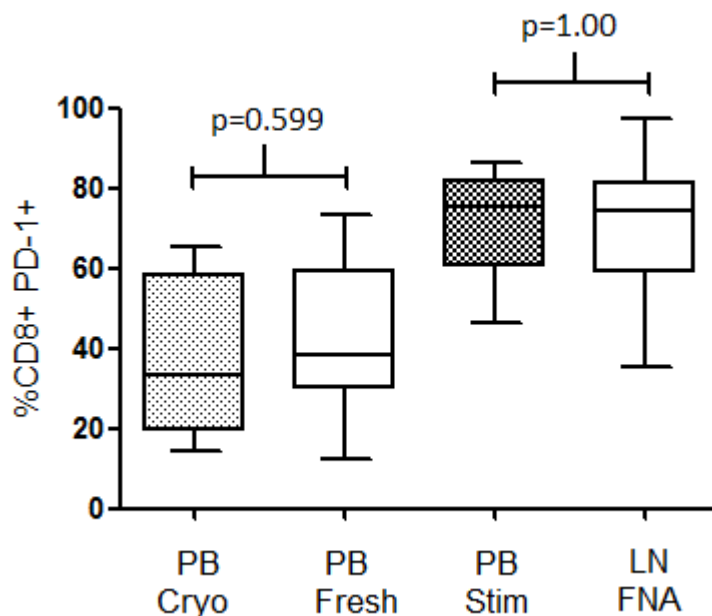
Figure 6-12 The level of PD-1 expression on CD8+ T-cells is unaffected by cryopreservation, and stimulation of T-cells with CD3/CD28 beads for 24 hours increases PD-1 levels on CD8+ T-cells to the same level as found on LN FNA derived CD8+ T-cells
In chapter 3 we reported by flow cytometry that 41.44% +/- 3.94 of PB CD8+ T-cells (PB fresh) were also PD-1+ (n=20). In the previously cryopreserved CD8+ T-cells presented here (PB Cryo) 37.87% +/- 7.13 of CD4+ T-cells express PD-1 (n=7). This was not statistically significantly different; p=0.599. CLL autologous PB T-cells were stimulated as in Figure 6-1. Levels of PD-1 were measured on CD8+ T-cells after 24 hours of stimulation (PB stim) (n=9). The level of PD-1 was compared to that found on the unstimulated fresh CD4+ T-cells from the LN of CLL patients (n=20) from Chapter 3 (LN FNA) and were found to be similar; p=1.00. Statistical analysis was with a D'Agostino and Pearson omnibus normality test and unpaired t-test.

6.5.8 PD-L1 can be induced on CLL cells by co-culture with stimulated T-cells

An interesting observation from chapter 3 was that in spite of the expression of PD-1 at significantly higher levels on the T-cells of CLL patients compared to normal controls, we found no evidence of PD-L1 expression on the tumour B-cell. Importantly we did not detect significant expression of PD-L1 on CLL cells derived from the LN microenvironment. In contrast there have been reports of PD-L1 expression on CLL cells (Grzywnowicz, Zaleska et al. 2012, Ramsay, Clear et al. 2012, Brusa, Serra et al. 2013). We have hypothesised that these apparently conflicting results may be as a result of *in vitro* CLL activation. We therefore sought to identify if T-cell stimulation would lead to expression of PD-L1 on CLL cells. In our study CD3/CD28 beads were added to unselected PBMCs, therefore we would predict the T-cells would be activated directly by the beads and the CLL cells indirectly by the activated T-cells. We compared baseline PD-L1 expression of the cohort of resting fresh CLL cells derived from the PB in chapter 3 and compared them to the previously cryopreserved CLL cells. PD-L1 expression levels were no different between fresh and cryopreserved CLL cells. PD-L1 on fresh PB CLL cells (n=8) vs cryopreserved PB CLL cells (n=10): 1.01% +/- 0.59 vs 0.25% +/- 0.13; n=8, p=0.435. See Figure 6-13.
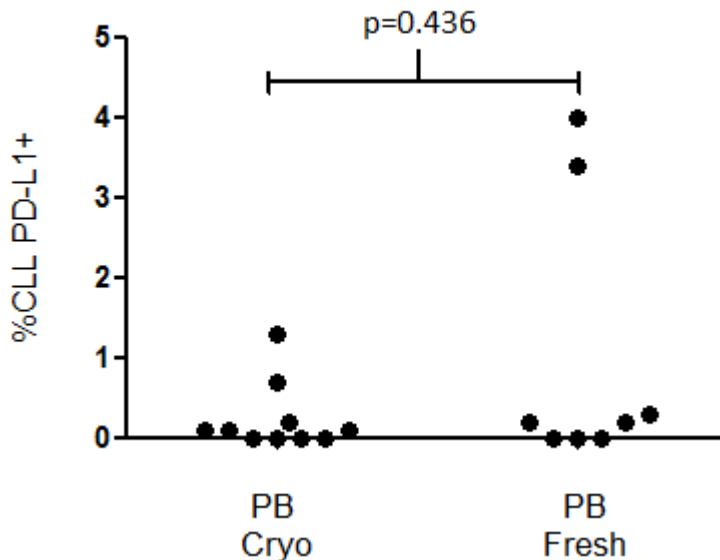
Figure 6-13 There was no difference in the baseline PD-L1 expression on fresh or previously cryopreserved CLL cells
In chapter 3 we reported by flow cytometry that 1.01% +/- 0.59 of PB CLL B-cells (PB fresh) were also PD-L1+ (n=8). In the previously cryopreserved CLL B-cells presented here (PB Cryo) 0.25% +/- 0.13 of CLL B-cells express PD-L1 (n=10). This was not statistically significant; p=0.436. Statistical analysis was with a D'Agostino and Pearson omnibus normality test and unpaired t-test.

Next we compared levels of PD-L1 from fresh LN FNA CLL cells and compared them to CLL cells co-cultured for 24 hours with CD3/CD28 stimulated T-cells. We found that PD-L1 could be upregulated on CLL cells, particularly after prolonged stimulation. See Figure 6-14. CLL PD-L1 24 hours unstimulated culture vs CLL PD-L1 CD3/CD28 co-culture; 0.24% +/- 0.11 vs 4.26% +/- 2.2; n=9, p=0.0078. CLL PD-L1 48 hours culture unstimulated vs CLL PD-L1 48 hours co-culture CD3/CD28 stimulated T-cells; 4.00% +/- 1.63 vs 21.32% +/- 6.24; n=9, p=0.027.
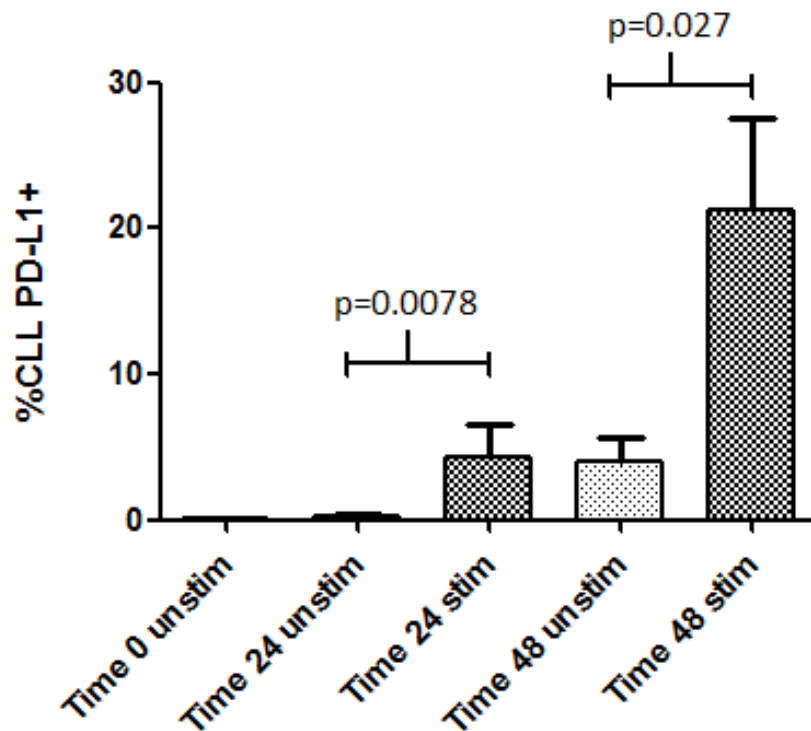
Figure 6-14 PD-L1 can be upregulated on CLL cells by co-culture with CD3/CD28 bead stimulated T-cells
CLL autologous PB T-cells were stimulated as in Figure 6-1. Levels of PD-L1 were measured on CLL B-cells at time 0 (Time 0), 24 hours (Time 24) and 48 hours (Time 48), with CD3/CD28 beads (stim) and without (unstim) by flow cytometry. The percentage of CLL B-cells that expressed PD-L1 increased after 24 hours of stimulation (n=9, p=0.0078) and further still after 48 hours (n=9, p=0.027). Statistical analysis as Figure 6-1.

Therefore we have shown that PD-L1 can be induced on CLL cells which are co-cultured with stimulated T-cells. The level of PD-L1 found on these CLL cells is much higher than that found on CLL LN derived cells from chapter 3 where very little expression was demonstrated on either these or PB derived CLL cells; p=0.0183. See Figure 6-15.
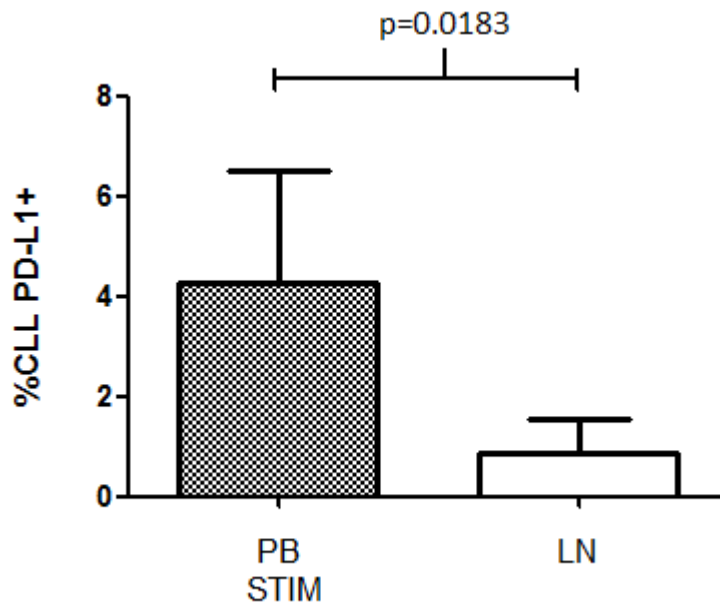
Figure 6-15 Indirect CD3/CD28 bead stimulation of T-cells in co-culture with CLL cells for 24 hours increases the PD-L1 on CLL cells from PB to levels above that found in the LN
CLL autologous PB T-cells were stimulated as in Figure 6-1. Levels of PD-L1 were measured on CLL B-cells after 24 hours of stimulation (PB stim). The level of PD-L1 was compared to that found on the unstimulated fresh CLL B-cells from the LN of CLL patients from Chapter 3 (LN). Statistical analysis was with a D'Agostino and Pearson omnibus normality test and unpaired t-test. There was statistically higher percentage of CLL/PD-L1+ B-cells in the PB stim sample than the LN FNA; p=0.0183.

6.5.9 PB T-cells upregulate PD-L1 following CD3/CD28 bead stimulation

It is becoming increasingly clear that the crosstalk between the activation and negative regulators of the immune system is complex and bidirectional. Therefore we chose to investigate whether the T-cells could also upregulate PD-L1 in response to stimulation and found that indeed was the case. We found PD-L1 is upregulated on the CD4+ and CD8+ T-cells. CD4+ PD-L1 24 hours unstimulated vs CD4+ PD-L1 24 hours CD3/CD28 bead stimulation; 5.63% +/- 1.61 vs 28.27% +/- 6.51; n=9, p=0.0078. The upregulation of PD-L1 was even more marked with prolonged stimulation. CD4+ PD-L1 48 hours unstimulated culture vs CD4+ PD-L1 48 hours CD3/CD28 bead stimulation culture; 11.61% +/- 2.72 vs 66.20% +/- 5.41; n=9, p=0.0039. See Figure 6-16.
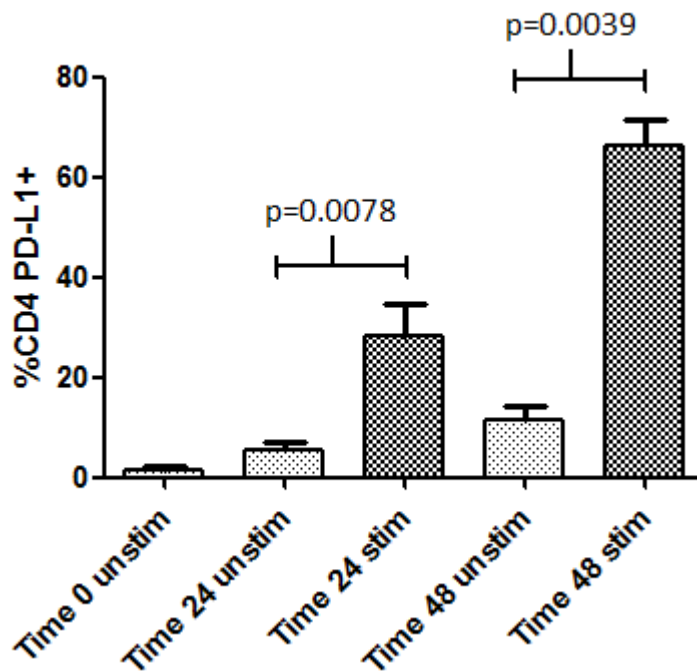
Figure 6-16 PD-L1 upregulates on CD4+ CLL T-cells following CD3/CD28 bead stimulation and the upregulation increases further still with prolonged stimulation
CLL autologous PB T-cells were stimulated as in Figure 6-1. Levels of PD-L1 were measured on CD4+ T-cells at time 0 (Time 0), 24 hours (Time 24) and 48 hours (Time 48), with CD3/CD28 beads (stim) and without (unstim) by flow cytometry. The percentage of CD4+ T-cells that expressed PD-L1 increased after 24 hours of stimulation (n=9, p=0.0078) and further still after 48 hours (n=9, p=0.0039). Statistical analysis as Figure 6-1.

The same is true from CD8+ T-cells which also upregulate PD-L1 upon CD3/CD8 bead stimulation. CD8+ PD-L1 24 hours unstimulated vs CD8+ PD-L1 24 hours CD3/CD28 bead stimulation; 8.03% +/- 2.12 vs 17.48% +/- 6.98; n=9, p=0.0234. Equally the levels of PD-L1 increase further with prolonged stimulation. CD8+ PD-L1 48 hours unstimulated vs CD8+ PD-L1+ 48 hours CD3/CD28 bead stimulation; 17.19% +/- 6.56 vs 62.09% +/- 8.56; n=9, p=0.0039. See Figure 6-17.
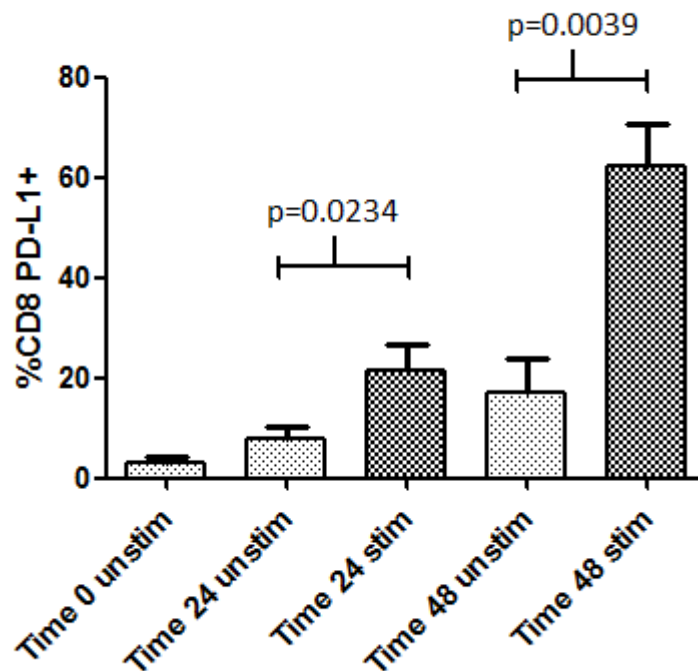
Figure 6-17 PD-L1 upregulates on CD8+ CLL T-cells following CD3/CD28 bead stimulation and the upregulation increases further still with prolonged stimulation
CLL autologous PB T-cells were stimulated as in Figure 6-1. Levels of PD-L1 were measured on CD8+ T-cells at time 0 (Time 0), 24 hours (Time 24) and 48 hours (Time 48), with CD3/CD28 beads (stim) and without (unstim) by flow cytometry. The percentage of CD8+ T-cells that expressed PD-L1 increased after 24 hours of stimulation (n=9, p=0.0234) and further still after 48 hours (n=9, p=0.0039). Statistical analysis as Figure 6-1.

6.5.10 PD-L2 is not expressed by PB CLL, CD4+ or CD8+ cells

PD-L2 was not expressed by resting CLL B-cells nor CD4+ or CD8+ T-cells in the PB or LN FNA. CLL PB stimulation with CD3/CD28 beads did not upregulate PD-L2 on any cell even after prolonged 48 hour stimulation, n=12 (data not shown).

6.5.11 Blocking the PD-1 / PD-L1 axis

Much interest has been generated in modulating immune checkpoint signalling pathways to reverse the negative T-cell regulation in cancer. Blocking the PD-1/PD-L1 axis has been shown to increase the cytotoxic T-cell responses in several cancers. The effect of blocking PD-1 or PD-L1 in CLL has not yet been fully elucidated. We chose to block PD-1 *in vitro* and look for phenotypic changes in the CD4+ and CD8+ T-cells and CLL cells by flow cytometry. The J116 monoclonal antibody blocks PD-1 signal transduction, but does not block its binding to PD-L1.

Blocking PD-1 signal transduction should increase the activation status of the T-cells. We undertook PD-1 blocking experiments on both the CD3/CD8 stimulated and unstimulated PB T-cells in culture at 24 and 48 hours as described in 6.3.5.

6.5.12 Effects of blocking PD-1 on CLL PB T-cell CD25 expression

Blocking PD-1 did not upregulate CD25 on resting PB CD4+. Pre-stimulated T-cells were also unaffected by PD-1 blockade at any time point. See Figure 6-18. CD4+ CD25+ unstimulated PB vs unstimulated PB + blocking antibody 24 hours: 11.41% +/- 4.09 vs 11.05% +/- 2.10; n=8, p=0.196. CD4+ CD25+ unstimulated PB vs unstimulated PB + blocking antibody 48 hours: 9.78% +/- 1.85 vs 7.49% +/- 1.022; n=8, p=0.979. CD4+ CD25+ stimulated CD3/CD28 PB vs stimulated PB + blocking antibody 24 hours: 60.09% +/- 6.39 vs 66.86% +/- 6.86; n=6, p=0.453. CD4+ CD25+ stimulated CD3/CD28 PB vs stimulated PB + blocking antibody 48 hours: 85.38% +/- 3.50 vs 82.31 +/- 5.43; n=7, p=0.183.
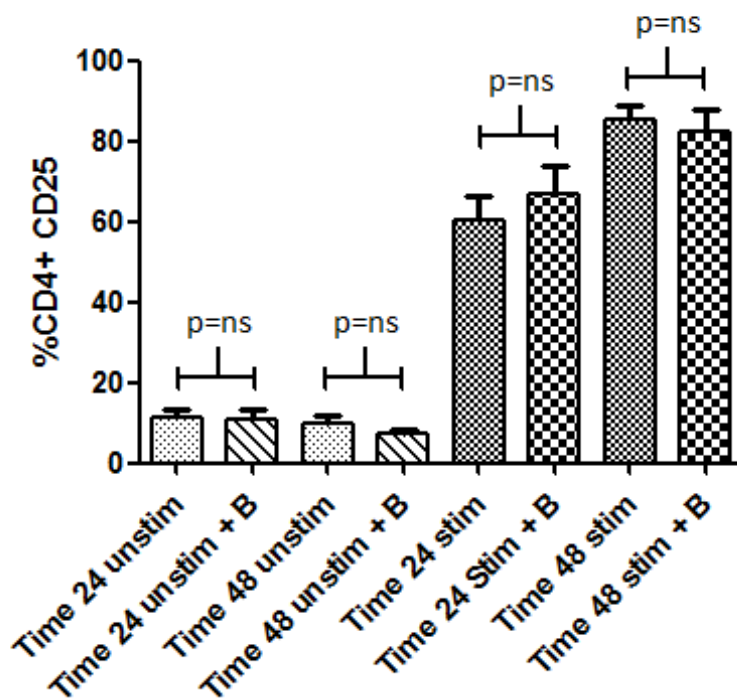
Figure 6-18 Blocking PD-1 signal transduction did not alter CD25 expression in CD4+ T-cells. CLL autologous PB T-cells were stimulated as in Figure 6-1. Functional grade anti-human PD-1 (eBioscience) was used to block PD-1 in culture. 10µg of anti-PD-1 was added per 1 x10^6 cells immediately prior to the anti-CD3/CD28 beads were added. Cultures were set up with (+B) and without the blocking antibody. Levels of CD25 were measured on CD4+ T-cells at time 0 (Time 0), 24 hours (Time 24) and 48 hours (Time 48), with CD3/CD28 beads (stim) and without (unstim) by flow cytometry. The percentage of CD4+ T-cells that expressed PD-L1 was unaffected by the addition of the blocking antibody at every time point.

PD-1 blockade did increase levels of CD25 on previously stimulated CD8+ T-cells at 24 hours. There was no change in phenotype at any other time point. See

Figure 6-19. CD8+ CD25+ stimulated CD3/CD28 PB vs stimulated PB + blocking antibody 24 hours: 37.88% +/- 6.32 vs 40.84. % +/- 7.87; n=6, p=0.031. CD8+ T-cells expressing CD25 unstimulated PB vs unstimulated PB + blocking antibody 24 hours: 3.67% +/- 1.16 vs 7.10% +/- 2.78; n=8, p=0.242. CD8+ T-cells expressing CD25 unstimulated PB vs unstimulated PB + blocking antibody 48 hours: 9.32% +/- 2.49 +/- 7.18% +/- 3.20; n=8, p=0.844. CD8+ CD25+ stimulated CD3/CD28 PB vs stimulated PB + blocking antibody 48 hours: 78.321% +/- 6.56 vs 82.21 +/- 6.31; n=7, p=0.954.
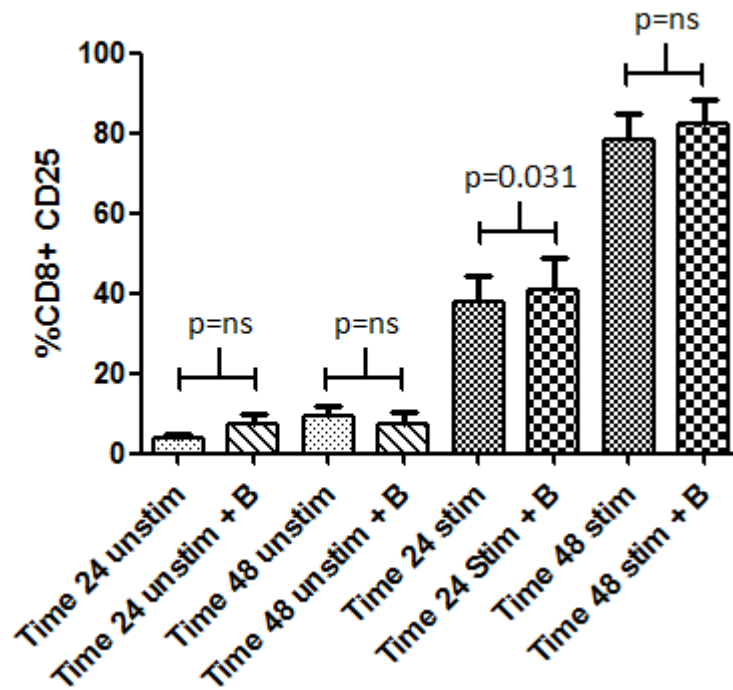
Figure 6-19 Blocking PD-1 signal transduction does not alter CD25 expression on CD8+ T-cells, except for pre-stimulated CD8+ T-cells at 24 hours
CLL autologous PB T-cells were stimulated as in Figure 6-1. Anti-human PD-1 was used to block PD-1 as described in Figure 6-18. Cultures were set up with (+B) and without the blocking antibody. Levels of CD25 were measured on CD8+ T-cells at time 0 (Time 0), 24 hours (Time 24) and 48 hours (Time 48), with CD3/CD28 beads (stim) and without (unstim) by flow cytometry. The percentage of CD8+ T-cells that expressed PD-L1 was unaffected by the addition of the blocking antibody at every time point except for pre-stimulated CD8+ T-cells at 24 hours (p=0.031).

6.5.13 Blocking PD-1 does not alter CD69 expression on CD4+ or CD8+ PB T-cells

Blocking PD-1 did not upregulate CD69 on resting PB CD4+ or CD8+ T-cells. Pre-stimulated T-cells were also unaffected by PD-1 blockade at any time point. See Figure 6-20. CD4+ CD69+ unstimulated PB vs unstimulated PB + blocking antibody 24 hours: 2.87% +/- 0.95 vs 2.35% +/- 1.47; n=8, p=0.54. CD4+ CD69+ unstimulated PB vs unstimulated PB + blocking antibody 48 hours: 3.45% +/- 1.02 vs 3.45% +/- 0.91; n=8, p=0.328. CD4+ CD69+ stimulated CD3/CD28 PB vs stimulated PB + blocking antibody 24 hours: 58.12% +/- 5.31 vs 57.70 +/- 7.67; n=7, p=0.105. CD4+ CD69+ stimulated CD3/CD28 PB vs stimulated PB + blocking antibody 48 hours: 68.82% +/- 5.25 vs 53.80% +/- 8.72; n=7, p=0.150.
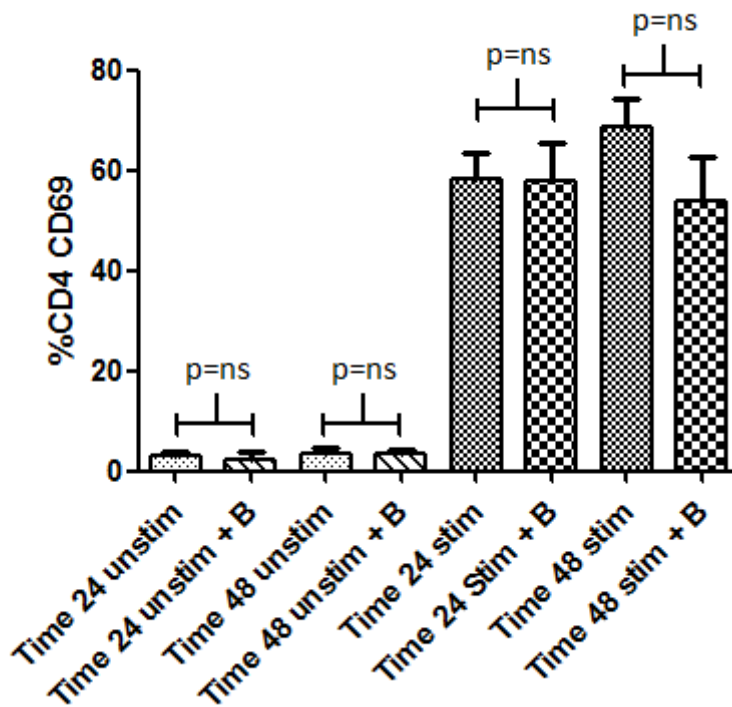
Figure 6-20 Blocking PD-1 signal transduction does not alter CD69 expression in CD4+ T-cells
CLL autologous PB T-cells were stimulated as in Figure 6-1. Anti-human PD-1 was used to block PD-1 as described in Figure 6-18. Cultures were set up with (+B) and without the blocking antibody. Levels of CD69 were measured on CD4+ T-cells at time 0 (Time 0), 24 hours (Time 24) and 48 hours (Time 48), with CD3/CD28 beads (stim) and without (unstim) by flow cytometry. The percentage of CD4+ T-cells that expressed CD69 was unaffected by the addition of the blocking antibody at every time point.

The same held true for CD8+ T-cells. See Figure 6-21. CD8+ CD69+ unstimulated PB vs unstimulated PB + blocking antibody 24 hours: 4.76% +/- 1.98 vs 5.05% +/- 2.35; n=8, p=0.056. CD8+ CD69+ unstimulated PB vs unstimulated PB + blocking antibody 48 hours:10.03% +/- 2.79 vs 7.39% +/- 2.48; n=8, p=0.700. CD8+ CD69+ stimulated CD3/CD28 PB vs stimulated PB + blocking antibody 24 hours: 52.07% +/- 6.09 vs 56.73% +/- 9.89; n=7, p=0.743. CD8+ CD69+ stimulated CD3/CD28 PB vs stimulated PB + blocking antibody 48 hours: 81.03% +/- 4.37 vs 78.94% +/- 4.25; n=7, p=0.121.
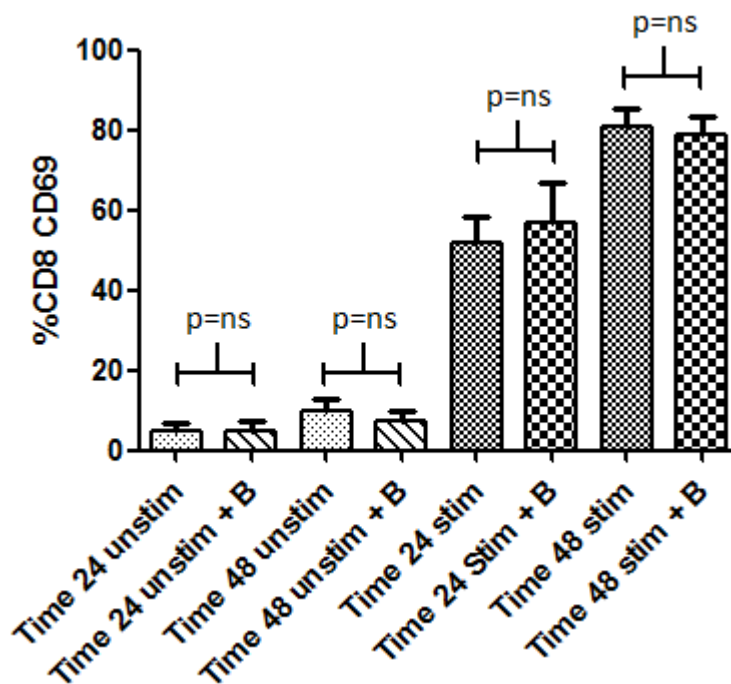
Figure 6-21 Blocking PD-1 signal transduction does not alter CD69 expression in CD8+ T-cells
CLL autologous PB T-cells were stimulated as in Figure 6-1. Anti-human PD-1 was used to block PD-1 as described in Figure 6-18. Cultures were set up with (+B) and without the blocking antibody. Levels of CD69 were measured on CD8+ T-cells at time 0 (Time 0), 24 hours (Time 24) and 48 hours (Time 48), with CD3/CD28 beads (stim) and without (unstim) by flow cytometry. The percentage of CD8+ T-cells that expressed CD69 was unaffected by the addition of the blocking antibody at every time point.

6.5.14 Blocking PD-1 does not alter CTLA-4 expression on CD4+ PB T-cells

Blocking PD-1 did not upregulate CTLA-4 on resting PB CD4 or CD8 T-cells. Pre-stimulated T-cells were also unaffected by PD-1 blockade at any time point. See Figure 6-22. CD4+ CTLA-4+ unstimulated PB vs unstimulated PB + blocking antibody 24 hours: 11.25% +/- 3.72 vs 7.33% +/- 2.76; n=8, p=0.988. CD4+ CTLA-4+ unstimulated PB vs unstimulated PB + blocking antibody 48 hours: 24.30% +/- 7.98 vs 29.48% +/- 11.80; n=8, p=0.842. CD4+ CTLA-4+ stimulated CD3/CD28 PB vs stimulated PB + blocking antibody 24 hours: 29.41% +/- 5.95 vs 27.45% +/- 9.96; n=8, p=0.551. CD4+ CTLA-4+ stimulated CD3/CD28 PB vs stimulated PB + blocking antibody 48 hours: 58.07% +/- 8.16 vs 62.81% +/- 9.04; n=8, p=0.631.
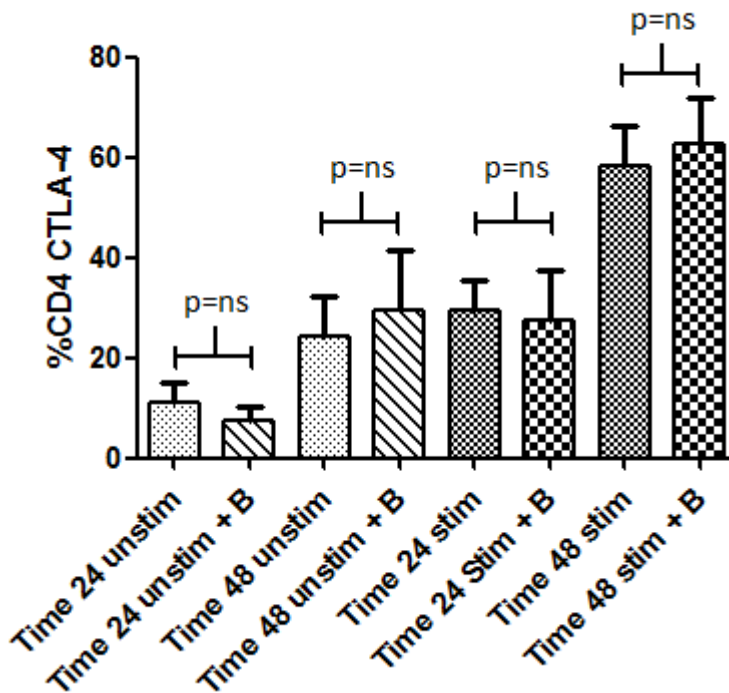
Figure 6-22 Blocking PD-1 signal transduction does not alter CTLA-4 expression in CD4+ T-cells
CLL autologous PB T-cells were stimulated as in Figure 6-1. Anti-human PD-1 was used to block PD-1 as described in Figure 6-18. Cultures were set up with (+B) and without the blocking antibody. Levels of CTLA-4 were measured on CD4+ T-cells at time 0 (Time 0), 24 hours (Time 24) and 48 hours (Time 48), with CD3/CD28 beads (stim) and without (unstim) by flow cytometry. The percentage of CD4+ T-cells that expressed CTLA-4 was unaffected by the addition of the blocking antibody at every time point.

The same held true for CD8+ T-cells, where PD-1 blockade unaffected CTLA-4 expression (data not shown).

6.5.15 Blocking PD-1 does not change PD-1 expression levels on PB T-cells or CLL cells

As for the stimulation experiments, the PD-1 blockade was performed on unselected CLL PB cells. Blocking PD-1 did not upregulate itself on resting PB CD4+ or CD8+ T-cells. Pre-stimulated T-cells were also unaffected by PD-1 blockade at any time point. In addition, there was no effect of the PD-1 blockade on CLL cells expression of PD-1. See Figure 6-23. CD4+ PD-1hi unstimulated PB vs unstimulated PB + blocking antibody 24 hours: 43.43% +/- 7.36 vs 47.47% +/- 10.11; n=6, p=0.729. CD4+ PD-1hi unstimulated PB vs unstimulated PB + blocking antibody 48 hours: 41.85% +/- 9.27 vs 41.88% +/- 10.99; n=5, p=0.696. CD4+ PD-1hi stimulated CD3/CD28 PB vs stimulated PB + blocking antibody 24 hours: 70.28% +/- 7.42 vs 74.88% +/- 8.89; n=5, p=0.085. CD4+ PD-1hi stimulated CD3/CD28 PB vs stimulated PB + blocking antibody 48 hours: 81.92% +/- 5.66 vs 80.94% +/- 6.19; n=5, p=0.695.
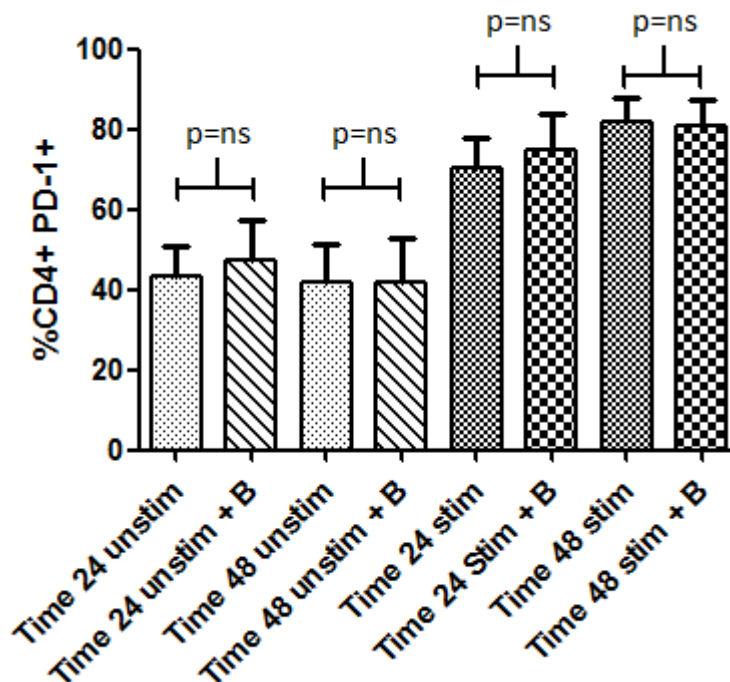
Figure 6-23 Blocking PD-1 signal transduction does not alter PD-1 expression in CD4+ T-cells CLL autologous PB T-cells were stimulated as in Figure 6-1. Anti-human PD-1 was used to block PD-1 as described in Figure 6-18. Cultures were set up with (+B) and without the blocking antibody. Levels of PD-1 were measured on CD4+ T-cells at time 0 (Time 0), 24 hours (Time 24) and 48 hours (Time 48), with CD3/CD28 beads (stim) and without (unstim) by flow cytometry. The percentage of CD4+ T-cells that expressed PD-1 was unaffected by the addition of the blocking antibody at every time point.

Again the same was true for CD8+ T-cells expressing PD-1. See Figure 6-24. CD8+ PD-1hi

unstimulated PB vs unstimulated PB + blocking antibody 24 hours: 55.65% +/- 5.53 vs 51.63%

+/- 7.94; n=6, p=0.869. CD8+ PD-1hi unstimulated PB vs unstimulated PB + blocking antibody

48 hours: 56.04% +/- 8.06 vs 57.54% +/- 13.42; n=5, p=0.515. CD8+ PD-1hi stimulated

CD3/CD28 PB vs stimulated PB + blocking antibody 24 hours: 71.47% +/- 4.59 vs 67.38% +/-

6.14; n=5, p=0.593. CD8+ PD-1hi stimulated CD3/CD28 PB vs stimulated PB + blocking

antibody 48 hours: 88.80% +/- 5.49 vs 92.76% +/- 2.76; n=5, p=0.730.
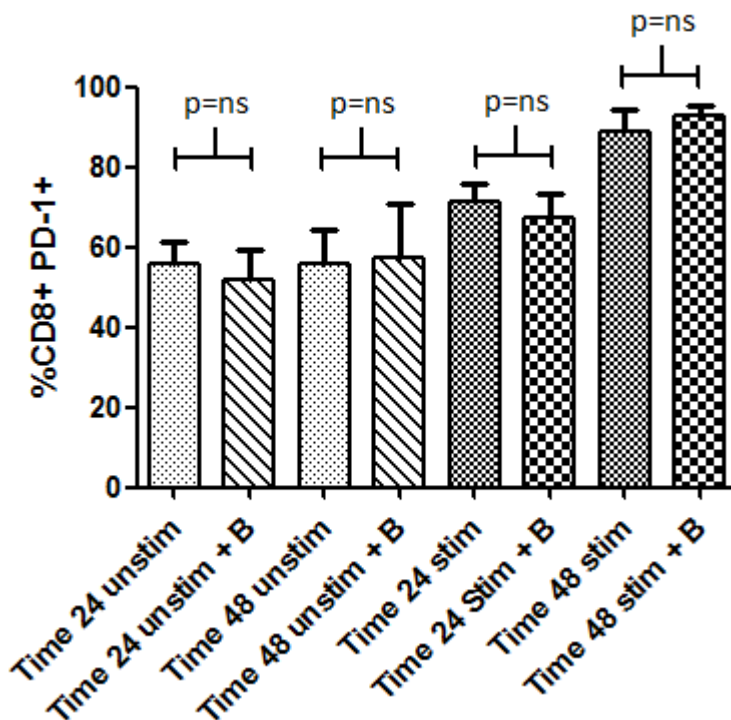
Figure 6-24 Blocking PD-1 signal transduction does not alter PD-1 expression on CD8+ T-cells
CLL autologous PB T-cells were stimulated as in Figure 6-1. Anti-human PD-1 was used to block PD-1 as described in Figure 6-18. Cultures were set up with (+B) and without the blocking antibody. Levels of PD-1 were measured on CD8+ T-cells at time 0 (Time 0), 24 hours (Time 24) and 48 hours (Time 48), with CD3/CD28 beads (stim) and without (unstim) by flow cytometry. The percentage of CD8+ T-cells that expressed PD-1 was unaffected by the addition of the blocking antibody at every time point.

Levels of PD-1 on CLL B-cells themselves were also unaffected. See Figure 6-25. CLL PD-1hi unstimulated PB vs unstimulated PB + blocking antibody 24 hours: 72.83% +/- 6.52 vs 77.62% +/- 9.63; n=6, p=0.306. CLL PD-1hi unstimulated PB vs unstimulated PB + blocking antibody 48 hours: 73.62% +/- 6.75 vs 77.78% +/- 8.39; n=5, p=0.659. CLL PD-1hi stimulated CD3/CD28 PB vs stimulated PB + blocking antibody 24 hours:74.37% +/- 6.39 vs 77.16 +/- 8.70; n=5, p=0.627. CLL PD-1hi stimulated CD3/CD28 PB vs stimulated PB + blocking antibody 48 hours: 79.74% +/- 7.72 vs 82.22% +/- 6.22; n=5, p=0.138.
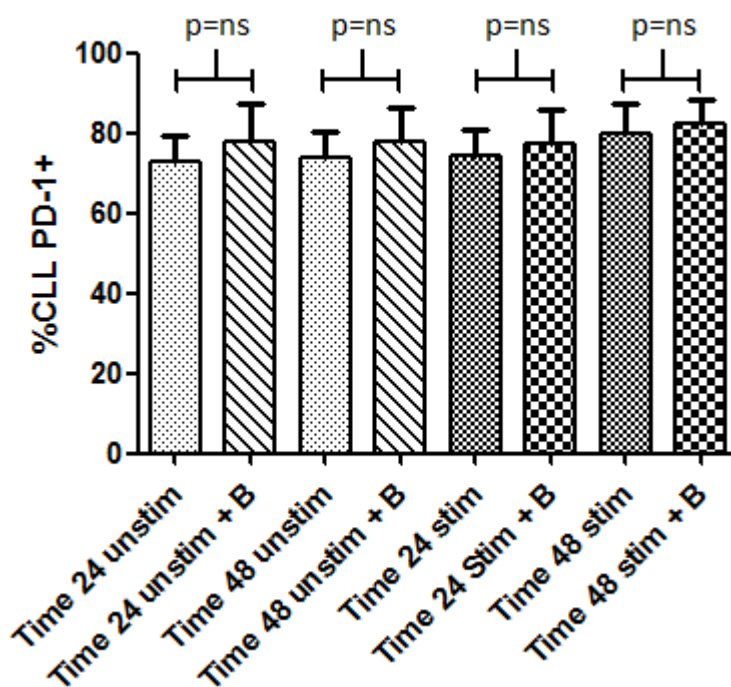

Figure 6-25 Blocking PD-1 signal transduction does not alter PD-1 expression on CLL cells
CLL autologous PB T-cells were stimulated as in Figure 6-1. Anti-human PD-1 was used to block PD-1 as described in Figure 6-18. Cultures were set up with (+B) and without the blocking antibody. Levels of PD-1 were measured on CLL B-cells at time 0 (Time 0), 24 hours (Time 24) and 48 hours (Time 48), with CD3/CD28 beads (stim) and without (unstim) by flow cytometry. The percentage of CLL B-cells that expressed PD-1 was unaffected by the addition of the blocking antibody at every time point.

6.5.16 Blocking PD-1 does not alter PD-L1 expression on PB CLL cells

Blocking PD-1 on CLL PBMCs did not upregulate PD-L1 on resting CLL cells. CLL cells in the presence of stimulated T-cells were also unaffected by PD-1 blockade at any time point. See Figure 6-26. CLL PD-L1+ unstimulated PB vs unstimulated PB + blocking antibody 24 hours: 0.24% +/- 0.11 vs 0.13% +/- 0.13; n=6, p=0.518. CLL PD-L1+ unstimulated PB vs unstimulated PB + blocking antibody 48 hours: 4.00% +/- 1.63 vs 1.56% +/- 0.46; n=5, p=0.542. CLL PD-L1+ stimulated CD3/CD28 PB vs stimulated PB + blocking antibody 24 hours: 4.26% +/- 2.26 vs 0.845 +/- 0.29; n=5, p=1.00. CLL PD-L1+ stimulated CD3/CD28 PB vs stimulated PB + blocking antibody 48 hours: 21.32% +/- 6.243 vs 14.10% +/- 4.78; n=5, p=0.134.
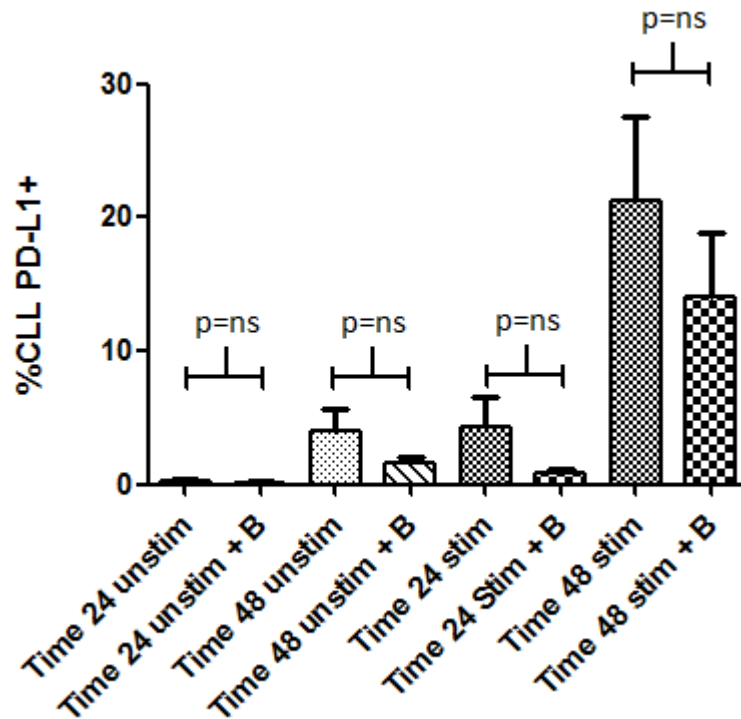
Figure 6-26 Blocking PD-1 signal transduction does not alter PD-L1 expression on CLL cells CLL autologous PB T-cells were stimulated as in Figure 6-1. Anti-human PD-1 was used to block PD-1 as described in Figure 6-18. Cultures were set up with (+B) and without the blocking antibody. Levels of PD-L1 were measured on CLL B-cells at time 0 (Time 0), 24 hours (Time 24) and 48 hours (Time 48), with CD3/CD28 beads (stim) and without (unstim) by flow cytometry. The percentage of CLL B-cells that expressed PD-L1 was unaffected by the addition of the blocking antibody at every time point.

The same was true for the CD4+ and CD8+ T-cells, where blocking PD-1 had no effect on levels of PD-L1 (data not shown).

6.5.17 Intracellular IFN-γ secretion

The PD-1 blocking experiments did not reveal consistent phenotypic changes in this study. We therefore went on to perform a preliminary experiment to look for changes in levels of intracellular IFN-γ in response to T-cell stimulation and PD-1 blockade as described in 6.3.6. This experiment showed an increase in IFN-γ following stimulation and that levels in this patient increased following PD-1 blockade. This work requires ongoing study using cells from a larger cohort of patients and is a fascinating area for future study. See Figure 6-27.
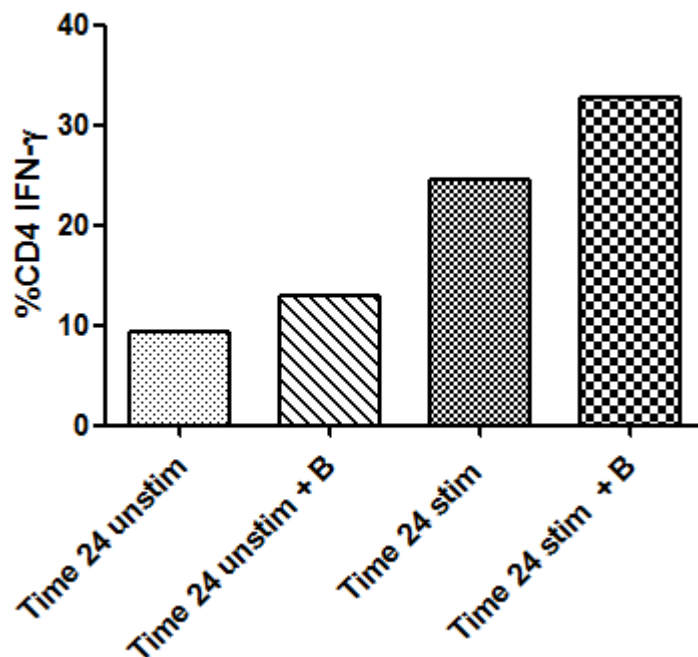
Figure 6-27 IFN-γ increased following stimulation and PD-1 blocking in this experiment
CLL autologous PB T-cells were stimulated as in Figure 6-1. Anti-human PD-1 was used to block PD-1 as described in Figure 6-18. Cultures were set up with (+B) and without the blocking antibody. Levels of IFN-γ were measured by intracellular cytokine staining of CD4+ T-cells at time point 24 hours (Time 24) with (stim) and without (unstim) CD3/CD28 beads as described. The percentage of CD4+ T-cells that positively labelled for intracellular IFN-γ increased following stimulation and PD-1 blocking in this single point of principle experiment.

6.6 Discussion

Having shown, in chapter 3, that LN derived T-cells appear to have undergone antigen induced activation, we have attempted to mimic the situation in the LN using CD3/CD28 bead stimulation of PB CLL T-cells. The results from this chapter have demonstrated that stimulating CLL T-cells from cryopreserved PB mononuclear cells can lead to phenotypic changes more similar to those found in CLL LN samples. To mimic APC dependent activation we used CD3/CD28 beads to stimulate the T-cells. This resulted in upregulation of PD-1 on PB CLL T-cells to levels consistent with those found in the LN. This provides further evidence that the phenotypic changes in CLL LNs may be a consequence of antigenic stimulation. Prolonged T-cell stimulation led to a greater level of T-cell activation than that seen in T-cells directly sampled from the CLL LN. This apparent overstimulation led to situation where the phenotypic markers of activation were increased to higher levels on the CD3/CD28 stimulated CLL PB T-cells than those found on the *in vivo* LN FNA T-cells. The TCR dependant negative T-cell regulator CTLA-4 was also expressed at higher levels on the *in vitro* cultured PB T-cells following CD3/CD28 stimulation than on the fresh LN FNA derived T-cells. This suggests, in this pilot study, that the *in vitro* stimulation method was too strong. Nonetheless these results indicate that further optimisation experiments could result in a model representative of LN derived T-cells. To address this we could have reduced the length of time of CD3/CD28 stimulation, considered CD3 stimulation alone or utilised alternate methods of T-cell stimulation. Stimulation with phytohaemagglutinin (PHA), a mitogenic lectin, could have been used although this is a very non-specific approach and we would predict that all T-cells would be non-specifically stimulated to express PD-1. CD3/CD28 stimulation is more akin to APC stimulation than PHA although it is still not entirely reflective of the *in vivo* situation. An alternate experimental approach could have been to activate T-cells by superantigen stimulation such as with Staphylococcal Enterotoxin B (SEB). Superantigen stimulation would have been of interest in light of the results of the data already presented here in this thesis; the spectratyping and HTS data from chapter 5 has shown that the PD-1hi T-cells in CLL are skewed across many TCRVβ families which could be in response to a superantigen. The ideal experiment would be to attempt to stimulate the T-cells with the candidate antigen, antigens or superantigen involved in the pathogenesis of CLL. Subsequent work in our laboratory has

been focused on stimulating CLL cells with a variety of autoantigens such as whole CLL cells and the cytoskeletal proteins, cofilin and vimentin.

A very significant result of this study was that TCR stimulation of T-cells co-cultured with CLL cells caused significant upregulation of PD-L1 on both the T-cells and the tumour cells in this *in vitro* model. We had not demonstrated PD-L1 expression on CLL cells derived from the fresh LN FNA in chapter 3. Dong et al have previously reported that PD-L1 can be upregulated, as a result of IFN-γ secreted by activated T-cells, on tumour cells, epithelial cells B-cells and the T-cells themselves (Dong, Strome et al. 2002). The upregulation of PD-L1 on the tumour CLL cells potentially has important clinical relevance and could be a target for therapy. In the normal immune response if PD-1 is blocked, T-cells are activated and produce IFN-γ, the IFN-γ in turn upregulates PD-L1 (Dong, Strome et al. 2002). We have shown that CLL T-cells can secrete IFN-γ upon stimulation and levels were increased further by PD-1 blockade. This clearly needs further study but nonetheless this preliminary work suggests that PD-1 blockade does increase IFN-γ secretion in CLL. Brusa et al have subsequently published supportive data whereby they found PD-L1 to be upregulated on CLL cells via interaction with CD3/CD28 stimulated T-cells (Brusa, Serra et al. 2013). They went on to co-culture primary CLL B-cells and stimulated T-cells with an anti-PD-L1 monoclonal antibody, which lead to an increase in CD8+ IFN-γ expression, and conversely co-culture with recombinant soluble PD-L1 decreased IFN-γ levels.

McClanahan et al have recently published a study of PD-L1 blockade in the Eμ-TCL-1 transgenic mouse model of CLL (McClanahan, Hanna et al. 2015). They found that the mice treated with PD-L1 blockade did not develop CLL in a transfer model, the CD8+ cytotoxic effector functions and immune synapse were restored and the T-cell proliferation normalised. Gassner previously published very similar findings in the same mouse model using a PD-1 blocker (Gassner, Zaborsky et al. 2015). This is of interest although, in contrast to our findings in primary human CLL cells, the murine model has constitutive expression of PD-L1. In this model the malignant B-cells in the mouse peritoneal cavity seemed to be unaffected by PD-L1 blockade, suggesting a protective niche and revealing there is a potential for tumour escape.

The major difficulty comes in unpicking the consequences of blocking the PD-1 / PD-L1 axis when all 3 of the main players of the hosts immune system, B-cells, CD4+ and CD8+ T-cells, all express PD-1 and PD-L1 to variable degrees. Butte et al have reported that PD-L1 is also a ligand of CD80, which is present on antigen resting cells, including CLL cells themselves, and that CD80 might bind PD-L1 preferentially over CD28 to downregulate immune responses (Butte, Keir et al. 2007). To add further to the complexity it is now increasingly understood that myeloid cells also express PD-L1 in response to IFN-γ secretion and play a role in T-cell suppression. This was first demonstrated in chronic hepatitis B infection (Chen, Zhang et al. 2007). PD-L1 has more recently been shown to be expressed by myeloid derived suppressor cells (MDSCs) in the PB of CLL patients (Ramsay, Clear et al. 2012, Jitschin, Braun et al. 2014). It is speculated that this suppression of T-cells by MDSCs is a further mechanism by which tumour cells are given the opportunity to proliferate (Curiel, Wei et al. 2003, Wilcox, Feldman et al. 2009). In the Eµ-TCL-1 mouse model McClanahan et al demonstrated that PD-L1 blockade increased the number of splenic macrophages, increased the levels of MHC Class II molecules on dendritic cells and reduced monocytes. Clearly there is a complex crosstalk between the co-stimulatory molecules and negative regulators in CLL, playing their part in disease proliferation, tumour clearance and T-cell immune dysfunction.

In the preliminary work presented here we blocked PD-1 directly using the monoclonal antibody J116. Although the PD-1 blockade did not, in general, alter the *in vitro* surface phenotype of the CD4+ T-cells, CD8+ T-cells or CLL cells, this is an area of great interest where there is clearly a need for further optimisation and study. There was one exception, where CD25 expression was upregulated on pre-stimulated CD8+ T-cells following co-culture with the anti-PD-1 antibody for 24 hours. There could be several explanations for these results. It is feasible that the blockade was not complete, and future experiments would include controls to prove the blocking was effective. If the PD-1 blockade here was partial, this would explain the change in surface expression of CD25 on pre-stimulated CD8+ T-cells and the increase IFN-γ secretion of CD4+ T-cells, following 24 incubation with anti-PD-1. This partial blockade may have been insufficient to fully overcome the negative regulation and therefore did not lead to other phenotypic changes. The amount of PD-1 antibody used is reported to block PD-1 signal transduction in a transfected cell line, and it is feasible that this is not the

same concentration as that is required to block PD-1 in primary patient cells. Future assays would include a titration experiment to identify the optimal concentration. In addition this preliminary work was performed on PBMCs where the T-cell to CLL ratio is not reflective of the LN microenvironment. Taking this work forward, T-cells could be selected and replaced at defined ratios to CLL cells to try and more closely mimic the situation found in CLL lymph nodes.

To date PD-1 blockade in primary CLL cells and *in vivo* is poorly studied. A single phase 1 clinical trial of Pidilizumab (CT-011) an anti-PD-1 monoclonal antibody, has been reported in patients with advanced haematological malignancies including a very small number of CLL patients (Berger, Rotem-Yehudar et al. 2008). Of the 3 CLL patients, 2 were reported to have stable disease. Such is the interest in harnessing the PD-1 / PD-L1 axis in CLL that a clinical trial has been given ethical approval in the United States (NCI-2015-00844). This study uses a combination of Nivolumab and Ibrutinib in relapsed refractory CLL. This trial follows the principle that PD-L1 blockade alone will not be sufficient to eradicate the established tumour and combination of BTK inhibition and PD-1 blockade seems an attractive proposition. This is particularly important in view of the data that BCR signalling may be negatively regulated by PD-1. The concern would be that blockade of PD-1 on the B-cells may in fact upregulate the BCR signalling pathway and give CLL a proliferative advantage. It of course remains to be elucidated what will be the effect of removing the brakes on the CD4+ and CD8+ T-cells, B-cells and MDSCs in CLL and future work should investigate the functional properties and cellular interactions further.

Chapter 7 Final Discussion

The overall aim of this thesis was to characterise the T-cell component of the CLL lymph node microenvironment. The role of the tumour microenvironment in CLL is of interest both to gain a better understanding of the pathobiology of the disease, and to identify potential therapeutic targets. Historically CLL was thought to be a disease of quiescent naïve B-cells with a defect in apoptosis and PB CLL B-cells were shown to be mainly in the G0 or G1 phase of the cell cycle supporting this hypothesis (Dameshek 1967, Andreeff, Darzynkiewicz et al. 1980). However *in vivo* studies using deuterium uptake revealed that CLL has a significant proliferative component with a tumour birth rate up to 1% per day (Messmer, Messmer et al. 2005). In addition, there is now increasing evidence that this proliferation take place within proliferation centres of the LN microenvironment (Swerdlow, Murray et al. 1984, Ben-Ezra, Burke et al. 1989). It is here that CLL tumour cells are in close contact with supportive elements of the tumour microenvironment. It is well documented that when cultured *in vitro* CLL cells die rapidly by apoptosis; but can be rescued by co-culture with a variety of elements of the microenvironment, including activated T-cells (Patten, Buggins et al. 2008, Pascutti, Jak et al. 2013), vascular endothelium (Buggins, Pepper et al. 2010), and stromal cells (Panayiotidis, Jones et al. 1996, Lagneaux, Delforge et al. 1999, Kay, Shanafelt et al. 2007). Our group has previously reported that within LN proliferating CLL cells are in close contact with activated CD4+ T-cells (Patten, Buggins et al. 2008).

Further evidence for the role of T-cells in CLL pathogenesis comes from the murine xenograft model of CLL where engraftment and proliferation of the B-cell clone is dependent upon the presence of activated human CD4+ T-cells (Bagnara, Kaufman et al. 2011). Taken together these findings support a disease model in which quiescent peripheral blood tumour cells transit into and out of secondary lymphoid tissues, where interactions that promote survival and proliferation of the malignant clone take place. Therefore we were especially interested in studying these CD4+ T-cells further.

To date there has been extensive study of the phenotype and functional abnormalities of PB derived T-cells in CLL, in contrast there has been little investigation of the T-cells from the LN microenvironment.

The first challenge of this study was to identify a method to access the T-cells of the LN in an unselected group of CLL patients. Previously published studies have focused primarily on LN tissue derived from FFPE; this approach has several shortcoming which have been extensively reviewed here. In summary patients that have a lymph node biopsy are a highly selected group, the material is fixed making RNA extraction challenging and only limited phenotyping can be undertaken on a slide based assay. We therefore utilised the technique of LN FNA and found this to be a feasible and safe method to obtain cells from the LN, allowing for multiparametric flow cytometry. This ethically approved study had no reported adverse incidents or any safety reports for the duration of the study.

In chapter 3 we present the phenotyping profile of the T-cells derived from the CLL LN tumour microenvironment using multiparameter flow cytometry. We found that up to 40% of the lymphocytes within the LN to be T-cells, compared to just 5% in the PB. Despite the small relative percentage of T-cells in the CLL PB this still represents a massive expansion in the total T-cell count compared to age matched healthy controls; confirming data from previously published series (Mellstedt and Choudhury 2006). We found the majority of the LN derived T-cells were CD4+ Th cells by immunophenotyping, a finding only previously reported on LN biopsy sections (Swerdlow, Murray et al. 1984, Schmid and Isaacson 1994, Bonato, Pittaluga et al. 1998). Interestingly we found the relative proportion of CD4+ T-cells to be much higher in the LN compartment compared to the PB of the same patient. It has been reported by several groups that the PB derived CD4+ T-cells in CLL have a phenotype of chronic activation and a bias towards effector memory phenotype with a relative decrease in naïve T-cells (Motta, Chiarini et al. 2010, Walton, Lydyard et al. 2010, Nunes, Wong et al. 2012). We found an even greater proportion of the LN CD4+ T-cells to be skewed towards an effector memory phenotype than in the PB, suggesting that it is within the LN microenvironment that the T-cells are subjected to antigenic stimulation. This is in contrast to the normal LN in which naïve and central memory T-cells predominate (Khan, Shariff et al. 2002). Additionally we have shown the LN derived T-cells to have higher levels of the costimulatory molecule CD28 and the negative regulators CTLA-4 and PD-1, than the T-cells of the PB. High levels of PD-1 expression on CLL PB T-cells compared to normal controls has now been confirmed by several other groups (Nunes, Wong et al. 2012, Brusa, Serra et al. 2013, Riches, Davies et

al. 2013). We report here for the first time the levels of PD-1 expression are even higher on CD4+ and CD8+ T-cells derived from the LN compared to those from the PB of the same patient taken at the same time. This strongly suggests that it interactions within the LN, most likely involving ongoing interaction with antigen(s), that are responsible for the high levels of PD-1 and other regulatory molecules found in patients with CLL.

In order to confirm these results we utilised the technique of multiparameter immunofluorescence microscopy on FFPE lymph nodes. Conventional immunohistochemistry on FFPE is limited in that only one antigen can be labelled at a time. The number of antigens that can be investigated simultaneously is superior when using fluorescently labelled antibodies, although not currently to the same magnitude as flow cytometry. The technology is rapidly changing and advances in confocal microscopy and availability of new fluorophores is making it increasingly feasible to label FFPE slide samples with more and more antigens. We confirmed by 3 colour immunofluorescence microscopy there was an accumulation within the CLL LN of CD4+ PD-1+ T-cells and that these were in close contact with Ki67+ proliferating tumour cells. This complements a recent study reporting that the PD-1 T-cells within the lymph node are in contact with PD-L1+ CLL cells (Brusa, Serra et al. 2013). In a normal germinal centre B-cell help is specifically offered by Tfh cells so we looked for evidence of a similar germinal centre like reaction in the CLL LN. We found that only a small proportion of the CD4+ PD-1+ T- cells co-expressed ICOS and therefore the majority were not Tfh cells; nonetheless they still accounted for approximately 9% of all CD4 T-cells in a CLL lymph node. The significance of this is not clear. A direct comparison with a normal LN was not available as here the Tfh cells here are very specifically distributed in the germinal centre. Ahearne et al have recently reported an increased number of circulating CD4+ CXCR5+ ICOS+ cells in CLL patients compared to normal controls and that IL-21 and IL-4 promotes CLL proliferation *in vitro*, which are the major cytokines secreted by Tfh cells (Ahearne, Willimott et al. 2013). We confirmed this phenotypic finding and additionally showed no clear differences between the relative proportions of Tfh cells between the PB and the LN FNA. The mechanism for the Tfh accumulation is unknown but may be as a result of the CLL cell secreting favourable cytokines into the tumour microenvironment. Our group has previously reported that CLL cells secrete high levels of IL-6 which is required for Tfh cell development (Buggins, Patten et al. 2008).

Taken together our results provide indirect evidence for antigenic stimulation of the CD4+ T-cells occurring within the lymph node; moreover, it can be hypothesised that the PD-1+ T-cells are specifically driven in response to the tumour. Supporting evidence for antigenic drive comes from studies of the malignant B-cell in CLL. It is now generally accepted that CLL are not naïve but have evidence of previous antigen experience, although the cell of origin is still debated (Seifert, Sellmann et al. 2012). Gene expression profiling of CLL B-cells have shown similarities to that of a normal memory B-cells and that the phenotype is that of an activated antigen experienced B-cell, including surface expression of CD23, CD25, CD69, CD71 and CD27 (Damle, Ghiotto et al. 2002). Further evidence for antigen drive in CLL comes from studies of the BCR. It is becoming increasingly clear that signalling through the BCR is of critical importance in CLL pathogenesis and it is subject to ongoing stimulation (Stevenson, Krysov et al. 2011, Woyach, Johnson et al. 2012). Gene expression profiling has shown that the BCR activation takes place preferentially within the CLL LN microenvironment (Herishanu, Perez-Galan et al. 2011). Non-random IGHV usage and the presence of homologous BCR subsets and stereotypes also suggest a specific antigen drive (Agathangelidis, Darzentas et al. 2012). CLL B-cells show significant skewing in their IGHV gene usage and several studies have shown that, in up to 20% of unrelated CLL patients, there is expression of BCRs with such striking homology to each other, that it would suggest specificity to the same antigen (Messmer, Albesiano et al. 2004, Tobin, Thunberg et al. 2004, Widhopf, Rassenti et al. 2004, Chiorazzi, Rai et al. 2005, Ghia, Stamatopoulos et al. 2005, Stamatopoulos, Belessi et al. 2007). This phenomenon could not possibly occur by random chance and the probability independent clones would carry the same BCR would be in the region of 1 in 10^{12}.

This has led investigators to try and identify putative candidate antigens. BCRs from unmutated CLL cases appear to be polyreactive and some BCRs show affinity for self-antigens including cytoskeletal proteins, non-muscle myosin heavy chain IIA and vimentin, which are expressed by cells undergoing apoptosis (Herve, Xu et al. 2005). Several groups have found affinity of BCRs for a variety of non-self-antigens including bacteria, fungal elements and viruses including CMV (Landgren, Rapkin et al. 2007, Kostareli, Hadzidimitriou et al. 2009, Steininger, Rassenti et al. 2009). CLL patients are immunosuppressed and have an increased incidence of bacterial, fungal and viral infections making this a plausible

hypothesis, although the cause and effect could be debated (Francis, Karanth et al. 2006). An interesting study, using an *in vitro* reconstitution system, suggested that CLL BCRs can possess an intrinsic antigen-independent capacity to elicit a calcium signal, which is a fascinating concept (Duhren-von Minden, Ubelhart et al. 2012).

Although the exact mechanism of BCR activation in CLL remains uncertain, there is good evidence that both antigen dependant and independent mechanisms could operate (Hewamana, Alghazal et al. 2008, Muzio, Apollonio et al. 2008, Gobessi, Laurenti et al. 2009, Zhuang, Hawkins et al. 2010, Le Roy, Deglesne et al. 2012). Our hypothesis is that the T-cell accumulation in CLL is as a result of specific antigenic stimulation. Investigation of the PB TCR repertoire from CLL patients supports this. Compared to age matched normal controls, the overall TCR repertoire in CLL PB shows oligoclonality in both the CD4+ and CD8+ T-cells (Wen, Mellstedt et al. 1990, Farace, Orlanducci et al. 1994, Serrano, Monteiro et al. 1997, Rezvany, Jeddi-Tehrani et al. 1999, Goolsby, Kuchnio et al. 2000). To date, however, no study has investigated the TCR repertoire in CLL LNs.

Having shown phenotypic evidence of T-cell interactions with antigen in CLL LNs, we went on to assess the TCR repertoire of the PB and LN, focusing on the CD4+ PD-1hi compartment; as it was this subset that we found to be co-localised with proliferating tumour cells. At the time this laboratory work was undertaken spectratyping was the gold standard technology for assessing the TCR repertoire. HTS is now becoming increasingly utilised although the technology and necessary bioinformatics techniques are still evolving. One of the major advantages of HTS is that it is quantitative, whereas spectratyping is can only identify gross changes within individual TCRVβ families. The advantage of spectratyping, however, is that it is informative regarding global changes in the repertoire and allows direct comparison of samples. We confirmed the finding of a skewed repertoire in CLL derived PB CD4+ T-cells compared to normal age matched controls. We additionally found that the CD4+ PD-1hi T-cell populations from the PB of normal individuals and CLL patients showed an even more skewed TCR repertoire compared to the PD-1lo counterparts. The CLL PD-1hi T-cells were skewed whether or not they were derived from the PB or LN, however as the frequency of PD-1hi cells is greater in the LN it is highly suggestive of antigen drive within this proliferative compartment.

Skewing of the spectratype was observed across numerous TCRVβ families, suggesting the T-cell response is not a clonal expansion to a single antigen. Data from HTS confirmed a skewed overall TCR repertoire in CLL and that within this repertoire there were a number of high frequency clonotypes. These clonotypes showed low homology between PB and LN but greater frequency of overlap between two LNs taken from the same patient, further supporting a role for a LN localised antigen(s). It is thus clear that CLL T-cells show evidence of oligoclonality and that the repertoire is more restricted in the LN than the PB. What remains unclear, however, is the nature of the putative antigen(s) and whether it could be the same as those involved in BCR activation. The number of changes we identified in the repertoire, however, make it more likely that multiple antigens are involved.

Confounding variables exist when studying the TCR repertoire of the PB and include the observation that there is a marked skewing of the TCR repertoire as a consequence of normal ageing and with previous exposure to common viral infections such as CMV. In a healthy elderly population CMV specific CD8+ T-cells can account for up to half the T-cell repertoire (Khan, Shariff et al. 2002, Savva, Pachnio et al. 2013). However CMV reactivation is rare in untreated CLL individuals suggesting an intact T-cell response to the virus remains, on a background of T-cell dysregulation (te Raa, Pascutti et al. 2014). It is also acknowledged that the T-cell abnormalities in CLL are not just restricted to CMV seropositive individuals and that there is still a vast T-cell expansion of dysregulated T-cells with abnormal phenotype even in CMV seronegative individuals (Riches, Davies et al. 2013, te Raa, Pascutti et al. 2014). The data we have presented here supports the observation that CMV alone cannot explain the T-cell phenotype changes or the TCRVβ repertoire skewing in CLL.

A plausible alternative hypothesis is that the TCR, like the BCR, is responding to self-derived antigens. Several groups have reported a definable population of T-cells in CLL PB with recognition of self-antigens including Rh antigen (Hall, Vickers et al. 2005), immunoglobulin framework (Trojan, Schultze et al. 2000) or CDR3 motifs (Rezvany, Jeddi-Tehrani et al. 2000). Others have demonstrated a small, but definable, population of anti-leukaemic CD8+ T-cells with a measurable specific tumour driven antigen response. CLL derived T-cells have shown *in vitro* responses to tumour idiotypes (Os, Burgler et al. 2013), tumour lysates (Goddard,

Prentice et al. 2003) and intact leukaemia cells themselves (Krackhardt, Harig et al. 2002). These have been the subject of interest especially with the possibility of expanding them by vaccination or indeed if they are "exhausted" PD-1hi cytotoxic T-cells they could be potentially be reinvigorated by PD-1 blockade.

PD-1 and PD-L1 blockade in cancer therapy is a rapidly expanding area of research. This field of study was opened up by the observation that PD-1 was expressed by "exhausted" CD8+ T-cells in response to chronic antigenic stimulation by viruses, such as hepatitis and HIV. Barber et al authored the seminal paper in Nature in 2006, where they blocked PD-L1 in mice and restored the function of the exhausted CD8 T-cells; which in turn cleared the animals of chronic LCMV infection (Barber, Wherry et al. 2006). It is now well described that CD8+ PD-1+ T-cells can be rescued from exhaustion and mount an anti-leukaemic effect in several cancers which has generated huge scientific interest. Anti PD-L1 antibodies have shown to promote tumour regression in melanoma, bladder cancer, renal carcinoma and non-small cell lung cancer (Brahmer 2012, Powles, Eder et al. 2014). Several anti-PD-1 drugs have reached the clinic since the work in this thesis was undertaken (Sharma and Allison 2015). Pembrolizumab was FDA approved in September 2014 for advanced metastatic melanoma (Hamid, Robert et al. 2013, Robert, Ribas et al. 2014). Nivolumab was FDA approved in December 2014 for melanoma, and in March 2015 for lung cancer (Robert, Ribas et al. 2014).

In order to study the functional PD-1 / PD-L1 axis in CLL PB we have presented here a small pilot study aimed at recapitulating the phenotype of the T-cells from the LN microenvironment in an *in vitro* model. Ideally we would have used cells directly obtained from the LN FNA but this was technically not feasible due to the relatively small numbers of T-cells obtained using this technique. Therefore we sought to identify a method to mimic the T-cell phenotype from the LN tumour microenvironment. We activated PB CLL derived T-cells with CD3/CD28 superparamagnetic polymer beads and found PD-1 was upregulated on both CD4+ and CD8+ T-cells to levels akin to those found in the LN. However, other activation and co-stimulation markers were raised to levels far in excess of those found *in vivo,* and therefore to take this work forward the method of stimulation needs to be optimised. One direction our group has

taken is to stimulate PB CLL T-cells with putative antigens involved in CLL pathogenesis including apoptosis derived proteins, cofilin and vimentin, and this work is on-going.

It has been previously reported that resting PB CLL cells express PD-L1, however, we were unable to confirm this (Ramsay, Clear et al. 2012). Interestingly we did find that CLL PB cells upregulate PD-L1 during *in vitro* co-culture with CD3/CD28 stimulated T-cells. A possible explanation for the apparent discrepancy in our results is that in the Ramsay paper there was manipulation of the CLL cells, which induced PD-L1 expression, which only became apparent in our study following co-culture with CD3/CD28 beads. The ability of PD-L1 to be upregulated on CLL cells does suggest the PD-1 / PD-L1 axis could be a potential therapeutic target in CLL. However, the precise effect of inhibiting these interactions remains unclear. The expression of PD-1 and PD-L1 on both T and B lymphocytes, as well as myeloid cells adds to the complexity, and inhibiting these interactions could unmask both pro and anti-tumour effects.

Early phase studies of the anti-PD-1 drug Nivolumab in Hodgkin lymphoma have shown an 87% response rate (Ansell, Lesokhin et al. 2015). However it must be remembered Hodgkin lymphoma is a very specific scenario where the Reed Sternberg cells constitutively express PD-L1 and therefore the mechanism of action may not be directly comparable. In our study we set out to block the PD-1 / PD-L1 axis in primary CLL PBMCs using an anti-PD-1 antibody. This antibody prevents PD-1 downstream signalling and looked for phenotypic changes on both the CD4+ and CD8+ T-cells. We did not demonstrate overall that blocking of the PD-1 changed the phenotype of the CD4+ or CD8+ T-cells, although we have shown that blocking PD-1 can increase IFN-γ expression and this clearly requires extensive future study. This is an important interaction to investigate, as the effects of immune checkpoint inhibition in CLL remain unknown, and as noted above, the critical unanswered question is what happens when T-cells are playing dual roles; with CD4+ T-cells potentially supporting the tumour survival and a proportion of cytotoxic T-cells may be directed against the tumour. Here PD-1 blockade may be a double edged sword and is thus a very exciting avenue for future research. It is also becoming increasingly clear that the crosstalk between the stimulation, co-stimulation and negative immune checkpoint regulators is complex and multidirectional. The molecules have

multiple ligand partners on many cell types whose interaction is yet to be fully elucidated and cannot be studied in isolation.

Although immune checkpoint inhibitors may be incorporated into treatment algorithms of CLL in the future, perhaps a more pertinent question currently is what effects will BCR inhibitors have on the T-cell compartment in CLL, and this is an exciting area for future research. The treatment paradigm for CLL is rapidly changing and drugs that specifically target B-cell signalling are already routinely used in clinical practice. Ibrutinib, a BTK inhibitor, and Idelalisib, a PI3kinase inhibitor, have shown very promising results even in patients with chemotherapy refractory disease. It would be of interest to study what T-cell changes are induced by these drugs, and to identify whether these influence, for example, response to treatment, disease progression and treatment failure.

Drugs that inhibit B-cell signalling may influence the T-cell component of CLL by direct and/or indirect mechanisms. As discussed in this thesis, it is well established that the CLL cells themselves induce changes in T-cells. Therefore quantitative and functional changes in the CLL B-cells, as a result of treatment with BCR inhibitors, would be predicted to lead to changes in T-cell numbers and function. Direct effects of these drugs on T-cells, also requires further evaluation. To date Ibrutinib is the most well studied. BTK is expressed in B-cells and myeloid cells but not in T-cells, however there is mounting evidence that Ibrutinib effects are not limited to targeting BTK. Several studies have shown that Ibrutinib has other off-target effects (Kokhaei, Jadidi-Niaragh et al. 2016). Dubovsky et al found that Ibrutinib inhibits IL-2 inducible tyrosine kinase (ITK) in T-cells (Dubovsky, Beckwith et al. 2013). This inhibits the proliferation of Th2 T-cells, and conversely Th1 T-cells are rescued by the activation of the resting lymphocyte kinase (RIK) compensatory signalling pathway which is not expressed by Th2 cells. This leads to a selective pressure and a drive towards a Th1 phenotype.

There is now also growing evidence that treatment of CLL patients with Ibrutinib can reverse some of the T-cell defects *in vivo* (Fraietta, Beckwith et al. 2016, Niemann, Herman et al. 2016). Niemann et al report that single agent Ibrutinib treatment significantly reduces the number of T-cells with a specific reduction in the number of Th17 T-cells. Interestingly they also report a reduction in the CD4+ PD-1+ population. *In vitro* murine studies revealed Ibrutinib

directly inhibits Th17 T-cells, confirming the drug's off-target effects. The inducible T-cell changes by Ibrutinib *in vivo* are of interest specifically when considering the emerging therapeutic field of CAR-T cells.

To generate a CAR-T cell, allogeneic or autologous, T-cells are expanded and manipulated to express a chimeric antigen receptor; in this case targeting CD19. All clinical CAR-T cell studies reported to date utilise T-cells from an autologous source. In CLL there is a discernible disadvantage of using autologous T-cells to manufacture a CAR-T product, as using dysfunctional exhausted T-cells with a reduced ability to proliferate *in vitro* would potentially render the CAR-T product suboptimal. Evidence to support this comes from the clinical trial data which show inferior results of autologous CD19 CAR-T trials in CLL compared to acute lymphoblastic leukaemia (ALL) (Brentjens, Riviere et al. 2011, Kochenderfer, Dudley et al. 2012, Davila, Riviere et al. 2014, Porter, Hwang et al. 2015). However, if Ibrutinib could overcome the T-cell dysfunction then this might enhance the ability to generate autologous CAR-T cells and their resultant efficacy may be increased. Fraietta et al have very recently reported that prior treatment of CLL patients with Ibrutinib did in fact enable the manufacture of a CD19 directed CAR-T product with superior efficacy (Fraietta, Beckwith et al. 2016). They showed that treatment of CLL patients with Ibrutinib for more than 5 months restored T-cell function to that of healthy controls *ex vivo*. This included a reduction in levels of PD-1 expression on CD8 T-cells. In 3 patients treated with prolonged Ibrutinib therapy they showed superior T-cell proliferation *ex vivo* and they were able to generate CAR-T cells with enhanced proliferation and engraftment in a xenograft model. They found that CD8+ T-cells with the lowest baseline expression of PD-1 were most able to expand and generate a successful CAR-T product. These results suggest that future therapeutics combining BCR inhibition and immune signalling blockade will be of significant interest.

It can be readily appreciated therefore that there are many potential avenues for future research in CLL. The ultimate aim would be to prevent individuals with MBL and early stage CLL progressing to advanced stage CLL and removing the need for therapy at all. It is clear that gaining a detailed understanding of the pathobiology of MBL and CLL and its complex interactions within the tumour microenvironment will play an important role in achieving that

aim. We need an understanding of these interactions to reveal under what circumstances a B-cell clone is allowed to expand, acquire deleterious genetic abnormalities and progress to an uncontrolled malignant proliferation. Then strategies could potentially be employed to prevent individuals from developing symptomatic CLL. Until such a time we need to continue research into drug therapeutics. Targeted therapies such as monoclonal antibodies, BCR inhibition, and immune checkpoint blockade all give promise for a chemotherapy free future for CLL patients. A specific understanding of the effects of these therapeutics, and a knowledge of how they disrupt the complex interactions in the tumour microenvironment, whether alone or in combination, is a research area of immediate need. It is imperative, therefore, that clinical trials utilising these agents incorporate laboratory research at every step and that clinicians and scientists work together to undertake truly translational research.

Taken together, understanding the CLL microenvironment is a challenge. The immune system is host, invader, defender, friend and foe. The lymph node is the niche in which all the players live in a complex milieu. We have demonstrated here some key new aspects in the understanding of CLL pathogenesis and importantly present data that supports the hypothesis that T-cell accumulation in CLL LNs is as a result of a yet unknown specific antigenic stimulation. It is hoped that this work, and that that follows on from it, will contribute further to the understanding of the pathobiology of CLL and ultimately benefit CLL patients.

References

Ademokun, A., Y. C. Wu, V. Martin, R. Mitra, U. Sack, H. Baxendale, D. Kipling and D. K. Dunn-Walters (2011). "Vaccination-induced changes in human B-cell repertoire and pneumococcal IgM and IgA antibody at different ages." Aging Cell **10**(6): 922-930.

Agata, Y., A. Kawasaki, H. Nishimura, Y. Ishida, T. Tsubata, H. Yagita and T. Honjo (1996). "Expression of the PD-1 antigen on the surface of stimulated mouse T and B lymphocytes." Int Immunol **8**(5): 765-772.

Agathangelidis, A., N. Darzentas, A. Hadzidimitriou, X. Brochet, F. Murray, X. J. Yan, Z. Davis, E. J. van Gastel-Mol, C. Tresoldi, C. C. Chu, N. Cahill, V. Giudicelli, B. Tichy, L. B. Pedersen, L. Foroni, L. Bonello, A. Janus, K. Smedby, A. Anagnostopoulos, H. Merle-Beral, N. Laoutaris, G. Juliusson, P. F. di Celle, S. Pospisilova, J. Jurlander, C. Geisler, A. Tsaftaris, M. P. Lefranc, A. W. Langerak, D. G. Oscier, N. Chiorazzi, C. Belessi, F. Davi, R. Rosenquist, P. Ghia and K. Stamatopoulos (2012). "Stereotyped B-cell receptors in one-third of chronic lymphocytic leukemia: a molecular classification with implications for targeted therapies." Blood **119**(19): 4467-4475.

Ahearne, M. J., S. Willimott, L. Pinon, D. B. Kennedy, F. Miall, M. J. Dyer and S. D. Wagner (2013). "Enhancement of CD154/IL4 proliferation by the T follicular helper (Tfh) cytokine, IL21 and increased numbers of circulating cells resembling Tfh cells in chronic lymphocytic leukaemia." Br J Haematol **162**(3): 360-370.

Akbar, A. N. (2010). "The silent war against CMV in CLL." Blood **116**(16): 2869-2870.

Akiba, H., K. Takeda, Y. Kojima, Y. Usui, N. Harada, T. Yamazaki, J. Ma, K. Tezuka, H. Yagita and K. Okumura (2005). "The role of ICOS in the CXCR5+ follicular B helper T cell maintenance in vivo." J Immunol **175**(4): 2340-2348.

Alegre, M. L., K. A. Frauwirth and C. B. Thompson (2001). "T-cell regulation by CD28 and CTLA-4." Nat Rev Immunol **1**(3): 220-228.

Andreeff, M., Z. Darzynkiewicz, T. K. Sharpless, B. D. Clarkson and M. R. Melamed (1980). "Discrimination of human leukemia subtypes by flow cytometric analysis of cellular DNA and RNA." Blood **55**(2): 282-293.

Anichini, A., A. Scarito, A. Molla, G. Parmiani and R. Mortarini (2003). "Differentiation of CD8+ T cells from tumor-invaded and tumor-free lymph nodes of melanoma patients: role of common gamma-chain cytokines." J Immunol **171**(4): 2134-2141.

Ansari-Lari, M. A., S. N. Jones, K. M. Timms and R. A. Gibbs (1996). "Improved ligation-anchored PCR strategy for identification of 5' ends of transcripts." Biotechniques **21**(1): 34-36, 38.

Ansell, S. M., A. M. Lesokhin, I. Borrello, A. Halwani, E. C. Scott, M. Gutierrez, S. J. Schuster, M. M. Millenson, D. Cattry, G. J. Freeman, S. J. Rodig, B. Chapuy, A. H. Ligon, L. Zhu, J. F. Grosso, S. Y. Kim, J. M. Timmerman, M. A. Shipp and P. Armand (2015). "PD-1 blockade with nivolumab in relapsed or refractory Hodgkin's lymphoma." N Engl J Med **372**(4): 311-319.

Arstila, T. P., A. Casrouge, V. Baron, J. Even, J. Kanellopoulos and P. Kourilsky (1999). "A direct estimate of the human alphabeta T cell receptor diversity." Science **286**(5441): 958-961.

Asplund, S. L., R. W. McKenna, M. S. Howard and S. H. Kroft (2002). "Immunophenotype does not correlate with lymph node histology in chronic lymphocytic leukemia/small lymphocytic lymphoma." Am J Surg Pathol **26**(5): 624-629.

Austen, B., J. E. Powell, A. Alvi, I. Edwards, L. Hooper, J. Starczynski, A. M. Taylor, C. Fegan, P. Moss and T. Stankovic (2005). "Mutations in the ATM gene lead to impaired overall and treatment-free survival that is independent of IGVH mutation status in patients with B-CLL." Blood **106**(9): 3175-3182.

Bagnara, D., M. S. Kaufman, C. Calissano, S. Marsilio, P. E. Patten, R. Simone, P. Chum, X. J. Yan, S. L. Allen, J. E. Kolitz, S. Baskar, C. Rader, H. Mellstedt, H. Rabbani, A. Lee, P. K. Gregersen, K. R. Rai and N. Chiorazzi (2011). "A novel adoptive transfer model of chronic lymphocytic leukemia suggests a key role for T lymphocytes in the disease." Blood **117**(20): 5463-5472.

Baitsch, L., A. Legat, L. Barba, S. A. Fuertes Marraco, J. P. Rivals, P. Baumgaertner, C. Christiansen-Jucht, H. Bouzourene, D. Rimoldi, H. Pircher, N. Rufer, M. Matter, O. Michielin and D. E. Speiser (2012). "Extended co-expression of inhibitory receptors by human CD8 T-cells depending on differentiation, antigen-specificity and anatomical localization." PLoS One **7**(2): e30852.

Bangerter, M., O. Brudler, B. Heinrich and M. Griesshamnuer (2007). "Fine needle aspiration cytology and flow cytometry in the diagnosis and subclassification of non-Hodgkin's lymphoma based on the World Health Organization classification." Acta Cytol **51**(3): 390-398.

Barber, D. L., E. J. Wherry, D. Masopust, B. Zhu, J. P. Allison, A. H. Sharpe, G. J. Freeman and R. Ahmed (2006). "Restoring function in exhausted CD8 T cells during chronic viral infection." Nature **439**(7077): 682-687.

Baum, P. D., V. Venturi and D. A. Price (2012). "Wrestling with the repertoire: the promise and perils of next generation sequencing for antigen receptors." Eur J Immunol **42**(11): 2834-2839.

Baumgarth, N. and M. Roederer (2000). "A practical approach to multicolor flow cytometry for immunophenotyping." J Immunol Methods **243**(1-2): 77-97.

Bechter, O. E., W. Eisterer, G. Pall, W. Hilbe, T. Kuhr and J. Thaler (1998). "Telomere length and telomerase activity predict survival in patients with B cell chronic lymphocytic leukemia." Cancer Res **58**(21): 4918-4922.

Ben-Aissa, H., S. Paulie, B. Gustafsson, L. Hakansson, M. Lagerkvist, H. Gustafson, C. Ahlstrand and P. Perlmann (1988). "Human bladder cancer associated antigens: evaluation of antigenicity in TCC tissues of different grades and in normal urothelium." Anticancer Res **8**(3): 443-449.

Ben-Ezra, J., J. S. Burke, W. G. Swartz, M. D. Brownell, R. K. Brynes, L. R. Hill, B. N. Nathwani, M. M. Oken, B. C. Wolf, R. Woodruff and et al. (1989). "Small lymphocytic lymphoma: a clinicopathologic analysis of 268 cases." Blood **73**(2): 579-587.

Bennett, F., A. Rawstron, M. Plummer, R. de Tute, P. Moreton, A. Jack and P. Hillmen (2007). "B-cell chronic lymphocytic leukaemia cells show specific changes in membrane protein expression during different stages of cell cycle." Br J Haematol **139**(4): 600-604.

Berger, R., R. Rotem-Yehudar, G. Slama, S. Landes, A. Kneller, M. Leiba, M. Koren-Michowitz, A. Shimoni and A. Nagler (2008). "Phase I safety and pharmacokinetic study of CT-011, a humanized antibody interacting with PD-1, in patients with advanced hematologic malignancies." Clin Cancer Res **14**(10): 3044-3051.

Beyer, M., M. Kochanek, K. Darabi, A. Popov, M. Jensen, E. Endl, P. A. Knolle, R. K. Thomas, M. von Bergwelt-Baildon, S. Debey, M. Hallek and J. L. Schultze (2005). "Reduced frequencies and suppressive function of CD4+CD25hi regulatory T cells in patients with chronic lymphocytic leukemia after therapy with fludarabine." Blood **106**(6): 2018-2025.

Bhalla, A. D., J. P. Gudikote, J. Wang, W. K. Chan, Y. F. Chang, O. R. Olivas and M. F. Wilkinson (2009). "Nonsense codons trigger an RNA partitioning shift." J Biol Chem **284**(7): 4062-4072.

Biancotto, A., P. K. Dagur, J. C. Fuchs, A. Wiestner, C. B. Bagwell and J. P. McCoy, Jr. (2012). "Phenotypic complexity of T regulatory subsets in patients with B-chronic lymphocytic leukemia." Mod Pathol **25**(2): 246-259.

Billinton, N. and A. W. Knight (2001). "Seeing the wood through the trees: a review of techniques for distinguishing green fluorescent protein from endogenous autofluorescence." Anal Biochem **291**(2): 175-197.

Binder, M., B. Lechenne, R. Ummanni, C. Scharf, S. Balabanov, M. Trusch, H. Schluter, I. Braren, E. Spillner and M. Trepel (2010). "Stereotypical chronic lymphocytic leukemia B-cell receptors recognize survival promoting antigens on stromal cells." PLoS One **5**(12): e15992.

Binet, J. L., A. Auquier, G. Dighiero, C. Chastang, H. Piguet, J. Goasguen, G. Vaugier, G. Potron, P. Colona, F. Oberling, M. Thomas, G. Tchernia, C. Jacquillat, P. Boivin, C. Lesty, M. T. Duault, M. Monconduit, S. Belabbes and F. Gremy (1981). "A new prognostic classification of chronic lymphocytic leukemia derived from a multivariate survival analysis." Cancer **48**(1): 198-206.

Bogen, B., Z. Dembic and S. Weiss (1993). "Clonal deletion of specific thymocytes by an immunoglobulin idiotype." EMBO J **12**(1): 357-363.

Bogen, B., B. Malissen and W. Haas (1986). "Idiotope-specific T cell clones that recognize syngeneic immunoglobulin fragments in the context of class II molecules." Eur J Immunol **16**(11): 1373-1378.

Bojarska-Junak, A., I. Hus, S. Chocholska, E. Wasik-Szczepanek, M. Sieklucka, A. Dmoszynska and J. Rolinski (2009). "BAFF and APRIL expression in B-cell chronic lymphocytic leukemia: correlation with biological and clinical features." Leuk Res **33**(10): 1319-1327.

Bojarska-Junak, A., I. Hus, E. W. Szczepanek, A. Dmoszynska and J. Rolinski (2008). "Peripheral blood and bone marrow TNF and TNF receptors in early and advanced stages of B-CLL in correlation with ZAP-70 protein and CD38 antigen." Leuk Res **32**(2): 225-233.

Bolotin, D. A., I. Z. Mamedov, O. V. Britanova, I. V. Zvyagin, D. Shagin, S. V. Ustyugova, M. A. Turchaninova, S. Lukyanov, Y. B. Lebedev and D. M. Chudakov (2012). "Next generation sequencing for TCR repertoire profiling: platform-specific features and correction algorithms." Eur J Immunol **42**(11): 3073-3083.

Bomberger, C., M. Singh-Jairam, G. Rodey, A. Guerriero, A. M. Yeager, W. H. Fleming, H. K. Holland and E. K. Waller (1998). "Lymphoid reconstitution after autologous PBSC transplantation with FACS-sorted CD34+ hematopoietic progenitors." Blood **91**(7): 2588-2600.

Bonato, M., S. Pittaluga, A. Tierens, A. Criel, G. Verhoef, I. Wlodarska, L. Vanutysel, L. Michaux, P. Vandekerckhove, H. Van den Berghe and C. De Wolf-Peeters (1998). "Lymph node histology in typical and atypical chronic lymphocytic leukemia." Am J Surg Pathol **22**(1): 49-56.

Bonyhadi, M., M. Frohlich, A. Rasmussen, C. Ferrand, L. Grosmaire, E. Robinet, J. Leis, R. T. Maziarz, P. Tiberghien and R. J. Berenson (2005). "In vitro engagement of CD3 and CD28 corrects T cell defects in chronic lymphocytic leukemia." J Immunol **174**(4): 2366-2375.

Borge, M., P. R. Nannini, J. G. Galletti, P. E. Morande, J. S. Avalos, R. F. Bezares, M. Giordano and R. Gamberale (2010). "CXCL12-induced chemotaxis is impaired in T cells from patients with ZAP-70-negative chronic lymphocytic leukemia." Haematologica **95**(5): 768-775.

Brahmer, J. R. (2012). "PD-1-targeted immunotherapy: recent clinical findings." Clin Adv Hematol Oncol **10**(10): 674-675.

Brentjens, R. J., I. Riviere, J. H. Park, M. L. Davila, X. Wang, J. Stefanski, C. Taylor, R. Yeh, S. Bartido, O. Borquez-Ojeda, M. Olszewska, Y. Bernal, H. Pegram, M. Przybylowski, D. Hollyman, Y. Usachenko, D. Pirraglia, J. Hosey, E. Santos, E. Halton, P. Maslak, D. Scheinberg, J. Jurcic, M. Heaney, G. Heller, M. Frattini and M. Sadelain (2011). "Safety and persistence of adoptively transferred autologous CD19-targeted T cells in patients with relapsed or chemotherapy refractory B-cell leukemias." Blood **118**(18): 4817-4828.

Britt-Compton, B., T. T. Lin, G. Ahmed, V. Weston, R. E. Jones, C. Fegan, D. G. Oscier, T. Stankovic, C. Pepper and D. M. Baird (2012). "Extreme telomere erosion in ATM-mutated and 11q-deleted CLL patients is independent of disease stage." Leukemia **26**(4): 826-830.

Brown, M. J., J. A. Hallam, E. Colucci-Guyon and S. Shaw (2001). "Rigidity of circulating lymphocytes is primarily conferred by vimentin intermediate filaments." J Immunol **166**(11): 6640-6646.

Brusa, D., S. Serra, M. Coscia, D. Rossi, G. D'Arena, L. Laurenti, O. Jaksic, G. Fedele, G. Inghirami, G. Gaidano, F. Malavasi and S. Deaglio (2013). "The PD-1/PD-L1 axis contributes to T-cell dysfunction in chronic lymphocytic leukemia." Haematologica **98**(6): 953-963.

Buggins, A. G., A. Levi, S. Gohil, K. Fishlock, P. E. Patten, Y. Calle, D. Yallop and S. Devereux (2011). "Evidence for a macromolecular complex in poor prognosis CLL that contains CD38, CD49d, CD44 and MMP-9." Br J Haematol **154**(2): 216-222.

Buggins, A. G., P. E. Patten, J. Richards, N. S. Thomas, G. J. Mufti and S. Devereux (2008). "Tumor-derived IL-6 may contribute to the immunological defect in CLL." Leukemia **22**(5): 1084-1087.

Buggins, A. G., C. Pepper, P. E. Patten, S. Hewamana, S. Gohil, J. Moorhead, N. Folarin, D. Yallop, N. S. Thomas, G. J. Mufti, C. Fegan and S. Devereux (2010). "Interaction with vascular endothelium enhances survival in primary chronic lymphocytic leukemia cells via NF-kappaB activation and de novo gene transcription." Cancer Res **70**(19): 7523-7533.

Bulian, P., T. D. Shanafelt, C. Fegan, A. Zucchetto, L. Cro, H. Nuckel, L. Baldini, A. V. Kurtova, A. Ferrajoli, J. A. Burger, G. Gaidano, G. Del Poeta, C. Pepper, D. Rossi and V. Gattei (2014). "CD49d is the strongest flow cytometry-based predictor of overall survival in chronic lymphocytic leukemia." J Clin Oncol **32**(9): 897-904.

Burger, J. A. (2010). "Chemokines and chemokine receptors in chronic lymphocytic leukemia (CLL): from understanding the basics towards therapeutic targeting." Semin Cancer Biol **20**(6): 424-430.

Burger, J. A. (2012). "Targeting the microenvironment in chronic lymphocytic leukemia is changing the therapeutic landscape." Curr Opin Oncol **24**(6): 643-649.

Burger, J. A., M. Burger and T. J. Kipps (1999). "Chronic lymphocytic leukemia B cells express functional CXCR4 chemokine receptors that mediate spontaneous migration beneath bone marrow stromal cells." Blood **94**(11): 3658-3667.

Burger, J. A., M. P. Quiroga, E. Hartmann, A. Burkle, W. G. Wierda, M. J. Keating and A. Rosenwald (2009). "High-level expression of the T-cell chemokines CCL3 and CCL4 by chronic lymphocytic leukemia B cells in nurselike cell cocultures and after BCR stimulation." Blood **113**(13): 3050-3058.

Burger, J. A., N. Tsukada, M. Burger, N. J. Zvaifler, M. Dell'Aquila and T. J. Kipps (2000). "Blood-derived nurse-like cells protect chronic lymphocytic leukemia B cells from spontaneous apoptosis through stromal cell-derived factor-1." Blood **96**(8): 2655-2663.

Burger, M., T. Hartmann, M. Krome, J. Rawluk, H. Tamamura, N. Fujii, T. J. Kipps and J. A. Burger (2005). "Small peptide inhibitors of the CXCR4 chemokine receptor (CD184) antagonize the activation, migration, and antiapoptotic responses of CXCL12 in chronic lymphocytic leukemia B cells." Blood **106**(5): 1824-1830.

Burkle, A., M. Niedermeier, A. Schmitt-Graff, W. G. Wierda, M. J. Keating and J. A. Burger (2007). "Overexpression of the CXCR5 chemokine receptor, and its ligand, CXCL13 in B-cell chronic lymphocytic leukemia." Blood **110**(9): 3316-3325.

Buschle, M., D. Campana, S. R. Carding, C. Richard, A. V. Hoffbrand and M. K. Brenner (1993). "Interferon gamma inhibits apoptotic cell death in B cell chronic lymphocytic leukemia." J Exp Med **177**(1): 213-218.

Butte, M. J., M. E. Keir, T. B. Phamduy, A. H. Sharpe and G. J. Freeman (2007). "Programmed death-1 ligand 1 interacts specifically with the B7-1 costimulatory molecule to inhibit T cell responses." Immunity **27**(1): 111-122.

Caligaris-Cappio, F. (1996). "B-chronic lymphocytic leukemia: a malignancy of anti-self B cells." Blood **87**(7): 2615-2620.

Calin, G. A., C. D. Dumitru, M. Shimizu, R. Bichi, S. Zupo, E. Noch, H. Aldler, S. Rattan, M. Keating, K. Rai, L. Rassenti, T. Kipps, M. Negrini, F. Bullrich and C. M. Croce (2002). "Frequent deletions and down-regulation of micro- RNA genes miR15 and miR16 at 13q14 in chronic lymphocytic leukemia." Proc Natl Acad Sci U S A **99**(24): 15524-15529.

Calissano, C., R. N. Damle, G. Hayes, E. J. Murphy, M. K. Hellerstein, C. Moreno, C. Sison, M. S. Kaufman, J. E. Kolitz, S. L. Allen, K. R. Rai and N. Chiorazzi (2009). "In vivo intraclonal and interclonal kinetic heterogeneity in B-cell chronic lymphocytic leukemia." Blood **114**(23): 4832-4842.

Cantwell, M., T. Hua, J. Pappas and T. J. Kipps (1997). "Acquired CD40-ligand deficiency in chronic lymphocytic leukemia." Nat Med **3**(9): 984-989.

Carlson, C. S., R. O. Emerson, A. M. Sherwood, C. Desmarais, M. W. Chung, J. M. Parsons, M. S. Steen, M. A. LaMadrid-Herrmannsfeldt, D. W. Williamson, R. J. Livingston, D. Wu, B. L. Wood, M. J. Rieder and H. Robins (2013). "Using synthetic templates to design an unbiased multiplex PCR assay." Nat Commun **4**: 2680.

Castle, B. E., K. Kishimoto, C. Stearns, M. L. Brown and M. R. Kehry (1993). "Regulation of expression of the ligand for CD40 on T helper lymphocytes." J Immunol **151**(4): 1777-1788.

Catera, R., G. J. Silverman, K. Hatzi, T. Seiler, S. Didier, L. Zhang, M. Herve, E. Meffre, D. G. Oscier, H. Vlassara, R. H. Scofield, Y. Chen, S. L. Allen, J. Kolitz, K. R. Rai, C. C. Chu and N. Chiorazzi (2008). "Chronic lymphocytic leukemia cells recognize conserved epitopes associated with apoptosis and oxidation." Mol Med **14**(11-12): 665-674.

Catovsky, D., E. Miliani, A. Okos and D. A. Galton (1974). "Clinical significance of T-cells in chronic lymphocytic leukaemia." Lancet **2**(7883): 751-752.

Cerutti, A., E. C. Kim, S. Shah, E. J. Schattner, H. Zan, A. Schaffer and P. Casali (2001). "Dysregulation of CD30+ T cells by leukemia impairs isotype switching in normal B cells." Nat Immunol **2**(2): 150-156.

Cha, Z., Y. Zang, H. Guo, J. R. Rechlic, L. M. Olasnova, H. Gu, X. Tu, H. Song and B. Qian (2013). "Association of peripheral CD4+ CXCR5+ T cells with chronic lymphocytic leukemia." Tumour Biol **34**(6): 3579-3585.

Chaouchi, N., C. Wallon, C. Goujard, G. Tertian, A. Rudent, D. Caput, P. Ferrera, A. Minty, A. Vazquez and J. F. Delfraissy (1996). "Interleukin-13 inhibits interleukin-2-induced proliferation

and protects chronic lymphocytic leukemia B cells from in vitro apoptosis." Blood **87**(3): 1022-1029.

Chaouchi, N., C. Wallon, J. Taieb, M. T. Auffredou, G. Tertian, F. M. Lemoine, J. F. Delfraissy and A. Vazquez (1994). "Interferon-alpha-mediated prevention of in vitro apoptosis of chronic lymphocytic leukemia B cells: role of bcl-2 and c-myc." Clin Immunol Immunopathol **73**(2): 197-204.

Chen, H., A. T. Treweeke, D. C. West, K. J. Till, J. C. Cawley, M. Zuzel and C. H. Toh (2000). "In vitro and in vivo production of vascular endothelial growth factor by chronic lymphocytic leukemia cells." Blood **96**(9): 3181-3187.

Chen, L., L. Huynh, J. Apgar, L. Tang, L. Rassenti, A. Weiss and T. J. Kipps (2008). "ZAP-70 enhances IgM signaling independent of its kinase activity in chronic lymphocytic leukemia." Blood **111**(5): 2685-2692.

Chen, L., Z. Zhang, W. Chen, Z. Zhang, Y. Li, M. Shi, J. Zhang, L. Chen, S. Wang and F. S. Wang (2007). "B7-H1 up-regulation on myeloid dendritic cells significantly suppresses T cell immune function in patients with chronic hepatitis B." J Immunol **178**(10): 6634-6641.

Chidrawar, S., N. Khan, W. Wei, A. McLarnon, N. Smith, L. Nayak and P. Moss (2009). "Cytomegalovirus-seropositivity has a profound influence on the magnitude of major lymphoid subsets within healthy individuals." Clin Exp Immunol **155**(3): 423-432.

Chilosi, M., G. Pizzolo, F. Caligaris-Cappio, A. Ambrosetti, F. Vinante, L. Morittu, F. Bonetti, L. Fiore-Donati and G. Janossy (1985). "Immunohistochemical demonstration of follicular dendritic cells in bone marrow involvement of B-cell chronic lymphocytic leukemia." Cancer **56**(2): 328-332.

Chiorazzi, N. and M. Ferrarini (2003). "B cell chronic lymphocytic leukemia: lessons learned from studies of the B cell antigen receptor." Annu Rev Immunol **21**: 841-894.

Chiorazzi, N. and M. Ferrarini (2011). "Cellular origin(s) of chronic lymphocytic leukemia: cautionary notes and additional considerations and possibilities." Blood **117**(6): 1781-1791.

Chiorazzi, N., S. M. Fu, G. Montazeri, H. G. Kunkel, K. Rai and T. Gee (1979). "T cell helper defect in patients with chronic lymphocytic leukemia." J Immunol **122**(3): 1087-1090.

Chiorazzi, N., K. R. Rai and M. Ferrarini (2005). "Chronic lymphocytic leukemia." N Engl J Med **352**(8): 804-815.

Chomczynski, P. and N. Sacchi (1987). "Single-step method of RNA isolation by acid guanidinium thiocyanate-phenol-chloroform extraction." Anal Biochem **162**(1): 156-159.

Christopoulos, P., D. Pfeifer, K. Bartholome, M. Follo, J. Timmer, P. Fisch and H. Veelken (2011). "Definition and characterization of the systemic T-cell dysregulation in untreated indolent B-cell lymphoma and very early CLL." Blood **117**(14): 3836-3846.

Chu, C. C., R. Catera, L. Zhang, S. Didier, B. M. Agagnina, R. N. Damle, M. S. Kaufman, J. E. Kolitz, S. L. Allen, K. R. Rai and N. Chiorazzi (2010). "Many chronic lymphocytic leukemia antibodies recognize apoptotic cells with exposed nonmuscle myosin heavy chain IIA: implications for patient outcome and cell of origin." Blood **115**(19): 3907-3915.

Ciupe, S. M., B. H. Devlin, M. L. Markert and T. B. Kepler (2013). "Quantification of total T-cell receptor diversity by flow cytometry and spectratyping." BMC Immunol **14**: 35.

Cochet, M., C. Pannetier, A. Regnault, S. Darche, C. Leclerc and P. Kourilsky (1992). "Molecular detection and in vivo analysis of the specific T cell response to a protein antigen." Eur J Immunol **22**(10): 2639-2647.

Coffman, R. L. and M. Cohn (1977). "The class of surface immunoglobulin on virgin and memory B lymphocytes." J Immunol **118**(5): 1806-1815.

Collins, R. J., L. A. Verschuer, B. V. Harmon, R. L. Prentice, J. H. Pope and J. F. Kerr (1989). "Spontaneous programmed death (apoptosis) of B-chronic lymphocytic leukaemia cells following their culture in vitro." Br J Haematol **71**(3): 343-350.

Cordingley, F. T., A. Bianchi, A. V. Hoffbrand, J. E. Reittie, H. E. Heslop, A. Vyakarnam, M. Turner, A. Meager and M. K. Brenner (1988). "Tumour necrosis factor as an autocrine tumour growth factor for chronic B-cell malignancies." Lancet **1**(8592): 969-971.

Crespo, M., N. Villamor, E. Gine, A. Muntanola, D. Colomer, T. Marafioti, M. Jones, M. Camos, E. Campo, E. Montserrat and F. Bosch (2006). "ZAP-70 expression in normal pro/pre B cells, mature B cells, and in B-cell acute lymphoblastic leukemia." Clin Cancer Res **12**(3 Pt 1): 726-734.

Curiel, T. J., S. Wei, H. Dong, X. Alvarez, P. Cheng, P. Mottram, R. Krzysiek, K. L. Knutson, B. Daniel, M. C. Zimmermann, O. David, M. Burow, A. Gordon, N. Dhurandhar, L. Myers, R. Berggren, A. Hemminki, R. D. Alvarez, D. Emilie, D. T. Curiel, L. Chen and W. Zou (2003). "Blockade of B7-H1 improves myeloid dendritic cell-mediated antitumor immunity." Nat Med **9**(5): 562-567.

Curran, M. A., W. Montalvo, H. Yagita and J. P. Allison (2010). "PD-1 and CTLA-4 combination blockade expands infiltrating T cells and reduces regulatory T and myeloid cells within B16 melanoma tumors." Proc Natl Acad Sci U S A **107**(9): 4275-4280.

Cutrona, G., M. Colombo, S. Matis, D. Reverberi, M. Dono, V. Tarantino, N. Chiorazzi and M. Ferrarini (2006). "B lymphocytes in humans express ZAP-70 when activated in vivo." Eur J Immunol **36**(3): 558-569.

D'Arena, G., F. D'Auria, V. Simeon, L. Laurenti, S. Deaglio, G. Mansueto, M. I. Del Principe, T. Statuto, G. Pietrantuono, R. Guariglia, I. Innocenti, M. C. Martorelli, O. Villani, V. De Feo, G. Del Poeta and P. Musto (2012). "A shorter time to the first treatment may be predicted by the absolute number of regulatory T-cells in patients with Rai stage 0 chronic lymphocytic leukemia." Am J Hematol **87**(6): 628-631.

D'Arena, G., L. Laurenti, M. M. Minervini, S. Deaglio, L. Bonello, L. De Martino, L. De Padua, L. Savino, M. Tarnani, V. De Feo and N. Cascavilla (2011). "Regulatory T-cell number is increased in chronic lymphocytic leukemia patients and correlates with progressive disease." Leuk Res **35**(3): 363-368.

D'Arena, G., V. Simeon, F. D'Auria, T. Statuto, P. D. Sanzo, L. D. Martino, A. Marandino, M. Sangiorgio, P. Musto and V. D. Feo (2013). "Regulatory T-cells in chronic lymphocytic leukemia: actor or innocent bystander?" Am J Blood Res **3**(1): 52-57.

Dameshek, W. (1967). "Chronic lymphocytic leukemia--an accumulative disease of immunolgically incompetent lymphocytes." Blood **29**(4): Suppl:566-584.

Damle, R. N., F. M. Batliwalla, F. Ghiotto, A. Valetto, E. Albesiano, C. Sison, S. L. Allen, J. Kolitz, V. P. Vinciguerra, P. Kudalkar, T. Wasil, K. R. Rai, M. Ferrarini, P. K. Gregersen and N. Chiorazzi (2004). "Telomere length and telomerase activity delineate distinctive replicative features of the B-CLL subgroups defined by immunoglobulin V gene mutations." Blood **103**(2): 375-382.

Damle, R. N., F. Ghiotto, A. Valetto, E. Albesiano, F. Fais, X. J. Yan, C. P. Sison, S. L. Allen, J. Kolitz, P. Schulman, V. P. Vinciguerra, P. Budde, J. Frey, K. R. Rai, M. Ferrarini and N. Chiorazzi (2002). "B-cell chronic lymphocytic leukemia cells express a surface membrane phenotype of activated, antigen-experienced B lymphocytes." Blood **99**(11): 4087-4093.

Damle, R. N., T. Wasil, F. Fais, F. Ghiotto, A. Valetto, S. L. Allen, A. Buchbinder, D. Budman, K. Dittmar, J. Kolitz, S. M. Lichtman, P. Schulman, V. P. Vinciguerra, K. R. Rai, M. Ferrarini and N. Chiorazzi (1999). "Ig V gene mutation status and CD38 expression as novel prognostic indicators in chronic lymphocytic leukemia." Blood **94**(6): 1840-1847.

Davila, M. L., I. Riviere, X. Wang, S. Bartido, J. Park, K. Curran, S. S. Chung, J. Stefanski, O. Borquez-Ojeda, M. Olszewska, J. Qu, T. Wasielewska, Q. He, M. Fink, H. Shinglot, M. Youssif, M. Satter, Y. Wang, J. Hosey, H. Quintanilla, E. Halton, Y. Bernal, D. C. Bouhassira, M. E. Arcila, M. Gonen, G. J. Roboz, P. Maslak, D. Douer, M. G. Frattini, S. Giralt, M. Sadelain and R. Brentjens (2014). "Efficacy and toxicity management of 19-28z CAR T cell therapy in B cell acute lymphoblastic leukemia." Sci Transl Med **6**(224): 224ra225.

De Fanis, U., L. Dalla Mora, C. Romano, A. Sellitto, A. Tirelli and G. Lucivero (2002). "Altered constitutive and activation-induced expression of CD95 by B- and T-cells in B-cell chronic lymphocytic leukemia." Haematologica **87**(3): 325-327.

De Silva, N. S. and U. Klein (2015). "Dynamics of B cells in germinal centres." Nat Rev Immunol **15**(3): 137-148.

Deaglio, S., S. Aydin, M. M. Grand, T. Vaisitti, L. Bergui, G. D'Arena, G. Chiorino and F. Malavasi (2010). "CD38/CD31 interactions activate genetic pathways leading to proliferation and migration in chronic lymphocytic leukemia cells." Mol Med **16**(3-4): 87-91.

Deaglio, S., T. Vaisitti, S. Aydin, L. Bergui, G. D'Arena, L. Bonello, P. Omede, M. Scatolini, O. Jaksic, G. Chiorino, D. Efremov and F. Malavasi (2007). "CD38 and ZAP-70 are functionally linked and mark CLL cells with high migratory potential." Blood **110**(12): 4012-4021.

Dearden, C. (2008). "Disease-specific complications of chronic lymphocytic leukemia." Hematology Am Soc Hematol Educ Program: 450-456.

Del Poeta, G., L. Maurillo, A. Venditti, F. Buccisano, A. M. Epiceno, G. Capelli, A. Tamburini, G. Suppo, A. Battaglia, M. I. Del Principe, B. Del Moro, M. Masi and S. Amadori (2001). "Clinical significance of CD38 expression in chronic lymphocytic leukemia." Blood **98**(9): 2633-2639.

Desjardins, P. and D. Conklin (2010). "NanoDrop microvolume quantitation of nucleic acids." J Vis Exp(45).

Desmarais, C. (2012). "High-throughput sequencing of Memory and Naïve T-cell receptor repertoires at the RNA and DNA levels reveals differences in relative expression of expanded TCR clones." J Immunol **188**((Meeting Abstract Supplement)): 178.112.

Deutsch, V., C. Perry and A. Polliack (2009). "Expansion of regulatory T cells in B chronic lymphocytic leukemia: enhanced 'brakes' on host immunity." Leuk Lymphoma **50**(5): 687-688.

Dewald, G. W., S. R. Brockman, S. F. Paternoster, N. D. Bone, J. R. O'Fallon, C. Allmer, C. D. James, D. F. Jelinek, R. C. Tschumper, C. A. Hanson, R. K. Pruthi, T. E. Witzig, T. G. Call and N. E. Kay (2003). "Chromosome anomalies detected by interphase fluorescence in situ hybridization: correlation with significant biological features of B-cell chronic lymphocytic leukaemia." Br J Haematol **121**(2): 287-295.

Dicker, F., S. Schnittger, T. Haferlach, W. Kern and C. Schoch (2006). "Immunostimulatory oligonucleotide-induced metaphase cytogenetics detect chromosomal aberrations in 80% of CLL patients: A study of 132 CLL cases with correlation to FISH, IgVH status, and CD38 expression." Blood **108**(9): 3152-3160.

Dighiero, G., P. Travade, S. Chevret, P. Fenaux, C. Chastang and J. L. Binet (1991). "B-cell chronic lymphocytic leukemia: present status and future directions. French Cooperative Group on CLL." Blood **78**(8): 1901-1914.

Ding, W., G. S. Nowakowski, T. R. Knox, J. C. Boysen, M. L. Maas, S. M. Schwager, W. Wu, L. E. Wellik, A. B. Dietz, A. K. Ghosh, C. R. Secreto, K. L. Medina, T. D. Shanafelt, C. S. Zent, T. G. Call and N. E. Kay (2009). "Bi-directional activation between mesenchymal stem cells and CLL B-cells: implication for CLL disease progression." Br J Haematol **147**(4): 471-483.

Dohner, H., K. Fischer, M. Bentz, K. Hansen, A. Benner, G. Cabot, D. Diehl, R. Schlenk, J. Coy, S. Stilgenbauer and et al. (1995). "p53 gene deletion predicts for poor survival and non-response to therapy with purine analogs in chronic B-cell leukemias." Blood **85**(6): 1580-1589.

Dohner, H., S. Stilgenbauer, A. Benner, E. Leupolt, A. Krober, L. Bullinger, K. Dohner, M. Bentz and P. Lichter (2000). "Genomic aberrations and survival in chronic lymphocytic leukemia." N Engl J Med **343**(26): 1910-1916.

Dong, H., S. E. Strome, D. R. Salomao, H. Tamura, F. Hirano, D. B. Flies, P. C. Roche, J. Lu, G. Zhu, K. Tamada, V. A. Lennon, E. Celis and L. Chen (2002). "Tumor-associated B7-H1 promotes T-cell apoptosis: a potential mechanism of immune evasion." Nat Med **8**(8): 793-800.

Dong, H. Y., N. L. Harris, F. I. Preffer and M. B. Pitman (2001). "Fine-needle aspiration biopsy in the diagnosis and classification of primary and recurrent lymphoma: a retrospective analysis of the utility of cytomorphology and flow cytometry." Mod Pathol **14**(5): 472-481.

Dono, M., V. L. Burgio, M. Colombo, S. Sciacchitano, D. Reverberi, V. Tarantino, G. Cutrona, N. Chiorazzi and M. Ferrarini (2007). "CD5+ B cells with the features of subepithelial B cells found in human tonsils." Eur J Immunol **37**(8): 2138-2147.

Dorfman, D. M., J. A. Brown, A. Shahsafaei and G. J. Freeman (2006). "Programmed death-1 (PD-1) is a marker of germinal center-associated T cells and angioimmunoblastic T-cell lymphoma." Am J Surg Pathol **30**(7): 802-810.

Dubovsky, J. A., K. A. Beckwith, G. Natarajan, J. A. Woyach, S. Jaglowski, Y. Zhong, J. D. Hessler, T. M. Liu, B. Y. Chang, K. M. Larkin, M. R. Stefanovski, D. L. Chappell, F. W. Frissora, L. L. Smith, K. A. Smucker, J. M. Flynn, J. A. Jones, L. A. Andritsos, K. Maddocks, A. M. Lehman, R. Furman, J. Sharman, A. Mishra, M. A. Caligiuri, A. R. Satoskar, J. J. Buggy, N. Muthusamy, A. J. Johnson and J. C. Byrd (2013). "Ibrutinib is an irreversible molecular inhibitor of ITK driving a Th1-selective pressure in T lymphocytes." Blood **122**(15): 2539-2549.

Duhren-von Minden, M., R. Ubelhart, D. Schneider, T. Wossning, M. P. Bach, M. Buchner, D. Hofmann, E. Surova, M. Follo, F. Kohler, H. Wardemann, K. Zirlik, H. Veelken and H. Jumaa (2012). "Chronic lymphocytic leukaemia is driven by antigen-independent cell-autonomous signalling." Nature **489**(7415): 309-312.

Durig, J., M. Naschar, U. Schmucker, K. Renzing-Kohler, T. Holter, A. Huttmann and U. Duhrsen (2002). "CD38 expression is an important prognostic marker in chronic lymphocytic leukaemia." Leukemia **16**(1): 30-35.

Endo, T., M. Nishio, T. Enzler, H. B. Cottam, T. Fukuda, D. F. James, M. Karin and T. J. Kipps (2007). "BAFF and APRIL support chronic lymphocytic leukemia B-cell survival through activation of the canonical NF-kappaB pathway." Blood **109**(2): 703-710.

Eto, D., C. Lao, D. DiToro, B. Barnett, T. C. Escobar, R. Kageyama, I. Yusuf and S. Crotty (2011). "IL-21 and IL-6 are critical for different aspects of B cell immunity and redundantly induce optimal follicular helper CD4 T cell (Tfh) differentiation." PLoS One **6**(3): e17739.

Eyerman, M. C., X. Zhang and L. J. Wysocki (1996). "T cell recognition and tolerance of antibody diversity." J Immunol **157**(3): 1037-1046.

Fabbri, G., S. Rasi, D. Rossi, V. Trifonov, H. Khiabanian, J. Ma, A. Grunn, M. Fangazio, D. Capello, S. Monti, S. Cresta, E. Gargiulo, F. Forconi, A. Guarini, L. Arcaini, M. Paulli, L. Laurenti, L. M. Larocca, R. Marasca, V. Gattei, D. Oscier, F. Bertoni, C. G. Mullighan, R. Foa,

L. Pasqualucci, R. Rabadan, R. Dalla-Favera and G. Gaidano (2011). "Analysis of the chronic lymphocytic leukemia coding genome: role of NOTCH1 mutational activation." J Exp Med **208**(7): 1389-1401.

Faint, J. M., D. Pilling, A. N. Akbar, G. D. Kitas, P. A. Bacon and M. Salmon (1999). "Quantitative flow cytometry for the analysis of T cell receptor Vbeta chain expression." J Immunol Methods **225**(1-2): 53-60.

Fais, F., F. Ghiotto, S. Hashimoto, B. Sellars, A. Valetto, S. L. Allen, P. Schulman, V. P. Vinciguerra, K. Rai, L. Z. Rassenti, T. J. Kipps, G. Dighiero, H. W. Schroeder, Jr., M. Ferrarini and N. Chiorazzi (1998). "Chronic lymphocytic leukemia B cells express restricted sets of mutated and unmutated antigen receptors." J Clin Invest **102**(8): 1515-1525.

Farace, F., F. Orlanducci, P. Y. Dietrich, C. Gaudin, E. Angevin, M. H. Courtier, C. Bayle, T. Hercend and F. Triebel (1994). "T cell repertoire in patients with B chronic lymphocytic leukemia. Evidence for multiple in vivo T cell clonal expansions." J Immunol **153**(9): 4281-4290.

Ferrajoli, A., T. Manshouri, Z. Estrov, M. J. Keating, S. O'Brien, S. Lerner, M. Beran, H. M. Kantarjian, E. J. Freireich and M. Albitar (2001). "High levels of vascular endothelial growth factor receptor-2 correlate with shortened survival in chronic lymphocytic leukemia." Clin Cancer Res **7**(4): 795-799.

Ferrand, C., E. Robinet, E. Contassot, J. M. Certoux, A. Lim, P. Herve and P. Tiberghien (2000). "Retrovirus-mediated gene transfer in primary T lymphocytes: influence of the transduction/selection process and of ex vivo expansion on the T cell receptor beta chain hypervariable region repertoire." Hum Gene Ther **11**(8): 1151-1164.

Forconi, F. and P. Moss (2015). "Perturbation of the normal immune system in patients with CLL." Blood **126**(5): 573-581.

Forconi, F., K. N. Potter, I. Wheatley, N. Darzentas, E. Sozzi, K. Stamatopoulos, C. I. Mockridge, G. Packham and F. K. Stevenson (2010). "The normal IGHV1-69-derived B-cell repertoire contains stereotypic patterns characteristic of unmutated CLL." Blood **115**(1): 71-77.

Fraietta, J. A., K. A. Beckwith, P. R. Patel, M. Ruella, Z. Zheng, D. M. Barrett, S. F. Lacey, J. J. Melenhorst, S. E. McGettigan, D. R. Cook, C. Zhang, J. Xu, P. Do, J. Hulitt, S. B. Kudchodkar, A. P. Cogdill, S. Gill, D. L. Porter, J. A. Woyach, M. Long, A. J. Johnson, K. Maddocks, N. Muthusamy, B. L. Levine, C. H. June, J. C. Byrd and M. V. Maus (2016). "Ibrutinib enhances chimeric antigen receptor T-cell engraftment and efficacy in leukemia." Blood **127**(9): 1117-1127.

Francia di Celle, P., S. Mariani, L. Riera, A. Stacchini, G. Reato and R. Foa (1996). "Interleukin-8 induces the accumulation of B-cell chronic lymphocytic leukemia cells by prolonging survival in an autocrine fashion." Blood **87**(10): 4382-4389.

Francis, S., M. Karanth, G. Pratt, J. Starczynski, L. Hooper, C. Fegan, C. Pepper, D. Valcarcel, D. W. Milligan and J. Delgado (2006). "The effect of immunoglobulin VH gene mutation status and other prognostic factors on the incidence of major infections in patients with chronic lymphocytic leukemia." Cancer **107**(5): 1023-1033.

Freeman, G. J., A. J. Long, Y. Iwai, K. Bourque, T. Chernova, H. Nishimura, L. J. Fitz, N. Malenkovich, T. Okazaki, M. C. Byrne, H. F. Horton, L. Fouser, L. Carter, V. Ling, M. R. Bowman, B. M. Carreno, M. Collins, C. R. Wood and T. Honjo (2000). "Engagement of the PD-1 immunoinhibitory receptor by a novel B7 family member leads to negative regulation of lymphocyte activation." J Exp Med **192**(7): 1027-1034.

Fridman, W. H., F. Pages, C. Sautes-Fridman and J. Galon (2012). "The immune contexture in human tumours: impact on clinical outcome." Nat Rev Cancer **12**(4): 298-306.

Frydecka, I., A. Kosmaczewska, D. Bocko, L. Ciszak, D. Wolowiec, K. Kuliczkowski and I. Kochanowska (2004). "Alterations of the expression of T-cell-related costimulatory CD28 and downregulatory CD152 (CTLA-4) molecules in patients with B-cell chronic lymphocytic leukaemia." Br J Cancer **90**(10): 2042-2048.

Fukuda, T., L. Chen, T. Endo, L. Tang, D. Lu, J. E. Castro, G. F. Widhopf, 2nd, L. Z. Rassenti, M. J. Cantwell, C. E. Prussak, D. A. Carson and T. J. Kipps (2008). "Antisera induced by infusions of autologous Ad-CD154-leukemia B cells identify ROR1 as an oncofetal antigen and receptor for Wnt5a." Proc Natl Acad Sci U S A **105**(8): 3047-3052.

Gallagher, S. R. and P. R. Desjardins (2006). "Quantitation of DNA and RNA with absorption and fluorescence spectroscopy." Curr Protoc Mol Biol **Appendix 3**: Appendix 3D.

Gassner, F. J., N. Zaborsky, K. Catakovic, S. Rebhandl, M. Huemer, A. Egle, T. N. Hartmann, R. Greil and R. Geisberger (2015). "Chronic lymphocytic leukaemia induces an exhausted T cell phenotype in the TCL1 transgenic mouse model." Br J Haematol.

Gassner, F. J., N. Zaborsky, K. Catakovic, S. Rebhandl, M. Huemer, A. Egle, T. N. Hartmann, R. Greil and R. Geisberger (2015). "Chronic lymphocytic leukaemia induces an exhausted T cell phenotype in the TCL1 transgenic mouse model." Br J Haematol **170**(4): 515-522.

Gattei, V., P. Bulian, M. I. Del Principe, A. Zucchetto, L. Maurillo, F. Buccisano, R. Bomben, M. Dal-Bo, F. Luciano, F. M. Rossi, M. Degan, S. Amadori and G. Del Poeta (2008). "Relevance of CD49d protein expression as overall survival and progressive disease prognosticator in chronic lymphocytic leukemia." Blood **111**(2): 865-873.

Ghia, P. and F. Caligaris-Cappio (2000). "The indispensable role of microenvironment in the natural history of low-grade B-cell neoplasms." Adv Cancer Res **79**: 157-173.

Ghia, P., P. Circosta, C. Scielzo, A. Vallario, A. Camporeale, L. Granziero and F. Caligaris-Cappio (2005). "Differential effects on CLL cell survival exerted by different microenvironmental elements." Curr Top Microbiol Immunol **294**: 135-145.

Ghia, P., G. Guida, S. Stella, D. Gottardi, M. Geuna, G. Strola, C. Scielzo and F. Caligaris-Cappio (2003). "The pattern of CD38 expression defines a distinct subset of chronic lymphocytic leukemia (CLL) patients at risk of disease progression." Blood **101**(4): 1262-1269.

Ghia, P., K. Stamatopoulos, C. Belessi, C. Moreno, S. Stella, G. Guida, A. Michel, M. Crespo, N. Laoutaris, E. Montserrat, A. Anagnostopoulos, G. Dighiero, A. Fassas, F. Caligaris-Cappio and F. Davi (2005). "Geographic patterns and pathogenetic implications of IGHV gene usage in chronic lymphocytic leukemia: the lesson of the IGHV3-21 gene." Blood **105**(4): 1678-1685.

Ghia, P., G. Strola, L. Granziero, M. Geuna, G. Guida, F. Sallusto, N. Ruffing, L. Montagna, P. Piccoli, M. Chilosi and F. Caligaris-Cappio (2002). "Chronic lymphocytic leukemia B cells are endowed with the capacity to attract CD4+, CD40L+ T cells by producing CCL22." Eur J Immunol **32**(5): 1403-1413.

Ghia, P. C. P. S. C. V. A. C. A. G. L. and F. Caligaris-Cappio (2005). "Differential effects on CLL cell survival exerted by different microenvironmental elements." Current Topics in Microbiology and Immunology **294**: 135-145.

Giannopoulos, K., M. Schmitt, M. Kowal, P. Wlasiuk, A. Bojarska-Junak, J. Chen, J. Rolinski and A. Dmoszynska (2008). "Characterization of regulatory T cells in patients with B-cell chronic lymphocytic leukemia." Oncol Rep **20**(3): 677-682.

Giannopoulos, K., M. Schmitt, P. Wlasiuk, J. Chen, A. Bojarska-Junak, M. Kowal, J. Rolinski and A. Dmoszynska (2008). "The high frequency of T regulatory cells in patients with B-cell chronic lymphocytic leukemia is diminished through treatment with thalidomide." Leukemia **22**(1): 222-224.

Gilling, C. E., A. K. Mittal, N. K. Chaturvedi, J. Iqbal, P. Aoun, P. J. Bierman, R. G. Bociek, D. D. Weisenburger and S. S. Joshi (2012). "Lymph node-induced immune tolerance in chronic lymphocytic leukaemia: a role for caveolin-1." Br J Haematol **158**(2): 216-231.

Gitelson, E., C. Hammond, J. Mena, M. Lorenzo, R. Buckstein, N. L. Berinstein, K. Imrie and D. E. Spaner (2003). "Chronic lymphocytic leukemia-reactive T cells during disease progression and after autologous tumor cell vaccines." Clin Cancer Res **9**(5): 1656-1665.

Glassman, A. B. and K. J. Hayes (2005). "The value of fluorescence in situ hybridization in the diagnosis and prognosis of chronic lymphocytic leukemia." Cancer Genet Cytogenet **158**(1): 88-91.

Gobessi, S., L. Laurenti, P. G. Longo, L. Carsetti, V. Berno, S. Sica, G. Leone and D. G. Efremov (2009). "Inhibition of constitutive and BCR-induced Syk activation downregulates Mcl-1 and induces apoptosis in chronic lymphocytic leukemia B cells." Leukemia **23**(4): 686-697.

Goddard, R., A. Prentice, A. Copplestone and E. Kaminski (2003). "A study of the proteins responsible for stimulating B-CLL-specific T-cell responses by autologous dendritic cells pulsed with tumour cell lysate." Hematol J **4**(4): 271-276.

Goddard, R. V., A. G. Prentice, J. A. Copplestone and E. R. Kaminski (2001). "Generation in vitro of B-cell chronic lymphocytic leukaemia-proliferative and specific HLA class-II-restricted cytotoxic T-cell responses using autologous dendritic cells pulsed with tumour cell lysate." Clin Exp Immunol **126**(1): 16-28.

Golab, K., D. Leveson-Gower, X. J. Wang, J. Grzanka, N. Marek-Trzonkowska, A. Krzystyniak, J. M. Millis, P. Trzonkowski and P. Witkowski (2013). "Challenges in cryopreservation of regulatory T cells (Tregs) for clinical therapeutic applications." Int Immunopharmacol **16**(3): 371-375.

Goldin, L. R., M. Bjorkholm, S. Y. Kristinsson, I. Turesson and O. Landgren (2009). "Elevated risk of chronic lymphocytic leukemia and other indolent non-Hodgkin's lymphomas among relatives of patients with chronic lymphocytic leukemia." Haematologica **94**(5): 647-653.

Goldin, L. R., O. Landgren, G. E. Marti and N. E. Caporaso (2010). "Familial Aspects of Chronic Lymphocytic Leukemia, Monoclonal B-Cell Lymphocytosis (MBL), and Related Lymphomas." European J Clin Med Oncol **2**(1): 119-126.

Goldin, L. R., M. Sgambati, G. E. Marti, L. Fontaine, N. Ishibe and N. Caporaso (1999). "Anticipation in familial chronic lymphocytic leukemia." Am J Hum Genet **65**(1): 265-269.

Gong, J. Z., D. C. Williams, Jr., K. Liu and C. Jones (2002). "Fine-needle aspiration in non-Hodgkin lymphoma: evaluation of cell size by cytomorphology and flow cytometry." Am J Clin Pathol **117**(6): 880-888.

Gonzalez-Rodriguez, A. P., J. Contesti, L. Huergo-Zapico, A. Lopez-Soto, A. Fernandez-Guizan, A. Acebes-Huerta, A. J. Gonzalez-Huerta, E. Gonzalez, C. Fernandez-Alvarez and S. Gonzalez (2010). "Prognostic significance of CD8 and CD4 T cells in chronic lymphocytic leukemia." Leuk Lymphoma **51**(10): 1829-1836.

Goolsby, C. L., M. Kuchnio, W. G. Finn and L. Peterson (2000). "Expansions of clonal and oligoclonal T cells in B-cell chronic lymphocytic leukemia are primarily restricted to the CD3(+)CD8(+) T-cell population." Cytometry **42**(3): 188-195.

Gorgun, G., T. A. Holderried, D. Zahrieh, D. Neuberg and J. G. Gribben (2005). "Chronic lymphocytic leukemia cells induce changes in gene expression of CD4 and CD8 T cells." J Clin Invest **115**(7): 1797-1805.

Grabowski, P., M. Hultdin, K. Karlsson, G. Tobin, A. Aleskog, U. Thunberg, A. Laurell, C. Sundstrom, R. Rosenquist and G. Roos (2005). "Telomere length as a prognostic parameter in chronic lymphocytic leukemia with special reference to VH gene mutation status." Blood 105(12): 4807-4812.

Granziero, L., P. Ghia, P. Circosta, D. Gottardi, G. Strola, M. Geuna, L. Montagna, P. Piccoli, M. Chilosi and F. Caligaris-Cappio (2001). "Survivin is expressed on CD40 stimulation and interfaces proliferation and apoptosis in B-cell chronic lymphocytic leukemia." Blood 97(9): 2777-2783.

Greil, R., C. Gattringer, W. Knapp and H. Huber (1986). "Growth fraction of tumour cells and infiltration density with natural killer-like (HNK1+) cells in non-Hodgkin lymphomas." Br J Haematol 62(2): 293-300.

Gros, A., P. F. Robbins, X. Yao, Y. F. Li, S. Turcotte, E. Tran, J. R. Wunderlich, A. Mixon, S. Farid, M. E. Dudley, K. Hanada, J. R. Almeida, S. Darko, D. C. Douek, J. C. Yang and S. A. Rosenberg (2014). "PD-1 identifies the patient-specific CD8(+) tumor-reactive repertoire infiltrating human tumors." J Clin Invest 124(5): 2246-2259.

Grzywnowicz, M., L. Karabon, A. Karczmarczyk, M. Zajac, K. Skorka, J. Zaleska, P. Wlasiuk, S. Chocholska, W. Tomczak, A. Bojarska-Junak, A. Dmoszynska, I. Frydecka and K. Giannopoulos (2015). "The function of a novel immunophenotype candidate molecule PD-1 in chronic lymphocytic leukemia." Leuk Lymphoma: 1-6.

Grzywnowicz, M., J. Zaleska, D. Mertens, W. Tomczak, P. Wlasiuk, K. Kosior, A. Piechnik, A. Bojarska-Junak, A. Dmoszynska and K. Giannopoulos (2012). "Programmed death-1 and its ligand are novel immunotolerant molecules expressed on leukemic B cells in chronic lymphocytic leukemia." PLoS One 7(4): e35178.

Hall, A. M., M. A. Vickers, E. McLeod and R. N. Barker (2005). "Rh autoantigen presentation to helper T cells in chronic lymphocytic leukemia by malignant B cells." Blood 105(5): 2007-2015.

Hallek, M., L. Wanders, M. Ostwald, R. Busch, R. Senekowitsch, S. Stern, H. D. Schick, I. Kuhn-Hallek and B. Emmerich (1996). "Serum beta(2)-microglobulin and serum thymidine kinase are independent predictors of progression-free survival in chronic lymphocytic leukemia and immunocytoma." Leuk Lymphoma 22(5-6): 439-447.

Hamblin, T. J. (1987). "Chronic lymphocytic leukaemia." Baillieres Clin Haematol 1(2): 449-491.

Hamblin, T. J., Z. Davis, A. Gardiner, D. G. Oscier and F. K. Stevenson (1999). "Unmutated Ig V(H) genes are associated with a more aggressive form of chronic lymphocytic leukemia." Blood 94(6): 1848-1854.

Hamblin, T. J., J. A. Orchard, R. E. Ibbotson, Z. Davis, P. W. Thomas, F. K. Stevenson and D. G. Oscier (2002). "CD38 expression and immunoglobulin variable region mutations are independent prognostic variables in chronic lymphocytic leukemia, but CD38 expression may vary during the course of the disease." Blood 99(3): 1023-1029.

Hamblin, T. J., D. G. Oscier and B. J. Young (1986). "Autoimmunity in chronic lymphocytic leukaemia." J Clin Pathol 39(7): 713-716.

Hamid, O., C. Robert, A. Daud, F. S. Hodi, W. J. Hwu, R. Kefford, J. D. Wolchok, P. Hersey, R. W. Joseph, J. S. Weber, R. Dronca, T. C. Gangadhar, A. Patnaik, H. Zarour, A. M. Joshua, K. Gergich, J. Elassaiss-Schaap, A. Algazi, C. Mateus, P. Boasberg, P. C. Tumeh, B. Chmielowski, S. W. Ebbinghaus, X. N. Li, S. P. Kang and A. Ribas (2013). "Safety and tumor responses with lambrolizumab (anti-PD-1) in melanoma." N Engl J Med 369(2): 134-144.

Han, T., M. Barcos, L. Emrich, H. Ozer, R. Gajera, G. A. Gomez, P. A. Reese, J. Minowada, M. L. Bloom, N. Sadamori and et al. (1984). "Bone marrow infiltration patterns and their prognostic significance in chronic lymphocytic leukemia: correlations with clinical, immunologic, phenotypic, and cytogenetic data." J Clin Oncol **2**(6): 562-570.

Hashimoto, S., M. Dono, M. Wakai, S. L. Allen, S. M. Lichtman, P. Schulman, V. P. Vinciguerra, M. Ferrarini, J. Silver and N. Chiorazzi (1995). "Somatic diversification and selection of immunoglobulin heavy and light chain variable region genes in IgG+ CD5+ chronic lymphocytic leukemia B cells." J Exp Med **181**(4): 1507-1517.

Hayat, A., D. O'Brien, P. O'Rourke, S. McGuckin, T. Fitzgerald, E. Conneally, P. V. Browne, S. R. McCann, M. P. Lawler and E. Vandenberghe (2006). "CD38 expression level and pattern of expression remains a reliable and robust marker of progressive disease in chronic lymphocytic leukemia." Leuk Lymphoma **47**(11): 2371-2379.

Haynes, N. M., C. D. Allen, R. Lesley, K. M. Ansel, N. Killeen and J. G. Cyster (2007). "Role of CXCR5 and CCR7 in follicular Th cell positioning and appearance of a programmed cell death gene-1high germinal center-associated subpopulation." J Immunol **179**(8): 5099-5108.

He, M., J. K. Tomfohr, B. H. Devlin, M. Sarzotti, M. L. Markert and T. B. Kepler (2005). "SpA: web-accessible spectratype analysis: data management, statistical analysis and visualization." Bioinformatics **21**(18): 3697-3699.

Hedegaard, J., K. Thorsen, M. K. Lund, A. M. Hein, S. J. Hamilton-Dutoit, S. Vang, I. Nordentoft, K. Birkenkamp-Demtroder, M. Kruhoffer, H. Hager, B. Knudsen, C. L. Andersen, K. D. Sorensen, J. S. Pedersen, T. F. Orntoft and L. Dyrskjot (2014). "Next-generation sequencing of RNA and DNA isolated from paired fresh-frozen and formalin-fixed paraffin-embedded samples of human cancer and normal tissue." PLoS One **9**(5): e98187.

Herishanu, Y., P. Perez-Galan, D. Liu, A. Biancotto, S. Pittaluga, B. Vire, F. Gibellini, N. Njuguna, E. Lee, L. Stennett, N. Raghavachari, P. Liu, J. P. McCoy, M. Raffeld, M. Stetler-Stevenson, C. Yuan, R. Sherry, D. C. Arthur, I. Maric, T. White, G. E. Marti, P. Munson, W. H. Wilson and A. Wiestner (2011). "The lymph node microenvironment promotes B-cell receptor signaling, NF-{kappa}B activation, and tumor proliferation in chronic lymphocytic leukemia." Blood **117**(2): 563-574.

Herishanu, Y., P. Perez-Galan, D. Liu, A. Biancotto, S. Pittaluga, B. Vire, F. Gibellini, N. Njuguna, E. Lee, L. Stennett, N. Raghavachari, P. Liu, J. P. McCoy, M. Raffeld, M. Stetler-Stevenson, C. Yuan, R. Sherry, D. C. Arthur, I. Maric, T. White, G. E. Marti, P. Munson, W. H. Wilson and A. Wiestner (2011). "The lymph node microenvironment promotes B-cell receptor signaling, NF-kappaB activation, and tumor proliferation in chronic lymphocytic leukemia." Blood **117**(2): 563-574.

Herrmann, F., A. Lochner, H. Philippen, B. Jauer and H. Ruhl (1982). "Imbalance of T cell subpopulations in patients with chronic lymphocytic leukaemia of the B cell type." Clin Exp Immunol **49**(1): 157-162.

Herve, M., K. Xu, Y. S. Ng, H. Wardemann, E. Albesiano, B. T. Messmer, N. Chiorazzi and E. Meffre (2005). "Unmutated and mutated chronic lymphocytic leukemias derive from self-reactive B cell precursors despite expressing different antibody reactivity." J Clin Invest **115**(6): 1636-1643.

Hewamana, S., S. Alghazal, T. T. Lin, M. Clement, C. Jenkins, M. L. Guzman, C. T. Jordan, S. Neelakantan, P. A. Crooks, A. K. Burnett, G. Pratt, C. Fegan, C. Rowntree, P. Brennan and C. Pepper (2008). "The NF-kappaB subunit Rel A is associated with in vitro survival and clinical disease progression in chronic lymphocytic leukemia and represents a promising therapeutic target." Blood **111**(9): 4681-4689.

Hodi, F. S., S. J. O'Day, D. F. McDermott, R. W. Weber, J. A. Sosman, J. B. Haanen, R. Gonzalez, C. Robert, D. Schadendorf, J. C. Hassel, W. Akerley, A. J. van den Eertwegh, J.

Lutzky, P. Lorigan, J. M. Vaubel, G. P. Linette, D. Hogg, C. H. Ottensmeier, C. Lebbe, C. Peschel, I. Quirt, J. I. Clark, J. D. Wolchok, J. S. Weber, J. Tian, M. J. Yellin, G. M. Nichol, A. Hoos and W. J. Urba (2010). "Improved survival with ipilimumab in patients with metastatic melanoma." N Engl J Med **363**(8): 711-723.

Hoogeboom, R., K. P. van Kessel, F. Hochstenbach, T. A. Wormhoudt, R. J. Reinten, K. Wagner, A. P. Kater, J. E. Guikema, R. J. Bende and C. J. van Noesel (2013). "A mutated B cell chronic lymphocytic leukemia subset that recognizes and responds to fungi." J Exp Med **210**(1): 59-70.

Huard, B., P. Schneider, D. Mauri, J. Tschopp and L. E. French (2001). "T cell costimulation by the TNF ligand BAFF." J Immunol **167**(11): 6225-6231.

Hulett, H. R., W. A. Bonner, R. G. Sweet and L. A. Herzenberg (1973). "Development and application of a rapid cell sorter." Clin Chem **19**(8): 813-816.

Hultdin, M., R. Rosenquist, U. Thunberg, G. Tobin, K. F. Norrback, A. Johnson, C. Sundstrom and G. Roos (2003). "Association between telomere length and V(H) gene mutation status in chronic lymphocytic leukaemia: clinical and biological implications." Br J Cancer **88**(4): 593-598.

Hurwitz, A. A., T. F. Yu, D. R. Leach and J. P. Allison (1998). "CTLA-4 blockade synergizes with tumor-derived granulocyte-macrophage colony-stimulating factor for treatment of an experimental mammary carcinoma." Proc Natl Acad Sci U S A **95**(17): 10067-10071.

Hus, I., A. Bojarska-Junak, S. Chocholska, W. Tomczak, J. Wos, A. Dmoszynska and J. Rolinski (2013). "Th17/IL-17A might play a protective role in chronic lymphocytic leukemia immunity." PLoS One **8**(11): e78091.

Hutchins, D. and C. M. Steel (1994). "Regulation of ICAM-1 (CD54) expression in human breast cancer cell lines by interleukin 6 and fibroblast-derived factors." Int J Cancer **58**(1): 80-84.

Ibrahim, S., M. Keating, K. A. Do, S. O'Brien, Y. O. Huh, I. Jilani, S. Lerner, H. M. Kantarjian and M. Albitar (2001). "CD38 expression as an important prognostic factor in B-cell chronic lymphocytic leukemia." Blood **98**(1): 181-186.

Isobe, K., J. Tamaru, T. Uno, S. Yasuda, T. Aruga, S. Itoyama, K. Harigaya, A. Mikata and H. Ito (2001). "Immunoglobulin heavy chain variable region (VH) genes of B cell chronic lymphocytic leukemia cells from lymph nodes show somatic mutations and intraclonal diversity irrespective of follicular dendritic cell network." Leuk Lymphoma **42**(3): 499-506.

Ito, M., S. Iida, H. Inagaki, K. Tsuboi, H. Komatsu, M. Yamaguchi, N. Nakamura, R. Suzuki, M. Seto, S. Nakamura, Y. Morishima and R. Ueda (2002). "MUM1/IRF4 expression is an unfavorable prognostic factor in B-cell chronic lymphocytic leukemia (CLL)/small lymphocytic lymphoma (SLL)." Jpn J Cancer Res **93**(6): 685-694.

Iwai, Y., S. Terawaki and T. Honjo (2005). "PD-1 blockade inhibits hematogenous spread of poorly immunogenic tumor cells by enhanced recruitment of effector T cells." Int Immunol **17**(2): 133-144.

Jackson, A. L., H. Matsumoto, M. Janszen, V. Maino, A. Blidy and S. Shye (1990). "Restricted expression of p55 interleukin 2 receptor (CD25) on normal T cells." Clin Immunol Immunopathol **54**(1): 126-133.

Jain, P., M. Javdan, F. K. Feger, P. Y. Chiu, C. Sison, R. N. Damle, T. A. Bhuiya, F. Sen, L. V. Abruzzo, J. A. Burger, A. Rosenwald, S. L. Allen, J. E. Kolitz, K. R. Rai, N. Chiorazzi and B. Sherry (2012). "Th17 and non-Th17 interleukin-17-expressing cells in chronic lymphocytic leukemia: delineation, distribution, and clinical relevance." Haematologica **97**(4): 599-607.

Jak, M., R. Mous, E. B. Remmerswaal, R. Spijker, A. Jaspers, A. Yague, E. Eldering, R. A. Van Lier and M. H. Van Oers (2009). "Enhanced formation and survival of CD4+ CD25hi Foxp3+ T-cells in chronic lymphocytic leukemia." Leuk Lymphoma **50**(5): 788-801.

Jaksic, B., B. Vitale, E. Hauptmann, A. Planinc-Peraica, S. Ostojic and R. Kusec (1991). "The roles of age and sex in the prognosis of chronic leukaemias. A study of 373 cases." Br J Cancer **64**(2): 345-348.

Jaksic, O., M. M. Paro, I. Kardum Skelin, R. Kusec, V. Pejsa and B. Jaksic (2004). "CD38 on B-cell chronic lymphocytic leukemia cells has higher expression in lymph nodes than in peripheral blood or bone marrow." Blood **103**(5): 1968-1969.

Jeffers, M. D., J. Milton, R. Herriot and M. McKean (1998). "Fine needle aspiration cytology in the investigation on non-Hodgkin's lymphoma." J Clin Pathol **51**(3): 189-196.

Jelinek, D. F., R. C. Tschumper, S. M. Geyer, N. D. Bone, G. W. Dewald, C. A. Hanson, M. J. Stenson, T. E. Witzig, A. Tefferi and N. E. Kay (2001). "Analysis of clonal B-cell CD38 and immunoglobulin variable region sequence status in relation to clinical outcome for B-chronic lymphocytic leukaemia." Br J Haematol **115**(4): 854-861.

Jitschin, R., M. Braun, M. Buttner, K. Dettmer-Wilde, J. Bricks, J. Berger, M. J. Eckart, S. W. Krause, P. J. Oefner, K. Le Blanc, A. Mackensen and D. Mougiakakos (2014). "CLL-cells induce IDOhi CD14+HLA-DRlo myeloid derived suppressor cells that inhibit T-cell responses and promote TRegs." Blood.

Jonuleit, H., E. Schmitt, M. Stassen, A. Tuettenberg, J. Knop and A. H. Enk (2001). "Identification and functional characterization of human CD4(+)CD25(+) T cells with regulatory properties isolated from peripheral blood." J Exp Med **193**(11): 1285-1294.

Juliusson, G., D. G. Oscier, M. Fitchett, F. M. Ross, G. Stockdill, M. J. Mackie, A. C. Parker, G. L. Castoldi, A. Guneo, S. Knuutila and et al. (1990). "Prognostic subgroups in B-cell chronic lymphocytic leukemia defined by specific chromosomal abnormalities." N Engl J Med **323**(11): 720-724.

Jurado, J. O., I. B. Alvarez, V. Pasquinelli, G. J. Martinez, M. F. Quiroga, E. Abbate, R. M. Musella, H. E. Chuluyan and V. E. Garcia (2008). "Programmed death (PD)-1:PD-ligand 1/PD-ligand 2 pathway inhibits T cell effector functions during human tuberculosis." J Immunol **181**(1): 116-125.

Jurlander, J., C. F. Lai, J. Tan, C. C. Chou, C. H. Geisler, J. Schriber, L. E. Blumenson, S. K. Narula, H. Baumann and M. A. Caligiuri (1997). "Characterization of interleukin-10 receptor expression on B-cell chronic lymphocytic leukemia cells." Blood **89**(11): 4146-4152.

Kabachinski, J. (2007). "TIFF, GIF, and PNG: get the picture?" Biomed Instrum Technol **41**(4): 297-300.

Kaleem, Z., G. White and R. T. Vollmer (2001). "Critical analysis and diagnostic usefulness of limited immunophenotyping of B-cell non-Hodgkin lymphomas by flow cytometry." Am J Clin Pathol **115**(1): 136-142.

Kalina, T., J. Flores-Montero, V. H. van der Velden, M. Martin-Ayuso, S. Bottcher, M. Ritgen, J. Almeida, L. Lhermitte, V. Asnafi, A. Mendonca, R. de Tute, M. Cullen, L. Sedek, M. B. Vidriales, J. J. Perez, J. G. te Marvelde, E. Mejstrikova, O. Hrusak, T. Szczepanski, J. J. van Dongen, A. Orfao and C. EuroFlow (2012). "EuroFlow standardization of flow cytometer instrument settings and immunophenotyping protocols." Leukemia **26**(9): 1986-2010.

Kay, N. E., T. D. Shanafelt, A. K. Strege, Y. K. Lee, N. D. Bone and A. Raza (2007). "Bone biopsy derived marrow stromal elements rescue chronic lymphocytic leukemia B-cells from spontaneous and drug induced cell death and facilitates an "angiogenic switch"." Leuk Res **31**(7): 899-906.

Kay, N. E. and J. Zarling (1987). "Restoration of impaired natural killer cell activity of B-chronic lymphocytic leukemia patients by recombinant interleukin-2." Am J Hematol **24**(2): 161-167.

Khan, N., N. Shariff, M. Cobbold, R. Bruton, J. A. Ainsworth, A. J. Sinclair, L. Nayak and P. A. Moss (2002). "Cytomegalovirus seropositivity drives the CD8 T cell repertoire toward greater clonality in healthy elderly individuals." J Immunol **169**(4): 1984-1992.

Kiaii, S., P. Kokhaei, F. Mozaffari, E. Rossmann, F. Pak, A. Moshfegh, M. Palma, L. Hansson, K. Mashayekhi, M. Hojjat-Farsangi, A. Osterborg, A. Choudhury and H. Mellstedt (2013). "T cells from indolent CLL patients prevent apoptosis of leukemic B cells in vitro and have altered gene expression profile." Cancer Immunol Immunother **62**(1): 51-63.

Kimby, E., H. Mellstedt, B. Nilsson, M. Bjorkholm and G. Holm (1987). "T lymphocyte subpopulations in chronic lymphocytic leukemia of B cell type in relation to immunoglobulin isotype(s) on the leukemic clone and to clinical features." Eur J Haematol **38**(3): 261-267.

Kini, A. R., N. E. Kay and L. C. Peterson (2000). "Increased bone marrow angiogenesis in B cell chronic lymphocytic leukemia." Leukemia **14**(8): 1414-1418.

Kircher, M. and J. Kelso (2010). "High-throughput DNA sequencing--concepts and limitations." Bioessays **32**(6): 524-536.

Klein, U., M. Lia, M. Crespo, R. Siegel, Q. Shen, T. Mo, A. Ambesi-Impiombato, A. Califano, A. Migliazza, G. Bhagat and R. Dalla-Favera (2010). "The DLEU2/miR-15a/16-1 cluster controls B cell proliferation and its deletion leads to chronic lymphocytic leukemia." Cancer Cell **17**(1): 28-40.

Klein, U., Y. Tu, G. A. Stolovitzky, M. Mattioli, G. Cattoretti, H. Husson, A. Freedman, G. Inghirami, L. Cro, L. Baldini, A. Neri, A. Califano and R. Dalla-Favera (2001). "Gene expression profiling of B cell chronic lymphocytic leukemia reveals a homogeneous phenotype related to memory B cells." J Exp Med **194**(11): 1625-1638.

Knauf, W. U., B. Ehlers, B. Mohr, E. Thiel, I. Langenmayer, M. Hallek, B. Emmerich, D. Adorf, C. Nerl and T. Zwingers (1997). "Prognostic impact of the serum levels of soluble CD23 in B-cell chronic lymphocytic leukemia." Blood **89**(11): 4241-4242.

Kneitz, C., M. Goller, M. Wilhelm, C. Mehringer, G. Wohlleben, A. Schimpl and H. P. Tony (1999). "Inhibition of T cell/B cell interaction by B-CLL cells." Leukemia **13**(1): 98-104.

Koch, S., A. Larbi, E. Derhovanessian, D. Ozcelik, E. Naumova and G. Pawelec (2008). "Multiparameter flow cytometric analysis of CD4 and CD8 T cell subsets in young and old people." Immun Ageing **5**: 6.

Kochenderfer, J. N., M. E. Dudley, S. A. Feldman, W. H. Wilson, D. E. Spaner, I. Maric, M. Stetler-Stevenson, G. Q. Phan, M. S. Hughes, R. M. Sherry, J. C. Yang, U. S. Kammula, L. Devillier, R. Carpenter, D. A. Nathan, R. A. Morgan, C. Laurencot and S. A. Rosenberg (2012). "B-cell depletion and remissions of malignancy along with cytokine-associated toxicity in a clinical trial of anti-CD19 chimeric-antigen-receptor-transduced T cells." Blood **119**(12): 2709-2720.

Kokhaei, P., F. Jadidi-Niaragh, A. Sotoodeh Jahromi, A. Osterborg, H. Mellstedt and M. Hojjat-Farsangi (2016). "Ibrutinib-A double-edge sword in cancer and autoimmune disorders." J Drug Target **24**(5): 373-385.

Konoplev, S. N., H. A. Fritsche, S. O'Brien, W. G. Wierda, M. J. Keating, T. G. Gornet, S. St Romain, X. Wang, K. Inamdar, M. R. Johnson, L. J. Medeiros and C. E. Bueso-Ramos (2010). "High serum thymidine kinase 1 level predicts poorer survival in patients with chronic lymphocytic leukemia." Am J Clin Pathol **134**(3): 472-477.

Kook, H., A. M. Risitano, W. Zeng, M. Wlodarski, C. Lottemann, R. Nakamura, J. Barrett, N. S. Young and J. P. Maciejewski (2002). "Changes in T-cell receptor VB repertoire in aplastic anemia: effects of different immunosuppressive regimens." Blood **99**(10): 3668-3675.

Kostareli, E., A. Hadzidimitriou, N. Stavroyianni, N. Darzentas, A. Athanasiadou, M. Gounari, V. Bikos, A. Agathagelidis, T. Touloumenidou, I. Zorbas, A. Kouvatsi, N. Laoutaris, A. Fassas, A. Anagnostopoulos, C. Belessi and K. Stamatopoulos (2009). "Molecular evidence for EBV and CMV persistence in a subset of patients with chronic lymphocytic leukemia expressing stereotyped IGHV4-34 B-cell receptors." Leukemia.

Krackhardt, A. M., S. Harig, M. Witzens, R. Broderick, P. Barrett and J. G. Gribben (2002). "T-cell responses against chronic lymphocytic leukemia cells: implications for immunotherapy." Blood **100**(1): 167-173.

Kretz-Rommel, A., F. Qin, N. Dakappagari, E. P. Ravey, J. McWhirter, D. Oltean, S. Frederickson, T. Maruyama, M. A. Wild, M. J. Nolan, D. Wu, J. Springhorn and K. S. Bowdish (2007). "CD200 expression on tumor cells suppresses antitumor immunity: new approaches to cancer immunotherapy." J Immunol **178**(9): 5595-5605.

Kriangkum, J., S. N. Motz, T. Mack, S. Beiggi, E. Baigorri, H. Kuppusamy, A. R. Belch, J. B. Johnston and L. M. Pilarski (2015). "Single-Cell Analysis and Next-Generation Immuno-Sequencing Show That Multiple Clones Persist in Patients with Chronic Lymphocytic Leukemia." PLoS One **10**(9): e0137232.

Krober, A., T. Seiler, A. Benner, L. Bullinger, E. Bruckle, P. Lichter, H. Dohner and S. Stilgenbauer (2002). "V(H) mutation status, CD38 expression level, genomic aberrations, and survival in chronic lymphocytic leukemia." Blood **100**(4): 1410-1416.

Kung, P., G. Goldstein, E. L. Reinherz and S. F. Schlossman (1979). "Monoclonal antibodies defining distinctive human T cell surface antigens." Science **206**(4416): 347-349.

Kuppers, R. (2003). "B cells under influence: transformation of B cells by Epstein-Barr virus." Nat Rev Immunol **3**(10): 801-812.

Kuppers, R. (2005). "Mechanisms of B-cell lymphoma pathogenesis." Nat Rev Cancer **5**(4): 251-262.

Lad, D. P., S. Varma, N. Varma, M. U. Sachdeva, P. Bose and P. Malhotra (2013). "Regulatory T-cells in B-cell chronic lymphocytic leukemia: their role in disease progression and autoimmune cytopenias." Leuk Lymphoma **54**(5): 1012-1019.

Lad, D. P., S. Varma, N. Varma, M. U. Sachdeva, P. Bose and P. Malhotra (2015). "Regulatory T-cell and T-helper 17 balance in chronic lymphocytic leukemia progression and autoimmune cytopenias." Leuk Lymphoma: 1-5.

Lagneaux, L., A. Delforge, C. De Bruyn, M. Bernier and D. Bron (1999). "Adhesion to bone marrow stroma inhibits apoptosis of chronic lymphocytic leukemia cells." Leuk Lymphoma **35**(5-6): 445-453.

Landgren, O., J. S. Rapkin, N. E. Caporaso, L. Mellemkjaer, G. Gridley, L. R. Goldin and E. A. Engels (2007). "Respiratory tract infections and subsequent risk of chronic lymphocytic leukemia." Blood **109**(5): 2198-2201.

Lanemo Myhrinder, A., E. Hellqvist, E. Sidorova, A. Soderberg, H. Baxendale, C. Dahle, K. Willander, G. Tobin, E. Backman, O. Soderberg, R. Rosenquist, S. Horkko and A. Rosen (2008). "A new perspective: molecular motifs on oxidized LDL, apoptotic cells, and bacteria are targets for chronic lymphocytic leukemia antibodies." Blood **111**(7): 3838-3848.

Latchman, Y., C. R. Wood, T. Chernova, D. Chaudhary, M. Borde, I. Chernova, Y. Iwai, A. J. Long, J. A. Brown, R. Nunes, E. A. Greenfield, K. Bourque, V. A. Boussiotis, L. L. Carter, B.

M. Carreno, N. Malenkovich, H. Nishimura, T. Okazaki, T. Honjo, A. H. Sharpe and G. J. Freeman (2001). "PD-L2 is a second ligand for PD-1 and inhibits T cell activation." Nat Immunol **2**(3): 261-268.

Le Gal, F. A., V. M. Widmer, V. Dutoit, V. Rubio-Godoy, J. Schrenzel, P. R. Walker, P. J. Romero, D. Valmori, D. E. Speiser and P. Y. Dietrich (2007). "Tissue homing and persistence of defined antigen-specific CD8+ tumor-reactive T-cell clones in long-term melanoma survivors." J Invest Dermatol **127**(3): 622-629.

Le Roy, C., P. A. Deglesne, N. Chevallier, T. Beitar, V. Eclache, M. Quettier, M. Boubaya, R. Letestu, V. Levy, F. Ajchenbaum-Cymbalista and N. Varin-Blank (2012). "The degree of BCR and NFAT activation predicts clinical outcomes in chronic lymphocytic leukemia." Blood **120**(2): 356-365.

Le, R. Q., J. J. Melenhorst, M. Battiwalla, B. Hill, S. Memon, B. N. Savani, A. Shenoy, N. F. Hensel, E. K. Koklanaris, K. Keyvanfar, F. T. Hakim, D. C. Douek and A. J. Barrett (2011). "Evolution of the donor T-cell repertoire in recipients in the second decade after allogeneic stem cell transplantation." Blood **117**(19): 5250-5256.

Leach, D. R., M. F. Krummel and J. P. Allison (1996). "Enhancement of antitumor immunity by CTLA-4 blockade." Science **271**(5256): 1734-1736.

Lee, J. S., D. O. Dixon, H. M. Kantarjian, M. J. Keating and M. Talpaz (1987). "Prognosis of chronic lymphocytic leukemia: a multivariate regression analysis of 325 untreated patients." Blood **69**(3): 929-936.

Lee, P. P., C. Yee, P. A. Savage, L. Fong, D. Brockstedt, J. S. Weber, D. Johnson, S. Swetter, J. Thompson, P. D. Greenberg, M. Roederer and M. M. Davis (1999). "Characterization of circulating T cells specific for tumor-associated antigens in melanoma patients." Nat Med **5**(6): 677-685.

Lin, K., S. Manocha, R. J. Harris, Z. Matrai, P. D. Sherrington and A. R. Pettitt (2003). "High frequency of p53 dysfunction and low level of VH mutation in chronic lymphocytic leukemia patients using the VH3-21 gene segment." Blood **102**(3): 1145-1146.

Lin, K., P. D. Sherrington, M. Dennis, Z. Matrai, J. C. Cawley and A. R. Pettitt (2002). "Relationship between p53 dysfunction, CD38 expression, and IgV(H) mutation in chronic lymphocytic leukemia." Blood **100**(4): 1404-1409.

Lin, S. J., C. D. Peacock, K. Bahl and R. M. Welsh (2007). "Programmed death-1 (PD-1) defines a transient and dysfunctional oligoclonal T cell population in acute homeostatic proliferation." J Exp Med **204**(10): 2321-2333.

Lin, T. T., B. T. Letsolo, R. E. Jones, J. Rowson, G. Pratt, S. Hewamana, C. Fegan, C. Pepper and D. M. Baird (2010). "Telomere dysfunction and fusion during the progression of chronic lymphocytic leukemia: evidence for a telomere crisis." Blood **116**(11): 1899-1907.

Lin, T. T., K. Norris, N. H. Heppel, G. Pratt, J. M. Allan, D. J. Allsup, J. Bailey, L. Cawkwell, R. Hills, J. W. Grimstead, R. E. Jones, B. Britt-Compton, C. Fegan, D. M. Baird and C. Pepper (2014). "Telomere dysfunction accurately predicts clinical outcome in chronic lymphocytic leukaemia, even in patients with early stage disease." Br J Haematol **167**(2): 214-223.

Linterman, M. A. (2014). "How T follicular helper cells and the germinal centre response change with age." Immunol Cell Biol **92**(1): 72-79.

Litjens, N. H., E. A. de Wit and M. G. Betjes (2011). "Differential effects of age, cytomegalovirus-seropositivity and end-stage renal disease (ESRD) on circulating T lymphocyte subsets." Immun Ageing **8**(1): 2.

Liu, K., R. C. Stern, R. T. Rogers, L. G. Dodd and K. P. Mann (2001). "Diagnosis of hematopoietic processes by fine-needle aspiration in conjunction with flow cytometry: A review of 127 cases." Diagn Cytopathol **24**(1): 1-10.

Liu, W., A. L. Putnam, Z. Xu-Yu, G. L. Szot, M. R. Lee, S. Zhu, P. A. Gottlieb, P. Kapranov, T. R. Gingeras, B. Fazekas de St Groth, C. Clayberger, D. M. Soper, S. F. Ziegler and J. A. Bluestone (2006). "CD127 expression inversely correlates with FoxP3 and suppressive function of human CD4+ T reg cells." J Exp Med **203**(7): 1701-1711.

Loman, N. J., R. V. Misra, T. J. Dallman, C. Constantinidou, S. E. Gharbia, J. Wain and M. J. Pallen (2012). "Performance comparison of benchtop high-throughput sequencing platforms." Nat Biotechnol **30**(5): 434-439.

Looney, R. J., A. Falsey, D. Campbell, A. Torres, J. Kolassa, C. Brower, R. McCann, M. Menegus, K. McCormick, M. Frampton, W. Hall and G. N. Abraham (1999). "Role of cytomegalovirus in the T cell changes seen in elderly individuals." Clin Immunol **90**(2): 213-219.

Lu, J., A. Basu, J. J. Melenhorst, N. S. Young and K. E. Brown (2004). "Analysis of T-cell repertoire in hepatitis-associated aplastic anemia." Blood **103**(12): 4588-4593.

Luo, H. Y., M. Rubio, G. Biron, G. Delespesse and M. Sarfati (1991). "Antiproliferative effect of interleukin-4 in B chronic lymphocytic leukemia." J Immunother (1991) **10**(6): 418-425.

Lutzny, G., T. Kocher, M. Schmidt-Supprian, M. Rudelius, L. Klein-Hitpass, A. J. Finch, J. Durig, M. Wagner, C. Haferlach, A. Kohlmann, S. Schnittger, M. Seifert, S. Wanninger, N. Zaborsky, R. Oostendorp, J. Ruland, M. Leitges, T. Kuhnt, Y. Schafer, B. Lampl, C. Peschel, A. Egle and I. Ringshausen (2013). "Protein kinase c-beta-dependent activation of NF-kappaB in stromal cells is indispensable for the survival of chronic lymphocytic leukemia B cells in vivo." Cancer Cell **23**(1): 77-92.

Mackus, W. J., F. N. Frakking, A. Grummels, L. E. Gamadia, G. J. De Bree, D. Hamann, R. A. Van Lier and M. H. Van Oers (2003). "Expansion of CMV-specific CD8+CD45RA+CD27- T cells in B-cell chronic lymphocytic leukemia." Blood **102**(3): 1057-1063.

Maecker, H. T., T. Frey, L. E. Nomura and J. Trotter (2004). "Selecting fluorochrome conjugates for maximum sensitivity." Cytometry A **62**(2): 169-173.

Maeda, A., A. M. Scharenberg, S. Tsukada, J. B. Bolen, J. P. Kinet and T. Kurosaki (1999). "Paired immunoglobulin-like receptor B (PIR-B) inhibits BCR-induced activation of Syk and Btk by SHP-1." Oncogene **18**(14): 2291-2297.

Mahnke, Y. D. and M. Roederer (2007). "Optimizing a multicolor immunophenotyping assay." Clin Lab Med **27**(3): 469-485, v.

Majid, A., T. T. Lin, G. Best, K. Fishlock, S. Hewamana, G. Pratt, D. Yallop, A. G. Buggins, S. Wagner, B. J. Kennedy, F. Miall, R. Hills, S. Devereux, D. G. Oscier, M. J. Dyer, C. Fegan and C. Pepper (2011). "CD49d is an independent prognostic marker that is associated with CXCR4 expression in CLL." Leuk Res **35**(6): 750-756.

Malavasi, F., S. Deaglio, A. Funaro, E. Ferrero, A. L. Horenstein, E. Ortolan, T. Vaisitti and S. Aydin (2008). "Evolution and function of the ADP ribosyl cyclase/CD38 gene family in physiology and pathology." Physiol Rev **88**(3): 841-886.

Matrai, Z. (2005). "CD38 as a prognostic marker in CLL." Hematology **10**(1): 39-46.

Matrai, Z., K. Lin, M. Dennis, P. Sherrington, M. Zuzel, A. R. Pettitt and J. C. Cawley (2001). "CD38 expression and Ig VH gene mutation in B-cell chronic lymphocytic leukemia." Blood **97**(6): 1902-1903.

Matsutani, T., C. Oishi, T. Kaneshige, H. Igimi, K. Uchida, Y. Tsuruta, T. Yoshioka, R. Suzuki and T. Sakata (1994). "Molecular analysis of T cell receptor V beta chain to detect leukemia cell clonality in patients by adaptor ligation-mediated polymerase chain reaction." J Immunol Methods **177**(1-2): 9-15.

Matsutani, T., K. Shiiba, T. Yoshioka, Y. Tsuruta, R. Suzuki, T. Ochi, T. Itoh, H. Musha, T. Mizoi and I. Sasaki (2004). "Evidence for existence of oligoclonal tumor-infiltrating lymphocytes and predominant production of T helper 1/T cytotoxic 1 type cytokines in gastric and colorectal tumors." Int J Oncol **25**(1): 133-141.

Matsutani, T., T. Yoshioka, Y. Tsuruta, S. Iwagami and R. Suzuki (1997). "Analysis of TCRAV and TCRBV repertoires in healthy individuals by microplate hybridization assay." Hum Immunol **56**(1-2): 57-69.

Matutes, E., K. Owusu-Ankomah, R. Morilla, J. Garcia Marco, A. Houlihan, T. H. Que and D. Catovsky (1994). "The immunological profile of B-cell disorders and proposal of a scoring system for the diagnosis of CLL." Leukemia **8**(10): 1640-1645.

McClanahan, F., B. Hanna, S. Miller, A. J. Clear, P. Lichter, J. G. Gribben and M. Seiffert (2015). "PD-L1 Checkpoint Blockade Prevents Immune Dysfunction and Leukemia Development in a Mouse Model of Chronic Lymphocytic Leukemia." Blood.

McLaughlin, B. E., N. Baumgarth, M. Bigos, M. Roederer, S. C. De Rosa, J. D. Altman, D. F. Nixon, J. Ottinger, C. Oxford, T. G. Evans and D. M. Asmuth (2008). "Nine-color flow cytometry for accurate measurement of T cell subsets and cytokine responses. Part I: Panel design by an empiric approach." Cytometry A **73**(5): 400-410.

Meda, B. A., D. H. Buss, R. D. Woodruff, J. O. Cappellari, R. O. Rainer, B. L. Powell and K. R. Geisinger (2000). "Diagnosis and subclassification of primary and recurrent lymphoma. The usefulness and limitations of combined fine-needle aspiration cytomorphology and flow cytometry." Am J Clin Pathol **113**(5): 688-699.

Mellstedt, H. and A. Choudhury (2006). "T and B cells in B-chronic lymphocytic leukaemia: Faust, Mephistopheles and the pact with the Devil." Cancer Immunol Immunother **55**(2): 210-220.

Messmer, B. T., E. Albesiano, D. G. Efremov, F. Ghiotto, S. L. Allen, J. Kolitz, R. Foa, R. N. Damle, F. Fais, D. Messmer, K. R. Rai, M. Ferrarini and N. Chiorazzi (2004). "Multiple distinct sets of stereotyped antigen receptors indicate a role for antigen in promoting chronic lymphocytic leukemia." J Exp Med **200**(4): 519-525.

Messmer, B. T., D. Messmer, S. L. Allen, J. E. Kolitz, P. Kudalkar, D. Cesar, E. J. Murphy, P. Koduru, M. Ferrarini, S. Zupo, G. Cutrona, R. N. Damle, T. Wasil, K. R. Rai, M. K. Hellerstein and N. Chiorazzi (2005). "In vivo measurements document the dynamic cellular kinetics of chronic lymphocytic leukemia B cells." J Clin Invest **115**(3): 755-764.

Mills, K. H. and J. C. Cawley (1982). "Suppressor T cells in B-cell chronic lymphocytic leukaemia: relationship to clinical stage." Leuk Res **6**(5): 653-657.

Mittal, A. K., N. K. Chaturvedi, K. J. Rai, C. E. Gilling, T. M. Nordgren, M. Moragues, R. Lu, R. Opavsky, G. R. Bociek, D. D. Weisenburger, J. Iqbal and S. S. Joshi (2014). "Chronic Lymphocytic Leukemia Cells in Lymph Node Microenvironment Depict Molecular Signature Associated with an Aggressive Disease." Mol Med.

Molica, S. (2006). "Sex differences in incidence and outcome of chronic lymphocytic leukemia patients." Leuk Lymphoma **47**(8): 1477-1480.

Molica, S., A. Vacca, D. Ribatti, A. Cuneo, F. Cavazzini, D. Levato, G. Vitelli, L. Tucci, A. M. Roccaro and F. Dammacco (2002). "Prognostic value of enhanced bone marrow angiogenesis in early B-cell chronic lymphocytic leukemia." Blood **100**(9): 3344-3351.

Molica, S., G. Vitelli, D. Levato, D. Giannarelli and G. M. Gandolfo (2001). "Elevated serum levels of soluble CD44 can identify a subgroup of patients with early B-cell chronic lymphocytic leukemia who are at high risk of disease progression." Cancer **92**(4): 713-719.

Momtaz, P. and M. A. Postow (2014). "Immunologic checkpoints in cancer therapy: focus on the programmed death-1 (PD-1) receptor pathway." Pharmgenomics Pers Med **7**: 357-365.

Montserrat, E., J. Sanchez-Bisono, N. Vinolas and C. Rozman (1986). "Lymphocyte doubling time in chronic lymphocytic leukaemia: analysis of its prognostic significance." Br J Haematol **62**(3): 567-575.

Morabito, F., M. Mangiola, B. Oliva, C. Stelitano, V. Callea, S. Deaglio, P. Iacopino, M. Brugiatelli and F. Malavasi (2001). "Peripheral blood CD38 expression predicts survival in B-cell chronic lymphocytic leukemia." Leuk Res **25**(11): 927-932.

Morabito, F., M. Mangiola, C. Stelitano, S. Deaglio, V. Callea and F. Malavasi (2002). "Peripheral blood CD38 expression predicts time to progression in B-cell chronic lymphocytic leukemia after first-line therapy with high-dose chlorambucil." Haematologica **87**(2): 217-218.

Moreau, E. J., E. Matutes, R. P. A'Hern, A. M. Morilla, R. M. Morilla, K. A. Owusu-Ankomah, B. K. Seon and D. Catovsky (1997). "Improvement of the chronic lymphocytic leukemia scoring system with the monoclonal antibody SN8 (CD79b)." Am J Clin Pathol **108**(4): 378-382.

Morrison, V. A. (2010). "Infectious complications of chronic lymphocytic leukaemia: pathogenesis, spectrum of infection, preventive approaches." Best Pract Res Clin Haematol **23**(1): 145-153.

Morse, H. C., 3rd, J. F. Kearney, P. G. Isaacson, M. Carroll, T. N. Fredrickson and E. S. Jaffe (2001). "Cells of the marginal zone--origins, function and neoplasia." Leuk Res **25**(2): 169-178.

Motta, M., M. Chiarini, C. Ghidini, C. Zanotti, C. Lamorgese, L. Caimi, G. Rossi and L. Imberti (2010). "Quantification of newly produced B and T lymphocytes in untreated chronic lymphocytic leukemia patients." J Transl Med **8**: 111.

Motta, M., L. Rassenti, B. J. Shelvin, S. Lerner, T. J. Kipps, M. J. Keating and W. G. Wierda (2005). "Increased expression of CD152 (CTLA-4) by normal T lymphocytes in untreated patients with B-cell chronic lymphocytic leukemia." Leukemia **19**(10): 1788-1793.

Muenst, S., S. Hoeller, S. Dirnhofer and A. Tzankov (2009). "Increased programmed death-1+ tumor-infiltrating lymphocytes in classical Hodgkin lymphoma substantiate reduced overall survival." Hum Pathol **40**(12): 1715-1722.

Muzio, M., B. Apollonio, C. Scielzo, M. Frenquelli, I. Vandoni, V. Boussiotis, F. Caligaris-Cappio and P. Ghia (2008). "Constitutive activation of distinct BCR-signaling pathways in a subset of CLL patients: a molecular signature of anergy." Blood **112**(1): 188-195.

Nakamura, K., T. Oshima, T. Morimoto, S. Ikeda, H. Yoshikawa, Y. Shiwa, S. Ishikawa, M. C. Linak, A. Hirai, H. Takahashi, M. Altaf-Ul-Amin, N. Ogasawara and S. Kanaya (2011). "Sequence-specific error profile of Illumina sequencers." Nucleic Acids Res **39**(13): e90.

Nicol, T. L., M. Silberman, D. L. Rosenthal and M. J. Borowitz (2000). "The accuracy of combined cytopathologic and flow cytometric analysis of fine-needle aspirates of lymph nodes." Am J Clin Pathol **114**(1): 18-28.

Niemann, C. U., S. E. Herman, I. Maric, J. Gomez-Rodriguez, A. Biancotto, B. Y. Chang, S. Martyr, M. Stetler-Stevenson, C. M. Yuan, K. R. Calvo, R. C. Braylan, J. Valdez, Y. S. Lee, D. H. Wong, J. Jones, C. Sun, G. E. Marti, M. Z. Farooqui and A. Wiestner (2016). "Disruption of in vivo Chronic Lymphocytic Leukemia Tumor-Microenvironment Interactions by Ibrutinib--Findings from an Investigator-Initiated Phase II Study." Clin Cancer Res **22**(7): 1572-1582.

Nishimura, H., M. Nose, H. Hiai, N. Minato and T. Honjo (1999). "Development of lupus-like autoimmune diseases by disruption of the PD-1 gene encoding an ITIM motif-carrying immunoreceptor." Immunity **11**(2): 141-151.

Nishio, M., T. Endo, N. Tsukada, J. Ohata, S. Kitada, J. C. Reed, N. J. Zvaifler and T. J. Kipps (2005). "Nurselike cells express BAFF and APRIL, which can promote survival of chronic lymphocytic leukemia cells via a paracrine pathway distinct from that of SDF-1alpha." Blood **106**(3): 1012-1020.

Nolz, J. C., R. C. Tschumper, B. T. Pittner, J. R. Darce, N. E. Kay and D. F. Jelinek (2005). "ZAP-70 is expressed by a subset of normal human B-lymphocytes displaying an activated phenotype." Leukemia **19**(6): 1018-1024.

Novak, A. J., R. J. Bram, N. E. Kay and D. F. Jelinek (2002). "Aberrant expression of B-lymphocyte stimulator by B chronic lymphocytic leukemia cells: a mechanism for survival." Blood **100**(8): 2973-2979.

Novak, M., V. Prochazka, P. Turcsanyi and T. Papajik (2015). "Numbers of CD8+PD-1+ and CD4+PD-1+ Cells in Peripheral Blood of Patients with Chronic Lymphocytic Leukemia Are Independent of Binet Stage and Are Significantly Higher Compared to Healthy Volunteers." Acta Haematol **134**(4): 208-214.

Nowakowski, G. S., J. D. Hoyer, T. D. Shanafelt, S. M. Geyer, B. R. LaPlant, T. G. Call, D. F. Jelinek, C. S. Zent and N. E. Kay (2007). "Using smudge cells on routine blood smears to predict clinical outcome in chronic lymphocytic leukemia: a universally available prognostic test." Mayo Clin Proc **82**(4): 449-453.

Nuckel, H., M. Switala, C. H. Collins, L. Sellmann, H. Grosse-Wilde, U. Duhrsen and V. Rebmann (2009). "High CD49d protein and mRNA expression predicts poor outcome in chronic lymphocytic leukemia." Clin Immunol.

Nunes, C., R. Wong, M. Mason, C. Fegan, S. Man and C. Pepper (2012). "Expansion of a CD8(+)PD-1(+) replicative senescence phenotype in early stage CLL patients is associated with inverted CD4:CD8 ratios and disease progression." Clin Cancer Res **18**(3): 678-687.

Nunes, C. T., K. L. Miners, G. Dolton, C. Pepper, C. Fegan, M. D. Mason and S. Man (2011). "A novel tumor antigen derived from enhanced degradation of bax protein in human cancers." Cancer Res **71**(16): 5435-5444.

O'Hayre, M., C. L. Salanga, T. J. Kipps, D. Messmer, P. C. Dorrestein and T. M. Handel (2010). "Elucidating the CXCL12/CXCR4 signaling network in chronic lymphocytic leukemia through phosphoproteomics analysis." PLoS One **5**(7): e11716.

O'Shea, U. D., K. M. Hollowood and A. W. Boylston (1996). "Demonstration of the oligoclonality of an enteropathy associated T-cell lymphoma by monoclonal antibodies and PCR analysis of the T-cell receptor V-beta repertoire on fixed tissue." Hum Pathol **27**(5): 509-513.

Ojha, J., J. Ayres, C. Secreto, R. Tschumper, K. Rabe, D. Van Dyke, S. Slager, T. Shanafelt, R. Fonseca, N. E. Kay and E. Braggio (2015). "Deep sequencing identifies genetic heterogeneity and recurrent convergent evolution in chronic lymphocytic leukemia." Blood **125**(3): 492-498.

Okazaki, T. and T. Honjo (2007). "PD-1 and PD-1 ligands: from discovery to clinical application." Int Immunol **19**(7): 813-824.

Okazaki, T., A. Maeda, H. Nishimura, T. Kurosaki and T. Honjo (2001). "PD-1 immunoreceptor inhibits B cell receptor-mediated signaling by recruiting src homology 2-domain-containing tyrosine phosphatase 2 to phosphotyrosine." Proc Natl Acad Sci U S A **98**(24): 13866-13871.

Os, A., S. Burgler, A. P. Ribes, A. Funderud, D. Wang, K. M. Thompson, G. E. Tjonnfjord, B. Bogen and L. A. Munthe (2013). "Chronic lymphocytic leukemia cells are activated and proliferate in response to specific T helper cells." Cell Rep **4**(3): 566-577.

Oscier, D., C. Dearden, E. Eren, C. Fegan, G. Follows, P. Hillmen, T. Illidge, E. Matutes, D. W. Milligan, A. Pettitt, A. Schuh, J. Wimperis and H. British Committee for Standards in (2012). "Guidelines on the diagnosis, investigation and management of chronic lymphocytic leukaemia." Br J Haematol **159**(5): 541-564.

Oscier, D., C. Fegan, P. Hillmen, T. Illidge, S. Johnson, P. Maguire, E. Matutes and D. Milligan (2004). "Guidelines on the diagnosis and management of chronic lymphocytic leukaemia." Br J Haematol **125**(3): 294-317.

Oscier, D., M. Fitchett, T. Herbert and R. Lambert (1991). "Karyotypic evolution in B-cell chronic lymphocytic leukaemia." Genes Chromosomes Cancer **3**(1): 16-20.

Oscier, D. G., A. Thompsett, D. Zhu and F. K. Stevenson (1997). "Differential rates of somatic hypermutation in V(H) genes among subsets of chronic lymphocytic leukemia defined by chromosomal abnormalities." Blood **89**(11): 4153-4160.

Paillard, F., G. Sterkers, G. Bismuth, E. Gomard and C. Vaquero (1988). "Lymphokine mRNA and T cell multireceptor mRNA of the Ig super gene family are reciprocally modulated during human T cell activation." Eur J Immunol **18**(10): 1643-1646.

Pallasch, C. P., S. Ulbrich, R. Brinker, M. Hallek, R. A. Uger and C. M. Wendtner (2009). "Disruption of T cell suppression in chronic lymphocytic leukemia by CD200 blockade." Leuk Res **33**(3): 460-464.

Palmer, S., C. A. Hanson, C. S. Zent, L. F. Porrata, B. Laplant, S. M. Geyer, S. N. Markovic, T. G. Call, D. A. Bowen, D. F. Jelinek, N. E. Kay and T. D. Shanafelt (2008). "Prognostic importance of T and NK-cells in a consecutive series of newly diagnosed patients with chronic lymphocytic leukaemia." Br J Haematol **141**(5): 607-614.

Pammer, J., A. Plettenberg, W. Weninger, B. Diller, M. Mildner, A. Uthman, W. Issing, M. Sturzl and E. Tschachler (1996). "CD40 antigen is expressed by endothelial cells and tumor cells in Kaposi's sarcoma." Am J Pathol **148**(5): 1387-1396.

Panayiotidis, P., K. Ganeshaguru, S. A. Jabbar and A. V. Hoffbrand (1993). "Interleukin-4 inhibits apoptotic cell death and loss of the bcl-2 protein in B-chronic lymphocytic leukaemia cells in vitro." Br J Haematol **85**(3): 439-445.

Panayiotidis, P., D. Jones, K. Ganeshaguru, L. Foroni and A. V. Hoffbrand (1996). "Human bone marrow stromal cells prevent apoptosis and support the survival of chronic lymphocytic leukaemia cells in vitro." Br J Haematol **92**(1): 97-103.

Pannetier, C., M. Cochet, S. Darche, A. Casrouge, M. Zoller and P. Kourilsky (1993). "The sizes of the CDR3 hypervariable regions of the murine T-cell receptor beta chains vary as a function of the recombined germ-line segments." Proc Natl Acad Sci U S A **90**(9): 4319-4323.

Pappas, J., W. J. Jung, A. K. Barda, W. L. Lin, J. E. Fincke, E. Purev, M. Radu, J. Gaughan, C. W. Helm, E. Hernandez, R. S. Freedman and C. D. Platsoucas (2005). "Substantial proportions of identical beta-chain T-cell receptor transcripts are present in epithelial ovarian carcinoma tumors." Cell Immunol **234**(2): 81-101.

Pascutti, M. F., M. Jak, J. M. Tromp, I. A. Derks, E. B. Remmerswaal, R. Thijssen, M. H. van Attekum, G. G. van Bochove, D. M. Luijks, S. T. Pals, R. A. van Lier, A. P. Kater, M. H. van Oers and E. Eldering (2013). "IL-21 and CD40L signals from autologous T cells can induce antigen-independent proliferation of CLL cells." Blood **122**(17): 3010-3019.

Patten, P., S. Devereux, A. Buggins, M. Bonyhadi, M. Frohlich and R. J. Berenson (2005). "Effect of CD3/CD28 bead-activated and expanded T cells on leukemic B cells in chronic lymphocytic leukemia." J Immunol **174**(11): 6562-6563; author reply 6563.

Patten, P. E., A. G. Buggins, J. Richards, A. Wotherspoon, J. Salisbury, G. J. Mufti, T. J. Hamblin and S. Devereux (2008). "CD38 expression in chronic lymphocytic leukemia is regulated by the tumor microenvironment." Blood **111**(10): 5173-5181.

Pedersen, I. M., S. Kitada, L. M. Leoni, J. M. Zapata, J. G. Karras, N. Tsukada, T. J. Kipps, Y. S. Choi, F. Bennett and J. C. Reed (2002). "Protection of CLL B cells by a follicular dendritic cell line is dependent on induction of Mcl-1." Blood **100**(5): 1795-1801.

Peggs, K. S., S. Verfuerth, S. D'Sa, K. Yong and S. Mackinnon (2003). "Assessing diversity: immune reconstitution and T-cell receptor BV spectratype analysis following stem cell transplantation." Br J Haematol **120**(1): 154-165.

Pepper, C., A. G. Buggins, C. H. Jones, E. J. Walsby, F. Forconi, G. Pratt, S. Devereux, F. K. Stevenson and C. Fegan (2015). "Phenotypic heterogeneity in IGHV-mutated CLL patients has prognostic impact and identifies a subset with increased sensitivity to BTK and PI3Kdelta inhibition." Leukemia **29**(3): 744-747.

Pepper, C., R. Ward, T. T. Lin, P. Brennan, J. Starczynski, M. Musson, C. Rowntree, P. Bentley, K. Mills, G. Pratt and C. Fegan (2007). "Highly purified CD38+ and CD38- sub-clones derived from the same chronic lymphocytic leukemia patient have distinct gene expression signatures despite their monoclonal origin." Leukemia **21**(4): 687-696.

Pflug, N., J. Bahlo, T. D. Shanafelt, B. F. Eichhorst, M. A. Bergmann, T. Elter, K. Bauer, G. Malchau, K. G. Rabe, S. Stilgenbauer, H. Dohner, U. Jager, M. J. Eckart, G. Hopfinger, R. Busch, A. M. Fink, C. M. Wendtner, K. Fischer, N. E. Kay and M. Hallek (2014). "Development of a comprehensive prognostic index for patients with chronic lymphocytic leukemia." Blood.

Philippen, A., S. Diener, T. Zenz, H. Dohner, S. Stilgenbauer and D. Mertens (2010). "SYK carries no activating point mutations in patients with chronic lymphocytic leukaemia (CLL)." Br J Haematol **150**(5): 633-636.

Pizzolo, G., M. Chilosi, A. Ambrosetti, G. Semenzato, L. Fiore-Donati and G. Perona (1983). "Immunohistologic study of bone marrow involvement in B-chronic lymphocytic leukemia." Blood **62**(6): 1289-1296.

Platsoucas, C. D., M. Galinski, S. Kempin, L. Reich, B. Clarkson and R. A. Good (1982). "Abnormal T lymphocyte subpopulations in patients with B cell chronic lymphocytic leukemia: an analysis by monoclonal antibodies." J Immunol **129**(5): 2305-2312.

Podhorecka, M., A. Dmoszynska, J. Rolinski and E. Wasik (2002). "T type 1/type 2 subsets balance in B-cell chronic lymphocytic leukemia--the three-color flow cytometry analysis." Leuk Res **26**(7): 657-660.

Poggi, A., C. Prevosto, S. Catellani, I. Rocco, A. Garuti and M. R. Zocchi (2010). "Engagement of CD31 delivers an activating signal that contributes to the survival of chronic lymphocytic leukaemia cells." Br J Haematol **151**(3): 252-264.

Pontikoglou, C., M. C. Kastrinaki, M. Klaus, C. Kalpadakis, P. Katonis, K. Alpantaki, G. A. Pangalis and H. A. Papadaki (2013). "Study of the quantitative, functional, cytogenetic, and immunoregulatory properties of bone marrow mesenchymal stem cells in patients with B-cell chronic lymphocytic leukemia." Stem Cells Dev **22**(9): 1329-1341.

Porakishvili, N., T. Roschupkina, T. Kalber, A. P. Jewell, K. Patterson, K. Yong and P. M. Lydyard (2001). "Expansion of CD4+ T cells with a cytotoxic phenotype in patients with B-chronic lymphocytic leukaemia (B-CLL)." Clin Exp Immunol **126**(1): 29-36.

Porter, D. L., W. T. Hwang, N. V. Frey, S. F. Lacey, P. A. Shaw, A. W. Loren, A. Bagg, K. T. Marcucci, A. Shen, V. Gonzalez, D. Ambrose, S. A. Grupp, A. Chew, Z. Zheng, M. C. Milone, B. L. Levine, J. J. Melenhorst and C. H. June (2015). "Chimeric antigen receptor T cells persist and induce sustained remissions in relapsed refractory chronic lymphocytic leukemia." Sci Transl Med **7**(303): 303ra139.

Pourgheysari, B., R. Bruton, H. Parry, L. Billingham, C. Fegan, J. Murray and P. Moss (2010). "The number of cytomegalovirus-specific CD4+ T cells is markedly expanded in patients with B-cell chronic lymphocytic leukemia and determines the total CD4+ T-cell repertoire." Blood **116**(16): 2968-2974.

Powles, T., J. P. Eder, G. D. Fine, F. S. Braiteh, Y. Loriot, C. Cruz, J. Bellmunt, H. A. Burris, D. P. Petrylak, S. L. Teng, X. Shen, Z. Boyd, P. S. Hegde, D. S. Chen and N. J. Vogelzang (2014). "MPDL3280A (anti-PD-L1) treatment leads to clinical activity in metastatic bladder cancer." Nature **515**(7528): 558-562.

Prieto, A., M. Sanchez, E. Perucha and M. Alvarez-Mon (2005). "Effect of CD3/CD28 bead-activated T cells on leukemic B cells in chronic lymphocytic leukemia." J Immunol **175**(4): 2042-2043.

Puente, X. S., M. Pinyol, V. Quesada, L. Conde, G. R. Ordonez, N. Villamor, G. Escaramis, P. Jares, S. Bea, M. Gonzalez-Diaz, L. Bassaganyas, T. Baumann, M. Juan, M. Lopez-Guerra, D. Colomer, J. M. Tubio, C. Lopez, A. Navarro, C. Tornador, M. Aymerich, M. Rozman, J. M. Hernandez, D. A. Puente, J. M. Freije, G. Velasco, A. Gutierrez-Fernandez, D. Costa, A. Carrio, S. Guijarro, A. Enjuanes, L. Hernandez, J. Yague, P. Nicolas, C. M. Romeo-Casabona, H. Himmelbauer, E. Castillo, J. C. Dohm, S. de Sanjose, M. A. Piris, E. de Alava, J. San Miguel, R. Royo, J. L. Gelpi, D. Torrents, M. Orozco, D. G. Pisano, A. Valencia, R. Guigo, M. Bayes, S. Heath, M. Gut, P. Klatt, J. Marshall, K. Raine, L. A. Stebbings, P. A. Futreal, M. R. Stratton, P. J. Campbell, I. Gut, A. Lopez-Guillermo, X. Estivill, E. Montserrat, C. Lopez-Otin and E. Campo (2011). "Whole-genome sequencing identifies recurrent mutations in chronic lymphocytic leukaemia." Nature **475**(7354): 101-105.

Quesada, V., L. Conde, N. Villamor, G. R. Ordonez, P. Jares, L. Bassaganyas, A. J. Ramsay, S. Bea, M. Pinyol, A. Martinez-Trillos, M. Lopez-Guerra, D. Colomer, A. Navarro, T. Baumann, M. Aymerich, M. Rozman, J. Delgado, E. Gine, J. M. Hernandez, M. Gonzalez-Diaz, D. A. Puente, G. Velasco, J. M. Freije, J. M. Tubio, R. Royo, J. L. Gelpi, M. Orozco, D. G. Pisano, J. Zamora, M. Vazquez, A. Valencia, H. Himmelbauer, M. Bayes, S. Heath, M. Gut, I. Gut, X. Estivill, A. Lopez-Guillermo, X. S. Puente, E. Campo and C. Lopez-Otin (2012). "Exome sequencing identifies recurrent mutations of the splicing factor SF3B1 gene in chronic lymphocytic leukemia." Nat Genet **44**(1): 47-52.

Quiroga, M. P., K. Balakrishnan, A. V. Kurtova, M. Sivina, M. J. Keating, W. G. Wierda, V. Gandhi and J. A. Burger (2009). "B-cell antigen receptor signaling enhances chronic lymphocytic leukemia cell migration and survival: specific targeting with a novel spleen tyrosine kinase inhibitor, R406." Blood **114**(5): 1029-1037.

Rai, K. R., A. Sawitsky, E. P. Cronkite, A. D. Chanana, R. N. Levy and B. S. Pasternack (1975). "Clinical staging of chronic lymphocytic leukemia." Blood **46**(2): 219-234.

Ramsay, A. G., A. J. Clear, R. Fatah and J. G. Gribben (2012). "Multiple inhibitory ligands induce impaired T-cell immunologic synapse function in chronic lymphocytic leukemia that can be blocked with lenalidomide: establishing a reversible immune evasion mechanism in human cancer." Blood **120**(7): 1412-1421.

Ramsay, A. G., A. J. Johnson, A. M. Lee, G. Gorgun, R. Le Dieu, W. Blum, J. C. Byrd and J. G. Gribben (2008). "Chronic lymphocytic leukemia T cells show impaired immunological synapse formation that can be reversed with an immunomodulating drug." J Clin Invest **118**(7): 2427-2437.

Ratech, H., K. Sheibani, B. N. Nathwani and H. Rappaport (1988). "Immunoarchitecture of the "pseudofollicles" of well-differentiated (small) lymphocytic lymphoma: a comparison with true follicles." Hum Pathol **19**(1): 89-94.

Ravinsky, E., C. Morales, E. Kutryk, A. Chrobak and F. Paraskevas (1999). "Cytodiagnosis of lymphoid proliferations by fine needle aspiration biopsy. Adjunctive value of flow cytometry." Acta Cytol **43**(6): 1070-1078.

Rawstron, A. C., M. R. Yuille, J. Fuller, M. Cullen, B. Kennedy, S. J. Richards, A. S. Jack, E. Matutes, D. Catovsky, P. Hillmen and R. S. Houlston (2002). "Inherited predisposition to CLL is detectable as subclinical monoclonal B-lymphocyte expansion." Blood **100**(7): 2289-2290.

Reittie, J. E., K. L. Yong, P. Panayiotidis and A. V. Hoffbrand (1996). "Interleukin-6 inhibits apoptosis and tumour necrosis factor induced proliferation of B-chronic lymphocytic leukaemia." Leuk Lymphoma **22**(1-2): 83-90, follow 186, color plate VI.

Rezvany, M. R., M. Jeddi-Tehrani, A. Osterborg, E. Kimby, H. Wigzell and H. Mellstedt (1999). "Oligoclonal TCRBV gene usage in B-cell chronic lymphocytic leukemia: major perturbations are preferentially seen within the CD4 T-cell subset." Blood **94**(3): 1063-1069.

Rezvany, M. R., M. Jeddi-Tehrani, H. Rabbani, N. Lewin, J. Avila-Carino, A. Osterborg, H. Wigzell and H. Mellstedt (2000). "Autologous T lymphocytes may specifically recognize leukaemic B cells in patients with chronic lymphocytic leukaemia." Br J Haematol **111**(2): 608-617.

Ricca, I., A. Rocci, D. Drandi, R. Francese, M. Compagno, C. Lobetti Bodoni, F. De Marco, M. Astolfi, L. Monitillo, S. Vallet, R. Calvi, F. Ficara, P. Omede, R. Rosato, A. Gallamini, C. Marinone, L. Bergui, M. Boccadoro, C. Tarella and M. Ladetto (2007). "Telomere length identifies two different prognostic subgroups among VH-unmutated B-cell chronic lymphocytic leukemia patients." Leukemia **21**(4): 697-705.

Riches, J. C., J. K. Davies, F. McClanahan, R. Fatah, S. Iqbal, S. Agrawal, A. G. Ramsay and J. G. Gribben (2013). "T cells from CLL patients exhibit features of T-cell exhaustion but retain capacity for cytokine production." Blood **121**(9): 1612-1621.

Riches, J. C. and J. G. Gribben (2014). "Immunomodulation and immune reconstitution in chronic lymphocytic leukemia." Semin Hematol **51**(3): 228-234.

Riley, J. L. (2009). "PD-1 signaling in primary T cells." Immunol Rev **229**(1): 114-125.

Rissiek, A., C. Schulze, U. Bacher, A. Schieferdecker, B. Thiele, A. Jacholkowski, A. Flammiger, C. Horn, F. Haag, G. Tiegs, K. Zirlik, M. Trepel, E. Tolosa and M. Binder (2014). "Multidimensional scaling analysis identifies pathological and prognostically relevant profiles of circulating T-cells in chronic lymphocytic leukemia." Int J Cancer.

Robert, C., A. Ribas, J. D. Wolchok, F. S. Hodi, O. Hamid, R. Kefford, J. S. Weber, A. M. Joshua, W. J. Hwu, T. C. Gangadhar, A. Patnaik, R. Dronca, H. Zarour, R. W. Joseph, P. Boasberg, B. Chmielowski, C. Mateus, M. A. Postow, K. Gergich, J. Elassaiss-Schaap, X. N. Li, R. Iannone, S. W. Ebbinghaus, S. P. Kang and A. Daud (2014). "Anti-programmed-death-receptor-1 treatment with pembrolizumab in ipilimumab-refractory advanced melanoma: a randomised dose-comparison cohort of a phase 1 trial." Lancet **384**(9948): 1109-1117.

Robert, C., L. Thomas, I. Bondarenko, S. O'Day, J. Weber, C. Garbe, C. Lebbe, J. F. Baurain, A. Testori, J. J. Grob, N. Davidson, J. Richards, M. Maio, A. Hauschild, W. H. Miller, Jr., P. Gascon, M. Lotem, K. Harmankaya, R. Ibrahim, S. Francis, T. T. Chen, R. Humphrey, A. Hoos and J. D. Wolchok (2011). "Ipilimumab plus dacarbazine for previously untreated metastatic melanoma." N Engl J Med **364**(26): 2517-2526.

Robins, H. (2013). "Immunosequencing: applications of immune repertoire deep sequencing." Curr Opin Immunol **25**(5): 646-652.

Robins, H., C. Desmarais, J. Matthis, R. Livingston, J. Andriesen, H. Reijonen, C. Carlson, G. Nepom, C. Yee and K. Cerosaletti (2012). "Ultra-sensitive detection of rare T cell clones." J Immunol Methods **375**(1-2): 14-19.

Robins, H. S., P. V. Campregher, S. K. Srivastava, A. Wacher, C. J. Turtle, O. Kahsai, S. R. Riddell, E. H. Warren and C. S. Carlson (2009). "Comprehensive assessment of T-cell receptor beta-chain diversity in alphabeta T cells." Blood **114**(19): 4099-4107.

Robins, H. S., N. G. Ericson, J. Guenthoer, K. C. O'Briant, M. Tewari, C. W. Drescher and J. H. Bielas (2013). "Digital genomic quantification of tumor-infiltrating lymphocytes." Sci Transl Med **5**(214): 214ra169.

Roederer, M. (2001). "Spectral compensation for flow cytometry: visualization artifacts, limitations, and caveats." Cytometry **45**(3): 194-205.

Roos, G., A. Krober, P. Grabowski, D. Kienle, A. Buhler, H. Dohner, R. Rosenquist and S. Stilgenbauer (2008). "Short telomeres are associated with genetic complexity, high-risk genomic aberrations, and short survival in chronic lymphocytic leukemia." Blood **111**(4): 2246-2252.

Rosenwald, A., A. A. Alizadeh, G. Widhopf, R. Simon, R. E. Davis, X. Yu, L. Yang, O. K. Pickeral, L. Z. Rassenti, J. Powell, D. Botstein, J. C. Byrd, M. R. Grever, B. D. Cheson, N. Chiorazzi, W. H. Wilson, T. J. Kipps, P. O. Brown and L. M. Staudt (2001). "Relation of gene expression phenotype to immunoglobulin mutation genotype in B cell chronic lymphocytic leukemia." J Exp Med **194**(11): 1639-1647.

Rossi, D., A. Bruscaggin, V. Spina, S. Rasi, H. Khiabanian, M. Messina, M. Fangazio, T. Vaisitti, S. Monti, S. Chiaretti, A. Guarini, I. Del Giudice, M. Cerri, S. Cresta, C. Deambrogi, E. Gargiulo, V. Gattei, F. Forconi, F. Bertoni, S. Deaglio, R. Rabadan, L. Pasqualucci, R. Foa, R. Dalla-Favera and G. Gaidano (2011). "Mutations of the SF3B1 splicing factor in chronic lymphocytic leukemia: association with progression and fludarabine-refractoriness." Blood **118**(26): 6904-6908.

Rossi, D., L. De Paoli, F. M. Rossi, M. Cerri, C. Deambrogi, S. Rasi, A. Zucchetto, D. Capello, V. Gattei and G. Gaidano (2008). "Early stage chronic lymphocytic leukaemia carrying unmutated IGHV genes is at risk of recurrent infections during watch and wait." Br J Haematol **141**(5): 734-736.

Rossi, D., M. Fangazio, S. Rasi, T. Vaisitti, S. Monti, S. Cresta, S. Chiaretti, I. Del Giudice, G. Fabbri, A. Bruscaggin, V. Spina, C. Deambrogi, M. Marinelli, R. Fama, M. Greco, G. Daniele, F. Forconi, V. Gattei, F. Bertoni, S. Deaglio, L. Pasqualucci, A. Guarini, R. Dalla-Favera, R. Foa and G. Gaidano (2012). "Disruption of BIRC3 associates with fludarabine chemorefractoriness in TP53 wild-type chronic lymphocytic leukemia." Blood **119**(12): 2854-2862.

Rossi, D., S. Rasi, G. Fabbri, V. Spina, M. Fangazio, F. Forconi, R. Marasca, L. Laurenti, A. Bruscaggin, M. Cerri, S. Monti, S. Cresta, R. Fama, L. De Paoli, P. Bulian, V. Gattei, A. Guarini, S. Deaglio, D. Capello, R. Rabadan, L. Pasqualucci, R. Dalla-Favera, R. Foa and G. Gaidano (2012). "Mutations of NOTCH1 are an independent predictor of survival in chronic lymphocytic leukemia." Blood **119**(2): 521-529.

Rossi, D., E. Sozzi, A. Puma, L. De Paoli, S. Rasi, V. Spina, A. Gozzetti, M. Tassi, E. Cencini, D. Raspadori, V. Pinto, F. Bertoni, V. Gattei, F. Lauria, G. Gaidano and F. Forconi (2009). "The prognosis of clinical monoclonal B cell lymphocytosis differs from prognosis of Rai 0 chronic lymphocytic leukaemia and is recapitulated by biological risk factors." Br J Haematol **146**(1): 64-75.

Rossi, D., A. Zucchetto, F. M. Rossi, D. Capello, M. Cerri, C. Deambrogi, S. Cresta, S. Rasi, L. De Paoli, C. L. Bodoni, P. Bulian, G. Del Poeta, M. Ladetto, V. Gattei and G. Gaidano

(2008). "CD49d expression is an independent risk factor of progressive disease in early stage chronic lymphocytic leukemia." Haematologica **93**(10): 1575-1579.

Rossi, E., E. Matutes, R. Morilla, K. Owusu-Ankomah, A. M. Heffernan and D. Catovsky (1996). "Zeta chain and CD28 are poorly expressed on T lymphocytes from chronic lymphocytic leukemia." Leukemia **10**(3): 494-497.

Rossmann, E. D., M. Jeddi-Tehrani, A. Osterborg and H. Mellstedt (2003). "T-cell signaling and costimulatory molecules in B-chronic lymphocytic leukemia (B-CLL): an increased abnormal expression by advancing stage." Leukemia **17**(11): 2252-2254.

Rossmann, E. D., N. Lewin, M. Jeddi-Tehrani, A. Osterborg and H. Mellstedt (2002). "Intracellular T cell cytokines in patients with B cell chronic lymphocytic leukaemia (B-CLL)." Eur J Haematol **68**(5): 299-306.

Roth, A., D. de Beer, H. Nuckel, L. Sellmann, U. Duhrsen, J. Durig and G. M. Baerlocher (2008). "Significantly shorter telomeres in T-cells of patients with ZAP-70+/CD38+ chronic lymphocytic leukaemia." Br J Haematol **143**(3): 383-386.

Roy, M., T. Waldschmidt, A. Aruffo, J. A. Ledbetter and R. J. Noelle (1993). "The regulation of the expression of gp39, the CD40 ligand, on normal and cloned CD4+ T cells." J Immunol **151**(5): 2497-2510.

Rozman, C., E. Montserrat, J. M. Rodriguez-Fernandez, R. Ayats, T. Vallespi, R. Parody, A. Rios, D. Prados, M. Morey, F. Gomis and et al. (1984). "Bone marrow histologic pattern--the best single prognostic parameter in chronic lymphocytic leukemia: a multivariate survival analysis of 329 cases." Blood **64**(3): 642-648.

Rozman, C., E. Montserrat and N. Vinolas (1988). "Serum immunoglobulins in B-chronic lymphocytic leukemia. Natural history and prognostic significance." Cancer **61**(2): 279-283.

Ruan, J., E. Hyjek, P. Kermani, P. J. Christos, A. T. Hooper, M. Coleman, B. Hempstead, J. P. Leonard, A. Chadburn and S. Rafii (2006). "Magnitude of stromal hemangiogenesis correlates with histologic subtype of non-Hodgkin's lymphoma." Clin Cancer Res **12**(19): 5622-5631.

Rusak, M., A. Eljaszewicz, L. Bolkun, E. Luksza, I. Lapuc, J. Piszcz, P. Singh, M. Dabrowska, A. Bodzenta-Lukaszyk, J. Kloczko and M. Moniuszko (2015). "Prognostic significance of PD-1 expression on peripheral blood CD4+ T cells in patients with newly diagnosed chronic lymphocytic leukemia." Pol Arch Med Wewn **125**(7-8): 553-559.

Saboorian, M. H. and R. Ashfaq (2001). "The use of fine needle aspiration biopsy in the evaluation of lymphadenopathy." Semin Diagn Pathol **18**(2): 110-123.

Sallusto, F., D. Lenig, R. Forster, M. Lipp and A. Lanzavecchia (1999). "Two subsets of memory T lymphocytes with distinct homing potentials and effector functions." Nature **401**(6754): 708-712.

Sandhaus, L. M. (2000). "Fine-needle aspiration cytology in the diagnosis of lymphoma. The next step." Am J Clin Pathol **113**(5): 623-627.

Sanger, F., S. Nicklen and A. R. Coulson (1977). "DNA sequencing with chain-terminating inhibitors." Proc Natl Acad Sci U S A **74**(12): 5463-5467.

Sarfati, M., S. Chevret, C. Chastang, G. Biron, P. Stryckmans, G. Delespesse, J. L. Binet, H. Merle-Beral and D. Bron (1996). "Prognostic importance of serum soluble CD23 level in chronic lymphocytic leukemia." Blood **88**(11): 4259-4264.

Saudemont, A., N. Jouy, D. Hetuin and B. Quesnel (2005). "NK cells that are activated by CXCL10 can kill dormant tumor cells that resist CTL-mediated lysis and can express B7-H1 that stimulates T cells." Blood **105**(6): 2428-2435.

Savva, G. M., A. Pachnio, B. Kaul, K. Morgan, F. A. Huppert, C. Brayne, P. A. Moss, F. Medical Research Council Cognitive and S. Ageing (2013). "Cytomegalovirus infection is associated with increased mortality in the older population." Aging Cell **12**(3): 381-387.

Schaerli, P., K. Willimann, A. B. Lang, M. Lipp, P. Loetscher and B. Moser (2000). "CXC chemokine receptor 5 expression defines follicular homing T cells with B cell helper function." J Exp Med **192**(11): 1553-1562.

Schietinger, A. and P. D. Greenberg (2014). "Tolerance and exhaustion: defining mechanisms of T cell dysfunction." Trends Immunol **35**(2): 51-60.

Schmid, C. and P. G. Isaacson (1994). "Proliferation centres in B-cell malignant lymphoma, lymphocytic (B-CLL): an immunophenotypic study." Histopathology **24**(5): 445-451.

Schmid, S., M. Tinguely, P. Cione, H. Moch and B. Bode (2010). "Flow cytometry as an accurate tool to complement fine needle aspiration cytology in the diagnosis of low grade malignant lymphomas." Cytopathology.

Schroeder, H. W., Jr. and G. Dighiero (1994). "The pathogenesis of chronic lymphocytic leukemia: analysis of the antibody repertoire." Immunol Today **15**(6): 288-294.

Schuh, A., J. Becq, S. Humphray, A. Alexa, A. Burns, R. Clifford, S. M. Feller, R. Grocock, S. Henderson, I. Khrebtukova, Z. Kingsbury, S. Luo, D. McBride, L. Murray, T. Menju, A. Timbs, M. Ross, J. Taylor and D. Bentley (2012). "Monitoring chronic lymphocytic leukemia progression by whole genome sequencing reveals heterogeneous clonal evolution patterns." Blood **120**(20): 4191-4196.

Scrivener, S., E. R. Kaminski, A. Demaine and A. G. Prentice (2001). "Analysis of the expression of critical activation/interaction markers on peripheral blood T cells in B-cell chronic lymphocytic leukaemia: evidence of immune dysregulation." Br J Haematol **112**(4): 959-964.

Seddiki, N., B. Santner-Nanan, J. Martinson, J. Zaunders, S. Sasson, A. Landay, M. Solomon, W. Selby, S. I. Alexander, R. Nanan, A. Kelleher and B. Fazekas de St Groth (2006). "Expression of interleukin (IL)-2 and IL-7 receptors discriminates between human regulatory and activated T cells." J Exp Med **203**(7): 1693-1700.

Seifert, M., L. Sellmann, J. Bloehdorn, F. Wein, S. Stilgenbauer, J. Durig and R. Kuppers (2012). "Cellular origin and pathophysiology of chronic lymphocytic leukemia." J Exp Med **209**(12): 2183-2198.

Sellmann, L., D. de Beer, M. Bartels, B. Opalka, H. Nuckel, U. Duhrsen, J. Durig, M. Seifert, D. Siemer, R. Kuppers, G. M. Baerlocher and A. Roth (2011). "Telomeres and prognosis in patients with chronic lymphocytic leukaemia." Int J Hematol **93**(1): 74-82.

Serrano, D., J. Monteiro, S. L. Allen, J. Kolitz, P. Schulman, S. M. Lichtman, A. Buchbinder, V. P. Vinciguerra, N. Chiorazzi and P. K. Gregersen (1997). "Clonal expansion within the CD4+CD57+ and CD8+CD57+ T cell subsets in chronic lymphocytic leukemia." J Immunol **158**(3): 1482-1489.

Sfanos, K. S., T. C. Bruno, A. K. Meeker, A. M. De Marzo, W. B. Isaacs and C. G. Drake (2009). "Human prostate-infiltrating CD8+ T lymphocytes are oligoclonal and PD-1+." Prostate **69**(15): 1694-1703.

Shaffer, A. L., 3rd, R. M. Young and L. M. Staudt (2012). "Pathogenesis of human B cell lymphomas." Annu Rev Immunol **30**: 565-610.

Shanafelt, T. D., S. M. Geyer, N. D. Bone, R. C. Tschumper, T. E. Witzig, G. S. Nowakowski, C. S. Zent, T. G. Call, B. Laplant, G. W. Dewald, D. F. Jelinek and N. E. Kay (2008). "CD49d expression is an independent predictor of overall survival in patients with chronic lymphocytic leukaemia: a prognostic parameter with therapeutic potential." Br J Haematol **140**(5): 537-546.

Shanafelt, T. D., N. E. Kay, T. G. Call, C. S. Zent, D. F. Jelinek, B. LaPlant, W. G. Morice and C. A. Hanson (2008). "MBL or CLL: which classification best categorizes the clinical course of patients with an absolute lymphocyte count >or= 5 x 10(9) L(-1) but a B-cell lymphocyte count <5 x 10(9) L(-1)?" Leuk Res **32**(9): 1458-1461.

Shanafelt, T. D., T. E. Witzig, S. R. Fink, R. B. Jenkins, S. F. Paternoster, S. A. Smoley, K. J. Stockero, D. M. Nast, H. C. Flynn, R. C. Tschumper, S. Geyer, C. S. Zent, T. G. Call, D. F. Jelinek, N. E. Kay and G. W. Dewald (2006). "Prospective evaluation of clonal evolution during long-term follow-up of patients with untreated early-stage chronic lymphocytic leukemia." J Clin Oncol **24**(28): 4634-4641.

Sharma, P. and J. P. Allison (2015). "The future of immune checkpoint therapy." Science **348**(6230): 56-61.

Sharpe, A. H. and G. J. Freeman (2002). "The B7-CD28 superfamily." Nat Rev Immunol **2**(2): 116-126.

Sheppard, K. A., L. J. Fitz, J. M. Lee, C. Benander, J. A. George, J. Wooters, Y. Qiu, J. M. Jussif, L. L. Carter, C. R. Wood and D. Chaudhary (2004). "PD-1 inhibits T-cell receptor induced phosphorylation of the ZAP70/CD3zeta signalosome and downstream signaling to PKCtheta." FEBS Lett **574**(1-3): 37-41.

Sherwood, A. M., C. Desmarais, R. J. Livingston, J. Andriesen, M. Haussler, C. S. Carlson and H. Robins (2011). "Deep sequencing of the human TCRgamma and TCRbeta repertoires suggests that TCRbeta rearranges after alphabeta and gammadelta T cell commitment." Sci Transl Med **3**(90): 90ra61.

Sherwood, A. M., R. O. Emerson, D. Scherer, N. Habermann, K. Buck, J. Staffa, C. Desmarais, N. Halama, D. Jaeger, P. Schirmacher, E. Herpel, M. Kloor, A. Ulrich, M. Schneider, C. M. Ulrich and H. Robins (2013). "Tumor-infiltrating lymphocytes in colorectal tumors display a diversity of T cell receptor sequences that differ from the T cells in adjacent mucosal tissue." Cancer Immunol Immunother **62**(9): 1453-1461.

Six, A., M. E. Mariotti-Ferrandiz, W. Chaara, S. Magadan, H. P. Pham, M. P. Lefranc, T. Mora, V. Thomas-Vaslin, A. M. Walczak and P. Boudinot (2013). "The Past, Present, and Future of Immune Repertoire Biology - The Rise of Next-Generation Repertoire Analysis." Front Immunol **4**: 413.

Smit, L. A., D. Y. Hallaert, R. Spijker, B. de Goeij, A. Jaspers, A. P. Kater, M. H. van Oers, C. J. van Noesel and E. Eldering (2007). "Differential Noxa/Mcl-1 balance in peripheral versus lymph node chronic lymphocytic leukemia cells correlates with survival capacity." Blood **109**(4): 1660-1668.

Smith, L. M., J. Z. Sanders, R. J. Kaiser, P. Hughes, C. Dodd, C. R. Connell, C. Heiner, S. B. Kent and L. E. Hood (1986). "Fluorescence detection in automated DNA sequence analysis." Nature **321**(6071): 674-679.

Snodgrass, H. R., A. M. Fisher, E. Bruyns and B. Bogen (1992). "Restricted alpha/beta receptor gene usage of idiotype-specific major histocompatibility complex-restricted T cells: selection for CDR3-related sequences." Eur J Immunol **22**(8): 2169-2172.

Solomon, B. M., K. G. Rabe, S. L. Slager, J. D. Brewer, J. R. Cerhan and T. D. Shanafelt (2013). "Overall and cancer-specific survival of patients with breast, colon, kidney, and lung

cancers with and without chronic lymphocytic leukemia: a SEER population-based study." J Clin Oncol **31**(7): 930-937.

Soma, L. A., F. E. Craig and S. H. Swerdlow (2006). "The proliferation center microenvironment and prognostic markers in chronic lymphocytic leukemia/small lymphocytic lymphoma." Hum Pathol **37**(2): 152-159.

Speedy, H. E., M. C. Di Bernardo, G. P. Sava, M. J. Dyer, A. Holroyd, Y. Wang, N. J. Sunter, L. Mansouri, G. Juliusson, K. E. Smedby, G. Roos, S. Jayne, A. Majid, C. Dearden, A. G. Hall, T. Mainou-Fowler, G. H. Jackson, G. Summerfield, R. J. Harris, A. R. Pettitt, D. J. Allsup, J. R. Bailey, G. Pratt, C. Pepper, C. Fegan, R. Rosenquist, D. Catovsky, J. M. Allan and R. S. Houlston (2014). "A genome-wide association study identifies multiple susceptibility loci for chronic lymphocytic leukemia." Nat Genet **46**(1): 56-60.

Stamatopoulos, K., C. Belessi, C. Moreno, M. Boudjograh, G. Guida, T. Smilevska, L. Belhoul, S. Stella, N. Stavroyianni, M. Crespo, A. Hadzidimitriou, L. Sutton, F. Bosch, N. Laoutaris, A. Anagnostopoulos, E. Montserrat, A. Fassas, G. Dighiero, F. Caligaris-Cappio, H. Merle-Beral, P. Ghia and F. Davi (2007). "Over 20% of patients with chronic lymphocytic leukemia carry stereotyped receptors: Pathogenetic implications and clinical correlations." Blood **109**(1): 259-270.

Stein, H., A. Bonk, G. Tolksdorf, K. Lennert, H. Rodt and J. Gerdes (1980). "Immunohistologic analysis of the organization of normal lymphoid tissue and non-Hodgkin's lymphomas." J Histochem Cytochem **28**(8): 746-760.

Stein, H., J. Gerdes and D. Y. Mason (1982). "The normal and malignant germinal centre." Clin Haematol **11**(3): 531-559.

Steininger, C., L. Z. Rassenti, K. Vanura, K. Eigenberger, U. Jager, T. J. Kipps, C. Mannhalter, S. Stilgenbauer and T. Popow-Kraupp (2009). "Relative seroprevalence of human herpes viruses in patients with chronic lymphocytic leukaemia." Eur J Clin Invest **39**(6): 497-506.

Stevenson, F. K., S. Krysov, A. J. Davies, A. J. Steele and G. Packham (2011). "B-cell receptor signaling in chronic lymphocytic leukemia." Blood **118**(16): 4313-4320.

Stilgenbauer, S., S. Sander, L. Bullinger, A. Benner, E. Leupolt, D. Winkler, A. Krober, D. Kienle, P. Lichter and H. Dohner (2007). "Clonal evolution in chronic lymphocytic leukemia: acquisition of high-risk genomic aberrations associated with unmutated VH, resistance to therapy, and short survival." Haematologica **92**(9): 1242-1245.

Strefford, J. C., L. Kadalayil, J. Forster, M. J. Rose-Zerilli, A. Parker, T. T. Lin, N. Heppel, K. Norris, A. Gardiner, Z. Davies, D. Gonzalez de Castro, M. Else, A. J. Steele, H. Parker, T. Stankovic, C. Pepper, C. Fegan, D. Baird, A. Collins, D. Catovsky and D. G. Oscier (2015). "Telomere length predicts progression and overall survival in chronic lymphocytic leukemia: data from the UK LRF CLL4 trial." Leukemia.

Swerdlow, S. H., L. J. Murray, J. A. Habeshaw and A. G. Stansfeld (1984). "Lymphocytic lymphoma/B-chronic lymphocytic leukaemia--an immunohistopathological study of peripheral B lymphocyte neoplasia." Br J Cancer **50**(5): 587-599.

Tang, D., Q. Niu, N. Jiang, J. Li, Q. Zheng and Y. Jia (2014). "Increased frequencies of Th17 in the peripheral blood of patients with chronic lymphocytic leukemia: A one year follow-up." Pak J Med Sci **30**(5): 1128-1133.

te Raa, G. D., M. F. Pascutti, J. J. Garcia-Vallejo, E. Reinen, E. B. Remmerswaal, I. J. ten Berge, R. A. van Lier, E. Eldering, M. H. van Oers, S. H. Tonino and A. P. Kater (2014). "CMV-specific CD8+ T-cell function is not impaired in chronic lymphocytic leukemia." Blood **123**(5): 717-724.

Terrin, L., L. Trentin, M. Degan, I. Corradini, R. Bertorelle, P. Carli, N. Maschio, M. D. Bo, F. Noventa, V. Gattei, G. Semenzato and A. De Rossi (2007). "Telomerase expression in B-cell chronic lymphocytic leukemia predicts survival and delineates subgroups of patients with the same igVH mutation status and different outcome." Leukemia **21**(5): 965-972.

Thorselius, M., A. Krober, F. Murray, U. Thunberg, G. Tobin, A. Buhler, D. Kienle, E. Albesiano, R. Maffei, L. P. Dao-Ung, J. Wiley, J. Vilpo, A. Laurell, M. Merup, G. Roos, K. Karlsson, N. Chiorazzi, R. Marasca, H. Dohner, S. Stilgenbauer and R. Rosenquist (2006). "Strikingly homologous immunoglobulin gene rearrangements and poor outcome in VH3-21-using chronic lymphocytic leukemia patients independent of geographic origin and mutational status." Blood **107**(7): 2889-2894.

Till, K. J., K. Lin, M. Zuzel and J. C. Cawley (2002). "The chemokine receptor CCR7 and alpha4 integrin are important for migration of chronic lymphocytic leukemia cells into lymph nodes." Blood **99**(8): 2977-2984.

Tobin, G., U. Thunberg, K. Karlsson, F. Murray, A. Laurell, K. Willander, G. Enblad, M. Merup, J. Vilpo, G. Juliusson, C. Sundstrom, O. Soderberg, G. Roos and R. Rosenquist (2004). "Subsets with restricted immunoglobulin gene rearrangement features indicate a role for antigen selection in the development of chronic lymphocytic leukemia." Blood **104**(9): 2879-2885.

Tobin, G., U. Thunberg, A. Laurell, K. Karlsson, A. Aleskog, K. Willander, O. Soderberg, M. Merup, J. Vilpo, M. Hultdin, C. Sundstrom, G. Roos and R. Rosenquist (2005). "Patients with chronic lymphocytic leukemia with mutated VH genes presenting with Binet stage B or C form a subgroup with a poor outcome." Haematologica **90**(4): 465-469.

Tonino, S. H., P. J. van de Berg, S. L. Yong, I. J. ten Berge, M. J. Kersten, R. A. van Lier, M. H. van Oers and A. P. Kater (2012). "Expansion of effector T cells associated with decreased PD-1 expression in patients with indolent B cell lymphomas and chronic lymphocytic leukemia." Leuk Lymphoma **53**(9): 1785-1794.

Totterman, T. H., M. Carlsson, B. Simonsson, M. Bengtsson and K. Nilsson (1989). "T-cell activation and subset patterns are altered in B-CLL and correlate with the stage of the disease." Blood **74**(2): 786-792.

Trautmann, L., L. Janbazian, N. Chomont, E. A. Said, S. Gimmig, B. Bessette, M. R. Boulassel, E. Delwart, H. Sepulveda, R. S. Balderas, J. P. Routy, E. K. Haddad and R. P. Sekaly (2006). "Upregulation of PD-1 expression on HIV-specific CD8+ T cells leads to reversible immune dysfunction." Nat Med **12**(10): 1198-1202.

Trentin, L., R. Zambello, C. Agostini, C. Enthammer, A. Cerutti, F. Adami, S. Zamboni and G. Semenzato (1994). "Expression and regulation of tumor necrosis factor, interleukin-2, and hematopoietic growth factor receptors in B-cell chronic lymphocytic leukemia." Blood **84**(12): 4249-4256.

Tretter, T., M. Schuler, F. Schneller, U. Brass, M. Esswein, M. J. Aman, C. Huber and C. Peschel (1998). "Direct cellular interaction with activated CD4(+) T cells overcomes hyporesponsiveness of B-cell chronic lymphocytic leukemia in vitro." Cell Immunol **189**(1): 41-50.

Trojan, A., J. L. Schultze, M. Witzens, R. H. Vonderheide, M. Ladetto, J. W. Donovan and J. G. Gribben (2000). "Immunoglobulin framework-derived peptides function as cytotoxic T-cell epitopes commonly expressed in B-cell malignancies." Nat Med **6**(6): 667-672.

Troutt, A. B., M. G. McHeyzer-Williams, B. Pulendran and G. J. Nossal (1992). "Ligation-anchored PCR: a simple amplification technique with single-sided specificity." Proc Natl Acad Sci U S A **89**(20): 9823-9825.

Tung, J. W., D. R. Parks, W. A. Moore, L. A. Herzenberg and L. A. Herzenberg (2004). "New approaches to fluorescence compensation and visualization of FACS data." Clin Immunol **110**(3): 277-283.

Vaisitti, T., S. Aydin, D. Rossi, F. Cottino, L. Bergui, G. D'Arena, L. Bonello, A. L. Horenstein, P. Brennan, C. Pepper, G. Gaidano, F. Malavasi and S. Deaglio (2010). "CD38 increases CXCL12-mediated signals and homing of chronic lymphocytic leukemia cells." Leukemia **24**(5): 958-969.

Van Bockstaele, F., B. Verhasselt and J. Philippe (2009). "Prognostic markers in chronic lymphocytic leukemia: a comprehensive review." Blood Rev **23**(1): 25-47.

Van de Lest, C. H., E. M. Versteeg, J. H. Veerkamp and T. H. Van Kuppevelt (1995). "Elimination of autofluorescence in immunofluorescence microscopy with digital image processing." J Histochem Cytochem **43**(7): 727-730.

van Elsas, A., A. A. Hurwitz and J. P. Allison (1999). "Combination immunotherapy of B16 melanoma using anti-cytotoxic T lymphocyte-associated antigen 4 (CTLA-4) and granulocyte/macrophage colony-stimulating factor (GM-CSF)-producing vaccines induces rejection of subcutaneous and metastatic tumors accompanied by autoimmune depigmentation." J Exp Med **190**(3): 355-366.

van Kooten, C., I. Rensink, L. Aarden and R. van Oers (1992). "Interleukin-4 inhibits both paracrine and autocrine tumor necrosis factor-alpha-induced proliferation of B chronic lymphocytic leukemia cells." Blood **80**(5): 1299-1306.

Vandenborre, K., J. Delabie, M. A. Boogaerts, R. De Vos, K. Lorre, C. De Wolf-Peeters and P. Vandenberghe (1998). "Human CTLA-4 is expressed in situ on T lymphocytes in germinal centers, in cutaneous graft-versus-host disease, and in Hodgkin's disease." Am J Pathol **152**(4): 963-973.

Vandewoestyne, M. L., V. C. Pede, K. Y. Lambein, M. F. Dhaenens, F. C. Offner, M. M. Praet, J. J. Philippe, T. J. Kipps and D. L. Deforce (2011). "Laser microdissection for the assessment of the clonal relationship between chronic lymphocytic leukemia/small lymphocytic lymphoma and proliferating B cells within lymph node pseudofollicles." Leukemia **25**(5): 883-888.

Vlad, A., P. A. Deglesne, R. Letestu, S. Saint-Georges, N. Chevallier, F. Baran-Marszak, N. Varin-Blank, F. Ajchenbaum-Cymbalista and D. Ledoux (2009). "Down-regulation of CXCR4 and CD62L in chronic lymphocytic leukemia cells is triggered by B-cell receptor ligation and associated with progressive disease." Cancer Res **69**(16): 6387-6395.

Vollbrecht, C., F. D. Mairinger, U. Koitzsch, M. Peifer, K. Koenig, L. C. Heukamp, G. Crispatzu, L. Wilden, K. A. Kreuzer, M. Hallek, M. Odenthal, C. D. Herling and R. Buettner (2015). "Comprehensive Analysis of Disease-Related Genes in Chronic Lymphocytic Leukemia by Multiplex PCR-Based Next Generation Sequencing." PLoS One **10**(6): e0129544.

Vuillier, F., P. Tortevoye, J. L. Binet and G. Dighiero (1988). "CD4, CD8 and NK subsets in B-CLL." Nouv Rev Fr Hematol **30**(5-6): 331-334.

Waitz, R., M. Fasso and J. P. Allison (2012). "CTLA-4 blockade synergizes with cryoablation to mediate tumor rejection." Oncoimmunology **1**(4): 544-546.

Wallace, M. E., M. B. Alcantara, Y. Minoda, G. Kannourakis and S. P. Berzins (2015). "tAn emerging role for immune regulatory subsets in chronic lymphocytic leukaemia." Int Immunopharmacol.

Walton, J. A., P. M. Lydyard, A. Nathwani, V. Emery, A. Akbar, M. J. Glennie and N. Porakishvili (2010). "Patients with B cell chronic lymphocytic leukaemia have an expanded population of CD4 perforin expressing T cells enriched for human cytomegalovirus specificity and an effector-memory phenotype." Br J Haematol **148**(2): 274-284.

Wang, C., P. Hillsamer and C. H. Kim (2011). "Phenotype, effector function, and tissue localization of PD-1-expressing human follicular helper T cell subsets." BMC Immunol **12**: 53.

Wang, J., V. M. Vock, S. Li, O. R. Olivas and M. F. Wilkinson (2002). "A quality control pathway that down-regulates aberrant T-cell receptor (TCR) transcripts by a mechanism requiring UPF2 and translation." J Biol Chem **277**(21): 18489-18493.

Wang, L., M. S. Lawrence, Y. Wan, P. Stojanov, C. Sougnez, K. Stevenson, L. Werner, A. Sivachenko, D. S. DeLuca, L. Zhang, W. Zhang, A. R. Vartanov, S. M. Fernandes, N. R. Goldstein, E. G. Folco, K. Cibulskis, B. Tesar, Q. L. Sievers, E. Shefler, S. Gabriel, N. Hacohen, R. Reed, M. Meyerson, T. R. Golub, E. S. Lander, D. Neuberg, J. R. Brown, G. Getz and C. J. Wu (2011). "SF3B1 and other novel cancer genes in chronic lymphocytic leukemia." N Engl J Med **365**(26): 2497-2506.

Waterhouse, P., J. M. Penninger, E. Timms, A. Wakeham, A. Shahinian, K. P. Lee, C. B. Thompson, H. Griesser and T. W. Mak (1995). "Lymphoproliferative disorders with early lethality in mice deficient in Ctla-4." Science **270**(5238): 985-988.

Weiss, L., T. Melchardt, A. Egle, C. Grabmer, R. Greil and I. Tinhofer (2011). "Regulatory T cells predict the time to initial treatment in early stage chronic lymphocytic leukemia." Cancer **117**(10): 2163-2169.

Wen, T., H. Mellstedt and M. Jondal (1990). "Presence of clonal T cell populations in chronic B lymphocytic leukemia and smoldering myeloma." J Exp Med **171**(3): 659-666.

Wherry, E. J. (2011). "T cell exhaustion." Nat Immunol **12**(6): 492-499.

Widhopf, G. F., 2nd, L. Z. Rassenti, T. L. Toy, J. G. Gribben, W. G. Wierda and T. J. Kipps (2004). "Chronic lymphocytic leukemia B cells of more than 1% of patients express virtually identical immunoglobulins." Blood **104**(8): 2499-2504.

Wikby, A., B. Johansson, J. Olsson, S. Lofgren, B. O. Nilsson and F. Ferguson (2002). "Expansions of peripheral blood CD8 T-lymphocyte subpopulations and an association with cytomegalovirus seropositivity in the elderly: the Swedish NONA immune study." Exp Gerontol **37**(2-3): 445-453.

Wilcox, R. A., A. L. Feldman, D. A. Wada, Z. Z. Yang, N. I. Comfere, H. Dong, E. D. Kwon, A. J. Novak, S. N. Markovic, M. R. Pittelkow, T. E. Witzig and S. M. Ansell (2009). "B7-H1 (PD-L1, CD274) suppresses host immunity in T-cell lymphoproliferative disorders." Blood **114**(10): 2149-2158.

Wolchok, J. D., F. S. Hodi, J. S. Weber, J. P. Allison, W. J. Urba, C. Robert, S. J. O'Day, A. Hoos, R. Humphrey, D. M. Berman, N. Lonberg and A. J. Korman (2013). "Development of ipilimumab: a novel immunotherapeutic approach for the treatment of advanced melanoma." Ann N Y Acad Sci **1291**: 1-13.

Wood, B. (2006). "9-color and 10-color flow cytometry in the clinical laboratory." Arch Pathol Lab Med **130**(5): 680-690.

Woyach, J. A., A. J. Johnson and J. C. Byrd (2012). "The B-cell receptor signaling pathway as a therapeutic target in CLL." Blood **120**(6): 1175-1184.

Wu, C. J. (2012). "CLL clonal heterogeneity: an ecology of competing subpopulations." Blood **120**(20): 4117-4118.

Wu, C. J., A. Chillemi, E. P. Alyea, E. Orsini, D. Neuberg, R. J. Soiffer and J. Ritz (2000). "Reconstitution of T-cell receptor repertoire diversity following T-cell depleted allogeneic bone marrow transplantation is related to hematopoietic chimerism." Blood **95**(1): 352-359.

Wybran, J., S. Chantler and H. H. Fudenberg (1973). "Isolation of normal T cells in chronic lymphatic leukaemia." Lancet **1**(7795): 126-129.

Xerri, L., B. Chetaille, N. Seriari, C. Attias, Y. Guillaume, C. Arnoulet and D. Olive (2008). "Programmed death 1 is a marker of angioimmunoblastic T-cell lymphoma and B-cell small lymphocytic lymphoma/chronic lymphocytic leukemia." Hum Pathol **39**(7): 1050-1058.

Xerri, L., B. Chetaille, N. Serriari, C. Attias, Y. Guillaume, C. Arnoulet and D. Olive (2008). "Programmed death 1 is a marker of angioimmunoblastic T-cell lymphoma and B-cell small lymphocytic lymphoma/chronic lymphocytic leukemia." Hum Pathol **39**(7): 1050-1058.

Xing, D., A. G. Ramsay, J. G. Gribben, W. K. Decker, J. K. Burks, M. Munsell, S. Li, S. N. Robinson, H. Yang, D. Steiner, N. Shah, J. D. McMannis, R. E. Champlin, C. Hosing, P. A. Zweidler-McKay, E. J. Shpall and C. M. Bollard (2010). "Cord blood natural killer cells exhibit impaired lytic immunological synapse formation that is reversed with IL-2 exvivo expansion." J Immunother **33**(7): 684-696.

Yassai, M. B., Y. N. Naumov, E. N. Naumova and J. Gorski (2009). "A clonotype nomenclature for T cell receptors." Immunogenetics **61**(7): 493-502.

Yi, J. S., M. A. Cox and A. J. Zajac (2010). "T-cell exhaustion: characteristics, causes and conversion." Immunology **129**(4): 474-481.

Yokosuka, T., M. Takamatsu, W. Kobayashi-Imanishi, A. Hashimoto-Tane, M. Azuma and T. Saito (2012). "Programmed cell death 1 forms negative costimulatory microclusters that directly inhibit T cell receptor signaling by recruiting phosphatase SHP2." J Exp Med **209**(6): 1201-1217.

Young, N. A., T. I. Al-Saleem, H. Ehya and M. R. Smith (1998). "Utilization of fine-needle aspiration cytology and flow cytometry in the diagnosis and subclassification of primary and recurrent lymphoma." Cancer **84**(4): 252-261.

Young, R. M. and L. M. Staudt (2013). "Targeting pathological B cell receptor signalling in lymphoid malignancies." Nat Rev Drug Discov **12**(3): 229-243.

Yousfi Monod, M., V. Giudicelli, D. Chaume and M. P. Lefranc (2004). "IMGT/JunctionAnalysis: the first tool for the analysis of the immunoglobulin and T cell receptor complex V-J and V-D-J JUNCTIONs." Bioinformatics **20 Suppl 1**: i379-385.

Yuille, M. R., R. S. Houlston and D. Catovsky (1998). "Anticipation in familial chronic lymphocytic leukaemia." Leukemia **12**(11): 1696-1698.

Zamarin, D., R. B. Holmgaard, S. K. Subudhi, J. S. Park, M. Mansour, P. Palese, T. Merghoub, J. D. Wolchok and J. P. Allison (2014). "Localized oncolytic virotherapy overcomes systemic tumor resistance to immune checkpoint blockade immunotherapy." Sci Transl Med **6**(226): 226ra232.

Zambrano-Zaragoza, J. F., E. J. Romo-Martinez, J. Duran-Avelar Mde, N. Garcia-Magallanes and N. Vibanco-Perez (2014). "Th17 cells in autoimmune and infectious diseases." Int J Inflam **2014**: 651503.

Zangani, M. M., M. Froyland, G. Y. Qiu, L. A. Meza-Zepeda, J. L. Kutok, K. M. Thompson, L. A. Munthe and B. Bogen (2007). "Lymphomas can develop from B cells chronically helped by idiotype-specific T cells." J Exp Med **204**(5): 1181-1191.

Zenz, T., J. G. Gribben, M. Hallek, H. Dohner, M. J. Keating and S. Stilgenbauer (2012). "Risk categories and refractory CLL in the era of chemoimmunotherapy." Blood **119**(18): 4101-4107.

Zenz, T., D. Mertens, R. Kuppers, H. Dohner and S. Stilgenbauer (2010). "From pathogenesis to treatment of chronic lymphocytic leukaemia." Nat Rev Cancer **10**(1): 37-50.

Zeppa, P., G. Marino, G. Troncone, F. Fulciniti, A. De Renzo, M. Picardi, G. Benincasa, B. Rotoli, A. Vetrani and L. Palombini (2004). "Fine-needle cytology and flow cytometry immunophenotyping and subclassification of non-Hodgkin lymphoma: a critical review of 307 cases with technical suggestions." Cancer **102**(1): 55-65.

Zhang, S., L. Chen, J. Wang-Rodriguez, L. Zhang, B. Cui, W. Frankel, R. Wu and T. J. Kipps (2012). "The onco-embryonic antigen ROR1 is expressed by a variety of human cancers." Am J Pathol **181**(6): 1903-1910.

Zhang, S., C. C. Wu, J. F. Fecteau, B. Cui, L. Chen, L. Zhang, R. Wu, L. Rassenti, F. Lao, S. Weigand and T. J. Kipps (2013). "Targeting chronic lymphocytic leukemia cells with a humanized monoclonal antibody specific for CD44." Proc Natl Acad Sci U S A **110**(15): 6127-6132.

Zhang, Y., M. Kaur, B. D. Price, S. Tetradis and G. M. Makrigiorgos (2002). "An amplification and ligation-based method to scan for unknown mutations in DNA." Hum Mutat **20**(2): 139-147.

Zhuang, J., S. F. Hawkins, M. A. Glenn, K. Lin, G. G. Johnson, A. Carter, J. C. Cawley and A. R. Pettitt (2010). "Akt is activated in chronic lymphocytic leukemia cells and delivers a pro-survival signal: the therapeutic potential of Akt inhibition." Haematologica **95**(1): 110-118.

Zucchetto, A., R. Bomben, M. Dal Bo, P. Bulian, D. Benedetti, P. Nanni, G. Del Poeta, M. Degan and V. Gattei (2006). "CD49d in B-cell chronic lymphocytic leukemia: correlated expression with CD38 and prognostic relevance." Leukemia **20**(3): 523-525; author reply 528-529.